



Syngas Fermentation to Biofuels

Evaluation of the Interplay of Kinetics and Thermodynamics for Directing Bioconversions based on Mixed Microbial Communities

Grimalt-Aleman, Antonio

Publication date:
2019

Document Version
Publisher's PDF, also known as Version of record

[Link back to DTU Orbit](#)

Citation (APA):

Grimalt-Aleman, A. (2019). *Syngas Fermentation to Biofuels: Evaluation of the Interplay of Kinetics and Thermodynamics for Directing Bioconversions based on Mixed Microbial Communities*. Technical University of Denmark.

General rights

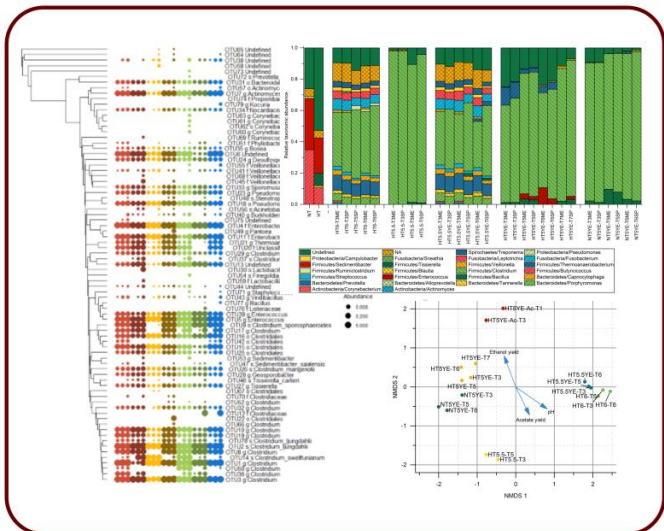
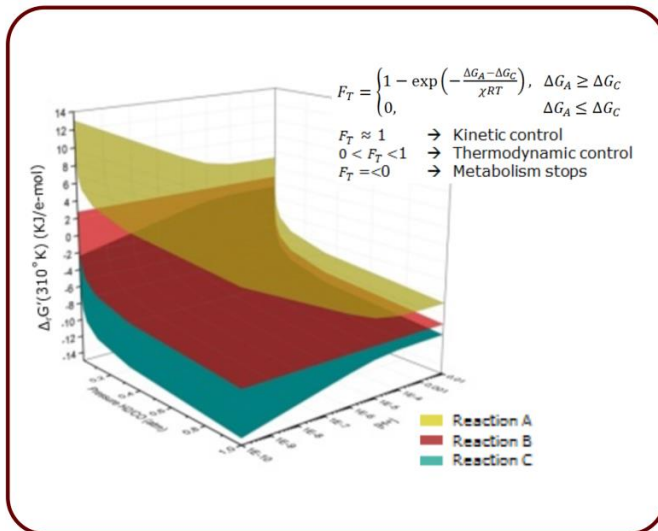
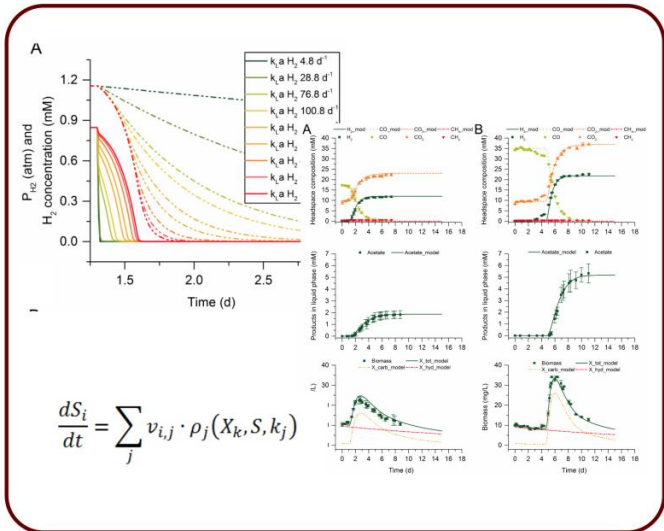
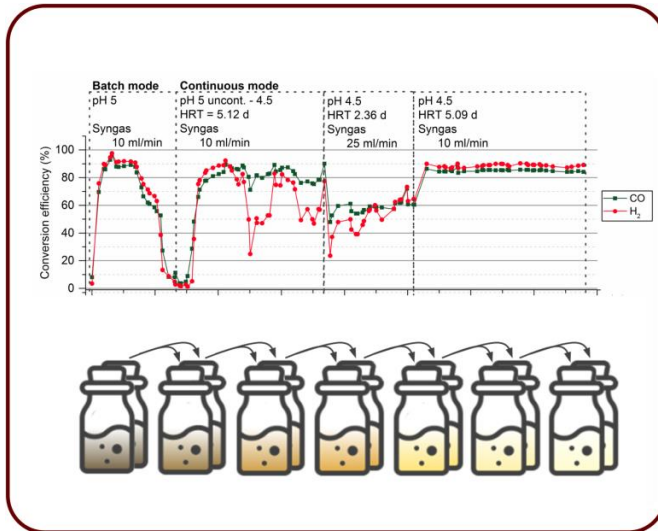
Copyright and moral rights for the publications made accessible in the public portal are retained by the authors and/or other copyright owners and it is a condition of accessing publications that users recognise and abide by the legal requirements associated with these rights.

- Users may download and print one copy of any publication from the public portal for the purpose of private study or research.
- You may not further distribute the material or use it for any profit-making activity or commercial gain
- You may freely distribute the URL identifying the publication in the public portal

If you believe that this document breaches copyright please contact us providing details, and we will remove access to the work immediately and investigate your claim.

SYNGAS FERMENTATION TO BIOFUELS:

Evaluation of the Interplay of Kinetics and Thermodynamics for Directing Bioconversions based on Mixed Microbial Communities



Antonio Grimalt-Alemany
PhD Thesis
September 2019



SYNGAS FERMENTATION TO BIOFUELS
*Evaluation of the Interplay of Kinetics and Thermodynamics for
Directing Bioconversions based on Mixed Microbial Communities*

Antonio Grimalt-Alemaný

PhD Thesis

September 2019

Supervisor: Associate Professor Hariklia N. Gavala

Co-supervisor: Associate Professor Ioannis V. Skiadas

Department of Chemical and Biochemical Engineering

Technical University of Denmark

DTU Chemical Engineering

Department of Chemical and Biochemical Engineering

SYNGAS FERMENTATION TO BIOFUELS
*Evaluation of the Interplay of Kinetics and Thermodynamics for
Directing Bioconversions based on Mixed Microbial Communities*

A dissertation

Presented to the Department of Chemical and Biochemical Engineering
of the Technical University of Denmark

In Partial Fulfillment of the Requirements for the Degree of
Doctor of Philosophy

By

Antonio Grimalt-Aleman

September 2019

Preface

This PhD dissertation is submitted to the Department of Chemical and Biochemical Engineering of the Technical University of Denmark (DTU) in partial fulfillment of the requirements for the degree of Doctor of Philosophy. The work presented in this dissertation was carried out in the period 2016-2019 as part of the SYNFERON project (Grant Acronym and Title: SYNFERON – Optimized syngas fermentation for biofuels production), coordinated by Professor G. K. Kontogeorgis and funded by Innovation Fund Denmark (Innovationsfonden). This work was supervised by Associate Professor Hariklia Gavala, and co-supervised by Associate Professor Ioannis Skiadas.

The thesis is structured in 7 chapters. In the 1st chapter, a general overview of biological syngas conversion processes, with special focus on syngas-converting mixed microbial communities, is given along with a short introduction of the different research topics covered in the thesis. The content of Chapter I is partially associated to Manuscript I. The scope, hypotheses and specific objectives of the thesis are defined in chapter 2. The main findings of the thesis are presented in thematic chapters; where the main findings of each manuscript related to the same research topic are discussed together in order to draw overall conclusions for each topic. Thus, in chapter 3, the potential of microbial enrichments for driving shifts in the metabolic activity and the microbial composition of syngas-converting microbial communities for production of CH₄ and ethanol is evaluated. Chapter 4 consists of an evaluation of the potential of thermodynamics as a tool for controlling the catabolic routes used by microbial communities converting syngas. In chapter 5, the main aspects of the syngas biomethanation models developed are discussed. Chapter 6 presents the main findings on the long-term cryopreservation of microbial communities. Lastly, the overall conclusions of the thesis are given in chapter 7.

The manuscripts included in the discussion of the previous chapters are provided in the appendix at the end of the document. The thesis (Chapters I-VII) is written as a stand-alone document. However, the reader is recommended to read the manuscripts related to the experimental work (Manuscripts II-VI) prior to reading the Chapters III-VI, as the latter cover only summaries of the main findings. Alternatively, the reader is referred to the manuscripts when detailed explanations and interpretations on the methods used and results obtained are needed.



Antonio Grimalt-Aleman
10th of September of 2019

List of publications

Collection of manuscripts included in the thesis:

- I. A. Grimalt-Alemany, I. V. Skiadas, and H. N. Gavala. Syngas biomethanation: State-of-the-art review and perspectives. *Biofuels, Bioprod Biorefining*, 2018; 12: 139–58.
- II. A. Grimalt-Alemany, M. Łężyk, L. Lange, I. V. Skiadas, and H. N. Gavala. Enrichment of syngas-converting mixed microbial consortia for ethanol production and thermodynamics-based design of enrichment strategies. *Biotechnol Biofuels*, 2018; 11, 198: 1–22.
- III. A. Grimalt-Alemany, M. Łężyk, D. M. Kennes-Veiga, I. V. Skiadas, and H. N. Gavala. Enrichment of mesophilic and thermophilic mixed microbial consortia for syngas biomethanation: the role of kinetic and thermodynamic competition. *Waste and Biomass Valorization*, 2019.
- IV. A. Grimalt-Alemany, K. Asimakopoulos, I. V. Skiadas, and H. N. Gavala. Modeling of Syngas Biomethanation and Control of Catabolic Routes of Mesophilic and Thermophilic Mixed Microbial Consortia. (Submitted).
- V. A. Grimalt-Alemany, M. Łężyk, K. Asimakopoulos, I. V. Skiadas, and H. N. Gavala. Cryopreservation and fast recovery of enriched syngas-converting microbial communities. (Submitted).
- VI. K. Asimakopoulos, A. Grimalt-Alemany, C. Lundholm-Høffner, H. N. Gavala and I. V. Skiadas Syngas Biomethanation with Exogenous H₂ Supply for the Production of Natural Gas Grade Biomethane. Contribution to sections 2.7 and 3.5. (Submitted).

Acknowledgements

First of all, I would like to thank my supervisors Associate Professor Hariklia N. Gavala and Associate Professor Ioannis V. Skiadas for giving me this opportunity. It has been a great personal and professional experience. I would also like to thank you for your good advice, support and interesting discussions we had during these 3½ years. Thanks also for always finding time for me and being open for discussion, despite your busy schedule.

I would like to thank Professor Georgios K. Kontogeorgis for the coordination of the SYNFERON project and for hosting me at CERE during the last part of this PhD project. Thanks also to Lene Lange, Peter K. Busk, Niels B. Rasmussen, Mauro Torli and other project partners for the collaboration and the interesting discussions during project meetings and other events.

I am especially grateful to Konstantinos, Mateusz, Christina and David for our collaboration during all these years. You made a great contribution to this work. Thanks for the time spent together in and outside the lab, for your good advice and all the interesting ideas and discussions we shared during this period. Special thanks to Konstantinos and Christina for all your efforts and hard work, for covering for me so many times, and for all the stressful and funny moments we went through together all this time. It was a great pleasure to spend these years with you.

I would also like to thank the people from the old BIOENG, and PROSYS and CERE centers of KT for welcoming and hosting me during this whole period, and for the nice time spent inside and outside the lab. Working in such a multicultural environment was an enriching experience both at a professional and personal level, where I had the opportunity to meet many interesting people. Thanks also to my former and present colleagues Cristiano, Stavros, Anna B. and Antonios for the nice time spent together during this journey. I would like to give special thanks to Georgios for his good advice, and our never-ending and always interesting conversations about science, life or any other topic we came across with.

Most of all, I would like to express my deepest gratitude and appreciation to Anna and Markos. Anna, you have been everything to me all these years. Thank you for your love and constant support, for being there when I most needed it, and for being so understanding during this whole journey. Thanks also for your always critic and constructive perspective on every single part of this work; you certainly helped me improving all my work. Lastly, I would like to thank you for your guidance and for everything I learned from you, your words were always valuable and inspiring to me. Gràcies a Markos per canviar-ho tot. Perquè sense dir una paraula, m'has donat la lliçó més important de la meua vida.

Summary

The climate crisis, the large production of waste worldwide and the foreseen depletion of fossil resources have fostered a paradigm shift towards the sustainable production of commodity chemicals, biofuels and biomaterials, and microbial production systems are expected to play an important role in this transition to a bio-based economy. Biotechnological applications have been traditionally based on the use of axenic cultures as biocatalysts. However, due to the large amount of waste to be potentially revalorized and the difficulty to treat these waste streams with axenic cultures, microbial communities started to be harnessed not only for waste treatment, but also for its conversion into valuable products, typically biogas through anaerobic digestion. The use of microbial communities is currently expanding from the conventional anaerobic digestion process towards other innovative technological platforms for expanding both the range of waste available to biological conversion and the range of possible products. Syngas fermentation is one of such innovative platforms where the potential of microbial communities can be harnessed for the synthesis of valuable products while lowering the operating costs. In this process, syngas (a mixture of mainly H₂, CO and CO₂) can be converted under anaerobic conditions into a range of products including CH₄, H₂, carboxylic acids (acetate, butyrate and caproate), and solvents (ethanol, butanol and hexanol).

Microbial communities may present a series of benefits derived from their inherent microbial diversity and functional redundancy, mainly including high resilience to process disturbances, the possibility of stable operation in continuous mode under non-sterile conditions and low costs of operation. Nevertheless, their high complexity also constitutes one of their major limitations, as the poor understanding of their complex network of metabolic interactions often results in limited control of their metabolism, ultimately hindering the control of the process and their product selectivity. Thus, this work attempted to address the limited control over their metabolic activity by evaluating the potential of several microbial community management strategies including directing the natural selection of microorganisms through microbial enrichments, the use of thermodynamic principles for designing operational strategies, and the use of modeling tools for ultimately improving the control over the activity of microbial communities. The production of ethanol and CH₄ were used as target products for evaluating the potential control of the metabolic activity of microbial communities using these tools. This work also attempted to deal with another of the challenges in microbial community driven processes, which is the reproducibility of the microbial activity and community structure of microbial communities after long-term frozen storage.

The microbial enrichment of microbial communities was found to drive a drastic reduction of complexity in the community structure, allowing the selection of the microbial trophic groups of interest and conditioning the catabolic routes used by the microbial community. Studying the effect of pH on the microbial selection of acetogenic microbial communities and their metabolic activity through microbial enrichments, a

maximum yield of ethanol of $59.15 \pm 0.18\%$ of the maximum theoretical was achieved. However, the changes in ethanol yield observed depending on the initial pH used could not be correlated with the microbial composition of the microbial communities, which indicated that the operating conditions were the main driver of the metabolic shift towards ethanol. In turn, the enrichment of methanogenic microbial communities at different incubation temperature resulted in microbial communities with drastic differences in their composition and activity rates. While the mesophilic enriched microbial community presented a rather intricate metabolic network and low specific CH_4 productivity (1.83 ± 0.27 mmol $\text{CH}_4/\text{g VSS/h}$), the thermophilic enriched microbial community resulted in a much simpler community structure and a much higher specific CH_4 productivity (33.48 ± 0.90 mmol $\text{CH}_4/\text{g VSS/h}$). Overall, microbial enrichments were found to be very effective for driving changes in the metabolic activity of microbial communities based on mutual exclusion interactions. However, the main limitation of this tool is that prior knowledge on the effect of the selective pressure applied is required, as the outcome of the microbial selection cannot be predicted otherwise.

Analyzing the interspecies metabolic network of the microbial communities based on the thermodynamic feasibility of prevailing net reactions during the fermentation of syngas alleviated partially the limitations of microbial enrichments, as it allowed for a more rational design of operational strategies targeting specific metabolic activities in the microbial communities. Using this approach, the maximum ethanol yield obtained in pH-based enrichments of acetogenic microbial communities was increased by 22.5% (reaching $72.44 \pm 2.11\%$ of the maximum theoretical) by increasing the initial concentration of acetate in the fermentation broth. In the case of methanogenic microbial communities, several catabolic route control strategies based on the modulation of the partial pressure of CO_2 for achieving higher product selectivity towards CH_4 were identified. The experimental results obtained for the mesophilic methanogenic microbial community when using a trickle bed reactor under continuous operation confirmed the catabolic route control, since the electron yield to acetate decreased from 3.4% to 0.4% by decreasing the partial pressure of CO_2 .

The syngas biomethanation process using mesophilic and thermophilic microbial communities was modelled by integrating thermodynamic and kinetic considerations in the growth models used. This allowed for an accurate description of the main cross-feeding, mutualistic and competitive interactions taking place during the fermentation. After model calibration, the models were able to predict changes in the catabolic routes used by the microbial communities and metabolic shifts for specific microbial trophic groups. Using these models, several catabolic route control strategies based on the modulation of the partial pressure of CO_2 (mentioned above) and the mass transfer were investigated through model simulations.

The long-term cryopreservation of syngas-converting microbial communities was studied based on the effect of the addition of several cryopreservation agents, namely glycerol, dimethylsulfoxide, polyvinylpyrrolidone,

Tween 80 and yeast extract, and also without cryopreservation agent addition. The results of the analysis of the microbial activity recovery and microbial community structure showed that the methods commonly applied, like adding glycerol or not adding any cryoprotective agent, were the least recommendable for long-term storage of microbial communities. Polyvinylpyrrolidone and Tween 80 were found to be the most effective cryopreservation agents for achieving a fast activity recovery and preservation of the microbial community structure. However, further work on the optimization of these methods and investigation of other possible cryopreservation agents is still needed.

Overall, the findings of this study suggested that the combination of all tools evaluated here are necessary for achieving some degree of control over the metabolic activity of microbial communities. Microbial enrichments are essential for the selection of the microbial trophic groups of interest and the exclusion of those with detrimental effects on the process. On the other hand, modeling tools integrating kinetic and thermodynamic constraints describing the performance of microbial communities as a function of the operating conditions are also necessary for an accurate design of operational strategies targeting specific biotransformations.

Dansk sammenfatning

Klimakrisen, den store produktion af affald verden over og den forudsete udtømmning af fossile ressourcer har fremmet et paradigmeskift mod en bæredygtig produktion af råvarekemikalier, biobrændstoffer og biomaterialer, og mikrobielle produktionssystemer forventes at spille en vigtig rolle i denne overgang til et biobaseret økonomi. Bioteknologiske anvendelser er traditionelt baseret på brugen af mono-kulturer som biokatalysatorer. På grund af den store mængde affald, der potentielt kunne genbruges, og vanskeligheden med at behandle disse affaldsstrømme med mono-kulturer, har mikrobielle samfund været brugt til affaldsbehandling, men også for omdannelse til værdifulde produkter, typisk biogas gennem anaerob fordøjelse. Brugen af mikrobielle samfund udvikles i øjeblikket fra den konventionelle anaerobe fordøjelsesproces mod andre innovative teknologiske platforme. Syngasfermentering er en af sådanne innovative platforme, hvor potentialet i mikrobielle samfund kan udnyttes til syntese af værdifulde produkter og samtidig sænke driftsomkostningerne. I denne proces kan syngas (en blanding af hovedsageligt H_2 , CO og CO_2) omdannes under anaerobe betingelser til en række produkter, herunder CH_4 , H_2 , carboxylsyrer (acetat, butyrat og caproat) og opløsningsmidler (ethanol, butanol og hexanol).

Mikrobielle samfund har en række fordele, der stammer fra deres mikrobielle mangfoldighed, såsom høj modstandsdygtighed over for processforstyrrelser, muligheden for stabil drift i kontinuerlig tilstand under ikke-sterile forhold og lave driftsomkostninger. Ikke desto mindre udgør deres høje kompleksitet også en af deres største begrænsninger, da den dårlige forståelse af deres komplekse netværk af metaboliske interaktioner ofte resulterer i begrænset kontrol af deres stofskifte, hvilket i sidste ende hindrer kontrollen med processen og deres produktivitet. Således forsøgte dette arbejde at tackle den begrænsede kontrol over deres metaboliske aktivitet ved at evaluere potentialet i adskillige mikrobielle samfundsstyringsstrategier. Herunder at styre den naturlige selektion af mikroorganismer gennem mikrobiel berigelse, brugen af termodynamiske principper til design af operationelle strategier og brugen af modellering værktøjer der i sidste ende at forbedre kontrollen over aktiviteten i mikrobielle samfund. Produktionen af ethanol og CH_4 blev anvendt som målprodukter til evaluering af den potentielle kontrol af den metaboliske aktivitet i mikrobielle samfund under anvendelse af disse værktøjer. Dette arbejde forsøgte også at tackle en anden af udfordringerne i mikrobielle samfundsdrivne processer, som er reproducerbarheden af mikrobiel aktivitet og samfundsstruktur i mikrobielle samfund efter langvarig frosset opbevaring.

Det viste sig, at mikrobiel berigelse af mikrobielle samfund driver en drastisk reduktion af kompleksitet i samfundsstrukturen, hvilket muliggjorde udvælgelse af de mikrobielle grupper af interesse og konditionering af de kataboliske ruter, der blev anvendt af det mikrobielle samfund. Undersøgelse af virkningen af pH på mikrobiel selektion af acetogene mikrobielle samfund og deres metaboliske aktivitet gennem mikrobiel berigelse blev et maksimalt udbytte af ethanol på $59,15 \pm 0,18\%$ af det maksimale teoretiske. Ændringerne i

ethanoludbytte, var påvirket af den indledende pH-værdi, men kunne imidlertid ikke korreleres med den mikrobielle sammensætning af de mikrobielle samfund. Hvilket indikerede, at driftsbetingelserne var den vigtigste drivkraft for det metaboliske skift mod ethanol. Til gengæld resulterede berigelse af methanogene mikrobielle samfund ved forskellige inkubationstemperaturer i mikrobielle samfund med drastiske forskelle i deres sammensætning og aktivitetshastighed. Mens det mesofile berigede mikrobielle samfund præsenterede et temmelig indviklet metabolisk netværk og lav specifik CH_4 -produktivitet ($1,83 \pm 0,27$ mmol $\text{CH}_4/\text{g VSS/h}$), resulterede det termofile berigede mikrobielle samfund i en meget enklere samfundsstruktur og en meget højere specifik CH_4 -produktivitet ($33,48 \pm 0,90$ mmol $\text{CH}_4/\text{g VSS/h}$). Generelt var mikrobielle berigelser meget effektive til at drive ændringer i den metaboliske aktivitet i mikrobielle samfund. Hovedbegrænsningen af dette værktøj er imidlertid, at for kendskab til virkningen af det anvendte selektive tryk er påkrævet, da resultatet af det mikrobielle valg ikke kan forudsiges på anden måde.

Analysen er baseret på termodynamiske principper af det metaboliske netværk af mikrobielle samfund, dette gør det muligt at overkomme begrænsningerne i mikrobielle berigelser. Det muliggør en mere rationel design af operationelle strategier, der er målrettet specifikke metaboliske aktiviteter i mikrobielle samfund. Ved anvendelse af denne fremgangsmåde blev det maksimale ethanoludbytte opnået i pH-baseret berigelse af acetogene mikrobielle samfund øget med 22,5% (når $72,44 \pm 2,11\%$ af det maksimale teoretiske) ved at øge den indledende koncentration af acetat i fermenteringsvæsken. I tilfælde af methanogene mikrobielle samfund blev der identificeret adskillige katabolske rute kontrol strategier baseret på kontrollen af det partielle tryk af CO_2 for at opnå højere produktselektivitet over for CH_4 . De eksperimentelle resultater opnået for det mesofile methanogene mikrobielle samfund ved anvendelse af en trickle-bedreaktor under kontinuerlig drift bekræftede den katabolske rutekontrol, da elektronudbyttet til acetat faldt fra 3,4% til 0,4% ved at sænke det partielle tryk af CO_2 .

Syngas-biomethanationsprocessen ved anvendelse af mesofile og termofile mikrobielle samfund blev modelleret ved at integrere termodynamiske og kinetiske overvejelser i de anvendte vækstmodeller. Dette muliggjorde en nøjagtig beskrivelse af de vigtigste interaktioner, der finder sted under gæringen. Efter modelkalibrering var modellerne i stand til at forudsige ændringer i de katabolske ruter, der blev anvendt af mikrobielle samfund og metaboliske skift for specifikke mikrobielle grupper. Under anvendelse af disse modeller blev adskillige katabolske rute kontrol strategier baseret på kontrollen af det partielle tryk af CO_2 (nævnt ovenfor) og masseoverførslen undersøgt ved hjælp af modelsimuleringer.

Den langvarige kryokonservering af syngas-omdannende mikrobielle samfund blev undersøgt baseret på virkningen af tilsætningen af flere kryokonservings midler, nemlig glycerol, dimethylsulfoxid, polyvinylpyrrolidon, Tween 80 og gærekstrakt og også uden kryopræserving midler. Resultaterne af analysen af genopretningen af mikrobiel aktivitet og den mikrobielle samfundsstruktur viste, at de metoder, der almindeligvis blev anvendt, som tilsætning af glycerol eller uden kryobeskyttelsesmiddel, var det mindst

anbefalede til langtidsopbevaring af mikrobielle samfund. Polyvinylpyrrolidon og Tween 80 viste sig at være de mest effektive kryokonserveringsmidler til at opnå en hurtig aktivitetsgenvinding og konservering af den mikrobielle samfundsstruktur. Imidlertid er der stadig behov for yderligere arbejde med optimering af disse metoder og undersøgelse af andre mulige kryokonserveringsmidler.

Generelt antydede resultaterne af denne undersøgelse, at kombinationen af alle værktøjer, der er evalueret her, er nødvendig for at opnå en vis grad af kontrol over den mikrobielle samfunds metaboliske aktivitet. Mikrobielle berigelser er vigtige for udvælgelsen af de mikrobielle grupper af interesse og udelukkelse af dem med skadelige virkninger på processen. På den anden side er modelleringsværktøjer, der integrerer kinetiske og termodynamiske begrænsninger, der beskriver ydelsen af mikrobielle samfund som funktion af driftsbetingelserne, også nødvendige for en nøjagtig design af driftsstrategier, der er målrettet mod specifikke biotransformationer.

Table of contents

Chapter I – Introduction	1
1.1. Sustainability and the role of biofuels.....	1
1.2. Biomass conversion routes.....	4
1.3. Syngas fermentation	6
1.3.1. Reactor design and configuration.....	7
1.3.2. Biocatalysts.....	8
1.4. Syngas-converting microbial trophic groups in microbial communities.....	10
1.4.1. Hydrogenogenic bacteria and archaea.....	10
1.4.2. Sulfate-reducing bacteria and archaea.....	12
1.4.3. Acetogenic bacteria.....	12
1.4.4. Methanogenic archaea.....	14
1.4.5. Other relevant microbial trophic groups.....	16
1.5. Microbial interactions in syngas-converting microbial communities	17
1.5.1. Cross-feeding interactions	18
1.5.2. Mutualistic interactions	19
1.5.3. Mutual exclusion interactions	20
1.6. Challenges and tools linked to mixed-culture-based systems.....	21
Chapter II – Scope of the thesis	27
2.1. Hypotheses.....	27
2.2. Specific objectives.....	28
Chapter III – Enrichment of Syngas-Converting Mixed Microbial Communities.....	29
3.1. Purpose	29
3.2. Hypotheses.....	29
3.3. Specific objectives.....	29
3.4. Related manuscripts.....	30
3.5. Experimental procedures	30
3.6. Summary of results.....	31
3.7. Conclusions.....	33
Chapter IV – Thermodynamics-based Selection of Operating Parameters and Catabolic Route Control Strategies.....	40
4.1. Purpose	40
4.2. Hypothesis	40
4.3. Specific objectives.....	40
4.4. Related manuscripts.....	40
4.5. Computational and experimental procedures	41
4.6. Summary of results.....	43
4.7. Conclusions.....	46
Chapter V – Modeling of Syngas Biomethanation and Catabolic Route Control	56
5.1. Purpose	56
5.2. Hypotheses.....	56
5.3. Specific objectives.....	56
5.4. Related manuscript	57
5.5. Models description and procedures	57
5.6. Summary of results.....	58
5.7. Conclusions.....	60
Chapter VI – Cryopreservation of Mixed Microbial Communities.....	69
6.1. Purpose	69
6.2. Hypothesis	69
6.3. Specific objectives.....	69
6.4. Related manuscript	69
6.5. Experimental procedures	69
6.6. Summary of results.....	70
6.7. Conclusions.....	72
Chapter VII – Overall conclusions and future perspectives	76

References	79
Appendix – Collection of Manuscripts.....	97
Manuscript I.....	99
Manuscript II.....	121
Manuscript III.....	153
Manuscript IV.....	179
Manuscript V.....	239
Manuscript VI.....	269

Chapter I – Introduction

1.1. Sustainability and the role of biofuels

The Paris agreement entered into force on 4 November 2016 and was ratified by 187 countries, which committed to holding the increase of global average temperature below 2°C above pre-industrial levels, pursuing efforts to limit this temperature increase to 1.5°C in order to reduce the risks and impacts of climate change [1]. The goals of the agreement were then subscribed by the 2030 Agenda for Sustainable Development and were included in the “Sustainable Development Goals” [2]. Despite the success that a global agreement on this matter represents, the fact that the Paris agreement was strictly based on voluntary country pledges was heavily criticized by their implicit lack of legally binding commitment and provisions. Some of the elements of the agreement brought into question were (i) the fact that there were no legally binding greenhouse gas (GHG) emission reduction targets, (ii) no specifics on financial support to developing countries for mitigation and adaptation measures, (iii) no liability provision related to financial compensation for damage from climate change to least developed countries, and (iv) no change in the basic policy premises [3]. Additionally, the latest predictions indicate that even accounting for the current national pledges already set within the agreement, the goal of limiting the increase of the global average temperature below 2°C will most likely not be met, unless national GHG emission reduction policies become stricter in the future (fig. 1.1).

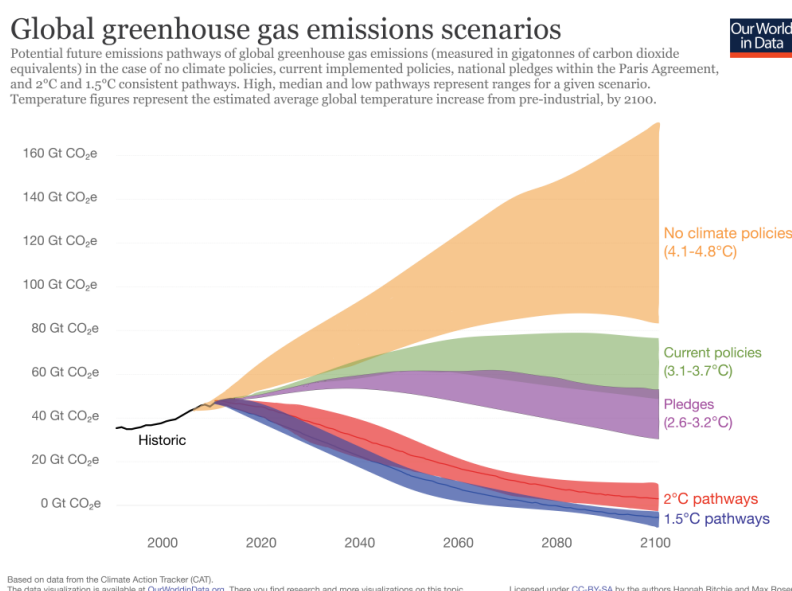


Figure 1.1. Global greenhouse gas emissions scenarios. Extracted from Ritchie & Roser [4].

The Paris agreement builds up on the vision of “Sustainable Development” as defined on by the Commission Brundtland in 1987 and the Declaration of Rio in 1992, which was established in response to the rising environmental awareness of the civil society during the 1960s and 1970s. During that time, the publication of scientific evidence of the harm caused to the environment by human activity in several books like *The silent spring* by Rachel Carson (1962) and *The population bomb* by Paul Ehrlich (1968), along with the oil crisis in the mid-1970s and several ecological disasters, raised an alarming mood in the civil society over the idea of an imminent ecological crisis. Additionally, the publication of the *The limits to growth* by Meadows and Rangers (1972) triggered a long debate where uncontrolled population growth and industrialization, and even the concept of unlimited economic growth, were brought into question after the realization of the finiteness of the resources of the planet and the fact that its maximum carrying capacity could be reached soon [5]. In that period, it became clear that the notion of development had to be redefined by including ideas associated with sustainability. Thus, the concept of “Sustainable Development” emerged as a compromise between economic growth and ecological conservation, and the notion of development started to be associated not only to economic growth and social equity, but to environmental preservation as well [5]. However, the necessity of economic growth was never questioned in this definition, and this ended up being a key aspect in defining the climate action strategies of the future, currently targeting the decarbonization of the economy by decoupling the increase in GDP and global energy demands from GHG emissions.

Within the frame of Sustainable Development, biofuels were expected to play an important role in reducing the GHG emissions and substituting fossil fuels mostly in the transportation sector [6]. However, the first policies fostering the production of biofuels were in fact motivated by the shortage in crude oil supplies and the rising prices of fossil fuels during the late 1970s. For example, the subsidization of ethanol in the US was prompted by the Energy Policy Act of 1978, which introduced a subsidy for blending ethanol into gasoline and established a higher taxation on foreign ethanol in order to stimulate the local production from corn, this way addressing energy security [7]. In turn, the implementation of policies in this direction in Europe did not take place until 2003, through the Directive 2003/30/EC. However, due to this delay, the main arguments of the European legislation were not limited to the diversification of energy supplies and the search of alternative outlets for the agricultural sector, and they also included the combat against climate change in response to the rising concerns of the civil society [8]. As a result of these policies, biofuels production rapidly gained relevance worldwide, both in developed and emerging countries, presenting a strong impact in the global market due to the key role of these regions in the international agricultural trade. According to the Food and Agriculture Organization (FAO), the world production of biofuels increased five times over the previous decade, rising from less than 20 billion liters per year in 2001 to over 100 billion liters per year in 2011 [8]. By the end of this period, the EU had become not only the largest producer of biofuels worldwide but also the largest net importer, accounting for a 45-fold increase in imported volume of biodiesel from 2006 to 2012 [9]. As this sharp increase was mostly based on first generation biodiesel, imported as fuel or

feedstock basically from Indonesia, Malaysia, US and Brazil [10], the increase in arable land required for farming these feedstocks had indirect implications on land use and food prices, bringing about a ripple effect with environmental and socio-economic impacts in these and other regions of the world [11]. Nevertheless, the adverse effects of the European “Biofuels Directive” were partially amended by the Directives 2009/28/EC and 2014/94/EU, which were built upon additional sustainability criteria on the exploitation of biomass and the deployment of an alternative fuel infrastructure. The Directive 2009/28/EC established legally binding targets for achieving a 20% share of energy from renewable sources on the overall European energy consumption by 2020 and a minimum share of 10% in the transport sector, emphasizing the need of promoting second generation biofuels. Similarly, US expanded the Renewable Fuel Standards (RFS) program through the Energy Independence and Security Act of 2007, which established a volume target for renewable fuels of 36 billion gallons by 2022 relying on a significant increase in the production of second generation biofuels.

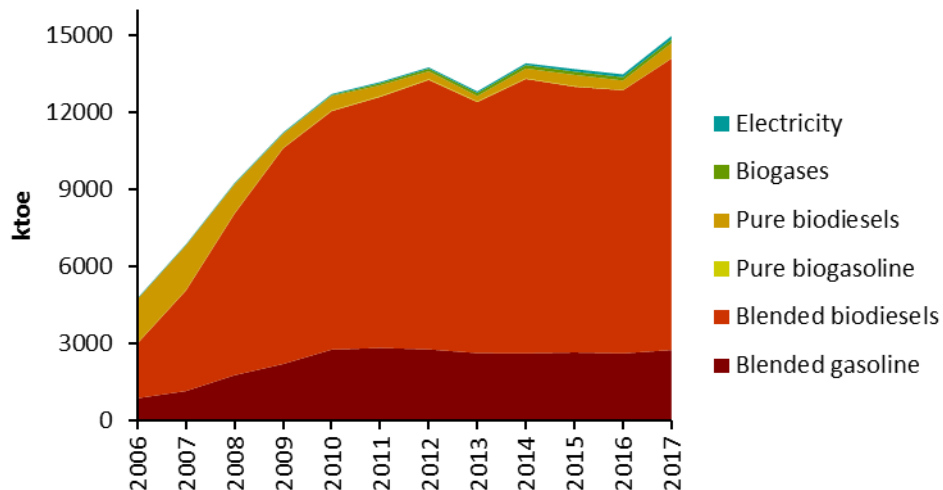


Figure 1.2. Energy consumption in road transport by type of renewable fuel. Data extracted from Eurostat [12].

In spite of the limitations of first generation biofuels in terms of resource efficiency and environmental performance, these are expected to dominate the renewable fuel sector in the coming years (fig. 1.2). However, at least in the EU, the current legal and regulatory framework poses an important opportunity for the development of an alternative technological infrastructure based on the use of waste streams as feedstock. Sweden is a notable example of this transition, in this case towards a biomethane-based transport fleet, where the consumption of biomethane (98,882 toe in 2016) is already comparable to that of bioethanol (109,057 toe in 2016) [13].

1.2. Biomass conversion routes

Second generation biofuels are considered a promising alternative for minimizing the negative impacts of first generation biofuels as these do not compete directly with conventional agriculture. This was shown in a study on the global land-use implications of first and second generation biofuels, which concluded that the latter have a better environmental performance provided that these are not sourced from dedicated energy crops directly competing with agricultural land [14]. Additionally, in contrast to first generation biofuels, mainly limited to sucrose-containing feedstocks and starchy materials, second generation biofuels are expected to exploit a much wider array of feedstocks such as industrial by-products (whey, glycerol, etc.), municipal solid wastes (food waste, paper, etc.), agricultural wastes (wheat straw, corn stalks, etc.), forest-based woody wastes (bark, sawdust, etc.), and industrial off-gases containing CO₂ and CO (from electricity and heat generation, iron and steel industry, etc.) [15,16], for which their GHG emission reduction potential should be higher. However, second generation biofuels face additional challenges associated with (i) the more recalcitrant nature of the lignocellulosic biomasses compared to the starchy materials typically employed in first generation biofuels, and (ii) the necessity of dealing with a huge variety of wastes of different nature that need to be processed independently. Overall, biomass and waste conversion routes being considered can be categorized in strictly biochemical methods, which would include the biological conversion of waste and lignocellulosic biomasses with or without a hydrolytic preprocessing step; and thermochemical methods, including e.g. pyrolysis and gasification, followed by a variety of catalytic and biological conversion processes (fig. 1.3).

Biochemical methods cover a wide range of raw materials and processes, within which a few examples are whey fermentation to ethanol by *Saccharomyces cerevisiae* [17], glycerol fermentation to butanol by *Clostridium pasterianum* [18], acetone-butanol-ethanol fermentation of municipal solid waste by *Clostridium acetobutylicum* [19] or anaerobic co-digestion of animal manures and lignocellulosic residues [20,21], among many others. However, ethanol fermentation of lignocellulosic biomasses such as wheat straw or corn stover is the most representative example as it is a mature technology with several commercial plants currently operational in US, Brazil and China [22]. In this case, the main advantages are related to the fast microbial growth, high microbial biomass titer and high product selectivity when considering commonly used yeasts, while the main challenges derive from the high content of lignin and hemicellulose in agricultural residues. Typically, agricultural residues are composed by 10-25% lignin, 20-30% hemicellulose and 40-50% cellulose [23], for which biomass pretreatment, enzymatic hydrolysis and additional unit operations for valorizing lignin and hemicellulose are often required prior to the fermentation. Another limitation may be the inhibition of the enzymatic hydrolysis and fermentation due to the generation of inhibitors like furfurals, hydroxymethylfurfurals and phenolic compounds during the pretreatment [24,25].

Thermochemical methods for biomass and waste conversion include processes like bio-oil production through liquefaction or pyrolysis, gasification followed by production of synthetic fuels from syngas (a gas mixture of mainly H₂, CO and CO₂) through Fischer-Tropsch (FT) processes, and gasification and further conversion of syngas into synthetic natural gas (bio-SNG) through catalytic methanation, among others [26,27]. Several demonstration and commercial scale plants for converting MSW and lignocellulosic biomasses into FT-fuels are currently under construction in US and Europe [28]. There is also a demonstration plant for bio-SNG production in Sweden [29]. The main advantage of many of these methods derives from the gasification step, which allows for a highly efficient conversion of the biomass including the more recalcitrant lignin fraction. The high feedstock flexibility, including biomasses with high lignin content such as forest residues and mixed wastes like MSW, is another key advantage. In turn, an important limitation in FT and catalytic methanation processes is the fact that the catalysts used are prone to poisoning and deactivation due to the presence of impurities in synthesis gas such as chlorine and sulfur compounds, ammonia, tars and particles, for which intensive raw syngas cleaning processes are required [30]. Furthermore, the additional water-gas shift reaction step often needed to obtain the correct ratio of C/H in syngas may increase the operation costs and complexity of the process, reducing its overall efficiency [31]. Another challenge generally encountered in these methods is the low product selectivity.

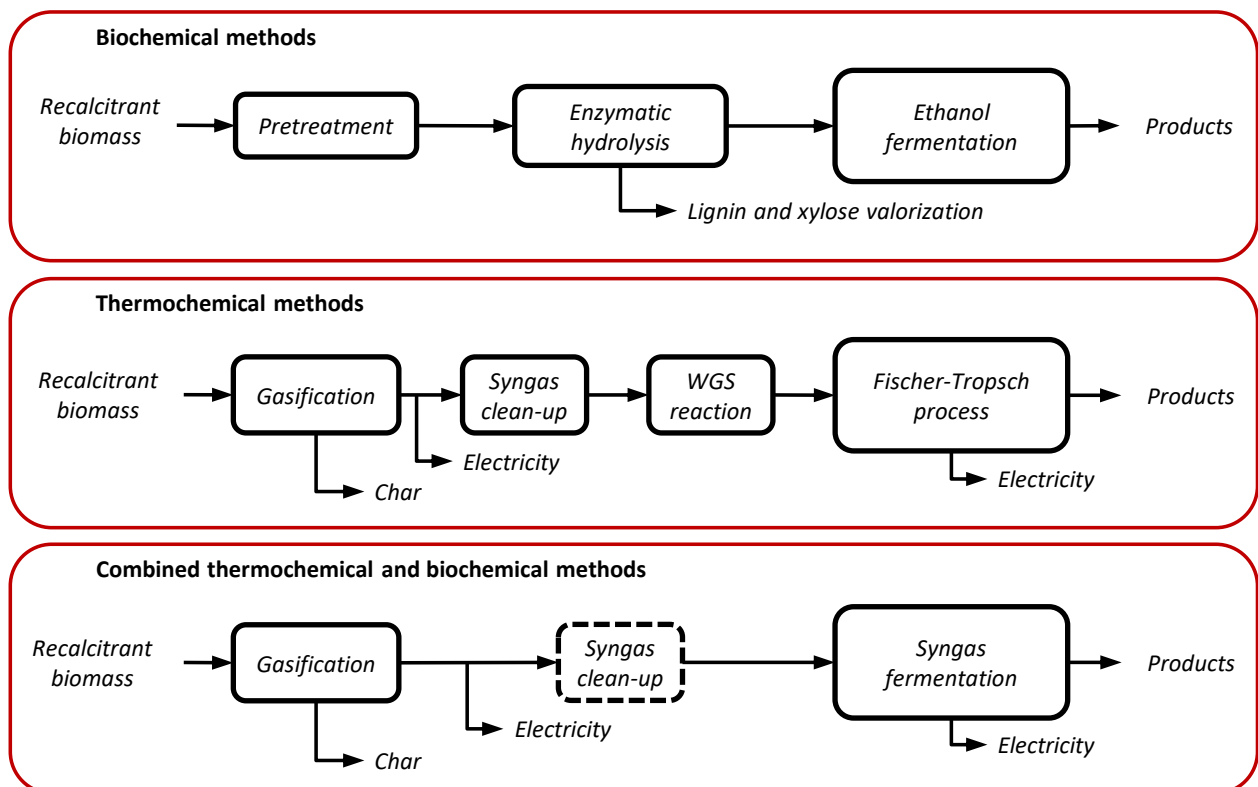


Figure 1.3. Overview of main biomass conversion routes.

The combination of thermochemical and biochemical methods, known as syngas fermentation, has also been proposed and consists of a first step where the biomass is gasified into syngas, followed by the biological conversion of syngas into a variety of fuels. This technology is less mature than ethanol fermentation or FT processes. However, as a result of this combination of methods, the process of syngas fermentation presents interesting features that make it a promising industrial application. On one hand, this process circumvents the limitations of the biological conversion of the lignocellulosic complex through the gasification of the biomass into a gas mixture that is directly fermentable. This enables the conversion of the lignin and hemicellulose fractions, which are typically not available in strictly biochemical methods. On the other hand, the operation at mild temperatures and pressures in syngas fermentation, and the use of inexpensive biocatalysts relatively tolerant to syngas impurities may result in a more cost-effective process when compared to FT processes [32]. Additionally, the fermentation of syngas can proceed independently of the ratio of C/H of syngas since the water-gas shift reaction is inherent to the autotrophic metabolism of the microorganisms used [33]. Another advantage is its high feedstock flexibility, since besides biomass-derived syngas, other CO/CO₂-rich industrial off-gases can also be used as substrate. In fact, the first commercial plant converting CO-rich waste gas into ethanol recently started its activity in China in 2018 [34]. However, the production of ethanol using biomass-derived syngas is still challenging. Other limitations typically encountered are the low growth rate of anaerobic microorganisms, the low microbial biomass concentration and the low gas-to-liquid mass transfer of the gaseous substrates, which limit the productivity of the process.

1.3. Syngas fermentation

The biological conversion of waste gases containing CO and syngas produced through gasification is typically carried out by anaerobic microorganisms. Acetogenic bacteria are currently the predominant microbial group studied in syngas fermentation processes, with *Clostridium ljungdahlii* and *Clostridium autoethanogenum* being the most common biocatalytic strains used for production of acetate and ethanol. These bacteria metabolize both H₂/CO₂ and CO as the sole carbon and energy source through the reductive acetyl-CoA or Wood-Ljungdahl pathway. Ethanol is undoubtedly the most common target product, for which a wide range of operational strategies aiming at the maximization of the ethanol yield and productivity have been investigated in the last decade using both pure and mixed cultures, mainly based on two-stage process operation [35,36], semi-continuous operation [37], glycerol as co-substrate [38], cyclic pH shifts [39,40], and the effect of nutrients, reducing agents and pH [41–46]. However, research on syngas fermentation has shifted over the past years towards broadening the product portfolio of *C. ljungdahlii* and *C. autoethanogenum* following three different approaches, i.e. metabolic engineering for synthesis of high value products, operational strategies targeting other natural products using alternative biocatalysts, and using microbial communities to expand the natural product portfolio of acetogenic bacteria and lower the

operating costs. In parallel, and independently of the targeted product, a large fraction of the studies conducted in syngas fermentation focused on reactor design and configuration in order to overcome the limitations derived from the low gas-to-liquid mass transfer and the low concentration of cells.

1.3.1. Reactor design and configuration

As stated above, syngas fermentation systems are often restricted by their low gas-to-liquid mass transfer and low cell concentration in the reactor, which ultimately reduce the volumetric productivity of the reactor. The volumetric mass transfer can be described by multiplying the difference between the real and the saturated gas concentration in the liquid phase (which is the driving force of the mass transfer) with the volumetric mass transfer coefficient ($k_{L,a}$), which depends on parameters like viscosity, surface tension, diffusivity of the gas and gas-liquid interfacial area. Therefore, the overall gas-to-liquid mass transfer could be enhanced by (i) increasing the mass transfer driving force, or (ii) increasing the $k_{L,a}$. Two studies reported an improved gas conversion and productivity of solvents when decreasing the incubation temperature from 37°C to 32°C and 25°C in each case, which was explained by the higher solubility (and higher mass transfer driving force) of H₂ and CO at these conditions [42,47]. Similarly, another study focusing on CH₄ production from CO reported improved CO consumption rates when increasing the total pressure of the reactor up to 14.6 atm, although CH₄ production was inhibited from 4 atm [48]. However, these studies are an exception, since most researchers focus on increasing the $k_{L,a}$ using different reactor types and configurations. Stirred tank reactors (STR) are the most commonly used, often equipped with a microbubble sparger to increase the $k_{L,a}$ [40,49–52]. Generally, $k_{L,a}$ values of the order of 14-35 h⁻¹ and 90-104 h⁻¹ have been measured for CO in STRs when using normal spargers and microbubble spargers, respectively, at different agitation rates [53]. However, high $k_{L,a}$ can only be obtained in STRs at the expense of high power input for mechanical mixing, which presents additional challenges and is generally considered not to be economically feasible in large scale. Alternative configurations considered in syngas fermentation with no mechanical mixing and relatively low cost of operation are bubble columns and gas-lift reactors [35,46]. A study comparing the mass transfer of CO between a bubble column and a gas-lift reactor, both equipped with a 20 μm bulb diffuser, reported maximum $k_{L,a}$ values of 78.8 h⁻¹ and 91.1 h⁻¹, respectively, when using a gas flow rate of 5000 sccm [54]. The highest $k_{L,a}$ value reported though, which corresponded to 1096.2 h⁻¹, was obtained by coupling a hollow fiber membrane module to a STR using a specific flow rate of 0.625 vvm of CO [55]. However, other hollow fiber membrane reactor configurations reported lower mass transfer for CO with a maximum $k_{L,a}$ value of 155.2 h⁻¹ [56]. A particularly interesting reactor type recently studied in syngas fermentation for production of ethanol and methane are trickle bed reactors [37,57]. Due to the fact that these are attached growth systems, these reactors address both the limitation of mass transfer and low concentration of cells simultaneously. Additionally, these generally require low energy input since there is neither mechanical mixing nor gas sparging at high pressure. Values of $k_{L,a}$ for O₂ reported for trickle bed reactors were within a

range of 178 h⁻¹ and 421 h⁻¹ [58]. Other reactor configurations studied for increasing the concentration of microbial biomass include a cell recycling system using hollow fiber membranes [35,59] and a reverse membrane bioreactor with total cell retention using membrane encased microorganisms [60].

1.3.2. Biocatalysts

Research on new syngas-fermenting biocatalysts can be categorized in three main approaches: metabolic engineering, novel wild-type strains and co-cultures, and mixed microbial communities.

Metabolic engineering

Metabolic engineering strategies aim at converting acetogenic bacteria in a microbial production platform for a wide range of chemicals and biofuels based on syngas as the sole carbon and energy source. Both rational design and directed evolution strain modification strategies have been used in *Clostridium* spp., although rational design strategies are more common [61,62]. The first genetically modified acetogen converting syngas was described by Köpke et al. [63], who transformed *C. ljungdahlii* with heterologous butanol production genes and demonstrated its production for the first time in *C. ljungdahlii*. Since then, several genetic engineering tools have been developed and more are under development. Examples of these tools are Clostron (for gene knockout), which was used for demonstrating energy conservation through electron bifurcation during H₂/CO₂ conversion into ethanol in *C. autoethanogenum* [64], and the CRISPR/Cas9 system, which was adapted for successful genome editing of *C. autoethanogenum* [65]. Other tools like genome-scale modeling, which allows to predict phenotypes and estimate intracellular flux patterns to ultimately improve rational design strategies [66], were also applied in *C. ljungdahlii* and *C. autoethanogenum* [67,68]. So far, these tools have been implemented for enhanced production of natural metabolites like acetate in *Acetobacterium woodii* [61] and ethanol in *C. autoethanogenum* [69], and for producing non-native products like butyrate [70], butanol [63] and 3-hydroxybutyrate [71] in *C. ljungdahlii*.

Novel wild-type strains and co-cultures

The acetogenic species *C. ljungdahlii* and *C. autoethanogenum*, able to convert syngas into mainly acetate and ethanol, and traces of 2,3-butanediol, were isolated in 1993 and 1994, respectively [72,73]. Since then, many other carboxydophilic species now considered for syngas- or waste gas-converting industrial applications were isolated, including further acetogenic bacteria [74], hydrogenogenic bacteria [75], methanogenic archaea [76] and even poly-3-hydroxyalkanoate-(bioplastic-)producing phototrophic bacteria [77]. Discovery of novel carboxydophilic hydrogenogenic species was especially fruitful since the discovery of *Carboxydotherrmus hydrogeniformans* in 1991 [78], as many other novel species were isolated including *Thermosinus carboxydivorans* [75], *Thermincola carboxydiphila* [79], *Thermococcus onnurineus* [80] and *Moorella stamsii* [81]. Some examples within the acetogenic microbial group are *C. coskatii* [74], *Alkalibaculum bacchi* [82], *C. ragsdalei* [83] and *C. carboxydivorans* [84]. Of these, *C. ragsdalei* and *C.*

carboxidivorans are particularly interesting due to their ability to synthesize butyrate, butanol, caproate and hexanol, among others, either directly from syngas or through re-assimilation of other metabolites [85,86]. Several studies have been published recently targeting the simultaneous production of ethanol, butanol and hexanol from syngas (H-B-E fermentation) using *C. carboxidivorans* [47,51,87–89].

An alternative approach for broadening the product portfolio of *C. ljungdahlii* and *C. autoethanogenum* is using co-cultures. One of the advantages of this approach is the fact that the microbial activity can be directed through specific catabolic pathways by selecting appropriate syntrophic partners. A good example can be found in the biomethanation of CO, which was shown to be directed through acetate as intermediate metabolite by using a co-culture of *Blautia producta* (formerly *Ruminococcus productus* and *Peptostreptococcus productus*) and *Methanotherix* sp. [48], or through H₂ as intermediate metabolite by using a co-culture of *Carboxydotherrnus hydrogenoformans* and *Methanothermobacter thermoautotrophicus* [90]. Other co-cultures composed by either *C. ljungdahlii* or *C. autoethanogenum*, and *C. kluyveri* have also been successfully used to combine the conversion of syngas into acetate and ethanol, carbon chain elongation of the latter to medium chain fatty acids (MCFAs), and further reduction of MCFAs into alcohols, resulting in a mixture of acetate, butyrate, caproate, caprylate, ethanol, butanol, hexanol and octanol [91,92]. However, in the latter example, one of the challenges often encountered is the difficulty of operating at optimal conditions (optimal pH) for the two species involved in the bioconversion. Thus, in order to overcome this limitation, two-stage process configurations have also been studied, where a mixture of acids is produced in the first stage by e.g. a mixed culture, and these acids are reduced into their corresponding alcohols in the second stage using *C. ragsdalei* and *C. ljungdahlii* [85,93].

Mixed cultures (mixed microbial consortia or mixed microbial communities)

The first study using syngas-converting mixed cultures on the perspective of a potential industrial application was carried out by Wise et al. in 1978, where the production of CH₄ and volatile fatty acids (VFAs) as by-products was demonstrated [94]. However, most of the studies on mixed-culture-based syngas fermentation were published after the 2000s, when syngas fermentation started gaining momentum as a future biotechnological application. The advantages associated with the use of mixed microbial communities in syngas fermentation are not limited to broadening the product spectrum of commonly used acetogenic bacteria, since these also offer the possibility of stable long-term continuous operation while lowering the operating costs due to fact that sterilization of the input streams is not required [95]. Their high stability when operating in continuous mode is especially convenient in attached growth systems like trickle bed reactors, which may be particularly prone to microbial contamination owing to the high cell residence time in the form of biofilm. Another potential advantage is their high resilience to disturbances and toxic compounds due to their inherent microbial diversity, which may lower the clean-up requirements of raw syngas when compared to axenic cultures. The product spectrum of mixed cultures is theoretically analogous to that of co-

culture systems as both of them are based on mainly cross-feeding microbial interactions for diverting the carbon to other products than acetate and ethanol. However, in this case, part of the research carried out has also focused on acetate and ethanol production. Using mixed cultures, the production of H₂ [96,97], CH₄ [57,60,98–103], volatile fatty acids (VFAs) (including acetate, propionate, butyrate, valerate, caproate, heptylate and caprylate) [104–111], ethanol [112–115] and other alcohols (including propanol, butanol and hexanol) [59,116–118] has been demonstrated. The conversion of syngas into CH₄ has been studied mostly in continuous operating mode using several reactor configurations, such as STR equipped with a spin-filter for cell retention [94], gas-lift reactors [99], trickle bed reactors [57], a multi-orifice baffled reactor [102] and a reverse membrane reactor [101]. A two-stage process with acetate as intermediate product was also proposed [98]. In turn, in the case of alcohols and VFAs production, STRs operated in batch mode are the most common set-up [104,105,113,116], although the possibility of using a packed-bubble flow reactor operated in continuous mode [109,111] and batch mode [110] was also studied for MCFAs production. As in the case of higher alcohol production using co-cultures, two-stage processes were also proposed using mixed cultures [117].

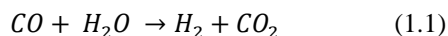
1.4. Syngas-converting microbial trophic groups in microbial communities

Syngas can support growth of a large variety of microorganisms including certain fungi [119], algae [120], phototrophic bacteria [121], hydrogenogenic bacteria [81] and archaea [122], sulfate-reducing bacteria [123] and archaea [124], acetogenic bacteria [125] and methanogenic archaea [126], among others. Nevertheless, in the absence of oxygen and light, CO and H₂/CO₂ can only be used as the sole carbon and energy source by acetogens, methanogens, sulfate reducers and hydrogenogens [127,128]. All these metabolic guilds have common metabolic features such as the fact that acetyl-CoA plays a central role in their anabolic metabolism and the fact that they all present CO dehydrogenases (CODH). However, the role of the CODHs is different in each metabolic guild, as these oxidize CO, synthesize acetyl-CoA or cleave acetyl-CoA in a variety of independent energy-yielding pathways [129]. A description of the main metabolic features of each of these microbial trophic groups is given in the next sections. Other microbial trophic groups playing a relevant role during the interspecies metabolism of syngas-converting microbial communities are also briefly described.

1.4.1. Hydrogenogenic bacteria and archaea

The carboxydrotrophic hydrogenogenic metabolism is based on the use of CO as the sole carbon and energy source in absence of other electron acceptors, resulting in the formation of equimolar amounts of H₂ and CO₂ according to eq. 1.1, which is the biological analogue to the catalytic water-gas shift reaction. The hydrogenogenic conversion of CO was first observed by Uffen in 1976 during the incubation of the phototroph *Rubrivivax gelatinosus* (f. *Rhodospseudomonas gelatinosa*), using CO as the only substrate in the

dark and under anaerobic conditions [130]. Since then, the amount of hydrogenogenic microorganisms isolated has increased significantly over the last decades, broadening the spectrum of prokaryotes with carboxydrotrophic hydrogenogenic abilities to other Gram-negative bacteria, thermophilic Gram-positive bacteria and thermophilic archaea [131,132].



All facultative anaerobes growing on hydrogenogenic conversion of CO are so far Gram-negative mesophilic bacteria, with the purple non-sulfur bacteria being the most predominant group [131]. Generally, this microbial group is limited by the poor growth rates exhibited in the dark. However, Kerby et al. [133] demonstrated that phototrophic bacteria are capable of rapid anaerobic growth on CO in the absence of light while working with *Rhodospirillum rubrum*. It was shown that *R. rubrum* was able to grow fast only when appropriate amounts of nickel were supplied with the medium, given that nickel was required for the synthesis of CODH.

The thermophilic hydrogenogenic bacterial group is formed by strict anaerobes belonging to the *Bacillus/Clostridium* sub-phylum [131]. So far, all isolated species are capable of growing on CO and inhibition due to high levels of CO has not been reported yet [131]. However, only two species have been found to be obligate carboxydrotrophs, namely *Carboxydocella thermoautotrophica* and *Thermincola carboxydiphila*, although the latter requires acetate as an additional carbon source [132,134]. Most hydrogenogenic thermophilic bacteria can grow fermentatively on a limited variety of substrates, and some also grow by reducing external electron acceptors such as Fe (III) or sulfate [132]. Generally, optimum growth in this microbial group takes place at temperatures ranging from 55°C to 80°C, exhibiting a rapid doubling time of around 1-2 h [135].

Lastly, the archaeal group of hydrogenogenic carboxydrotrophs is more limited in terms of isolates. To date, there are only a few hyperthermophilic archaea species capable of hydrogenogenic growth on CO, most of them belonging to the genus *Thermococcus* such as *Thermococcus AM4*, [122] *T. onnurineus* NA1 [80], and strains MP, Ch1 and Ch5 from the phylogenetic group of *T. barophilus* [136], among others. However, the hydrogenogenic growth of these microorganisms is not strictly linked to their carboxydrotrophic metabolism as some are also capable of growing on formate and starch producing H₂ as the main end product such as *T. onnurineus* NA1. Generally, this microbial group is able to grow on a rather wide range of temperature and pH conditions, although both *Thermococcus AM4* and *T. onnurineus* NA1 exhibit optimum hydrogenogenic growth on CO at temperatures and pH values around 80-82°C and 6.5, respectively [122,137].

As a microbial group, all hydrogenogenic carboxydrotrophs exhibit mechanisms of energy conservation through the formation of H₂ as an end product. This microbial group catalyzes the oxidation of CO by means of monofunctional CODH, which couple the oxidation of CO with the transfer of electrons to energy-

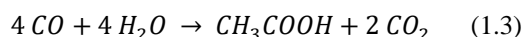
converting hydrogenases (Ech) to synthesize H₂ [138]. Concurrently, the electron transfer to Ech is coupled to the translocation of protons or sodium ions across the membrane, driving the synthesis of ATP by chemiosmotic phosphorylation [138,139]. Therefore, the energy conserving mechanisms of this microbial group are independent of the acetyl-CoA pathway. However, hydrogenogenic carboxydrotrophs use this pathway for the synthesis of cellular carbon through a bifunctional CODH/ACS complex [140].

1.4.2. Sulfate-reducing bacteria and archaea

The sulfate-reducing microbial group consists of both mesophilic and thermophilic obligate anaerobes able to conserve energy for biosynthesis by coupling the oxidation of organic compounds or H₂ with the reduction of sulfate. This microbial group is known to utilize a large variety of organic compounds as electron donor including carboxylic aliphatic acids, polar aromatic compounds, alcohols and even hydrocarbons [141]. Additionally, some species have been reported to use alternative electron acceptors such as sulfite, thiosulfate, sulfur or nitrate [141]. Growth on CO usually takes place through the conversion of CO and H₂O to CO₂ and H₂, subsequently using H₂ as an electron donor for the reduction of sulfate into sulfide [131,132,142]. Generally, carboxydrotrophic sulfate-reducers tolerate rather low partial pressure of CO (P_{CO}). For instance, the strains *Desulfotomaculum nigrificans* DSM 574 and *Desulfotomaculum sp.* RHT-3 were not able to grow on CO at levels exceeding 0.2 atm and 0.5 atm, respectively [123]. However, there are some exceptions such as *Desulfotomaculum carboxydivorans* (strain CO-1-SRB) and a strain of *Archaeoglobus fulgidus*, which are able to grow in absence of sulfate at high levels of CO as a hydrogenogen and as an acetogen, respectively [123,124]. Additionally, other sulfate-reducers such as *D. kuznetsovii* and *D. thermobenzoicum* shift their metabolism towards the production of acetate while increasing concentrations of CO during growth on CO, H₂ and CO₂ [143]. The carboxydrotrophic metabolism of the sulfate-reducing microbial group is based on the acetyl-CoA pathway for the fixation of carbon and the formation of acetate; however, the exact mechanism of electron funneling through the respiratory chain still remains unclear [142].

1.4.3. Acetogenic bacteria

Acetogenic bacteria are a phylogenetically diverse microbial group that can be found in a wide range of habitats growing on a variety of different substrates such as hexoses, C₂ and C₁ compounds [144]. However, this microbial group is defined by its ability to use the reductive acetyl-CoA pathway for the assimilation of CO₂ as the sole source of carbon and energy [145]. The formation of acetate from H₂/CO₂ and CO, according to eq. 1.2 and 1.3, was first reported by Fischer et al. in 1932 while working with enrichment cultures from sewage sludge [146]. Shortly after that, in 1936, Wieringa successfully isolated the first acetogenic anaerobe, *Clostridium aceticum*, growing on H₂ and CO₂ as the sole substrate [147].



To date, many of the acetogens isolated are able to grow on both H₂/CO₂ and CO such as *Moorella thermoacetica* (formerly *Clostridium thermoaceticum*) [148,149], *Clostridium autoethanogenum* [150], *Blautia producta* (f. *Ruminococcus productus* and *Peptostreptococcus productus*) [151], *Acetobacterium woodii* [152], *Eubacterium limosum* [152] and *Butyribacterium methylotrophicum* [153], among many others. As mentioned above, the autotrophic metabolism of acetogens is based on the reductive acetyl-CoA or Wood-Ljungdahl pathway, which consists of a methyl and a carbonyl branch for the synthesis of acetyl-CoA as a building block for the formation of cellular carbon and energy. In the methyl branch, CO₂ is reduced to formate and bound to tetrahydrofolate, which is subsequently reduced to methyl-tetrahydrofolate. Thereafter, the methyl group is transferred to the corronoid enzyme before being incorporated to acetyl-CoA. In turn, the formation of the carbonyl group of acetyl-CoA is carried out by a bifunctional CODH/ACS, which catalyzes the reduction of CO₂ to CO and subsequently fixes it into acetyl-CoA [154–156]. As shown in fig. 1.4, formyl-tetrahydrofolate is formed from formate at the expense of one mol of ATP, which is balanced by the gain of a mol of ATP by substrate-level phosphorylation in the acetate kinase reaction. Thus, the production of acetate through this pathway results in no net gain of energy by substrate level phosphorylation. This indicates that acetogens are able to conserve energy by means of alternative processes based on chemiosmosis [144,145]. However, the exact enzymatic complex behind the generation of these electrochemical gradients remained unknown until recently. This changed with the discovery of the Rnf complex, which was found to couple the oxidation of the reduced ferredoxin with the reduction of NAD⁺ and transmembrane ion export [157–159]. Additionally, an alternative energy-conserving module based on the Ech complex has been proposed recently for those acetogens lacking the Rnf complex such as *M. thermoacetica* [160]. Thus, the bioenergetics of all acetogens are strictly based on chemiosmotic processes, relying upon either (i) sodium-dependent ATP synthesis as found in *Acetobacterium woodii* or *Eubacterium limosum*, or (ii) proton-dependent ATP synthesis as found in *Clostridium ljungdahlii* or *Moorella thermoacetica* [157,161].

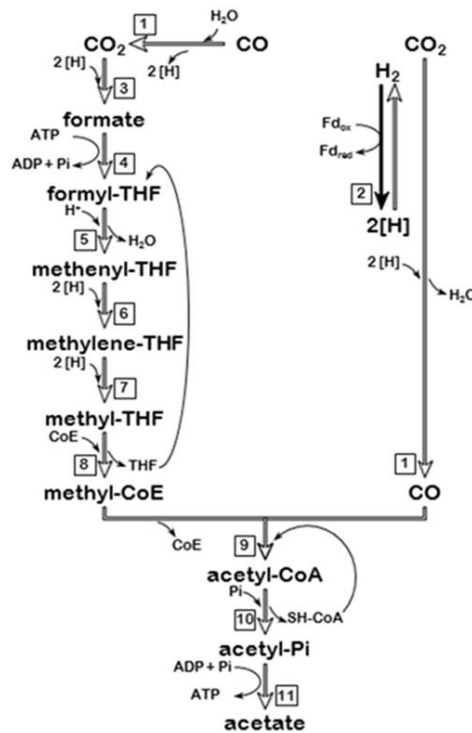


Figure 1.4. Acetyl-CoA pathway of acetogenic bacteria. 1, CO dehydrogenase; 2, hydrogenase; 3, formate dehydrogenase; 4, formyl-THF synthetase; 5, methenyl-THF cylohydrolase; 6, methylene-THF dehydrogenase; 7, methylene-THF reductase; 8, methyltransferase; 9, CO dehydrogenase/acetyl-CoA synthase; 10, phosphotransacetylase; 11, acetate kinase.

1.4.4. Methanogenic archaea

The biological conversion of CO into CH₄ was first discovered by Fischer et al. in 1932 while working with a methanogenic undefined mixed culture [162]. They observed that CO was metabolized through H₂ and CO₂ as intermediary products prior to their conversion into CH₄ according to eq. 1.1 and eq. 1.4, resulting in the overall stoichiometric reaction given in eq. 1.5.



These biochemical reactions were shortly after confirmed by Stephenson and Stickland using a pure culture capable of converting CO and H₂ to CH₄ [163]. However, Daniels et al. [164] were the first providing evidence of methanogenic growth on CO as the sole carbon and electron source using *Methanothermobacter thermoautotrophicus*. To date, only a few species of methanogenic archaea have been shown to utilize CO as the only substrate for growth including the aforementioned *Methanothermobacter thermoautotrophicus* [164], *Methanosarcina barkeri* [165], *Methanosarcina acetivorans* [126], and the recently discovered *Methanothermobacter marburgensis* [76], among others. However, the carboxydrotrophic growth of these species is strongly inhibited upon exposure to high P_{CO}. Both *M. thermoautotrophicus* and *M. marburgensis* can grow on P_{CO} up to 0.5 atm, where the first exhibits a doubling time of 200 h [76,164]. *M. barkeri* can

tolerate a P_{CO} of 1 atm, growing at a doubling time of 65 h [165]. In turn, *M. acetivorans* is so far the most tolerant and the fastest species growing on CO, presenting a doubling time of 24 h and withstanding a P_{CO} above 1 atm [126]. However, the authors of this study observed that *M. acetivorans* shifts its metabolism towards the production of substantial amounts of formate and acetate as end products upon CO inhibition, using the reductive acetyl-CoA pathway as an alternative energy conservation mechanism to methanogenesis [126]. This unusual metabolic capability illustrates the versatility of the energy conserving processes in methanogens.

As a microbial group, methanogens can produce CH_4 from a variety of substrates such as CO_2 , chlorinated compounds, methylated compounds or acetate. Methane is formed via three distinct metabolic pathways including the hydrogenotrophic pathway, the methylotrophic pathway and the acetoclastic pathway [166]. The mechanisms for conservation of energy along any of these pathways are based on chemiosmotic processes, in which an ion motive force is formed across the membrane [167]. In the hydrogenotrophic pathway, H_2 is used as an electron donor for the stepwise reduction of CO_2 to CH_4 through coenzyme-bound intermediates as shown in fig. 1.5 [142]. The methylotrophic pathway starts with the transfer of the methyl groups to the coenzyme M. In this pathway, three out of four methyl groups are diverted to the reductive branch for their reduction to CH_4 , while one out of four methyl groups is transferred through the reversed CO_2 reduction route for the generation of reducing equivalents needed for the reduction of $CH_3-S-CoM$ to CH_4 [166]. Lastly, the acetoclastic methanogenesis takes place through the reverse acetyl-CoA pathway, where acetate is converted to acetyl-CoA by acetate kinase and phosphotransacetylase. Thereafter, acetyl-CoA is split by a bifunctional CODH/ACS into CO and CH_3-H_4MPT , where the reducing equivalents obtained from the oxidation of CO to CO_2 are coupled to the reduction of the methyl group into CH_4 . To date, most carboxydrotrophic methanogens metabolize CO through the hydrogenotrophic pathway, for which carboxydrotrophic growth is basically hydrogenotrophic coupled to the oxidation of CO to CO_2 and H_2 by CODH and ferredoxin. However, *M. acetivorans* is able to metabolize CO through this pathway circumventing the formation of H_2 by means of mechanisms that still remain unclear [126].

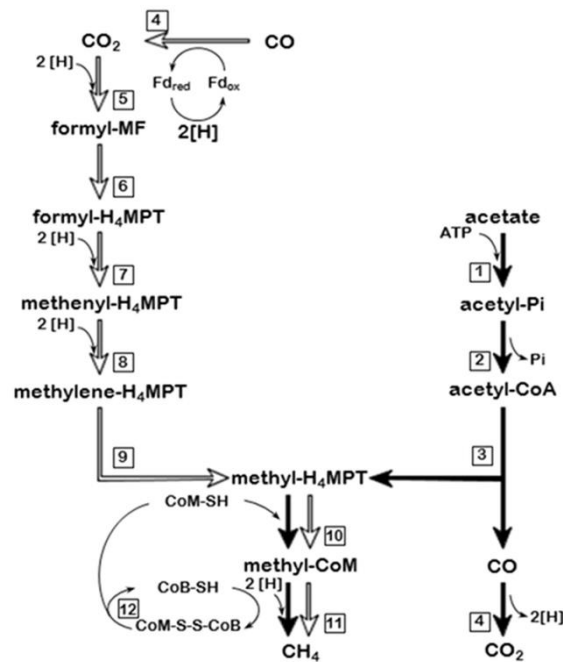


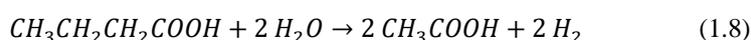
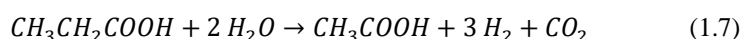
Figure 5. Pathways of carboxydrotrophic, hydrogenotrophic (empty arrows) and acetate-clastic (bold arrows) methanogenesis. 1, acetate kinase; 2, phosphotransacetylase; 3, CO dehydrogenase/acetyl-CoA synthase (CODH/ACS); 4, CO dehydrogenase(/acetyl-CoA synthase); 5, formyl-methanofuran (MF) dehydrogenase; 6, formyl-MF:tetrahydromethanopterin (H₄MPT) formyltransferase; 7, methenyl-H₄MPT cyclohydrolase; 8, methylene-H₄MPT dehydrogenase; 9, methylene-H₄MPT reductase; 10, methyl-H₄MPT:HS-CoM methyl transferase; 11, methyl-CoM reductase; 12, heterodisulfide reductase.

1.4.5. Other relevant microbial trophic groups

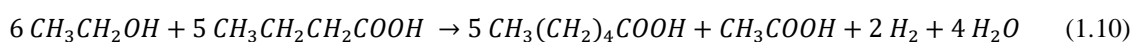
Besides acetate-clastic methanogens described above, there are other microbial groups that, despite they are not able to metabolize neither H₂/CO₂ (with few exceptions) nor CO, may play a significant role in microbial communities growing on syngas.

The first microbial group can be broadly defined as syntrophic fatty acid oxidizing bacteria, which is formed by a phylogenetically and metabolically diverse group of bacteria performing the syntrophic acetate, propionate and butyrate oxidation according to eq. 1.6, 1.7 and 1.8, respectively. Although each group carries out a different metabolic function, all of them share an intrinsic thermodynamic limitation in their main metabolic activity. Consequently, all of them are obligate syntrophic bacteria, since the continuous removal of their secreted products by a syntrophic partner is required to maintain their activity within the limits of thermodynamic feasibility. Despite syntrophic acetate oxidizers are known to play an important role in the conversion of acetate in anaerobic digesters under specific conditions [168,169], the number of isolates is still very limited and include *Clostridium ultunense* [170], *Syntrophaceticus schinkii* [171], *Tepidanaerobacter acetatoxydans* [172], *Thermacetogenium phaeum* [173], *Thermotoga lettingae* [174] and *Geobacter sulfurreducens*[175]. Most of them oxidize acetate through the oxidative acetyl-CoA pathway, except for *T. acetatoxydans*, *T. lettingae* and *G. sulfurreducens*, which most probably metabolize acetate

through the oxidative citric acid cycle [176,177]. In turn, all syntrophic butyrate-oxidizing bacteria metabolize butyrate through the β -oxidation pathway and belong to the order Clostridiales and Syntrophobacterales, including species like *Syntrophomonas wolfei* and *Syntrophus aciditrophicus* [178]. Syntrophic propionate oxidizers also belong to the order Clostridiales and Syntrophobacterales and include species like *Syntrophobacter fumaroxidans* and *Pelotomaculum propionicicum* [178]. All of them metabolize propionate through the methylmalonyl-CoA pathway, except for *Smithella propionica*, which uses a dismutating pathway to acetate and butyrate and later on oxidizes butyrate to acetate [179].



Another relevant microbial activity in mixed microbial communities is the carbon chain elongation, which consists in the conversion of short-chain fatty acids into MCFAs and H_2 through the reverse β -oxidation pathway, using a variety of electron donors such as methanol, ethanol or lactate (eq. 1.9 and 1.10) [180]. So far, a limited number of species belonging to the Clostridia class are known to utilize this pathway, including *Megasphaera elsdenii*, *Clostridium kluyveri*, *Pseudoramibacter alactolyticus*, *Eubacterium limosum*, *Eubacterium pyruvativorans*, and *Ruminococcaceae* bacterium CPB6 [181]. However, *Clostridium kluyveri* is considered the model organism for carbon chain elongation as it was the first to be isolated. This bacterium grows within a temperature range of 25-43°C and a pH range of 5.2-8, with optima at 35-37 °C and a pH of 6.4 [182].



1.5. Microbial interactions in syngas-converting microbial communities

Syngas fermentation systems operated with co-cultures generally exploit the association of two syntrophic partners based on cross-feeding interactions, where one species feeds upon the product of the other. This is also the case in syngas-converting methanogenic and acetogenic microbial communities used for production of CH_4 , ethanol or MCFAs, as these are produced through a network of interconnected biochemical reactions involving several microbial trophic groups (fig. 1.6). However, microbial communities generally present a higher level of complexity in their microbial interactions since, regardless their degree of specialization, they originate from natural microbial communities sustained not only based on cross-feeding interactions, but on a wide range of other symbiotic and mutual exclusion interactions. Since these are generally carried over to

engineered microbial communities, a few examples of microbial interactions known to take place during syngas biomethanation and syngas fermentation to ethanol and MCFAs are discussed here.

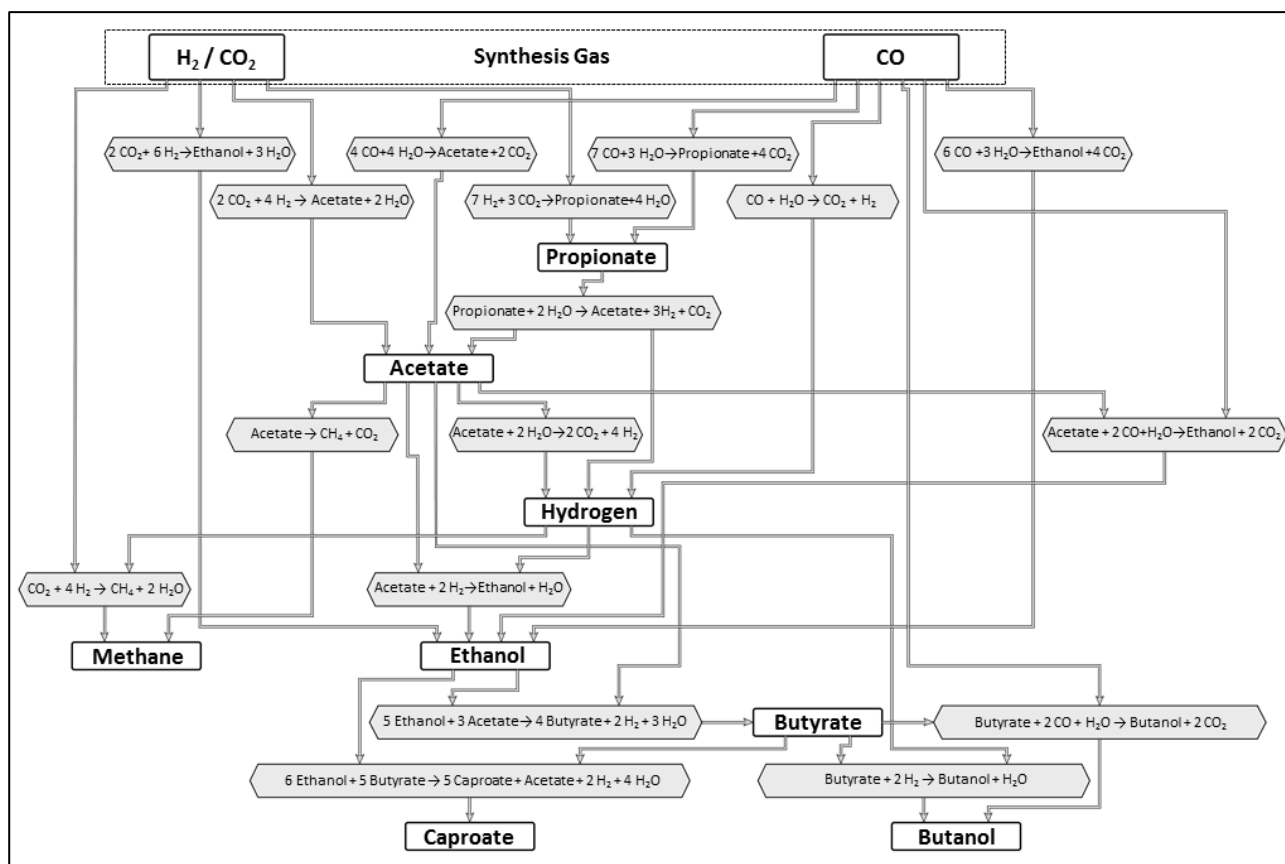


Figure 1.6. Interspecies metabolic network of syngas-converting methanogenic and acetogenic microbial communities. MCFAs with odd number of carbons, direct carboxydrotrophic methanogenesis and direct production of butyrate and butanol were left out of the figure for simplicity.

1.5.1. Cross-feeding interactions

As shown in fig. 1.6, there are multiple catabolic routes leading to ethanol and MCFAs when using mixed microbial communities. The production of ethanol can take place either directly from CO and H₂/CO₂, or indirectly through the reduction of acetate using either H₂ or CO as electron donor. In parallel, acetate may also be converted into butyrate and caproate in presence of ethanol through carbon chain elongation. Additionally, these MCFAs can be further reduced to their corresponding alcohols using either H₂ or CO as electron donor. As discussed above, there are a few acetogenic species such as *C. carboxidivorans*, which are able to perform all these reactions [47]. However, in a mixed microbial community, each of these reactions could also be carried out by different species given that each of them constitutes an independent energy-yielding metabolic bioconversion [183].

As opposed to acetogenic microbial communities, where the product spectrum tends to expand with each bioconversion step, methanogenic microbial communities typically produce a rather wide range of products

at first, and as the fermentation proceeds, these are sequentially converted into CH₄ as the only end product. In this case, CO can be converted into CH₄, acetate and H₂ by carboxydrotrophic methanogens, acetogens and hydrogenogens, respectively. In turn, H₂/CO₂ can be converted into CH₄ and acetate by hydrogenotrophic methanogens and homoacetogens, respectively. Then, depending on the intermediate metabolite, the last step of methanogenesis is carried out by either acetoclastic or hydrogenotrophic methanogens. Despite the multiple possible catabolic routes, not all of them seem to be equally important since several studies reported the preferential use of certain pathways depending on the operating conditions. Sipma et al. [184] studied the effect of the incubation temperature during the conversion of CO by an anaerobic sludge and found that acetate was the predominant intermediate product at mesophilic conditions, while at thermophilic conditions, H₂ was the main intermediate. This was confirmed by Navarro et al. [185] studying the biomethanation of CO using a granular sludge, who also found that the production of acetate was the predominant activity at mesophilic conditions. Additionally, these studies concluded that direct carboxydrotrophic methanogenic activity is either not present or negligible when using anaerobic sludge as biocatalyst [99,184,185], as carboxydrotrophic methanogens are most likely outcompeted by other carboxydrotrophs.

1.5.2. Mutualistic interactions

Interspecies diffusion of electron carriers like H₂ and formate between syntrophic fatty acid oxidizers and hydrogenotrophic methanogens or sulfate reducers is perhaps the most illustrative example of mutualistic interactions within anaerobic microbial communities, as the syntrophic oxidation of acetate or other VFAs can only take place in presence of syntrophic partners able to keep the concentration of H₂ (and acetate) low enough to make the anaerobic oxidation reaction thermodynamically feasible. A recent study showed that direct interspecies electron transfer is also possible using *Geobacter* spp. and *Methanosaeta* spp. [186]. Typically, these symbiotic interactions remain unnoticed due to the fast turnover and low concentration of H₂ and formate [187]. Nonetheless, syntrophic acetate oxidizers were found in significant amounts in 10 out of 13 randomly selected industrial anaerobic digesters, which demonstrates the importance that syntrophic fatty acid-oxidizing bacteria, and mutualistic interactions in general, may have in anaerobic microbial communities [168]. These syntrophic interactions have not been thoroughly investigated in syngas biomethanation processes yet. However, Wang et al. [188] found that *Smithella* spp. were relatively dominant during the simultaneous biomethanation of sewage sludge and CO. Similarly, Navarro et al. [100] found that the abundance of the syntrophic acetate oxidizer *Geobacter unaniireducens* increased after long-term exposure of a granular anaerobic sludge to CO.

Further symbiotic interactions related to the protection of sensitive bacteria against the toxicity of CO have also been observed. This type of mutualistic interaction was clearly exemplified in Parshina et al. [143], as axenic cultures of *Desulfotomaculum kuznetsovii* and *Desulfotomaculum thermobenzoicum* subsp. *Thermosyntrophicum* were not able to grow above a P_{CO} of 0.7 atm in presence of sulfate, but they grew at a

P_{CO} of up to 1 atm when co-cultured with *C. hydrogeniformans*. In this case, the sulfate reducers benefited from the removal of CO while the carboxydophilic hydrogenogen benefited from the continuous removal of H_2 . Similar symbiotic interactions were also observed in syngas-converting microbial communities. However, in the latter case, the protection against the toxicity of CO originated from the higher organizational structure of the microbial community when growing in anaerobic granules, as it was found that crushed granular sludge presented a lower methanogenic activity than the intact granular sludge when converting CO [100].

1.5.3. Mutual exclusion interactions

Additional microbial interactions with strong impact on the structure of microbial communities are mutual exclusion interactions, which may take place at metabolic guild level and at species level within each metabolic guild. In presence of sulfate, all microbial trophic groups described in the previous section compete for common substrates like CO, H_2 and acetate. Generally, sulfate reducers are expected to dominate the competition for H_2 with homoacetogens and hydrogenotrophic methanogens, given that the growth kinetics and the thermodynamics of the sulfate reduction are more favorable [189,190]. Nevertheless, in fermentation processes, the sulfate-reducing activity may be easily controlled by adjusting the content of sulfate in the growth medium. Based on the findings of Liu et al. [191], the competition for H_2 between homoacetogens and hydrogenotrophic methanogens is expected to favor the latter, since hydrogenotrophic methanogens were found to have four times higher maximum specific growth rate and higher substrate affinity than homoacetogens. However, this study also reported that homoacetogens were able to outcompete methanogens when working at high P_{H_2} (0.96 bar). In turn, when competing for CO, carboxydophilic methanogens are expected to be easily outcompeted by carboxydophilic acetogens and hydrogenogens in a mixed microbial community since the former present the longest doubling time of all, generally ranging from 24 h to 200 h [126,164]. Carboxydophilic hydrogenogens and acetogens exhibit relatively similar doubling times ranging from 1-2 h to 8.4 h and from 1.5 h to 16 h, respectively [133,135,149,151,192]. Of course, the outcome of the competition for common substrates is strongly influenced by the operating conditions, as changes in several operating parameters, such as pH, temperature, nutrients content, VFAs concentration, ionic strength, etc., may affect differently the growth rate of each species. This is obvious e.g. within the acetogenic microbial trophic group, where the pH seems to be a major factor driving the microbial selection of different species. For instance, several enrichment studies operating at a pH range of 6.8-7.6 reported that *Acetobacterium* spp. and *Geosporobacter* spp. were dominant [112,193], while in another study operating at a pH range of 4.5-6.0, *Clostridium* spp. became the dominant species [116].

1.6. Challenges and tools linked to mixed-culture-based systems

As outlined above, mixed microbial communities present several unique features that make them an attractive option for industrial applications (e.g. in waste treatment, bioenergy, biochemical and biofuel production), such as non-sterile operation, resistance, resilience and adaptive capacity when facing process disturbances, and high long-term functional stability. The possibility of operating under non-sterile conditions derives from the high microbial diversity and evenness generally found in microbial communities, as these properties contribute to maintaining the functionality of the community upon invasion of foreign species [194]. Resistance and resilience also lie on microbial diversity, but are mainly related to the high metabolic flexibility and physiological tolerance of some microbial groups, especially bacteria, which provide the microbial community with the ability to resist or recover from environmental disturbances [195]. Lastly, the long-term stable activity of the microbial community despite changes in microbial composition is mainly attributed to its functional redundancy, which is ensured by a reservoir of latent species with the same ecological function that can take over after an environmental disturbance [196]. Coyte et al. [197] also highlighted the role of microbial competition in functionally stable microbial communities. Additionally, other processes like auxotrophic interactions and horizontal gene transfer may also contribute to increasing the microbial diversity and adaptability of the microbial community [195,198–200].

This assemblage of complex cooperative and competitive microbial interactions and metabolic processes shaping the microbial community allows them to thrive in harsh environments and perform difficult tasks like degrading highly complex substrate mixtures. However, their high complexity constitutes their main advantage and their main limitation at the same time, as the still poor understanding of the underlying mechanisms governing the performance of microbial communities often results in limited process control, ultimately translated into low yields or low product selectivity. The acetogenic metabolism of microbial communities is an example of this (fig. 1.6), as all chain elongation and VFA-reduction (to alcohols) reactions compete for the same substrates, typically resulting in a mixture of acids and alcohols of different length. Thus, tools for integrating the regulation of the community metabolic function, population dynamics and microbial interactions, and the effect of operating parameters on the latter are fundamental for the control and optimization of mixed-culture-based processes. Another issue typically argued against the use of mixed cultures in industrial processes (excepting wastewater treatment and anaerobic digestion) is related to the reproducibility of the complexity of microbial communities and the lack of long-term preservation methods. Although cryopreservation methods are well established for axenic cultures, the long-term preservation of the structure and functionality of microbial communities has not been thoroughly investigated. In fact, neither natural nor engineered microbial communities are available in any culture collections yet [201–203]. However, the development of such techniques is a prerequisite for the further advancing of mixed-culture-based biotechnological applications.

There are several approaches or tools currently being considered for addressing the limited control in mixed-culture-based fermentation processes. These include mainly microbial enrichment and bioaugmentation techniques, modeling tools, the use of thermodynamic principles for describing and potentially predicting the function of microbial communities, and the use of microbial indicators of process stability (fig. 1.7).

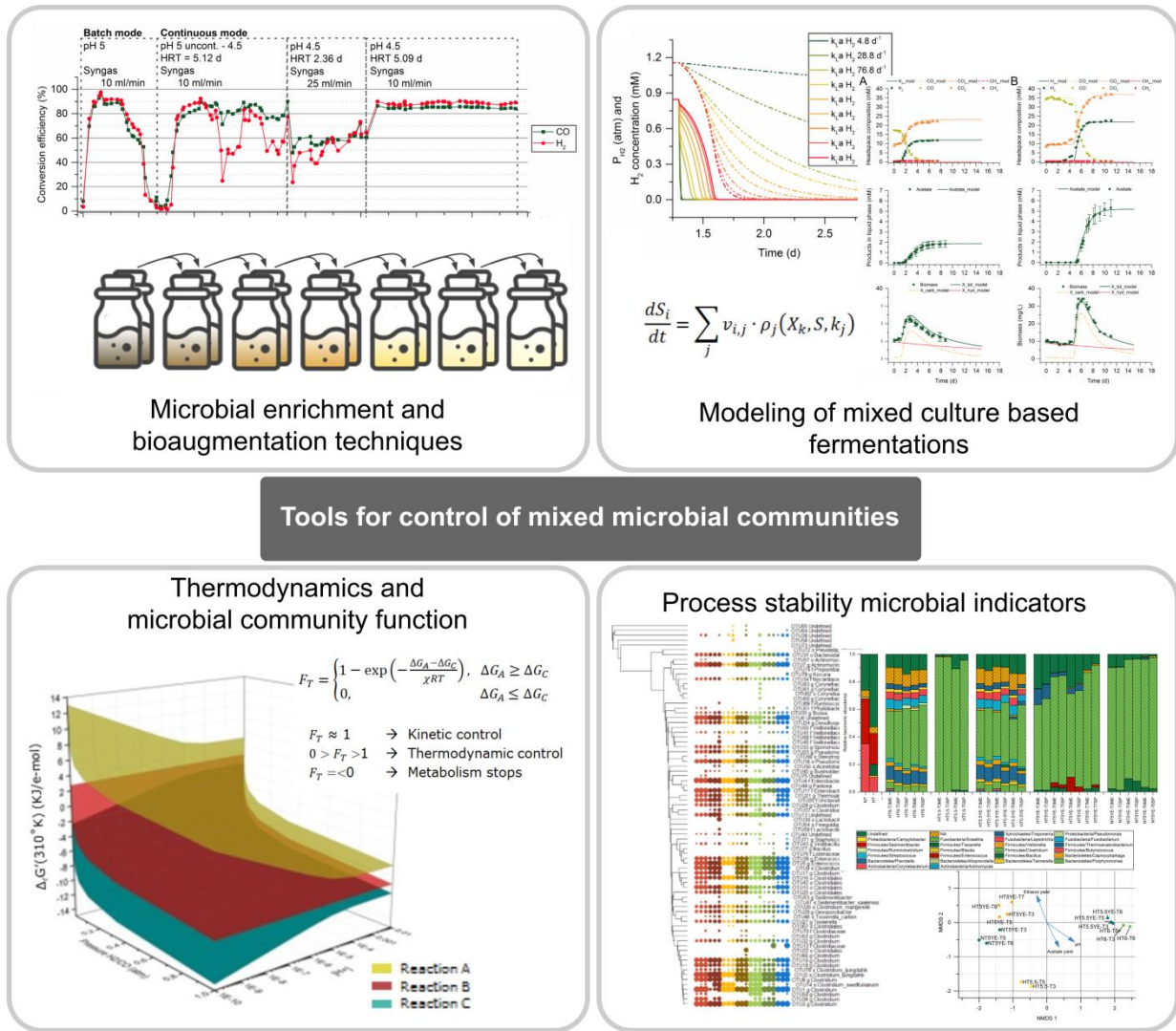


Figure 1.7. Potential tools for addressing the limited control on the metabolic activity of microbial community.

Microbial enrichments and bioaugmentation

Both microbial enrichments and bioaugmentation are based on the idea of steering the microbial community structure towards a specific metabolic function. However, microbial enrichments rely on the application of a selective pressure to drive the natural selection of specific microbial groups, while bioaugmentation consists in the direct addition of exogenous microorganisms to enhance a specific metabolic function or property of the microbial community.

Microbial enrichment techniques are typically used for (i) reducing the complexity of microbial communities and shaping their function so that the target product yield and productivity is enhanced, and (ii) increasing the resistance of microbial communities to certain inhibitors or harsh conditions through adaptation. This technique can also be used for the selection of species or microbial groups with specific properties, e.g. selection of R-strategists (high μ_{\max} and low substrate affinity) or K-strategists (low μ_{\max} and high substrate affinity) [204]. Both sequential batch and continuous operating mode can be used. In syngas fermentation, batch mode microbial enrichments have been successfully applied in several studies for generating specialized microbial communities targeting the production of CH₄, ethanol, and mixtures of MCFAs and higher alcohols [102,114,116,205].

Bioaugmentation has not been used in syngas fermentation processes, but several studies on anaerobic digestion and biohydrogen production through dark fermentation have demonstrated its effectiveness. This technique has been applied for achieving a fast activity recovery after process disturbances, for increasing the methane and hydrogen yield, and for alleviating the inhibitory effect of ammonia-rich substrates, among other purposes [206–210].

Both techniques have proven to be effective for driving important shifts in the microbial community structure. However, the impact of these methods on the composition of the microbial community is limited to the time frame during which the selective pressure (or the addition of exogenous microorganisms) is present. As soon as the selective pressure disappears, the pre-existing environmental conditions will eventually drive new shifts in the composition of the microbial community, tending to its original state in most cases.

Modeling of mixed-culture-based fermentations

Mathematical modeling of biological processes has proven to be a valuable tool for predicting the outcome of different process configurations, easing operation and process parameter optimization tasks, and ultimately providing a better understanding and control over these processes. The process of syngas fermentation has been modelled using several acetogenic and hydrogenogenic strains, mostly based on Monod and modified Monod models [140,211–214]. However, a model able to describe the performance of mixed cultures in syngas fermentation processes has not been developed yet. Such a model, including the main microbial interactions within the microbial community (e.g. cross-feeding, competition and other symbiotic interactions) and the effect of operating parameters on the latter would certainly simplify process parameter optimization tasks and could possibly allow for a certain degree of control over the catabolic routes used by the microbial community. Nevertheless, a more complex model structure than the ones used so far would be needed.

More structured models like the Anaerobic Digestion Model no. 1 have been proposed for modelling anaerobic microbial communities and are currently applied not only in anaerobic digestion, but also in e.g.

biohydrogen production through dark fermentation [215–218]. The higher predictive capacity of this model, when compared to much simpler models like the Gompertz model [217], derives from the more complex model structure, which in this case considers cross-feeding interactions between different metabolic guilds within the microbial community. A similar approach would probably be well suited for simulating e.g. the syngas biomethanation process, which also involves the synergistic action of different metabolic guilds for the complete conversion of syngas into CH₄. Other processes like the fermentation of syngas into MCFAs and alcohols would probably be better described by other models focusing on intracellular metabolic processes, as the intracellular regulation of the metabolism of the species composing the microbial community probably play a more important role determining the final product distribution than the microbial composition. These type of models have been successfully applied for describing the product distribution of mixed-culture-based glucose fermentation by combining kinetic, thermodynamic and bioenergetic considerations, e.g. variable proton motive potential and active transport energy costs [219–221].

Other modeling approaches, more common of the synthetic ecology field and mainly consisting of flux balance models based on genome-scale network reconstructions, have also been put forward and could be applied in the future to predict community-wide behaviors or for rationally designing synthetic microbial communities [222,223]. This approach has been applied so far in simple synthetic co-cultures for describing mutualistic interactions like direct interspecies electron transfer and diffusion of electron carriers like H₂ and formate [224,225]. However, whether these models will be able to handle the myriad of mutualistic and competitive microbial interactions taking place in natural microbial communities is still an open question.

Thermodynamics and microbial community function

Thermodynamics have been extensively used to describe many aspects of the metabolism of microorganisms including the thermodynamic feasibility and reversibility of metabolic pathways, and growth rate and biomass yield predictions, among others [183,226]. One of the main applications in microbial ecology and mixed-culture-based bioprocesses has been the prediction of the biomass yield for a given catabolic reaction. Several methods have been proposed including the Gibbs free energy dissipation method, the ATP-balancing method and the thermodynamic electron equivalents model, all of them based on the balance between the free energy released by catabolic reactions (ΔG_{rxn}) and the free energy required for anabolic reactions (ΔG_{C}) [227–229]. Tijhuis et al. [230] also showed that the Gibbs free energy dissipation for maintenance could be correlated with the incubation temperature in a single equation independently of the type of metabolism, ultimately allowing for predicting the actual biomass yield as a function of carbon and nitrogen source, electron donor and acceptor, growth rate and temperature. These biomass yield predictions, together with mass and energy balances defining the reaction stoichiometry, are commonly used in dynamic modeling of mixed-culture-based fermentations.

A significant contribution of thermodynamics to our understanding of microbial interactions is the concept of thermodynamic competition between different species or metabolic guilds within a microbial community. This concept is based on the fact that all microorganisms require a minimum concentration of substrate in order to gain metabolically convertible energy, which is given by the minimum Gibbs free energy threshold. The minimum quantum of metabolically convertible energy (ΔG_{\min}) is theoretically defined by the free energy needed for translocating of one proton across the membrane, approximately -20 kJ/mol [231]. However, more recent studies have demonstrated that microbial metabolism can be sustained at much lower ΔG_{\min} , varying quite importantly depending on the species [232–234]. Consequently, microbial trophic groups carrying out more exergonic metabolic functions are likely to be able to keep the concentration of electron donors below the thermodynamic feasibility limits of more endergonic reactions performed by other microbial groups competing for the same substrate. An extension to the concept of thermodynamic competition is the idea that metabolic activity rates are controlled by thermodynamics rather than kinetics when ΔG_{rxn} approaches ΔG_{\min} . Several modified kinetic models have been proposed for simulating the thermodynamic control of the metabolic activity rates, with most of them considering both ΔG_{rxn} and ΔG_c [234–239]. The additional thermodynamic considerations of these models have important implications as, e.g. these allow for explaining the coexistence of diverse microbial trophic groups (with different growth kinetics) competing for the same substrates in microbial communities [240]. These models have been typically used for describing the metabolic activity of microbial communities in oligotrophic geochemical environments. However, the simulation of thermodynamic competition dynamics in microbial communities offered by these models could also constitute a solid basis for shaping the structure of microbial communities by engineering environmental conditions favoring specific metabolic activities.

Process stability microbial indicators

Bioinformatic tools relying on high throughput sequencing have undergone a rapid development over the last years. These tools have certainly become a part of the routine analyses in mixed-culture-based bioprocesses, also in syngas fermentation processes, as these can provide valuable insights on prevailing metabolic processes and microbial interactions taking place within the microbial community [57,102,107,112,115,118,241]. Much work has been carried out in the field of anaerobic digestion correlating phylogenetic traits, metabolic function and operating conditions by using exploratory data analysis tools like PCA, PCoA and NMDS [242,243]. However, their use has been so far limited to retrospective analyses.

Proactive management of microbial communities based on early microbial indicators of future process failure after a disturbance has been proposed [244]. A variety of tools could be applied for microbial community diagnostics including molecular techniques (e.g. DGGE, high throughput sequencing or microarray technologies) and single cell based techniques (e.g. FISH probes or flow cytometry) [244].

Carballa et al. [206] suggested that certain traits of the microbial community structure, like microbial diversity or evenness in specific microbial trophic groups, could be potential microbial indicators. Nevertheless, the development of such microbial indicators will require (i) an extensive and exhaustive characterization of the microbial production systems and their response to environmental disturbances, and (ii) that analyses of the microbial community become much quicker and more accessible in the future.

Chapter II – Scope of the Thesis

Over the last decades, the fermentation of syngas originating from biomass gasification has attracted considerable scientific attention as a possible alternative to strictly biochemical and thermochemical biomass conversion processes. The syngas fermentation process has been typically studied using axenic cultures of acetogenic bacteria, mainly *Clostridium ljungdahlii* and *Clostridium autoethanogenum*, with ethanol being the most commonly targeted product. Over the last years though, the focus in the syngas fermentation studies has shifted towards expanding the product portfolio of these commonly used strains. One of the alternatives to broaden their product spectrum to other products, like H₂, CH₄, medium chain fatty acids and higher alcohols, is the use of syngas-converting microbial communities, as these may offer a series of additional benefits such as lower operating costs derived from non-sterile operation, resilience to process disturbances and stable operation in continuous mode with low risk of contamination. However, the control of the metabolic activity of microbial communities still remains challenging owing to the high complexity of their microbial interactions, which often entail a poor understanding of the underlying mechanisms regulating their metabolism and result in poor product selectivity, especially in the case of syngas fermentation to ethanol. Another issue generating reluctance on the industrial application of mixed microbial communities is the low reproducibility of the complexity of microbial communities and the lack of validated methods for the long-term preservation of their structure and function.

The main goal of this thesis is to evaluate the potential of different microbial community management strategies, including directed natural selection through microbial enrichments, thermodynamics-based selection of operational conditions, and modeling tools, for driving targeted metabolic and structural shifts in the microbial community. The production of ethanol and CH₄ by syngas-converting microbial communities were used as case studies in this thesis. Finally, the effectiveness of several frozen storage methods on the long-term preservation of the microbial community structure and function was also evaluated.

2.1. Hypotheses

This work is based on the following hypotheses:

- ❖ The application of a selective pressure, given by a set of operating conditions, in microbial enrichments can direct the catabolic routes used by syngas-converting microbial communities through the selection and exclusion of specific microbial trophic groups.
- ❖ Operational conditions overwrite the role of the microbial composition on the regulation of the solventogenic metabolism of syngas-converting microbial communities.

- ❖ Thermodynamic principles can be used for steering the metabolic activity of specific microbial trophic groups by regulating either the intracellular or the interspecies metabolism of microbial communities.
- ❖ The simulation of the syngas biomethanation process through “grey box” models, accounting for the main microbial trophic groups and interactions of the microbial community, can successfully describe the performance of microbial communities with relatively high predictive capacity.
- ❖ The combination of thermodynamic and kinetic considerations in dynamic models allows for designing detailed catabolic route control strategies.
- ❖ Cryopreservation methods based on cryoprotectants, alternative to those commonly used like glycerol and no addition of cryoprotectant, may allow for more reliable long-term preservation of the microbial community structure and its functional redundancy.

2.2. Specific objectives

In order to test the validity of the hypotheses above stated, the following specific objectives were defined:

- ❖ To characterize the catabolic routes employed by syngas-converting methanogenic microbial communities enriched at different incubation temperatures, namely 37°C and 60°C.
- ❖ To evaluate the effect of pH, yeast extract addition and hydraulic retention time on the microbial composition and the solventogenic activity of syngas-converting acetogenic microbial communities through microbial enrichments.
- ❖ To investigate whether operating conditions or microbial composition determine the solventogenic potential of enriched microbial communities.
- ❖ To analyze the thermodynamics of net biochemical reactions composing the metabolic network of methanogenic and acetogenic microbial communities based on their thermodynamic feasibility in order to identify reactions subject to thermodynamic control.
- ❖ To define catabolic route control strategies and operational strategies allowing for targeted control of specific bioconversions.
- ❖ To develop dynamic models able to describe the performance of mesophilic and thermophilic enriched microbial communities during syngas biomethanation.
- ❖ To define the structure of the models based on experimental observations and thermodynamic considerations in order to include specific mutualistic, competitive and cross-feeding interactions and improve the overall predictive capacity of the models.
- ❖ To investigate the effect of several cryopreservation agents on the long-term cryopreservation of the microbial community structure and functionality based on microbial composition and microbial activity recovery.

Chapter III – Enrichment of Syngas-Converting Mixed Microbial Communities

3.1. Purpose

The goal of this study was to evaluate the potential of microbial enrichment techniques for directing the metabolic activity of the microbial community towards ethanol and CH₄. The exposure to syngas and specific operating conditions, favoring methanogenic and solventogenic activity, were applied during the enrichments as selective pressure for driving a reduction of the complexity of the microbial community while steering its metabolic activity towards the targeted products. Both microbial community structure and fermentation products were used for monitoring the evolution of the microbial community along the enrichment processes.

3.2. Hypotheses

- ❖ The application of a selective pressure, given by a set of operating conditions, in microbial enrichments can direct the catabolic routes used by syngas-converting microbial communities through the selection and exclusion of specific microbial trophic groups.
- ❖ Operational conditions overwrite the role of the microbial composition on the regulation of the solventogenic metabolism of syngas-converting microbial communities.

3.3. Specific objectives

- ❖ To characterize the catabolic routes employed by syngas-converting methanogenic microbial communities enriched at different incubation temperatures, namely 37°C and 60°C.
- ❖ To evaluate the effect of pH, yeast extract addition and HRT on the microbial composition and the solventogenic activity of syngas-converting acetogenic microbial communities through microbial enrichments.
- ❖ To investigate whether operating conditions or microbial composition determine the solventogenic potential of enriched microbial communities.

3.4. Related manuscripts

- II. A. Grimalt-Alemany, M. Łężyk, L. Lange, I. V. Skiadas, and H. N. Gavala. Enrichment of syngas-converting mixed microbial consortia for ethanol production and thermodynamics-based design of enrichment strategies. *Biotechnol Biofuels*, 2018; 11, 198: 1–22.
- III. A. Grimalt-Alemany, M. Łężyk, D. M. Kennes-Veiga, I. V. Skiadas, and H. N. Gavala. Enrichment of mesophilic and thermophilic mixed microbial consortia for syngas biomethanation: the role of kinetic and thermodynamic competition. *Waste and Biomass Valorization*, 2019.
- V. A. Grimalt-Alemany, M. Łężyk, K. Asimakopoulos, I. V. Skiadas, and H. N. Gavala. Cryopreservation and fast recovery of enriched syngas-converting microbial communities. (Submitted).

3.5. Experimental procedures

The enrichment of syngas-converting methanogenic microbial communities was carried out using a sequential batch enrichment technique for studying the effect of different incubation temperatures on the microbial selection, namely 37°C and 60°C. An anaerobic sludge was used as starting inoculum and the enriched community was considered stable after 5 successive transfers. The catabolic routes employed by each enriched microbial community were then characterized through specific activity tests and 16S rRNA gene amplicon sequencing.

The enrichments of mesophilic (37°C) solventogenic microbial communities were performed both in sequential batch mode, consisting of 6 successive transfers, and continuous mode in order to study the effect of different operational parameters, including pH, yeast extract and hydraulic retention time (HRT), on the microbial selection and the metabolic activity of the microbial community. Sequential batch enrichments focused on the effect of initial pH and yeast extract addition, while the enrichment in continuous mode evaluated the effect of pH and HRT. The specific enrichment conditions in sequential batch mode were pH 6, 5.5 and 5, with and without yeast extract addition. The operating conditions in the enrichment in continuous mode were pH 4.5 and HRT of 5.1 d and 2.4 d. The anaerobic sludge used as starting inoculum was heat-shock treated prior to inoculation in most cases in order to inhibit the methanogenic activity. However, the possibility of using a non-treated anaerobic sludge was also evaluated in one of the sequential batch enrichments. The microbial composition was analyzed based on 16S rRNA gene amplicon sequencing during and at the end of the enrichment in all cases.

3.6. Summary of results

The anaerobic sludge used in all experiments was able to convert syngas without pre-acclimation and with no apparent inhibition in its hydrogenotrophic and carboxydrotrophic activity due to the initial partial pressure of CO (0.40-0.47 atm). However, not all carboxydrotrophic microbial groups were present in the enriched microbial communities as, in all enrichments, CO was found to be strictly converted by either carboxydrotrophic acetogens or hydrogenogens depending on the operating conditions.

In the methanogenic enrichments, the analysis of the patterns of activity of the mesophilic and thermophilic microbial communities revealed that the enrichment at different incubation temperatures led to microbial communities with drastic differences in the complexity of their community structure and their activity rates (Manuscript III). The mesophilic enriched microbial community presented a rather intricate metabolic network, where CO was strictly converted into acetate and propionate by carboxydrotrophic acetogens, and H₂/CO₂ was simultaneously converted into acetate and CH₄ as a result of the competition between the homoacetogenic and the hydrogenotrophic methanogenic microbial groups. Acetate was then further converted into CH₄ by aceticlastic methanogens, although syntrophic acetate and propionate oxidation possibly took place as well to a limited extent diverting a small part of the carbon through hydrogenotrophic methanogenesis. In turn, the thermophilic enriched microbial community was much simpler as it was composed by only two functional microbial groups, where CO was strictly converted into H₂/CO₂ by carboxydrotrophic hydrogenogens (in presence of hydrogenotrophic methanogens) and H₂/CO₂ was directly converted into CH₄ by hydrogenotrophic methanogens. These differences in the putative composition of the microbial communities led to significant differences in their productivities, as the maximum specific CH₄ productivity of the thermophilic microbial community was one order of magnitude higher than that of the mesophilic due to the faster turnover rates of H₂ compared to acetate (table 3.1).

The results of the specific activity tests determining the catabolic routes utilized by each methanogenic microbial community were confirmed by the analysis of their microbial composition, as all microbial trophic groups expected to be present in the microbial communities were identified through 16S rRNA gene amplicon sequencing. The mesophilic microbial community was found to be dominated by *Acetobacterium* spp. (with 26.0% of reads mapped to the corresponding OTUs), which likely converted CO and H₂/CO₂ into acetate, and *Methanospirillum* spp. (with 23.3% of reads mapped), converting H₂/CO₂ into CH₄ (fig. 3.1). Other expected microbial groups corresponding to aceticlastic methanogens (*Methanosarcinales* spp.) and syntrophic acetate oxidizers (*Geobacter* spp.) were also identified. On the other hand, the thermophilic microbial community was composed by the obligate carboxydrotrophic hydrogenogenic species *Thermincola carboxydiphila* (with 47.9% of reads mapped) and a hydrogenotrophic methanogenic microbial group corresponding to *Methanothermobacter* spp. (with 14.8% of reads mapped) (fig.3.1).

The sequential batch solventogenic enrichments applied at different initial pH with/without yeast extract addition resulted in the successful selection of acetogenic bacteria from both untreated and heat-shock treated anaerobic sludges, resulting in 5 enriched microbial communities with variable solventogenic potential and microbial diversity as a function of the enrichment conditions (Manuscript II). The acetate and ethanol yield was found to decrease and increase, respectively, with decreasing initial pH, with the microbial community enriched at pH 5 with heat-shock treated inoculum presenting the highest ethanol yield corresponding to $59.15 \pm 0.18\%$ of the stoichiometric maximum (fig. 3.2). In turn, the addition of yeast extract did not affect the ethanol yield, but triggered a significant production of butyrate, butanol and small amounts of caproate (fig. 3.2 C, D and E). Analyzing the composition of the microbial communities along the enrichments revealed that the composition shifted rapidly along the enrichment, reaching a stable community structure dominated by *Clostridium* spp. in all cases (fig. 3.3).

Both pH and yeast extract addition were found to be determinant operational parameters affecting the microbial diversity and composition of the microbial communities. On one hand, the decrease in initial pH was clearly detrimental for the microbial diversity of the enriched cultures (fig. 3.4A). This drop in microbial diversity could be amended by the addition of yeast extract, as this allowed for the microbial community enriched at pH 5.5 with yeast extract to have a microbial diversity similar to that of the community enriched at pH 6 without yeast extract (fig. 3.3). However, further decreasing the initial pH to 5 resulted in a significant drop in the microbial diversity even though yeast extract was added (fig. 3.4A). On the other hand, the addition of yeast extract was found to determine the outcome of the competition for H_2/CO_2 and CO at species level. While enrichments without addition of yeast extract were dominated by the putative species *Clostridium ljungdahlii*, enrichments with yeast extract addition favored the dominance of the putative species *Clostridium carboxidivorans*. This can be explained by the fact that *C. carboxidivorans* shows poor activity synthesizing amino acids, and consequently, needs a rich medium to grow efficiently [245]. Furthermore, the dominance of different *Clostridium* spp. is consistent with the change in carbon chain length of the products observed, as those enrichments with *C. ljungdahlii* as dominant species produced exclusively acetate and ethanol, whereas enrichments dominated by *C. carboxidivorans* resulted in the production of butyrate and butanol as well.

The microbial enrichment in continuous mode also showed important differences in the metabolic activity of the microbial community upon changing the operating conditions (Manuscript V). In this case, the pH was adjusted to 4.5 in order to prevent a significant carbon chain elongation of acetate and ethanol to butyrate and obtain an enriched microbial community with a higher product selectivity towards C₂ compounds (acetate and ethanol), based on the inhibition of the chain elongation reaction at pH below 5 [116,182,246,247]. When the enrichment was switched to continuous mode, the production of acetate remained at a relatively constant concentration of around 100-125 mM independently of the HRT and syngas inflow used (fig. 3.5).

In turn, the concentration of ethanol was found to be strongly affected by the change in HRT from 5.1 d to 2.4 d, as it varied from 40.9 ± 1.6 mM at steady state with 5.1 days of HRT (4th experimental condition) to a minimum of 17.5 ± 0.1 mM at steady state with 2.4 days of HRT (3rd experimental condition) (fig. 3.5). This indicated that ethanol was probably produced through the reduction of acetate using H₂ or CO as electron donors, since a higher HRT should favor a higher extent of this reaction. The low pH applied during the enrichment successfully suppressed the carbon chain elongation activity during the beginning of the enrichment. However, after 25 days of operation, butyrate started to increase gradually until a maximum yield of $8.0 \pm 1.0\%$ of the stoichiometric maximum was reached on day 33 (fig. 3.5). Decreasing the HRT to 2.4 d temporarily though, allowed for a nearly complete suppression of the chain elongation activity.

The microbial composition analysis showed a clear dominance of acetogenic bacteria from the family *Clostridiaceae* (fig. 3.6). Other families of bacteria with a considerable representation in the microbial community corresponded to *Enterobacteriaceae* and *Pseudomonadaceae*. The microbial community was dominated by the putative species *C. ljungdahlii* during the whole enrichment (from 45.5% to 83.4% of reads mapped). However, between days 13 and 51, this species was found to be partially displaced by a species closely related to *Clostridium luticellari*, reaching a maximum of 28.0% of reads mapping to this species. The syngas conversion was mainly attributed to *C. ljungdahlii*, while the temporary occurrence of the chain elongation reaction was attributed to *Clostridium luticellari*. Similarly to the sequential batch enrichments, when the microbial community enriched in continuous mode was inoculated in batch fermentation flasks, the composition of the community shifted towards dominance of species with closest but low similarity to *C. carboxidivorans* and *Clostridium nitrophenolicum*, together with *C. ljungdahlii*, resulting in the production of acetate, ethanol, butyrate, butanol and small amounts of caproate. This indicated that the microbial community presented high functional redundancy despite the drastic reduction in structure complexity after the enrichment.

3.7. Conclusions

The microbial enrichments performed in these studies demonstrated that directing the natural selection through the application of specific environmental pressures is an effective tool for driving a reduction of the complexity of the microbial community structure and redirecting the carbon flux through specific pathways of its metabolic network. These studies showed that the microbial selection could be directed towards specific microbial trophic groups based on mutual exclusion interactions within the community, as these should favor the dominance of the most competitive species depending on the operating conditions applied, and eventually, the wash-out of least competitive species. The enrichment of methanogenic microbial communities is a clear example of this mutual exclusion at microbial trophic group level, as the incubation at different temperatures led to microbial communities where CO was strictly metabolized through acetate by

carboxydrotrophic acetogens or through H_2/CO_2 by carboxydrotrophic hydrogenogens, with important implications in their metabolic activity rates. The acetogenic microbial communities developed here also demonstrated the exclusion of methanogenic and hydrogenogenic microbial trophic groups.

The microbial competition at species level within a specific microbial group was also studied through sequential batch mode and continuous mode enrichments of acetogenic microbial communities. These studies showed that nutrient supplementation and the operating mode were crucial factors determining the dominant species of the microbial community. In the enrichments in sequential batch mode, the putative species *C. ljungdahlii* was shown to be outcompeted by a species closely related to *C. carboxidivorans* when the growth medium was supplemented with yeast extract, which indicated that the latter has a higher μ_{max} provided that certain amino acids are supplied. However, the substrate-limiting conditions found under continuous operating mode favored the dominance of *C. ljungdahlii* even though the medium was supplemented with the same concentration of yeast extract, which indicated that the latter either is more tolerant to low pH conditions or has a higher substrate affinity. This reasserts that enrichment strategies targeting the selection of species with specific kinetic properties or physiological traits are also possible. However, as opposed to the competition at microbial trophic group level where permanent changes in the microbial community are more likely, the outcome of the competition at species level is inherently more dynamic and subject to the fine tuning of the operating conditions due to the more similar physiological traits among species of the same metabolic guild and the functional redundancy of microbial communities.

The relation between operational parameters, composition of the microbial community and metabolic activity was studied in acetogenic enrichments performed in sequential batch mode. In this case, the yield of the target product in acetogenic enrichments, ethanol, was found to be dependent on the operating conditions rather than on the microbial composition. Enrichments at initial pH 5.5 with and without yeast extract addition were found to present drastic differences in their microbial diversity and different dominant species (either *C. ljungdahlii* or *C. carboxidivorans*), but resulted in a very similar ethanol yield corresponding to 0.028 mol/e-mol and 0.025 mol/e-mol with and without yeast extract addition, respectively (fig. 3.2 B and C). Additionally, the increase in ethanol yield with decreasing initial pH was consistent regardless of the microbial diversity and dominant species of each enriched microbial community. This was further supported by the ordination of microbial community samples through non-metric multidimensional scaling (nMDS), where a statistically significant correlation was found between the ordination of the samples and the acetate yield, ethanol yield and initial pH (fig. 3.4B). Therefore, all results indicated that the pH acted on the composition of the microbial community and on the regulation of their metabolism in independent ways. However, changes in the yield of other products like butyrate and butanol were, in fact, not dependent solely on the operating conditions but on the microbial composition as well, as the presence of *C. carboxidivorans* most probably triggered their production.

Overall, the microbial enrichment technique used was found to be an effective tool for driving important changes in the composition of the microbial communities studied, which could enable the design of operational strategies targeting specific metabolic activities. However, one of the main limitations of this technique is that these operational strategies can only be based on prior knowledge of the effect of certain operational parameters on the microbial community, as the outcome of the enrichment cannot be predicted otherwise, with few exceptions. This might limit its applicability or its effectiveness in novel microbial conversion processes without extensive experimental work.

Table 3.1. Biomass yield and specific activities and productivities for the different microbial groups present in the mesophilic and the thermophilic enriched microbial consortia. Extracted from Grimalt-Aleman et al. [248] (Manuscript III).

	Biomass yield (g VSS/mol substrate)	Max. Specific activity (mmol substrate/g VSS/h)			Max. Specific productivity (mmol product/g VSS/h)			
		H ₂	CO	Acetate	Acetate	Propionate	H ₂	CH ₄
<i>Mesophilic enriched consortium</i>								
Carboxydrotrophic acetogens	2.45±0.06	14.18±2.31			2.53±0.64	0.18±0.03		
Homoacetogens	0.54±0.03	49.14±10.70			7.36±1.62			
Hydrogenotrophic methanogens ^a	0.72±0.03 ^a	46.12±5.50 ^a			11.00±1.31 ^a			
Aceticlastic methanogens	0.57±0.06	6.65±1.77			6.44±0.54			
All microbial groups	0.87±0.02	27.45±1.23	14.87±0.59		5.26±0.91	0.10±0.00		1.83±0.27
<i>Thermophilic enriched consortium</i>								
Carboxydrotrophic hydrogenogens	0.82±0.01	52.35±1.72			1.61±0.42	44.95±4.11		
Hydrogenotrophic methanogens	0.51±0.01	244.26±12.87			43.46±1.52			
All microbial groups	0.66±0.01	165.75±4.53	12.43±1.16		33.48±0.90			

^aThe biomass yield, the maximum specific activity and productivity for hydrogenotrophic methanogens was estimated based on the biomass and acetate yield of homoacetogens determined in the experiments with H₂/CO₂ with BES addition.

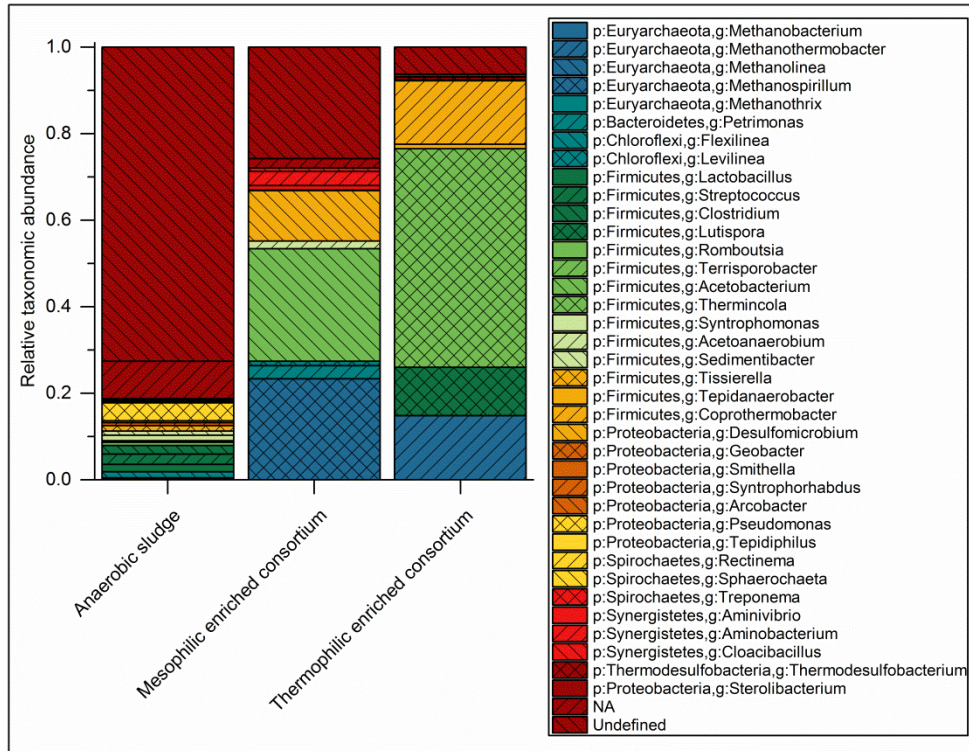


Figure 3.1. Average relative taxonomic abundance of triplicate samples for the initial inoculum used and the mesophilic and thermophilic enriched microbial consortia at genus level using the V3-V4 region primer set. NA corresponds to the sum of all genera with relative abundance below 0.5% in the individual samples before calculating the average. Extracted from Grimalt-Alemanly et al. [248] (Manuscript III).

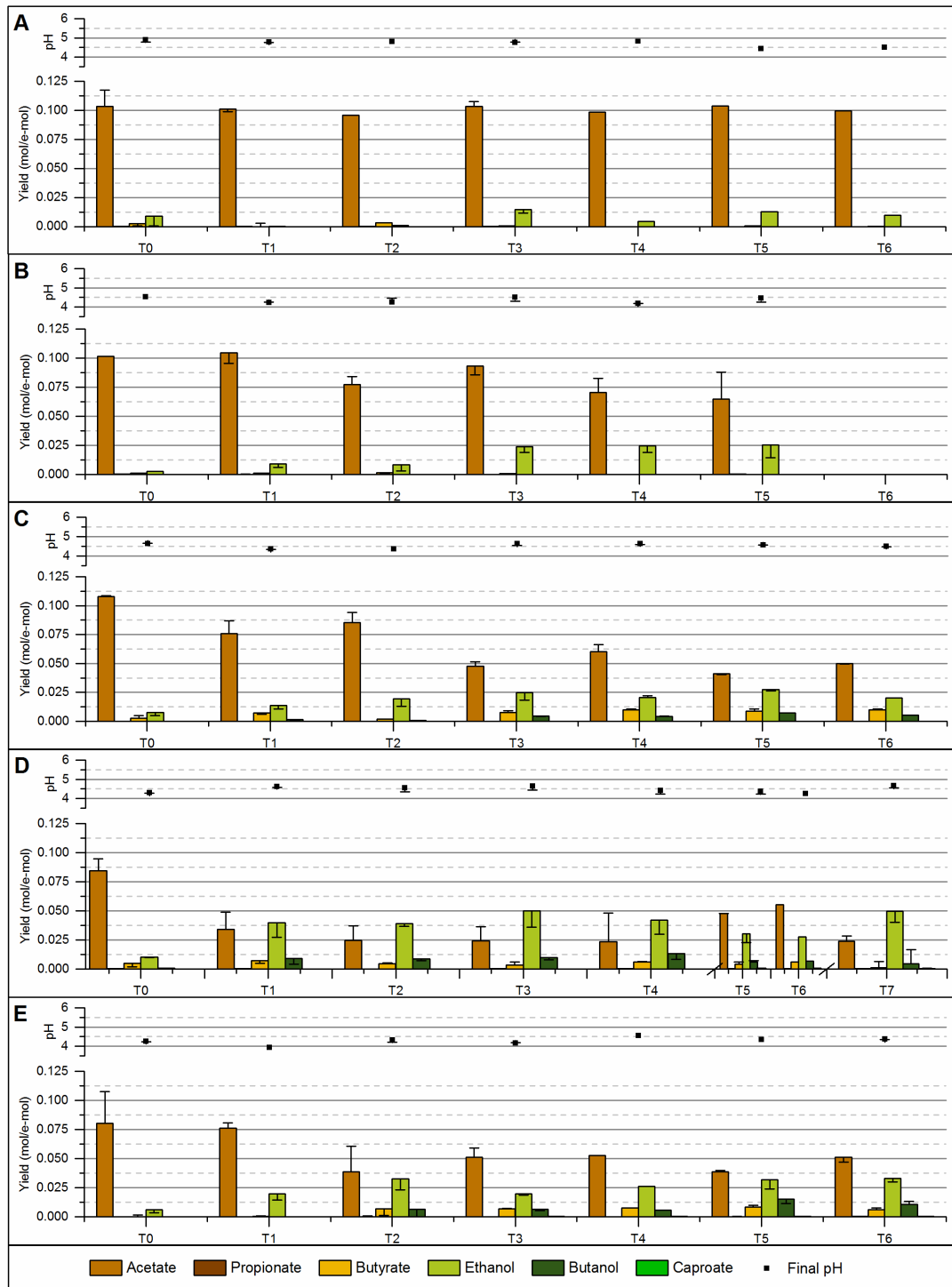


Figure 3.2. Product yields (mol/e-mol) obtained in each transfer for all enrichment conditions and final pH at the moment of the transfer. The columns show the values for the fermentation transferred and the error bars indicate the corresponding values of the duplicate experiment. Additional information on substrate consumption and apparent biomass yields can be found in the additional file 1 (fig. 5). **A** Enrichment HT6 at an initial pH of 6; **B** Enrichment HT5.5 at an initial pH of 5.5; **C** Enrichment HT5.5YE at an initial pH of 5.5 with YE (0.5 g/L); **D** Enrichment HT5YE at an initial pH of 5 with YE (0.5 g/L); **E** Enrichment NT5YE at an initial pH of 5 with YE (0.5 g/L). Extracted from Grimalt-Alemany et al. [249] (Manuscript II).

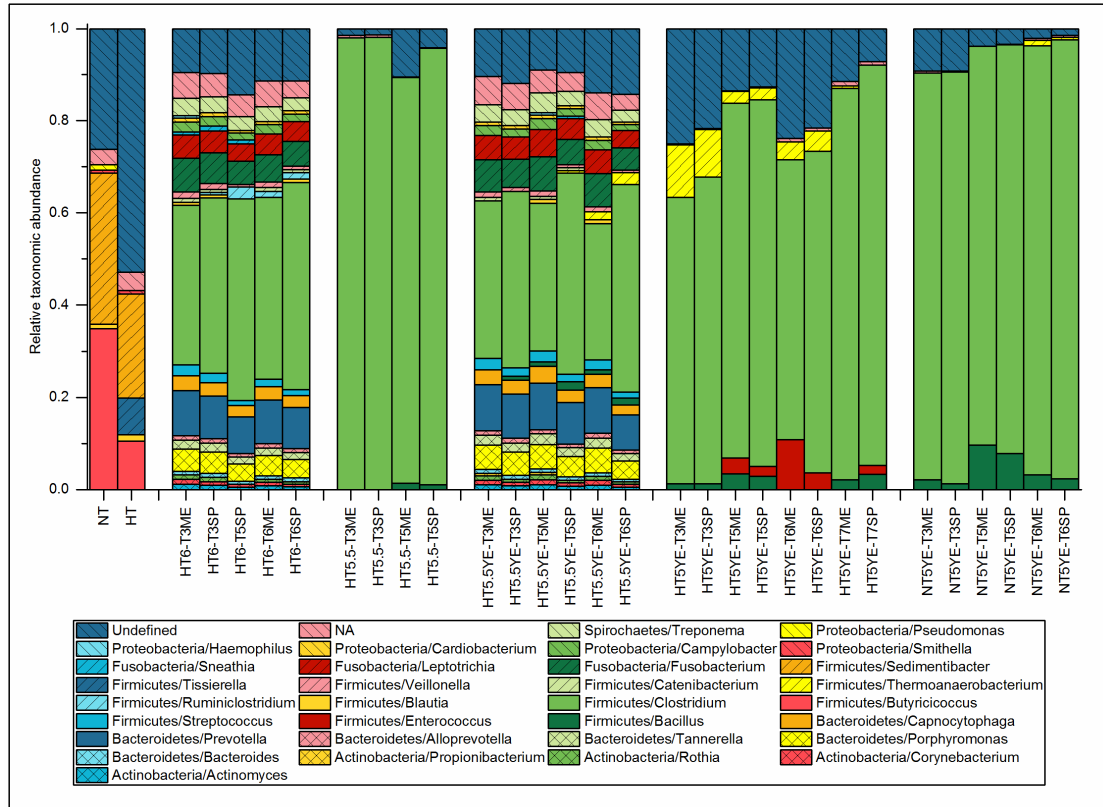


Figure 3.3. Relative taxonomic abundance of the analyzed microbial consortia in pH-based enrichments at genus level. The label of the samples is encoded according to the enrichment name, transfer number and growth phase at the moment of the sampling. ME and SP stand for mid-exponential and stationary growth phase, respectively. The label NA corresponds to the sum of all genera with a relative abundance below 1%. Extracted from Grimalt-Alemany et al. [249] (Manuscript II).

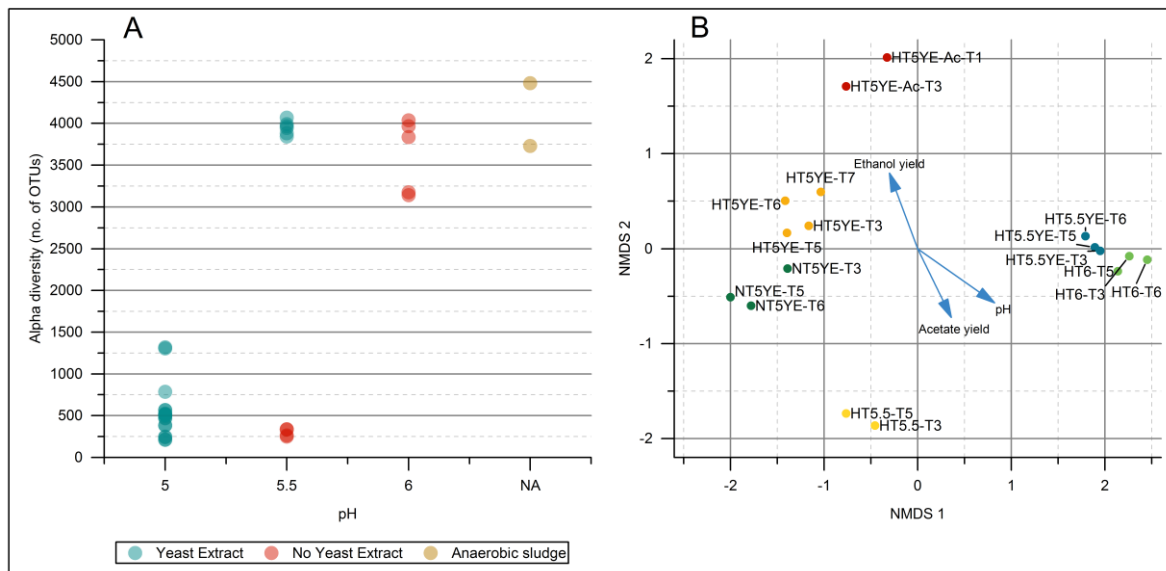


Figure 3.4. **A** Dependence of alpha-diversity (measured as number of unique OTUs) on pH for all enrichment samples. NA corresponds to samples from the starting inocula. **B** Non-metric multidimensional scaling (nMDS) unconstrained ordination. The arrows represent the direction and strength of the correlation between the variables and the unconstrained ordination of samples. The label of the samples is encoded according to the enrichment series name and transfer number. Extracted from Grimalt-Alemany et al. [249] (Manuscript II).

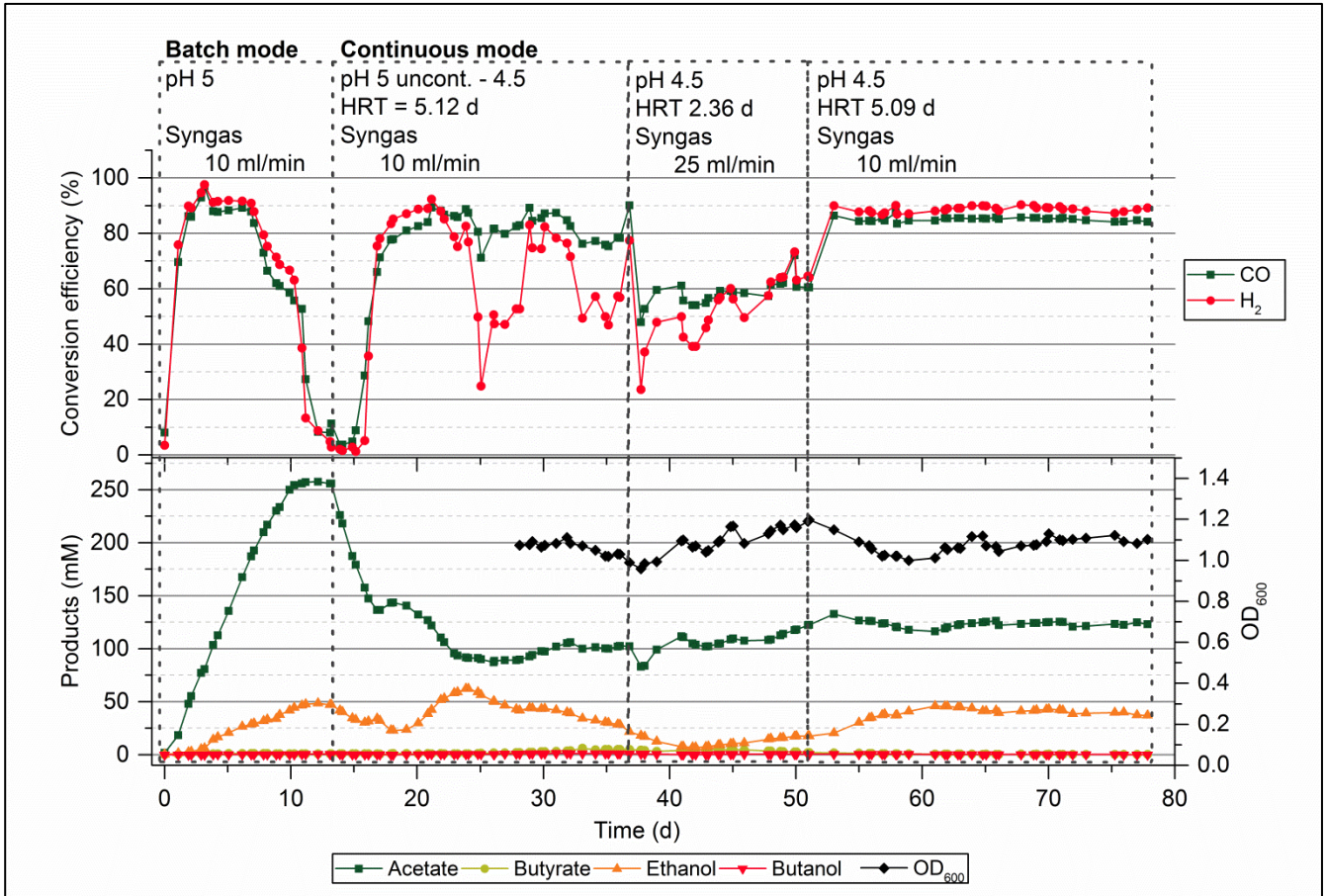


Figure 3.5. Conversion efficiency and product concentration profile during the microbial enrichment under batch and continuous operation. Changes in operating conditions are noted above the graph. The initial lag phase of the anaerobic sludge after inoculation is not included in the graph. Extracted from Manuscript V.

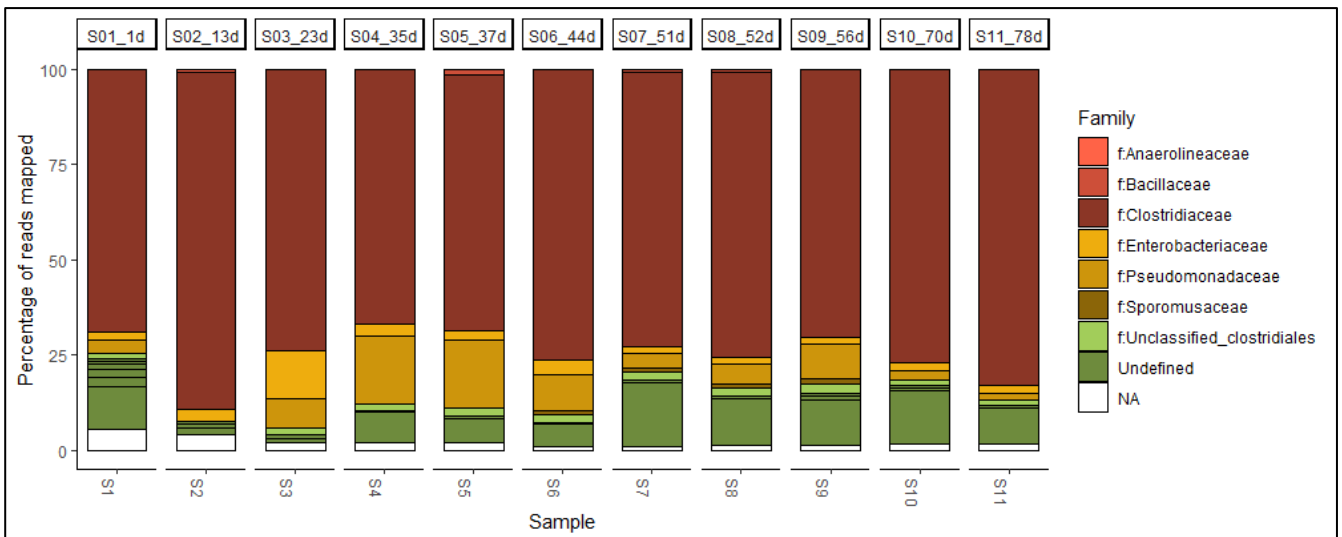


Figure 3.6. Relative abundance of reads mapped to OTUs at family taxonomic level during the microbial enrichment. The corresponding day when the sample was taken is given above the columns. NA corresponds to reads mapped to OTUs assigned to families with a percentage of reads below 0.5%. Extracted from Manuscript V.

Chapter IV – Thermodynamics-based Selection of Operating Parameters and Catabolic Route Control Strategies

4.1. Purpose

In this chapter, the thermodynamics of the network of net biochemical reactions of acetogenic and methanogenic syngas-converting microbial communities is investigated on the perspective of identifying operational strategies allowing for the control of their metabolic activity. The metabolic network of these microbial communities is first analyzed based on the thermodynamic feasibility of their reactions, focusing on several aspects of their metabolism like syntrophic interactions and thermodynamic competition. Key reactions subject to thermodynamic control at the given operating conditions are then identified through the thermodynamic potential factor (F_T), derived by Jin & Bethke [237]. Finally, possible operational strategies targeting specific metabolic activities in the microbial community are defined and tested experimentally for confirmation.

4.2. Hypothesis

- ❖ Thermodynamic principles can be used for steering the metabolic activity of specific microbial trophic groups by regulating either the intracellular or the interspecies metabolism of microbial communities.

4.3. Specific objectives

- ❖ To analyze the thermodynamics of net biochemical reactions composing the metabolic network of methanogenic and acetogenic microbial communities based on their thermodynamic feasibility in order to identify reactions subject to thermodynamic control.
- ❖ To design catabolic route control strategies and operational strategies allowing for targeted control of specific bioconversions.

4.4. Related manuscripts

- II. A. Grimalt-Alemany, M. Łężyk, L. Lange, I. V. Skiadas, and H. N. Gavala. Enrichment of syngas-converting mixed microbial consortia for ethanol production and thermodynamics-based design of enrichment strategies. *Biotechnol Biofuels*, 2018; 11, 198: 1–22.

- III. A. Grimalt-Alemany, M. Łężyk, D. M. Kennes-Veiga, I. V. Skiadas, and H. N. Gavala. Enrichment of mesophilic and thermophilic mixed microbial consortia for syngas biomethanation: the role of kinetic and thermodynamic competition. *Waste and Biomass Valorization*, 2019.
- IV. A. Grimalt-Alemany, K. Asimakopoulos, I. V. Skiadas, and H. N. Gavala. Modeling of Syngas Biomethanation and Control of Catabolic Routes of Mesophilic and Thermophilic Mixed Microbial Consortia. (Submitted).
- VI. K. Asimakopoulos, A. Grimalt-Alemany, C. Lundholm-Høffner, H. N. Gavala and I. V. Skiadas. Syngas Biomethanation with Exogenous H₂ Supply for the Production of Natural Gas Grade Biomethane. (Submitted).

4.5. Computational and experimental procedures

The metabolic network of acetogenic and methanogenic microbial communities was first analyzed based on the Gibbs free energy change (ΔG_{rxn}) for all reactions occurring during the fermentation of syngas (table 4.1 and 4.2). The ΔG_{rxn} was corrected for the concentration of substrates and products, pH, temperature and ionic strength. Corrections for temperature were made through the Gibbs-Helmholtz equation, and the ionic strength was corrected based on the extended Debye-Hückel equation according to Alberty [250]. The thermodynamic feasibility of each of these reactions and the possibility of applying thermodynamic control on the microbial activity rates were evaluated through F_T according to eq. 4.1, where ΔG_A corresponds to $-\Delta G_{\text{rxn}}$ in kJ per reaction; ΔG_C is the energy conserved calculated based on the ATP yield of each metabolic pathway multiplied by the Gibbs free energy of phosphorylation (ΔG_p) according to eq. 4.2; and χ is the average stoichiometric number, which can be approximated by the number of times a rate-determining step takes place through a metabolic pathway.

$$F_T = 1 - \exp\left(-\frac{\Delta G_A - \Delta G_C}{\chi RT}\right) \quad (4.1)$$

$$\Delta G_C = Y_{ATP} \cdot \Delta G_p \quad (4.2)$$

F_T was originally intended to make kinetic models thermodynamically consistent (e.g. $\frac{dX}{dt} = \frac{\mu_{\text{max}} \cdot S}{K_s + S} \cdot X \cdot F_T$). However, F_T is used here independently in order to evaluate the role of thermodynamic control, thermodynamic competition between microbial trophic groups and the feasibility of syntrophic interactions. When $\Delta G_A \gg \Delta G_C$, F_T approaches 1, indicating that the rate of the reaction is strictly kinetically controlled. Conversely, when ΔG_A approaches ΔG_C , the reaction starts to be thermodynamically limited and F_T takes values between 0 and 1, indicating that the rate of the reaction is thermodynamically controlled. Lastly, when ΔG_A is equal to or lower than ΔG_C , F_T is 0 or negative and the metabolism ceases. Since the intracellular ratio ATP/ADP was not known, F_T calculations were made using different ΔG_p values in order to give an

idea of the sensitivity of F_T . The ΔG_p values used in the calculations for analyzing the acetogenic metabolic network were 45, 57.5 and 70 kJ/mol ATP, and for the methanogenic metabolic network were 45, 50 and 55 kJ/mol ATP [232,251–253].

Possible operational strategies identified for increasing the yield and selectivity towards ethanol and CH_4 were tested experimentally. Strategies targeting higher ethanol production through a higher acetate-reducing activity using H_2 or CO as electron donor were confirmed experimentally through an additional enrichment in sequential batch mode at initial pH 5 with increased initial concentration of acetate (20 mM). Operational strategies targeting higher product selectivity towards CH_4 through catabolic route control were tested experimentally at mesophilic and thermophilic conditions using a trickle bed reactor operated in continuous mode, where the partial pressure of CO_2 (P_{CO_2}) was controlled by adding exogenous H_2 .

Table 4.1. Biochemical reactions composing the methanogenic metabolic network along with the ATP yield and average stoichiometric number (χ) used in thermodynamic potential factor (F_T) calculations. Extracted from Grimalt-Alemany et al. [248] (Manuscript III).

Stoichiometry of biochemical reactions	ATP yield (mol per reaction)	χ	Ref.
Acetogenesis			
$4 H_2 + 2 CO_2 \rightarrow CH_3COOH + 2 H_2O$	0.33	1	[254]
$4 CO + 2 H_2O \rightarrow CH_3COOH + 2 CO_2$	1.66	5	[254]
Hydrogenogenesis			
$CO + H_2O \rightarrow H_2 + CO_2$	0.33	1	Calculated
Syntrophic fatty acid oxidation			
$CH_3CH_2COOH + 2 H_2O \rightarrow CH_3COOH + 3 H_2 + CO_2$	0.33	1	[255]
$CH_3COOH + 2 H_2O \rightarrow 4 H_2 + 2 CO_2$	0.33	1	[255]
Methanogenesis			
$4 H_2 + CO_2 \rightarrow CH_4 + 2 H_2O$	0.5	2	[252]
$CH_3COOH \rightarrow CO_2 + CH_4$	0.5	2	Calculated

Table 4.2. Biochemical reactions composing the acetogenic metabolic network along with the ATP yield and average stoichiometric number (χ) used in the thermodynamic potential factor (F_T) calculation. Extracted from Grimalt-Alemany et al. [249] (Manuscript II).

Stoichiometry of biochemical reactions	ATP yield (mol per reaction)	χ	Ref.
H_2/CO_2 conversion into acetate/ethanol			
$4 H_2 + 2 CO_2 \rightarrow CH_3COO^- + H^+ + H_2O$	0.3	2	[254]
$6 H_2 + 2 CO_2 \rightarrow CH_3CH_2OH + 2 H_2O$	-0.1 // 0.3 ^a	3	[254]
CO conversion into acetate/ethanol			
$4 CO + 2 H_2O \rightarrow CH_3COO^- + H^+ + 2 CO_2$	1.5	4	[254]
$6 CO + 3 H_2O \rightarrow CH_3CH_2OH + 4 CO_2$	1.7	6	[254]
VFA reduction to corresponding alcohols			
$CH_3COO^- + H^+ + 2 H_2 \rightarrow CH_3CH_2OH + H_2O$	0.33	4	[183]
$CH_3(CH_2)_2COO^- + H^+ + 2 H_2 \rightarrow CH_3(CH_2)_2CH_2OH + H_2O$	0.33	4	[183]
$CH_3COO^- + H^+ + 2 CO + H_2O \rightarrow CH_3CH_2OH + 2 CO_2$	0.66	5	Calculated
$CH_3(CH_2)_2COO^- + H^+ + 2 CO + H_2O \rightarrow CH_3(CH_2)_2CH_2OH + 2 CO_2$	0.66	5	Calculated
Chain elongation			
$5 CH_3CH_2OH + 3 CH_3COO^- \rightarrow 4 CH_3(CH_2)_2COO^- + H^+ + 3 H_2O + 2 H_2$	1	1	[180]

^a Bertsch & Müller [254] predicted an ATP yield of -0.1, however the possibility of a positive ATP yield was also evaluated.

4.6. Summary of results

The acetogenic metabolic network was first analyzed based on ΔG_{rxn} and F_T as a function of pH in order to confirm that the metabolic activity of the acetogenic microbial communities enriched at different initial pH conditions (described in the Chapter III) was consistent with the thermodynamic analysis (Manuscript II). The results indicated that, despite the ΔG_{rxn} of most of the reactions is affected by the change of pH, only a few would be expected to be thermodynamically controlled under the given initial operational conditions. As shown in fig. 4.1A, all acetate-producing reactions become less exergonic with decreasing pH, while VFA-reducing reactions are significantly favored by the pH decrease, and direct ethanol-producing reactions remain unaffected. However, the analysis of the F_T shows that not all reactions are equally sensitive to changes in the ΔG_{rxn} liberated. The F_T of acetate- and ethanol-producing reactions from H_2/CO_2 and CO approach 1 at all pH conditions, which suggests that these reactions are kinetically controlled rather than thermodynamically controlled (fig. 4.1B). Thus, the direct production of either acetate or ethanol probably depends strictly on the kinetic competition between the different intracellular enzymatic reactions of their metabolic pathways, as these reactions provide enough thermodynamic driving force to proceed forward without being affected by the change in ΔG_{rxn} . On the other hand, all VFA-reducing reactions present F_T values below 1, indicating that the rate of these reactions could be thermodynamically controlled. According to this, the rate of acetate- and butyrate-reducing reactions would be expected to increase with the decrease in pH, as the F_T increases considerably in all reactions (fig. 4.1B). The boundaries of thermodynamic feasibility of these reactions cannot be accurately determined though, due to the uncertainties in ΔG_c . For example, using a ΔG_p of 45 kJ/mol of ATP and an ATP yield of 0.33 moles per reaction, the reduction of acetate to ethanol using H_2 as electron donor would become feasible below a pH of 5.6, while this reaction would not be feasible at any pH when using a ΔG_p of 70 kJ/mol of ATP (fig. 4.1B). However, despite the uncertainties, it is clear that a high pH in the fermentation broth would render this reaction unfeasible, while decreasing the pH would favor it. There is less uncertainty associated to the acetate-reducing activity using CO as electron donor as it is thermodynamically feasible at all relevant pH conditions regardless of the ΔG_p used. Decreasing the pH from 6 to 5 would then be expected to boost the rate of this reaction as F_T increases from 0.68 to 0.79 when using a ΔG_p of 57.5 kJ/mol of ATP (fig. 4.1B). These results are fully consistent with the increasing trend in ethanol and butanol yield observed when decreasing the initial pH during the solventogenic enrichments described in Chapter III, which allow concluding that VFA-reducing reactions played a fundamental role on the solventogenic activity of the enriched microbial communities. Accordingly, operational strategies for further improving the ethanol yield should target boosting the rates of acetate-reducing reactions.

According to the stoichiometry of acetate-reducing reactions, F_T , and consequently the activity rate of these reactions, could be boosted by increasing the P_{CO} and P_{H_2} , increasing the initial acetate concentration,

removing ethanol in-situ and decreasing the P_{CO_2} . In this case, the increase of initial acetate concentration was chosen as it was the simplest option for selectively targeting a higher activity of acetate-reducing reactions. As shown in fig. 4.2A, changes in the initial concentration of acetate have a strong effect on the ΔG_{rxn} of most reactions. However, only acetate-reducing reactions using H_2 and CO as electron donors would be highly sensitive to changes in ΔG_{rxn} , with F_T increasing significantly with the increase of acetate concentration (fig. 4.2B). Therefore, an enrichment at pH 5 with an initial acetate concentration of 20 mM would be expected to boost the ethanologenic potential of the microbial community by enhancing its acetate-reducing activity. The higher ethanologenic potential of the enriched community, when compared to the base case (enrichment at pH 5 without acetate addition), was obvious given that ethanol was the main product of the fermentation from the first transfer (fig. 4.3). By the end of the enrichment, the fermentation carried out by this microbial community resulted in an ethanol yield of $72.44 \pm 2.11\%$ of the stoichiometric maximum, which corresponded to a 22.49% increase of the maximum ethanol yield obtained previously (enrichment at pH 5). The higher acetate-reducing activity of this microbial community was apparent during the fermentation even though the latter took place during the exponential growth phase (fig. 4.4).

The thermodynamics of the metabolic network of methanogenic microbial communities was initially analyzed based on the ΔG_{rxn} and F_T as a function of temperature in order to identify possible bioenergetic limitations conditioning the metabolic activity of specific microbial trophic groups (Manuscript III). As shown in fig. 4.5a, the increase of temperature has a negative effect on ΔG_{rxn} for most reactions, with the exception of aceticlastic methanogenesis, syntrophic acetate oxidation (not shown in figure 4.5a) and carboxydrotrophic hydrogenogenesis. Based on F_T calculations considering the initial fermentation conditions, these are also the only reactions with an increasingly compromised thermodynamic feasibility with decreasing temperature (non-feasible in the case of syntrophic acetate oxidation) (fig. 4.5b). In the case of aceticlastic methanogenesis, the thermodynamic limitation is caused by the low acetate concentration at the initial fermentation conditions (1 mM), which would disappear as soon as acetate started to be produced during the course of the fermentation and would have no further implications. However, the thermodynamic limitation of the carboxydrotrophic hydrogenogenesis could have had implications in the microbial selection of carboxydrotrophic acetogens during the mesophilic enrichment (described in Chapter III), as the latter probably had an initial advantage derived from the partial thermodynamic inhibition of the hydrogenogenesis. The microbial selection of different carboxydrotrophic microbial groups can be further explained by the increasing and decreasing doubling times for carboxydrotrophic acetogens and hydrogenogens, respectively, with the increase of temperature [133,151,256,257]. The thermodynamic competition between these microbial groups follows the same trend, since carboxydrotrophic hydrogenogens would be clearly outcompeted by acetogens at low CO concentrations in the liquid at mesophilic conditions (fig. 4.6a), while they should be able to compete for CO at thermophilic conditions (fig. 4.6b). In turn, the competition for H_2/CO_2 was found to be strictly kinetically driven at the initial conditions of the

fermentation, as F_T approaches 1 at all temperatures for both homoacetogenesis and hydrogenotrophic methanogenesis (fig. 4.5b). Nevertheless, thermodynamic competition among these microbial trophic groups also played a role during the fermentation when the concentration of H_2 in the liquid started to be limiting, given that hydrogenotrophic methanogens present a much lower minimum threshold P_{H_2} than homoacetogens (fig. 4.6 and 4.7a).

Two reactions of the methanogenic metabolic network were especially interesting due to the possibility of applying thermodynamic control on the metabolic activity of their corresponding microbial trophic groups, namely, syntrophic acetate oxidation and carboxydrotrophic hydrogenogenesis.

Syntrophic fatty acid oxidizers are a classic example of microbial metabolism severely affected by thermodynamic constraints due to the intrinsically compromised thermodynamic feasibility of these reactions. As shown in fig. 4.7, the syntrophic interaction between syntrophic acetate and propionate oxidizers with hydrogenotrophic methanogens was not possible under the operating conditions found during the batch experiments at mesophilic conditions; although a limited contribution of these reactions cannot be ruled out. However, the main acetate conversion catabolic route, aceticlastic methanogenesis, has been repeatedly reported to be inhibited by the toxicity of CO , even resulting in complete wash-out from the reactor in continuous processes and in accumulation of VFAs that remained unconverted (representing up to 20-25% of e-mols from syngas in some cases) [57,100,258,259]. Therefore, from an application perspective, it would be interesting to be able to drive a shift in the acetate conversion catabolic routes from aceticlastic methanogenesis to syntrophic acetate oxidation in order to achieve a complete conversion of VFAs and increase the product selectivity towards CH_4 . Analyzing the effect of P_{CO_2} on the thermodynamic feasibility of syntrophic acetate oxidation indicated that it would be feasible to engineer operating conditions favoring the syntrophic interaction between syntrophic acetate oxidizers and hydrogenotrophic methanogens by decreasing the P_{CO_2} e.g. adding exogenous H_2 (Manuscript VI). This can be seen in fig. 4.8, where both reactions become thermodynamically feasible within a common H_2 concentration range in the liquid phase at the lowest P_{CO_2} evaluated. When this was tested experimentally using a mesophilic trickle bed reactor, decreasing the P_{CO_2} from 0.12 atm to 0.016 atm (and the P_{H_2} from 0.11 atm to around 0.02 atm) resulted in a twelve-fold decrease in the acetate concentration in the reactor, corresponding to a drop in the e-mols diverted to acetate from 3.4% to 0.4% (fig. 4.9).

In the thermophilic microbial community, the carboxydrotrophic hydrogenogenic microbial group was found to shift its metabolism towards acetate depending on the operating conditions. CO was converted strictly into H_2 and CO_2 when carboxydrotrophic hydrogenogens were grown in syntrophic association with hydrogenotrophic methanogens, while the conversion of CO was partially diverted to acetate when hydrogenotrophic methanogens were inhibited and H_2/CO_2 started to accumulate in the gas phase. This is consistent with the literature, as even when using a co-culture composed by *C. hydrogenoformans* and *M.*

thermoautotrophicus converting CO in continuous operating mode, the carbon diverted towards acetate accounted for 7.9-15.4% (Cmol basis) of the product distribution [90]. Analyzing the thermodynamic limitation of the carboxydrotrophic hydrogenogenesis through the F_T revealed that the dynamic yield of H_2/CO_2 and acetate of this microbial trophic group was directly proportional to the degree of thermodynamic limitation of the hydrogenogenesis given by F_T (Manuscript IV – see also Chapter V for further details). The high sensitivity of the thermodynamic feasibility of the carboxydrotrophic hydrogenogenesis to changes in the operational conditions is shown in fig. 4.10, where it can be seen that the minimum threshold P_{CO} changes 6 orders of magnitude depending on the value of P_{H_2} and P_{CO_2} . Thus, decreasing the P_{CO_2} by adding exogenous H_2 would be expected to result in lower concentration of acetate in the liquid phase of the reactor due to the higher thermodynamic feasibility of the carboxydrotrophic hydrogenogenesis. When testing this experimentally, the decrease in P_{CO_2} from 0.23 atm to 0.07 atm resulted in a relatively low drop in acetate concentration from 16.8 mM (3.1% e-mols diverted to acetate) to 11.4 mM (2.0% e-mols diverted to acetate), which could be explained by the fact that P_{CO_2} was not low enough to avoid a partial production of acetate (fig. 4.11). Subsequently, adding excess H_2 caused the complete inhibition of the hydrogenogenesis due to the increase in P_{H_2} in the gas phase (fig. 4.11).

4.7. Conclusions

Although thermodynamic feasibility analyses constitute an indispensable tool for the reconstruction of the intracellular metabolic network of microorganisms through genome-scale models, these are rarely applied to analyze the interspecies metabolism of microbial communities in fermentation studies. However, as shown here, thermodynamics can provide valuable information on several metabolic features and processes taking place during microbial community driven bioconversions, such as the thermodynamic competition among microbial groups under substrate-limiting conditions, the feasibility of certain syntrophic interactions and the regulation of the metabolism of specific microbial trophic groups inherently conditioned by thermodynamic constraints. Additionally, the possibility of engineering operating conditions favoring specific metabolic activities in the microbial community, based on thermodynamic control of key reactions, was also demonstrated through fermentations targeting ethanol and CH_4 using different approaches.

The thermodynamic analysis carried out here, based on both ΔG_{rxn} and F_T , contributed to a better understanding of the metabolic response of the microbial community to different operating conditions at both intracellular and interspecies level. On one hand, the evaluation of the thermodynamic competition through minimum substrate threshold concentrations allowed a more complete interpretation of the mechanisms driving the microbial selection of specific carboxydrotrophic, hydrogenotrophic and acetate-converting microbial trophic groups during the methanogenic enrichments. On the other hand, the metabolic shifts towards acetate in the carboxydrotrophic hydrogenogenic microbial group, and towards ethanol in the case of

acetogenic microbial communities, could also be explained from a thermodynamic perspective. This shows that the thermodynamic interpretation of the metabolic network of microbial communities often offers complementary information to other routine analyses (e.g. kinetic interpretations or analysis of specific physiological traits of microbial communities) and should be included in the analytical toolkit of mixed-culture-based conversion processes.

The thermodynamic potential factor (F_T) proved to be an interesting tool for dealing with the complexity of the metabolic network of microbial communities, as it allowed for identifying candidate reactions to be thermodynamically controlled, this way simplifying the design of operational strategies favoring specific metabolic activities. The approach adopted in the acetogenic microbial community, considering each reaction as an independent and competing energy-yielding metabolic conversion, demonstrated an enhanced ethanol yield through the thermodynamic control of the activity rates of acetate-reducing reactions (by giving them an initial competitive advantage). This showed that the reduction of acids to their corresponding alcohols, typically taking place during stationary phase, can be induced during exponential growth phase through the selection of appropriate operating parameters. In turn, the approach adopted in the mesophilic methanogenic microbial community, based on studying the thermodynamic feasibility of the syntrophic interaction between syntrophic acetate oxidizers and hydrogenotrophic methanogens as a function of P_{CO_2} , demonstrated that controlling the catabolic routes used by microbial communities is possible and may be an effective strategy for improving their product selectivity, in this case towards CH_4 . The control of P_{CO_2} for increasing the product selectivity of carboxydrotrophic hydrogenogens could not be properly confirmed experimentally as it required a finer tuning of the P_{CO_2} . However, this control strategy, further explained and demonstrated in Chapter V, constitutes an example of thermodynamics-driven regulation of the intracellular metabolism.

Despite the simplicity of the method used, considering net biochemical reactions rather than intracellular processes, the results demonstrated that the product selectivity towards ethanol and CH_4 can be enhanced by using thermodynamic principles to steering the activity of microbial communities. Nonetheless, several limitations were identified. One of the most important is the fact that this method, as used here, can only guide the design of operational strategies targeting a specific activity, as accurate predictions on the dynamics of the activity of the microbial community during batch fermentations are not possible. This method is based on “snapshots” at key time points of the fermentation, while accurate predictions would require e.g. the integration of F_T with dynamic modelling tools accounting for changing conditions and kinetic considerations as well. Another important limitation derived from the fact that the ATP yield for each reaction and the ΔG_p were calculated assuming a fixed stoichiometry and constant parameters according to model metabolic pathways, although these have been shown to be dynamic [232]. An alternative to increase the accuracy of these calculations would be determining experimentally the minimum threshold Gibbs free

energy change (ΔG_{\min}) for each reaction, which could substitute ΔG_C in F_T calculations. The determination of ΔG_{\min} is rather straightforward for microbial trophic groups with a sole product, e.g. hydrogenotrophic and acetivlastic methanogens. However, this might be more challenging for acetogenic bacteria, as these tend to produce variable amounts of several products depending on the operating conditions.

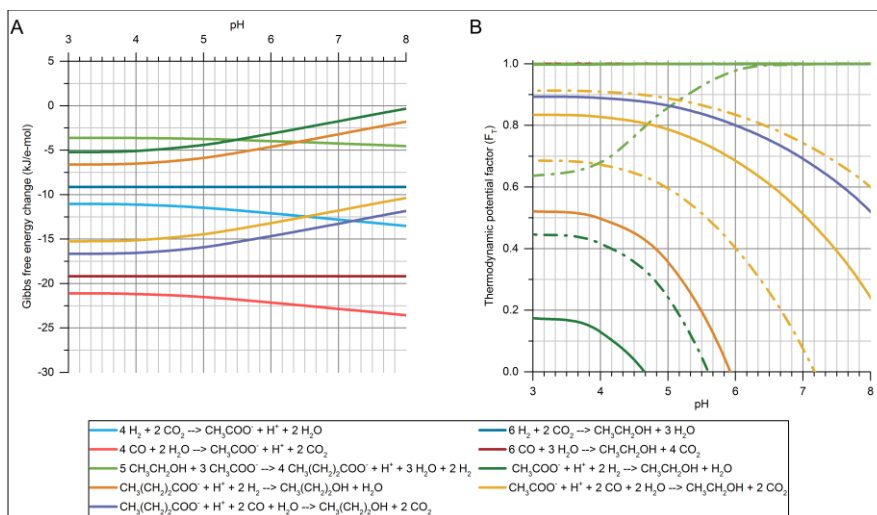


Figure 4.1. **A** Calculated $\Delta_r G'_{310K}$ for the metabolic network of microbial consortia as a function of pH, normalized for e-mol transferred per reaction. Process conditions considered were a temperature of 310.15 K, ionic strength of 0.08 M, P_{H_2} of 1.05 atm, P_{CO_2} of 0.6 atm, P_{CO} of 0.45 atm and concentration of metabolites of 0.001 M. **B** Thermodynamic potential factor calculated for all reactions as a function of pH. Solid lines represent F_T calculated using a ΔG_p of 57.5 kJ/mol of ATP. Dashed lines represent the upper and lower bound of F_T when using a ΔG_p of 45 and 70 kJ/mol of ATP, respectively. The upper and lower bounds are shown only for acetate-reducing reactions and the chain elongation reaction. Extracted from Grimalt-Alemayn et al. [249] (Manuscript II).

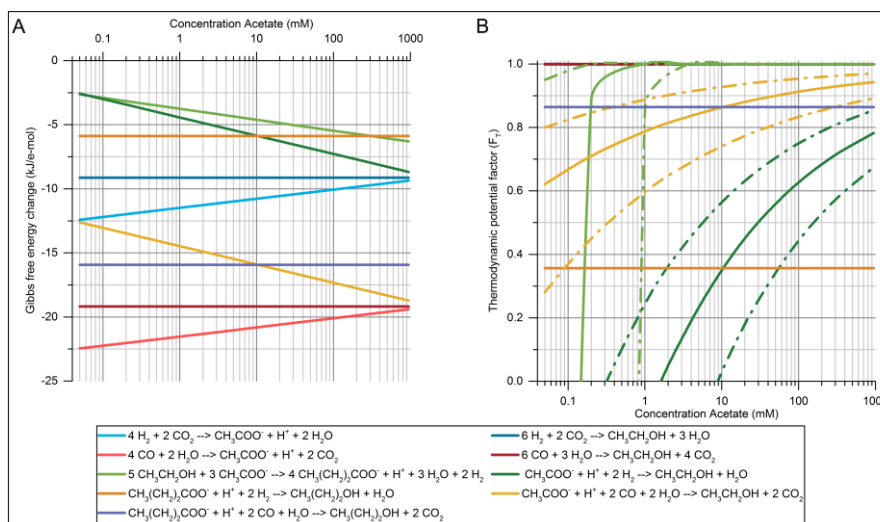


Figure 4.2. **A** Calculated $\Delta_r G'_{310K}$ for the metabolic network of microbial consortia as a function of acetate concentration, normalized for e-mol transferred per reaction. Process conditions considered were a temperature of 310.15 K, ionic strength of 0.08 M, P_{H_2} of 1.05 atm, P_{CO_2} of 0.6 atm, P_{CO} of 0.45 atm, concentration of other metabolites of 0.001 M and pH 5. **B** Thermodynamic potential factor calculated for all reactions as a function of pH. Solid lines represent F_T calculated using a ΔG_p of 57.5 kJ/mol of ATP. Dashed lines represent the upper and lower bound of F_T when using a ΔG_p of 45 and 70 kJ/mol of ATP, respectively. The upper and lower bounds are shown only for acetate-reducing reactions and the chain elongation reaction. Extracted from Grimalt-Alemayn et al. [249] (Manuscript II).

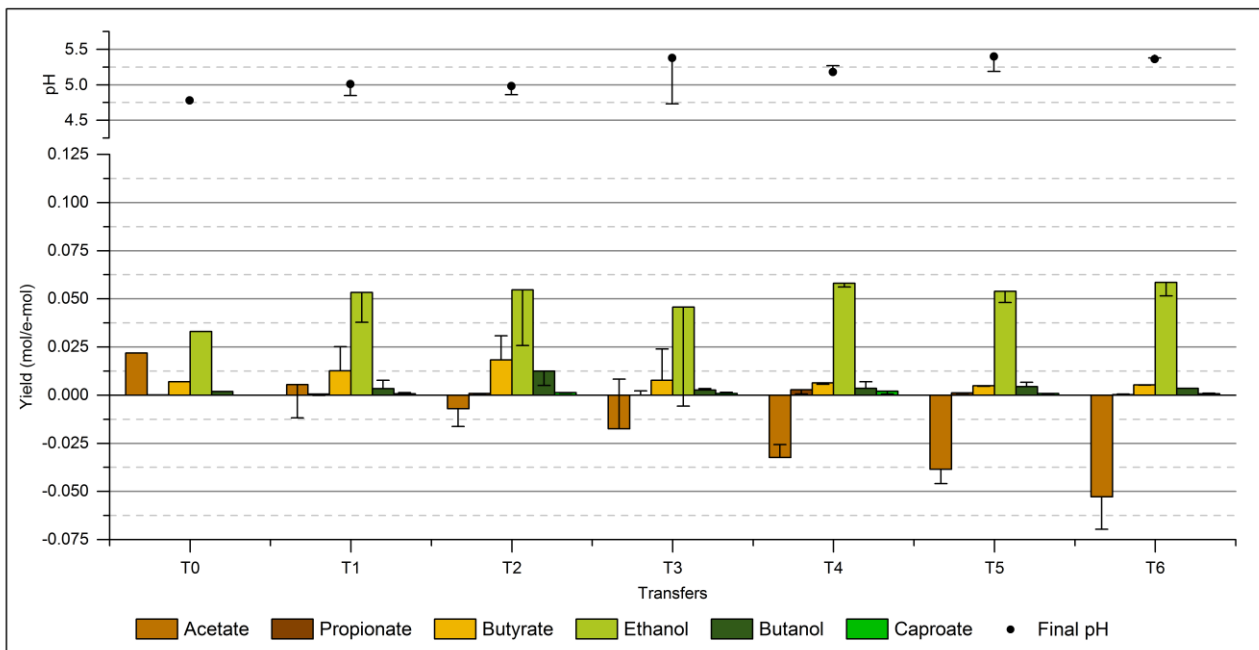


Figure 4.3. Product yields (mol/e-mol), net consumption/production of acetate (mol /e-mol of syngas consumed) and final pH for each fermentation in enrichment at pH 5 with addition of acetate (20 mM). The maximum theoretical net consumption of acetate corresponds to 0.25 mol acetate consumed/e-mol of syngas consumed. The columns show the values for the fermentation transferred and the error bars indicate the corresponding values of the duplicate experiment. Additional information on substrate consumption can be found in the additional file 1 (fig. 8). Extracted from Grimalt-Alemany et al. [249] (Manuscript II).

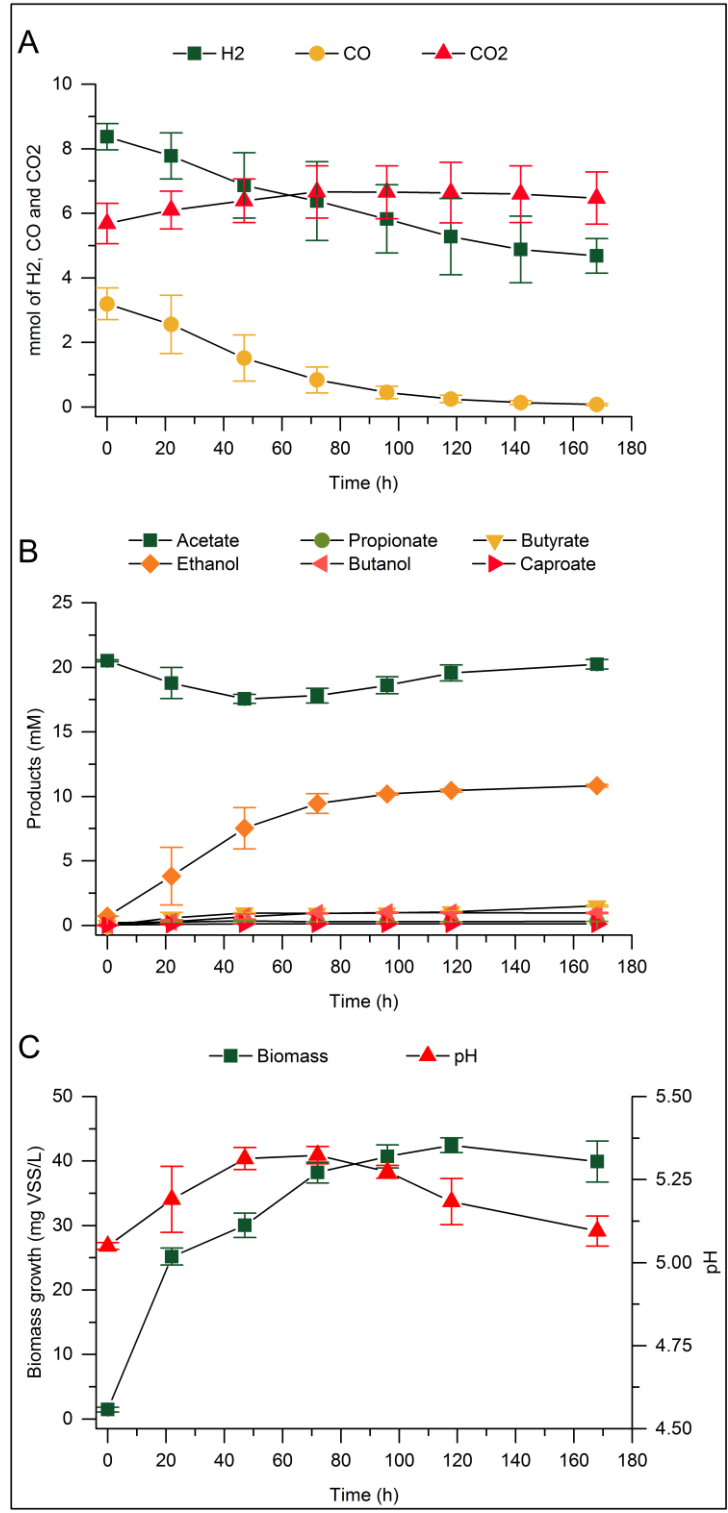


Figure 4.4. Fermentation profile of the enriched consortium HT5YE-Ac. **A** Gas composition of the headspace (mmol). **B** Concentration of products in the fermentation broth (mM). **C** Microbial growth and pH of the fermentation broth. Extracted from Grimalt-Aleman et al. [249] (Manuscript II).

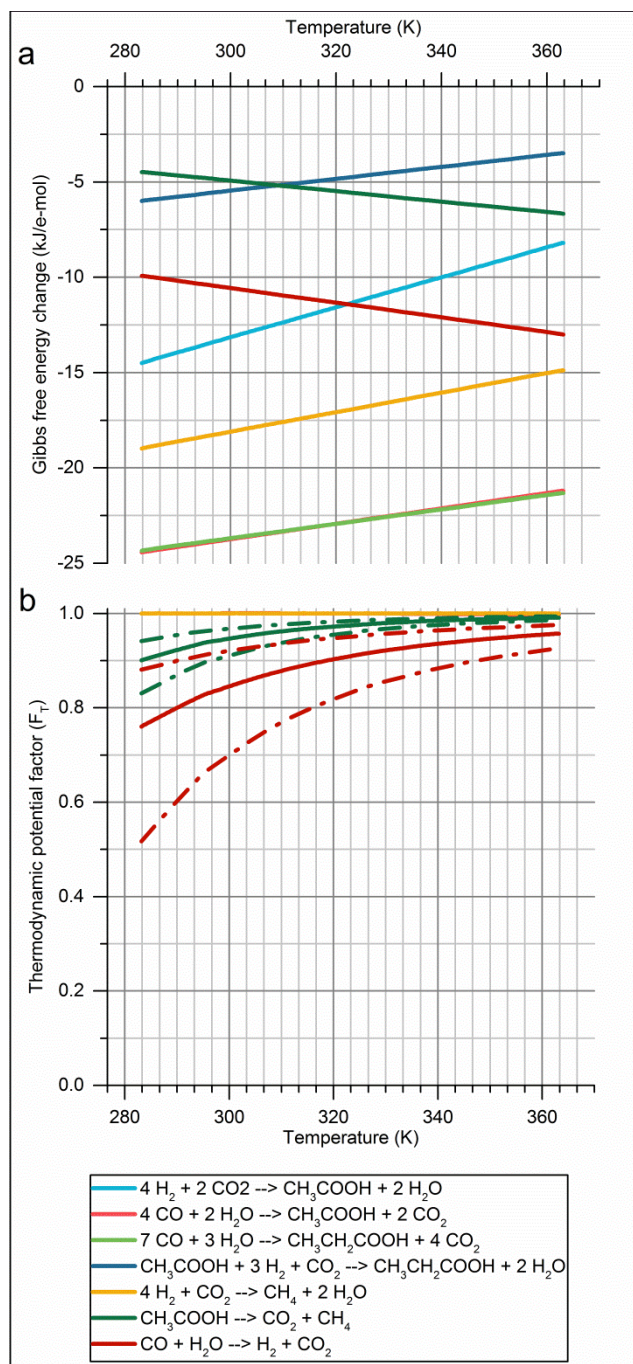


Figure 4.5. a. Gibbs free energy change as a function of temperature normalized to e-mol of electron donor for each of the biochemical reactions considered at the initial enrichment conditions. The operating conditions considered were P_{H_2} of 1.3 atm, P_{CO_2} of 0.2 atm, P_{CO} of 0.4 atm, acetic acid concentration of 0.001 M, propionate concentration of 0.0001 M, pH 7 and ionic strength of 0.08 M. **b.** Thermodynamic potential factor (F_T) as a function of temperature for each of the biochemical reactions considered at the initial enrichment conditions. Solid lines represent F_T calculated using a ΔG_p of 50 kJ/mol of ATP. Dashed lines represent the upper and lower boundaries of F_T when using a ΔG_p of 45 and 55 kJ/mol of ATP, respectively. Extracted from Grimalt-Alemany et al. [248] (Manuscript III).

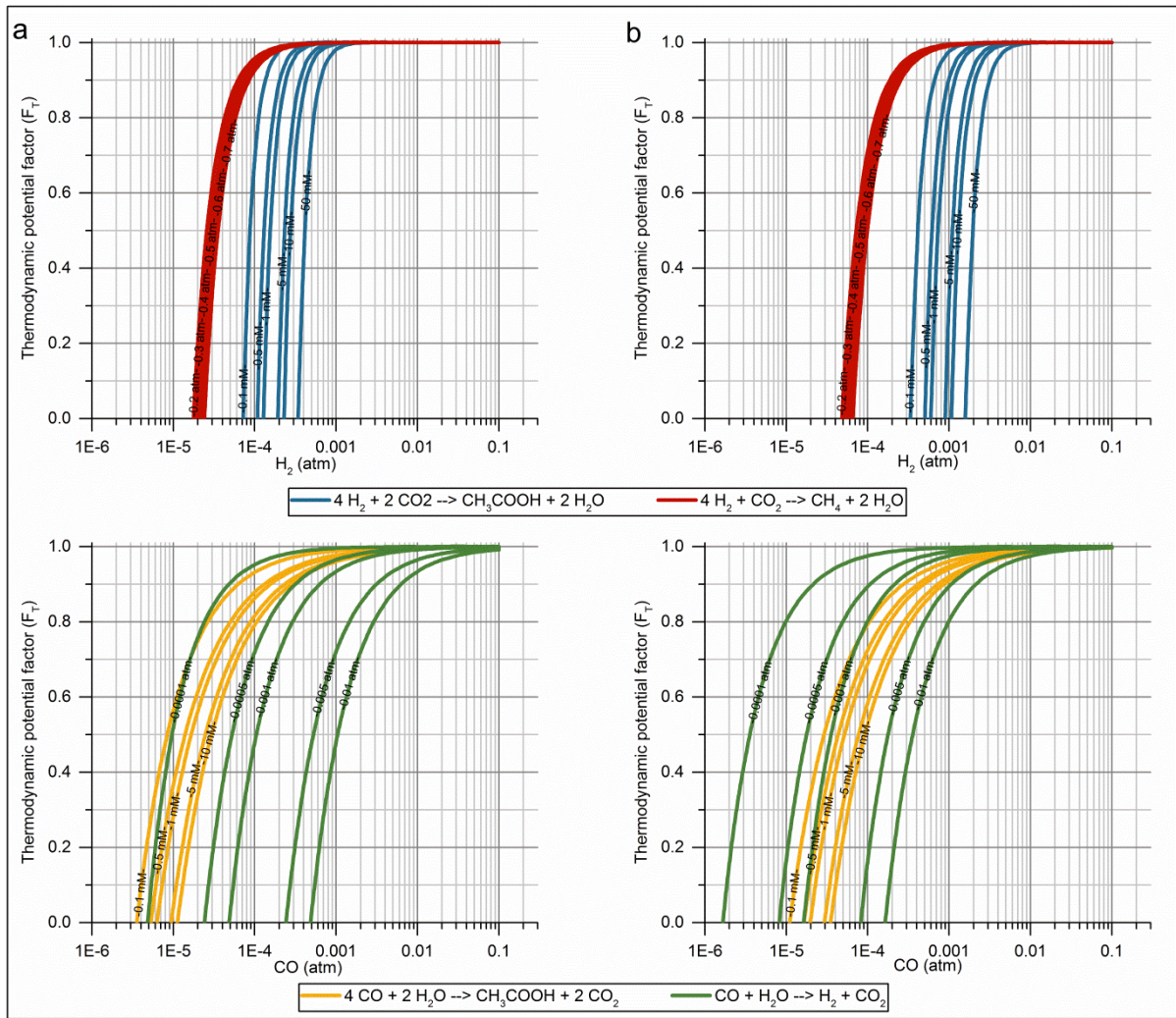


Figure 4.6. **a.** Minimum threshold partial pressure of CO and H₂ for carboxydutrophic acetogens, carboxydutrophic hydrogenogens, hydrogenotrophic methanogens and homoacetogens at mesophilic conditions (37 °C). **b.** Minimum threshold partial pressure of CO and H₂ for carboxydutrophic acetogens, carboxydutrophic hydrogenogens, hydrogenotrophic methanogens and homoacetogens at thermophilic conditions (60 °C). All calculations of F_T were made using a ΔGp of 50 kJ/mol of ATP. The different lines for each reaction correspond to different product concentrations for each reaction. The process conditions considered for determining the minimum threshold for CO were P_{H2} of 0.0001-0.01 atm, acetate concentration of 0.0001-0.01 M, P_{CO2} of 0.2 atm, pH 7 and ionic strength of 0.08 M. The process conditions considered for determining the minimum threshold of H₂ were P_{CH4} of 0.2-0.7 atm, acetate concentration of 0.0001-0.05 M, P_{CO2} of 0.5 atm, pH 7 and ionic strength of 0.08 M.

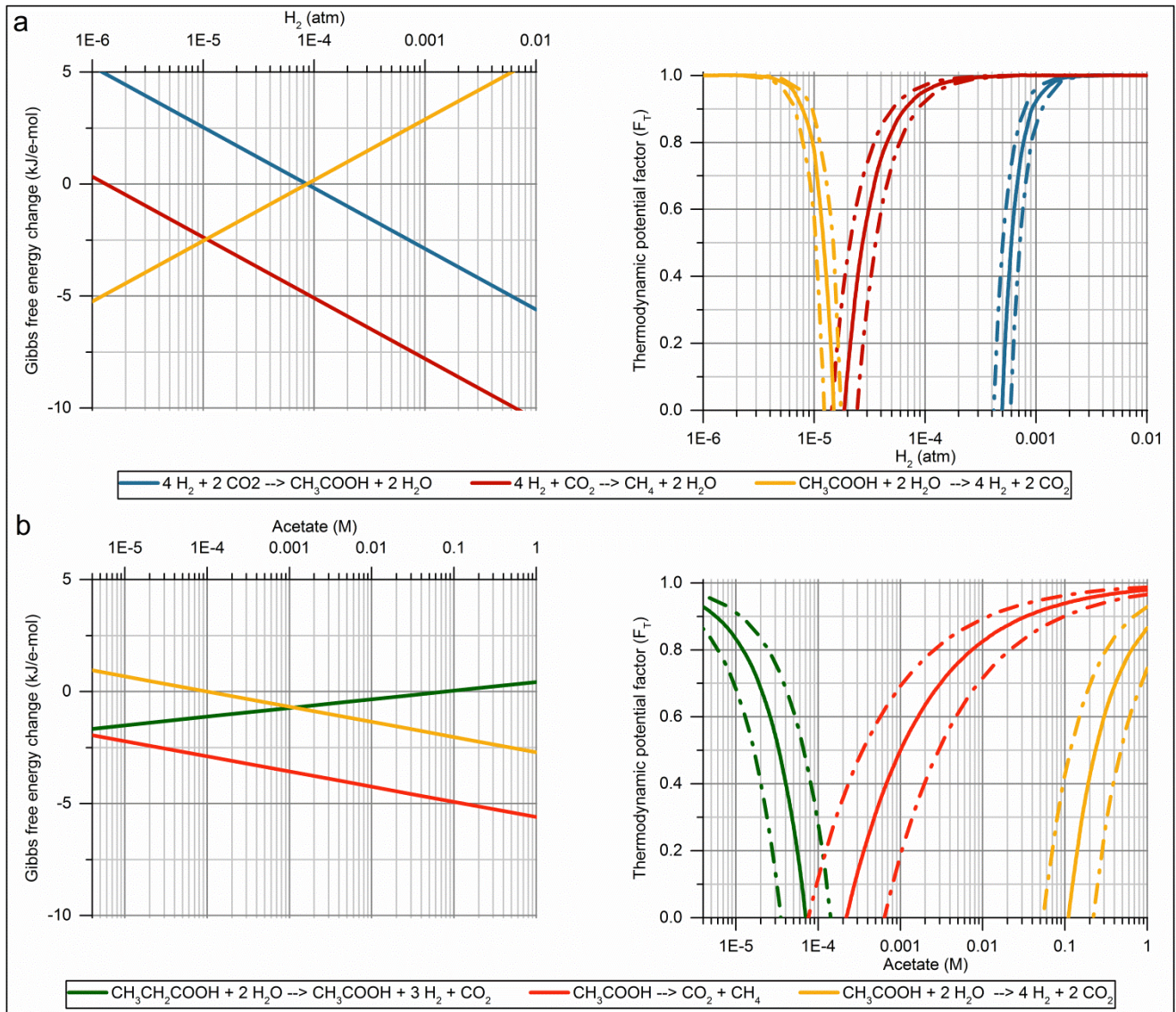


Figure 4.7. a. Gibbs free energy change ($\Delta_r G'_T$) and thermodynamic potential factor (F_T) as a function of P_{H_2} for hydrogenotrophic methanogenesis, homoacetogenesis and syntrophic acetate oxidation at the fermentation time with maximum acetate concentration. The operating conditions considered were P_{CO_2} of 0.2 atm, P_{CH_4} of 0.1 atm, acetate concentration of 0.022 M, temperature of 37 °C, pH 6.8 and ionic strength of 0.08 M. **b.** Gibbs free energy change ($\Delta_r G'_T$) and thermodynamic potential factor (F_T) as a function of acetate concentration for aceticlastic methanogenesis and syntrophic propionate and acetate oxidation at the final fermentation conditions. The operating conditions considered were P_{H_2} of 0.00002 atm (determined by the minimum threshold of H_2 for hydrogenotrophic methanogens), P_{CO_2} of 0.2 atm, P_{CH_4} of 0.28 atm, propionate concentration of 0.0006 M, temperature of 37 °C, pH 7 and ionic strength of 0.08 M. The $\Delta_r G'_T$ shown was normalized to e-mol of electron donor for each of the biochemical reactions considered. Solid lines for F_T represent F_T calculated using a ΔG_p of 50 kJ/mol of ATP. Dashed lines represent the upper and lower boundaries of F_T when using a ΔG_p of 45 and 55 kJ/mol of ATP, respectively. Extracted from Grimalt-Alemany et al. [248] (Manuscript III).

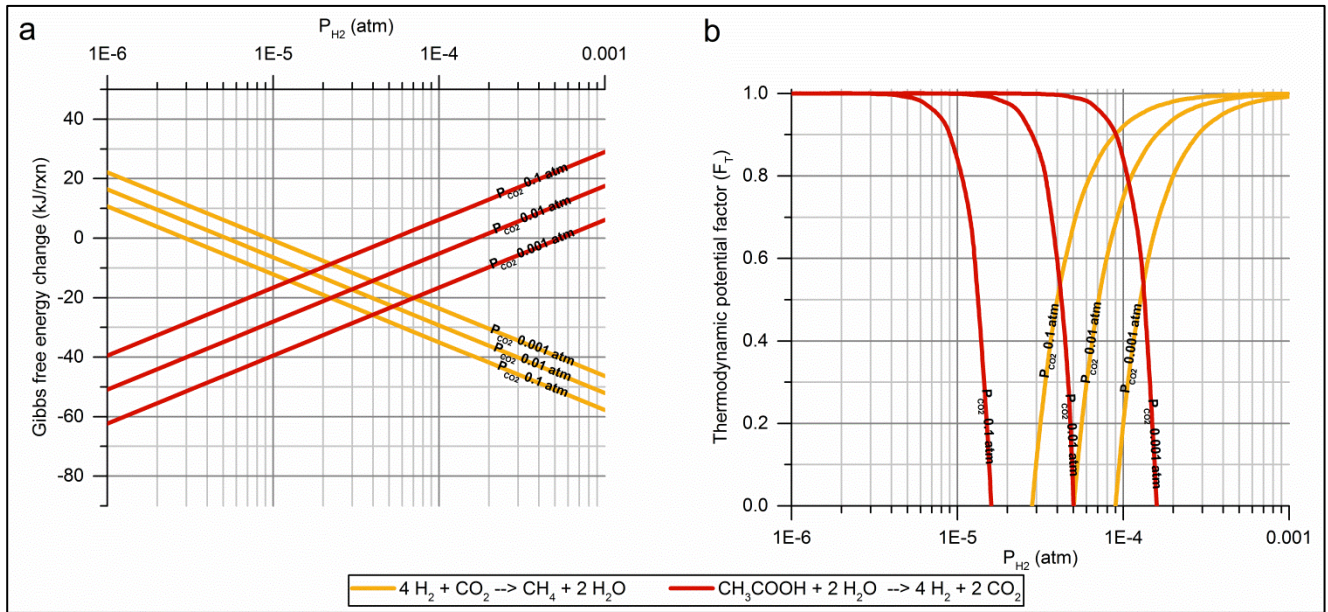


Figure 4.8. (a) Gibbs free energy change ($\Delta_r G'_{310K}$) as a function of P_{H_2} in kJ per reaction for hydrogenotrophic methanogenesis and syntrophic acetate oxidation calculated at different P_{CO_2} . (b) Thermodynamic potential factor (F_T) as a function of P_{H_2} for hydrogenotrophic methanogenesis and syntrophic acetate oxidation calculated at different P_{CO_2} . The operating conditions considered in the calculations were P_{CO_2} of 0.1 atm, 0.01 atm and 0.001 atm; P_{CH_4} of 0.6 atm; acetate concentration of 17 mM; temperature of 310 K; pH 7.4; and ionic strength of 0.25 M. Note that P_{H_2} and P_{CO_2} are lower than those reported in fig. 4.9, as these represent the theoretical partial pressure in equilibrium with the concentration of H_2 and CO_2 in the liquid phase. Extracted from Manuscript VI.

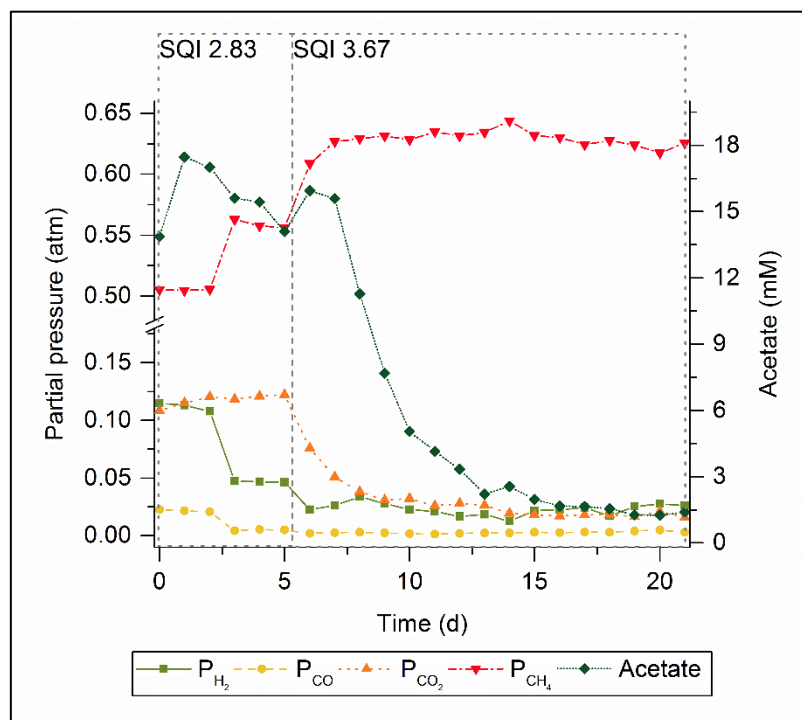


Figure 4.9. Partial pressure of gases in the effluent and acetate concentration profile of the mesophilic trickle bed reactor operated in continuous mode at SQI 2.83 and 3.67. SQI represents the ratio of electron donors/carbon calculated as $\frac{(mol H_2 + mol CO)}{(mol CO + mol CO_2)}$, where a value of 4 represents ideal syngas composition for its conversion into methane. Extracted from Manuscript VI.

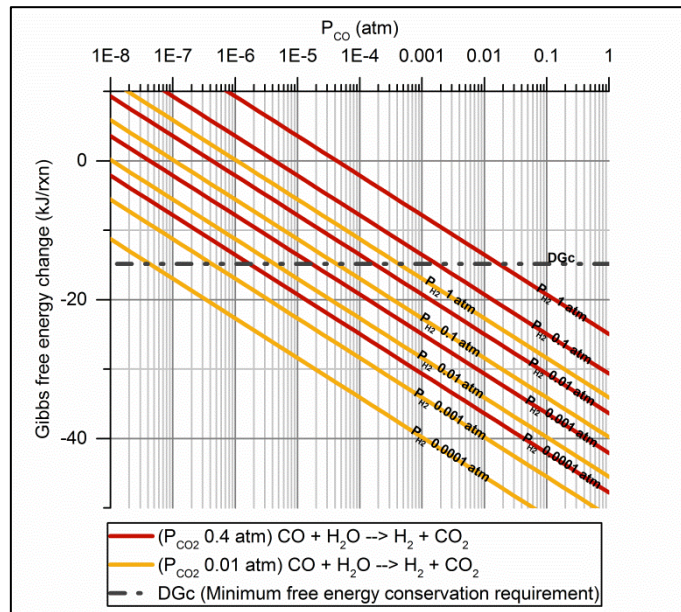


Figure 4.10. Gibbs free energy change ($\Delta_r G'_{333K}$) as a function of P_{CO} in kJ per reaction for carboxydrotrophic hydrogenogenesis calculated using different P_{H_2} and P_{CO_2} . The dashed line indicates the minimum energy conservation requirements (ΔG_c or ΔG_{min}) assumed for carboxydrotrophic hydrogenogenesis and the minimum threshold P_{CO} at each of the conditions considered. The calculations were made using a P_{H_2} of 1 atm, 0.1 atm, 0.01 atm, 0.001 atm and 0.0001 atm; P_{CO_2} of 0.4 atm and 0.01 atm; and temperature of 333 K. Extracted from Manuscript VI.

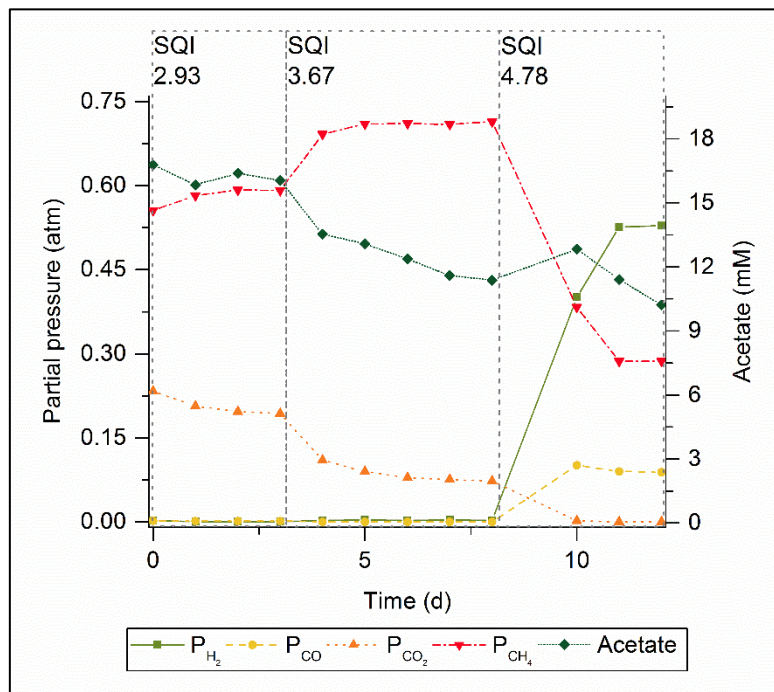


Figure 4.11. Partial pressure of gases and acetate concentration profile of the thermophilic trickle bed reactor operated in continuous mode at SQI 2.93, 3.67 and 4.78. SQI represents the ratio of electron donors/carbon calculated as $\frac{(mol H_2 + mol CO)}{(mol CO + mol CO_2)}$, where a value of 4 represents ideal syngas composition for its conversion into methane. Extracted from Manuscript VI.

Chapter V – Modeling of Syngas Biomethanation and Catabolic Route Control

5.1. Purpose

In this chapter, the development of two models for simulation of the syngas biomethanation process in batch mode is described. In order to correct initial model mismatches with the experimental measurements during the simulations, several model parameters were either estimated by fitting to experimental data through the least squares method, determined experimentally or fixed manually based on data from the literature. After validation with additional experimental data, these models were used to demonstrate possible catabolic route control strategies through kinetic and thermodynamic control based on model simulations.

5.2. Hypotheses

- ❖ The simulation of the syngas biomethanation process through “grey box” models, accounting for the main microbial trophic groups and interactions of the microbial community, can successfully describe the performance of microbial communities with relatively high predictive capacity.
- ❖ The combination of thermodynamic and kinetic considerations in dynamic models allows for designing detailed catabolic route control strategies.

5.3. Specific objectives

- ❖ To develop dynamic models able to describe the performance of mesophilic and thermophilic enriched microbial communities during syngas biomethanation.
- ❖ To define the structure of the models based on experimental observations and thermodynamic considerations in order to include specific mutualistic, competitive and cross-feeding interactions and improve the overall predictive capacity of the models.
- ❖ To evaluate the parameter importance and identifiability in each model based on sensitivity analyses for optimal experimental and computational parameter estimation.
- ❖ To design catabolic route control strategies and operational strategies allowing for targeted control of specific bioconversions.

5.4. Related manuscript

- IV. A. Grimalt-Alemany, K. Asimakopoulos, I. V. Skiadas, and H. N. Gavala. Modeling of Syngas Biomethanation and Control of Catabolic Routes of Mesophilic and Thermophilic Mixed Microbial Consortia. (Submitted).

5.5. Models description and procedures

Two structured models were developed for simulating the syngas biomethanation process at mesophilic and thermophilic conditions. The structure of the models was in agreement with the catabolic routes employed by the enriched microbial communities described in Chapter III and Chapter IV, and consequently, accounted for simultaneous growth of different microbial trophic groups. The microbial trophic groups included in the mesophilic model corresponded to carboxydrotrophic acetogens, homoacetogens, hydrogenotrophic methanogens, aceticlastic methanogens and syntrophic acetate and propionate oxidizers. In turn, the thermophilic model accounted for simultaneous growth of carboxydrotrophic hydrogenogens and hydrogenotrophic methanogens. Other physicochemical processes such as acid dissociation and gas-to-liquid mass transfer were also included. All growth models were based on the Monod growth model. However, in order to add thermodynamic consistency to the models, the Monod growth kinetic expression was modified by adding the thermodynamic potential factor (F_T) (eq. 5.1), with which microbial trophic groups are active only within the limits of thermodynamic feasibility of their metabolic activity. A generalized model used for all microbial trophic groups is described by eq. 5.2, which includes several control functions like pH inhibition (I_{pH} - used only for mesophilic methanogens), lag phase (f_{lag}) and presence of the methanogenic inhibitor sodium 2-bromoethanesulfonate (BES) (f_{BES} - used only for methanogens).

$$F_T = \begin{cases} 1 - \exp\left(-\frac{\Delta G_A - \Delta G_C}{\chi RT}\right), & \Delta G_A \geq \Delta G_C \\ 0, & \Delta G_A \leq \Delta G_C \end{cases} \quad (5.1)$$

$$\mu = \frac{\mu_{max} \cdot S}{k_s + S} \cdot F_T \cdot I_{pH} \cdot f_{lag} \cdot f_{BES} \quad (5.2)$$

The growth models used for syntrophic fatty acid oxidizers and carboxydrotrophic hydrogenogens presented some particularities. Growth of syntrophic fatty acid oxidizers was modelled by substituting the Monod rate control function $\left(\frac{S}{k_s + S}\right)$ by F_T according to eq. 5.3 to avoid redundant control of the activity rate. The carboxydrotrophic hydrogenogenic microbial groups also needed some additional equations (eq. 5.4-5.6) for modeling the dynamic H_2 and acetate yield, where $F_{T,carb_hyd}$ corresponds to the F_T of the conversion of CO into H_2/CO_2 ; $Y_{e-mol/CO}$ represents the total product yield expressed in e-mols of product per mol of CO; and

$n_{e-mol/mol\ Ac\ or\ H_2}$ corresponds to the number of e-mols needed to synthesize one mol of acetate or H_2 . The dynamic biomass yield of this microbial group was modelled including a specific maintenance rate, described by eq. 5.7, assuming that acetate production may not result in biomass synthesis, where a_{carb_hyd} represents the severity of the maintenance cost. When $0 < a_{carb_hyd} < 1$, there is growth associated with acetate production; $a_{carb_hyd} = 1$ indicates no growth associated to acetate production; and $a_{carb_hyd} > 1$ indicates a specific maintenance cost associated with acetate production.

$$\mu = \mu_{max} \cdot F_T \quad (5.3)$$

$$\mu_{carb_hyd} = \frac{\mu_{max,carb_hyd} \cdot CO_{aq}}{k_{s,carb_hyd} + CO_{aq}} \cdot F_{T,carb_ac} \cdot f_{lag,carb_hyd} \quad (5.4)$$

$$Y_{H_2,carb_hyd} = F_{T,carb_hyd} \cdot Y_{e-mol/CO} / n_{e-mol/mol\ H_2} \quad (5.5)$$

$$Y_{Ac,carb_hyd} = (1 - F_{T,carb_hyd}) \cdot Y_{e-mol/CO} / n_{e-mol/mol\ Ac} \quad (5.6)$$

$$m_{s,carb_hyd} = a_{carb_hyd} \cdot \mu_{carb_hyd} \cdot (1 - F_{T,carb_hyd}) \quad (5.7)$$

The dataset used for model calibration corresponded to specific activity tests using H_2/CO_2 , CO and acetate as the only substrates with and without BES. Other experiments using syngas with varying initial P_{CO} were used for validation of the models. After performing a parameter identifiability analysis based on a local sensitivity analysis, the models were calibrated through least squares parameter estimation and experimental determination of specific mass transfer coefficients (k_{LA}), and validated with experimental data outside of the region used for model calibration. Possible catabolic route control strategies through kinetic and thermodynamic control for improving the product selectivity towards CH_4 in continuous processes were evaluated based on model simulations.

5.6. Summary of results

The parameter significance analysis through the sensitivity measure ∂_j^{msqr} showed common trends in the parameter importance ranking for both the mesophilic and the thermophilic models. In both models, the mass transfer coefficients for H_2 (k_{LAH_2}) and CO (k_{LACO}) were found to exert a strong influence on several model outputs, and the maximum specific growth rates (μ_{max}) were systematically more important than the half-saturation constants for each microbial trophic group (fig. 5.1). Besides k_{LAH_2} , k_{LACO} and μ_{max} of all groups, other important parameters for the thermophilic syngas biomethanation model were $\Delta G_{C,carb_hyd}$, a_{carb_hyd} and χ_{carb_hyd} , which are related to the maintenance cost and the dynamic yield of H_2 and acetate of the carboxydotrophic hydrogenogenic microbial group (fig. 5.1). However, the identifiability analysis performed based on the collinearity index (γ_K) indicated that not all parameters could be estimated simultaneously.

Accordingly, the parameters $\mu_{\max,\text{carb}}$, $\mu_{\max,\text{hyd}}$ and $\mu_{\max,\text{ac}}$ of the mesophilic model, and $\mu_{\max,\text{carb_hyd}}$, $\mu_{\max,\text{hyd}}$, $\Delta G_{\text{C,carb_hyd}}$ and $a_{\text{carb_hyd}}$ of the thermophilic model, were selected for least squares parameter estimation, while the k_{La} for all gases was determined experimentally.

The values obtained experimentally for k_{LaCO} corresponded to 2.59 h^{-1} and 2.61 h^{-1} at mesophilic and thermophilic conditions, respectively (fig. 5.2). Values obtained for k_{LaH_2} were 4.18 h^{-1} and 3.81 h^{-1} at mesophilic and thermophilic conditions, respectively (fig. 5.2). The results of the least squares parameter estimation are shown in table 5.1, where it can be seen that all parameters presented a low correlation among them, with the maximum correlation factor corresponding to 0.373 (table 5.1). This confirmed that the parameters were uniquely identifiable.

After model calibration, both mesophilic and thermophilic models were able to describe satisfactorily the performance of the microbial communities during syngas biomethanation, as it can be seen that all model variables follow closely the experimental data (fig. 5.3, 5.4 and 5.5). The mesophilic syngas biomethanation model was able to describe the combined kinetic and thermodynamic competition between homoacetogens and hydrogenotrophic methanogens. Homoacetogens were found to dominate the microbial community during the initial stage of the fermentation when the P_{H_2} was still high, while hydrogenotrophic methanogens took over the community once the mass transfer of H_2 became limiting due to the fact that hydrogenotrophic methanogens were able to keep the H_2 concentration in the liquid phase below the minimum H_2 threshold concentration for homoacetogens (fig. 5.3 and 5.4A). According to the model fittings, the conversion of acetate was exclusively carried out by acetoclastic methanogens, since syntrophic acetate oxidation was not thermodynamically feasible during the experiments used for calibration, excepting when acetate was used as the only substrate.

In the thermophilic model, it was hypothesized that the dynamic product and biomass yield observed experimentally could be modelled based on the thermodynamic feasibility of the hydrogenogenesis as described in eq. 5.4-5.7. The model assumed that H_2 was the main product from the conversion of CO and that acetate was produced only as a result of the thermodynamic limitation of the hydrogenogenesis. An additional assumption was that the production of acetate would not result in biomass formation. This was confirmed by the value of the estimated kinetic parameters ($a_{\text{carb_hyd}} > 1$) and the good fit to the experimental data in all cases, as the model could describe the behavior of carboxydophilic hydrogenogens when grown alone and in syntrophic association (fig. 5.4 and 5.5).

The structure of the models, considering simultaneous growth of several microbial groups, along with the addition of F_{T} in the specific growth models allowed for modeling cross-feeding, mutualistic and mutual exclusion interactions. Based on these interactions, three possible catabolic route control strategies based on kinetic and thermodynamic control were evaluated through model simulations. The possibility of controlling

the competition for H_2 between homoacetogens and hydrogenotrophic methanogens through the modulation of k_{LA} was identified, where it was found that decreasing the k_{LAH_2} should result in a clear dominance of the hydrogenotrophic methanogenic microbial group (fig. 5.6). The modulation of the P_{CO_2} could also be used as a catabolic route control strategy at mesophilic conditions (as described and confirmed experimentally in Chapter IV). In this case, decreasing significantly the P_{CO_2} should favor the dominance of syntrophic acetate oxidizers over aceticlastic methanogens as shown in fig. 5.7 through the F_T . Lastly, adjusting the P_{CO_2} at thermophilic conditions could allow a better control of the acetogenic metabolic shift observed in carboxydrotrophic hydrogenogens. This is shown in fig. 5.8, where it can be seen that the drop in P_{CO_2} would result in an increase of the thermodynamic drive of the hydrogenogenesis, minimizing in this way the production of acetate as by-product.

5.7. Conclusions

These models demonstrated the successful simulation of the performance of microbial communities during syngas biomethanation. Including thermodynamic considerations in the models was found to improve the simulations, and potentially the predictive capacity of the models, as these allowed predicting the feasibility of mutualistic interactions between syntrophic acetate oxidizers and hydrogenotrophic methanogens, the competition for H_2 between homoacetogens and hydrogenotrophic methanogens, and the acetogenic metabolic shift of carboxydrotrophic hydrogenogens.

The consideration of the dynamics of the microbial interactions and metabolic processes taking place during the mesophilic and thermophilic process offered the possibility of describing the process much more accurately than when using previously described methods (Chapter III and Chapter IV). This allowed, not only identifying possible catabolic route control strategies based on the modulation of specific operating parameters, but predicting quantitatively the degree of affection of the microbial community, e.g. through changes in the dominance of specific microbial trophic groups, or the specific final acetate and H_2 yield of carboxydrotrophic hydrogenogens as a function of the operating conditions. The kinetic control strategy identified (based on the limitation of the mass transfer) would have limited industrial applications, as the limitation of the mass transfer would prevent a high CH_4 productivity. However, this strategy could have some interesting applications in isolation of novel hydrogenotrophic methanogenic species or in the development of bioaugmentation operational strategies. In turn, the thermodynamic control strategies based on the modulation of P_{CO_2} through addition of exogenous H_2 would have clear industrial applications, bringing about a dual benefit as these strategies could allow the simultaneous control of catabolic routes and upgrading of the biogas produced to biomethane.

Using dynamic modeling tools integrating kinetic and thermodynamic considerations in “grey box” models opens good perspectives for achieving a more accurate control of the metabolic activity of microbial communities. However, much work is still needed in this direction. For example, in the case of the models developed here, it is likely that the kinetic parameters determined still need further confirmation or refinement in order to allow accurate simulations under other operating modes and reactor configurations. Other processes or microbial interactions like direct interspecies electron transfer, which may play an important role during this process, were as well overlooked in these models.

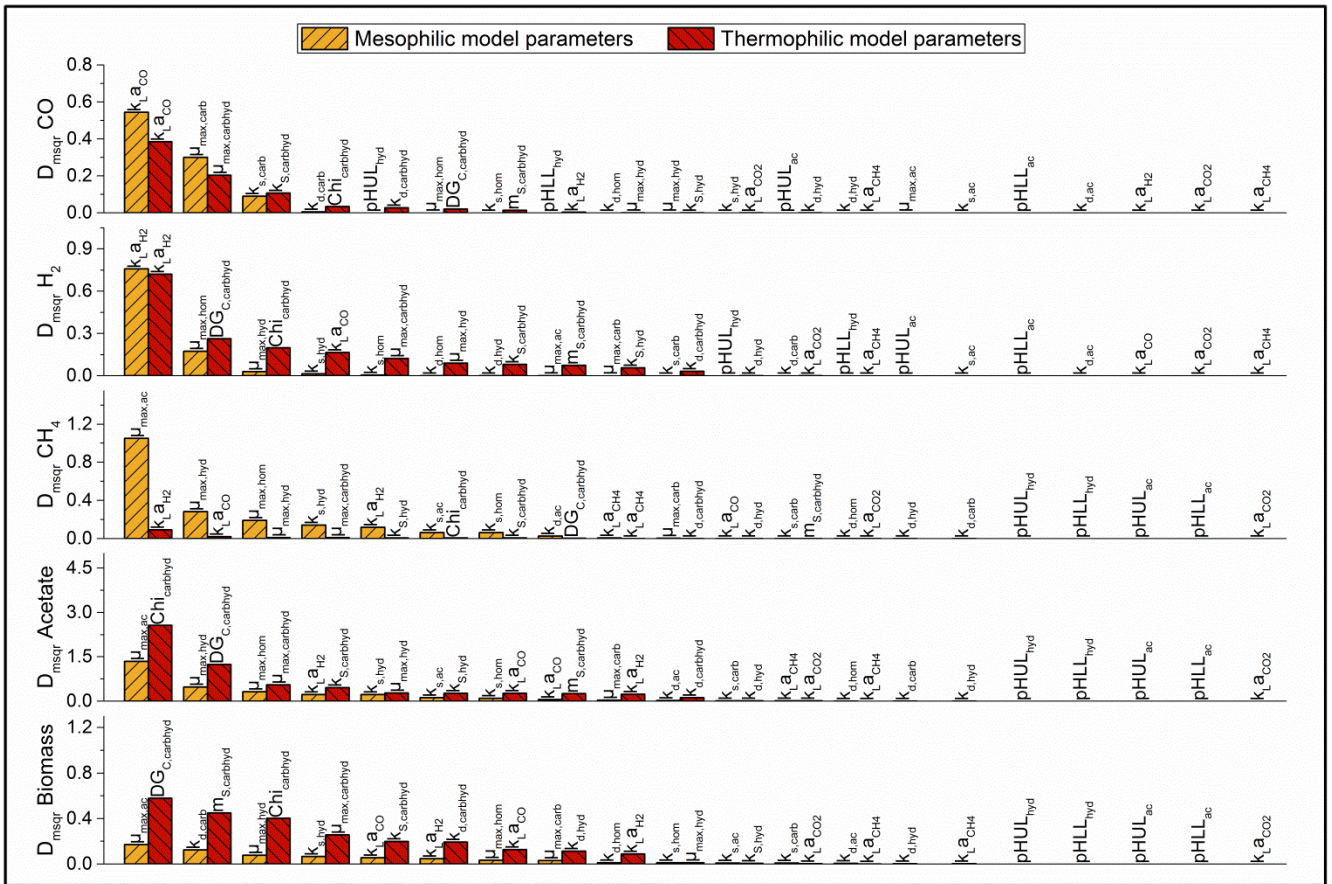


Figure 5.1. Parameter significance ranking based on the sensitivity measure ∂_j^{msqr} for the model outputs used for parameter estimation in both mesophilic and thermophilic syngas biometanation model.

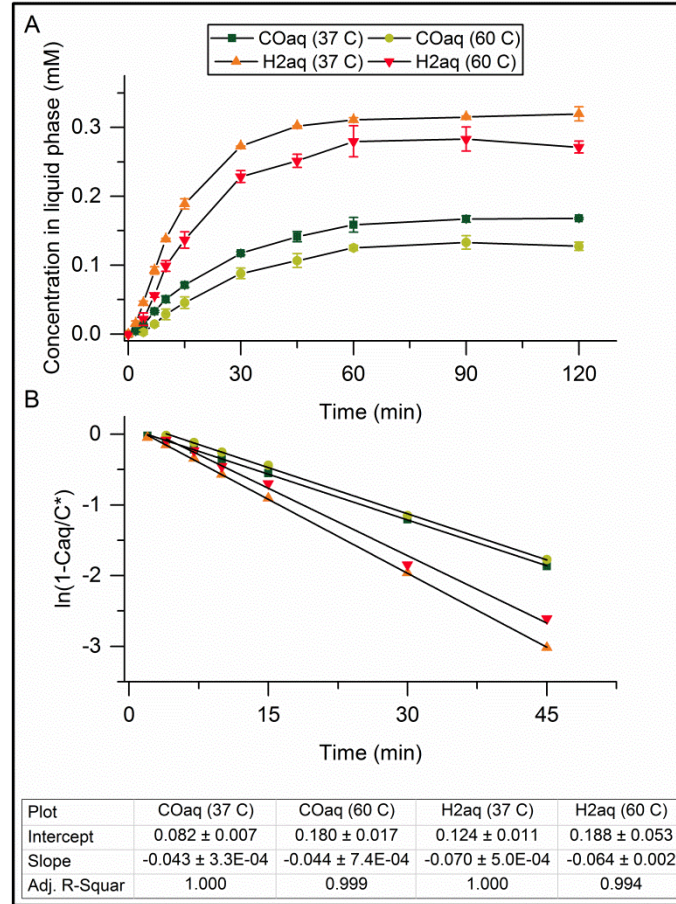


Figure 5.2. **A** Concentration of H₂ and CO in the liquid phase over time at mesophilic and thermophilic conditions. **B** Linearized plot ($\ln(1-C_{aq}/C^*) = -k_{La}t$) for determination of k_{LaCO} and k_{LaH_2} at mesophilic and thermophilic conditions. C_{aq} and C^* correspond to the actual concentration and the saturated concentration of gas in the liquid, and the slope of the linear fit corresponds to $-k_{La}$ for each gas in min^{-1} .

Table 5.1. Value of estimated parameters for the mesophilic and thermophilic MMC along with their standard deviation (SD), 95% confidence intervals (CI 95) and correlation matrix. Values for $\mu_{\max, \text{hom}}$, $k_{s, \text{carb_hyd}}$ and $\chi_{\text{carb_hyd}}$ were fixed manually prior to the least squares parameter estimation.

Parameters	Estimated parameters	SD	Lower CI 95	Upper CI 95	Correlation matrix			
Mesophilic microbial consortium								
$\mu_{\max, \text{carb}} (\text{d}^{-1})$	3.910	0.001	3.908	3.911	1.000			
$\mu_{\max, \text{hyd}} (\text{d}^{-1})$	5.026	0.029	4.969	5.083	-0.024	1.000		
$\mu_{\max, \text{ac}} (\text{d}^{-1})$	0.667	0.001	0.665	0.669	-0.031	-0.265	1.000	
$\mu_{\max, \text{hom}} (\text{d}^{-1})$	8.140							
Thermophilic microbial consortium								
$\mu_{\max, \text{carb_hyd}} (\text{d}^{-1})$	10.927	0.050	10.828	11.025	1.000			
$\mu_{\max, \text{hyd}} (\text{d}^{-1})$	11.106	0.009	11.089	11.124	0.373	1.000		
$\Delta G_{C, \text{carb_hyd}} (\text{kJ/mol H}_2)$	8.288	0.039	8.211	8.365	-0.283	0.088	1.000	
$a_{\text{carb_hyd}}$	2.390	0.001	2.388	2.392	0.116	-0.079	-0.027	1.000
$\chi_{\text{carb_hyd}}$	2							
$k_{s, \text{carb_hyd}} (\text{M})$	1.45e-4							

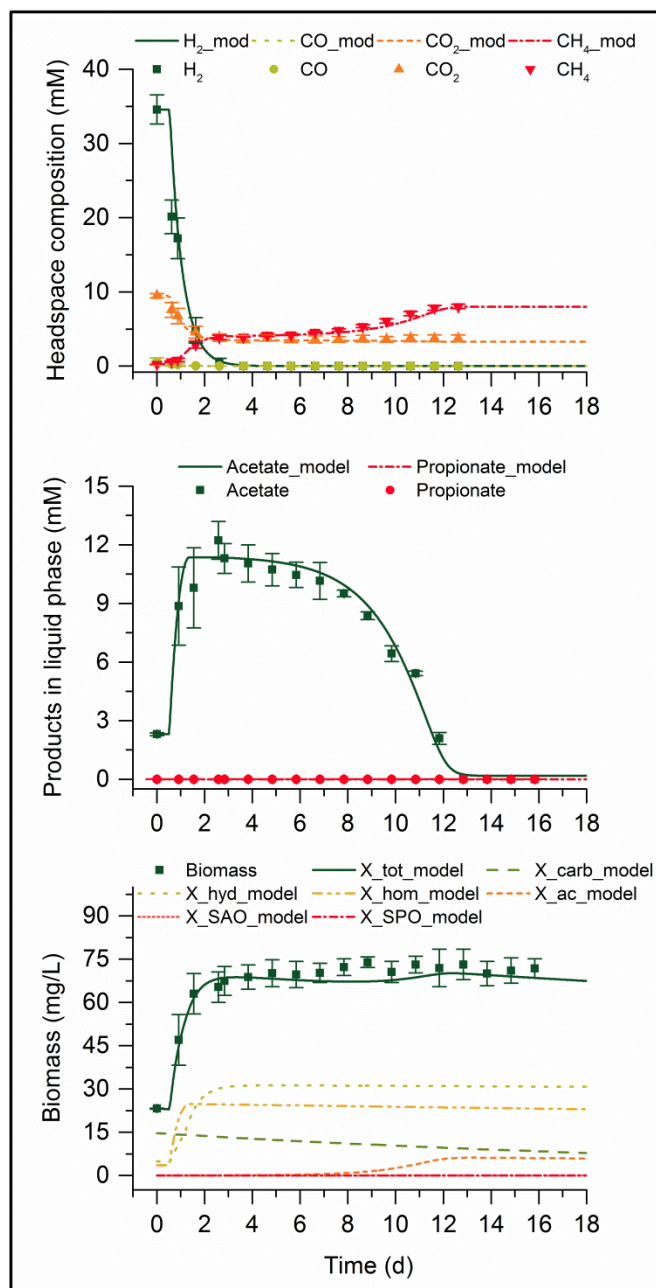


Figure 5.3. Model fitting to experiment at mesophilic conditions with initial P_{H_2} and P_{CO_2} of 0.8 atm and 0.2 atm, respectively.

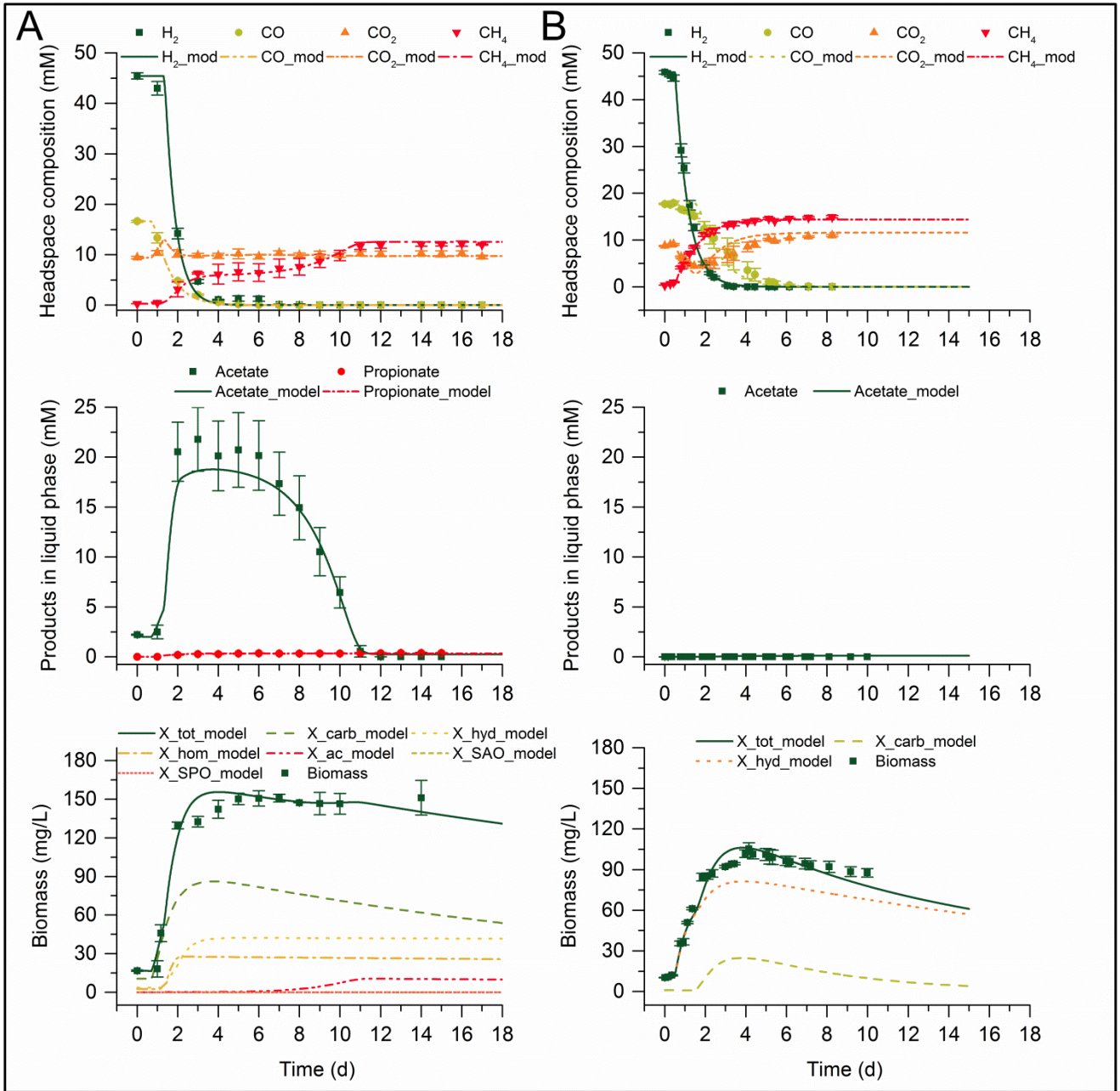


Figure 5.4. **A** Model fitting to experiment at mesophilic conditions with P_{H_2} , P_{CO} and P_{CO_2} of 1.0 atm, 0.4 atm and 0.2 atm, respectively. **B** Model fitting to experiment at thermophilic conditions with P_{H_2} , P_{CO} and P_{CO_2} of 1.0 atm, 0.4 atm and 0.2 atm, respectively.

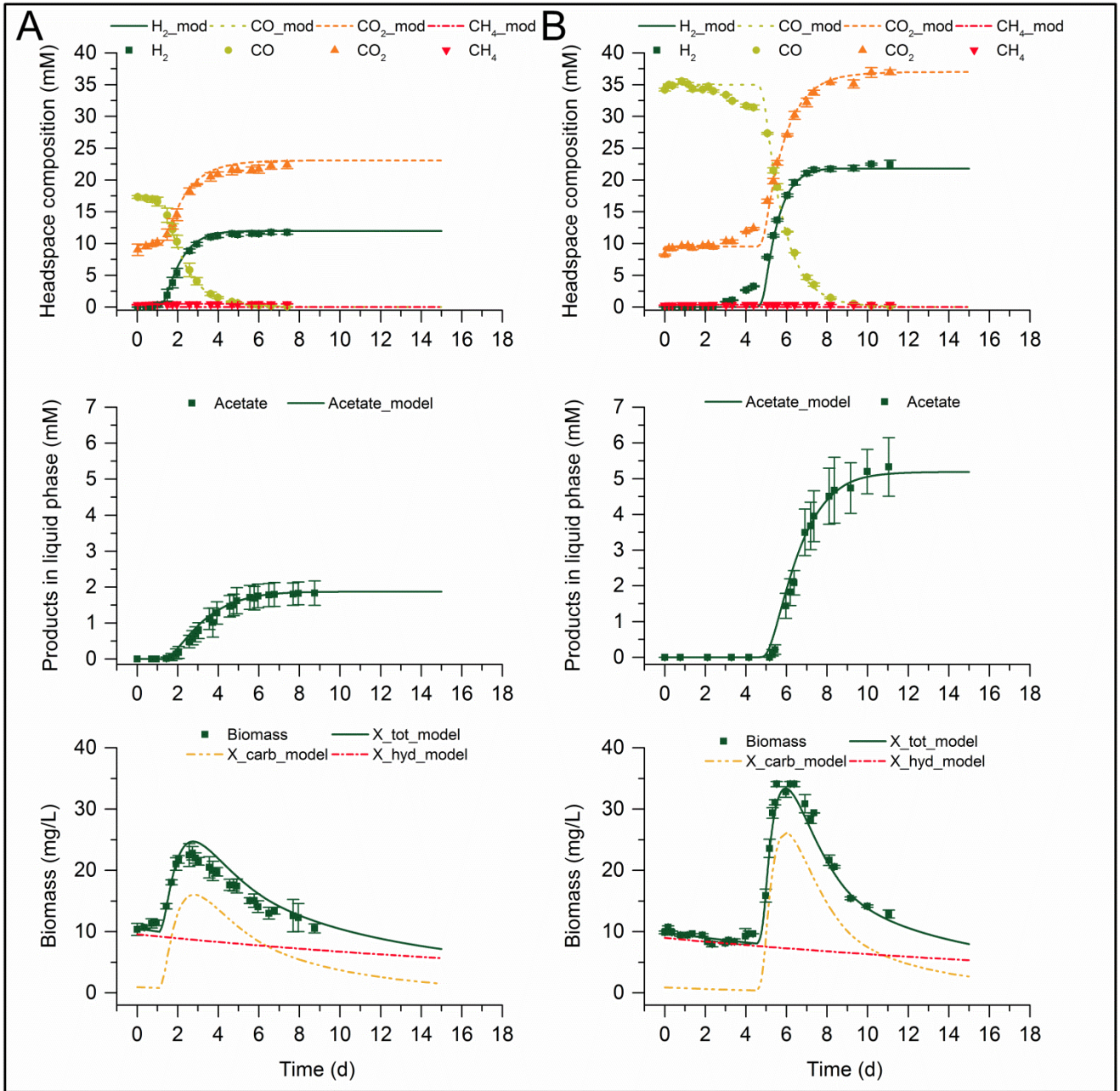


Figure 5.5. **A** Model fitting to experiment with initial P_{CO} of 0.4 atm and BES addition at thermophilic conditions. **B** Model fitting to experiment with initial P_{CO} of 0.8 atm and BES addition at thermophilic conditions.

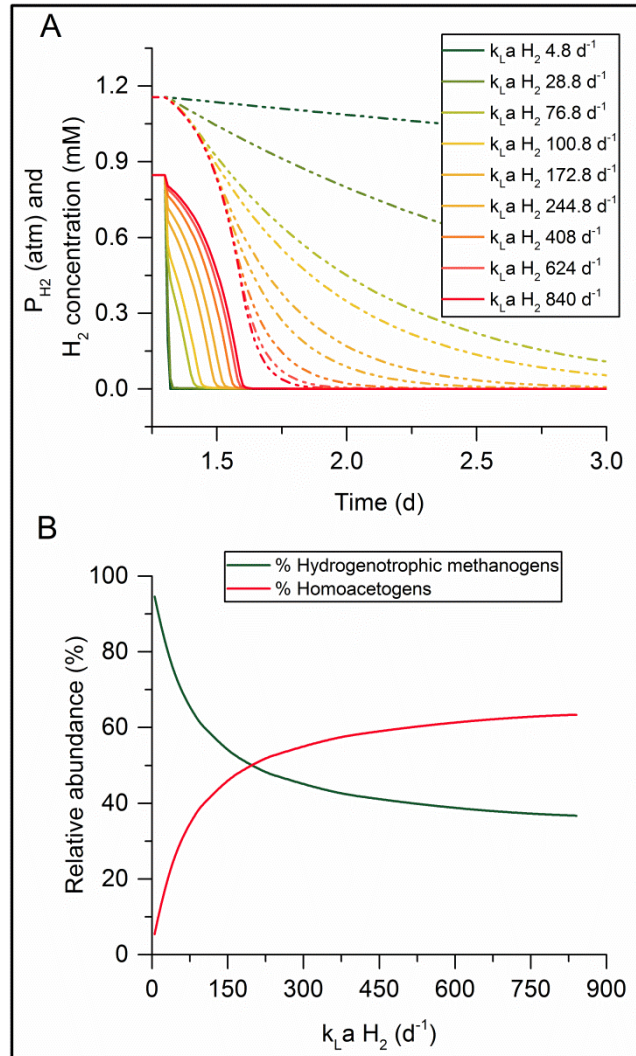


Figure 5.6. A Simulation of the conversion of H_2 over time by homoacetogens and hydrogenotrophic methanogens using different k_{LAH_2} values. Dashed lines represent the P_{H_2} of the headspace and solid lines represent the concentration of H_2 in the liquid phase. **B** Relative abundance of hydrogenotrophic methanogens and homoacetogens at the end of the fermentation plotted as a function of k_{LAH_2} .

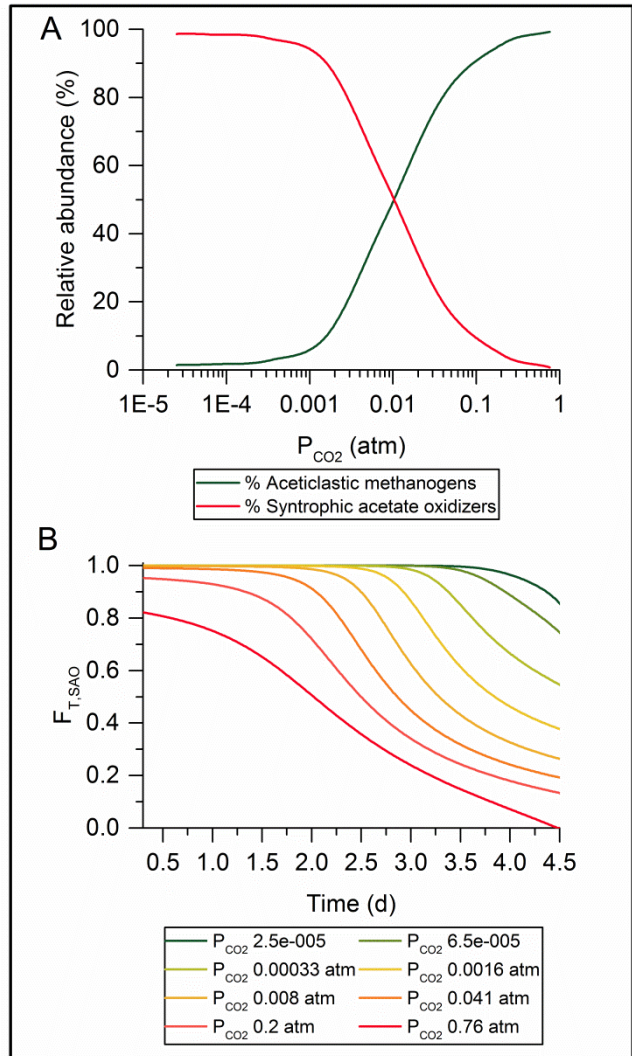


Figure 5.7. A Relative abundance of aceticlastic methanogens and syntrophic acetate oxidizers as a function of P_{CO_2} in both fermentation using acetate as the only substrate. **B** Simulation of the evolution of the thermodynamic potential factor for syntrophic acetate oxidation ($F_{T,SAO}$) during the course of acetate fermentations using different fixed P_{CO_2} .

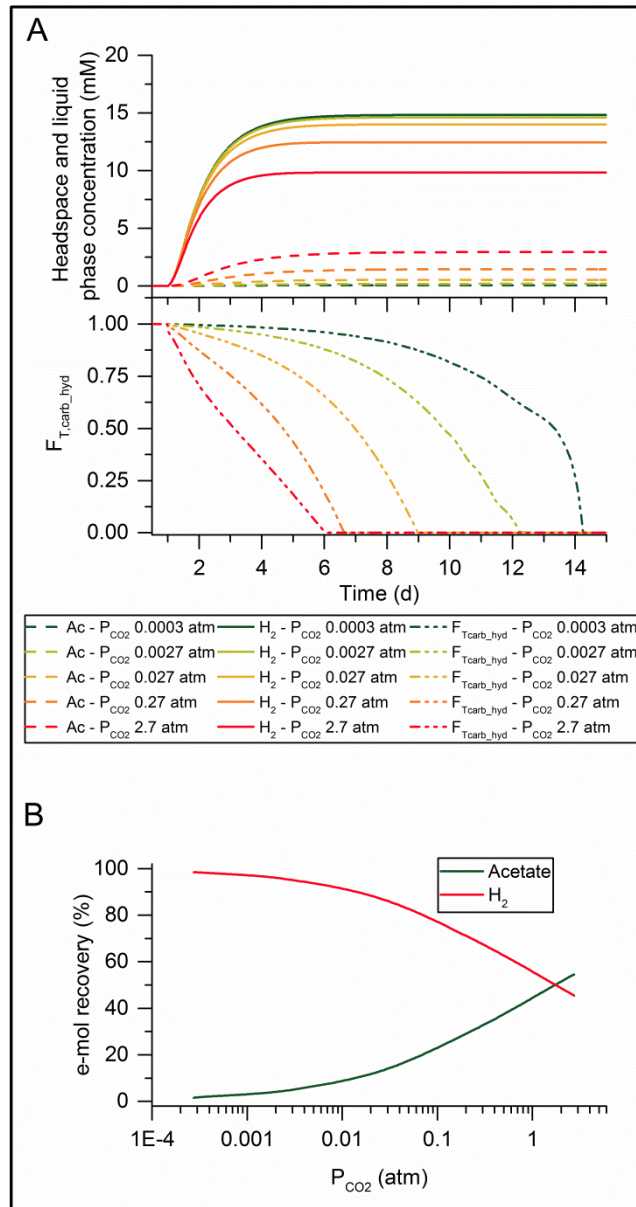


Figure 5.8. A Simulation of H₂ and acetate concentration profiles and evolution of the thermodynamic potential factor for carboxydrotrophic hydrogenogenesis ($F_{T,carb_hyd}$) during the fermentation of CO with BES addition using different fixed P_{CO_2} . **B** Percentage of e-mols recovered as H₂ and acetate as a function of P_{CO_2} when fermenting CO with addition of BES to inhibit methanogenic archaea.

Chapter VI – Cryopreservation of Mixed Microbial Communities

6.1. Purpose

In this last chapter, the effect of several cryopreservation agents (CPA) on the long-term frozen storage of microbial communities is evaluated with the purpose of improving the reliability of commonly employed cryopreservation methods, either using glycerol as CPA or with no CPA addition. The effectiveness of the cryopreservation was evaluated based on the recovery of the microbial community structure and functionality upon revival.

6.2. Hypothesis

- ❖ Cryopreservation methods based on cryoprotectants, alternative to those commonly used like glycerol and no addition of cryoprotectant, may allow for more reliable long-term preservation of the microbial community structure and its functional redundancy.

6.3. Specific objectives

- ❖ To investigate the effect of several cryopreservation agents on the long-term cryopreservation of the microbial community structure and functionality based on microbial composition and microbial activity recovery.

6.4. Related manuscript

- V. A. Grimalt-Aleman, M. Łężyk, K. Asimakopoulos, I. V. Skiadas, and H. N. Gavala. Cryopreservation and fast recovery of enriched syngas-converting microbial communities. (Submitted).

6.5. Experimental procedures

The long-term cryopreservation of microbial communities was carried out using an enriched syngas-converting microbial community as case study. The microbial community was enriched for over 70 days in a stirred tank reactor (STR) operated in continuous mode using syngas as the only carbon and energy source. The enrichment started in batch mode with a pH of 5. Once the batch fermentation finished, the process

started to be operated in continuous mode with a pH of 4.5 and either a hydraulic retention time (HRT) of 5.1 days and syngas inflow of 10 ml/min or with a HRT of 2.4 days and 25 ml/min. At day 78, the enriched microbial community was used as inoculum (1% v/v) for a batch fermentation test in 330 ml fermentation flasks, and at the same time, it was stored at -80°C after equilibration in several CPA solutions. All fermentations were incubated at 37°C using syngas as the only carbon and energy source at an initial pH of 5.7±0.1. The microbial activity and composition of the community after the batch fermentation would then serve as reference for the reactivated microbial communities after 7 months of frozen storage.

The enriched microbial community was fast frozen with liquid nitrogen and kept at -80°C after equilibration with several CPAs, namely glycerol, dimethylsulfoxide (DMSO), polyvinylpyrrolidone (PVP), Tween 80 and yeast extract, and also without CPA addition. All microbial community samples were kept in 10 ml anaerobic serum vials with a CPA solution volume of 2 ml, and were inoculated with 5 ml of actively growing culture with a cell density of $1.23 \cdot 10^8 \pm 0.22 \cdot 10^8$ cells/ml measured with a hemocytometer. All frozen microbial communities were reactivated after 7 months of storage by inoculating them into triplicate fermentation flasks with an inoculum size of 1.4% v/v. The volumetric productivity and maximum products yield of each reactivated microbial community was then compared to that of the reference experiment. Samples for microbial community analysis through 16S rRNA gene amplicon sequencing were taken at the end of all fermentations performed. The microbial composition of the reactivated microbial communities was also compared to the reference microbial community.

6.6. Summary of results

The reference batch fermentation inoculated with fresh inoculum from the bioreactor presented some differences in the product distribution compared to that of the bioreactor. These differences can be easily explained though from the change in operating conditions, as (i) the pH was increased from 4.5 to 5.7 in order to prevent a possible acid crash during the batch fermentation, and (ii) the operating mode changed from continuous to batch. As a result, acetate and ethanol were not the only products of the batch fermentation, since these were partially converted into butyrate and butanol. The maximum yield of each product during the fermentation corresponded to 60.0±7.6% for acetate (88 h), 38.0±6.8% for ethanol (111 h), 22.5±5.8% for butyrate (126 h) and 12.2±2.1% for butanol (126 h) in e-mol basis (fig. 6.1). The microbial community structure of the reference batch fermentation also presented some differences when compared to that of the bioreactor, although the community was still dominated by *Clostridiaceae* spp. and *Enterobacteriaceae* spp. (fig. 6.2). Family *Clostridiaceae* presented the biggest differences since instead of being dominated by a single species, closely related to *C. ljungdahlii*, the microbial community of the reference batch fermentation presented a more even structure, with this being composed by a species closely related to *C. ljungdahlii* (100% sequence similarity) and two *Clostridium* spp. with closest but low similarity

to *C. carboxidivorans* (53% sequence similarity) and *C. nitrophenolicum* (48% sequence similarity) (fig. 6.2). This rapid shift in the composition of the family *Clostridiaceae* was also proof of the high functional redundancy of the microbial community, despite its reduction in complexity along the enrichment, since it quickly adapted to the change in operating conditions with rearrangements in its community structure at species level. The reactivated microbial communities were also expected to undergo the same changes in metabolic activity and microbial composition.

The ability of the microbial community to convert syngas in to produce acetate and ethanol from syngas was successfully preserved using all CPAs. However, all of them presented differences. When DMSO, PVP, Tween 80, yeast extract and no CPA were used, the maximum yield of acetate and ethanol oscillated between 77.3-99.5% and 87.9-96.6% of the maximum yield obtained in reference experiments, respectively (fig. 6.1). When glycerol was used as CPA, more important differences were found in the maximum yield of acetate and ethanol, corresponding to 59.9% and 18.1% of that of the reference experiment, respectively. The biggest differences though were observed in the rest of the products as, when considering all CPAs but glycerol, the best activity recovery corresponded to 23.0% and 30.9% for butyrate and butanol, respectively, obtained using PVP as CPA. Notable differences were found when no CPA was added and when glycerol was used. Not adding CPA resulted in negligible production of butyrate and butanol, while when glycerol was used as CPA, syngas and glycerol were co-metabolized resulting in a very different product distribution, with 1,3-propanediol being the second major product of the fermentation. Based on the Euclidean distance of the maximum product yields to the reference fermentation ($D_{Y,ref}$), PVP was the most effective CPA. However, the difference between the $D_{Y,ref}$ of PVP, and Tween 80 and yeast extract was found to be not statistically significant.

All reactivated microbial communities presented a similar community structure at family level, despite a few differences in the relative abundance of *Clostridiaceae* spp., *Enterobacteriaceae* spp. and *Enterococcaceae* spp. (fig. 6.2). This suggested that all CPAs preserved appropriately the most abundant species of the microbial communities. However, a more detailed analysis of the family *Clostridiaceae* revealed considerable differences in the preservation of the dominant species depending on the CPA used. The most notable differences were found when glycerol and no CPA were used. When no CPA was used, the percentage of reads mapping to the *Clostridium* sp. with closest similarity to *C. carboxidivorans* corresponded to 3.7%, 0.006% and 0.002% in the triplicates compared to 34.4-48.4% in the reference microbial community (fig. 6.2), which could explain the negligible butyrate- and butanol-producing activity of this reactivated microbial community. In turn, using glycerol as CPA was found to be ineffective preserving the *Clostridium* sp. with closest similarity to *C. nitrophenolicum*, since reads mapping to this OTU corresponded to 0.07-0.20% compared to 10.7-17.6% in the reference microbial community (fig. 6.2). Using DMSO and yeast extract as CPA resulted in the successful preservation of the three dominant

Clostridium spp., although a high variability in the relative abundance of reads mapping to these species was observed across triplicates. Overall, PVP and Tween 80 were the only CPAs able to reproduce the relative abundance of reads mapping to the three dominant species with small variations across triplicates and also compared to the reference microbial community (fig. 6.2). This was confirmed by the PCoA analysis based on Unifrac distances between samples, which showed that the microbial communities preserved with PVP and especially with Tween 80 presented the shortest distances to the reference microbial community (fig. 6.3).

6.7. Conclusions

Fast activity recovery and maintenance of the microbial community diversity and functionality are indispensable requirements for cryopreservation methods for microbial communities, as these characteristics may allow for minimizing the start-up time and maintaining the resiliency of microbial communities in mixed-culture-based bioprocesses after an eventual process shutdown. This work showed that overall more effective cryopreservation methods than those commonly used, such as using glycerol as CPA or not adding CPA, are possible. In this case, using glycerol and not adding CPA during the cryopreservation of microbial communities were found to be the least recommendable methods. DMSO, which is also commonly used to a lesser extent, was found to be more effective than the latter. However, PVP and Tween 80 were the CPAs offering the best reproducibility in terms of fast activity recovery and preservation of the microbial community structure after long-term storage. None of these methods was optimized though, for which future efforts should focus on optimizing these methods for preservation of minority microbial groups in microbial communities, as well as on studying the effectiveness of other CPAs known to be effective for axenic cultures.

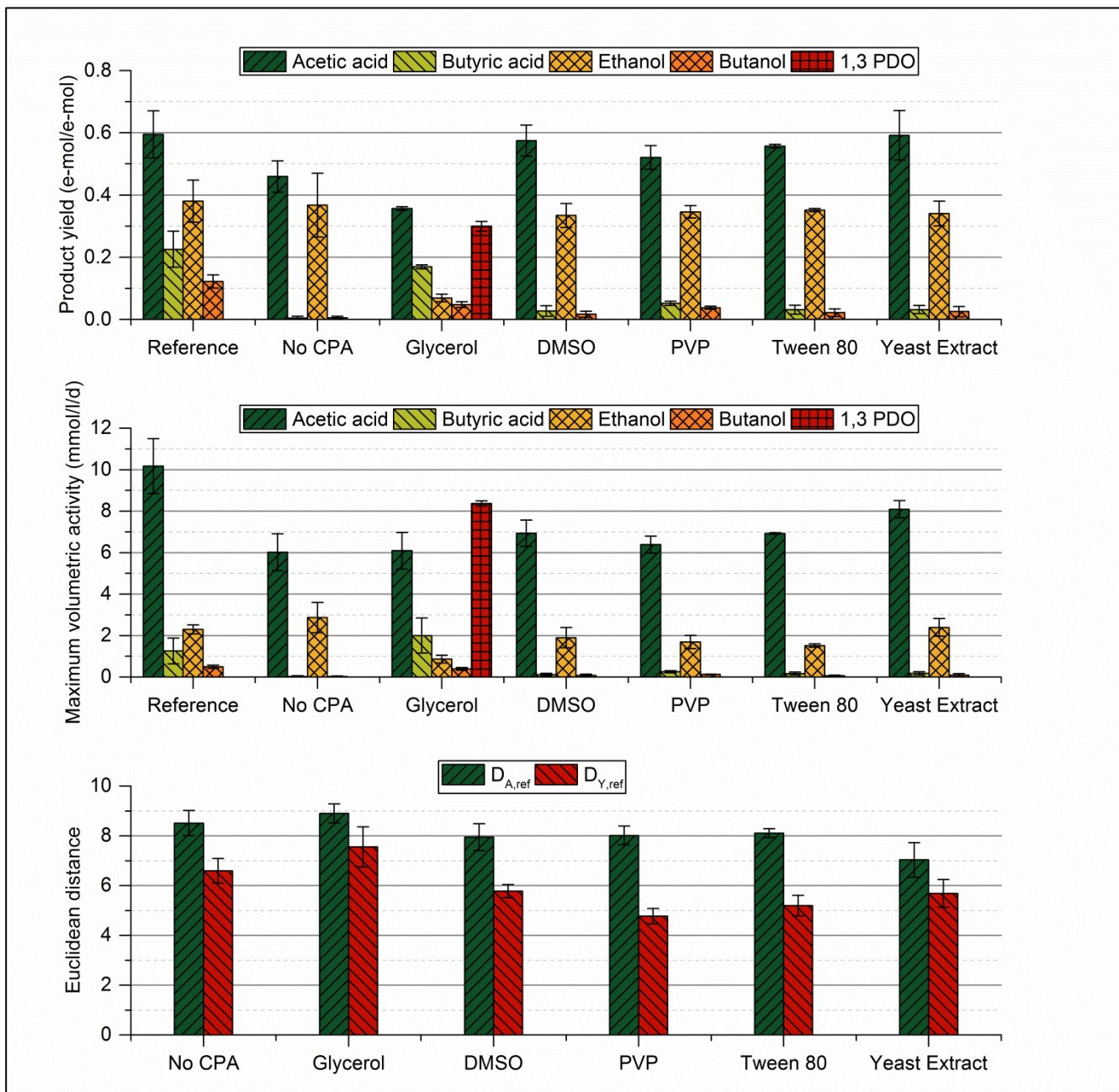


Figure 6.1. Maximum apparent product yield and maximum volumetric productivity of each product for reference experiments (fresh microbial community) and reactivated microbial communities after long-term frozen storage using different CPAs, and Euclidean distance to the reference for each CPA based on the maximum product yields ($D_{Y,ref}$) and maximum productivities ($D_{A,ref}$). Note that the maximum product yields do not correspond to the final product yields, but to the yield in the time points where the maximum concentration of each product was observed. The maximum product yields were corrected for the production from control experiments.

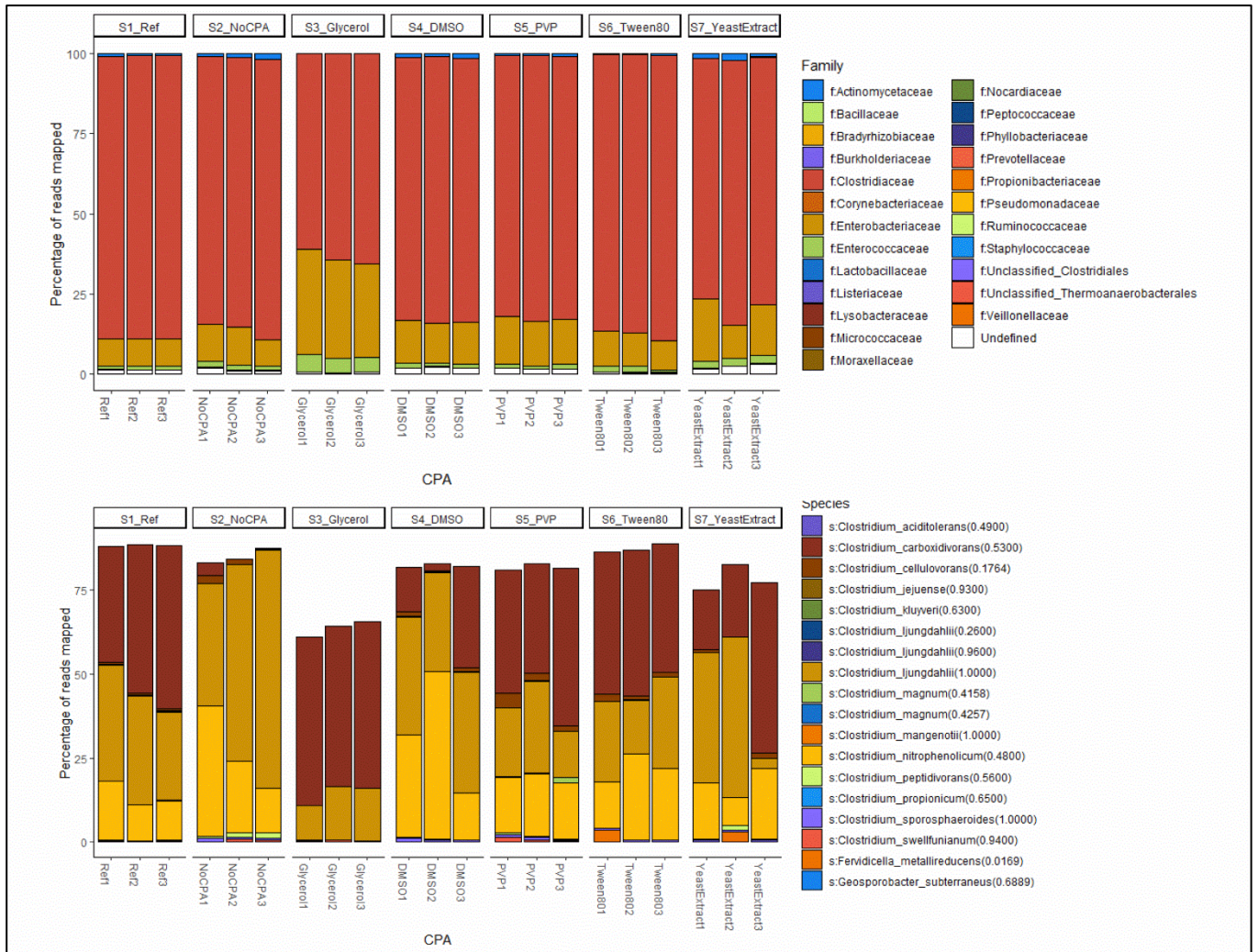


Figure 6.2. **A** Relative abundance of reads mapped to OTUs at family taxonomic level in reference microbial community and reactivated microbial communities after long-term frozen storage using different CPAs. **B** Relative abundance of reads mapping to *Clostridiaceae* spp. in reference microbial community and reactivated microbial communities after long-term frozen storage using different CPAs. The sequence similarity index (from 0 to 1) is given in brackets. Note that the taxonomic assignment to OTUs at species level correspond to the closest species based on the 16S rRNA sequence similarity, independently of the sequence similarity index.

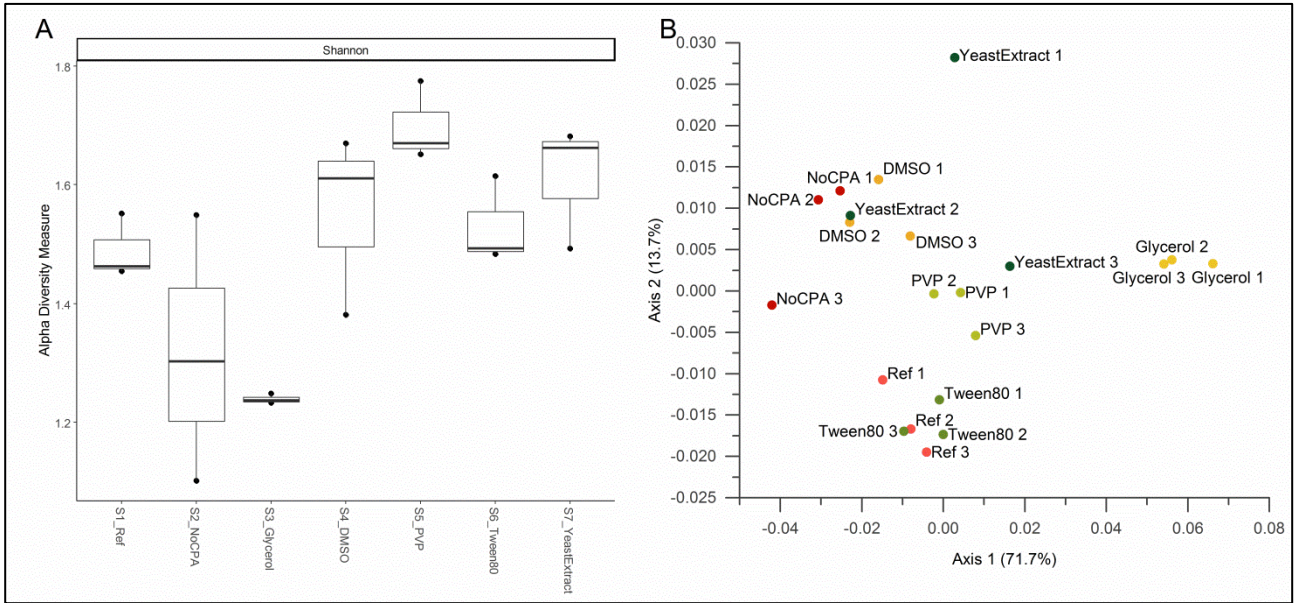


Figure 6.3. **A** Alpha diversity measure based on the Shannon diversity index for the reference microbial community and all reactivated microbial communities after cryopreservation using different CPAs. **B** Principal Coordinate Analysis (PCoA) on Unifrac distances between samples from the reference microbial community and all reactivated microbial communities. The percentage of variability explained in the ordination of samples by each axis is given in the axis label.

Chapter VII – Overall conclusions and future perspectives

Microbial diversity and functional redundancy constitute the main assets of microbial communities, as these features provide them with high resilience when facing process disturbances, and consequently allow for long-term process stability. Microbial communities are currently exploited for several purposes, including the simultaneous waste treatment, nutrients recovery and even bioenergy production. However, their use in biotechnological applications aiming at the production of commodity chemicals, biomaterials and biofuels is still challenging due to the limited control achieved so far over their metabolic activity. The main goal of this study was therefore to evaluate the potential of different microbial community management tools for improving the control over the microbial composition of microbial communities, their microbial interactions and their overall metabolic activity when targeting specific products. In this case, all methods were implemented in syngas-converting microbial communities and targeted the production of CH₄ and ethanol. The long-term cryopreservation of microbial communities was also studied to evaluate the effectiveness of different methods typically employed for axenic cultures.

The findings of this study suggest that a combination of all tools evaluated here is necessary to achieve some degree of control over the metabolic activity of microbial communities. Microbial enrichments seem to be an indispensable tool for driving the natural selection of microbial trophic groups conducting specific bioconversions. As shown in this study, all enrichments presented a strong impact on the metabolic activity and the microbial composition of the microbial community, which varied depending on the enrichment conditions applied. For example, the enrichment of acetogenic microbial communities in sequential batch mode resulted in an increase of the ethanol yield from nearly 8.16±0.49% to 59.15±0.18% of the theoretical maximum when decreasing the initial pH from 6 to 5. However, this method requires considerable experimental work for assessing the effect of different operational parameters on the activity of the microbial community prior to its implementation in the lab-scale production process, given that it is not possible to predict the specific outcome of the microbial selection beforehand without prior knowledge. The enrichments of methanogenic microbial communities at different temperatures carried out in this study are an example of this, as these resulted in enriched microbial communities with drastic differences in their community structure and activity rates, which could not be predicted without prior experimentation. Additionally, microbial enrichments were found to be very effective directing the selection of microbial trophic groups consuming the primary substrate based on mutual exclusion interactions, but were less effective controlling cross-feeding interactions developed afterwards, as e.g. it was not possible to wash-out species performing the chain elongation from the acetogenic microbial communities in sequential batch enrichments. This could be partially amended though by using thermodynamic principles to analyze the

thermodynamic feasibility of certain metabolic activities of interest beforehand and eventually, to design operational strategies promoting or demoting specific metabolic activities in the microbial community.

The thermodynamic potential factor (F_T) was found to be an interesting tool for identifying biochemical reactions potentially subject to thermodynamic control, and boosting their activity rates through the selection of appropriate operational parameters. This was shown e.g. in acetogenic microbial communities producing ethanol through the reduction of acetate, where an ethanol yield of 72.44% of the maximum theoretical was achieved; and in methanogenic microbial communities by controlling the syntrophic interaction between syntrophic acetate oxidizers and hydrogenotrophic methanogens through the P_{CO_2} , which resulted in 0.4% of e-mols diverted to by-products. This method could have some interesting applications in other anaerobic fermentation processes as well, since the metabolic network of anaerobic microbial communities often presents several reactions taking place intrinsically at the edge of their thermodynamic feasibility. However, one of the limitations of this method is that thermodynamic control only applies to certain reactions (operating close to thermodynamic equilibrium), and that it needs to be combined with kinetic considerations in order to allow a more complete interpretation of the overall behavior of microbial communities. Further work on improving the accuracy of the thermodynamic feasibility predictions through better estimation of the parameters of F_T , e.g. the free energy conservation requirements, is also needed.

Dynamic modeling tools combining kinetic and thermodynamic control of the rates were found to have a high potential for designing operational strategies targeting the expression of specific physiological traits in the microbial community, as these allowed e.g. accounting for the changing conditions and cumulative effects of batch fermentation processes. This was shown through the models of syngas biomethanation process developed in this thesis. Some examples of this kinetic and thermodynamic control were the successful simulation of the combined kinetic and thermodynamic competition for H_2/CO_2 between homoacetogens and hydrogenotrophic methanogens, and the prediction of the total acetate produced as by-product of the carboxydrotrophic hydrogenogenesis, which was modelled strictly based on the thermodynamic constraints of the hydrogenogenesis. This allowed identifying several opportunities for catabolic route control, which could target a higher selectivity towards CH_4 in continuous processes through e.g. bioaugmentation strategies or in-situ biogas bio-upgrading with simultaneous reduction of by-product formation.

The “grey box” models developed here allowed for the successful simulation of the syngas biomethanation process by considering the stepwise conversion of syngas into CH_4 involving several microbial trophic groups and their corresponding cross-feeding, mutualistic and competitive interactions. Nevertheless, this model structure would not be applicable to all processes driven by microbial communities, as there are cases where the regulation of the intracellular metabolism plays a more important role than the specific microbial composition. The enriched acetogenic microbial communities developed in this study are a good example of

this, since it was found that their solventogenic metabolism was regulated by the operational parameters rather than by their interspecies metabolism. In this case, a model structure accounting for the regulation of intracellular processes would therefore be at least as important as accounting for possible microbial interactions. A few models have already been developed for modeling the anaerobic fermentation of glucose by microbial communities following a similar approach. However, in these models, changes in the product distribution as a function of operational parameters are considered to be dictated solely by intracellular processes, while the interspecies metabolism of the microbial community is neglected. Further research on modelling approaches merging these two types of models is still needed.

Finally, the study of the long-term preservation of microbial communities showed that some of the methods investigated were considerably better than the most commonly used cryopreservation methods, like using glycerol as CPA or not adding CPA at all. The use of PVP and Tween 80 as CPA were found to be the most reliable in terms of microbial activity recovery and preservation of the microbial community structure among the CPAs tested. However, all microbial communities presented some degree of activity loss upon reactivation regardless the CPA used, especially in butyrate- and butanol-producing activity, when compared to the reference microbial community. Further work on the optimization of the methods investigated here may address some of the limitations found. Further studying other potential cryopreservation methods for the long-term storage of microbial communities is also recommended.

References

- [1] UNFCCC. Conference of the Parties (COP). Adoption of the Paris agreement. 2015. <https://unfccc.int/process-and-meetings/the-paris-agreement/the-paris-agreement> (accessed August 4, 2019).
- [2] UN General Assembly. Transforming our world: the 2030 Agenda for Sustainable Development. 21 October 2015, A/RES/70/1.
- [3] Cléménçon R. The Two Sides of the Paris Climate Agreement: Dismal Failure or Historic Breakthrough? *J Environ Dev* 2016;25:3–24. doi:10.1177/1070496516631362.
- [4] Ritchie H, Roser M. CO₂ and other Greenhouse Gas Emissions. Published online at OurWorldInData.org, 2019. <https://ourworldindata.org/co2-and-other-greenhouse-gas-emissions> (accessed August 4, 2019).
- [5] Du Pisani JA. Sustainable development – historical roots of the concept. *Environ Sci* 2006;3:83–96. doi:10.1080/15693430600688831.
- [6] Ghosh P, Westhoff P, Debnath D. Biofuels, food security, and sustainability. *Biofuels, Bioenergy Food Secur.*, Elsevier Inc.; 2019, p. 211–29. doi:10.1016/b978-0-12-803954-0.00012-7.
- [7] Hertel TW, Tyner WE, Birur DK. The Global Impacts of Biofuel Mandates. *Energy J* 2010;31:75–100. doi:10.5547/ISSN0195-6574-EJ-Vol31-No1-4.
- [8] HLPE. Biofuels and food security. A report by the High Level Panel of Experts on Food Security and Nutrition of the Committee on World Food Security. Rome: 2013. doi:10.1111/j.1467-9353.2008.00425.x.
- [9] Pacini H, Sanches-Pereira A, Durleva M, Malick K, Bhutani A. The state of the biofuels market: regulatory, trade and development perspectives. 2014.
- [10] Charles C, Gerasimchuk I, Bridle R, Moerenhout T, Asmelash E, Laan T. Biofuels - At what cost? A review of costs and benefits of EU biofuel policies. International Institute for Sustainable Development. 2013.
- [11] Naylor RL, Liska A, Burke MB, Falcon WP, Gaskell JC, Rozelle SD, et al. The Ripple Effect: Biofuels, Food Security, and the Environment. *Environ Sci Policy Sustain Dev* 2007;49:30–43. doi:10.3200/ENVT.49.9.30-43.
- [12] Eurostat. Energy statistics - main indicators. Final energy consumption in road transport by type of fuel 2019. <https://ec.europa.eu/eurostat/data/database> (accessed August 5, 2019).
- [13] EUROBSERV'ER. Biofuels barometer. 2018.
- [14] Havlík P, Schneider U a., Schmid E, Böttcher H, Fritz S, Skalský R, et al. Global land-use implications of first and second generation biofuel targets. *Energy Policy* 2011;39:5690–702. doi:10.1016/j.enpol.2010.03.030.
- [15] Robak K, Balcerek M. Review of second generation bioethanol production from residual biomass. *Food Technol Biotechnol* 2018;56:174–87. doi:10.17113/ftb.56.02.18.5428.
- [16] Redl S, Diender M, Ølshøj T, Sousa DZ, Toftgaard A. Exploiting the potential of gas fermentation. *Ind Crop Prod* 2017;106:21–30. doi:10.1016/j.indcrop.2016.11.015.

- [17] Tomaszewska M, Białończyk L. Ethanol production from whey in a bioreactor coupled with direct contact membrane distillation. *Catal Today* 2016;268:156–63. doi:10.1016/j.cattod.2016.01.059.
- [18] Garlapati VK, Shankar U, Budhiraja A. Bioconversion technologies of crude glycerol to value added industrial products. *Biotechnol Reports* 2016;9:9–14. doi:10.1016/j.btre.2015.11.002.
- [19] Farmanbordar S, Karimi K, Amiri H. Municipal solid waste as a suitable substrate for butanol production as an advanced biofuel. *Energy Convers Manag* 2018;157:396–408. doi:10.1016/j.enconman.2017.12.020.
- [20] Neshat SA, Mohammadi M, Najafpour GD, Lahijani P. Anaerobic co-digestion of animal manures and lignocellulosic residues as a potent approach for sustainable biogas production. *Renew Sustain Energy Rev* 2017;79:308–22. doi:10.1016/j.rser.2017.05.137.
- [21] Lymperatou A, Gavala HN, Skiadas I V. Optimization of Aqueous Ammonia Soaking of manure fibers by Response Surface Methodology for unlocking the methane potential of swine manure. *Bioresour Technol* 2017;244:509–16. doi:10.1016/j.biortech.2017.07.147.
- [22] European Technology and Innovation Platform. Cellulosic Ethanol. http://www.etipbioenergy.eu/index.php?option=com_content&view=article&id=273 (accessed August 6, 2019).
- [23] Anwar Z, Gulfranz M, Irshad M. Agro-industrial lignocellulosic biomass a key to unlock the future bio-energy: A brief review. *J Radiat Res Appl Sci* 2014;7:163–73. doi:10.1016/j.jrras.2014.02.003.
- [24] García-Aparicio MP, Ballesteros I, González A, Oliva JM, Ballesteros M, Negro MJ. Effect of Inhibitors Released During Steam-Explosion Pretreatment of Barley Straw on Enzymatic Hydrolysis. *Appl Biochem Biotechnol* 2006;129:278–88.
- [25] Hendriks ATWM, Zeeman G. Pretreatments to enhance the digestibility of lignocellulosic biomass. *Bioresour Technol* 2009;100:10–8. doi:10.1016/j.biortech.2008.05.027.
- [26] Naik SN, Goud V V., Rout PK, Dalai AK. Production of first and second generation biofuels: A comprehensive review. *Renew Sustain Energy Rev* 2010;14:578–97. doi:10.1016/j.rser.2009.10.003.
- [27] Kopyscinski J, Schildhauer TJ, Biollaz SMA. Production of synthetic natural gas (SNG) from coal and dry biomass – A technology review from 1950 to 2009. *Fuel* 2010;89:1763–83. doi:10.1016/j.fuel.2010.01.027.
- [28] European Technology and Innovation Platform. FT-Liquids & Biomass to Liquids (BtL). http://www.etipbioenergy.eu/index.php?option=com_content&view=article&id=277 (accessed August 7, 2019).
- [29] Danish Energy Agency, Energinet. Technology Data for Renewable Fuels. 2017.
- [30] Rönsch S, Schneider J, Matthischke S, Schlüter M, Götz M, Lefebvre J, et al. Review on methanation - From fundamentals to current projects. *Fuel* 2016;166:276–96. doi:10.1016/j.fuel.2015.10.111.
- [31] Li H, Larsson E, Thorin E, Dahlquist E, Yu X. Feasibility study on combining anaerobic digestion and biomass gasification to increase the production of biomethane. *Energy Convers Manag* 2015;100:212–9. doi:10.1016/j.enconman.2015.05.007.
- [32] Grimalt-Alemany A, Skiadas I V., Gavala HN. Syngas biomethanation: State-of-the-art review and perspectives. *Biofuels, Bioprod Biorefining* 2018;12:139–58. doi:10.1002/bbb.1826.
- [33] Brown RC. Hybrid Thermochemical / Biological Processing. Putting the Cart Before the Horse? *Appl*

Biochem Biotechnol 2007;136:947–56.

- [34] LanzaTech. World's First Commercial Waste Gas to Ethanol Plant Starts Up. <https://www.lanzatech.com/2018/06/08/worlds-first-commercial-waste-gas-ethanol-plant-starts/> (accessed August 7, 2019).
- [35] Richter H, Martin ME, Angenent LT. A two-stage continuous fermentation system for conversion of syngas into ethanol. *Energies* 2013;6:3987–4000. doi:10.3390/en6083987.
- [36] Perez JM, Richter H, Loftus SE, Angenent LT. Biocatalytic reduction of short-chain carboxylic acids into their corresponding alcohols with syngas fermentation. *Biotechnol Bioeng* 2013;110. doi:10.1002/bit.24786.
- [37] Devarapalli M, Atiyeh HK, Phillips JR, Lewis RS, Huhnke RL. Ethanol production during semi-continuous syngas fermentation in a trickle bed reactor using *Clostridium ragsdalei*. *Bioresour Technol* 2016;209:56–65. doi:10.1016/j.biortech.2016.02.086.
- [38] Kimura Z ichiro, Kita A, Iwasaki Y, Nakashimada Y, Hoshino T, Murakami K. Glycerol acts as alternative electron sink during syngas fermentation by thermophilic anaerobe *Moorella thermoacetica*. *J Biosci Bioeng* 2016;121:268–73. doi:10.1016/j.jbiosc.2015.07.003.
- [39] Abubackar HN, Fernández-Naveira Á, Veiga MC, Kennes C. Impact of cyclic pH shifts on carbon monoxide fermentation to ethanol by *Clostridium autoethanogenum*. *Fuel* 2016;178:56–62. doi:10.1016/j.fuel.2016.03.048.
- [40] Abubackar HN, Bengelsdorf FR, Dürre P, Veiga MC, Kennes C. Improved operating strategy for continuous fermentation of carbon monoxide to fuel-ethanol by clostridia. *Appl Energy* 2016;169:210–7. doi:http://dx.doi.org/10.1016/j.apenergy.2016.02.021.
- [41] Gao J, Atiyeh HK, Phillips JR, Wilkins MR, Huhnke RL. Development of low cost medium for ethanol production from syngas by *Clostridium ragsdalei*. *Bioresour Technol* 2013;147:508–15. doi:10.1016/j.biortech.2013.08.075.
- [42] Kundiyana DK, Wilkins MR, Maddipati P, Huhnke RL. Effect of temperature, pH and buffer presence on ethanol production from synthesis gas by “*Clostridium ragsdalei*”. *Bioresour Technol* 2011;102:5794–9. doi:10.1016/j.biortech.2011.02.032.
- [43] Abubackar HN, Veiga MC, Kennes C. Biological conversion of carbon monoxide to ethanol: effect of pH, gas pressure, reducing agent and yeast extract. *Bioresour Technol* 2012;114:518–22. doi:10.1016/j.biortech.2012.03.027.
- [44] Panneerselvam A, Wilkins MR, Delorme MJM, Atiyeh HK, Huhnke RL. Effects of Various Reducing Agents on Syngas Fermentation by “*Clostridium ragsdalei*”. *Biol Eng* 2010;2:135–44.
- [45] Babu BK, Atiyeh HK, Wilkins MR, Huhnke RL. Effect of the Reducing Agent Dithiothreitol on Ethanol and Acetic Acid Production by *Clostridium* Strain P11 Using Simulated Biomass-Based Syngas. *Biol Eng* 2010;3:19–35. doi:10.13031/2013.35924.
- [46] Hu P. Thermodynamic, Sulfide, Redox Potential, and pH Effects on Syngas Fermentation. Brigham Young University, 2011.
- [47] Ramió-pujol S, Ganigué R, Bañeras L, Colprim J. Incubation at 25 ° C prevents acid crash and enhances alcohol production in *Clostridium carboxidivorans* P7. *Bioresour Technol* 2015;192:296–303. doi:10.1016/j.biortech.2015.05.077.
- [48] Ko CW, Vega JL, Clausen EC, Gaddy JL. Effects of high pressure on a co-culture for the production

of methane from coal synthesis gas. Chem Eng Comm 1989;77:155–69.

- [49] Ungerman AJ, Heindel TJ. Carbon Monoxide Mass Transfer for Syngas Fermentation in a Stirred Tank Reactor with Dual Impeller Configurations. Biotechnol Prog 2007;23:613–20. doi:10.1021/bp060311z.
- [50] Mohammadi M, Younesi H, Najafpour G, Mohamed AR. Sustainable ethanol fermentation from synthesis gas by *Clostridium ljungdahlii* in a continuous stirred tank bioreactor. J Chem Technol Biotechnol 2012;87:837–43. doi:10.1002/jctb.3712.
- [51] Fernández-Naveira Á, Abubackar HN, Veiga MC, Kennes C. Efficient butanol-ethanol (B-E) production from carbon monoxide fermentation by *Clostridium carboxidivorans*. Appl Microbiol Biotechnol 2016;100:3361–70. doi:10.1007/s00253-015-7238-1.
- [52] Klasson KT, Ackerson MD, Clausen EC, Gaddy JL. Bioconversion of synthesis gas into liquid or gaseous fuels. Enzyme Microb Technol 1992;14:602–8. doi:10.1016/0141-0229(92)90033-K.
- [53] Bredwell MD, Srivastava P, Worden RM. Reactor design issues for synthesis-gas fermentations. Biotechnol Prog 1999;15:834–44. doi:10.1021/bp990108m.
- [54] Munasinghe PC, Khanal SK. Syngas fermentation to biofuel: Evaluation of carbon monoxide mass transfer coefficient (k_{La}) in different reactor configurations. Biotechnol Prog 2010;26:1616–21. doi:10.1002/btpr.473.
- [55] Shen Y, Brown R, Wen Z. Syngas fermentation of *Clostridium carboxidivorans* P7 in a hollow fiber membrane biofilm reactor: Evaluating the mass transfer coefficient and ethanol production performance. Biochem Eng J 2014;85:21–9. doi:10.1016/j.bej.2014.01.010.
- [56] Yasin M, Park S, Jeong Y, Lee EY, Lee J, Chang IS. Effect of internal pressure and gas/liquid interface area on the CO mass transfer coefficient using hollow fibre membranes as a high mass transfer gas diffusing system for microbial syngas fermentation. Bioresour Technol 2014;169:637–43. doi:10.1016/j.biortech.2014.07.026.
- [57] Asimakopoulos K, Gavala HN, Skiadas I V. Biomethanation of Syngas by Enriched Mixed Anaerobic Consortia in Trickle Bed Reactors. Waste and Biomass Valorization 2019. doi:10.1007/s12649-019-00649-2.
- [58] Orgill JJ, Atiyeh HK, Devarapalli M, Phillips JR, Lewis RS, Huhnke RL. A comparison of mass transfer coefficients between trickle-bed, Hollow fiber membrane and stirred tank reactors. Bioresour Technol 2013;133:340–6. doi:10.1016/j.biortech.2013.01.124.
- [59] Liu K, Atiyeh HK, Stevenson BS, Tanner RS, Wilkins MR, Huhnke RL. Continuous syngas fermentation for the production of ethanol, n-propanol and n-butanol. Bioresour Technol 2014;151:69–77. doi:10.1016/j.biortech.2013.10.059.
- [60] Westman S, Chandolias K, Taherzadeh M. Syngas Biomethanation in a Semi-Continuous Reverse Membrane Bioreactor (RMBR). Fermentation 2016;2:1–12. doi:10.3390/fermentation2020008.
- [61] Straub M, Demler M, Weuster-Botz D, Dürre P. Selective enhancement of autotrophic acetate production with genetically modified *Acetobacterium woodii*. J Biotechnol 2014;178:67–72. doi:10.1016/j.jbiotec.2014.03.005.
- [62] Patankar S, Dudhane A, Paradh AD, Patil S. Improved bioethanol production using genome-shuffled *Clostridium ragsdalei* (DSM 15248) strains through syngas fermentation. Biofuels 2018;7:269:1–9. doi:10.1080/17597269.2018.1457313.

- [63] Köpke M, Held C, Hujer S, Liesegang H, Wiezer A, Wollherr A, et al. *Clostridium ljungdahlii* represents a microbial production platform based on syngas. *Proc Natl Acad Sci* 2010;107:13087–92. doi:10.1073/pnas.1011320107.
- [64] Mock J, Zheng Y, Mueller AP, Ly S, Tran L, Segovia S. Energy conservation associated with ethanol formation from H₂ and CO₂ in *Clostridium autoethanogenum* involving electron bifurcation. *J Bacteriol* 2015;197:2965–80. doi:10.1128/JB.00399-15.
- [65] Nagaraju S, Davies NK, Walker DJF, Köpke M, Simpson SD. Genome editing of *Clostridium autoethanogenum* using CRISPR/Cas9. *Biotechnol Biofuels* 2016;9:1–8. doi:10.1186/s13068-016-0638-3.
- [66] Molitor B, Marcellin E, Angenent LT. Overcoming the energetic limitations of syngas fermentation. *Curr Opin Chem Biol* 2017;41:84–92. doi:10.1016/j.cbpa.2017.10.003.
- [67] Nagarajan H, Sahin M, Nogales J, Latif H, Lovley DR, Ebrahim A, et al. Characterizing acetogenic metabolism using a genome-scale metabolic reconstruction of *Clostridium ljungdahlii*. *Microb Cell Fact* 2013;12:1–13. doi:10.1186/1475-2859-12-118.
- [68] Marcellin E, Behrendorff JB, Nagaraju S, DeTissera S, Segovia S, Palfreyman RW, et al. Low carbon fuels and commodity chemicals from waste gases – systematic approach to understand energy metabolism in a model acetogen. *Green Chem* 2016;18:3020–8. doi:10.1039/C5GC02708J.
- [69] Liew F, Henstra AM, Köpke M, Winzer K, Simpson SD, Minton NP. Metabolic engineering of *Clostridium autoethanogenum* for selective alcohol production. *Metab Eng* 2017;40:104–14. doi:10.1016/j.ymben.2017.01.007.
- [70] Ueki T, Nevin KP, Woodard TL, Lovley DR. Converting Carbon Dioxide to Butyrate with an Engineered Strain of *Clostridium ljungdahlii*. *MBio* 2014;5:1–10. doi:10.1128/mBio.01636-14.Editor.
- [71] Woolston BM, Emerson DF, Currie DH, Stephanopoulos G. Rediverting carbon flux in *Clostridium ljungdahlii* using CRISPR interference (CRISPRi). *Metab Eng* 2018;48:243–53. doi:10.1016/j.ymben.2018.06.006.
- [72] Tanner RS, Miller LM, Yang D. *Clostridium ljungdahlii* sp. nov., an Acetogenic Species in Clostridial rRNA Homology Group I. *Int J Syst Bacteriol* 1993;43:232–6.
- [73] Abrini J, Naveau H, Nyns E. *Clostridium autoethanogenum*, sp. nov., an anaerobic bacterium that produces ethanol from carbon monoxide. *Arch Microbiol* 1994;161:345–51.
- [74] Zahn JA, Saxena J. ETHANOLOGENIC CLOSTRIDIUM SPECIES, *CLOSTRIDIUM COSKATII*. US008143037B2, 2012.
- [75] Sokolova TG, González JM, Kostrikina NA, Chernyh NA, Slepova T V., Bonch-Osmolovskaya EA, et al. *Thermosinus carboxydivorans* gen. nov., sp. nov., a new anaerobic, thermophilic, carbon-monoxide-oxidizing, hydrogenogenic bacterium from a hot pool of Yellowstone National Park. *Int J Syst Evol Microbiol* 2004;54:2353–9. doi:10.1099/ijs.0.63186-0.
- [76] Diender M, Pereira R, Wessels HJCT, Stams AJM, Sousa DZ. Proteomic Analysis of the Hydrogen and Carbon Monoxide Metabolism of *Methanothermobacter marburgensis*. *Front Microbiol* 2016;7:1–10. doi:10.3389/fmicb.2016.01049.
- [77] Maness PC, Weaver PF. Production of poly-3-hydroxyalkanoates from CO and H₂ by a novel photosynthetic bacterium. *Appl Biochem Biotechnol* 1994;45–46:395–406. doi:10.1007/BF02941814.

- [78] Svetlichny VA, Sokolova TG, Gerhardt M, Ringpfeil M, Kostrikina NA, Zavarzin GA. *Carboxydotherrmus hydrogeniformans* gen. nov., sp. nov., a CO-utilizing Thermophilic Anaerobic Bacterium from Hydrothermal Environments of Kunashir Island. *Syst Appl Microbiol* 1991;14:254–60. doi:10.1016/S0723-2020(11)80377-2.
- [79] Sokolova TG, Kostrikina NA, Chernyh NA, Kolganova T V, Tourova TP, Bonch-osmolovskaya EA. *Thermincola carboxydiphila* gen. nov., sp. nov., a novel anaerobic, carboxydotrophic, hydrogenogenic bacterium from a hot spring of the Lake Baikal area. *Int J Syst Evol Microbiol* 2005;55:2069–73. doi:10.1099/ijs.0.63299-0.
- [80] Bae SS, Kim YJ, Yang SH, Lim JK, Jeon JH, Lee HS, et al. *Thermococcus onnurineus* sp. nov., a hyperthermophilic archaeon isolated from a deep-sea hydrothermal vent area at the PACMANUS field. *J Microbiol Biotechnol* 2006;16:1826–31.
- [81] Alves JI, van Gelder AH, Alves MM, Sousa DZ, Plugge CM. *Moorella stamsii* sp. nov., a new anaerobic thermophilic hydrogenogenic carboxydotroph isolated from digester sludge. *Int J Syst Evol Microbiol* 2013;63:4072–6. doi:10.1099/ijs.0.050369-0.
- [82] Allen TD, Caldwell ME, Lawson PA, Huhnke RL, Tanner RS. *Alkalibaculum bacchi* gen. nov., sp. nov., a CO-oxidizing, ethanol-producing acetogen isolated from livestock-impacted soil. *Int J Syst Evol Microbiol* 2010;60:2483–9. doi:10.1099/ijs.0.018507-0.
- [83] Huhnke RL, Lewis RS, Tanner RS. ISOLATION AND CHARACTERIZATION OF NOVEL CLOSTRIDIAL SPECIES. US007704723B2, 2010. doi:10.1016/j.
- [84] Liou JSC, Balkwill DL, Drake GR, Tanner RS. *Clostridium carboxidivorans* sp. nov., a solvent-producing clostridium isolated from an agricultural settling lagoon, and reclassification of the acetogen *Clostridium scatologenes* strain SL1 as *Clostridium drakei* sp. nov. *Int J Syst Evol Microbiol* 2005;55:2085–91. doi:10.1099/ijs.0.63482-0.
- [85] Isom CE, Nanny MA, Tanner RS. Improved conversion efficiencies for n-fatty acid reduction to primary alcohols by the solventogenic acetogen “*Clostridium ragsdalei*.” *J Ind Microbiol Biotechnol* 2015;42:29–38. doi:10.1007/s10295-014-1543-z.
- [86] Ukpong MN, Atiyeh HK, De Lorme MJM, Liu K, Zhu X, Tanner RS, et al. Physiological response of *Clostridium carboxidivorans* during conversion of synthesis gas to solvents in a gas-fed bioreactor. *Biotechnol Bioeng* 2012;109:2720–8. doi:10.1002/bit.24549.
- [87] Phillips JR, Atiyeh HK, Tanner RS, Torres JR, Saxena J, Wilkins MR, et al. Butanol and hexanol production in *Clostridium carboxidivorans* syngas fermentation: Medium development and culture techniques. *Bioresour Technol* 2015;190:114–21. doi:10.1016/j.biortech.2015.04.043.
- [88] Fernández-Naveira Á, Veiga MC, Kennes C. Selective anaerobic fermentation of syngas into either C2-C6 organic acids or ethanol and higher alcohols. *Bioresour Technol* 2019;280:387–95. doi:10.1016/j.biortech.2019.02.018.
- [89] Zhang J, Taylor S, Wang Y. Effects of end products on fermentation profiles in *Clostridium carboxidivorans* P7 for syngas fermentation. *Bioresour Technol* 2016;218:1055–63. doi:10.1016/j.biortech.2016.07.071.
- [90] Diender M, Uhl PS, Bitter JH, Stams AJM, Sousa DZ. High Rate Biomethanation of Carbon Monoxide-Rich Gases via a Thermophilic Synthetic Coculture. *ACS Sustain Chem Eng* 2018;6:2169–76. doi:10.1021/acssuschemeng.7b03601.
- [91] Diender M, Stams AJM, Sousa DZ. Production of medium-chain fatty acids and higher alcohols by a

synthetic co-culture grown on carbon monoxide or syngas. *Biotechnol Biofuels* 2016;9:82. doi:10.1186/s13068-016-0495-0.

- [92] Richter H, Molitor B, Diender M, Sousa DZ. A Narrow pH Range Supports Butanol , Hexanol , and Octanol Production from Syngas in a Continuous Co-culture of *Clostridium ljungdahlii* and *Clostridium kluyveri* with In-Line Product Extraction 2016;7. doi:10.3389/fmicb.2016.01773.
- [93] Perez JM, Richter H, Loftus SE, Angenent LT. Biocatalytic reduction of short-chain carboxylic acids into their corresponding alcohols with syngas fermentation. *Biotechnol Bioeng* 2013;110:1066–77. doi:10.1002/bit.24786.
- [94] Wise DL, Cooney CL, Augenstein DC. Biomethanation: Anaerobic fermentation of CO₂, H₂ and CO to methane. *Biotechnol Bioeng* 1978;20:1153–72. doi:10.1002/bit.260200804.
- [95] Kleerebezem R, van Loosdrecht MC. Mixed culture biotechnology for bioenergy production. *Curr Opin Biotechnol* 2007;18:207–12. doi:10.1016/j.copbio.2007.05.001.
- [96] Liu Y, Wan J, Han S, Zhang S, Luo G. Selective conversion of carbon monoxide to hydrogen by anaerobic mixed culture. *Bioresour Technol* 2016;202:1–7. doi:10.1016/j.biortech.2015.11.071.
- [97] Chandolias K, Wainaina S, Niklasson C, Taherzadeh MJ. Effects of Heavy Metals and pH on the Conversion of Biomass to Hydrogen via Syngas Fermentation 2018;13:4455–69.
- [98] Luo G, Jing Y, Lin Y, Zhang S, An D. A novel concept for syngas biomethanation by two-stage process: Focusing on the selective conversion of syngas to acetate. *Sci Total Environ* 2018;645:1194–200. doi:10.1016/j.scitotenv.2018.07.263.
- [99] Guiot SR, Cimpioia R. Potential of Wastewater-Treating Anaerobic Granules for Biomethanation of Synthesis Gas. *Environ Sci Technol* 2011;45:2006–12.
- [100] Navarro SS, Cimpioia R, Bruant G, Guiot SR. Biomethanation of Syngas Using Anaerobic Sludge: Shift in the Catabolic Routes with the CO Partial Pressure Increase. *Front Microbiol* 2016;7:1–13. doi:10.3389/fmicb.2016.01188.
- [101] Youngsukkasem S, Chandolias K, Taherzadeh MJ. Rapid bio-methanation of syngas in a reverse membrane bioreactor: Membrane encased microorganisms. *Bioresour Technol* 2014;178:334–40. doi:10.1016/j.biortech.2014.07.071.
- [102] Arantes AL, Alves JI, Alfons JM, Alves MM, Sousa DZ. Enrichment of syngas-converting communities from a multi-orifice baffled bioreactor. *Microb Biotechnol* 2017. doi:10.1111/1751-7915.12864.
- [103] Chandolias K, Pekgenc E, Taherzadeh MJ. Floating Membrane Bioreactors with High Gas Hold-Up for Syngas-to-Biomethane Conversion. *Energies* 2019;12:1–14. doi:10.3390/en12061046.
- [104] Park S, Yasin M, Kim D, Park H-D, Kang CM, Kim DJ, et al. Rapid enrichment of (homo)acetogenic consortia from animal feces using a high mass-transfer gas-lift reactor fed with syngas. *J Ind Microbiol Biotechnol* 2013;40:995–1003. doi:10.1007/s10295-013-1292-4.
- [105] Woo C, Jung KA, Moon J. Biological carbon monoxide conversion to acetate production by mixed culture. *Bioresour Technol* 2016;211:478–85. doi:10.1016/j.biortech.2016.03.100.
- [106] El-gammal M, Abou-shanab R, Angelidaki I, Omar B. High efficient ethanol and VFA production from gas fermentation: Effect of acetate, gas and inoculum microbial composition. *Biomass and Bioenergy* 2017;105:32–40. doi:10.1016/j.biombioe.2017.06.020.

- [107] Singla A, Kumar S, Lavania M, Chhipa H, Kapardar R, Rastogi S, et al. Optimization and Molecular Characterization of Syngas Fermenting Anaerobic Mixed Microbial Consortium TERI SA1. *Int J Renew Energy Dev* 2017;6:241–51.
- [108] Esquivel-elizondo S, Krajmalnik-brown R, Miceli J, Cesar III. Impact of carbon monoxide partial pressures on methanogenesis and medium chain fatty acids production during ethanol fermentation. *Biotechnol Bioeng* 2017;1–10. doi:10.1002/bit.26471.
- [109] Vasudevan D, Richter H, Angenent LT. Upgrading dilute ethanol from syngas fermentation to n-caproate with reactor microbiomes. *Bioresour Technol* 2014;151:378–82. doi:10.1016/j.biortech.2013.09.105.
- [110] He P, Han W, Shao L, Lü F. One-step production of C6-C8 carboxylates by mixed culture solely grown on CO. *Biotechnol Biofuels* 2018;11:1–13. doi:10.1186/s13068-017-1005-8.
- [111] Grootsholten TIM, Steinbusch KJJ, Hamelers HVM, Buisman CJN. Chain elongation of acetate and ethanol in an upflow anaerobic filter for high rate MCFA production. *Bioresour Technol* 2013;135:440–5. doi:10.1016/j.biortech.2012.10.165.
- [112] Esquivel-Elizondo S, Delgado AG, Rittmann BE, Brown RK. The effects of CO₂ and H₂ on CO metabolism by pure and mixed microbial cultures. *Biotechnol Biofuels* 2017;10:1–13. doi:10.1186/s13068-017-0910-1.
- [113] Chakraborty S, Rene ER, Lens PNL, Veiga MC, Kennes C. Enrichment of a solventogenic anaerobic sludge converting carbon monoxide and syngas into acids and alcohols. *Bioresour Technol* 2019;272:130–6. doi:10.1016/j.biortech.2018.10.002.
- [114] Singla A, Verma D, Lal B, Sarma PM. Enrichment and optimization of anaerobic bacterial mixed culture for conversion of syngas to ethanol. *Bioresour Technol* 2014;172:41–9. doi:10.1016/j.biortech.2014.08.083.
- [115] Xu S, Fu B, Zhang L, Liu H. Bioconversion of H₂/CO₂ by acetogen enriched cultures for acetate and ethanol production: the impact of pH. *World J Microbiol Biotechnol* 2015;31:941–50. doi:10.1007/s11274-015-1848-8.
- [116] Ganigué R, Sánchez-paredes P, Bañeras L, Colprim J. Low Fermentation pH Is a Trigger to Alcohol Production , but a Killer to Chain Elongation. *Front Microbiol* 2016;7:1–11. doi:10.3389/fmicb.2016.00702.
- [117] Liu K, Atiyeh HK, Stevenson BS, Tanner RS, Wilkins MR, Huhnke RL. Mixed culture syngas fermentation and conversion of carboxylic acids into alcohols. *Bioresour Technol* 2014;152:337–46. doi:10.1016/j.biortech.2013.11.015.
- [118] Ganigué R, Ramió-Pujol S, Sánchez P, Bañeras L. Conversion of sewage sludge to commodity chemicals via syngas fermentation. *Water Sci Technol* 2015;72:415–20. doi:10.2166/wst.2015.222.
- [119] Inman RE, Ingersoll RB. Note on the Uptake of Carbon Monoxide by Soil Fungi. *J Air Pollut Control Assoc* 1971;21:646–7. doi:10.1080/00022470.1971.10469582.
- [120] Chappelle EW. Carbon monoxide oxidation by algae. *Biochim Biophys Acta* 1962;62:45–62.
- [121] Pakpour F, Najafpour G, Tabatabaei M, Tohidfar M, Younesi H. Biohydrogen production from CO-rich syngas via a locally isolated *Rhodospseudomonas palustris* PT. *Bioprocess Biosyst Eng* 2014;37:923–30. doi:10.1007/s00449-013-1064-6.
- [122] Sokolova TG, Jeanthon C, Kostrikina NA, Chernyh NA, Lebedinsky A V., Stackebrandt E, et al. The

first evidence of anaerobic CO oxidation coupled with H₂ production by a hyperthermophilic archaeon isolated from a deep-sea hydrothermal vent. *Extremophiles* 2004;8:317–23. doi:10.1007/s00792-004-0389-0.

- [123] Parshina SN, Sipma J, Nakashimada Y, Henstra AM, Smidt H, Lysenko AM, et al. *Desulfotoculum carboxydivorans* sp. nov., a novel sulfate-reducing bacterium capable of growth at 100% CO. *Int J Syst Evol Microbiol* 2005;55:2159–65. doi:10.1099/ijs.0.63780-0.
- [124] Henstra AM, Dijkema C, Stams AJM. *Archaeoglobus fulgidus* couples CO oxidation to sulfate reduction and acetogenesis with transient formate accumulation. *Environ Microbiol* 2007;9:1836–41. doi:10.1111/j.1462-2920.2007.01306.x.
- [125] Bernalier A, Willems A, Leclerc M, Rochet V, Collins MD. *Ruminococcus hydrogenotrophicus* sp. nov., a new H₂/CO₂-utilizing acetogenic bacterium isolated from human feces. *Arch Microbiol* 1996;166:176–83.
- [126] Rother M, Metcalf WW. Anaerobic growth of *Methanosarcina acetivorans* C2A on carbon monoxide: an unusual way of life for a methanogenic archaeon. *Proc Natl Acad Sci U S A* 2004;101:16929–34. doi:10.1073/pnas.0407486101.
- [127] Cord-Ruwisch R, Seitz H-J, Conrad R. The capacity of hydrogenotrophic anaerobic bacteria to compete for traces of hydrogen depends on the redox potential of the electron acceptor. *Arch Microbiol* 1988;149:350–7.
- [128] Mörsdorf G, Frunzke K, Gadkari D, Meyer O. Microbial growth on carbon monoxide. *Biodegradation* 1992;3:61–82.
- [129] Ferry JG. CO Dehydrogenase. *Annu Rev Microbiol* 1995;49:305–33.
- [130] Uffen RL. Anaerobic growth of a *Rhodospseudomonas* species in the dark with carbon monoxide as sole carbon and energy substrate. *Proc Natl Acad Sci USA* 1976;73:3298–302. doi:10.1073/pnas.73.9.3298.
- [131] Sipma J, Henstra AM, Parshina SM, Lens PN, Lettinga G, Stams AJM. Microbial CO conversions with applications in synthesis gas purification and bio-desulfurization. *Crit Rev Biotechnol* 2006;26:41–65. doi:10.1080/07388550500513974.
- [132] Sokolova TG, Henstra AM, Sipma J, Parshina SN, Stams AJM, Lebedinsky A V. Diversity and ecophysiological features of thermophilic carboxydophilic anaerobes. *FEMS Microbiol Ecol* 2009;68:131–41. doi:10.1111/j.1574-6941.2009.00663.x.
- [133] Kerby RL, Ludden PW, Roberts GP. Carbon monoxide-dependent growth of *Rhodospirillum rubrum*. *J Bacteriol* 1995;177:2241–4.
- [134] Sokolova TG, Kostrikina NA, Chernyh NA, Kolganova T V., Tourova TP, Bonch-Osmolovskaya EA. *Thermincola carboxydiphila* gen. nov., sp. nov., a novel anaerobic, carboxydophilic, hydrogenogenic bacterium from a hot spring of the Kae Baikal area. *Int J Syst Evol Microbiol* 2005;55:2069–73. doi:10.1099/ijs.0.63299-0.
- [135] Henstra AM, Sipma J, Rinzema A, Stams AJM. Microbiology of synthesis gas fermentation for biofuel production. *Curr Opin Biotechnol* 2007;18:200–6. doi:10.1016/j.copbio.2007.03.008.
- [136] Kozhevnikova DA, Taranov EA, Lebedinsky A V., Bonch-Osmolovskaya EA, Sokolova TG. Hydrogenogenic and sulfidogenic growth of *Thermococcus* archaea on carbon monoxide and formate. *Microbiology* 2016;85:400–10. doi:10.1134/S0026261716040135.

- [137] Bae SS, Kim TW, Lee HS, Kwon KK, Kim YJ, Kim MS, et al. H₂ production from CO, formate or starch using the hyperthermophilic archaeon, *Thermococcus onnurineus*. *Biotechnol Lett* 2012;34:75–9. doi:10.1007/s10529-011-0732-3.
- [138] Hedderich R. Energy-Converting [NiFe] Hydrogenases from Archaea and Extremophiles: Ancestors of Complex I. *J Bioenerg Biomembr* 2004;36:65–75. doi:10.1023/B:JOB.0000019599.43969.33.
- [139] Maness PC, Huang J, Smolinski S, Tek V, Vanzin G. Energy generation from the CO oxidation-hydrogen production pathway in *Rubrivivax gelatinosus*. *Appl Environ Microbiol* 2005;71:2870–4. doi:10.1128/AEM.71.6.2870-2874.2005.
- [140] Zhao Y, Cimpoaia R, Liu Z, Guiot SR. Kinetics of CO conversion into H₂ by *Carboxydothemus hydrogenoformans*. *Appl Microbiol Biotechnol* 2011;91:1677–84. doi:10.1007/s00253-011-3509-7.
- [141] Rabus R, Hansen TA, Widdel F. Dissimilatory Sulfate- and Sulfur-Reducing Prokaryotes. The prokaryotes, New York: Springer; 2006, p. 659–768.
- [142] Oelgeschläger E, Rother M. Carbon monoxide-dependent energy metabolism in anaerobic bacteria and archaea. *Arch Microbiol* 2008;190:257–69. doi:10.1007/s00203-008-0382-6.
- [143] Parshina SN, Kijlstra S, Henstra AM, Sipma J, Plugge CM, Stams AJM. Carbon monoxide conversion by thermophilic sulfate-reducing bacteria in pure culture and in co-culture with *Carboxydothemus hydrogenoformans*. *Appl Microbiol Biotechnol* 2005;68:390–6. doi:10.1007/s00253-004-1878-x.
- [144] Müller V. Energy Conservation in Acetogenic Bacteria. *Appl Environ Microbiol* 2003;69:6345–53. doi:10.1128/AEM.69.11.6345.
- [145] Drake HL, Küsel K, Matthies C. Acetogenic Prokaryotes. *Prokaryotes*, New York: Springer; 2006, p. 354–420. doi:10.1007/0-387-30742-7_13.
- [146] Fischer F, Lieske R, Winzer K. Biologische Gasreaktionen. II. Mitteilung: über die Bildung von Essigsäure bei der biologischen Umsetzung von Kohlenoxyd und Kohlensäure mit Wasserstoff zu Methan. *Biochem Z* 1932;245:2–12.
- [147] Wieringa KT. Over het verdwijnen van waterstof en koolzuur onder anaerobe voorwaarden. *Antonie Van Leeuwenhoek* 1936;3:263–73. doi:10.1007/BF02059556.
- [148] Fontaine FE, Peterson WH, Johnson MJ, George J. A New Type of Glucose Fermentation by *Clostridium thermoaceticum*. *J Appl Toxicol* 1942;43:701–15.
- [149] Kerby R, Zeikus JG. Growth of *Clostridium thermoaceticum* on H₂/CO₂ or CO as energy source. *Curr Microbiol* 1983;8:27–30. doi:10.1007/bf01567310.
- [150] Abrini J, Naveau H, Nyns E. *Clostridium autoethanogenum*, sp. nov., an anaerobic bacterium that produces ethanol from carbon monoxide. *Arch Microbiol* 1994:345–51.
- [151] Lorowitz WH, Bryant MP. *Peptostreptococcus productus* strain that grows rapidly with CO as the energy source. *Appl Environ Microbiol* 1984;47:961–4.
- [152] Genthner BRS, Bryant MP. Additional characteristics of one-carbon-compound utilization by *Eubacterium limosum* and *Acetobacterium woodii*. *Appl Environ Microbiol* 1987;53:471–6.
- [153] Worden RM, Grethlein AJ, Zeikus JG, Datta R. Butyrate Production from Carbon Monoxide by *Butyribacterium methylothrophicum*. *Appl Biochem Biotechnol* 1989;20:687–99.

- [154] Diekert G, Wohlfarth G. Metabolism of homoacetogens. *Antonie Van Leeuwenhoek* 1994;66:209–21.
- [155] Ljungdahl LG. The autotrophic pathway of acetate synthesis in acetogenic bacteria. *Annu Rev Microbiol* 1986;40:415–50.
- [156] Ragsdale SW, Pierce E. Acetogenesis and the Wood-Ljungdahl pathway of CO₂ fixation. *Biochim Biophys Acta* 2008;1784:1873–98. doi:10.1016/j.bbapap.2008.08.012.
- [157] Müller V, Imkamp F, Biegel E, Schmidt S, Dilling S. Discovery of a ferredoxin:NAD⁺-oxidoreductase (Rnf) in *Acetobacterium woodii*: A novel potential coupling site in acetogens. *Ann N Y Acad Sci* 2008;1125:137–46. doi:10.1196/annals.1419.011.
- [158] Poehlein A, Schmidt S, Kaster A-K, Goenrich M, Vollmers J, Thürmer A, et al. An ancient pathway combining carbon dioxide fixation with the generation and utilization of a sodium ion gradient for ATP synthesis. *PLoS One* 2012;7:e33439. doi:10.1371/journal.pone.0033439.
- [159] Tremblay P, Zhang T, Dar SA. The Rnf Complex of *Clostridium ljungdahlii* Is a Proton-Translocating Ferredoxin: NAD⁺ Oxidoreductase Essential for Autotrophic growth 2013;4:1–8. doi:10.1128/mBio.00406-12.Editor.
- [160] Schuchmann K, Müller V. Autotrophy at the thermodynamic limit of life: a model for energy conservation in acetogenic bacteria. *Nat Rev Microbiol* 2014;12:809–21. doi:10.1038/nrmicro3365.
- [161] Hess V, Gallegos R, Jones JA, Barquera B, Malamy MH, Müller V. Occurrence of ferredoxin:NAD⁺ oxidoreductase activity and its ion specificity in several Gram-positive and Gram-negative bacteria. *PeerJ* 2016;4:e1515. doi:10.7717/peerj.1515.
- [162] Fischer F, Lieske R, Winzer K. Die umsetzungen des kohlenoxyds. *Biochem Z* 1931;236:247–67.
- [163] Stephenson M, Stickland LH. The bacterial formation of methane by the reduction of one-carbon compounds by molecular hydrogen. *Biochem J* 1933;27:1517–27.
- [164] Daniels L, Fuchs G, Thauer RK, Zeikus JG. Carbon Monoxide Oxidation by Methanogenic Bacteria. *J Bacteriol* 1977;132:118–26.
- [165] O'Brien JM, Wolkin RH, Moench TT, Morgan JB, Zeikus JG. Association of hydrogen metabolism with unitrophic or mixotrophic growth of *Methanosarcina barkeri* on carbon monoxide. *J Bacteriol* 1984;158:373–5.
- [166] Deppenmeier U, Lienard T, Gottschalk G. Novel reactions involved in energy conservation by methanogenic archaea. *Febs Lett* 1999;457:291–7.
- [167] Tiquia-Arashiro SM. Thermophilic Carboxydrotrophs and their Applications in Biotechnology. Springer International Publishing; 2014. doi:10.1007/978-3-319-11873-4.
- [168] Sun L, Müller B, Westerholm M, Schnürer A. Syntrophic acetate oxidation in industrial CSTR biogas digesters. *J Biotechnol* 2014;171:39–44. doi:10.1016/j.jbiotec.2013.11.016.
- [169] Schnürer A, Zellner G, Svensson BH. Mesophilic syntrophic acetate oxidation during methane formation in biogas reactors. *FEMS Microbiol Ecol* 1999;29:249–61. doi:10.1016/S0168-6496(99)00016-1.
- [170] Schnürer A, Schink B, Svensson BH. *Clostridium ultunense* sp. nov., a mesophilic bacterium oxidizing acetate in syntrophic association with a hydrogenotrophic methanogenic bacterium. *Int J Syst Bacteriol* 1996;46:1145–52. doi:10.1099/00207713-46-4-1145.

- [171] Westerholm M, Roos S, Schnürer A. *Syntrophaceticus schinkii* gen. nov., sp. nov., an anaerobic, syntrophic acetate-oxidizing bacterium isolated from a mesophilic anaerobic filter. *FEMS Microbiol Lett* 2010;309:100–4. doi:10.1111/j.1574-6968.2010.02023.x.
- [172] Westerholm M, Roos S, Schnürer A. *Tepidanaerobacter acetatoxydans* sp. nov., an anaerobic, syntrophic acetate-oxidizing bacterium isolated from two ammonium-enriched mesophilic methanogenic processes. *Syst Appl Microbiol* 2011;34:260–6. doi:10.1016/j.syapm.2010.11.018.
- [173] Hattori S, Kamagata Y, Hanada S. *Thermacetogenium phaeum* gen. nov., sp. nov., a Strictly Anaerobic, Thermophilic, Syntrophic Acetate-Oxidizing Bacterium. *Int J Syst Evol Microbiol* 2000:1601–9.
- [174] Stams AJM, Balk M, Weijma J. *Thermotoga lettingae* sp. nov., a novel thermophilic, methanol-degrading bacterium isolated from a thermophilic anaerobic reactor. *Int J Syst Evol Microbiol* 2002;52:1361–8. doi:10.1099/00207713-52-4-1361.
- [175] Cord-ruwisch R, Lovley DR. Growth of *Geobacter sulfurreducens* with Acetate in Syntrophic Cooperation with Hydrogen-Oxidizing Anaerobic Partners. *Appl Environ Microbiol* 1998;64:2232–6.
- [176] Hattori S. Syntrophic Acetate-Oxidizing Microbes in Methanogenic Environments. *Microbes Environ* 2008;23:118–27. doi:10.1264/jsme2.23.118.
- [177] Müller B, Manzoor S, Niazi A, Bongcam-Rudloff E, Schnürer A. Genome-guided analysis of physiological capacities of *Tepidanaerobacter acetatoxydans* provides insights into environmental adaptations and syntrophic acetate oxidation. *PLoS One* 2015;10:1–21. doi:10.1371/journal.pone.0121237.
- [178] Müller N, Worm P, Schink B, Stams AJM, Plugge CM. Syntrophic butyrate and propionate oxidation processes: From genomes to reaction mechanisms. *Environ Microbiol Rep* 2010;2:489–99. doi:10.1111/j.1758-2229.2010.00147.x.
- [179] de Bok F, Stams A, Dijkema C, Boone D. Pathway of Propionate Oxidation by a Syntrophic Culture of *Smithella propionica* and *Methanospirillum hungatei*. *Appl Environ Microbiol* 2001;67:1800–4. doi:10.1128/AEM.67.4.1800.
- [180] Angenent LT, Richter H, Buckel W, Spirito CM, Steinbusch KJ, Plugge C, et al. Chain elongation with reactor microbiomes: open-culture biotechnology to produce biochemicals. *Environ Sci Technol* 2016;50:2796–810. doi:10.1021/acs.est.5b04847.
- [181] Scarborough MJ, Lawson CE, Hamilton JJ, Donohue TJ, Noguera DR. Metatranscriptomic and Thermodynamic Insights into Medium-Chain Fatty Acid Production Using an Anaerobic Microbiome. *MSystems* 2018;3:1–21. doi:10.1128/msystems.00221-18.
- [182] Kenealy WR, Waselefsky DM. Studies on the substrate range of *Clostridium kluveri*; the use of propanol and succinate. *Arch Microbiol* 1985;141:187–94. doi:10.1007/BF00408056.
- [183] González-Cabaleiro R, Lema JM, Rodríguez J, Kleerebezem R. Linking thermodynamics and kinetics to assess pathway reversibility in anaerobic bioprocesses. *Energy Environ Sci* 2013;6:3780–9. doi:10.1039/c3ee42754d.
- [184] Sipma J, Lens PNL, Stams a. JM, Lettinga G. Carbon monoxide conversion by anaerobic bioreactor sludges. *FEMS Microbiol Ecol* 2003;44:271–7. doi:10.1016/S0168-6496(03)00033-3.
- [185] Navarro SS, Cimpioia R, Bruant G, Guiot SR. Specific inhibitors for identifying pathways for methane production from carbon monoxide by a nonadapted anaerobic mixed culture. *Can J Microbiol* 2014;415:407–15. doi:10.1139/cjm-2013-0843.

- [186] Rotaru A-E, Shrestha PM, Liu F, Shrestha M, Shrestha D, Embree M, et al. A new model for electron flow during anaerobic digestion: direct interspecies electron transfer to *Methanosaeta* for the reduction of carbon dioxide to methane. *Energy Environ Sci* 2014;7:408–15. doi:10.1039/c3ee42189a.
- [187] Boone DR, Johnson RL, Liu Y. Diffusion of the interspecies electron carriers H₂ and formate in methanogenic ecosystems and its implications in the measurement of K_m for H₂ or formate uptake. *Appl Environ Microbiol* 1989;55:1735–41. doi:0099-2240/89/071735-07\$02.00/0.
- [188] Wang W, Xie L, Luo G, Zhou Q, Angelidaki I. Performance and microbial community analysis of the anaerobic reactor with coke oven gas biomethanation and in situ biogas upgrading. *Bioresour Technol* 2013;146:234–9. doi:10.1016/j.biortech.2013.07.049.
- [189] Stams AJM, Elferink SJWH, Westermann P. Metabolic Interactions Between Methanogenic Consortia and Anaerobic Respiring Bacteria. *Adv Biochem Eng Biotechnol* 2003;81:31–56.
- [190] Stams a. JM, Plugge CM, de Bok F a M, van Houten BHGW, Lens P, Dijkman H, et al. Metabolic interactions in methanogenic and sulfate-reducing bioreactors. *Water Sci Technol* 2005;52:13–20.
- [191] Liu R, Hao X, Wei J. Function of homoacetogenesis on the heterotrophic methane production with exogenous H₂/CO₂ involved. *Chem Eng J* 2015;284:1196–203. doi:10.1016/j.cej.2015.09.081.
- [192] Sipma J, Lettinga G, Stams AJM, Lens PNL. Hydrogenogenic CO conversion in a moderately thermophilic (55 C) sulfate-fed gas lift reactor: Competition for CO-derived H₂. *Biotechnol Prog* 2006;22:1327–34. doi:10.1021/bp0601084.
- [193] Esquivel-Elizondo S, Delgado AG, Krajmalnik-Brown R. Evolution of microbial communities growing with carbon monoxide, hydrogen, and carbon dioxide. *FEMS Microbiol Ecol* 2017;93:1–12. doi:10.1093/femsec/fix076.
- [194] De Roy K, Marzorati M, Negroni A, Thas O, Balloi A, Fava F, et al. Environmental conditions and community evenness determine the outcome of biological invasion. *Nat Commun* 2013;4:1383–5. doi:10.1038/ncomms2392.
- [195] Allison SD, Martiny JBH. Resistance, resilience, and redundancy in microbial communities. *Proc Natl Acad Sci USA* 2008;105:11512–9. doi:10.17226/12501.
- [196] Briones A, Raskin L. Diversity and dynamics of microbial communities in engineered environments and their implications for process stability. *Curr Opin Biotechnol* 2003;14:270–6. doi:10.1016/S0958-1669(03)00065-X.
- [197] Coyte KZ, Schluter J, Foster KR. The ecology of the microbiome: Networks, competition, and stability. *Science (80-)* 2015;350:663–6. doi:10.1126/science.aad2602.
- [198] Top EM, Springael D. The role of mobile genetic elements in bacterial adaptation to xenobiotic organic compounds. *Curr Opin Biotechnol* 2003;14:262–9. doi:10.1016/S0958-1669(03)00066-1.
- [199] Mee MT, Collins JJ, Church GM, Wang HH. Syntrophic exchange in synthetic microbial communities. *Proc Natl Acad Sci U S A* 2014;111. doi:10.1073/pnas.1405641111.
- [200] Zengler K, Zaramela LS. The social network of microorganisms — how auxotrophies shape complex communities. *Nat Rev Microbiol* 2018;16:383–90. doi:10.1038/nbt.3301.Mammalian.
- [201] Emerson D, Wilson W. Giving microbial diversity a home. *Nat Rev Microbiol* 2009;7:758. doi:10.1038/nrmicro2246.

- [202] Sievers M. Culture Collections in the Study of Microbial Diversity, Importance. *Encycl Metagenomics* 2013;1–5. doi:10.1007/978-1-4614-6418-1.
- [203] Dominguez Bello MG, Knight R, Gilbert JA, Blaser MJ. Ensure the Health of Future Generations. *Science* (80-) 2018;362:33–5.
- [204] Jörg Overmann. Principles of Enrichment, Isolation, Cultivation, and Preservation of Prokaryotes. In: Rosenberg E, DeLong EF, Lory S, Stackebrandt E, Thompson F, editors. *The Prokaryotes*. 4th ed., Springer-Verlag Berlin Heidelberg; 2013, p. 149–207.
- [205] Alves JI, Stams AJM, Plugge CM, Alves MM, Sousa DZ. Enrichment of anaerobic syngas-converting bacteria from thermophilic bioreactor sludge. *FEMS Microbiol Ecol* 2013;86:590–7. doi:10.1111/1574-6941.12185.
- [206] Carballa M, Regueiro L, Lema JM. Microbial management of anaerobic digestion: Exploiting the microbiome-functionality nexus. *Curr Opin Biotechnol* 2015;33:103–11. doi:10.1016/j.copbio.2015.01.008.
- [207] Schauer-Gimenez AE, Zitomer DH, Maki JS, Struble CA. Bioaugmentation for improved recovery of anaerobic digesters after toxicant exposure. *Water Res* 2010;44:3555–64. doi:10.1016/j.watres.2010.03.037.
- [208] Nielsen HB, Mladenovska Z, Ahring BK. Bioaugmentation of a two-stage thermophilic (68°C/55°C) anaerobic digestion concept for improvement of the methane yield from cattle manure. *Biotechnol Bioeng* 2007;97:1638–43. doi:10.1002/bit.21342.
- [209] Fotidis IA, Wang H, Fiedel NR, Luo G, Karakashev DB, Angelidaki I. Bioaugmentation as a solution to increase methane production from an ammonia-rich substrate. *Environ Sci Technol* 2014;48:7669–76. doi:10.1021/es5017075.
- [210] Kotay SM, Das D. Novel dark fermentation involving bioaugmentation with constructed bacterial consortium for enhanced biohydrogen production from pretreated sewage sludge. *Int J Hydrogen Energy* 2009;34:7489–96. doi:10.1016/j.ijhydene.2009.05.109.
- [211] Vega JL, Clausen EC, Gaddy JL. Design of bioreactors for coal synthesis gas fermentations. *Resour Conserv Recycl* 1990;3:149–60. doi:10.1016/0921-3449(90)90052-6.
- [212] Mohammadi M, Mohamed AR, Najafpour GD, Younesi H, Uzir MH. Kinetic studies on fermentative production of biofuel from synthesis gas using *Clostridium ljungdahlii*. *Sci World J* 2014;2014:1–8. doi:10.1155/2014/910590.
- [213] Younesi H, Najafpour G, Mohamed AR. Ethanol and acetate production from synthesis gas via fermentation processes using anaerobic bacterium, *Clostridium ljungdahlii*. *Biochem Eng J* 2005;27:110–9. doi:10.1016/j.bej.2005.08.015.
- [214] Najafpour G, Younesi H, Mohamed AR. Continuous Hydrogen Production Via Fermentation of Synthesis Gas. *Pet Coal* 2003;45:154–8.
- [215] Batstone DJ, Keller J, Angelidaki I, Kalyuzhnyi S., Pavlostathis S., Rozzi A, et al. The IWA Anaerobic Digestion Model No 1 (ADM1). *Water Sci Technol* 2002;45:65–73. doi:10.2166/wst.2008.678.
- [216] Antonopoulou G, Gavala HN, Skiadas I V., Lyberatos G. Modeling of fermentative hydrogen production from sweet sorghum extract based on modified ADM1. *Int J Hydrogen Energy* 2012;37:191–208. doi:10.1016/j.ijhydene.2011.09.081.

- [217] Gadhamshetty V, Arudchelvam Y, Nirmalakhandan N, Johnson DC. Modeling dark fermentation for biohydrogen production: ADM1-based model vs. Gompertz model. *Int J Hydrogen Energy* 2010;35:479–90. doi:10.1016/j.ijhydene.2009.11.007.
- [218] Penumathsa BKV, Premier GC, Kyazze G, Dinsdale R, Guwy AJ, Esteves S, et al. ADM1 can be applied to continuous bio-hydrogen production using a variable stoichiometry approach. *Water Res* 2008;42:4379–85. doi:10.1016/j.watres.2008.07.030.
- [219] Rodríguez J, Kleerebezem R, Lema JM, Van Loosdrecht MCM. Modeling product formation in anaerobic mixed culture fermentations. *Biotechnol Bioeng* 2006;93:592–606. doi:10.1002/bit.20765.
- [220] Regueira A, González-Cabaleiro R, Ofițeru ID, Rodríguez J, Lema JM. Electron bifurcation mechanism and homoacetogenesis explain products yields in mixed culture anaerobic fermentations. *Water Res* 2018;141:349–56. doi:10.1016/j.watres.2018.05.013.
- [221] González-Cabaleiro R, Lema JM, Rodríguez J. Metabolic energy-based modelling explains product yielding in anaerobic mixed culture fermentations. *PLoS One* 2015;10:1–17. doi:10.1371/journal.pone.0126739.
- [222] Klitgord N, Segrè D. Ecosystems biology of microbial metabolism. *Curr Opin Biotechnol* 2011;22:541–6. doi:10.1016/j.copbio.2011.04.018.
- [223] Johns NI, Blazejewski T, Gomes ALC, Wang HH. Principles for designing synthetic microbial communities. *Curr Opin Microbiol* 2016;31:146–53. doi:10.1016/j.mib.2016.03.010.
- [224] Stolyar S, Van Dien S, Hillesland KL, Pinel N, Lie TJ, Leigh JA, et al. Metabolic modeling of a mutualistic microbial community. *Mol Syst Biol* 2007;3:1–14. doi:10.1038/msb4100131.
- [225] Nagarajan H, Embree M, Rotaru AE, Shrestha PM, Feist AM, Palsson B, et al. Characterization and modelling of interspecies electron transfer mechanisms and microbial community dynamics of a syntrophic association. *Nat Commun* 2013;4:1–10. doi:10.1038/ncomms3809.
- [226] Pfeiffer T, Bonhoeffer S. Evolution of cross-feeding in microbial populations. *Am Nat* 2004;163.
- [227] McCarty PL. Thermodynamic electron equivalents model for bacterial yield prediction: Modifications and comparative evaluations. *Biotechnol Bioeng* 2007;97:377–88. doi:10.1002/bit.21250.
- [228] Hoijnen JJ, van Loosdrecht MCM, Tijhuis L. A black box mathematical model to calculate auto- and heterotrophic biomass yields based on Gibbs energy dissipation. *Biotechnol Bioeng* 1992;40:1139–54. doi:10.1002/bit.260401003.
- [229] Kleerebezem R, Van Loosdrecht MC. A Generalized Method for Thermodynamic State Analysis of Environmental Systems. *Crit Rev Environ Sci Technol* 2010;40:1–54. doi:10.1080/10643380802000974.
- [230] Tijhuis L, van Loosdrecht M, Heijnen J. A Thermodynamically Based Correlation for Maintenance Gibbs Energy Requirements in Aerobic and Anaerobic Chemotrophic Growth. *Biotechnol Bioeng* 1993;42:509–19.
- [231] Schink B, Friedrich M. Energetics of syntrophic fatty acid oxidation. *FEMS Microbiol Rev* 1994;15:85–94. doi:10.1111/j.1574-6976.1994.tb00127.x.
- [232] Jackson BE, McInerney MJ. Anaerobic microbial metabolism can proceed close to thermodynamic limits. *Nature* 2002;415:454–6.
- [233] Hoehler TM, Alperin MJ, Albert DB, Martens CS. Apparent minimum free energy requirements for

methanogenic Archaea and sulfate-reducing bacteria in an anoxic marine sediment. *FEMS Microbiol Ecol* 2001;38:33–41. doi:10.1016/S0168-6496(01)00175-1.

- [234] Kleerebezem R, Stams AJM. Kinetics of Syntrophic Cultures : A Theoretical Treatise on Butyrate Fermentation 2000.
- [235] Hoh CY, Cord-Ruwisch R. A practical kinetic model that considers endproduct inhibition in anaerobic digestion processes by including the equilibrium constant. *Biotechnol Bioeng* 1996;51:597–604. doi:10.1002/(SICI)1097-0290(19960905)51:5<597::AID-BIT12>3.3.CO;2-E.
- [236] Jin Q, Bethke CM. Predicting the rate of microbial respiration in geochemical environments. *Geochim Cosmochim Acta* 2005;69:1133–43. doi:10.1016/j.gca.2004.08.010.
- [237] Jin Q, Bethke CM. The thermodynamics and kinetics of microbial metabolism. *Am J Sci* 2007;307:643–77. doi:10.2475/04.2007.01.
- [238] Blodau C. Thermodynamic control on terminal electron transfer and methanogenesis. *ACS Symp Ser* 2011;1071:65–83. doi:10.1021/bk-2011-1071.ch004.
- [239] Liu C, Kota S, Zachara JM, Fredrickson JK, Brinkman CK. Kinetic analysis of the bacterial reduction of goethite. *Environ Sci Technol* 2001;35:2482–90. doi:10.1021/es001956c.
- [240] Großkopf T, Soyer OS. Microbial diversity arising from thermodynamic constraints. *Int Soc Microb Ecol* 2016;10:2725–33. doi:10.1038/ismej.2016.49.
- [241] Alves J, Visser M, Stams A, Plugge C, Alves M, Sousa D. Enrichment and microbial characterization of syngas converting anaerobic cultures. 13th World Congr Anaerob Dig 2013:2–5.
- [242] Ziganshin AM, Liebetrau J, Pröter J, Kleinsteuber S. Microbial community structure and dynamics during anaerobic digestion of various agricultural waste materials. *Appl Microbiol Biotechnol* 2013;97:5161–74. doi:10.1007/s00253-013-4867-0.
- [243] Sundberg C, Al-Soud WA, Larsson M, Alm E, Yekta SS, Svensson BH, et al. 454 Pyrosequencing Analyses of Bacterial and Archaeal Richness in 21 Full-Scale Biogas Digesters. *FEMS Microbiol Ecol* 2013;85:612–26. doi:10.1111/1574-6941.12148.
- [244] Koch C, Müller S, Harms H, Harnisch F. Microbiomes in bioenergy production: From analysis to management. *Curr Opin Biotechnol* 2014;27:65–72. doi:10.1016/j.copbio.2013.11.006.
- [245] Wan N, Sathish A, You L, Tang YJ, Wen Z. Deciphering Clostridium metabolism and its responses to bioreactor mass transfer during syngas fermentation. *Sci Rep* 2017;1–11. doi:10.1038/s41598-017-10312-2.
- [246] Grootsholten TIM, Kinsky dal Borgo F, Hamelers HVM, Buisman CJN. Promoting chain elongation in mixed culture acidification reactors by addition of ethanol. *Biomass and Bioenergy* 2013;48:10–6. doi:10.1016/j.biombioe.2012.11.019.
- [247] Richter H, Molitor B, Diender M, Sousa DZ. A Narrow pH Range Supports Butanol , Hexanol , and Octanol Production from Syngas in a Continuous Co-culture of *Clostridium ljungdahlii* and *Clostridium kluyveri* with In-Line Product Extraction. *Front Microbiol* 2016;7:1–13. doi:10.3389/fmicb.2016.01773.
- [248] Grimalt-Alemany A, Łężyk M, Kennes-Veiga DM, Skiadas I V., Gavala HN. Enrichment of mesophilic and thermophilic mixed microbial consortia for syngas biomethanation: the role of kinetic and thermodynamic competition. *Waste and Biomass Valorization* 2019. doi:10.1007/s12649-019-00595-z.

- [249] Grimalt-Alemany A, Łężyk M, Lange L, Skiadas I V, Gavala HN. Enrichment of syngas-converting mixed microbial consortia for ethanol production and thermodynamics-based design of enrichment strategies. *Biotechnol Biofuels* 2018;11:1–22. doi:10.1186/s13068-018-1189-6.
- [250] Alberty RA. *Thermodynamics of Biochemical Reactions*. New Jersey: John Wiley & Sons, Inc; 2003.
- [251] Jin Q. Energy conservation of anaerobic respiration. *Am J Sci* 2012;312:573–628. doi:10.2475/06.2012.01.
- [252] Kaster A, Moll J, Parey K, Thauer RK. Coupling of ferredoxin and heterodisulfide reduction via electron bifurcation in hydrogenotrophic methanogenic archaea 2011;108:2981–6. doi:10.1073/pnas.1016761108.
- [253] Schlegel K, Welte C, Deppenmeier U, Mu V. Electron transport during acetoclastic methanogenesis by *Methanosarcina acetivorans* involves a sodium-translocating Rnf complex 2012;279:4444–52. doi:10.1111/febs.12031.
- [254] Bertsch J, Müller V. Bioenergetic constraints for conversion of syngas to biofuels in acetogenic bacteria. *Biotechnol Biofuels* 2015;8:1–12. doi:10.1186/s13068-015-0393-x.
- [255] Lingen HJ Van, Plugge CM, Fadel JG, Kebreab E. Thermodynamic Driving Force of Hydrogen on Rumen Microbial Metabolism: A Theoretical Investigation. *PLoS One* 2016;11 (10):1–18. doi:10.1371/journal.pone.0161362.
- [256] Savage MD, Wu Z, Daniel SL, Lundie LL, Drake HL. Carbon monoxide dependent chemolithotrophic growth of *Clostridium thermoautotrophicum*. *Appl Environ Microbiol* 1987;53:1902–6.
- [257] Slepova T V., Sokolova TG, Lysenko AM, Tourova TP, Kolganova T V., Kamzolkina O V., et al. *Carboxydocella sporoproducens* sp. nov., a novel anaerobic CO-utilizing/H₂-producing thermophilic bacterium from a Kamchatka hot spring. *Int J Syst Evol Microbiol* 2006;56:797–800. doi:10.1099/ijs.0.63961-0.
- [258] Esquivel-elizondo S, Krajmalnik-brown R, Miceli J, Cesar III. Impact of carbon monoxide partial pressures on methanogenesis and medium chain fatty acids production during ethanol fermentation. *Biotechnol Bioeng* 2018;115:341–50. doi:10.1002/bit.26471.
- [259] Luo G, Wang W, Angelidaki I. Anaerobic digestion for simultaneous sewage sludge treatment and CO biomethanation: process performance and microbial ecology. *Environ Sci Technol* 2013;47:10685–93. doi:10.1021/es401018d.

Appendix – Collection of Manuscripts

Manuscript I

“Syngas biomethanation: State-of-the-art review and perspectives”

Syngas biomethanation: state-of-the-art review and perspectives

Antonio Grimalt-Alemany,¹ Center for Bioprocess Engineering, Department of Chemical and Biochemical Engineering, Technical University of Denmark, Lyngby, Denmark

Ioannis V. Skiadas, PILOT PLANT, Department of Chemical and Biochemical Engineering, Technical University of Denmark, Lyngby, Denmark

Hariklia N. Gavala, Center for Bioprocess Engineering, Department of Chemical and Biochemical Engineering, Technical University of Denmark, Lyngby, Denmark

Received June 23, 2017; revised August 24, 2017; and accepted August 25, 2017

View online at October 10, 2017 Wiley Online Library (wileyonlinelibrary.com);

DOI: 10.1002/bbb.1826; *Biofuels, Bioprod. Bioref.* 12:139–158 (2018)

Abstract: Significant research efforts are currently being made worldwide to develop more efficient biomethane production processes from a variety of waste streams. The biomethanation of biomass-derived syngas can contribute to increasing the potential of methane production as it opens the way for the conversion of recalcitrant biomasses, generally not fully exploitable by anaerobic digestion systems. Additionally, this biological process presents several advantages over its analogous process of catalytic methanation such as the use of inexpensive biocatalysts, milder operational conditions, higher tolerance to the impurities of syngas, and higher product selectivity. However, there are still several challenges to be addressed for this technology to reach commercial stage. This work reviews the progress made over the last few years in syngas biomethanation processes in order to provide an overview of the current state of the art of this technology. The most relevant aspects determining the performance of syngas biomethanation processes are extensively discussed here, including microbial diversity and metabolic interactions in mixed microbial consortia, the influence of operating parameters and bioreactor designs, and the potential of modelling as a tool for the design and control of this bioprocess. © 2017 Society of Chemical Industry and John Wiley & Sons, Ltd

Keywords: biomethanation; synthesis gas; carbon monoxide; methane; microbial consortia; mixed cultures

Introduction

The increase in energy demand over the last few decades along with the foreseen future scarcity of fossil fuels and the climate crisis have driven policymakers to foster the production of biofuels as an alternative energy source. Currently, the EU and several countries with an important role in the global market have implemented policies in this direction, including the USA,

Brazil, China, and India, among others.¹ An example of such policies is the European Directive 2009/28/EC, which established binding targets for achieving a 20% share of energy from renewable sources on the overall European energy consumption by 2020, and a minimum share of 10% in the transport sector emphasizing the need of promoting second-generation biofuels. Therefore, the current legal and regulatory framework poses an important window of opportunity for the development of an alternative

Correspondence to: Hariklia N. Gavala, Center for Bioprocess Engineering, Department of Chemical and Biochemical Engineering, Technical University of Denmark, Søltofts Plads 229, 2800 Kgs. Lyngby, Denmark. E-mail: hnga@kt.dtu.dk, hari_gavala@yahoo.com

technological infrastructure based on the use of non-food biomasses and waste streams as feedstock.

One of the most promising approaches within second- and third-generation biofuel technologies is the process of gas fermentation, which has gained increasing interest in recent years for the conversion of both industrial off-gases and recalcitrant feedstocks when coupled to their gasification into synthesis gas. This process consists in the fermentation of a gaseous substrate, mainly composed by H₂, CO, and CO₂, carried out by anaerobic micro-organisms able to utilize these gases as a carbon and energy source. Acetogenic bacteria are currently the predominant microbial group subject to study in syngas fermentation processes, with ethanol being the most commonly targeted product. Syngas fermentation processes for the production of ethanol^{2–8} and other products, such as acetone, butanol, 2,3-butanediol, and even biopolymers, have been extensively reviewed recently including several process-development related aspects such as bioreactor design, relevant operational parameters, and genetic tools for broadening the product portfolio of the syngas bioconversion.^{9–15} However, the biological process of syngas conversion into methane is often overlooked in these reviews despite the research carried out in this field in recent years. Therefore, the scope of this paper is to perform a comprehensive review of the knowledge available up to date in syngas biomethanation processes in order to provide an overview of the current state of the art of this technology, as well as to discuss about its future application perspectives.

As a potential product, biogas (or biomethane when upgraded) presents a significant potential for its integration into the current biofuel landscape due to its versatility as an energy carrier. To date, the most common practice is to exploit biogas *in situ* for production of combined heat and power as the quality standards for this application are generally lower. However, biogas upgrading to biomethane provides a more flexible application of this fuel, as biomethane and natural gas are fully miscible in the natural gas grid. As a transportation fuel, the use of biomethane in bi-fuel cars is a rather attractive alternative to liquid fuels in terms of energy content (Table 1). Additionally, the fact that it is fully miscible with its fossil analog, natural gas, is a clear advantage over other liquid biofuels such as bioethanol or biodiesel, which are usually blended to some extent in conventional cars.¹⁶ On the other hand, its further development as an automotive fuel is currently hindered by several factors such as the early stage of its commercial market, the limited number of filling stations, and the high cost of the technological transfer to bi-fuel vehicles compared to vehicles fueled solely by ethanol.^{17,18}

Table 1. Energy content of various fuels.²⁰

Fuel	Higher Heating Value (MJ/kg)
Gasoline	46.5
Diesel	45.4 ^a
Ethanol	29.7
Biodiesel	42.2 ^a
Methane	55.5
Hydrogen	141.8
Butanol	36.6 ^a
Dimethyl Ether	31.7
Methanol	22.7 ^a

^aExtracted from Demirel²¹

However, the positive trend in the use of biomethane as a vehicle fuel in several European countries, for example Sweden, France, or Denmark,¹⁹ anticipates the expansion of this emerging market, which could foster the development of more efficient production processes.

An additional aspect of biomethane is its flexibility in terms of production paths and biomass sources, as it can be produced by both biochemical and thermochemical methods which separately and in combination may cover a wide range of feedstocks of a different nature. Anaerobic digestion is a well-established technology currently processing several feedstock types from the agricultural sector and other organic industrial waste streams.²² On the other hand, catalytic methanation technologies for synthetic natural gas (SNG) production have been revisited over the last 10 years due to the rising prices of natural gas and the need to address energy security issues, which has promoted the development of several new catalytic methanation processes based on biomass gasification.²³ These facts suggest that the process of syngas biomethanation would also have a potential market for its future application once it reached commercial scale. As will be discussed in the next section, this technology presents several advantages over the analogous catalytic methanation process and is also well suited for coupling to current anaerobic digestion systems, opening thus good perspectives for further development of this technology.

Overview of the syngas biomethanation process

The biomethanation of biomass-derived syngas is a robust bioconversion route combining the benefits of

thermochemical and biochemical conversion processes, as it circumvents the limitations of the biological degradation of complex substrates by gasifying the biomass into a directly fermentable gas. The thermochemical conversion of the feedstock through gasification constitutes one of the main advantages since any type of biomass can be gasified including agricultural residues, forestry residues, non-fermentable byproducts from biorefineries, byproducts of any bioprocessing facility, and even organic municipal wastes.²⁴ However, the substrate of the syngas biomethanation process is not limited to biomass-derived syngas, as there are other potential sources of CO-rich industrial off-gases in the iron and steel sector.²⁵ Alternatively, other industrial CO₂-rich off-gases could also be used as substrate along with H₂ derived from the surplus of renewable electricity, opening another potential application as a means of storing renewable electricity.²⁶ Therefore, there is a rather wide range of industrial off-gas sources and biomasses that could be used as feedstock for this process.

The biomethanation of syngas involves the synergistic action of micro-organisms, integrated in a mixed microbial consortium, for the utilization of syngas as a carbon and energy source to synthesize a mixture of methane and carbon dioxide. The biomethanation of syngas is a strictly anaerobic process that can be carried out at both mesophilic and thermophilic conditions. Synthesis gas is converted into methane both directly and stepwise through intermediary products by several microbial groups such as methanogenic archaea, acetogenic bacteria, and hydrogenogenic bacteria among others, with all of them thriving in syntrophic association. As a result, the biomethanation of syngas comprises a complex network of biochemical reactions mainly based on the water-gas shift reaction, acetogenesis, hydrogenotrophic methanation, carboxydrotrophic methanation, and acetoclastic methanation. Despite the higher complexity of microbial consortia compared to pure cultures, the adoption of this mixed-culture approach presents a series of inherent merits such as non-sterile operation, higher adaptation capacity, higher tolerance to the impurities of the raw syngas, and resiliency after a disturbance in the operating conditions, which represent a crucial advantage when it comes to maintain the productivity of a continuous process.^{12,27,28} Additionally, using undefined mixed microbial consortia renders continuous processes more robust, as their adaptation to the substrate selects the most efficient and effective biocatalysts leading to a long-term improved performance of the microbial consortium.²⁸

Syngas biomethanation versus catalytic methanation

The catalytic methanation is an exothermic process using hydrogen and carbon oxides present in syngas for the catalytic production of methane and water. This process operates at temperatures above 250°C and high pressures, using previously activated metallic catalysts to drive the catalytic reduction of carbon oxides into methane. The catalysts used in methanation are very sensitive to the impurities present in synthesis gas such as chlorine and sulfur compounds, ammonia, tars, and particles, which ultimately cause poisoning and deactivation of the catalysts.²⁹ Therefore, the catalytic methanation requires an intensive gas cleaning process of the raw syngas before entering the reactor. Furthermore, an additional water-gas shift reaction process is often needed in order to correct the ratio of C/H in syngas, which reduces the overall efficiency of the process while increasing the complexity and the cost of operation.³⁰ The use of biocatalysts in syngas biomethanation is anticipated to result in a more cost-effective process as these present a higher tolerance to the impurities of syngas and operate at mild temperatures. As opposed to the catalytic process, the biological process is not sensitive to the ratio of C/H since the water-gas shift reaction is inherent to the autotrophic metabolism of most microbial groups³¹ conducting the biomethanation of syngas. Additionally, the biomethanation presents a higher selectivity as methane and carbon dioxide are the only end-products of the fermentation, whereas the catalytic process produces higher hydrocarbons as byproducts. Lastly, the irreversible character of the biochemical reactions during biomethanation allows the complete conversion of the substrates, this way avoiding the thermodynamic equilibrium limitations of the catalytic process.³²

Coupling syngas biomethanation and anaerobic digestion

Anaerobic digestion is so far the default technology for biological production of methane, holding the dual role of waste treatment and production of biofuels process.³³ The degradation of organic residues in anaerobic digestion is carried out by undefined mixed microbial consortia in four consecutive stages, namely hydrolysis, acidogenesis, acetogenesis and methanogenesis. Continuous anaerobic digestion processes are generally characterized by long hydraulic retention times due to the presence of refractory compounds in the biomass, which make hydrolysis the

main rate-limiting step of the digestion.³⁴ Nevertheless, the main limiting factor is often the low biomass conversion efficiency due to the low degradability of some specific biomasses. Thus, pre-treatments are usually needed to enhance the digestibility of the biomass and improve the hydrolysis yield. In turn, the syngas biomethanation process circumvents the limitations of the biological degradation of complex substrates by gasifying the biomass into a directly fermentable gas, overcoming the aforementioned shortcomings. Nonetheless, these technologies are not necessarily alternative as their integration in a combined process seems a promising configuration for achieving a more efficient production of methane. Li *et al.*³⁰ studied the feasibility of combining the anaerobic digestion of source-separated organic waste with the gasification and biomethanation of wood pellets to increase both quality and productivity of biomethane, obtaining a potential increase of 161% in the production of biomethane compared to the stand-alone anaerobic digestion process. Similarly, Guiot *et al.*³⁵ estimated the potential of the conversion of municipal solid waste through anaerobic digestion of the easily digestible organic fraction and syngas biomethanation of the non-digestible organic fraction, resulting in a production of biomethane of about five times higher than the stand-alone anaerobic digestion of municipal solid waste. Other potential benefits are the use of biochar produced during the thermochemical treatment of the biomass as a support for biofilm formation or as an *in situ* biogas upgrading agent during the anaerobic digestion process.^{36,37} Therefore, there are several synergies that could be exploited upon the combination of these technologies.

Progress in syngas biomethanation and ongoing research

Despite the potential benefits of the syngas biomethanation process, there are still important bottlenecks that need to be addressed in order for this technology to be commercially applicable. One of the main shortcomings of continuous syngas fermentation processes is the limited mass transfer rate of H₂ and CO due to the low solubility of these gases in the liquid medium. The low cell growth rate of anaerobic micro-organisms is another limiting factor since the low cell productivities of continuous processes result in low volumetric productivities of CH₄. The fundamental aspects of the microbial metabolism of the micro-organisms carrying out the biomethanation of syngas have been thoroughly studied over the last

few decades. Yet, studies on the behavior of microbial consortia under different operating conditions still need to be conducted to improve our understanding of the microbial interactions within microbial consortia and achieve an optimal performance in microbial consortia-driven processes. The effect of operational parameters such as pH, temperature, gas partial pressure and syngas impurities were recently reviewed in the frame of syngas fermentation to ethanol and other products.^{2,4,5,38,39} Thus, this review focuses on the progress made in the above-mentioned aspects of syngas biomethanation processes over the last years, laying special emphasis on the role of microbial interactions within syngas-converting mixed microbial consortia.

Microbial growth on synthesis gas and syntrophic relationships in undefined mixed microbial consortia

The main components of synthesis gas (H₂, CO₂, and CO) can sustain growth of a wide array of micro-organisms belonging to different ecological niches such as certain fungi,⁴⁰ algae,⁴¹ photosynthetic bacteria,⁴² hydrogenogenic bacteria⁴³ and archaea,⁴⁴ sulfate-reducing bacteria⁴⁵ and archaea,⁴⁶ acetogenic bacteria⁴⁷ and methanogenic archaea⁴⁸ among others. However, during anaerobic growth only acetogens, methanogens, sulfate-reducers, and hydrogenogens can use either CO or H₂/CO₂ as the sole carbon and energy source.^{49,50} These groups are physiologically and phylogenetically diverse, although they all share common metabolic features such as the fact that acetyl-CoA plays a central role during the assimilation of both H₂/CO₂ and CO in all of them, and CO itself is a necessary intermediate for the fixation of CO₂ by acetogens and methanogens.⁵¹⁻⁵³ Therefore, the presence of CO dehydrogenases (CODH) is also a common thread in the metabolism of these micro-organisms. However, the function of their CODH differs in that they can either oxidize CO, synthesize acetyl-CoA or cleave acetyl-CoA in a variety of independent energy-yielding pathways in each of these microbial groups.⁵⁴

The anaerobic assimilation of CO and H₂/CO₂ can be categorized in the following four distinct activities according to their final metabolic product: hydrogenogenesis (including hydrogenogenic bacteria and archaea, and carboxydrotrophic hydrogenogenic sulfate-reducers⁵⁵), sulfidogenesis (including carboxydrotrophic sulfidogenic sulfate-reducers^{52,55}), carboxydrotrophic and hydrogenotrophic acetogenesis,^{56,57} and carboxydrotrophic and hydrogenotrophic methanogenesis.^{52,58} The biochemistry

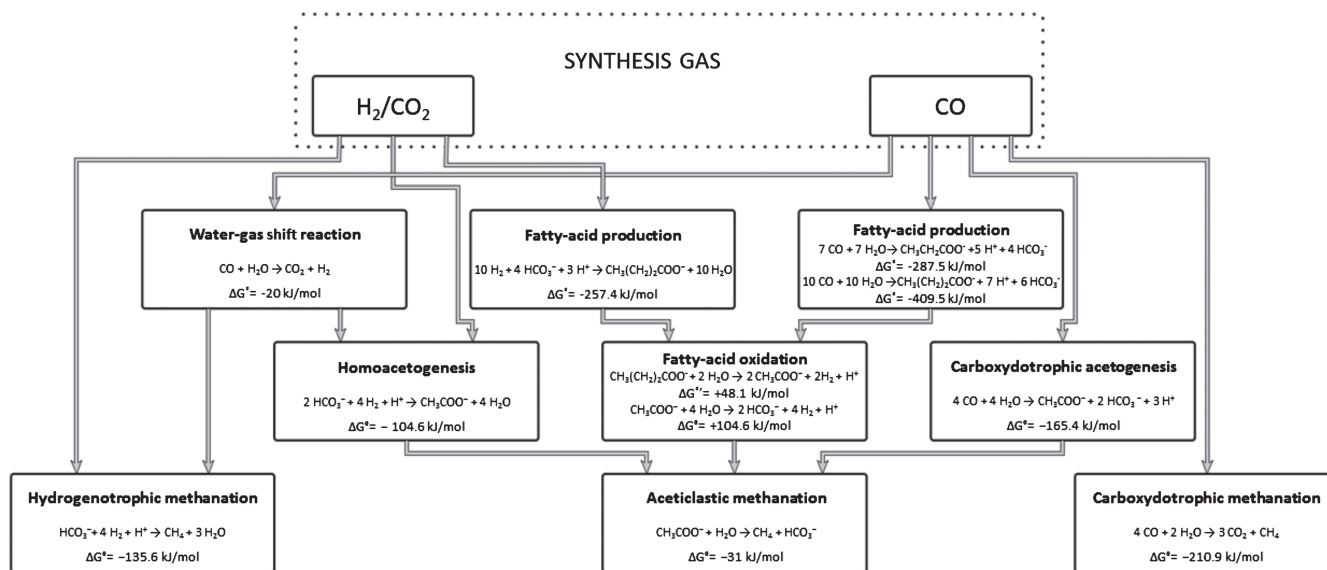


Figure 1. Pathways leading to the production of methane. The standard Gibbs free energy change (ΔG°) was calculated according to Thauer *et al.*⁸⁹

of these respiratory processes has been extensively reviewed by several researchers in recent years.^{52,53,55–59}

Thus, this section focuses on the microbial interactions prevailing in syngas-converting microbial consortia during the production of methane.

A microbial consortia-driven process of syngas biomethanation sustains a variety of microbial groups, such as those mentioned, which develop a chain of syntrophic interactions resulting in the production of CH_4 as the only end product of the fermentation. Thus, the conversion of syngas into CH_4 can take place either directly through the conversion of both CO and H_2/CO_2 by carboxydrotrophic and hydrogenotrophic methanogenesis, or indirectly through the conversion of syngas into methanogenic precursors such as acetate, H_2 and formate, followed by aceticlastic and hydrogenotrophic methanogenesis. Additionally, acetogenic bacteria have been reported to produce other by-products besides acetate, like ethanol,⁶⁰ butyrate,⁶¹ and butanol,⁶² which could be further converted into acetate and ultimately into CH_4 . Therefore, a microbial consortium may convert syngas into CH_4 through a complex network of interconnected biochemical reactions as shown in Fig. 1. However, the microbial interactions within a stable and structured microbial consortium do not simply consist of cross-feeding relationships, as there are other possible microbial interactions besides cross-feeding, like synergistic interactions between different species and mutual exclusion relationships between metabolically competitive populations.

Cross-feeding relationships

Despite the multiple pathways through which syngas can be converted into CH_4 , several studies have reported the preferential use of certain pathways within the consortium during the biomethanation of syngas. Guiot and Cimpoia⁶⁴ evaluated the mesophilic and thermophilic methanogenic potential of anaerobic granules from a UASB plant during the conversion of CO and syngas, observing that CO was predominantly converted through hydrogenotrophic methanogenesis combined with CO -dependent H_2 formation. In this study, formation of volatile fatty acids (VFA) was also observed, although only in trace amounts consisting of mainly acetate; however, when H_2 and CO_2 were also added as substrates, the amount of VFA's produced increased. In turn, Navarro *et al.*⁶⁵ found that CO was converted into CH_4 through acetate as a main intermediary product during inhibition experiments (based on the use of BES and vancomycin for inhibiting the methanogenesis and acetogenesis, respectively) at mesophilic conditions using a similar anaerobic granular sludge. These results are in line with the findings of other studies using the same inhibitors, in which acetate was found to be the main intermediate product during the conversion of CO into CH_4 at mesophilic conditions, and H_2 at thermophilic conditions.⁶⁶ All these studies concluded that the carboxydrotrophic methanogenic activity was negligible for the anaerobic sludges tested. Similar results were obtained while studying the structure and diversity of microbial

consortia on a simultaneous process of thermophilic anaerobic digestion of sewage sludge and CO biomethanation, in which the population of hydrogenotrophic methanogens increased upon addition of CO into the bioreactor due to the higher production of H₂ from CO.⁶⁷ In turn, in a similar study at mesophilic conditions, Wang *et al.*⁶⁸ found that the addition of CO in the bioreactor resulted in a clear increase of hydrogenotrophic microbial groups while the population of acetoclastic methanogens remained at high levels. They concluded that CO was converted to both H₂ and acetate, which were further converted into CH₄ by both direct hydrogenotrophic methanogenesis, and indirect acetogenesis and acetoclastic methanogenesis. Thus, it appears that the biomethanation of syngas by mixed microbial consortia generally takes place through indirect conversion rather than direct, with acetate and H₂ being the most common methanogenic precursors.

Mutualistic interactions

There are still other possible metabolic interactions exhibiting mutualistic properties that could be developed among different members of a mixed microbial consortium. An example of such mutualistic relationships is the interspecies diffusion of electron carriers like H₂ or formate between syntrophic bacteria and methanogenic archaea, which could remain unnoticed due to the low concentration and fast turnover of these compounds.⁶⁹ The syntrophic bacterial genus *Smithella*, a fatty acid-oxidizer, was found to be relatively dominant during the simultaneous biomethanation of sewage sludge and CO; however, whether its function was relevant to the biomethanation of CO was not determined.⁶⁸ Similarly, Navarro *et al.*⁷⁰ found that the population of *Geobacter unaniireducens*, a syntrophic acetate-oxidizing bacterium, increased in a granular sludge after a long-term exposure to CO. The process of interspecies diffusion of electron carriers was studied by Boone *et al.*⁶⁹ in co-culture experiments with the fatty acid-oxidizing bacterium *S. wolfei* and the methanogen *M. formicicum* using butyrate as substrate. When these species were co-cultured, the production of CH₄ proceeded exponentially while the concentration of H₂ remained constant at 63 nM until depletion of butyrate, after which the concentration of H₂ dropped to 35 nM.⁶⁹ Similarly in the same study, a co-culture of *S. wolfei* and *Desulfovibrio* sp. strain GII was incubated with butyrate and sulfate as substrates, where the concentration of H₂ stabilized at 27 nM for 2 days until sulfate was depleted. This illustrates the importance that such interspecies diffusion of electron carriers may have during the conversion of fatty acids to

methanogenic precursors in mixed microbial consortia. However, the Gibbs free-energy change for, for example, butyrate oxidation to acetate, H₂ and CO₂ is only favorable at very low P_{H₂} (<10⁻⁴ atm). This type of symbiotic relationship is thus only feasible in those cases in which H₂ is kept at low concentrations due to the continuous removal of H₂ by, for example, hydrogenotrophic methanogens. Nonetheless, recent studies have demonstrated that *Geobacter* species and *Methanosaeta* species are capable of direct interspecies electron transfer as an alternative mechanism to H₂ or formate transfer.⁷¹

Further symbiotic interactions have also been reported in other co-culture experiments. Parshina *et al.*⁷² found that the pure cultures of *D. kuznetsovii* and *D. thermobenzoicum* subsp. *thermosyntrophicum* were capable of chemolithotrophic growth on CO levels up to 0.70 atm when cultivated in presence of sulfate. However, when these species were co-cultured with *C. hydrogenoformans*, they were able to grow at 1 atm of CO through the reduction of sulfate using the H₂ produced by the hydrogenogen.⁷² Similar results were obtained by Rajagopal *et al.*⁷³ who studied the co-culture of *D. vulgaris* and *M. barkeri* in the absence of sulfate. The pure culture of *D. vulgaris* exhibited partial inhibition of the production of H₂ from pyruvate upon addition of CO to the culture, as the rate of H₂ production from pyruvate alone and from both substrates remained unchanged. Nonetheless, when *D. vulgaris* was co-cultured with *M. barkeri* using lactate as substrate, the injection of CO resulted in a H₂ burst along with a parallel increase in the rate of CH₄ production with no apparent inhibitory effect of CO.⁷³ Additional symbiotic interactions have also been observed in experiments using undefined mixed microbial consortia. Navarro *et al.*⁷⁰ compared the performance of crushed granular sludge and whole sludge granules fed on CO, finding that the higher organization of the granular sludge enhanced the CH₄ production rate due to the protection of the inner layers of the granule against the toxicity of CO. Therefore, these cases show that the metabolic interaction between microbial groups can generate synergistic effects due to the lower concentration of CO in the medium or in the inner layers of the granules, enhancing both the growth and the resiliency of the microbial community as a whole.

Mutual exclusion interactions

The structure of a microbial consortium is not only determined by interactions of mutualistic nature since mutual exclusion relationships, based on competition for common substrates, also play an important role on the definition of

the community structure. In presence of sulfate, all active microbial groups during syngas biomethanation including acetogens, methanogens, sulfate-reducers and hydrogenogens compete for common substrates such as CO, H₂ or acetate. The competition for H₂ is generally ruled by sulfate-reducers, since both the kinetic properties of this group and the thermodynamics of sulfate reduction are more favorable than in homoacetogenesis and methanogenesis.^{74,75} However, in most cases the activity of sulfate-reducers can be easily suppressed by controlling the sulfate content in the medium in order to favor the methanogenesis given the low content of sulfur oxides in syngas. According to Xu *et al.*,³⁸ the highest concentration of sulfur compounds reported in biomass-derived syngas corresponds to 0.055 mol% for SO₂, and 0.0001 mol% for H₂S and COS. Moreover, the outcome of the competition for H₂ appears to depend on additional factors, since in contrast to the previous statement hydrogenotrophic methanogens have also been reported to outcompete sulfate-reducers. Sipma *et al.*⁷⁶ observed that sulfate-reducers were clearly outcompeted by hydrogenotrophic methanogens during operation of a gas-lift reactor fed on CO and sulfate at thermophilic conditions. In this study, the dominance of hydrogenotrophic methanogens was attributed to the higher growth rates of this microbial group at the operating conditions investigated.⁷⁶ The competition between homoacetogens and hydrogenotrophic methanogens for H₂ was studied by Liu *et al.*,⁷⁷ finding that the kinetic constants K_s and μ_{max} of homoacetogens were respectively 10 times higher and 4 times lower than those of hydrogenotrophic methanogens. Hence, homoacetogens were clearly outcompeted by the latter group under substrate-limiting conditions (low P_{H₂}). However, homoacetogens were able to compete for H₂ at high P_{H₂}, contributing through aceticlastic methanogenesis to the formation of 40% of the CH₄ produced.⁷⁷

The competition for CO in mixed microbial consortia has not been thoroughly studied, although the outcome of the competition can be predicted based on the kinetic properties reported for these microbial groups. Carboxydophilic methanogens typically have long doubling times ranging from 24 h to 200 h.^{48,78} In turn, the doubling times exhibited by acetogenic bacteria generally oscillate between 1.5 h and 16 h reported for *R. Productus* and *C. thermoaceticum*, respectively.^{79,80} Hydrogenogenic growth supports different doubling times depending on the microbial group, being 1–2 h for thermophilic hydrogenogens and 4.8–8.4 h for phototrophic bacteria.^{81,82,76} Therefore, the comparison of the growth kinetics on CO of these microbial groups indicates that methanogens will

be easily outcompeted in a mixed microbial consortium. However, it is likely that the outcome of the competition between hydrogenogenic and acetogenic bacteria is not ultimately dependent upon their kinetics given the similarity of the doubling times reported.

All these microbial interactions can have an influence, either positive or negative, on the structure and diversity of a microbial community, ultimately affecting the performance of the consortium. Therefore, knowledge on the type of interactions prevailing among the members of a microbial consortium is fundamental for the control and optimization of the process.⁸³ However, the performance of a consortium is also strongly influenced by the operating conditions of the process, thus requiring the integration of all aspects determining the outcome of the process for optimal process control.

Influencing factors in syngas biomethanation

The operating parameters of biological processes have a strong impact on the performance of the culture in terms of productivity as these affect several aspects of microbial growth. Pure culture-based processes are generally operated at conditions favoring optimal growth and productivity based on the characteristics and requirements of a particular strain. However, the members composing a mixed microbial consortium for syngas biomethanation rarely share the same optimal growth conditions, which make the selection of operational parameters a critical step when it comes to optimizing the process. In this section, the influence of parameters such as temperature, pH and gas composition on the CH₄ yield and production rate of syngas-converting consortia is reviewed.

pH

The pH is an important parameter for microbial growth due to its influence on the regulation of the metabolism and the bioenergetics of micro-organisms as it causes changes in the intracellular pH and the electrochemical gradient across the membrane. Acetogenic bacteria are perhaps the most versatile microbial group as they are able to tolerate a wide range of pH including both acidic and alkaline conditions,⁵⁶ although they are known to shift their generally acidogenic metabolism towards solventogenesis when decreasing the pH.^{84,85} The hydrogenogenic microbial group including phototrophic and hydrogenogenic bacteria generally exhibit optimal growth at neutral pH.⁵⁵ In turn, most methanogens grow

optimally at either neutral or slightly alkaline pH ranging from 6.8 to 8.5,⁵⁸ being partially inhibited when decreasing the pH. Consequently, most syngas biomethanation processes are operated at pH close to neutrality, between 7.0 and 7.6, to favor the methanogenesis and avoid the accumulation of liquid products (Table 2). Nevertheless, the influence of the pH has not been thoroughly studied in syngas biomethanation processes. So far, only Pereira *et al.*⁸⁶ have investigated the biomethanation of syngas using a mixed culture approach under different pH conditions. This study reported that the combination of low pH and high pressures of syngas (2.5 atm) resulted in high inhibition of the methanogenic activity, obtaining the lowest production of CH₄ among all conditions tested.⁸⁶

Temperature

The temperature is one of the most influential factors in syngas biomethanation processes as it affects several aspects of the performance of mixed microbial consortia. As mentioned already, the temperature of the broth has been reported to have an effect on the microbial interactions among members of microbial consortia as it appears to determine the predominant metabolic pathways used by the consortia. Several studies on biomethanation of CO indicate that acetate is the main precursor of the methanogenesis at mesophilic conditions, whereas H₂ is a more relevant precursor at thermophilic conditions. This could be explained by the higher diversity of carboxydrotrophic hydrogenogenic bacteria in thermophilic environments. However, another possible explanation could be the fact that H₂-producing reactions become more exergonic with increasing temperatures,⁸⁷ favoring a higher hydrogenogenic conversion of CO at thermophilic conditions. In either case, it has been shown that these changes in the microbial structure of the consortia due to higher temperatures lead to higher conversion rates in syngas biomethanation processes. Guiot and Cimpoia⁶⁴ compared the rates of CH₄ production of a granular sludge at mesophilic and thermophilic conditions, finding that the CH₄ productivity at thermophilic conditions (5.6 mmol/g VSS/d at 60°C) was much higher than that at mesophilic conditions (1 mmol/g VSS/d at 35°C). Similarly, another study investigated the correlation between the rates of conversion of CO and the temperature, observing that the rates of conversion of CO and the productivity of CH₄ increased gradually from 40°C onwards until a maximum was reached at 55°C.⁶⁶ Nonetheless, despite the higher conversion rate and productivity, the increase in temperature also poses certain drawbacks related to the lower solubility

of the gases, which could lead to mass transfer limitations in thermophilic processes.

Gas partial pressure

The effects of the composition of synthesis gas are mainly associated with mass transfer processes of the constituents of syngas, which are dependent on both the mass transfer coefficient ($k_L a$) and consequently on the characteristics of the reactor, and the partial pressure of these gases as the driving force for their transportation to the liquid phase. In this section, the effects of the partial pressures of the main components of syngas are discussed, while the effects of the mass transfer rates are addressed in the section for process configurations.

Carbon monoxide, besides being a substrate for carboxydrotrophs, is also a well-known inhibitor for most carboxydrotrophic microbial groups. Carboxydrotrophic methanogens and sulfate-reducers appear to be the most sensitive, tolerating partial pressures of CO (P_{CO}) between 0.5 and 1.0 atm and 0.2–0.5 atm respectively, with some exceptions.^{45,48,78,88} In turn, both acetogens and hydrogenogens exhibit a higher tolerance to CO, generally being able to grow at P_{CO} higher than 1 atm.^{4,55} Nevertheless, the effects of CO on syngas biomethanation processes are not limited to direct inhibition of carboxydrotrophic growth, as other non-carboxydrotrophic microbial groups with a significant role might also be affected, including fatty-acid oxidizing bacteria, aceticlastic and hydrogenotrophic methanogenic archaea.

In syngas biomethanation processes, the increase in P_{CO} generally results in partial inhibition, ultimately affecting the yield and the productivity of CH₄. The effects on the CH₄ yield were evaluated on a mesophilic granular sludge fed on syngas, in which a decline in the CH₄ yield was observed while increasing the total pressure of syngas from 1 to 2.5 atm due to the inhibition of the methanogenic activity.⁸⁶ In turn, the specific carboxydrotrophic and methanogenic activities of a mesophilic granular sludge under different initial P_{CO} were studied by Navarro *et al.*,⁷⁰ observing that the rate of consumption of CO increased with the amount of CO supplied until a maximum was reached at a P_{CO} of 0.5 atm. However, the rate of production of CH₄ reached its maximum at 0.2 atm of CO, followed by a gradual decline along with the increase of P_{CO} until the methanogenic activity was totally inhibited at 1 atm of CO.⁷⁰ Additionally, in this study a shift in the metabolic pathways with increasing P_{CO} was observed, in which aceticlastic methanogenesis was displaced by hydrogenotrophic methanogenesis between 0.5 and 1 atm.

Table 2. Overview of syngas biomethanation process configurations and operating conditions.

Micro-organism	Reactor	Operation mode	Gas composition (%)	Co-substrate	Gas rec. rate (ml/min)	Gas flow rate (ml/min)	H ₂ flow rate (mmol/l/d)	CO flow rate (mmol/l/d)	CH ₄ prod. (mmol/l/d)	Yield ⁱ (mol/mol)	T (C°)	pH	Ref.
Cow pasture sludge	BC ^a	Batch	H ₂ /CO ₂ (-)	-	300	-	1380	-	300	0.22-0.26	55	7.4	Bugante et al. ¹⁰⁷
Cow pasture sludge	BC ^a	Batch	CO (40)	-	300	-	-	480	120	0.25	55	7.4	Bugante et al. ¹⁰⁷
Sewage plant anaerobic sludge	TB ^b	Cont.	H ₂ /CO ₂ (-)	-	-	n.d.	268	-	66.5	0.248	37	7.2	Burkhardt et al. ¹⁰³
Fruit processing plant granular sludge	GL ^c	Cont.	CO (41)	-	1150	57.5	n.d.	-	2.92 ^h	0.228	35	7.1	Guiot et al. ⁶⁴
Triculture (<i>R. rubrum</i> , <i>M. barkeri</i> , <i>M. formicicum</i>)	TB ^b	Cont.	CO/CO ₂ /H ₂ 55.6/9.7/19.7	light	n.d.	70	n.d.	n.d.	48-72	0.2	37	n.d.	Kimmel et al. ¹⁰⁵
Triculture (<i>R. rubrum</i> , <i>M. barkeri</i> , <i>M. formicicum</i>)	TB ^b	Cont.	CO/CO ₂ /H ₂ 54.4/9.7/21.1	light	n.d.	174	n.d.	n.d.	9.6	0.2	37	n.d.	Kimmel et al. ¹⁰⁵
Granular sludge	MOBB ^d	Cont.	CO/CO ₂ /H ₂ (60/10/30)	-	600	100	24.2	54	73	0.6-0.8	35-37	5.8-6.7	Pereira ¹⁰⁹
MSW sludge	RMB ^e	Semi-Cont.	CO/CO ₂ /H ₂ (55/10/20)	3.4 g COD VFAs/l/d	300	n.d.	7	15	8.3	n.d.	55	n.d.	Westman ¹¹⁰
Anaerobic sewage sludge	STR ^f	Cont.	H ₂ /CO ₂ (-)	-	n.d.	700	1344	-	352.8	n.d.	37	n.d.	Wise ¹⁰²
Triculture (<i>R. rubrum</i> , <i>M. barkeri</i> , <i>M. formicicum</i>)	TB ^b	Cont.	CO/CO ₂ /H ₂ (55.6/9.9/19.7)	light	n.d.	300	n.d.	n.d.	72	0.214	37	6.8-7.2	Klasson ¹⁰⁸
Triculture (<i>R. rubrum</i> , <i>M. barkeri</i> , <i>M. formicicum</i>)	PBC ^g	Cont.	CO/CO ₂ /H ₂ (55/9.6/20.4)	light	n.d.	80	n.d.	n.d.	4.8-7.2	0.214	34	6.8-7.2	Klasson ¹⁰⁸

^abubble column; ^btrickle-bed; ^cgas-lift; ^dmulti-orifice oscillatory baffled bioreactor; ^ereverse membrane bioreactor; ^fstirred tank reactor; ^gpacked bubble column; ^hmmol/g VSS/d.

ⁱYield expressed in mol CH₄/mol syngas (H₂ + CO)

Thus, these studies clearly show that CO exerts a strong inhibitory effect over all microbial groups of the microbial consortium. Nevertheless, the differences observed between the carboxydrotrophic and the methanogenic activities illustrate a distinctive inhibition over acetoclastic methanogens, which appear to be less tolerant than acetogenic, hydrogenogenic bacteria, and hydrogenotrophic methanogenic archaea. The lower tolerance of the methanogenic group was also evident during the enrichment of a thermophilic methanogenic microbial consortium using increasing amounts of syngas along the successive transfers.⁸⁹ In these experiments, both H₂/CO₂ and CO were initially converted into CH₄ as the only end product. However, the enriched consortium lost its methanogenic activity at the fourth transfer due to the inhibition caused by the increasing partial pressure of syngas, resulting in the production of H₂ as an intermediate product and the accumulation of acetate and propionate as end products.⁸⁹

The concentration of H₂ seems to have a milder influence on the performance of the consortium, although changes in the P_{H₂} have been reported to have an effect on the microbial activity. The activity of the hydrogenase of a clostridial species denoted as P11 was studied under increasing P_{H₂}, finding that higher P_{H₂} enhanced the activity of the hydrogenase.⁹⁰ However, the efficiency of the hydrogenase decreased as the pressure of H₂ built up due to the saturation of the enzyme.⁹⁰ These findings are in line with the results of other experiments using a mixed culture approach, in which the production rate of CH₄ increased sensibly from 0.035 mmol/h to 0.072 mmol/h upon an increase of the initial pressure of H₂/CO₂ from 1 to 5 atm,⁹¹ as it can be noted that the increase in the productivity appears not to correspond proportionally to the increase of pressure. Therefore, it is likely that the hydrogenases of other H₂-utilizing micro-organisms, for example hydrogenotrophic methanogens, are also affected by high P_{H₂} resulting in lower rates of conversion. Additionally, in this study the structure of the microbial community was found to be affected by the P_{H₂}, reducing its diversity as the P_{H₂} increased due to the more stringent conditions.⁹¹

Impurities of synthesis gas

An additional aspect of the composition of syngas is the content of impurities typically found in the raw syngas, which may affect the process of syngas biomethanation either causing perturbations in the performance of the consortia or altering the operating parameters such as pH or redox. Impurities such as tars, NO_x and NH₃ have

been found to inhibit the activity of several enzymes in acetogenic bacteria.^{38,92,93} On the other hand, the sulfur gases H₂S and COS barely affected the growth and the substrate uptake rate of the acetogen *R. productus* and the methanogen *M. barkeri*, whereas the hydrogenogen *R. rubrum* and the methanogen *M. formicicum* were strongly inhibited even at low concentrations of these gases.⁹⁴ Thus, each of the microbial groups appears to be affected differently by the impurities. Guiot *et al.*⁹⁵ studied the effects of HCN, NH₃, H₂S and aromatic hydrocarbons on the overall performance of a methanogenic anaerobic sludge. The results of this study showed that the performance of the mixed culture was not significantly affected at levels below 500 ppm, 50 ppm, and 1 ppm of NH₃, H₂S and aromatic hydrocarbons, respectively. However, HCN was found to inhibit the acetoclastic methanogenic activity at levels below 15 ppm. It was thus concluded that acetoclastic methanogens were generally the most sensitive microbial group, although the activity of all microbial groups was inhibited at higher levels of these impurities. Despite it has been shown that the activity of microbial consortia is not significantly affected by low levels of impurities, further research in this area is still necessary in order to establish the minimum gas clean-up requirements of raw syngas as these may have an important influence on the overall efficiency of syngas biomethanation processes.

Some of the influencing factors discussed here, such as the effect of the temperature and the growth inhibition due to high P_{CO}, have been studied thoroughly in microbial consortia-driven syngas biomethanation processes. Nevertheless, studies on the influence of pH and the impurities of syngas are still very limited. Additionally, other factors such as the redox potential and the trace metal content of the media that have been studied in pure culture experiments,^{96,97} have not been investigated yet in microbial consortia. Studying the potential interactions among the influencing factors discussed in this section could also provide more insights on possible synergistic effects on the behavior of microbial consortia. Therefore, further research on both the influencing factors and their potential interactions is still necessary in order to fully comprehend their influence over the performance of each microbial group and the consortium as a whole.

Process configurations

Besides the limitations related to the inhibitory effects of CO and other aforementioned factors, syngas biomethanation processes are often restricted by poor gas-to-liquid mass transfer and low cell concentrations in the reactor,

which ultimately reduce the volumetric productivity of CH₄. In an attempt to address these shortcomings, syngas biomethanation processes have been studied in a number of process configurations including both batch and continuous operating modes and several reactor designs, each one of them having specific drawbacks and advantages. The main characteristics, yields and CH₄ productivities obtained in such process configurations are summarized in Table 2. Different syngas fermentation process configurations and bioreactor design issues have been reviewed before for the production of H₂, ethanol and other potential products.^{2,4,9,98} Therefore, this paper covers only the findings related to syngas biomethanation.

Stirred-tank reactors

The traditional stirred-tank reactors have been widely used in syngas fermentation processes.^{60,99–101} In this type of reactor, the volumetric mass transfer coefficient (K_La) is affected by several factors such as the geometry of the reactor, the impeller configuration, the agitation speed, and the gas flow rate. Typically, higher mass-transfer rates are attained by increasing both the agitation speed and the gas flow rate, which increase the gas-liquid interfacial area due to the smaller size of the bubbles. Klasson *et al.*³² studied the influence of these parameters on the K_La during the biomethanation of CO using a triculture of *R. rubrum*, *M. formicicum* and *M. barkeri*. The K_La was observed to increase from 28.1 h⁻¹ to 101.1 h⁻¹ when increasing the agitation speed from 300 rpm to 450 rpm. However, the authors also observed that the efficiency in the conversion of CO decreased sharply while the gas loading rate increased, being 90% the maximum conversion efficiency reported at a gas loading rate of around 0.2 h⁻¹. It can be thus concluded that although relatively high K_La values are attainable in this type of reactors, a high productivity of CH₄ can only be achieved at the expense of low conversion efficiencies owing to the high gas flow rate needed. An alternative strategy for increasing the productivity of CH₄ is to increase of the concentration of microbial biomass in the bioreactor. This possibility was studied in a continuous process of biomethanation of H₂ and CO₂ using a mixed culture from sewage sludge by including a cell recycling stream into the bioreactor.¹⁰² The cell recycle resulted in an increase of the cell concentration from 2.5 g/L to 8.3 g/L, boosting the volumetric productivity of CH₄ from 1.3 L_{CH₄}/L/h to 4 L_{CH₄}/L/h. Therefore, an increase in the productivity of CH₄ can be achieved through both cells recycling and enhancing the gas-to-liquid mass transfer. Other considerations such as the cost of operation should

also be accounted when scaling up a process as the high energy requirements of maintaining a high mixing regime in large scale stirred tank reactors often can render this process not economically feasible.⁹

Trickle-bed reactors

Trickle-bed reactors are a suitable alternative to stirred tank reactors in terms of costs of operation as this type of reactors do not require mechanical mixing. These reactors generally offer a more efficient gas-to-liquid mass transfer while maintaining low gas and liquid flow rates due to the higher contact surface area between the gaseous substrate and the liquid film on the packing material. The influence of the liquid recirculation rate and the thickness of the liquid film on the mass transfer and the productivity of CH₄ was studied during the biomethanation of H₂ and CO₂ using anaerobic sewage sludge as inoculum.¹⁰³ A correlation between increasing productivities of CH₄ and decreasing liquid recirculation rates was observed in this study, concluding that a high conversion (nearly 100%) and productivity (1.49 L_{CH₄}/L/d) could be achieved without gas recirculation by just increasing the H₂ loading rate while decreasing the liquid recirculation rate. Thus, trickle bed reactors seem a promising option for their application in syngas biomethanation as the plug flow regime of these reactors allows high gas loading rates while maintaining high productivities and conversion efficiencies. Nevertheless, as found in other processes, compromised stability of continuous processes due to channeling of the gaseous substrate through the packing material attributed to the excessive accumulation of microbial biofilm was observed during the biomethanation of H₂ and CO₂.¹⁰⁴ Kimmel *et al.*¹⁰⁵ compared the performance of two trickle bed reactors with different diameters on the process of syngas biomethanation using a triculture of *R. rubrum*, *M. formicicum* and *M. barkeri*. The productivity of CH₄ in the smaller reactor was observed to increase as the gas loading rate increased, reaching a maximum productivity of 2–3 mmol CH₄/L/h. However, the productivity of the larger reactor barely reached 0.4 mmol CH₄/L/h at very low gas loading rates, showing a decreasing trend as the gas loading rate was raised. Apparently, the lower porosity along with the smaller size of the packing material used in the smaller reactor favored an enhanced productivity as the lower pore size of the packing promoted a better distribution of the liquid medium. Therefore, trickle bed reactors have been successfully applied to syngas biomethanation processes achieving high productivities and conversion efficiencies. Nevertheless, there are still certain

aspects of the continuous operation of these reactors such as biofilm accumulation, porosity and the size of the packing material that need further study for attaining full exploitation of their potential.

Bubble column and gas-lift reactors

The use of bubble columns and gas-lift reactors has also been studied in syngas biomethanation processes as they offer a number of benefits such as high gas-liquid interfacial area, high volumetric mass transfer coefficient, non-mechanical mixing, and relatively low cost of operation. As there is no mechanical mixing, the mass transfer coefficient of these reactors generally depends on the gas flow rate and the size of the bubbles. The effect of these operational parameters on the mass transfer of CO was studied in both a bubble column and a gas-lift reactor, showing that the K_La increases along with the increase of the gas flow rate and the decrease of the pore size of the column diffuser.¹⁰⁶ The maximum K_La values reported for the bubble column and the gas-lift reactor were 78.8 h^{-1} and 91.1 h^{-1} , respectively, when a gas flow rate of 5000 sccm was combined with a 20 μm bulb diffuser.¹⁰⁶ Another common feature of these reactors is the need of applying a high gas recirculation rate in order to attain a relatively high conversion efficiency for sparingly soluble gases such as H_2 and CO. Guiot *et al.*⁶⁴ studied the effects of different gas recirculation rates during the biomethanation of CO in a gas-lift reactor using granular sludge. In these experiments, the insufficient gas holdup when gas recirculation was not applied resulted in a CO conversion efficiency as low as 4%; however, when the gas recirculation-to-feed ratio was set to 18:1 the conversion efficiency increased to 70%, obtaining an improvement of the productivity from 0.49 $\text{mmol CH}_4/\text{g VSS/d}$ to 2.55 $\text{mmol CH}_4/\text{g VSS/d}$. The increase in partial pressure of CO in the feed was also observed to have a positive impact on the productivity, although when both high gas recirculation rates and high CO partial pressure were applied the conversion efficiency dropped significantly due to the inhibitory effects of CO.⁶⁴ Similar results were obtained in batch experiments using a bubble column, as the productivity of CH_4 from H_2 and CO_2 increased from 480 mmol/L/d to 660 mmol/L/h while raising the gas recirculation rate from 18 L/h to 40 L/h .¹⁰⁷ The continuous biomethanation of syngas has also been tested in a packed bed bubble column using a triculture of *R. rubrum*, *M. formicicum* and *M. barkeri*.¹⁰⁸ A maximum conversion efficiency of 79% was reached at the lowest gas flow rate tested (1.3 sccm) without gas recirculation, obtaining a rather low productivity of CH_4 of around

0.2 mmol/L/h .¹⁰⁸ Higher productivities (0.4 $\text{mmol CH}_4/\text{L/h}$) could be achieved when raising the gas flow rate to 13.3–16.6 sccm; this however had a dramatic impact on the conversion efficiency as it dropped from 79% to 20–25%. The authors concluded that the low productivity was caused by mass transfer limitations and the high porosity of the packing material given the low K_La value obtained (3.5 h^{-1}). It seems that despite the simplicity of the design of these reactors, each of them has a good potential for their application in syngas biomethanation processes. However, there are several key operational parameters that need to be optimized in order to achieve a high productivity of CH_4 while maintaining relatively high conversion efficiencies.

Other reactor designs

Other reactor designs have also been studied for improving the productivity of CH_4 in syngas biomethanation processes by either overcoming the mass transfer limitations or increasing the concentration of cells in the bioreactor. A novel multi-orifice oscillatory baffled bioreactor with a unique baffle design for improving both mixing and mass transfer rates was fully characterized and tested for the biomethanation of syngas using a mesophilic granular sludge as inoculum.¹⁰⁹ The maximum productivity achieved with this bioreactor was 73 $\text{mmol CH}_4/\text{L/d}$ at the maximum flow rate tested (100 sccm). Nonetheless, as the gas loading rate was raised the conversion efficiency dropped as a result of the intensive mixing at high flow rates. Another reactor design intended to achieve total retention of cells into the bioreactor was also studied for its application in syngas biomethanation. This design consisted in a reverse membrane bioreactor, in which the micro-organisms from a thermophilic MSW sludge were membrane encased prior to their inoculation in the bioreactor.¹¹⁰ The maximum productivity of CH_4 reported for the biomethanation of solely syngas was 0.109 $\text{L}_{\text{CH}_4}/\text{L/d}$ when using a gas flow rate of 200 sccm, which was comparable to the productivity of an analogous reactor operated with free cells.¹¹⁰ However, the increase of the gas loading rate and the organic loading rate by addition of VFA's as co-substrate resulted in a sharp increase in the productivity of CH_4 (0.186 L/L/d) in the reverse membrane reactor, whereas in the free cells reactor the productivity gradually decreased to 0.046 $\text{L}_{\text{CH}_4}/\text{L/d}$ as the cells were washed out due to the more stringent conditions.¹¹⁰ Thus, the use of these membranes seems to effectively maintain a high concentration of cells in the bioreactor under harsh conditions, yet the effect of the membranes on the transport

of the gaseous substrates to the micro-organisms still remains to be investigated.

As shown in this section, the productivity of CH_4 is highly dependent on the particular process configuration and type of reactor. A high productivity of CH_4 can be achieved in each type of reactor under specific process configurations. Generally, the most influential parameters affecting the productivity in continuous processes are the concentration of cells, the gas-to-liquid mass transfer, the gas and liquid flow rates, the recycle of these streams and the mixing regime. Nevertheless, the relevance of these parameters is different for each type of reactor. A common feature of stirred tank reactors, bubble columns and gas-lift reactors is that for a given gas loading rate there is a maximum conversion efficiency threshold as a result of the mixed-flow regime of these reactors when high gas inflow and gas recirculation rates are applied. In turn, trickle-bed reactors seem to outperform the other type of reactors in several aspects due to their plug-flow regime. However, the application of microbubble dispersion in stirred tank reactors, bubble columns and gas-lift reactors, not studied yet in syngas biomethanation processes, could enhance significantly the mass transfer and hence the performance of these reactors. Other aspects of the operation of these reactors such as scaling-up issues or economic considerations for each of the process configurations discussed, which have not been accounted for here, may also play a crucial role when it comes to determine the feasibility of these processes.

Kinetics and modeling of syngas biomethanation processes

Mathematical modeling of bioprocesses is usually applied in order to simulate and predict the outcome of different process configurations, as well as to optimize the process in terms of yield and productivity of the desirable product(s). Unstructured models are perhaps the most simplistic expression of mathematical models, using only a few state variables for describing the concentration profiles of microbial biomass, substrates and products.¹¹¹ However, unstructured kinetic models are frequently used as they are simple and can successfully simulate the effects of the main variables on the microbial growth and the productivity in batch and continuous processes, being thus a valuable tool for design and operation of bioprocesses.

Kinetic models used so far for the determination of the kinetic properties of several syngas-converting pure cultures under different fermentation conditions and process configurations are shown in Table 3. Vega *et al.*¹¹²

determined the kinetics of the growth of the acetogen *R. productus* on CO using a modified Monod equation in order to simulate the inhibitory effects of high P_{CO} . This model was then used for studying the conversion rate of CO as a function of the gas loading rate and the volumetric mass transfer coefficient in a stirred tank reactor and a bubble column. The growth kinetics of the acetogen *C. ljungdahlii* were determined using several dual-substrate kinetic models in order to study the effects of the initial pressure of syngas on the simultaneous consumption of H_2 and CO.¹¹³ Among all kinetic models tested in this study, the combination of Luong and Monod kinetics was found to give the best fitting for simulating growth on mixed substrates. Other kinetic models based on different equations have also been proposed. For instance, the kinetic parameters of the growth of *C. ljungdahlii* on CO and syngas were also determined using the Andrew equation and a novel equation for simulating microbial growth, cell decay and the inhibition of CO.¹¹⁴ Hydrogenogenic cultures have also been studied using kinetic models in order to determine the optimum process parameters for the continuous production of H_2 . A Monod chemostat model was used to determine the kinetic parameters of *R. rubrum* growing on CO during washout experiments in a stirred tank reactor with dual impellers.⁹⁹ The productivity of H_2 was then optimized by using this model to determine the optimum dilution rate for the particular process configuration of this reactor. Another hydrogenogen, *C. hydrogenoformans*, was characterized kinetically using the Han and Levenspiel model in order to study the effects of the P_{CO} and the influence of the ratio of substrate/biomass on the activity of the culture.¹¹⁵ The growth kinetics of other relevant microbial groups in syngas biomethanation processes such as methanogenic archaea have also been evaluated using a number of kinetic models based on Monod kinetics, the Andrew equation and a modified Gompertz model, among others.^{116–119} However, the influence of the partial pressure of CO on the kinetics of this microbial group has not been determined yet, as most of these studies have been carried out in the frame of anaerobic digestion processes.

Despite all microbial groups typically found in a syngas-converting microbial consortium have been characterized using kinetic models, a kinetic model able to describe the simultaneous growth of these microbial groups in syngas biomethanation processes has not been developed yet. The development of such a model, including, for example, the kinetic competition among microbial groups or the effects of the operating parameters on the growth of each microbial group, could contribute to improving

Table 3. Unstructured kinetic models used for several acetogens, hydrogenogens and methanogens.

Micro-organism	Kinetic model	Growth rate/Substrate-uptake rate equation	Empirical constants			Ref.
			μ_{max}	K_S	K_i	
<i>R. productus</i>	Andrew	$\mu = \frac{\mu_{max} P_{CO}^L}{K_S + P_{CO}^L + W}$	0.21 h ⁻¹	0.044 atm	$P_{CO}^L < 0.6$ atm; $W = \infty$ $P_{CO}^L < 0.6$ atm; $W = 3$ atm	Vega et al. ¹¹²
<i>C. ljungdahlii</i>	Luong + Monod	$\mu = \frac{\mu_{max}}{2 \left[\left(\frac{S_{CO}}{K_{S,CO} + S_{CO}} \right) \left(1 - \frac{S_{CO}}{S_m} \right)^n + \frac{S_{H_2}}{K_{S,H_2} + S_{H_2}} \right]}$	0.195 h ⁻¹	CO = 0.855 atm H ₂ = 0.412 atm	$S_m = 0.743$ atm $n = 0.465$	Mohammadi et al. ¹¹³
<i>C. ljungdahlii</i>	Andrew	$\mu = \frac{\mu_{max,CO} C_{CO}^*}{K_{CO} + C_{CO}^* + (C_{CO}^*)^2 / K_i}$	0.022 h ⁻¹	0.078 mmol CO/l	2 mmol CO/l	Younesi et al. ¹¹⁴
<i>R. rubrum</i>	Monod	$\mu = \frac{\mu_{max} C_S}{K_S + C_S}$	0.0225 h ⁻¹	0.13 gCO/l	–	Najafpour et al. ⁹⁹
<i>C. hydrogeniformans</i>	Han and Levenspiel	$k = k_{max} \left(1 - \frac{S}{S_I} \right)^n \frac{S}{S + K_m \left(1 - \frac{S}{S_I} \right)^m}$	8.2 molCO/gVSS/d	2.1 mM	SI = 1.37 mM $n = 1.4$ $m = 4.7$	Zhao et al. ¹¹⁵
<i>M. barkeri</i> 227	Andrew	$\mu = \frac{\mu_{max,ac} S_{ac}}{K_{S,ac} + S_{ac} + (S_{ac})^2 / K_i}$	0.038 h ⁻¹	1.75 g ac/l	7.37 g ac/l	Yang et al. ¹¹⁷
<i>M. barkeri</i> MS	Andrew	$\mu = \frac{\mu_{max,ac} S_{ac}}{K_{S,ac} + S_{ac} + (S_{ac})^2 / K_i}$	0.63 h ⁻¹	100 g ac/l	0.46 g ac/l	Yang et al. ¹¹⁷
<i>M. mazei</i> S6	Andrew	$\mu = \frac{\mu_{max,ac} S_{ac}}{K_{S,ac} + S_{ac} + (S_{ac})^2 / K_i}$	0.029 h ⁻¹	1.00 g ac/l	48.66 g ac/l	Yang et al. ¹¹⁷
<i>M. thermoautotrophicum</i>	Monod	$\mu = \frac{\mu_{max} C_S}{K_S + C_S}$	0.69 h ⁻¹	H ₂ = 20% CO ₂ = 11%	–	Schönheit et al. ¹¹⁶

the criteria for the selection of operational parameters and easing optimization tasks in syngas biomethanation processes. Additionally, the inclusion of microbial interactions in the model could provide a certain control over the metabolic pathways dominating the microbial consortium. Nonetheless, a more complex model structure would be required in order to include the microbial interactions, thus complicating the estimation of the kinetic parameters describing the behavior of the microbial consortium. More structured modeling approaches that intended to describe the metabolic network of mixed culture-based processes have been proposed on the perspective of modeling anaerobic digestion processes¹²⁰ or the product distribution in mixed culture fermentations.¹²¹ The only attempt of modeling the metabolic network of syngas biomethanation processes has been carried out based on a flux balance analysis approach, although the low number of components of the metabolic network monitored over time limited the accuracy of the model.¹⁰⁹ However, this work sets a precedent in modeling of syngas biomethanation processes. Research in this direction is thus encouraged here given the potential of these models for the control and optimization of syngas biomethanation processes.

Future perspectives

A significant research effort is being made worldwide in order to develop efficient processes for the production of biomethane from agricultural, domestic and industrial waste streams. This is of particular importance to several European countries currently showing an increasing interest in the production of biomethane, as it can contribute to offset the decreasing trend of production of natural gas and reduce their dependency on imported natural gas supplies. Several process configurations based on the syngas platform are being explored for increasing the share of biomethane to be used as a vehicle fuel or injected into the natural gas grid. A combined process of gasification and syngas biomethanation presents a significant potential as it offers the possibility of producing renewable methane from a wide array of waste streams regardless of their recalcitrance, broadening the spectrum of biomasses currently available to anaerobic digestion systems. In the near future, the biomethanation of syngas could become a suitable alternative for increasing the flexibility of gasification plants exploiting syngas for heat and electricity production. As opposed to the catalytic methanation process, the biological conversion of syngas to methane could be economically feasible for small-scale gasification plants

due to its lower operational costs, which would provide an alternative outlet to the excess energy generated during periods of low heat and electricity demand. Other process configurations considered include the integration of anaerobic digestion and syngas biomethanation processes as their combination could result in a much higher biomass conversion efficiency and methane productivity. The gasification of either source-separated organic waste or solid digestate and re-injection of syngas into the bioreactor would certainly enhance the productivity of methane, achieving a nearly complete conversion of the biomass. However, the overall efficiency of the process could be compromised by the high moisture content of the solid digestate as an intensive drying process would be required in order to lower its moisture content to the optimal range. Therefore, regardless of the process configuration considered, there are still several challenges to be overcome in both the gasification of biomass and the biomethanation of syngas in order for these technologies to be commercially applicable.

Research on syngas biomethanation processes have undergone a considerable progress over the last years, evolving from the early pure culture-based studies aiming at understanding the metabolism of carboxydophilic micro-organisms to the current mixed culture-based approach for its industrial exploitation in the bioenergy sector. The continuous biomethanation of syngas has so far been successfully applied in a number of bioreactor designs and process configurations, achieving high yield and conversion efficiency for both CO and H₂/CO₂. Nevertheless, the performance of the bioreactors could still be further improved in order to achieve a higher conversion efficiency and productivity. Recent advances in the design of hollow fiber membrane reactors and microbubble spargers have been applied in other syngas fermentation processes, and seem a promising way for overcoming the mass transfer limitation. More research is also necessary in order to improve our knowledge on microbial consortia-driven processes. In this sense, adopting a cross-disciplinary approach is crucial for understanding the nature of the metabolic interactions in microbial consortia, and how these are affected by changes in the operational conditions of continuous processes. Important advances have been made so far in characterizing the effects of the operating conditions on the performance of microbial consortia, finding common patterns of activity on microbial consortia originated from different sources. However, further studies are still necessary in this area in order to find possible interactions between influencing factors, and to correlate these effects to the behavior of the

population dynamics of microbial consortia. The potential of modelling tools for the control and optimization of mixed culture-based bioprocesses has also been discussed here. This area still remains practically unexplored in syngas biomethanation processes. However, the development of new models capable of describing the effects of the operating conditions on the behavior of mixed cultures could contribute to achieve a higher level of control over the performance of continuous processes.

The progress achieved over the last years opens good perspectives for the further development of syngas biomethanation processes. However, this technology has not reached commercial application yet, mainly due to the relatively high sales prices that are needed to supporting it.¹²² This can be overcome if (i) syngas biomethanation occurs in the frame of an already industrial gasification activity, i.e., in combined heat and power plants and (ii) further advancing the syngas biomethanation process targeting higher productivities than the ones achieved so far. Nowadays, where exploitation of the residual biomass is more than ever imperative, syngas biomethanation should be re-visited. Future advances in the areas outlined here will contribute to overcome the current limitations of the process, unlocking thus the potential of this technological application.

Acknowledgements

This work was financially supported by the Technical University of Denmark (DTU) and Innovation Foundation-DK in the frame of SYNFERON project.

References

- Sorda G, Banse M and Kemfert C, An overview of biofuel policies across the world. *Energy Policy* **38**:6977–6988 (2010).
- Munasinghe PC and Khanal SK, Biomass-derived syngas fermentation into biofuels: Opportunities and challenges. *Bioresour Technol* **101**:5013–5022 (2010).
- Köpke M, Mihalcea C, Bromley JC and Simpson SD, Fermentative production of ethanol from carbon monoxide. *Curr Opin Biotechnol* **22**(3):320–325 (2011).
- Mohammadi M, Najafpour GD, Younesi H, Lahijani P, Uzir MH and Mohamed AR, Bioconversion of synthesis gas to second generation biofuels: A review. *Renew Sustain Energy Rev* **15**:4255–4273 (n2011).
- Devarapalli M and Atiyeh HK, A review of conversion processes for bioethanol production with a focus on syngas fermentation. *Biofuel Res J* **7**:268–280 (2015).
- Kennes D, Abubackar HN, Diaz M, Veiga MC and Kennes C, Bioethanol production from biomass: Carbohydrate vs syngas fermentation. *J Chem Technol Biotechnol* **91**(2):304–317 (2016).
- Verma D, Singla A, Lal B and Sarma PM, Conversion of biomass-generated syngas into next-generation liquid transport fuels through microbial intervention: potential and current status. *Curr Sci* **110**(3):329–336 (2016).
- Rittmann SKMR, Lee HS, Lim JK, Kim TW, Lee JH and Kang SG, One-carbon substrate-based biohydrogen production: Microbes, mechanism, and productivity. *Biotechnol Adv* **33**:165–177 (2015).
- Bredwell MD, Srivastava P and Worden RM, Reactor design issues for synthesis-gas fermentations. *Biotechnol Prog* **15**:834–844 (1999).
- Daniell J, Köpke M and Simpson S, Commercial biomass syngas fermentation. *Energies* **5**:5372–5417 (2012).
- Bengelsdorf FR, Straub M and Dürre P, Bacterial synthesis gas (syngas) fermentation. *Environ Technol* **34**:1639–1651 (2013).
- Drzyzga O, Revelles O, Durante-rodríguez G, Díaz E, García JL and Prieto A, New challenges for syngas fermentation: towards production of biopolymers. *J Chem Technol Biotechnol* **90**:1735–1751 (2015).
- Bertsch J and Müller V, Bioenergetic constraints for conversion of syngas to biofuels in acetogenic bacteria. *Biotechnol Biofuel* **8**(210):1–12 (2015).
- Liew F, Martin E, Tappel R, Heijstra B, Mihalcea C and Köpke M, Gas fermentation – a flexible platform for commercial scale production of low carbon fuels and chemicals from waste and renewable feedstocks. *Front Microbiol* **7**:1–28 (2016).
- Dürre P, Butanol formation from gaseous substrates. *FEMS Microbiol Lett* **363**(6):1–7 (2016).
- Thrän D, Billig E, Persson T, Svensson M, Daniel-Gromke J, Ponitka J *et al.*, Biomethane - status and factors affecting market development and trade. [Online]. IEA Task 40 and Task 37 Joint Study (2014). Available at: <http://publications.jrc.ec.europa.eu/repository/handle/JRC91580> [September 16, 2016].
- Lantz M, Svensson M, Björnsson L and Börjesson P, The prospects for an expansion of biogas systems in Sweden - Incentives, barriers and potentials. *Energy Policy* **35**:1819–1829 (2007).
- Börjesson P and Mattiasson B, Biogas as a resource-efficient vehicle fuel. *Trends Biotechnol* **26**:7–13 (2008).
- IEA Bioenergy Task 37 - Country Reports Summary 2015. [Online]. IEA Bioenergy Task 37 (2016). Available at: <http://www.iea-biogas.net/country-reports.html> [October 4, 2016].
- Lide DR, *CRC Handbook of Chemistry and Physics*. 90th ed., ed by Lide DR and Haynes WM. CRC Press, Boca Raton, FL (2009).
- Demirel Y, *Energy: Production, Conversion, Storage, Conservation, and Coupling*. Springer-Verlag, London, UK, 508 p. (2012).
- Holm-Nielsen JB, Al Seadi T and Oleskowicz-Popiel P, The future of anaerobic digestion and biogas utilization. *Bioresour Technol* **100**:5478–84 (2009).
- Kopyscinski J, Schildhauer TJ and Biollaz SMA, Production of synthetic natural gas (SNG) from coal and dry biomass – A technology review from 1950 to 2009. *Fuel* **89**:1763–83 (2010).
- Kumar A, Jones DD and Hanna M, Thermochemical biomass gasification: a review of the current status of the technology. *Energies* **2**:556–581 (2009).
- Redl S, Diender M, Ølshøj T, Sousa DZ and Toftgaard A, Exploiting the potential of gas fermentation. *Ind Crop Prod* **106**:21–30 (2017).

26. Xia A, Cheng J and Murphy JD, Innovation in biological production and upgrading of methane and hydrogen for use as gaseous transport biofuel. *Biotechnol Adv* **34**(5):451–472 (2016).
27. Kleerebezem R and van Loosdrecht MC, Mixed culture biotechnology for bioenergy production. *Curr Opin Biotechnol* **18**:207–212 (2007).
28. Marshall CW, LaBelle EV and May HD, Production of fuels and chemicals from waste by microbiomes. *Curr Opin Biotechnol* **24**:391–397 (2013).
29. Rönsch S, Schneider J, Matthischke S, Schlüter M, Götz M, Lefebvre J *et al.*, Review on methanation - From fundamentals to current projects. *Fuel* **166**:276–296 (2016).
30. Li H, Larsson E, Thorin E, Dahlquist E and Yu X, Feasibility study on combining anaerobic digestion and biomass gasification to increase the production of biomethane. *Energy Convers Manag* **100**:212–219 (2015).
31. Brown RC, Hybrid thermochemical / biological processing. Putting the cart before the horse? *Biotechnol Appl Biochem* **136**:947–956 (2007).
32. Klasson KT, Ackerson MD, Clausen EC and Gaddy JL, Bioconversion of synthesis gas into liquid or gaseous fuels. *Enzyme Microb Technol* **14**:602–608 (1992).
33. Batstone DJ and Virdis B, The role of anaerobic digestion in the emerging energy economy. *Curr Opin Biotechnol* **27**:142–149 (2014).
34. Noike T, Endo G, Chang JE, Yaguchi J and Matsumoto J, Characteristics of carbohydrate degradation and the rate-limiting step in anaerobic digestion. *Biotechnol Bioeng* **27**:1482–1489 (1985).
35. Guiot SR, Cimpoia R, Dath L, Ollier J, Das R and Sancho Navarro S, Chapter 1.10. Anaerobic digestion fully enhanced by merging the biomethanation of syngas from solid digestate, in *Environmental Biotechnology and Engineering*, ed by Poggi-Varaldo HM, Bretón-Deval LM, Camacho-Pérez B, Escamilla-Alvarado C, Escobedo-Acuña G, Hernández-Flores G *et al.* Ed. Cinves. Mexico D.F., Mexico, p. 84–91 (2014).
36. Shen Y, Linville JL, Urgan-Demirtas M, Schoene RP and Snyder SW, Producing pipeline-quality biomethane via anaerobic digestion of sludge amended with corn stover biochar with in-situ CO₂ removal. *Appl Energy* **158**:300–309 (2015).
37. Fabbri D and Torri C, Linking pyrolysis and anaerobic digestion (Py-AD) for the conversion of lignocellulosic biomass. *Curr Opin Biotechnol* **38**:167–173 (2016).
38. Xu D, Tree DR and Lewis RS, The effects of syngas impurities on syngas fermentation to liquid fuels. *Biomass Bioenergy* **35**:2690–2696 (2011).
39. Ramachandriya KD, Kundiyana DK, Sharma AM, Kumar A, Atiyeh HK, Huhnke RL *et al.*, Critical factors affecting the integration of biomass gasification and syngas fermentation technology. *AIMS Bioeng* **3**:188–210 (2016).
40. Inman RE and Ingersoll RB, Note on the Uptake of Carbon Monoxide by Soil Fungi. *J Air Pollut Control Assoc* **21**:646–647 (1971).
41. Chappelle EW, Carbon monoxide oxidation by algae. *Biochim Biophys Acta* **62**:45–62 (1962).
42. Pakpour F, Najafpour G, Tabatabaei M, Tohidfar M and Younesi H, Biohydrogen production from CO-rich syngas via a locally isolated *Rhodospseudomonas palustris* PT. *Bioprocess Biosyst Eng* **37**:923–930 (2014).
43. Alves JI, van Gelder AH, Alves MM, Sousa DZ and Plugge CM, *Moorella stamsii* sp. nov., a new anaerobic thermophilic hydrogenogenic carboxydrotroph isolated from digester sludge. *Int J Syst Evol Microbiol* **63**:4072–4076 (2013).
44. Sokolova TG, Jeanthon C, Kostrikina NA, Chernyh NA, Lebedinsky AV, Stackebrandt E *et al.*, The first evidence of anaerobic CO oxidation coupled with H₂ production by a hyperthermophilic archaeon isolated from a deep-sea hydrothermal vent. *Extremophiles* **8**:317–323 (2004).
45. Parshina SN, Sipma J, Nakashimada Y, Henstra AM, Smidt H, Lysenko AM *et al.*, *Desulfotoculum carboxydivorans* sp. nov., a novel sulfate-reducing bacterium capable of growth at 100% CO. *Int J Syst Evol Microbiol* **55**:2159–2165 (2005).
46. Henstra AM, Dijkema C and Stams AJM, *Archaeoglobus fulgidus* couples CO oxidation to sulfate reduction and acetogenesis with transient formate accumulation. *Environ Microbiol* **9**:1836–1841 (2007).
47. Bernalier A, Willems A, Leclerc M, Rochet V and Collins MD, *Ruminococcus hydrogenotrophicus* sp. nov., a new H₂/CO₂-utilizing acetogenic bacterium isolated from human feces. *Arch Microbiol* **166**:176–183 (1996).
48. Rother M and Metcalf WW, Anaerobic growth of *Methanosarcina acetivorans* C2A on carbon monoxide: an unusual way of life for a methanogenic archaeon. *Proc Natl Acad Sci USA* **101**:16929–16934 (2004).
49. Cord-Ruwisch R, Seitz H-J and Conrad R, The capacity of hydrogenotrophic anaerobic bacteria to compete for traces of hydrogen depends on the redox potential of the electron acceptor. *Arch Microbiol* **149**:350–357 (1988).
50. Mörsdorf G, Frunzke K, Gadkari D and Meyer O, Microbial growth on carbon monoxide. *Biodegradation* **3**:61–82 (1992).
51. Diekert G, Hansch M and Conrad R, Acetate synthesis from 2 CO₂ in acetogenic bacteria: is carbon monoxide an intermediate? *Arch Microbiol* **138**:224–228 (1984).
52. Oelgeschläger E and Rother M, Carbon monoxide-dependent energy metabolism in anaerobic bacteria and archaea. *Arch Microbiol* **190**:257–269 (2008).
53. Techtmann SM, Colman AS and Robb FT, “That which does not kill us only makes us stronger”: The role of carbon monoxide in thermophilic microbial consortia. *Environ Microbiol* **11**:1027–1037 (2009).
54. Ferry JG, CO Dehydrogenase. *Ann Rev Microbiol* **49**:305–333 (1995).
55. Sipma J, Henstra AM, Parshina SM, Lens PN, Lettinga G and Stams AJM, Microbial CO conversions with applications in synthesis gas purification and bio-desulfurization. *Crit Rev Biotechnol* **26**:41–65 (2006).
56. Drake HL, Küsel K and Matthies C, Acetogenic Prokaryotes, in *Prokaryotes*. Springer, New York, p. 354–420 (2006).
57. Zeikus AJG, Kerby R and Krzycki JA, Single-carbon chemistry of acetogenic and methanogenic bacteria. *Am Assoc Adv Sci* **227**(4691):1167–1173 (2011).
58. Liu Y and Whitman WB, Metabolic, phylogenetic, and ecological diversity of the Methanogenic Archaea. *Ann N Y Acad Sci* **1125**:171–189 (2008).
59. Tiquia-Arashiro SM, *Thermophilic Carboxydrotrophs and their Applications in Biotechnology*. Springer International Publishing, Cham, p. 131 (2014).
60. Mohammadi M, Younesi H, Najafpour G and Mohamed AR, Sustainable ethanol fermentation from synthesis gas by *Clostridium ljungdahlii* in a continuous stirred tank bioreactor. *J Chem Technol Biotechnol* **87**(6):837–843 (2012).

61. Worden RM, Grethlein AJ, Zeikus JG and Datta R, Butyrate production from carbon monoxide by *Butyribacterium methylophilum*. *Appl Biochem Biotechnol* **20**(1): 687–699 (1989).
62. Fernández-Naveira Á, Abubackar HN, Veiga MC and Kennes C, Efficient butanol-ethanol (B-E) production from carbon monoxide fermentation by *Clostridium carboxidivorans*. *Appl Microbiol Biotechnol* **100**:3361–3370 (2016).
63. Thauer RK, Jungermann K and Decker K, Energy conservation in chemotrophic anaerobic bacteria. *Bacteriol Rev* **41**:100–180 (1977).
64. Guiot SR and Cimpioia R, Potential of wastewater-treating anaerobic granules for biomethanation of synthesis gas. *Environ Sci Technol* **45**:2006–2012 (2011).
65. Navarro SS, Cimpioia R, Bruant G and Guiot SR, Specific inhibitors for identifying pathways for methane production from carbon monoxide by a nonadapted anaerobic mixed culture. *Can J Microbiol* **415**:407–415 (2014).
66. Sipma J, Lens PNL, Stams JM and Lettinga G, Carbon monoxide conversion by anaerobic bioreactor sludges. *FEMS Microbiol Ecol* **44**:271–277 (2003).
67. Luo G, Wang W and Angelidaki I, Anaerobic digestion for simultaneous sewage sludge treatment and CO biomethanation: process performance and microbial ecology. *Environ Sci Technol* **47**:10685–106193 (2013).
68. Wang W, Xie L, Luo G, Zhou Q and Angelidaki I, Performance and microbial community analysis of the anaerobic reactor with coke oven gas biomethanation and in situ biogas upgrading. *Bioresour Technol* **146**:234–239 (2013).
69. Boone DR, Johnson RL and Liu Y, Diffusion of the interspecies electron carriers H₂ and formate in methanogenic ecosystems and its implications in the measurement of Km for H₂ or formate uptake. *Appl Env Microbiol* **55**:1735–1741 (1989).
70. Navarro SS, Cimpioia R, Bruant G and Guiot SR, Biomethanation of syngas using anaerobic sludge: shift in the catabolic routes with the CO partial pressure increase. *Front Microbiol* **7**:1–13 (2016).
71. Rotaru A-E, Shrestha PM, Liu F, Shrestha M, Shrestha D, Embree M *et al.*, A new model for electron flow during anaerobic digestion: direct interspecies electron transfer to *Methanosaeta* for the reduction of carbon dioxide to methane. *Energy Environ Sci* **7**:408–415 (2014).
72. Parshina SN, Kijlstra S, Henstra AM, Sipma J, Plugge CM and Stams AJM, Carbon monoxide conversion by thermophilic sulfate-reducing bacteria in pure culture and in co-culture with *Carboxydotherrmus hydrogeniformans*. *Appl Microbiol Biotechnol* **68**:390–396 (2005).
73. Rajagopal BS, Lespinat PA, Fauque G, LeGall J and Berlier YM, Mass-spectrometric studies of the interrelations among hydrogenase, carbon monoxide dehydrogenase, and methane-forming activities in pure and mixed cultures of *Desulfovibrio vulgaris*, *Desulfovibrio desulfuricans*, and *Methanosarcina barkeri*. *Appl Environ Microbiol* **55**:2123–2139 (1989).
74. Stams AJM, Elferink SJWH and Westermann P, Metabolic Interactions Between Methanogenic Consortia and Anaerobic Respiring Bacteria. *Adv Biochem Eng Biotechnol* **81**:31–56 (2003).
75. Stams a. JM, Plugge CM, de Bok F a M, van Houten BHGW, Lens P, Dijkman H *et al.*, Metabolic interactions in methanogenic and sulfate-reducing bioreactors. *Water Sci Technol* **52**:13–20 (2005).
76. Sipma J, Lettinga G, Stams AJM and Lens PNL, Hydrogenogenic CO conversion in a moderately thermophilic (55 C) sulfate-fed gas lift reactor: Competition for CO-derived H₂. *Biotechnol Prog* **22**:1327–1334 (2006).
77. Liu R, Hao X and Wei J, Function of homoacetogenesis on the heterotrophic methane production with exogenous H₂/CO₂ involved. *Chem Eng J* **284**:1196–1203 (2015).
78. Daniels L, Fuchs G, Thauer RK and Zeikus JG, Carbon monoxide oxidation by methanogenic bacteria. *J Bacteriol* **132**:118–126 (1977).
79. Kerby R and Zeikus JG, Growth of *Clostridium thermoacetatum* on H₂/CO₂ or CO as energy source. *Curr Microbiol* **8**:27–30 (1983).
80. Lorowitz WH and Bryant MP, *Peptostreptococcus productus* strain that grows rapidly with CO as the energy source. *Appl Environ Microbiol* **47**:961–964 (1984).
81. Kerby RL, Ludden PW and Roberts GP, Carbon monoxide-dependent growth of *Rhodospirillum rubrum*. *J Bacteriol* **177**:2241–2244 (1995).
82. Henstra AM, Sipma J, Rinzema A and Stams AJM, Microbiology of synthesis gas fermentation for biofuel production. *Curr Opin Biotechnol* **18**:200–206 (2007).
83. Ghosh S, Chowdhury R and Bhattacharya P, Mixed consortia in bioprocesses: role of microbial interactions. *Appl Microbiol Biotechnol* **100**:4283–4295 (2016).
84. Kundiya DK, Wilkins MR, Maddipati P and Huhnke RL, Effect of temperature, pH and buffer presence on ethanol production from synthesis gas by “*Clostridium ragsdalei*”. *Bioresour Technol* **102**:5794–5799 (2011).
85. Abubackar HN, Veiga MC and Kennes C, Biological conversion of carbon monoxide to ethanol: effect of pH, gas pressure, reducing agent and yeast extract. *Bioresour Technol* **114**:518–522 (2012).
86. Pereira FM, Alves MM and Sousa DZ, Effect of pH and pressure on syngas fermentation by anaerobic mixed cultures, in *13th World Congress on Anaerobic Digestion*, p. 1–4 (2013).
87. Conrad R and Wetter B, Influence of temperature on energetics of hydrogen metabolism in homoacetogenic, methanogenic, and other anaerobic bacteria. *Arch Microbiol* **155**(1):94–98 (1990).
88. Diender M, Pereira R, Wessels HJCT, Stams AJM and Sousa DZ, Proteomic Analysis of the Hydrogen and Carbon Monoxide Metabolism of *Methanothermobacter marburgensis*. *Front Microbiol* **7**:1–10 (2016).
89. Alves JI, Stams AJM, Plugge CM, Alves MM and Sousa DZ, Enrichment of anaerobic syngas-converting bacteria from thermophilic bioreactor sludge. *FEMS Microbiol Ecol* **86**:590–597 (2013).
90. Skidmore BE, Baker R a., Banjade DR, Bray JM, Tree DR and Lewis RS, Syngas fermentation to biofuels: Effects of hydrogen partial pressure on hydrogenase efficiency. *Biomass Bioenerg* **55**:156–162 (2013).
91. Lopes M, Alves JI, Arantes AL, Belo I, Sousa DZ and Alves MM, Hydrogenotrophic activity under increased H₂/CO₂ pressure: Effect on methane production and microbial community. *J Biotechnol* **208**:S5–S120 (2015).
92. Ahmed A, Cateni BG, Huhnke RL and Lewis RS, Effects of biomass-generated producer gas constituents on cell growth, product distribution and hydrogenase activity of *Clostridium carboxidivorans* P7^T. *Biomass Bioenerg* **30**:665–672 (2006).

93. Xu D and Lewis RS, Syngas fermentation to biofuels: Effects of ammonia impurity in raw syngas on hydrogenase activity. *Biomass Bioenerg* **45**:303–310 (2012).
94. Vega JL, Klasson KT, Kimmel DE, Clausen EC and Gaddy JL, Sulfur gas tolerance and toxicity of co-utilizing and methanogenic bacteria. *Appl Biochem Biotechnol* **24–25**:329–340 (1990).
95. Guiot S, Cimpoia R, Sancho Navarro S, Prudhomme A and Filiatrault M, Anaerobic digestion for bio-upgrading syngas into renewable natural gas (methane), in *Proceedings of the 13th World Congress on Anaerobic Digestion*. Santiago de Compostela, p. 1–5 (2013).
96. Saxena J and Tanner RS, Effect of trace metals on ethanol production from synthesis gas by the ethanologenic acetogen, *Clostridium ragsdalei*. *J Ind Microbiol Biotechnol* **38**:513–521 (2011).
97. Hu P, Thermodynamic, Sulfide, Redox Potential, and pH Effects on Syngas Fermentation. All Theses and Dissertations. Paper 2919. Brigham Young University, Provo, Utah (2011).
98. Orgill JJ, Atiyeh HK, Devarapalli M, Phillips JR, Lewis RS and Huhnke RL, A comparison of mass transfer coefficients between trickle-bed, hollow fiber membrane and stirred tank reactors. *Bioresour Technol* **133**:340–346 (2013).
99. Najafpour G, Younesi H and Mohamed AR, Continuous hydrogen production via fermentation of synthesis gas. *Pet Coal* **45**:154–158 (2003).
100. Groher A and Weuster-botsch D, Comparative reaction engineering analysis of different acetogenic bacteria for gas fermentation. *J Biotechnol* **228**:82–94 (2016).
101. Ungerman AJ and Heindel TJ, Carbon monoxide mass transfer for syngas fermentation in a stirred tank reactor with dual impeller configurations. *Biotechnol Prog* **23**:613–620 (2007).
102. Wise DL, Cooney CL and Augenstein DC, Biomethanation: Anaerobic fermentation of CO₂, H₂ and CO to methane. *Biotechnol Bioeng* **20**:1153–1172 (1978).
103. Burkhardt M, Koschack T and Busch G, Biocatalytic methanation of hydrogen and carbon dioxide in an anaerobic three-phase system. *Bioresour Technol* **178**:330–333 (2015).
104. Jee HS, Nishio N and Nagai S, Continuous methane production from hydrogen and carbon dioxide by *Methanobacterium thermoautotrophicum* in a fixed-bed reactor. *J Ferment Technol* **66**:235–238 (1988).
105. Kimmel DE, Klasson KT, Clausen EC and Gaddy JL, Performance of trickle-bed bioreactors for converting synthesis gas to methane. *Appl Biochem Biotechnol* **28–29**:457–469 (1991).
106. Munasinghe PC and Khanal SK, Syngas fermentation to biofuel: Evaluation of carbon monoxide mass transfer coefficient ($k_L a$) in different reactor configurations. *Biotechnol Prog* **26**:1616–1621 (2010).
107. Bugante EC, Shimomura Y, Tanaka T, Taniguchi M and Oi S, Methane production from hydrogen and carbon dioxide and monoxide in a column bioreactor of thermophilic methanogens by gas recirculation. *J Ferment Bioeng* **67**:419–421 (1989).
108. Klasson KT, Cowger JP, Ko CW, Vega JL, Clausen EC and Gaddy JL, Methane production from synthesis gas using a mixed culture of *R. rubrum*, *M. barkeri*, and *M. formicicum*. *Appl Biochem Biotechnol* **24–25**:317–328 (1990).
109. Pereira FM Intensified Bioprocess for the Anaerobic Conversion of Syngas to Biofuels. Universidade do Minho, Braga (2014).
110. Westman S, Chandolias K and Taherzadeh M, Syngas biomethanation in a semi-continuous Reverse Membrane Bioreactor (RMBR). *Fermentation* **2**:1–12 (2016).
111. Almquist J, Cvijovic M, Hatzimanikatis V, Nielsen J and Jirstrand M, Kinetic models in industrial biotechnology - Improving cell factory performance. *Metab Eng* **24**:38–60 (2014).
112. Vega JL, Clausen EC and Gaddy JL, Design of bioreactors for coal synthesis gas fermentations. *Resour Conserv Recycl* **3**:149–160 (1990).
113. Mohammadi M, Mohamed AR, Najafpour GD, Younesi H and Uzir MH, Kinetic studies on fermentative production of biofuel from synthesis gas using *Clostridium ljungdahlii*. *Sci World J* **2014**:1–8 (2014).
114. Younesi H, Najafpour G and Mohamed AR, Ethanol and acetate production from synthesis gas via fermentation processes using anaerobic bacterium, *Clostridium ljungdahlii*. *Biochem Eng J* **27**(2):110–119 (2005).
115. Zhao Y, Cimpoia R, Liu Z and Guiot SR, Kinetics of CO conversion into H₂ by *Carboxydotherrmus hydrogenoformans*. *Appl Microbiol Biotechnol* **91**:1677–1684 (2011).
116. Schönheit P, Moll J and Thauer RK, Growth parameters (K_s , μ_{max} , Y_s) of *Methanobacterium thermoautotrophicum*. *Arch Microbiol* **127**:59–65 (1980).
117. Yang ST and Okos MR, Kinetic Study and Mathematical Modeling of Methanogenesis of Acetate Using Pure Cultures of Methanogens. *Biotechnol Bioeng* **30**: 661–667 (1987).
118. Ako OY, Kitamura Y, Intabon K and Satake T, Steady state characteristics of acclimated hydrogenotrophic methanogens on inorganic substrate in continuous chemostat reactors. *Bioresour Technol* **99**: 6305–6310 (2008).
119. Pan X, Angelidaki I, Alvarado-Morales M, Liu H, Liu Y, Huang X *et al.*, Methane Production from formate, acetate and H₂/CO₂; focusing on kinetics and microbial characterization. *Bioresour Technol* **218**:796–806 (2016).
120. Batstone D, Keller J, Angelidaki I, Kalyuzhnyi S, Pavlostathis S, Rozzi A *et al.*, The IWA Anaerobic Digestion Model No 1 (ADM1). *Water Sci Technol* **45**(10):65–73 (2002).
121. Rodríguez J, Kleerebezem R, Lema JM and Van Loosdrecht MCM, Modeling product formation in anaerobic mixed culture fermentations. *Biotechnol Bioeng* **93**:592–606 (2006).
122. Hoogendoorn A and van Kasteren H, *Transportation Biofuels: Novel Pathways for the Production of Ethanol, Biogas and Biodiesel*. Royal Society of Chemistry, Cambridge, 202 p. (2010).



Antonio Grimalt-Alemanly

Antonio Grimalt-Alemanly is a PhD candidate at the Technical University of Denmark currently working on biofuels production through syngas fermentation using open mixed microbial consortia. His research interests focus on fermentation-based processes for waste valorization.



Dr Ioannis V. Skiadas

Dr Ioannis V. Skiadas is a chemical engineer and works as associate professor at the Chemical Engineering department at the Technical University of Denmark where he teaches biotechnology, process design, fermentation technology and unit operations. His research lies in the area of biological conversion of biomass to chemicals and fuels. He holds a PhD in Chemical Engineering from the University of Patras, Greece.



Hariklia N. Gavala

Hariklia N. Gavala is an associate professor at the Department of Chemical and Biochemical Engineering at Technical University of Denmark. Her expertise lies in the field of Bioprocess Engineering and her current research focuses on harnessing the potential of mixed microbial consortia by optimizing the selection and enrichment process as well as the fermentation operating strategy toward the development of innovative and cost-efficient processes for production of chemicals, materials, and biofuels. She holds a PhD in Chemical and Biochemical Engineering from University of Patras, Greece.

Manuscript II

“Enrichment of syngas–converting mixed microbial consortia for ethanol production and thermodynamics–based design of enrichment strategies”

RESEARCH

Open Access



Enrichment of syngas-converting mixed microbial consortia for ethanol production and thermodynamics-based design of enrichment strategies

Antonio Grimalt-Alemany, Mateusz Łężyk, Lene Lange, Ioannis V. Skiadas and Hariklia N. Gavala*

Abstract

Background: The production of ethanol through the biochemical conversion of syngas, a mixture of H₂, CO and CO₂, has been typically studied using pure cultures. However, mixed microbial consortia may offer a series of benefits such as higher resilience and adaptive capacity, and non-sterile operation, all of which contribute to reducing the utility consumption when compared to pure culture-based processes. This work focuses on the study of strategies for the enrichment of mixed microbial consortia with high ethanologenic potential, investigating the effect of the operational conditions (pH and yeast extract addition) on both the ethanol yield and evolution of the microbial community along the enrichment process. The pH was selected as the main driver of the enrichment as it was expected to be a crucial parameter for the selection of carboxydophilic bacteria with high ethanologenic potential. Additionally, a thermodynamic analysis of the network of biochemical reactions carried out by syngas-converting microbial consortia was performed and the potential of using thermodynamics as a basis for the selection of operational parameters favoring a specific microbial activity was evaluated.

Results: All enriched consortia were dominated by the genus *Clostridium* with variable microbial diversity and species composition as a function of the enrichment conditions. The ethanologenic potential of the enriched consortia was observed to increase as the initial pH was lowered, achieving an ethanol yield of $59.2 \pm 0.2\%$ of the theoretical maximum in the enrichment at pH 5. On the other hand, yeast extract addition did not affect the ethanol yield, but triggered the production of medium-chain fatty acids and alcohols. The thermodynamic analysis of the occurring biochemical reactions allowed a qualitative prediction of the activity of microbial consortia, thus enabling a more rational design of the enrichment strategies targeting specific activities. Using this approach, an improvement of 22.5% over the maximum ethanol yield previously obtained was achieved, reaching an ethanol yield of $72.4 \pm 2.1\%$ of the theoretical maximum by increasing the initial acetate concentration in the fermentation broth.

Conclusions: This study demonstrated high product selectivity towards ethanol using mixed microbial consortia. The thermodynamic analysis carried out proved to be a valuable tool for interpreting the metabolic network of microbial consortia-driven processes and designing microbial-enrichment strategies targeting specific biotransformations.

Keywords: Enrichment, Syngas, Carbon monoxide, Mixed culture, Microbial consortia, Ethanol, Thermodynamics

*Correspondence: hnga@kt.dtu.dk; hari_gavala@yahoo.com
Department of Chemical and Biochemical Engineering, Technical
University of Denmark, Søtofts Plads 229, 2800 Kgs. Lyngby, Denmark



Background

Over the past decades, the rising concerns about climate change and the depletion of fossil fuels, along with the ever increasing demand of transportation fuels, have led to the global implementation of policies fostering biofuel production. As a result of these policies, the biofuel market underwent a rapid expansion rising from less than 20 billion liters/year in 2001 to over 100 billion liters/year in 2011 [1]. However, the rapid growth of this market, strictly based on first generation biofuels, brought along a series of environmental and socioeconomic impacts derived from the competition with food crops such as land use change, rising food and feed prices, and poor greenhouse gas emission savings [2, 3]. Developing second-generation biofuel technologies is thus considered an important step forward as these are based on the use of non-food biomasses and waste streams as feedstock, and are expected to overcome the limitations of first-generation biofuels in terms of environmental impacts and range of exploitable feedstocks.

Among the different approaches within second-generation biofuel technologies, syngas fermentation is one of the most promising as it combines the benefits of both thermochemical and biochemical biomass conversion processes. Typically, this process comprises thermochemical conversion of the biomass through gasification into synthesis gas, a mixture of mainly H_2 , CO_2 and CO , followed by its biological conversion into a variety of chemicals and fuels [4–7]. The fermentation of syngas is carried out by anaerobic acetogenic bacteria, which are able to use both CO and H_2/CO_2 as the sole carbon and energy source through the Wood–Ljungdahl pathway. So far, mostly pure cultures have been employed in syngas fermentation processes, with the most common wild-type strains being *C. autoethanogenum* [8], *C. ljungdahlii* [9], *C. ragsdalei* [10] and *C. carboxidivorans* [11]. However, several studies have reported that microbial growth on CO and H_2/CO_2 can be significantly inhibited by the impurities of syngas [12, 13], which may result in decreased productivity of syngas fermentation systems and/or higher raw syngas clean-up requirements. Another limitation is the fact that sterile operation is necessary to avoid a possible microbial contamination of the monoculture, which increases the energy input requirements.

A possible alternative to overcome these limitations is to use open-mixed microbial consortia. Developing microbial consortia-driven processes may allow reducing the cleaning requirements of raw syngas as they present a higher resilience and adaptive capacity due to their microbial diversity [14]. Additionally, sterilization is not necessary when using microbial consortia [15], which contributes to reducing the utility consumption.

Nonetheless, their higher complexity often entails an inadequate understanding of the microbial interactions within the consortium, resulting in limited process control. Low product selectivity is another challenge generally encountered in microbial consortia-driven processes, ultimately lowering the yield of the desired product.

Although the use of open-mixed microbial consortia in syngas fermentation processes is still rather limited compared to pure cultures, the potential of microbial consortia for producing H_2 [16], CH_4 [17], carboxylic acids [18–20] and higher alcohols [21] has been demonstrated in a number of studies. The production of solvents through the reduction of carboxylic acids using either syngas or H_2 as electron donor has also been studied [22, 23]. However, scientific literature on the production of ethanol by mixed microbial consortia using syngas as the sole carbon source is scarce, with only two studies showing a significant ethanogenic potential. Singla et al. [24] were the first demonstrating a high ethanol production using an enriched mixed culture from the culture collection of TERI University. In their study, the operating conditions were optimized for maximizing the ethanol yield in batch experiments, obtaining a maximum concentration of 1.54 and 0.9 g/l of ethanol and acetic acid, respectively. In turn, Ganigué et al. [21] studied the enrichment of a pre-acclimatized open-mixed microbial consortium using 2-bromoethanesulfonate for inhibiting methanogenic activity, where significant amounts of ethanol, butanol and hexanol were produced through syngas fermentation and chain elongation. Nevertheless, a dedicated study on enrichment of mixed microbial consortia aiming at enhancing the product selectivity towards ethanol has not been conducted yet.

This work focuses on the study of selective enrichment strategies for developing microbial consortia with high ethanogenic potential, laying special emphasis on the effect of the enrichment conditions on both the ethanol yield and selectivity, and the evolution of the microbial community along the enrichment process. Additionally, the thermodynamics of the network of biochemical reactions of microbial consortia is evaluated based on the Gibbs free energy change at different enrichment conditions with the perspective of using thermodynamics as a tool for developing selective enrichment strategies targeting specific biotransformations.

Methods

Inoculum source

The inoculum used was a combination of two different types of anaerobic sludge collected from the Lundtofte wastewater treatment plant (Denmark) and from a lab-scale anaerobic digester fed with manure (at Chemical and Biochemical Engineering Department, Technical

University of Denmark). The inoculum was prepared by mixing the two anaerobic sludges in equal amounts (50/50 v/v) and adjusting the pH to 6 with 1 M HCl while flushing with N₂ to ensure anaerobic conditions.

Unless otherwise stated, the starting inoculum used in the enrichments (see “[Enrichment experiments and conditions](#)”) underwent a heat-shock treatment to suppress the methanogenic activity. The heat-shock treatment was carried out by heating the mixture of anaerobic sludges up to 90 °C for 15 min while flushing with N₂.

Growth medium composition

A modified basal anaerobic (BA) medium was used in all experiments, which consisted of six stock solutions containing phosphate buffer, vitamins, trace elements, salts, chelating agents and reducing agents. The stock solutions had the following composition: solution A (NH₄Cl, 100 g/l; NaCl, 10 g/l; MgCl₂·6H₂O, 10 g/l; CaCl₂·2H₂O, 5 g/l), vitamins solution according to Wolin et al. [25], trace metal solution (FeCl₂·4H₂O, 2000 mg/l; H₃BO₃, 50 mg/l; ZnCl₂, 50 mg/l; CuCl₂, 30 mg/l; MnCl₂·4 H₂O, 50 mg/l; (NH₄)₆Mo₇O₂₄·4 H₂O, 50 mg/l; AlCl₃, 50 mg/l; CoCl₂·6H₂O, 50 mg/l; NiCl₂, 50 mg/l; Na₂SeO₃·5H₂O, 100 mg/l; Na₂WO₄·2H₂O, 60 mg/l), chelating agent solution (Nitrilotriacetic acid, 1 g/l) and reducing agent solution (Na₂S·9H₂O, 25 g/l).

The medium was prepared by adding 10 ml/l of solution A, 1 ml/l of trace metal solution, 10 ml/l of vitamins solution, 10 ml/l of reducing agent solution, 20 ml/l of chelating agent solution and distilled water up to 1 l. The pH was adjusted with phosphate buffer (50 mM) using three stock solutions (K₂HPO₄·3H₂O, 200 g/l; KH₂PO₄, 136 g/l; H₃PO₄, 98 g/l). When relevant, yeast extract (YE) and sodium acetate were added to the medium with a final concentration of 0.5 g/l and 20 mM, respectively.

Enrichment experiments and conditions

All enrichment experiments were performed in 330 ml serum flasks with an active volume of 100 ml and an

inoculum size of 15% v/v (15 ml). The medium (85 ml) was added to the flasks and was flushed with H₂ to create anaerobic conditions. After the flasks were sealed with rubber stoppers and screw plugs, the remaining gases (CO and CO₂) were added up to a total pressure of 2 atm prior to inoculation using a precision pressure indicator (model CPH6400, WIKA, Germany). All gases used had purity above 99.9%, and were purchased from AGA (Denmark). After inoculation, the total initial pressure increased to 2.14 atm and the final gas composition of the headspace corresponded to approximately 10.1 mmol of H₂, 4.5 mmol of CO and 5.5 mmol of CO₂ at 25 °C. The fermentation flasks were incubated in the dark at 37 °C and 100 rpm. Control experiments were performed at the same incubation conditions with no addition of gaseous substrates, adjusting the gaseous composition of the headspace to 1.44 atm of N₂ and 0.56 atm of CO₂ prior to inoculation.

A batch-enrichment technique was used in all enrichment series, consisting in the successive transfer of a fraction of the fermented broth (used as inoculum) into a new flask with fresh medium and substrate (Fig. 1). Each enrichment series comprised a total of six transfers and seven fermentations using a 15% v/v inoculum size for each transfer. The enrichments were performed in duplicates with the best performing one being used as inoculum for the next transfer. The selection of the individual duplicate to be transferred was based on the ethanol yield, i.e., only the best ethanol-producing consortium was transferred to the next set of duplicates. The enrichment strategies were based on the pH conditions and the presence of syngas as the main drivers for selecting the most effective and efficient ethanologenic consortia. Yeast extract was also added to selected enrichment series to improve growth at low pH conditions. The enrichment conditions used, including starting inoculum, pH, substrates and nutrient supplements, are given in Table 1.

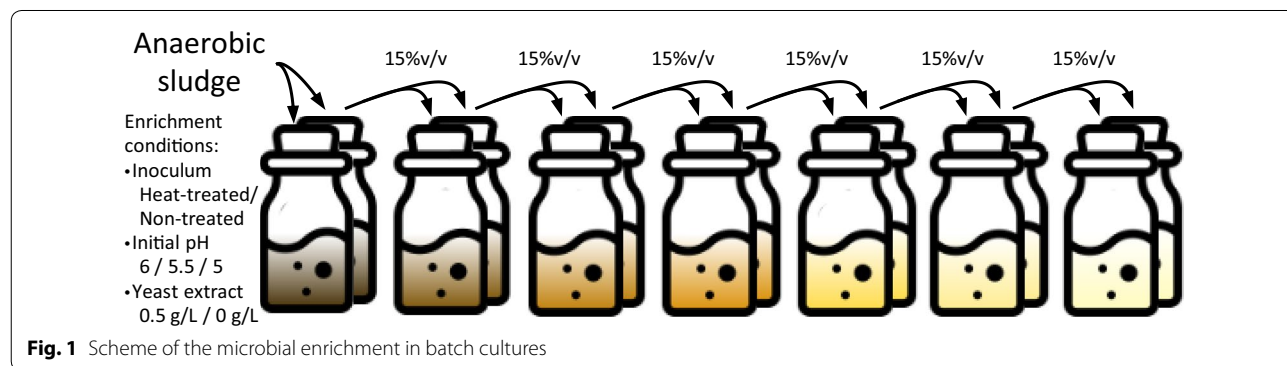


Table 1 Enrichment conditions based on initial pH and initial addition of acetate

Enrichment series	Inoculum treatment	Initial pH	Syngas composition (%H ₂ , %CO, %CO ₂)	Co-substrate	YE (g/l)
HT6	Heat-shock	5.95 ± 0.06	50%, 22.2%, 27.8%	–	–
HT5.5	Heat-shock	5.51 ± 0.09	50%, 22.2%, 27.8%	–	–
HT5	Heat-shock	5.05 ± 0.02	50%, 22.2%, 27.8%	–	–
HT5.5YE	Heat-shock	5.43 ± 0.13	50%, 22.2%, 27.8%	–	0.5
HT5YE	Heat-shock	5.02 ± 0.10	50%, 22.2%, 27.8%	–	0.5
NT5YE	Non-treated	5.04 ± 0.13	50%, 22.2%, 27.8%	–	0.5
HT5YE-Ac	Heat-shock	4.99 ± 0.08	50%, 22.2%, 27.8%	NaCH ₃ COO (20 mM)	0.5

The pH was not stable during the course of the fermentations

The enrichment series HT5YE was interrupted at transfer T4 and presented a significant loss of solventogenic activity upon resuming the enrichment. Thus, this enrichment was extended for one more transfer to confirm the recovery of the previous activity.

Samples for the determination of the metabolites concentration and yield in each transfer were taken at the beginning of the experiments and after the culture reached the stationary phase. Samples for microbial growth determination were taken from transfer T3, when the solids from the anaerobic sludge were completely diluted and did not interfere with the absorbance of the fermentation broth. As it was not possible to measure microbial growth during the first transfers of the enrichments, the distinction between exponential and stationary growth phase was based on the profile of the consumption of H₂ and CO over time.

DNA extraction, sequencing and microbial population analysis

For analysis of microbial composition, selected fermentation steps during enrichments were sampled at both exponential and stationary growth phase. 5 ml of culture was spun down and genomic DNA was isolated using DNeasy Blood & Tissue Kit, following manufacturer recommendations for Gram-positive bacteria (Qiagen, Copenhagen).

The DNA sample was submitted to Macrogen Inc. (Korea) for 16S rRNA amplicon library preparation and sequencing using Illumina Miseq instrument (300 bp paired-end sequencing). Amplification of V3 and V4 region of 16S rRNA gene was done with Pro341F 5'-CCTACGGGNBGCASCAG-3' and Pro805R 5'-GACTACNVGGGTATCTAATCC-3' [26]. Sequences containing primers were trimmed with cutadapt and all other reads filtered out [27]. Subsequently, filtering, generation of operational taxonomic units (OTUs) and mapping of reads to OTUs were performed using the UPARSE/unoise3 pipeline [28]. Taxonomy was assigned to OTUs using SINTAX and NCBI database of 18421 16S

ribosomal RNA sequences from NCBI RefSeq Targeted Loci Project [29]. Subsequently, OTU table was corrected using the UNCROSS algorithm [30], normalized with respect to 16S copy number and primer mismatches with UNBIAS algorithm [31]. Each sample was normalized to the depth of the sample with least counts. OTUs with overall count less than 100 were filtered out and sample data from available replicate runs have been collapsed based on the mean count. Downstream analyses were performed with Phyloseq R [32] package and MicrobiomeAnalyst web service, available at <http://www.microbiomeanalyst.ca/> [33]. Fitting of environmental variables onto ordination plots was performed with R Vegan package [34].

Analytical methods

The gaseous composition of the headspace (H₂, CO, CO₂ and CH₄) was determined using a gas chromatograph (model 8610C, SRI Instruments, USA) equipped with a thermal conductivity detector and two packed columns, a 6' × 1/8" Molsieve 13× column and a 6' × 1/8" silica gel column connected in series through a rotating valve. The column temperature was maintained at 65 °C for 3 min, followed by a temperature ramp of 10 °C/min to 95 °C and 24 °C/min from 95 to 140 °C. Gaseous samples of 50 µl were collected with a gas-tight syringe (model 1750SL, Hamilton). Volatile fatty acids (VFA) (acetate, propionate, iso-butyrate, butyrate and caproate) and alcohols (ethanol and 1-butanol) were determined using a high performance liquid chromatograph (Shimadzu, USA) equipped with a refractive index detector and an Aminex HPX-87H column (Bio-Rad, USA) at 63 °C. A solution of 12 mM H₂SO₄ was used as eluent at a flow rate of 0.6 ml/min. Volatile Suspended Solids (VSS) concentration in the fermentation broth was determined according to standard methods [35]. Microbial biomass growth was monitored by measuring the absorbance of liquid samples at 600 nm using a spectrophotometer (DR2800, Hach Lange), and was correlated to the volatile

suspended solids (VSS) concentration of the fermentation broth.

Product yield and efficiency calculations

The product yields were calculated using CO, H₂ and acetate (when applicable) as substrates and are given in mol product/e-mol substrate for them to be expressed on a common basis for all substrates according to:

$$Y_i \left(\frac{\text{mol}}{\text{e-mol}} \right) = \frac{n_{(i)} \text{produced}}{n_{\text{H}_2} \text{consumed} \cdot n_{e-\text{H}_2} + n_{\text{CO}} \text{consumed} \cdot n_{e-\text{CO}} + n_{\text{Acetate}} \text{consumed} \cdot n_{e-\text{Acetate}}} \tag{1}$$

where $n_{(i)}$ is the number of moles of compound i , and $n_{e-\text{H}_2}$, $n_{e-\text{CO}}$ and $n_{e-\text{Acetate}}$ are the number of e-mol per mol of H₂, CO and acetate, respectively. Acetate was included as substrate in the calculations only for enrichments and fermentations with initial addition of acetate that resulted in net consumption of acetate.

The efficiency of the enriched mixed microbial consortia was calculated based on the recovery of e-mol and carbon from the different substrates (H₂, CO and CO₂) in the products. The recovery of e-mol from H₂ and CO in products was corrected by subtracting the total e-mol produced in control experiments according to:

$$\text{e-mol recovery (\%)} = \frac{\sum_{i=1}^N (n_{(i)} \text{produced} - n_{(i)} \text{control}) \cdot n_{e-(i)}}{n_{\text{H}_2} \text{consumed} \cdot n_{e-\text{H}_2} + n_{\text{CO}} \text{consumed} \cdot n_{e-\text{CO}}} \cdot 100 \tag{2}$$

where $n_{e-(i)}$ is the number of e-mol per mol of compound i . Similarly, the recovery of carbon from CO and CO₂ in the products was calculated taking into account the production in control experiments and the concentration of CO₂ (aq), HCO₃⁻, CO₃⁻² as a function of the initial and the final pH according to Eqs. 3, 4, 5 and 6.

$$\text{Cmol recovery (\%)} = \frac{\sum_{i=1}^N \text{Cmol}_{(i)} \text{produced} - \text{Cmol}_{(i)} \text{control}}{n_{\text{CO}} \text{consumed} + n_{\text{CO}_2} \text{consumed} + n_{\text{HCO}_3^-} \text{consumed} + n_{\text{CO}_3^{2-}} \text{consumed}} \cdot 100 \tag{3}$$

$$[\text{CO}_2(\text{aq})] = K_{\text{HCO}_2} \cdot P_{\text{CO}_2} \tag{4}$$

$$[\text{HCO}_3^-] = \frac{[\text{CO}_2(\text{aq})] \cdot K_{a1}}{[\text{H}^+]} \tag{5}$$

$$[\text{CO}_3^{2-}] = \frac{K_{a2} \cdot [\text{CO}_2(\text{aq})] \cdot K_{a1}}{[\text{H}^+]^2} \tag{6}$$

The dissociation constants K_{a1} and K_{a2} were corrected for the ionic strength of BA medium ($I=0.08$ M) by solving Eq. 7 for K_a . The standard Gibbs free energy of formation ($\Delta_f G^\circ$) of the carbonate species was extracted from Alberty [36] and corrected using the extended Debye–Hückel equation (Eq. 8) prior to calculating the Gibbs free energy change of the dissociation reactions ($\Delta_r G^\circ$) [37].

$$0 = \Delta_r G^\circ (I = 0.08M) + RT \ln K_a \tag{7}$$

Thermodynamic calculations

The thermodynamics of the net biochemical reactions was evaluated through the Gibbs free energy change ($\Delta_r G^\circ$) of reactions under the specific operating conditions of the enrichment series. To study the effect of the enrichment conditions on the feasibility of each biochemical reaction, the $\Delta_r G^\circ$ of all reactions was corrected for ionic strength, pH, temperature and concentration of substrates and products. Standard Gibbs free energies of formation ($\Delta_f G^\circ$) and standard enthalpies of forma-

tion ($\Delta_f H^\circ$) were extracted from Amend and Shock [38] and Alberty [36]. The $\Delta_f G^\circ$ and $\Delta_f H^\circ$ were corrected for the ionic strength of BA medium ($I=0.08$ M) using the extended Debye–Hückel equation:

$$\Delta_f G_i^\circ (I) = \Delta_f G_i^\circ (I = 0) - \frac{RTAz_i^2 I^{1/2}}{1 + BI^{1/2}} \tag{8}$$

$$\Delta_f H_i^\circ (I) = \Delta_f H_i^\circ (I = 0) + \frac{1.4775z_i^2 I^{1/2}}{1 + BI^{1/2}} \tag{9}$$

where z_i is the charge number of compound i , A equals 1.1758 kg^{1/2}/mol^{1/2} in water at 25 °C and B is an empirical constant that equals 1.6 L^{1/2}/mol^{1/2} within a ionic strength range of 0.05–0.25 M [36]. Next, the initial concentration of products and substrates in the medium and partial pressure of gases was corrected using Eq. 10,

and the pH was taken into account according to Steinbusch et al. [22]. Note that the reaction quotient in Eq. 10 denotes the concentration of products and reactants of the general reaction $aA + bB \leftrightarrow cC + dD$. Finally, $\Delta_r G'$ of all reactions was adjusted to the incubation temperature of the enrichment experiments (310.15 K) using the Gibbs–Helmholtz Eq. 11. The reactions considered in the thermodynamic analysis are given in Table 2.

$$\Delta_r G' = \Delta_r G^\circ (I = 0.08M) + RT \ln \frac{[C]^c [D]^d}{[A]^a [B]^b} \quad (10)$$

$$\Delta_r G'_T = \Delta_r G'_{298.15K} \cdot \frac{T}{298.15K} + \Delta_r H'_{298.15K} \cdot \frac{298.15K - T}{298.15K} \quad (11)$$

Thermodynamic potential factor (F_T)

The thermodynamic potential factor (F_T), introduced by Jin and Bethke [39], was calculated with the purpose of identifying a possible thermodynamic control on the rates of the biochemical reactions considered. Jin and Bethke [39] introduced this factor as a modification of usually employed rate laws, e.g., Monod equation ($r = \frac{k_{max} \cdot S}{K_s + S} \cdot X \cdot F_T$), to make them thermodynamically consistent by taking into account the energy available and the energy conserved along a particular metabolic pathway. Thus, the thermodynamic potential factor (F_T) determines whether the net biochemical reactions are subject to either thermodynamic or kinetic control depending on the thermodynamic driving force of each reaction, and is calculated according to the following equation:

$$F_T = 1 - \exp\left(\frac{\Delta G_A + \Delta G_C}{\chi RT}\right) \quad (12)$$

where ΔG_A corresponds to the energy available through each biochemical reaction ($-\Delta_r G'_{310 K}$ calculated as described in “[Thermodynamic calculations](#)”) in kJ per reaction; ΔG_C is the energy conserved determined by the number of ATP produced in each metabolic pathway multiplied by the Gibbs free energy of phosphorylation (ΔG_p); and χ is the average stoichiometric number and represents the number of times a rate-determining step takes place in the overall reaction or metabolic pathway. When $\Delta G_A \gg \Delta G_C$, there is a strong thermodynamic driving force for the forward reaction and F_T approaches 1, indicating that the rate of the reaction is strictly dependent on the kinetics of the biochemical reaction. Conversely, when ΔG_A approaches ΔG_C , there is a small thermodynamic drive and F_T approaches 0, indicating a thermodynamic control of the reaction as F_T exerts a

strong effect on the reaction rate. Finally, ΔG_A equal to or lower than ΔG_C results in a F_T of 0 or negative, respectively, indicating that the thermodynamic drive vanishes and the metabolism ceases.

The calculations of the F_T for the direct conversion of H_2/CO_2 and CO into acetate and ethanol were carried out using ATP yields given by Bertsch and Müller [40]. The chain elongation reaction was assumed to yield 1 mol ATP per reaction, obtained through substrate level phosphorylation, according to Angenent et al. [41]. The reduction of acetic acid into ethanol with H_2 as electron donor was assumed to follow the acetate activation pathway via acetyl-CoA at the expense of 1 ATP, which would be compensated through the translocation of four protons across the membrane resulting in 0.33 mol ATP per reaction, as suggested by González-Cabaleiro et al. [42]. The analogous acetic acid reduction to ethanol using CO was assumed to follow the same pathway; however, a tentative yield of 0.66 mol of ATP per reaction was used, as the ATP yield of this reaction would be expected to be higher due to the oxidation of the additional reduced ferredoxin produced by CO dehydrogenase. The stoichiometry of the ATP synthesis through ion translocation used for the calculated ATP yields corresponded to a fixed ratio of 3 mol of H^+/Na^+ per mol of ATP. The average stoichiometric number (χ) was determined by the number of ions translocated across the membrane for all reactions, except for the chain elongation, in which the substrate level phosphorylation was used instead. It should be noted that the ATP yields used here were not determined experimentally, and thus, are subject to uncertainties derived from the assumptions made in each case. To account partially for these uncertainties and give an idea of the sensitivity of the thermodynamic potential factor (F_T) to the energy conservation parameter, a rather broad range of Gibbs free energy of phosphorylation was used for the calculations corresponding to 45 kJ/mol ATP [43], 57.5 kJ/mol ATP and 70 kJ/mol ATP [44]. The values used for the calculations are summarized in Table 2.

Results and discussion

Enrichment of syngas-converting microbial consortia based on pH

Ethanologenic potential of enriched consortia

A number of enrichment strategies using the pH as the main selective driver were designed to study the evolution of the ethanologenic activity during the enrichment of microbial consortia at different initial conditions. Different initial pH conditions were tested using a heat-shock-treated inoculum (pH 6, 5.5 and 5) and a non-treated inoculum (pH 5).

All enrichment strategies successfully suppressed the methanogenic activity of the anaerobic sludge as

Table 2 Biochemical reactions, ATP yield and average stoichiometric number used in the thermodynamic potential factor calculation

Stoichiometry of biochemical reactions	ATP yield (mol per reaction)	χ	Refs.
H ₂ /CO ₂ conversion into acetate/ethanol			
4 H ₂ + 2 CO ₂ → CH ₃ COO ⁻ + H ⁺ + 2 H ₂ O	0.3	2	[40]
6 H ₂ + 2 CO ₂ → CH ₃ CH ₂ OH + 3 H ₂ O	-0.1/0.3 ^a	3	[40]
CO conversion into acetate/ethanol			
4 CO + 2 H ₂ O → CH ₃ COO ⁻ + H ⁺ + 2 CO ₂	1.5	4	[40]
6 CO + 3 H ₂ O → CH ₃ CH ₂ OH + 4 CO ₂	1.7	6	[40]
VFA reduction to corresponding alcohols			
CH ₃ COO ⁻ + H ⁺ + 2 H ₂ → CH ₃ CH ₂ OH + H ₂ O	0.33	4	[42]
CH ₃ (CH ₂) ₂ COO ⁻ + H ⁺ + 2 H ₂ → CH ₃ (CH ₂) ₂ CH ₂ OH + H ₂ O	0.33	4	[42]
CH ₃ COO ⁻ + H ⁺ + 2 CO + H ₂ O → CH ₃ CH ₂ OH + 2 CO ₂	0.66	5	
CH ₃ (CH ₂) ₂ COO ⁻ + H ⁺ + 2 CO + H ₂ O → CH ₃ (CH ₂) ₂ CH ₂ OH + 2 CO ₂	0.66	5	
Chain elongation			
5 CH ₃ CH ₂ OH + 3 CH ₃ COO ⁻ → 4 CH ₃ (CH ₂) ₂ COO ⁻ + H ⁺ + 3 H ₂ O + 2 H ₂	1	1	[41]

^a Bertsch and Müller [40] predicted an ATP yield of -0.1; however, the possibility of a positive ATP yield was also evaluated

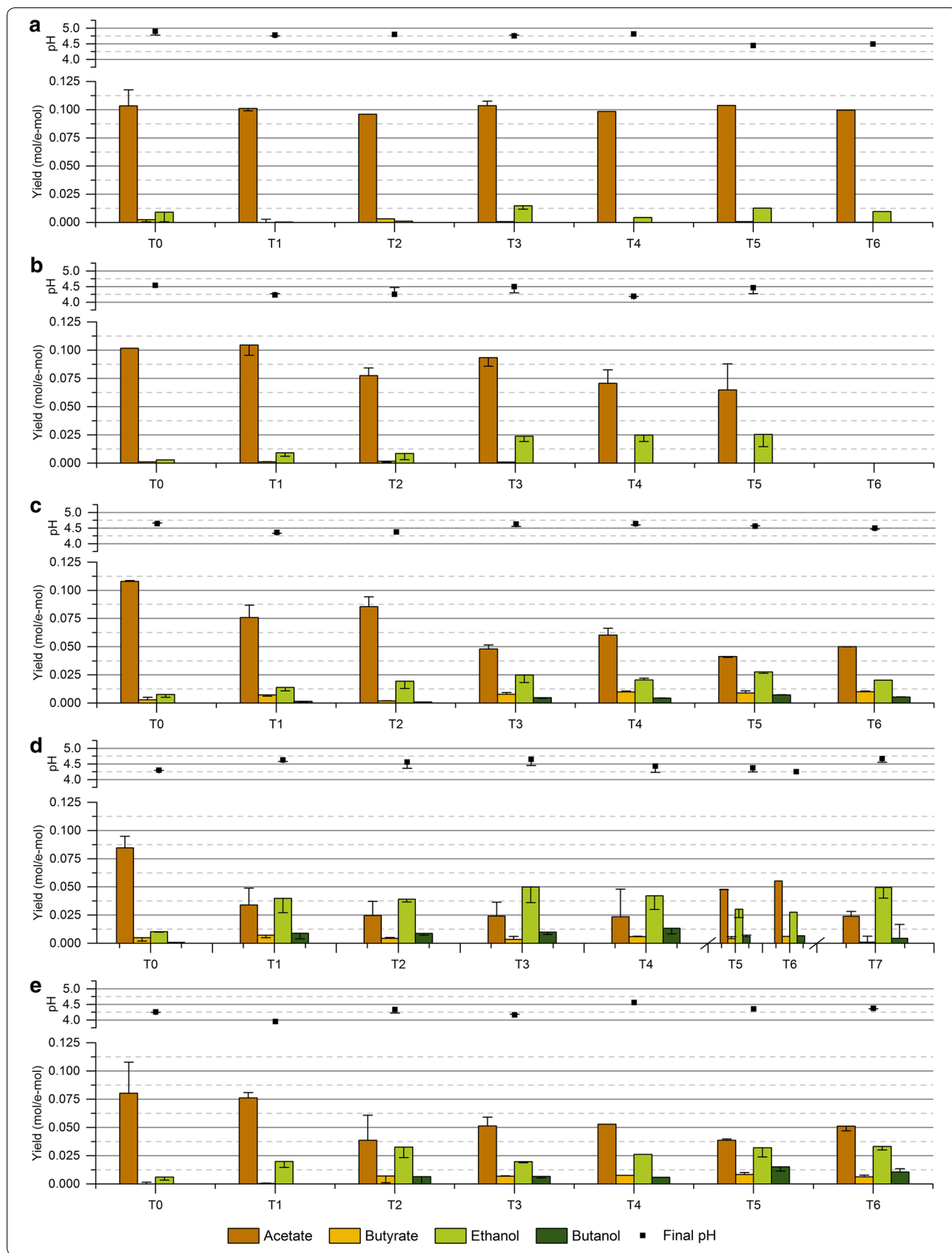
methane was not detected in any transfer of the enrichments. This was expected in the enrichments using a heat-shock-treated inoculum, since spore-forming bacteria should be predominant in the anaerobic sludge as a result of the heat treatment [45]. In turn, small amounts of methane were expected when using the non-treated inoculum due to the abundance of methanogenic archaea in the anaerobic sludge, as observed by Steinbusch et al. [46]. However, in this study, the low initial pH (pH 5) of experiments using the non-treated inoculum inhibited both methanogenic and acetogenic growth when YE was not added to the growth medium, whereas experiments with YE addition presented exclusively acetogenic growth. This indicates that the methanogenic activity of the sludge was inhibited by the combination of low pH and toxicity of CO. Thus, open-mixed cultures could be used in syngas fermentation processes with no need of heat treatment or methanogenic inhibitors, just by operating at harsh conditions for methanogenic archaea.

All enrichment conditions presented a very low ethanol production in the first transfer, with the product spectrum being initially dominated by acetate (Fig. 2). However, as the enrichments progressed, the distribution of products rapidly shifted following different trends depending on the operating conditions and seemed to be relatively stable after two to three transfers in most of

the enrichments. The enrichment with initial pH 6 (HT6) resulted in the narrowest product spectrum with acetate as the main end product, and small amounts of ethanol and butyrate produced irregularly during the enrichment (Fig. 2a). As expected, decreasing the initial pH to 5.5 (HT5.5) improved the production of ethanol, which increased gradually along the enrichment reaching a maximum ethanol yield of 0.025 mol/e-mol (30.4% of the stoichiometric maximum) and an average of duplicates of 0.020 ± 0.005 mol/e-mol at transfer T5 (Fig. 2b). Nevertheless, the lower initial pH of this enrichment negatively affected the growth of the microbial consortium as the enrichment advanced until transfer T5, at which the culture could not be reactivated anymore. The enrichment with initial pH 5 (HT5) did not present any growth (data not shown); indicating that the microbial activity of the inoculum used was inhibited by the low initial pH of this enrichment. Consequently, enrichments with initial pH 5.5 and 5 were restarted and supplemented with YE to favor a better microbial growth. The addition of YE to the enrichment with initial pH 5.5 (HT5.5YE) indeed allowed a much better microbial growth as the lag phase of the culture was significantly reduced (Additional file 1: Figures S1–S4), and did not have any effect on the final ethanol yield when compared to enrichment HT5.5 (Fig. 2b, c). Further decreasing the initial pH to 5 significantly

(See figure on next page.)

Fig. 2 Product yields (mol/e-mol) obtained in each transfer for all enrichment conditions and final pH at the moment of the transfer. The columns show the values for the fermentation transferred and the error bars indicate the corresponding values of the duplicate experiment. Additional information on substrate consumption and apparent biomass yields can be found in Additional file 1: Figure S5. **a** Enrichment HT6 at an initial pH of 6; **b** enrichment HT5.5 at an initial pH of 5.5; **c** enrichment HT5.5YE at an initial pH of 5.5 with YE (0.5 g/l); **d** enrichment HT5YE at an initial pH of 5 with YE (0.5 g/l); **e** enrichment NT5YE at an initial pH of 5 with YE (0.5 g/l)



enhanced the solventogenic activity in enrichment HT5YE, with ethanol becoming the main end product and obtaining a maximum ethanol yield of 0.050 mol/e-mol (59.5% of the stoichiometric maximum) and an average of 0.045 ± 0.005 mol/e-mol at transfer T7 (Fig. 2d).

The enrichment with initial pH 5 using the non-treated inoculum (NT5YE) presented a similar trend with enrichment HT5YE, as the solventogenic activity was rapidly boosted along the successive transfers (Fig. 2e). However, the maximum ethanol yield obtained in enrichment NT5YE at transfer T6, namely, 0.033 mol/e-mol and 39.7% of the stoichiometric maximum (average of 0.032 ± 0.002 mol/e-mol), was not as high as that of enrichment HT5YE. An explanation for this difference in the product yields could be based on the heat treatment of the inoculum, as the enrichment HT5YE presented a more abrupt response upon exposure to the enrichment conditions (from T0 to T1) compared to enrichment NT5YE, where changes in the product profile took place gradually (from T0 to T2). Thus, it is possible that the higher degree of sporulation derived from the heat treatment of the initial inoculum favored a faster microbial selection process ultimately resulting in a different ethanologenic activity in these two enriched consortia. Besides the quantitative difference in the final ethanol yield, the high similarity in the behavioral traits of these microbial consortia is also supported by their common response upon reactivation of the cultures. As shown in Fig. 2d, e, a noticeable decrease of solventogenic activity was observed in both enrichments after stopping them for 2 months at transfer T4 (HT5YE) and T2 (NT5YE). Additionally, a very similar or even higher solventogenic activity was recovered after two transfers upon resuming the enrichments in both microbial consortia.

The apparent biomass yield was observed to be affected by both the initial pH of the enrichments and the addition of YE. Generally, the average biomass yield along the enrichments varied between 1.7 and 2.8 mg VSS/e-mol, with enrichment HT5.5 presenting the lowest biomass yield and enrichments HT5YE and NT5YE exhibiting the highest biomass yields (Additional file 1: Figure S5). No statistically significant differences were found between the average biomass yield of the enrichments at different pH, with *P* values above 0.05 in all cases when comparing HT6 to the rest of the enrichments (Additional file 1: Figure S5 and Table S1). However, the fact that the enrichment HT5.5 could not be reactivated at transfer T6 and that enrichment HT5 did not present any growth indicates a clear negative effect of the pH on microbial growth. In turn, the addition of YE was observed to improve the biomass yield of the enrichment cultures as statistically significant differences with *P* values below 0.05 were found between enrichment HT5.5 and all

enrichments with YE addition, namely, HT5.5YE, HT5YE and NT5YE (Additional file 1: Table S1).

A low pH is commonly applied in syngas fermentation studies [47, 48] based on the hypothesis that the higher diffusion of VFAs through the cell membrane at acidic pH triggers solventogenesis as a means of preventing a further intracellular pH drop [49, 50]. The observations made in this study are in agreement with this hypothesis as (i) the highest ethanol yields were obtained in the enrichments at the lowest initial pH tested, and (ii) the final pH of the fermentations oscillated around 4.3–4.6 in most enrichment conditions and seemed not to be related to the initial pH conditions (Fig. 2c, d). Thus, it is likely that intracellular pH homeostasis may have driven a higher ethanol production by the enriched consortia.

The addition of YE appeared to have no effect on the final yield of ethanol in enrichments at an initial pH of 5.5 (Fig. 2b, c), but triggered the production of butyrate, butanol and small amounts of caproate leading to a broader product spectrum in all YE-supplemented enrichments (Fig. 2c–e). The production of butyrate and butanol was observed to take place in a two-step reaction, which indicates that they were produced through chain elongation and reduction of VFAs (Additional file 1: Figures S6, S7). The potential of microbial consortia for producing medium-chain fatty acids (MCFAs) through chain elongation has been shown in a number of studies [18, 51]. However, when it comes to ethanol production, the chain elongation process is often regarded as a major drawback as it reduces the selectivity of the mixed culture towards ethanol due to the conversion of ethanol and VFAs into MCFAs, as found in El-gammal et al. [52]. In this study, a significant chain-elongating activity appeared to be prevented by the low pH of the fermentations (generally ranging between 4.3 and 4.6 at the end of the experiments), since both acetate and ethanol remained as the major end products at all enrichment conditions. Ganigué et al. [21] reached similar conclusions in a study targeting the production of higher alcohols, in which low pH was found to affect negatively the chain elongation process. Nevertheless, the reduced chain-elongating activity found in the present study allowed achieving high ethanol yield in enrichments at pH 5.

A maximum ethanol yield of 0.050 mol/e-mol (59.5% of e-mol recovery) and an ethanol-to-acetate ratio of 1.58 g/g was achieved in enrichment HT5YE. The maximum ethanol-to-acetate ratio obtained was significantly higher than those often reported in other batch experiments using pure cultures such as *C. ragsdalei* (1.30 g/g) [10], *C. autoethanogenum* (0.39 g/g) [8] and *C. ljungdahlii* (0.70 g/g) [53], and in other mixed-culture studies with ratios below 0.4 g/g [20, 52]. Yet, higher

Table 3 Efficiency calculated in terms of e-mol and Cmol recovery and product yields for all enriched microbial consortia

	HT6	HT5.5 ^a	HT5.5YE	HT5YE	NT5YE
Recovery (%) ^b					
e-mol	92.92 ± 0.54	85.83 ± 2.46	89.84 ± 1.80	88.57 ± 1.77	95.01 ± 3.29
Cmol	83.16 ± 0.70	77.33 ± 2.31	93.18 ± 1.69	80.29 ± 0.83	91.60 ± 6.41
Product yield (% e-mol/e-mol)					
Acetate	83.32 ± 0.81	61.15 ± 7.41	41.38 ± 1.75	29.29 ± 0.63	27.68 ± 1.67
Propionate	0.00 ± 0.00	0.11 ± 0.20	0.01 ± 0.08	2.11 ± 0.38	0.26 ± 0.04
Iso-butyrate	1.55 ± 0.09	0.00 ± 0.00	1.82 ± 0.78	0.00 ± 0.00	1.17 ± 0.31
Butyrate	0.00 ± 0.00	0.00 ± 0.00	11.59 ± 4.82	2.05 ± 0.74	16.51 ± 1.07
Ethanol	8.16 ± 0.49	25.20 ± 5.32	29.40 ± 5.36	59.15 ± 0.18	34.81 ± 2.27
Butanol	0.00 ± 0.00	0.00 ± 0.00	15.37 ± 1.55	3.50 ± 0.64	21.82 ± 1.45
Caproate	0.00 ± 0.00	0.00 ± 0.00	1.39 ± 0.03	3.33 ± 0.20	1.09 ± 0.09
Biomass yield (g VSS/e-mol)	2.10 ± 0.11	1.83 ± 0.42	3.21 ± 0.51	3.13 ± 0.20	2.85 ± 1.06

^a The efficiency and product yields of HT5.5 were calculated using the results for transfers T4 and T5 of the enrichment

^b Additional information on the production of control experiments is provided in Additional file 1: Table S3

ethanol-to-acetate ratios were reported by Singla et al. (2014) using the enriched culture TERI-SA1 (2.46 g/g).

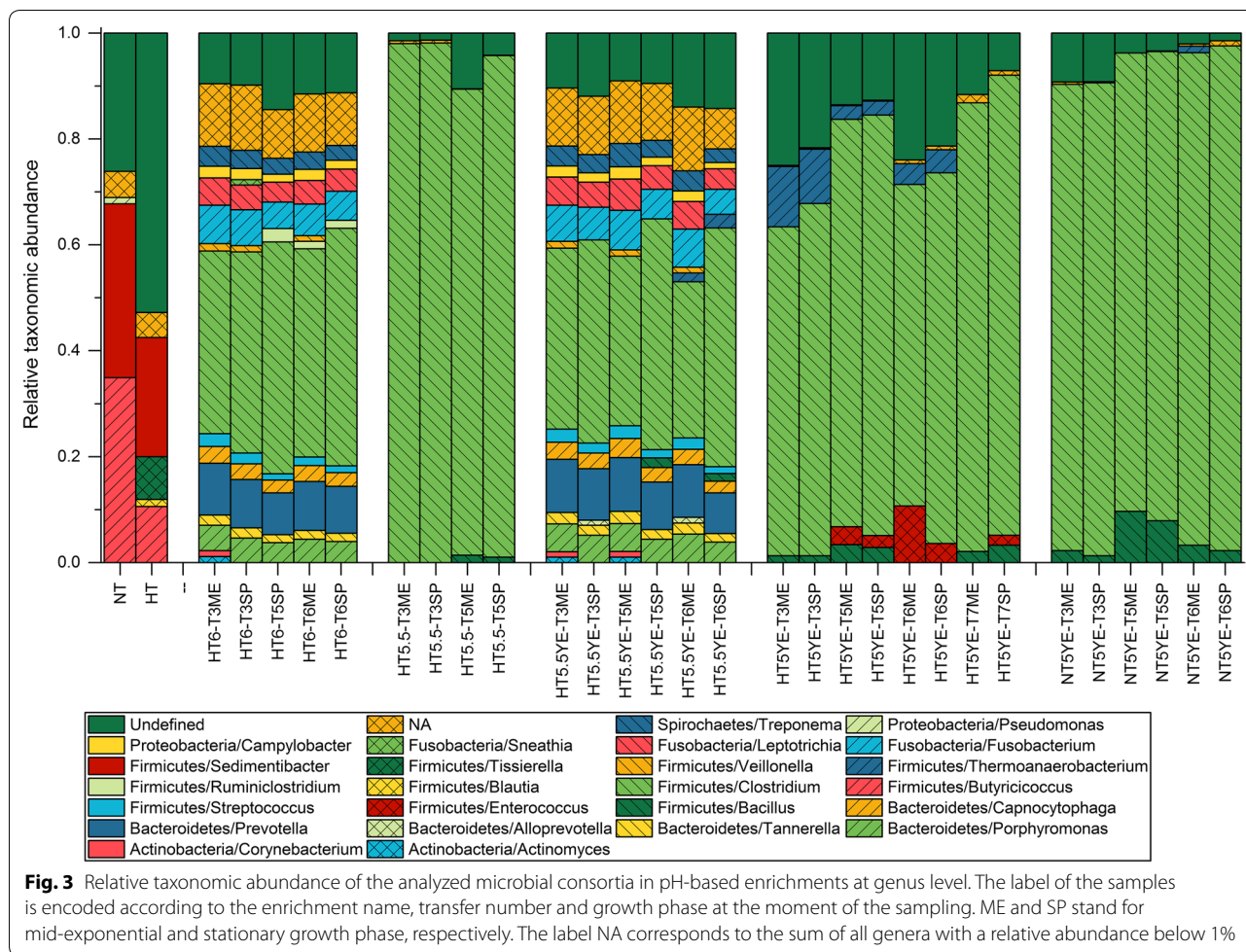
The analysis of the production efficiency on fermentations carried out by the enriched consortia showed that both the pH and YE had a significant effect on the performance of the cultures. Table 3 shows the production efficiencies, calculated on a Cmol and e-mol recovery basis, for all enriched consortia. The calculated Cmol and e-mol recoveries were in relatively good agreement, with a maximum deviation of 10% corresponding to the enriched consortium HT6. Generally, the efficiency of the fermentations remained at a high levels for all enriched consortia and was consistent with previously reported e-mol recoveries [54]. Nonetheless, differences can be observed in Table 3, where the production efficiency of the enriched consortium HT5.5 resulted to be much lower than that of the consortia HT6 and HT5.5YE. A statistically significant difference was found when comparing the Cmol recovery of the enriched cultures HT5.5 and HT5.5YE (*P* value of 0.0003), indicating that the addition of YE had a positive effect on the production efficiency. On the other hand, the decrease in pH had an adverse effect on the production efficiency since a statistically significant difference (*P* value of 0.017 and 0.012 for Cmol and e-mol recovery, respectively) was found between the product recovery of the consortia enriched at pH 5.5 (HT5.5) and at pH 6 (HT6). However, the negative effects of reducing the initial pH were not significant as long as YE was added to the medium (Additional file 1: Table S2). These effects of pH and YE on the production efficiency were in fact anticipated as increasing both pH (in the range tested) and YE has been previously reported to favor biomass growth [8], which in turn reduces the

maintenance requirements for cell metabolism and allows a higher production efficiency. Interestingly, the product distribution had no effect on the production efficiency of the fermentations, indicating that the latter was strictly dependent on the growth conditions.

Microbial characterization of enrichment cultures

A total of 49,736,621 sequences were obtained from all investigated samples after quality checking and data filtering, with an average of 956,473 reads per sample (range 309,337–8,985,816 reads per sample). Replication, error correction, denoising with unoise algorithm and filtering of OTU table resulted in 6183 OTUs with all but one OTUs belonging to bacteria domain. Considering all sequences retrieved in the present study, Firmicutes accounted for the largest fraction (78% of the total), mainly represented by the classes *Clostridia*, *Tissierella* and *Bacilli*.

The analysis of the microbial composition of the enrichment samples at genus level revealed significant differences between the initial inocula and the different enrichment cultures. The untreated (NT) and heat-shock-treated (HT) inocula were initially dominated by the genera *Sedimentibacter* (32.8% and 22.5% of reads mapping to corresponding OTUs for NT and HT, respectively) and *Butyrivicoccus* (34.9 and 10.6% for NT and HT, respectively), while other genera like *Clostridium* represented only a minor fraction (below 1% in both cases) (Additional file 2: Table S1). However, upon exposure to the different operating conditions, the composition of all enrichment cultures rapidly shifted with a clear and stable dominance of the genus *Clostridium* from transfer T3. As shown in Fig. 3, the degree of dominance of the genus *Clostridium*



was variable across the different enrichment conditions. Samples from enrichments HT6 and HT5.5YE presented the highest diversity in terms of genera, with the genus *Clostridium* representing an average of $41.5 \pm 3.3\%$ and $37.1 \pm 6.3\%$ of the total reads mapped, respectively. In turn, samples from enrichments HT5.5, HT5YE and NT5YE exhibited a lower diversity at genus level with a much larger representation of the reads mapping to OTUs corresponding to *Clostridium* with an average of $94.7 \pm 4.7\%$, $73.4 \pm 10.0\%$ and $90.2 \pm 3.3\%$, respectively. These results show that *Clostridium* was among the most resilient genera found in the microbial consortia since its dominance increased with harsher enrichment conditions, i.e., decreasing pH or absence of YE.

Despite the clear dominance of OTUs belonging to the genus *Clostridium* in all enrichments, the abundance of individual OTUs found in the enrichment samples varied depending on the enrichment conditions (Additional file 2: Table S3). The mean relative frequencies between the OTU abundances were compared across all samples with and without addition of YE. It was found that

representative sequences of abundant OTUs identified solely in enrichments without addition of YE (HT6 and HT5.5), aligned with high identity (98.4–100%) to 16S rRNA genes from *Clostridium autoethanogenum* and *Clostridium ljungdahlii*. Abundances of these OTUs (2;1302;1233;1249;1983) were 81.5% and 41.4% in samples HT5.5T5SP and HT6T6SP, respectively (Additional file 2: Table S3). In turn, reads mapping to these OTUs were negligible in YE-supplemented enrichments. Moreover, identified OTUs exclusively present in YE-supplemented enrichments and their representative sequences exhibited the best alignment (97–100% identity) with 16S rRNA sequences of *Clostridium drakei* and *Clostridium carboxidivorans*. Abundance of these OTUs (1;337;434;359) was up to 87.5% in sample NT5YET6SP (Additional file 2: Table S3). These differences indicate that the addition of YE, besides promoting better growth conditions for the entire microbial consortium, also played a determining role as a selection factor in addition to the pH conditions and the substrate composition.

The range of metabolites found in each of the enrichment series was in agreement with the product portfolio of the putative dominant species identified in the enrichment samples. As mentioned above, acetate and ethanol were the main metabolites in enrichments HT6 and HT5.5 where the putative dominant species were *C. autoethanogenum* and *C. ljungdahlii*, while longer carbon chain products such as butyrate and butanol were also found in YE-supplemented enrichments (HT5.5YE, HT5YE and NT5YE) with *C. drakei* and *C. carboxidivorans* as putative dominant species. Both *C. autoethanogenum* and *C. ljungdahlii* have been reported to produce only acetate and ethanol when fermenting syngas in batch cultures [55, 56]. In turn, *C. drakei* and *C. carboxidivorans* present a broader product spectrum including butyrate, butanol, and even caproate and hexanol in the case of *C. carboxidivorans* [57, 58], which are produced through re-assimilation, chain elongation and reduction of the primary metabolites [59]. Additionally, the optimum growth conditions for all these species vary between a pH of 5.5 and 6.2 and temperatures around 37 °C, which explains the dominance of these species during the enrichments. Therefore, most likely the dominant species identified were the major contributors to the formation of products observed during the enrichments.

The ethanol yield seemed to be independent of the microbial composition of the enrichment cultures at genus level. Enrichments HT6 and HT5.5YE resulted in a similar microbial composition (Fig. 3) and presented a maximum ethanol yield along the enrichment of 0.015 and 0.028 mol/e-mol, respectively (Fig. 2). Similarly, enrichments HT5.5, HT5YE and NT5YE also presented similar microbial composition with a clear dominance of the genus *Clostridium* (Fig. 3) and resulted in a maximum ethanol yield of 0.025 mol/e-mol, 0.050 mol/e-mol and 0.034 mol/e-mol, respectively (Fig. 2). On the contrary, enrichments at similar operating conditions and different microbial composition (HT5.5 and HT5.5YE) resulted in similar maximum ethanol yields. Thus, despite the clear effect of the pH on the microbial composition of the enriched consortia, it can be concluded that the shift towards ethanol observed in the enrichment experiments was probably the result of the metabolic response to the different initial pH conditions and not so dependent on the microbial composition of the enrichment cultures.

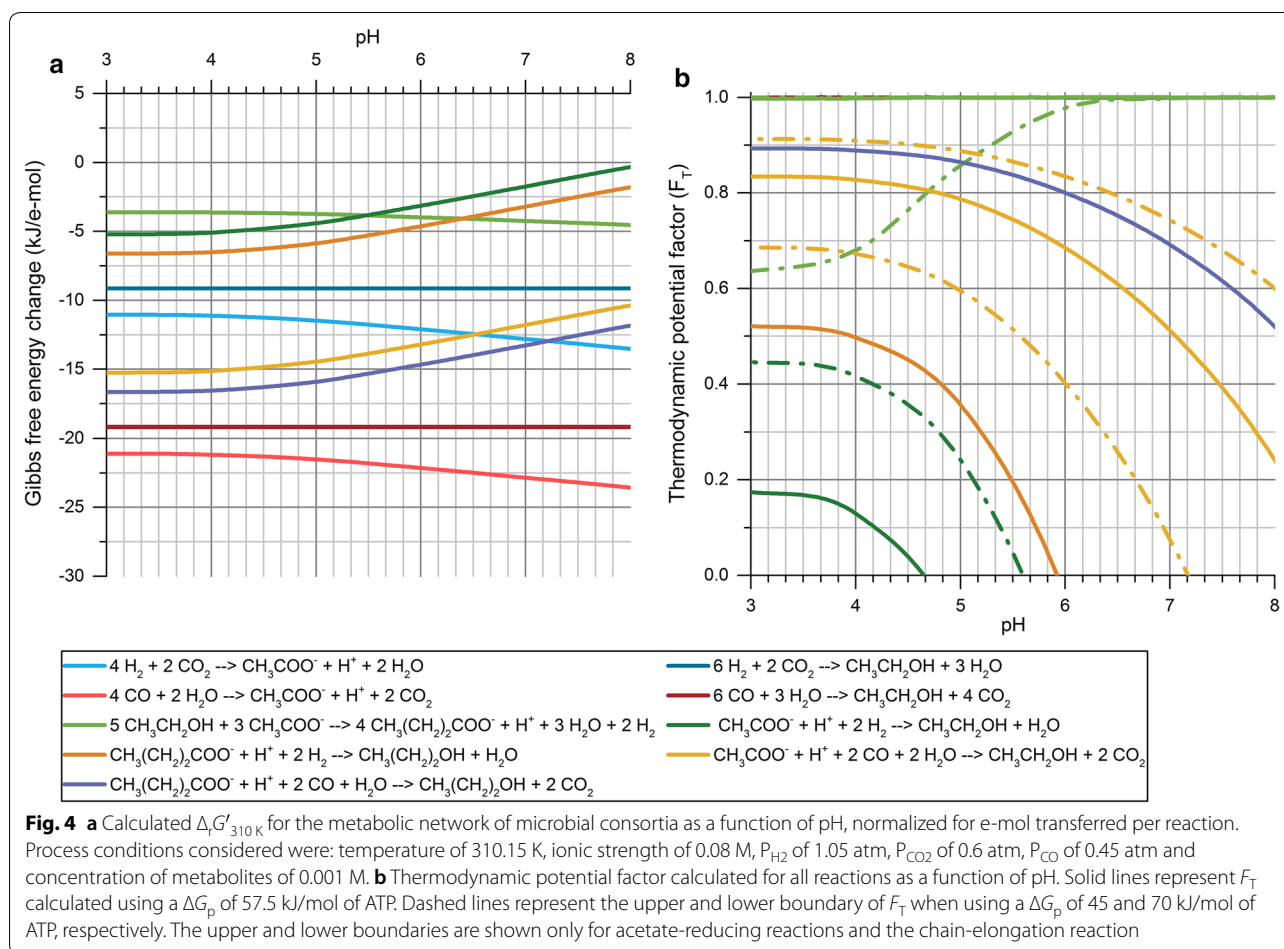
A direct comparison with the literature is not possible since the only quantitative analysis of the composition of a syngas-converting microbial consortium using a 16S rRNA amplicon-based sequencing method was performed under higher pH conditions (pH 7.5), and thus, resulted in significantly different microbial composition [54]. However, the species identified in other studies carried out at a comparable pH range (pH 6.2–6.0) which were entirely consistent

with the results found here [21, 24]. Ganigué et al. (2016) studied the composition of a microbial consortium during the conversion of syngas into higher alcohols using PCR-DGGE analysis and identified both of the putative dominant species reported here (*C. autoethanogenum*/*C. ljungdahlii* and *C. drakei*/*C. carboxidivorans*). In their study, *C. autoethanogenum*/*C. ljungdahlii* were found to be the main species carrying out the carbon fixation. In turn, Singla et al. [60] found that *C. drakei* and *C. scatalogenes* were either the main or possibly the only members of the enriched microbial consortium TERI-SA1. Interestingly, YE was not added in the medium used by Ganigué et al. [21] during the enrichment, while Singla et al. [60] added 1 g/l of YE to the medium. Taking this into consideration, the findings reported in the literature and the results reported here follow the same trend, with the putative dominant species of the enrichment cultures being *C. autoethanogenum*/*C. ljungdahlii* when YE was absent in the growth medium and *C. drakei*/*C. carboxidivorans* when YE was added to the medium.

Thermodynamic analysis of the metabolic network of the enriched consortia

The enriched consortia developed through pH-based enrichments were observed to produce ethanol with relatively high selectivity. However, the production of ethanol took place during the exponential phase of the fermentations, and thus, it was not possible to distinguish between direct production of ethanol and reduction of acetic acid to ethanol. Therefore, a thermodynamic analysis of the metabolic network of net biochemical reactions taking place during the activity of the enriched consortia was performed to identify possible bioenergetic drivers of the metabolic shift observed under different enrichment conditions. Based on experimental observations, the reactions considered for evaluating the $\Delta_r G'_{310\text{K}}$ and the thermodynamic potential factor (F_T) under changing process conditions were the production of ethanol and acetic acid from H_2/CO_2 and CO, the production of butyric acid through chain elongation, and the reduction of both acetic and butyric acid into their corresponding alcohols using either H_2 or CO as electron donor.

Analyzing the $\Delta_r G'_{310\text{K}}$ of the metabolic network of the enriched microbial consortia revealed that several reactions could be affected upon changing the initial pH conditions. As shown in Fig. 4a, the production of acetate would be favored over ethanol when considering the direct conversion of either H_2/CO_2 or CO, as the $\Delta_r G'_{310\text{K}}$ of acetate-producing reactions are always below that of ethanol regardless the pH conditions. However, acetate-producing reactions from both substrates become less exergonic as the pH decreases, while the analogous ethanol-producing reactions remain unaffected by pH



changes. The chain elongation to butyrate follows a similar trend with acetate production, becoming thermodynamically less favorable upon decreasing the pH. In turn, the reduction of acetic and butyric acid using either H_2 or CO as electron donor is significantly boosted by the pH decrease until the $\Delta_r G'_{310\text{K}}$ stabilizes at around pH 3.5–4. Overall, besides the fact that acid-producing reactions are negatively affected by the lower pH, it seems that the only reactions clearly favored upon decreasing the initial pH conditions are the reduction of VFAs into their corresponding alcohols. However, the analysis of the thermodynamic potential factor (F_T) shows that not all reactions are equally affected by the changes in $\Delta_r G'_{310\text{K}}$ liberated. The F_T of both acetate- and ethanol-producing reactions from H_2/CO_2 and CO approach 1 at all pH conditions, indicating that these reactions would provide enough thermodynamic driving force to proceed forward regardless of the pH conditions considered and would not be significantly affected by the changes in $\Delta_r G'_{310\text{K}}$ (Fig. 4). Therefore, rather than being thermodynamically controlled, the rates of direct production of either acetate or ethanol would be ultimately controlled by the specific

enzyme kinetics of each metabolic pathway, which in turn would be dependent on the concentration of intermediate metabolites and reduced cofactors during the fermentation. On the other hand, the evaluation of the F_T for the reduction of VFAs into their corresponding alcohols, using either H_2 or CO, and the chain elongation reaction resulted in values between 0 and 1 depending on the pH conditions considered (Fig. 4b). This implies that the energy generated through these reactions is close to their energy conservation requirements, and as a result, the thermodynamic drive for these reactions to proceed forward is limited and pH-dependent. As opposed to direct acetate- and ethanol-producing reactions, the feasibility and the rate of VFA-reducing and chain elongation reactions are very sensitive to the changes in $\Delta_r G'_{310\text{K}}$ obtained at different pH conditions (Fig. 4a).

According to the thermodynamic analysis, the direct conversion of H_2/CO_2 and CO into either acetate or ethanol is not expected to be thermodynamically controlled until these substrates become severely depleted. However, the higher thermodynamic driving force (lower $\Delta_r G'_{310\text{K}}$) and ATP yield per mol of substrate for

acetate-producing reactions suggest that these would prevail over direct ethanol-producing reactions under kinetic control. Besides, calculations carried out by Bertsch and Müller [40] for the model organism *Acetobacterium woodii* indicate that the production of ethanol from H_2/CO_2 might not be possible, as this reaction would require a net input of 0.1 mol of ATP per mol of ethanol.

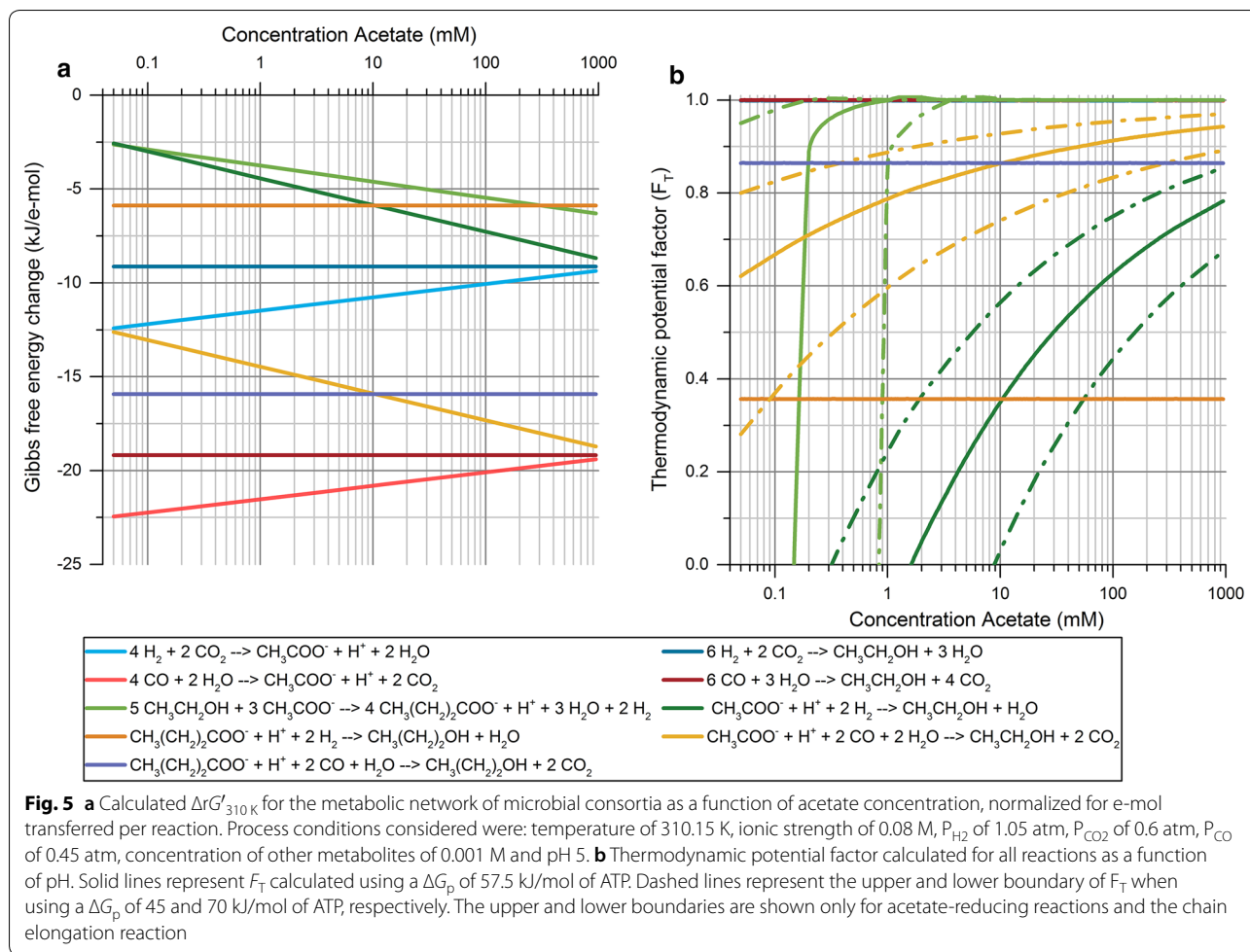
As opposed to direct conversion route from H_2/CO_2 and CO to liquid products, VFA-reducing reactions are subject to thermodynamic control under the operating conditions considered and are clearly favored upon decreasing the pH. The F_T values for all VFA-reducing reactions show that changes in $\Delta_r G'_{310 K}$ at the pH range studied have a strong effect on the rates of these reactions, which could explain the higher ethanol yield obtained in the enrichment experiments at an initial pH of 5. As illustrated in Fig. 4b, a high pH in the fermentation broth renders the reduction of acetate with H_2 unfeasible (negative F_T values). However, the boundaries of feasibility for this reaction cannot be accurately delimited due to the high sensitivity of F_T to the values of ATP yield and Gibbs free energy of phosphorylation (ΔG_p) used in the calculations. Considering an ATP yield of 0.33 mol per reaction and a ΔG_p of 45 kJ/mol of ATP, the reduction of acetate would be feasible below a pH of 5.6, whereas using a ΔG_p of 70 kJ/mol of ATP would render this reaction unfeasible at any pH resulting in a maximum F_T of -0.23 at pH 3. Thus, detailed conclusions on whether this reaction is possible as a function of pH cannot be drawn, although it is obvious that this reaction is more likely to occur at the lower range of pH studied. On the other hand, using CO as electron donor for the reduction of acetate provides a much lower $\Delta_r G'_{310 K}$, reducing the uncertainties on the activity of this reaction. In this case, the use of CO as electron donor is possible at all conditions regardless of the ΔG_p considered (Fig. 4b). Furthermore, decreasing the pH from 6 to 5 causes the F_T of this reaction to increase from 0.68 to 0.79 (Fig. 4b), indicating that the acetate-reducing activity is significantly boosted as the pH decreases. Thus, it can be concluded that acetate-reducing reactions played an important role on the solventogenic activity observed in the enrichment experiments. Additionally, based on the F_T for these reactions, the acetate-reducing activity using CO rather than H_2 as electron donor was probably more significant during the enrichments. This is in line with the observations made by Hu et al. [61] while studying the thermodynamics of the oxidation of CO and H_2 , where it was concluded that the use of CO as a source of electrons is thermodynamically more favorable than H_2 at all conditions.

In “[Ethanologenic potential of enriched consortia](#),” it was hypothesized that the chain elongation reaction was

inhibited by the decrease of pH during the fermentation, as both acetate and ethanol remained as the main products of the fermentation and were only partially converted into butyrate (Additional file 1: Figures S6, S7). However, the results of the F_T for this reaction at different pH conditions show that the chain elongating activity is negatively affected by the decrease of pH when considering a ΔG_p of 70 kJ/mol, with F_T values corresponding to 0.98, 0.86 and 0.68 at pH 6, 5 and 4, respectively (Fig. 4b). Therefore, the inhibition due to pH drop observed experimentally could be grounded on a limitation in the thermodynamic driving force for this reaction to proceed forward.

The thermodynamic analysis carried out here suggests that a significant amount of ethanol was produced via a two-step reaction, where direct production of acetic acid was initially favored followed by its reduction into ethanol in a second step. This is consistent with the distinction between acidogenic and solventogenic growth phases commonly applied in syngas fermentation processes [48, 62]. Furthermore, the limited thermodynamic drive for chain-elongating activity found when decreasing the pH could explain the high selectivity towards ethanol observed in enrichments at pH 5. Thus, the methodological approach used here proved to be useful for a qualitative interpretation of how the metabolic network of mixed microbial consortia responds when changing operational conditions. Of course, microbial growth inhibition phenomena due to high VFAs/solvents concentration are not taken into account in this method and need to be considered from a microbiological perspective; however, the enrichment experiments took place at low substrate and product concentration and were not expected to present such inhibition phenomena. This method presented low accuracy when attempting to draw definite boundaries on the feasibility of the acetate reduction with H_2 due to the broad range of ΔG_p used in the calculations. Other limitations identified were the fact that the energy conservation requirements, determined by the ATP yield and the ΔG_p , were assumed to be constant regardless of the reaction and operating conditions considered. The stoichiometry of ATP synthesis was also assumed to have a fixed ratio of 3 ions translocated per mol of ATP. Nevertheless, both the ΔG_p and the stoichiometry of ATP synthesis have been shown to be subject to variation depending on several factors such as intracellular ATP/ADP ratio, electrochemical membrane potential, electron donors and acceptors considered, or even the species carrying out the reaction [44].

Despite the limitations outlined above, the thermodynamic analysis allowed for interpretation of the effects of operating conditions on the network of biochemical reactions prevailing in mixed microbial consortia.



Thus, this method could be used for the selection of operational conditions with the aim of boosting specific reactions. To test the validity of this method for predicting changes in the microbial activity of enriched consortia and improving further the ethanol yield obtained previously, an additional experiment series was performed.

Enrichment strategies based on thermodynamics of the metabolic network

Thermodynamic predictions of the microbial activity

From a thermodynamic perspective, the metabolic network of microbial consortia can be affected by several operating parameters such as the partial pressure of gases, the concentration of products or the pH. Several of these parameters could potentially enhance the production of ethanol due to their distinct effect on different reactions such as the pH already discussed, the partial pressure of CO_2 given the distinct stoichiometric CO_2 formation in acetate- and ethanol-producing

reactions, the partial pressure of H_2 and CO affecting acetate-reducing reactions, and the initial concentration of acetate and ethanol affecting the whole metabolic network. In this case, given the effect of the pH on the acetate-reducing activity discussed in “[Thermodynamic analysis of the metabolic network of the enriched consortia](#)”, it was decided to study the effect of the initial acetate concentration in the medium to boost these reactions even further. However, this can be regarded as a proof-of-concept since this method could be used to evaluate the effect of the abovementioned parameters on any reactions taking place under thermodynamic control, e.g., in systems operating in continuous mode under substrate-limiting conditions.

The analysis of the $\Delta_r G'_{310K}$ indicated that the results obtained at pH 5 could be further improved by changing the initial concentration of acetate as several reactions would be significantly affected. As shown in Fig. 5a, the $\Delta_r G'_{310K}$ of ethanol-producing reactions from H_2/CO_2 and CO would be neither positively nor negatively

affected by the initial concentration of acetate. In turn, all reactions involving the use of acetate as product or substrate present significant variations in the $\Delta_r G'_{310\text{K}}$ upon changes in acetate concentration. While acetate-producing reactions are negatively affected by the increase of acetate, the reactions consuming acetate become thermodynamically favored. However, based on the F_T obtained for each reaction, only acetate-reducing reactions and the chain elongation could be thermodynamically controlled upon changing the initial acetate concentration (Fig. 5b). The production of acetate from both H_2/CO_2 and CO would not be sensitive to changes in $\Delta_r G'_{310\text{K}}$ as the free energy liberated would be high enough to drive these reactions forward independently of the concentration of acetate (Fig. 5b).

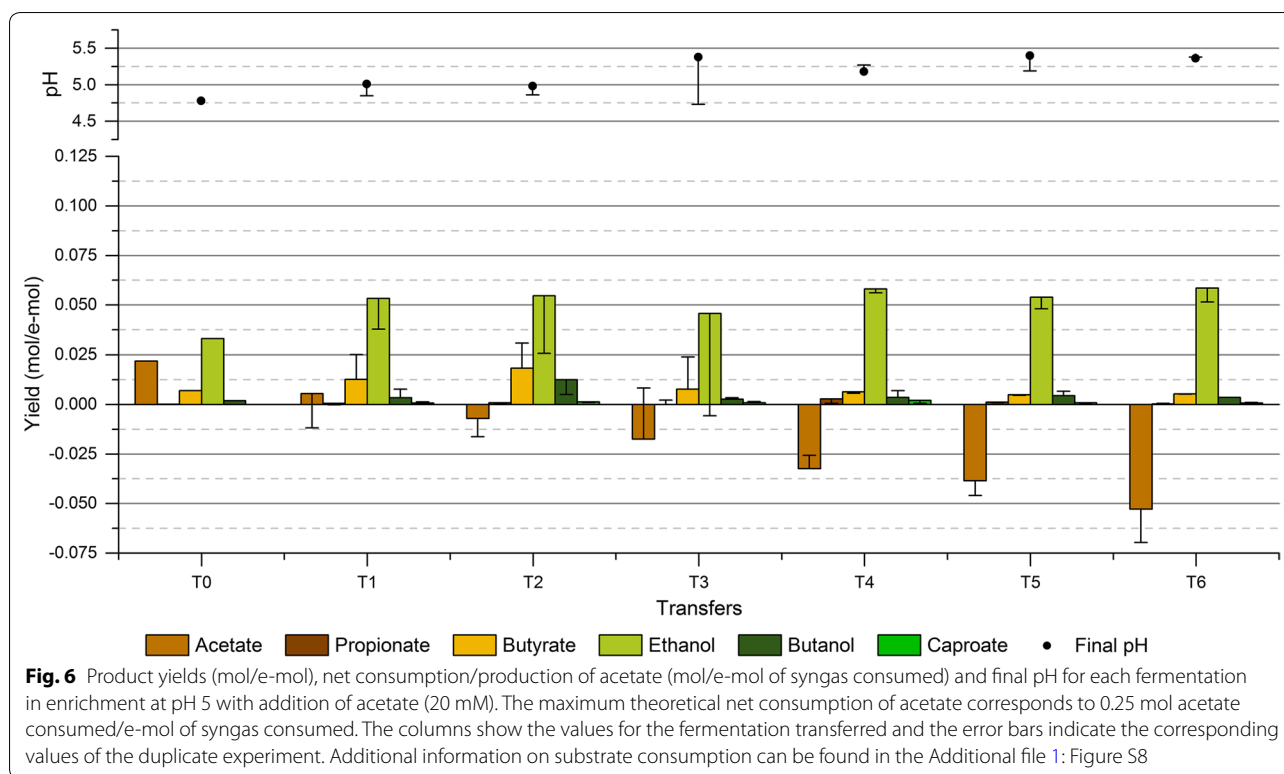
Comparing the effect of the pH and the initial acetate concentration on acetate-reducing reactions, the analysis of the changes in $\Delta_r G'_{310\text{K}}$ and F_T shows that the concentration of acetate has a stronger effect on the activity rates of these reactions. An increase in acetate concentration from 1 mM to 20 mM would significantly boost the acetate-reducing activity as the F_T would increase from 0.79 to 0.88 when using CO as electron donor, and from -0.13 to 0.45 when using H_2 . In this case, at an initial acetate concentration of 20 mM, both reactions would be clearly feasible regardless of the ΔG_p considered, even when using the more conservative ΔG_p of 70 kJ/mol of ATP (Fig. 5b). Thus, according to these calculations, an enrichment at pH 5 and 20 mM of initial concentration of acetate would be expected to boost the ethanologenic potential of the microbial consortium by increasing its acetate-reducing activity.

As opposed to lowering the pH, increasing the initial concentration of acetate would favor the chain-elongating activity. In this case, the F_T for chain elongation would remain constant at values approaching 1 by increasing the initial concentration of acetate from 1 mM to 20 mM when using a ΔG_p of 57.5 kJ/mol of ATP (Fig. 5b). Considering the most conservative ΔG_p of 70 kJ/mol of ATP, the F_T would increase from 0.86 to approx. 1. Therefore, the rate of this reaction would be clearly boosted by the increase of initial acetate concentration in the fermentation broth. This would theoretically decrease the ethanologenic potential of the microbial consortium, as also shown experimentally by El-gammal et al. [52]. However, as the pH was anticipated to decrease during the course of the fermentation, the inhibition of the chain-elongating activity due to the low pH observed in this and other studies [21] was expected to play an important role in such enrichment conditions by preventing a significant activity.

Enrichment with acetate addition: ethanol yield and microbial community

The results of the enrichment showed that the production of ethanol was enhanced by the addition of acetate. The higher ethanologenic potential of the microbial consortium at these enrichment conditions was evident as, at the first transfer, ethanol was already the main product of the fermentation and the ethanol yield was significantly higher than that of enrichment HT5YE without acetate addition (Fig. 6). As the enrichment proceeded, the ethanol production rapidly improved reaching an ethanol yield of 0.055 mol/e-mol (65.58% of the stoichiometric maximum) at transfer T2. Nevertheless, from transfer T0, both acetate and ethanol started to be used as substrates for the chain elongation reaction, resulting in increasing amounts of butyrate produced from transfer T0 to T3. Figure 6 shows the product yields obtained along the enrichment for the two replicates, where a high disparity between replicates and a high tendency for chain elongation can be observed, with butyrate even becoming the main product in one of the replicates at transfer T3. The large variations observed in transfer T3 derive from the fact that butyrate was produced through a two-step reaction, thus causing high deviations depending upon when the chain-elongation reaction started during the fermentation (fermentation profiles of transfer T3 can be found in Additional file 1: Figures S9 and S10). Although it was possible to perform the transfers while ethanol was still the main product of the fermentation in at least one of the replicates, at transfer T2 it was obvious that the chain-elongating microbial group was being enriched in the microbial consortium. Therefore, the enrichment strategy was modified from transfer T2 in an attempt to wash out the chain-elongating microbial group by transferring the cultures as soon as consumption of both CO and H_2 started. This strategy was expected to select exclusively for carboxydrotrophic microorganisms as these would be the only microbial group able to reach exponential growth phase at the moment of the transfer, favoring a gradual wash out of the chain-elongating microbial group. As expected, changing the enrichment strategy allowed reducing the chain-elongating activity of the microbial consortium, yet a complete wash out of this microbial group was not achieved since a residual amount of butyrate was still produced by the end of the enrichment. However, the decline in chain-elongating activity enabled increasing further the ethanol yields obtained during the enrichment, reaching a maximum of 0.059 mol/e-mol (70.24% of stoichiometric maximum) at transfer T6.

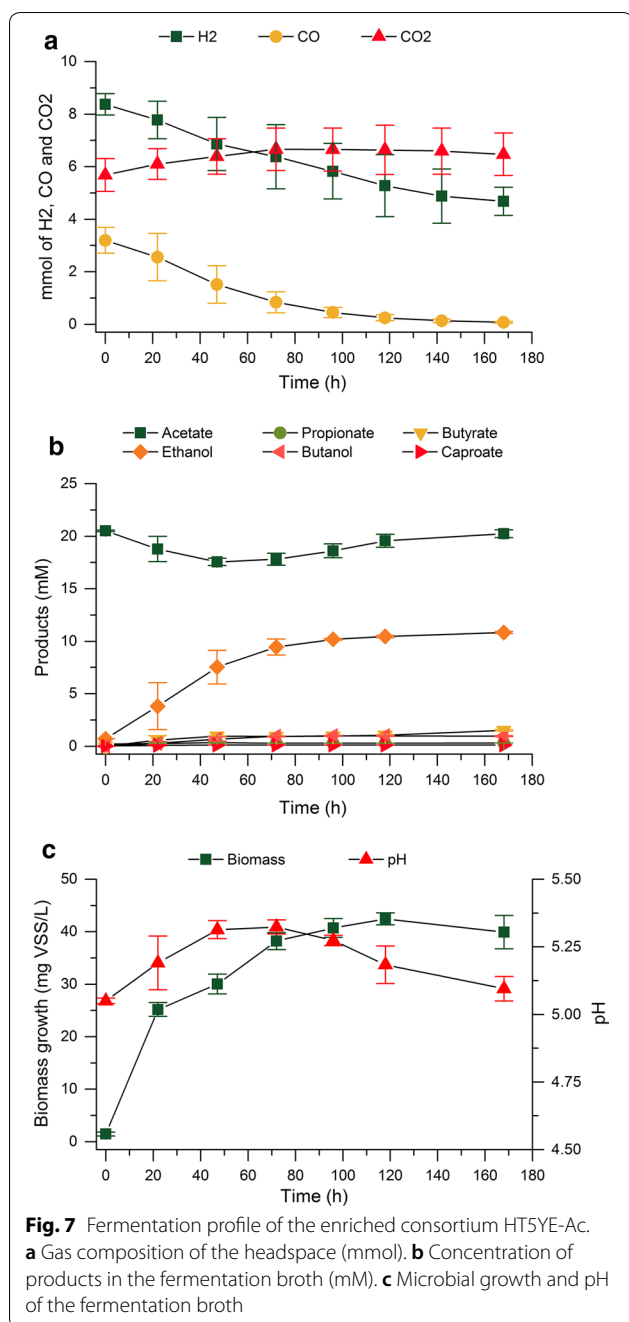
The thermodynamic analysis predicted a much higher acetate-reducing and chain-elongating activity in the microbial consortium enriched with acetate (HT5YE-Ac) when compared to the enrichment at pH 5 (HT5YE). The higher acetate-reducing activity could be clearly



observed in the fermentation profile shown in Fig. 7, where the consumption of H_2 , CO and acetate with concomitant ethanol production was apparent. This emphasizes the bioenergetic component of the metabolic shift towards ethanol, as increasing the initial acetate concentration clearly boosted the activity of acetate-reducing reactions. On the other hand, the chain elongation was expected to be inhibited by the decrease of pH along the fermentations even though this reaction would be thermodynamically favored by the addition of acetate. Nevertheless, during the course of the fermentations, the pH of the fermentation broth increased significantly as a result of the acetate conversion into ethanol (Fig. 7), which probably favored the fact that the pH inhibition of the chain-elongating activity did not operate during the enrichment. Thus, it seems that an automated pH control would be necessary to successfully prevent the chain-elongating activity through pH inhibition under these enrichment conditions. The results obtained here differed significantly from those reported by El-gammal et al. [52] since, in their study, acetate-reducing reactions were not enhanced upon addition of acetate, resulting in net acetate production at all times. However, in their study a pH of 6 and an initial acetate concentration of 13 mM was used, which reduced the effect on the $\Delta_r G'_{310 K}$ for acetate-reducing reactions. In this study, the fermentation carried out by the enriched consortium

HT5YE-Ac (Fig. 7) resulted in a net consumption of 0.021 ± 0.004 mol of acetate/e-mol of syngas and an ethanol yield of 0.060 ± 0.002 mol/e-mol (72.44 \pm 2.11% of the stoichiometric maximum), increasing the ethanol yield obtained with the enriched consortium HT5YE by 22.49%. Similar yields, corresponding to $58.6 \pm 7.4\%$ of the stoichiometric maximum, were reported by Steinbusch et al. [22] while studying the reduction of acetate into ethanol with H_2 as electron donor using a heat-shock-treated anaerobic sludge as inoculum. Additionally, a high chain-elongating activity was also reported in their study, where ethanol was produced in the first stage of the fermentation and was subsequently converted into butyrate.

The analysis of the microbial composition revealed strong similarities with the pH-based enrichment samples analyzed. In this case, the samples were withdrawn at transfers T1 and T3, which allowed evaluating the evolution of the microbial composition at an earlier stage in the enrichment. Interestingly, the results showed that the composition of the microbial community at genus level had already changed drastically at transfer T1 and remained stable until transfer T3 (Fig. 8). As in the pH-based enrichments, all enrichment samples were clearly dominated by the genus *Clostridium* with an average abundance of $63.2 \pm 5.4\%$. However, it was not possible to identify the dominant species. There was a significant



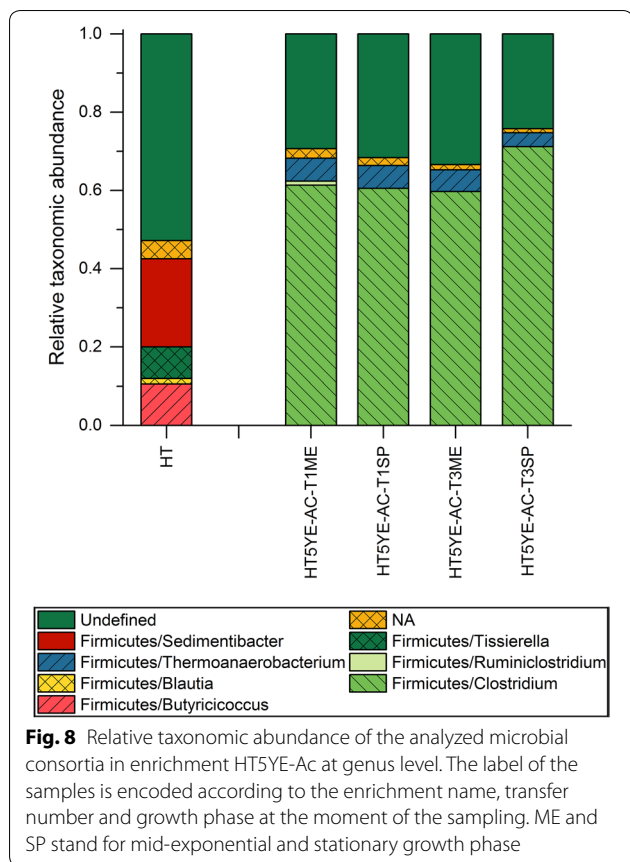
proportion of diverse OTUs (between 79.9 and 85.9% in all samples) that could not be reliably classified at this level (bootstrap value of 80% using SINTAX) (Additional file 2: Table S2). SINTAX-classified OTUs with relatively high abundance were classified as *C. nitrophenolicum* and *C. kluyveri* and were present in the enrichment samples within a range of 10.6–18.4% and 0–2.8%, respectively. This magnitude of abundances suggests a possible role during the fermentations. *C. nitrophenolicum* has

never been described to consume neither CO nor H₂. The only mention of *C. nitrophenolicum* in gas fermentation-related literature corresponds to a study on bio-H₂-mediated production of commodity chemicals using bioelectrochemical systems, where this species had a relative abundance between 2.7% and 3.6% in the cathode biofilm [63]. In turn, *C. kluyveri* is generally referred to as the model organism for the chain elongation process in several studies using both co- and mixed cultures [51, 64]. Additionally, *C. kluyveri* was identified in an enrichment study aiming at the conversion of syngas into higher alcohols, in which this species was found to participate in the chain elongation of acetate and ethanol [21]. In this study, the relative abundance of selected OTUs corresponding to *C. kluyveri* increased from transfer T1 to T3 during the enrichment, where butyrate was observed to be produced through chain elongation (Additional file 1: Figures S9 and S10). It can be thus concluded that this species clearly contributed to the increasing chain-elongating activity observed during the early stage of this enrichment.

Effect of enrichment conditions on microbial diversity

Comparing the microbial diversity of all enrichment samples revealed important differences across enrichment conditions. Figure 9a shows the alpha diversity calculated for all samples sorted by initial pH conditions. The results show that both inocula used presented among the highest alpha diversity, which gradually decreased with harsher enrichment conditions. The comparison across enrichment conditions shows a clear decreasing trend in alpha diversity as the pH decreases. Although the addition of YE contributed to a higher diversity, as it can be seen by comparing the two enrichments at pH 5.5 (HT5.5 and HT5.5YE), further decreasing the pH to 5 resulted in a drastic drop in diversity despite YE addition. Thus, the pH seems to be the major factor driving the reduction of complexity observed in the enrichment cultures. Similar trends were observed when studying the microbial diversity during a hydrogenotrophic enrichment at different pH conditions using cow manure as inoculum, where it was shown that pH 5 and pH 7 sustained the lowest and the highest microbial diversity among all conditions studied [65].

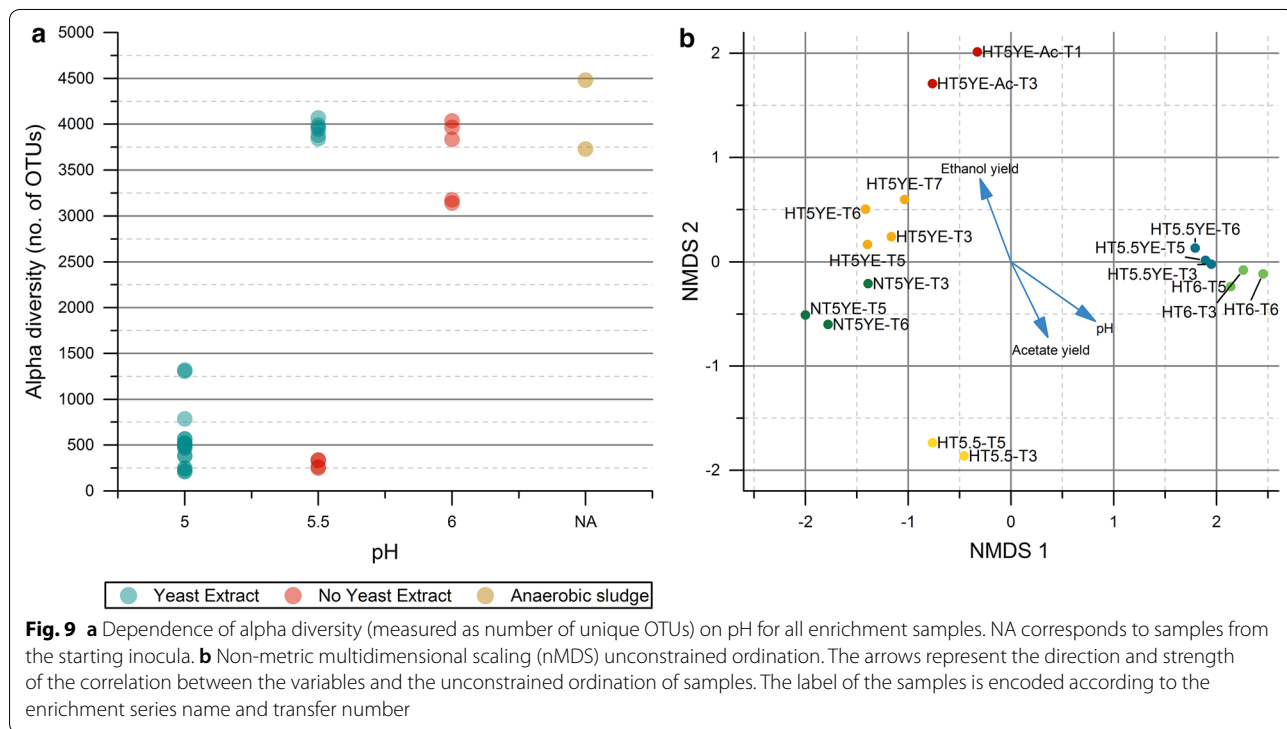
The non-metric multidimensional scaling (nMDS) analysis (Fig. 9b) illustrates the degree of microbial composition similarity between enrichment samples based on their relative distance. The results show that the samples from each enrichment are grouped together as a result of their higher similarity, which indicates that the enrichment cultures had reached a stable microbial composition at transfer T3. Comparing across enrichment conditions, it can be seen that enrichments HT6



and HT5.5YE, on one hand, and enrichments HT5YE, NT5YE and HT5YE-Ac on the other, developed closely related microbial communities, although a more widespread distribution can be observed in the latter group (Fig. 9b). In turn, the microbial consortium from enrichment HT5.5 was less related to other enrichments, probably due to the drastic drop in alpha diversity as compared to HT5.5YE. A statistically significant correlation was found between the initial pH conditions of each enrichment series and their microbial composition with a R^2 corresponding to 0.90 (P value < 0.001), which indicates that the microbial composition found in the enrichment cultures was pH-dependent (Fig. 9b). Similarly, the ethanol and acetate yields were also found to be correlated with the ordination of the samples (with a R^2 of 0.73 and 0.65, respectively, P value < 0.001) and followed a similar gradient direction with the pH (Fig. 9b). Thus, these results show that both the microbial composition and the yield of the main products were affected by the pH conditions of each enrichment series.

Conclusions

The enrichment strategies studied resulted in the successful selection of acetogenic bacteria from both untreated and heat-shock-treated anaerobic sludge, obtaining a number of enriched mixed microbial consortia with variable ethanologenic potential and microbial



diversity as a function of the enrichment conditions applied. The composition of the microbial community was shown to shift rapidly along the enrichments, reaching a stable microbial composition dominated by the genus *Clostridium* in all cases, with a single dominant species in most of the enrichments. Both pH and nutrient supplements (YE) were found to be determinant operational parameters affecting the specific composition of the consortia and their microbial diversity. The ethanologenic potential of the enriched consortia was strongly dependent on the pH conditions applied, where an ethanol yield of $59.15 \pm 0.18\%$ of the stoichiometric maximum was achieved in pH-based enrichments at the lowest pH tested (pH 5). On the other hand, the addition of YE triggered the production of C4 compounds, opening the way for the production of MCFAs and higher alcohols. The thermodynamic approach used for the analysis of the metabolic network of reactions carried out by syngas-converting microbial consortia proved to be highly useful for assisting the design and interpretation of enrichment strategies. Based on the qualitative predictions of the thermodynamic analysis, it was possible to improve the product selectivity and enhance the maximum ethanol yield obtained in pH-based enrichments by 22.5% ($72.44 \pm 2.11\%$ of the stoichiometric maximum) through an increase of the initial acetate concentration (enrichment HT5YE-Ac). Thus, this work demonstrated that a highly selective microbial activity towards the production of ethanol is possible using open-mixed microbial consortia. However, given the experimental observations made here, the ethanol yield obtained in enrichment HT5YE-Ac in batch mode cannot be extrapolated to processes in continuous mode as the long-term exposure of the enriched consortium to elevated ethanol and acetate concentrations would likely promote a high chain-elongating activity, lowering the product selectivity towards ethanol. Further work in this area is still needed to develop operational strategies able to control the chain-elongation reaction in syngas-converting microbial consortia.

Additional files

Additional file 1: Table S1. t-test for comparing the biomass yields of the enrichment experiments. **Table S2.** t-test for comparing the production efficiency of the enriched consortia. **Table S3.** Metabolite production in control experiments. **Figures S1–S4.** Fermentation profiles from enrichment cultures HT5.5 and HT5.5YE. **Figure S5.** Biomass yield and substrate consumption in enrichment experiments. **Figures S6, S7.** Fermentation profiles from enrichment cultures HT5.5YE and HT5YE. **Figure S8.** Biomass yield and substrate consumption in enrichment HT5YE-Ac. **Figures S9, S10.** Fermentation profiles from enrichment HT5YE-Ac at transfer T3.

Additional file 2. Tables S1, S2. Relative taxonomic abundance at genus and species level for initial inocula and enrichment samples. **Table S3.** Normalized read counts mapping in all samples to Operational Taxonomic Units (OTUs) and their taxonomy classification.

Authors' contributions

AG performed the enrichment experiments, analyzed the data from enrichment experiments, carried out the thermodynamic analysis and wrote the manuscript. ML analyzed the microbial composition of enrichment samples, wrote the corresponding section and reviewed the manuscript. LL reviewed the microbial composition data and the manuscript. HNG and IVS guided the experimental design and interpretation of the data and reviewed the manuscript. All authors read and approved the final manuscript.

Acknowledgements

This work was financially supported by the Technical University of Denmark (DTU) and Innovation Foundation-DK in the frame of SYNFERON project.

Competing interests

The authors declare that they have no competing interests.

Availability of data

The datasets used and analyzed in the current study are included either in the main text of the article, in the additional files, or are available upon reasonable request to AG and ML. Raw sequences were submitted to NCBI Sequence Read Archive (SRA) database and are available under the project ID PRJNA439372 (BioSample accessions SAMN08765035-SAMN08765086).

Funding

Not applicable.

Publisher's Note

Springer Nature remains neutral with regard to jurisdictional claims in published maps and institutional affiliations.

Received: 25 March 2018 Accepted: 27 June 2018

Published online: 19 July 2018

References

- HLPE. Biofuels and food security. A report by the High Level Panel of Experts on Food Security and Nutrition of the Committee on World Food Security. Rome, 2013.
- Havlik P, et al. Global land-use implications of first and second generation biofuel targets. *Energy Policy*. 2011;39:5690–702.
- Rosegrant MW, Msangi S. Consensus and contention in the food-versus-fuel debate. *Annu Rev Environ Resour*. 2014;39:271–94.
- Henstra AM, Sipma J, Rinzema A, Stams AJM. Microbiology of synthesis gas fermentation for biofuel production. *Curr Opin Biotechnol*. 2007;18:200–6.
- Kennes D, Abubackar HN, Diaz M, Veiga MC, Kennes C. Bioethanol production from biomass: carbohydrate vs syngas fermentation. *J Chem Technol Biotechnol*. 2016;91:304–17.
- Grimalt-Alemany A, Skiadas IV, Gavala HN. Syngas biomethanation: state-of-the-art review and perspectives. *Biofuels Bioprod Biorefining*. 2018;12:139–58.
- Wainaina S, Horváth IS, Taherzadeh MJ. Biochemicals from food waste and recalcitrant biomass via syngas fermentation: a review. *Bioresour Technol*. 2018;248:113–21.
- Abubackar HN, Veiga MC, Kennes C. Biological conversion of carbon monoxide to ethanol: effect of pH, gas pressure, reducing agent and yeast extract. *Bioresour Technol*. 2012;144:518–22.
- Mohammadi M, Younesi H, Najafpour G, Mohamed AR. Sustainable ethanol fermentation from synthesis gas by *Clostridium ljungdahlii* in a continuous stirred tank bioreactor. *J Chem Technol Biotechnol*. 2012;87:837–43.
- Kundiyan DK, Wilkins MR, Maddipati P, Huhnke RL. Effect of temperature, pH and buffer presence on ethanol production from synthesis gas by "*Clostridium ragsdalei*". *Bioresour Technol*. 2011;102:5794–9.
- Shen Y, Brown R, Wen Z. Syngas fermentation of *Clostridium carboxidivorans* P7 in a hollow fiber membrane biofilm reactor: evaluating the mass transfer coefficient and ethanol production performance. *Biochem Eng J*. 2014;85:21–9.

12. Xu D, Tree DR, Lewis RS. The effects of syngas impurities on syngas fermentation to liquid fuels. *Biomass Bioenergy*. 2011;35(7):2690–6.
13. Ramachandriya KD, et al. Critical factors affecting the integration of biomass gasification and syngas fermentation technology. *AIMS Bioeng*. 2016;3:188–210.
14. Kleerebezem R, van Loosdrecht MC. Mixed culture biotechnology for bioenergy production. *Curr Opin Biotechnol*. 2007;18:207–12.
15. Redl S, Diender M, Ølshøj T, Sousa DZ, Toftgaard A. Exploiting the potential of gas fermentation. *Ind Crop Prod*. 2017;106:21–30.
16. Liu Y, Wan J, Han S, Zhang S, Luo G. Selective conversion of carbon monoxide to hydrogen by anaerobic mixed culture. *Bioresour Technol*. 2016;202:1–7.
17. Navarro SS, Cimpoia R, Bruant G, Guiot SR. Biomethanation of syngas using anaerobic sludge: shift in the catabolic routes with the CO partial pressure increase. *Front Microbiol*. 2016;7:1–13.
18. Vasudevan D, Richter H, Angenent LT. Upgrading dilute ethanol from syngas fermentation to n-caproate with reactor microbiomes. *Bioresour Technol*. 2014;151:378–82.
19. Ganigué R, Ramió-Pujol S, Sánchez P, Bañeras L. Conversion of sewage sludge to commodity chemicals via syngas fermentation. *Water Sci Technol*. 2015;72(3):415–20.
20. Woo C, Jung KA, Moon J. Biological carbon monoxide conversion to acetate production by mixed culture. *Bioresour Technol*. 2016;211:478–85.
21. Ganigué R, Sánchez-Paredes P, Bañeras L, Colprim J. Low fermentation pH is a trigger for alcohol production, but a killer to chain elongation. *Front Microbiol*. 2016;7(702):1–11.
22. Steinbusch KJJ, Hamelers HVM, Buisman CJN. Alcohol production through volatile fatty acids reduction with hydrogen as electron donor by mixed cultures. *Water Res*. 2008;42:4059–66.
23. Liu K, Atiyeh HK, Stevenson BS, Tanner RS, Wilkins MR, Huhnke RL. Mixed culture syngas fermentation and conversion of carboxylic acids into alcohols. *Bioresour Technol*. 2014;152:337–46.
24. Singla A, Verma D, Lal B, Sarma PM. Enrichment and optimization of anaerobic bacterial mixed culture for conversion of syngas to ethanol. *Bioresour Technol*. 2014;172:41–9.
25. Wolin EA, Wolin MJ, Wolfe RS. Formation of methane by bacterial extracts. *J Biol Chem*. 1963;238(8):2882–6.
26. Takahashi S, Tomita J, Nishioka K, Hisada T, Nishijima M. Development of a prokaryotic universal primer for simultaneous analysis of bacteria and archaea using next-generation sequencing. *PLoS ONE*. 2014;9(8):e105592.
27. Martin M. Cutadapt removes adapter sequences from high-throughput sequencing reads. *EMBnet J*. 2011;17(1):10–2.
28. Edgar RC. UNOISE2: improved error-correction for Illumina 16S and ITS amplicon sequencing. *BioRxiv*. 2016. <https://doi.org/10.1101/003723>.
29. Edgar RC. SINTAX: a simple non-Bayesian taxonomy classifier for 16S and ITS sequences. *BioRxiv*. 2016. <https://doi.org/10.1101/074161>.
30. Edgar RC. UNCRSS: filtering of high-frequency cross-talk in 16S amplicon reads. *BioRxiv*. 2016. <https://doi.org/10.1101/088666>.
31. Edgar RC. UNBIAS: an attempt to correct abundance bias in 16S sequencing, with limited success. *BioRxiv*. 2017. <https://doi.org/10.1101/124149>.
32. McMurdie PJ, Holmes S. Phyloseq: an R package for reproducible interactive analysis and graphics of microbiome census data. *PLoS ONE*. 2013;8(4):e61217.
33. Dhariwal A, Chong J, Habib S, King IL, Agellon LB, Xia J. MicrobiomeAnalyst: a web-based tool for comprehensive statistical, visual and meta-analysis of microbiome data. *Nucleic Acids Res*. 2018;45:180–8.
34. Oksanen J et al. Vegan: community ecology package., R package version 2.4-6. 2018.
35. APHA. Standard methods for the examination of water and wastewater. Washington DC: American Public Health Association/American Water Works Association/Water Pollution Control Federation; 2005.
36. Alberty RA. Thermodynamics of biochemical reactions. Hoboken: Wiley; 2003.
37. Alberty RA. Effect of temperature on standard transformed Gibbs energies of formation of reactants at specified pH and ionic strength and apparent equilibrium constants of biochemical reactions. *J Phys Chem B*. 2001;105:7865–70.
38. Amend JP, Shock EL. Energetics of overall metabolic reactions of thermophilic and hyperthermophilic Archaea and bacteria. *FEMS Microbiol Rev*. 2001;25(2):175–243.
39. Jin Q, Bethke CM. The thermodynamics and kinetics of microbial metabolism. *Am J Sci*. 2007;307:643–77.
40. Bertsch J, Müller V. Bioenergetic constraints for conversion of syngas to biofuels in acetogenic bacteria. *Biotechnol Biofuels*. 2015;8(210):1–12.
41. Angenent LT, et al. Chain elongation with reactor microbiomes: open-culture biotechnology to produce biochemicals. *Environ Sci Technol*. 2016;50:2796–810.
42. González-Cabaleiro R, Lema JM, Rodríguez J, Kleerebezem R. Linking thermodynamics and kinetics to assess pathway reversibility in anaerobic bioprocesses. *Energy Environ Sci*. 2013;6:3780–9.
43. Jin Q. Energy conservation of anaerobic respiration. *Am J Sci*. 2012;312:573–628.
44. Jackson BE, McInerney MJ. Anaerobic microbial metabolism can proceed close to thermodynamic limits. *Nature*. 2002;415:454–6.
45. Varrone C, et al. Comparison of different strategies for selection/adaptation of mixed microbial cultures able to ferment crude glycerol derived from second-generation biodiesel. *Hindawi*. 2015;2015:1–14.
46. Steinbusch KJJ, Arvaniti E, Hamelers HVM, Buisman CJN. Selective inhibition of methanogenesis to enhance ethanol and n-butyrate production through acetate reduction in mixed culture fermentation. *Bioresour Technol*. 2009;100(13):3261–7.
47. Phillips JR, Klasson KT, Clausen EC, Gaddy JL. Biological production of ethanol from coal synthesis gas. *Appl Biochem Biotechnol*. 1993;39–40:559–71.
48. Abubackar HN, Fernández-Naveira Á, Veiga MC, Kennes C. Impact of cyclic pH shifts on carbon monoxide fermentation to ethanol by *Clostridium autoethanogenum*. *Fuel*. 2016;178:56–62.
49. Gottwald M, Gottsehalck G. The internal pH of *Clostridium acetobutylicum* and its effect on the shift from acid to solvent formation Matthias. *Arch Microbiol*. 1985;143:42–6.
50. Huang LI, Forsberg CW, Gibbins LN. Influence of external pH and fermentation products on *Clostridium acetobutylicum* intracellular pH and cellular distribution of fermentation products. *Appl Environ Microbiol*. 1986;51:1230–4.
51. Grootsholten TIM, Steinbusch KJJ, Hamelers HVM, Buisman CJN. Chain elongation of acetate and ethanol in an upflow anaerobic filter for high rate MCFAs production. *Bioresour Technol*. 2013;135:440–5.
52. El-gammal M, Abou-shanab R, Angelidaki I, Omar B. High efficient ethanol and VFA production from gas fermentation: effect of acetate, gas and inoculum microbial composition. *Biomass Bioenergy*. 2017;105:32–40.
53. Younesi H, Najafpour G, Mohamed AR. Ethanol and acetate production from synthesis gas via fermentation processes using anaerobic bacterium, *Clostridium ljungdahlii*. *Biochem Eng J*. 2005;27(2):110–9.
54. Esquivel-Elizondo S, Delgado AG, Rittmann BE, Brown RK. The effects of CO₂ and H₂ on CO metabolism by pure and mixed microbial cultures. *Biotechnol Biofuels*. 2017;10(220):1–13.
55. Najafpour GD, Younesi H. Ethanol and acetate synthesis from waste gas using batch culture of *Clostridium ljungdahlii*. *Enzym Microb Technol*. 2006;38:223–8.
56. Abrini J, Naveau H, Nyns E. *Clostridium autoethanogenum*, sp. nov., an anaerobic bacterium that produces ethanol from carbon monoxide. *Arch Microbiol*. 1994;161:345–51.
57. Liou JS, Balkwill DL, Drake GR, Tanner RS. *Clostridium carboxidivorans* sp. nov., a solvent-producing clostridium isolated from an agricultural settling lagoon, and reclassification of the acetogen *Clostridium scatologenes* strain SL1 as *Clostridium drakei* sp. nov. *Int J Syst Evol Microbiol*. 2005;55:2085–91.
58. Ramió-pujol S, Ganigué R, Bañeras L, Colprim J. Incubation at 25 °C prevents acid crash and enhances alcohol production in *Clostridium carboxidivorans* P7. *Bioresour Technol*. 2015;192:296–303.
59. Zhang J, Taylor S, Wang Y. Effects of end products on fermentation profiles in *Clostridium carboxidivorans* P7 for syngas fermentation. *Bioresour Technol*. 2016;218:1055–63.
60. Singla A, et al. Optimization and molecular characterization of syngas fermenting anaerobic mixed microbial consortium TERI SA1. *Int J Renew Energy Dev*. 2017;6(3):241–51.
61. Hu P, Bowen SH, Lewis RS. A thermodynamic analysis of electron production during syngas fermentation. *Bioresour Technol*. 2011;102(17):8071–6.
62. Richter H, Martin ME, Angenent LT. A two-stage continuous fermentation system for conversion of syngas into ethanol. *Energies*. 2013;6(8):3987–4000.

63. Puig S, Ganigué R, Batlle-Vilanova P, Balaguer MD, Bañeras L. Tracking bio-hydrogen-mediated production of commodity chemicals from carbon dioxide and renewable electricity. *Bioresour Technol.* 2017;228:201–9.
64. Diender M, Stams AJM, Sousa DZ. Production of medium-chain fatty acids and higher alcohols by a synthetic co-culture grown on carbon monoxide or syngas. *Biotechnol Biofuels.* 2016;9(82):1–11.
65. Xu S, Fu B, Zhang L, Liu H. Bioconversion of H₂/CO₂ by acetogen enriched cultures for acetate and ethanol production: the impact of pH. *World J Microbiol Biotechnol.* 2015;31:941–50.

Ready to submit your research? Choose BMC and benefit from:

- fast, convenient online submission
- thorough peer review by experienced researchers in your field
- rapid publication on acceptance
- support for research data, including large and complex data types
- gold Open Access which fosters wider collaboration and increased citations
- maximum visibility for your research: over 100M website views per year

At BMC, research is always in progress.

Learn more biomedcentral.com/submissions



Enrichment of syngas-converting mixed microbial consortia for ethanol production and thermodynamics-based design of enrichment strategies – Additional file 1.

Table 1. Average apparent biomass yield for enrichment experiments from transfer T3 to T6 and p-values from t-test analysis.

	Biomass yield (mg VSS/e-mol)	P-value	HT6	HT5.5	HT5.5YE	HT5YE	NT5YE
HT6	0.216±0.042	HT6					
HT5.5*	0.168±0.040	HT5.5	0.121				
HT5.5YE	0.221±0.026	HT5.5YE	0.844	0.035			
HT5YE	0.279±0.071	HT5YE	0.077	0.016	0.054		
NT5YE	0.262±0.036	NT5YE	0.110	0.002	0.039	0.563	

*Average apparent biomass yield of enrichment series HT5.5 was calculated using values from transfer T3 to T5.

Table 2. Average production efficiency calculated in Cmol and e-mol recovery, and p-values from t-test analysis.

		Production efficiency (%)	P-value	HT6	HT5.5	HT5.5YE	HT5YE	NT5YE
HT6	Cmol	83.16±0.70%	HT6	Cmol				
	e-mol	92.92±0.54%		e-mol				
HT5.5	Cmol	77.33±2.31%	HT5.5	Cmol	0.017			
	e-mol	85.83±2.46%		e-mol	0.012			
HT5.5YE	Cmol	93.18±1.69%	HT5.5YE	Cmol	0.007	0.000		
	e-mol	89.84±1.80%		e-mol	0.128	0.090		
HT5YE	Cmol	80.29±0.83%	HT5YE	Cmol	0.115	0.133	0.003	
	e-mol	88.57±1.77%		e-mol	0.234	0.334	0.618	
NT5YE	Cmol	91.60±6.41%	NT5YE	Cmol	0.203	0.077	0.764	0.126
	e-mol	95.01±3.29%		e-mol	0.464	0.035	0.144	0.115

*Production efficiency of HT5.5 calculated using data from transfer T4 and T5 of enrichment experiments.

Table 3. Net production/consumption in control experiments and total Cmol (Cmmol) and e-mol (e-mmol) production.

	Acetate (mmol)	Propionate (mmol)	Butyrate (mmol)	Ethanol (mmol)	Butanol (mmol)	Caproate (mmol)	Total Cmmol	Total e-mmol
HT6	0.004	0.000	0.000	0.000	0.000	0.000	0.007	0.029
HT5.5	0.024	0.000	0.000	-0.005	0.000	0.000	0.039	0.137
HT5.5YE	0.332	0.018	0.020	-0.109	-0.020	0.000	0.496	1.498
HT5YE	0.066	0.013	0.037	-0.038	0.000	-0.002	0.230	0.926
NT5YE	0.324	0.027	0.024	-0.110	-0.019	0.013	0.606	2.088

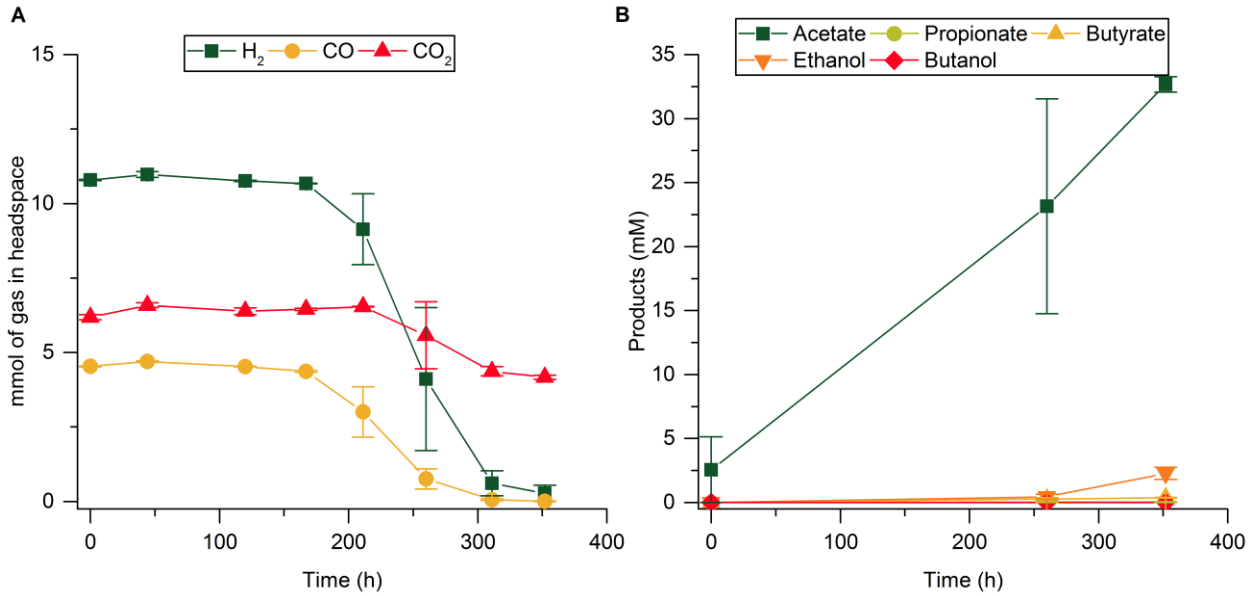


Figure 1. Fermentation profile of enrichment HT5.5 at transfer T1 (average of duplicates). **A** Gas composition of the headspace (mmol). **B** Concentration of products in the fermentation broth (mM) and microbial growth (mg VSS/L).

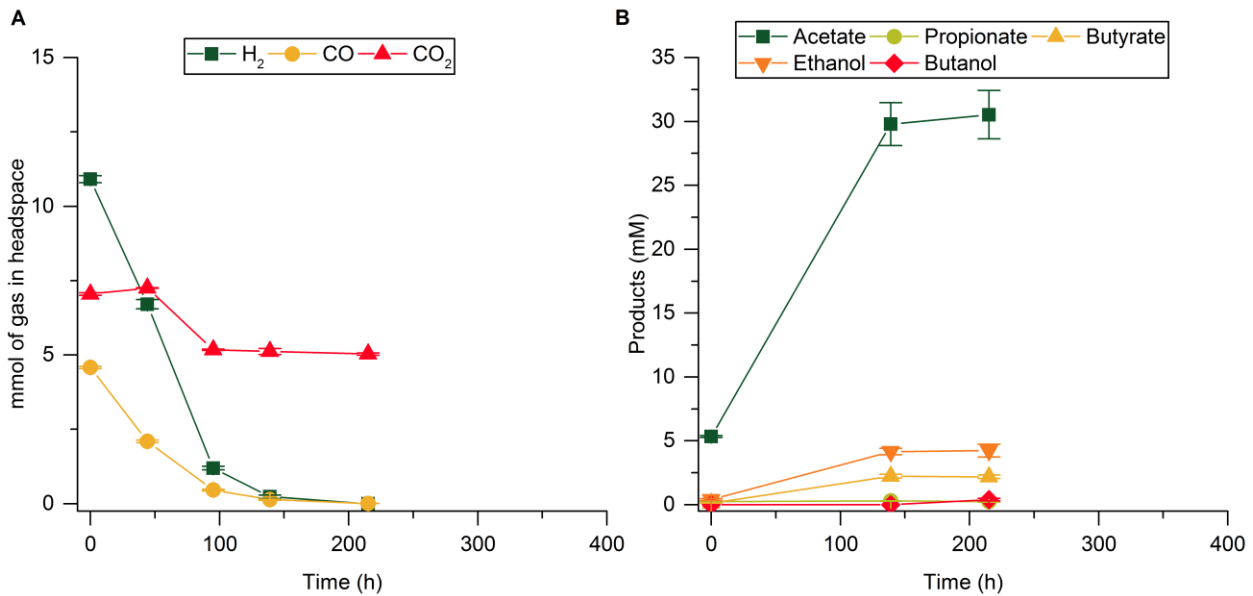


Figure 2. Fermentation profile of enrichment HT5.5YE at transfer T1 (average of duplicates). **A** Gas composition of the headspace (mmol). **B** Concentration of products in the fermentation broth (mM) and microbial growth (mg VSS/L).

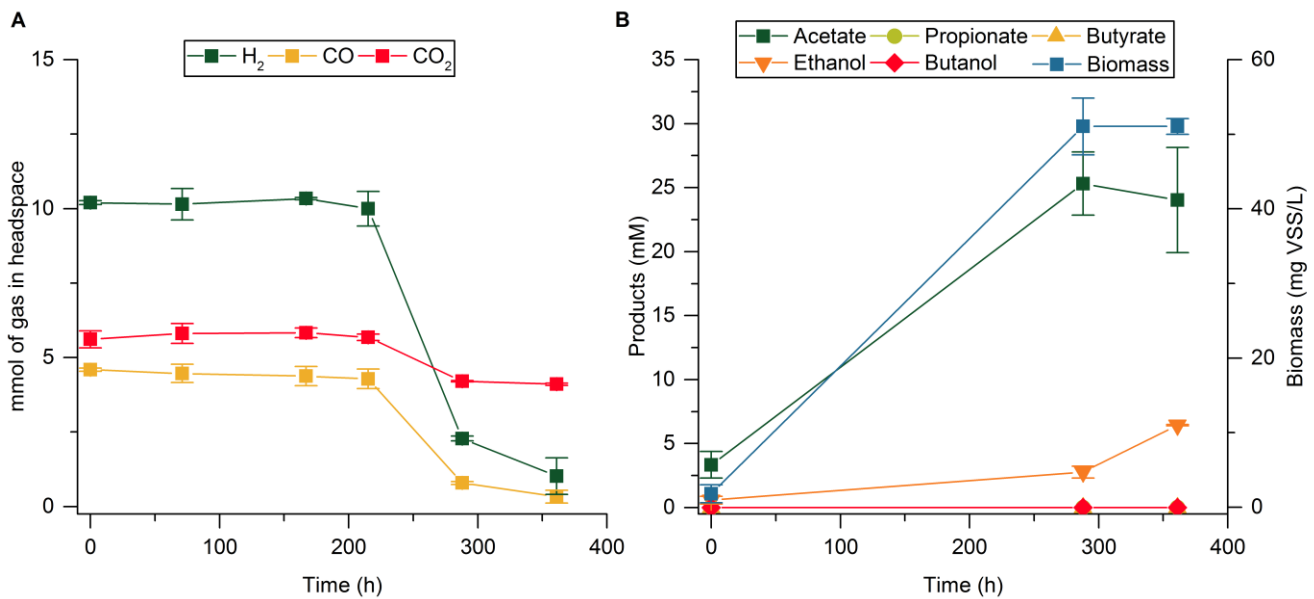


Figure 3. Fermentation profile of enrichment HT5.5 at transfer T4 (average of duplicates). **A** Gas composition of the headspace (mmol). **B** Concentration of products in the fermentation broth (mM) and microbial growth (mg VSS/L).

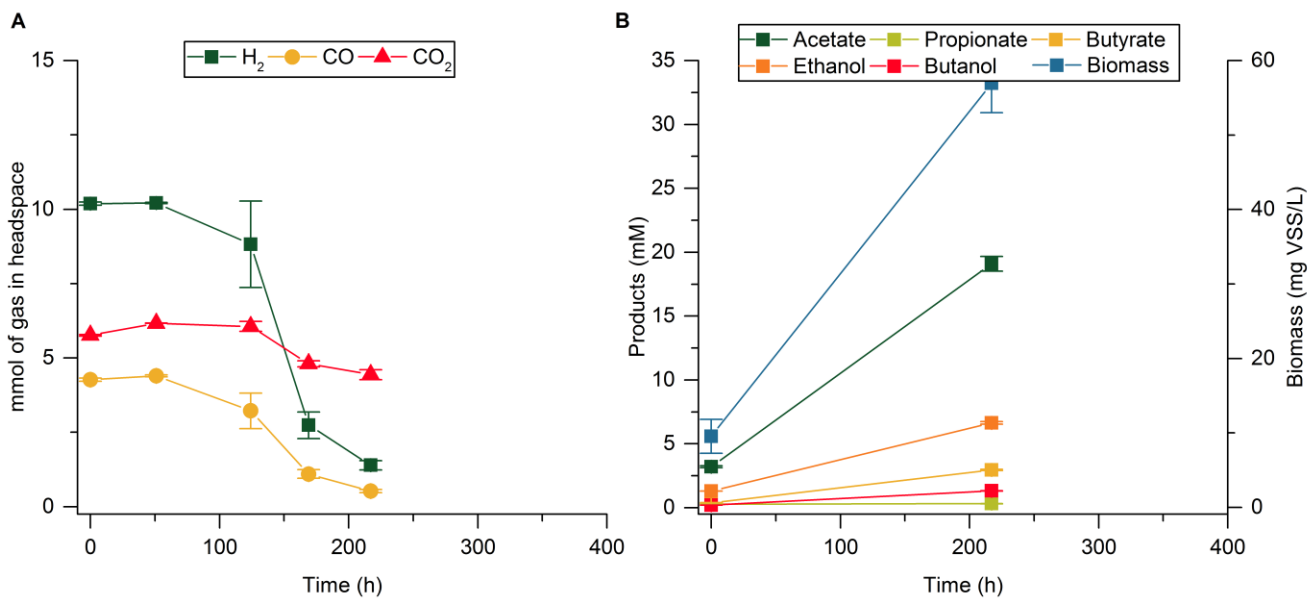


Figure 4. Fermentation profile of enrichment HT5.5YE at transfer T4 (average of duplicates). **A** Gas composition of the headspace (mmol). **B** Concentration of products in the fermentation broth (mM) and microbial growth (mg VSS/L).

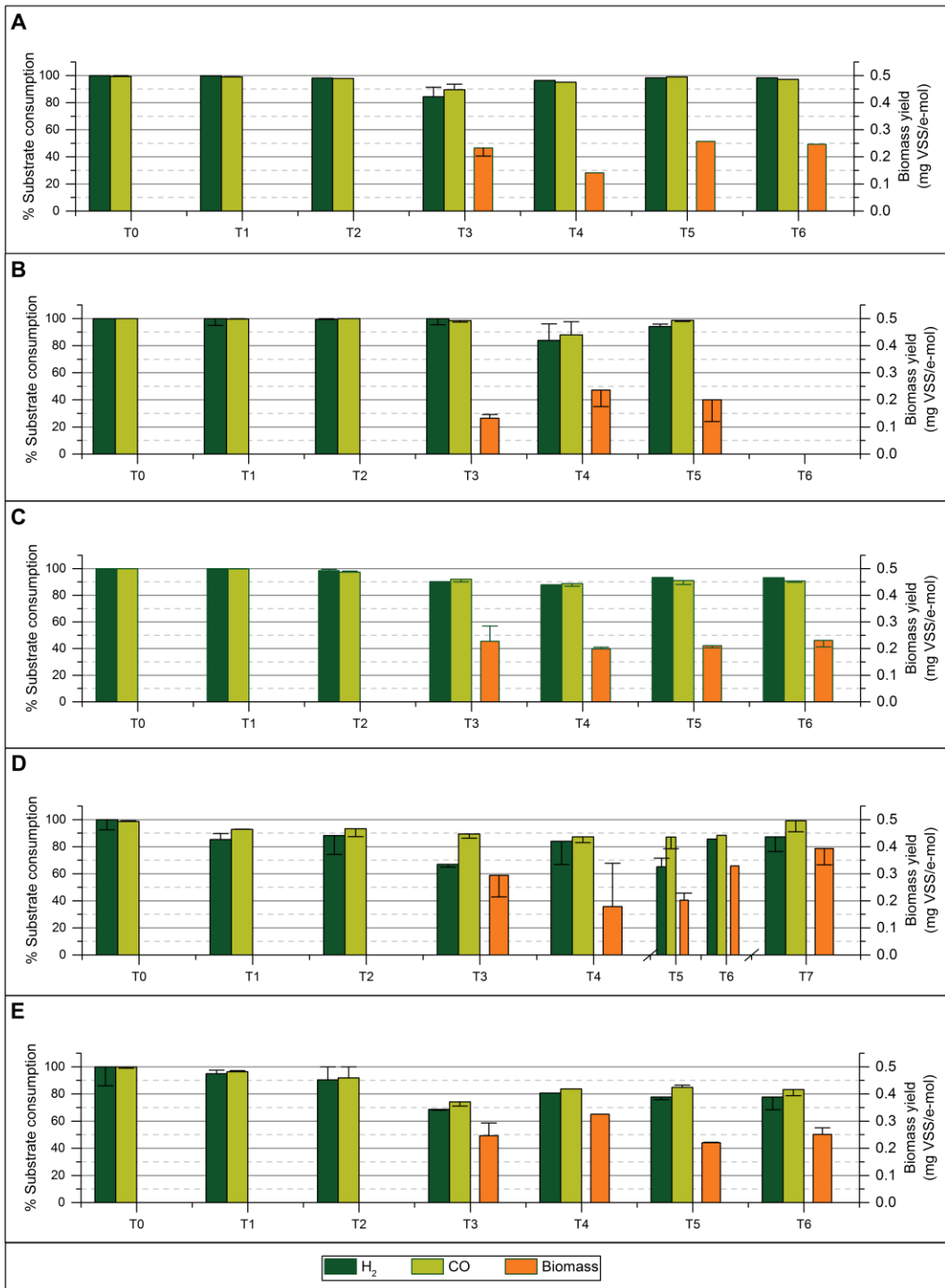


Figure 5. Apparent biomass yield in enrichment experiments from transfer T3, and percentage of H₂ and CO conversion for each batch experiment. The columns show the values for the fermentation transferred and the error bars indicate the corresponding values of the duplicate experiment. **A** Enrichment HT6 at an initial pH of 6; **B** Enrichment HT5.5 at an initial pH of 5.5; **C** Enrichment HT5.5YE at an initial pH of 5.5 with YE (0.5 g/L); **D** Enrichment HT5YE at an initial pH of 5 with YE (0.5 g/L); **E** Enrichment NT5YE at an initial pH of 5 with YE (0.5 g/L).

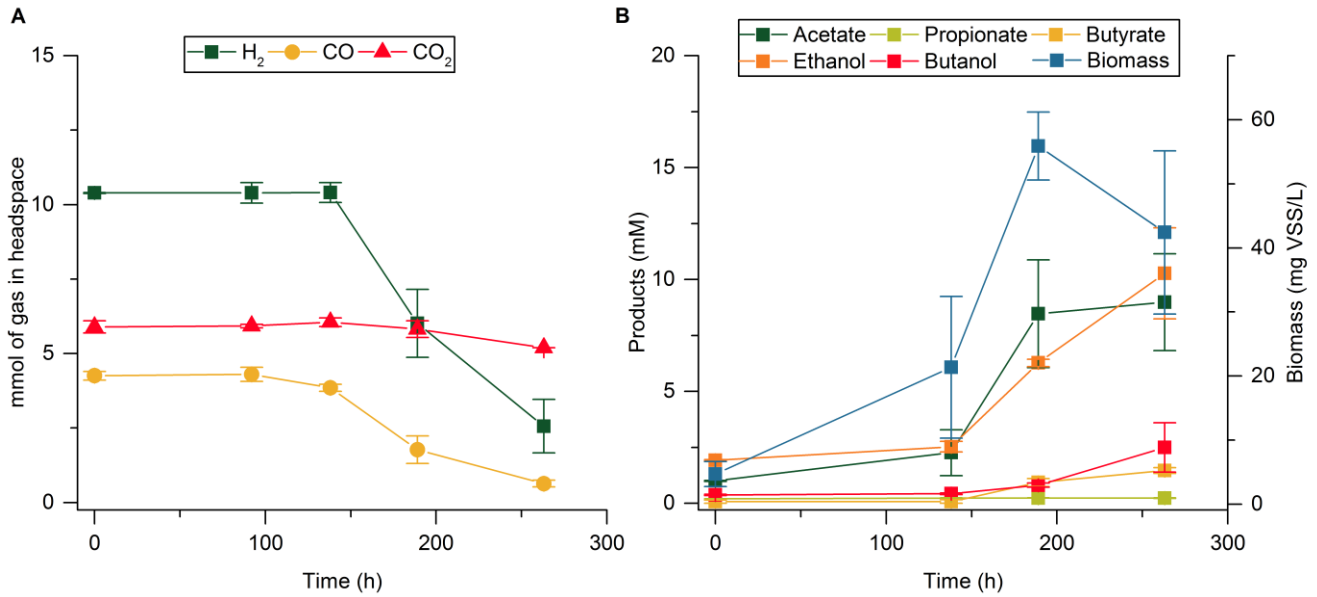


Figure 6. Fermentation profile of enrichment HT5YE at transfer T4 (average of duplicates). **A** Gas composition of the headspace (mmol). **B** Concentration of products in the fermentation broth (mM) and microbial growth (mg VSS/L).

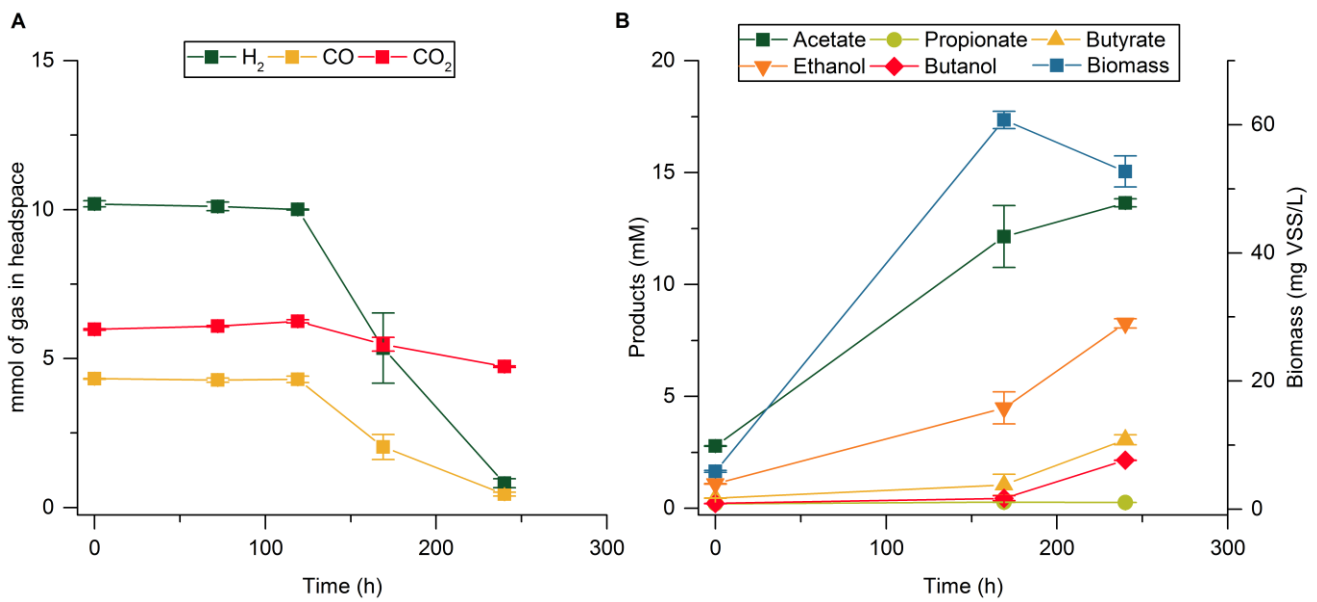


Figure 7. Fermentation profile of enrichment HT5.5YE at transfer T5 (average of duplicates). **A** Gas composition of the headspace (mmol). **B** Concentration of products in the fermentation broth (mM) and microbial growth (mg VSS/L).

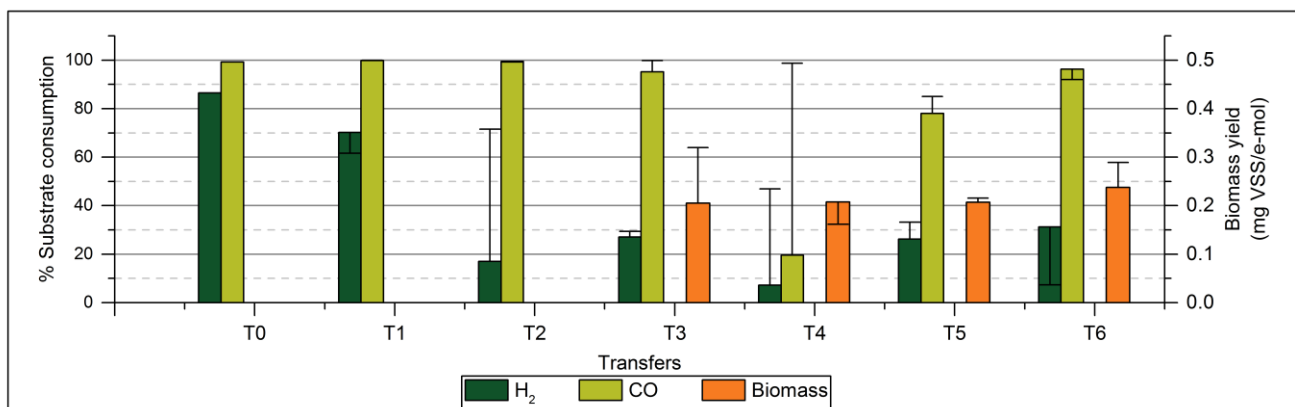


Figure 8. Apparent biomass yield for enrichment HT5YE-Ac from transfer T3, and percentage of H₂ and CO conversion. The columns show the values for the fermentation transferred and the error bars indicate the corresponding values of the duplicate experiment.

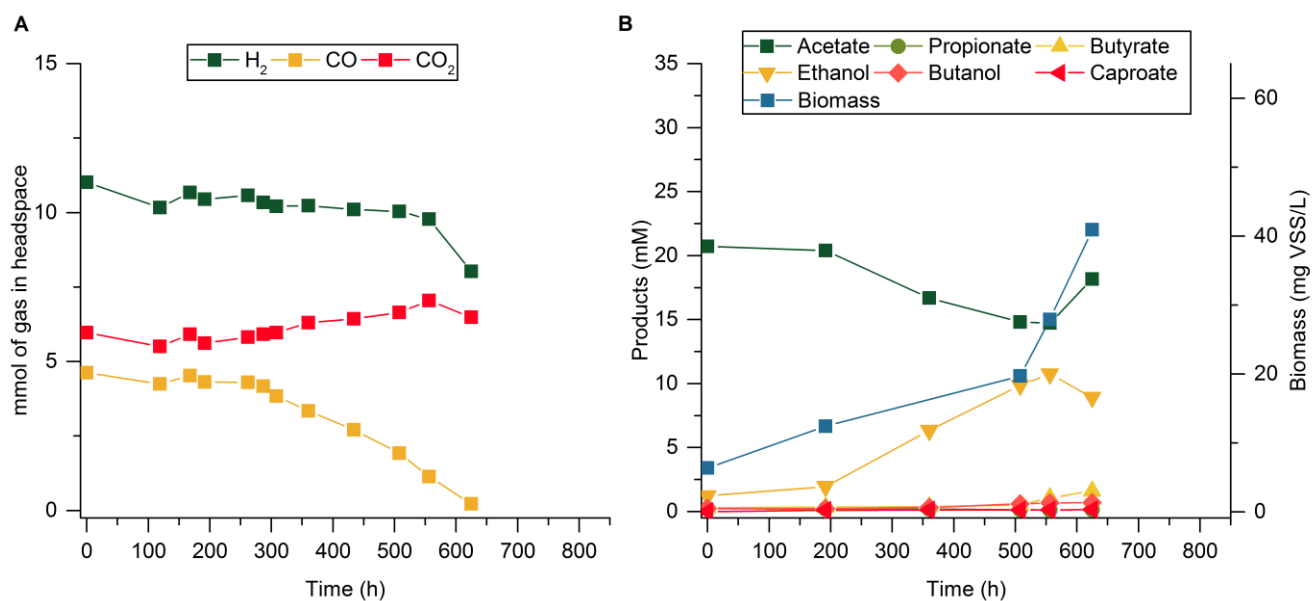


Figure 9. Fermentation profile of enrichment HT5YE-Ac at transfer T3 (replicate 1). **A** Gas composition of the headspace (mmol). **B** Concentration of products in the fermentation broth (mM) and microbial growth (mg VSS/L).

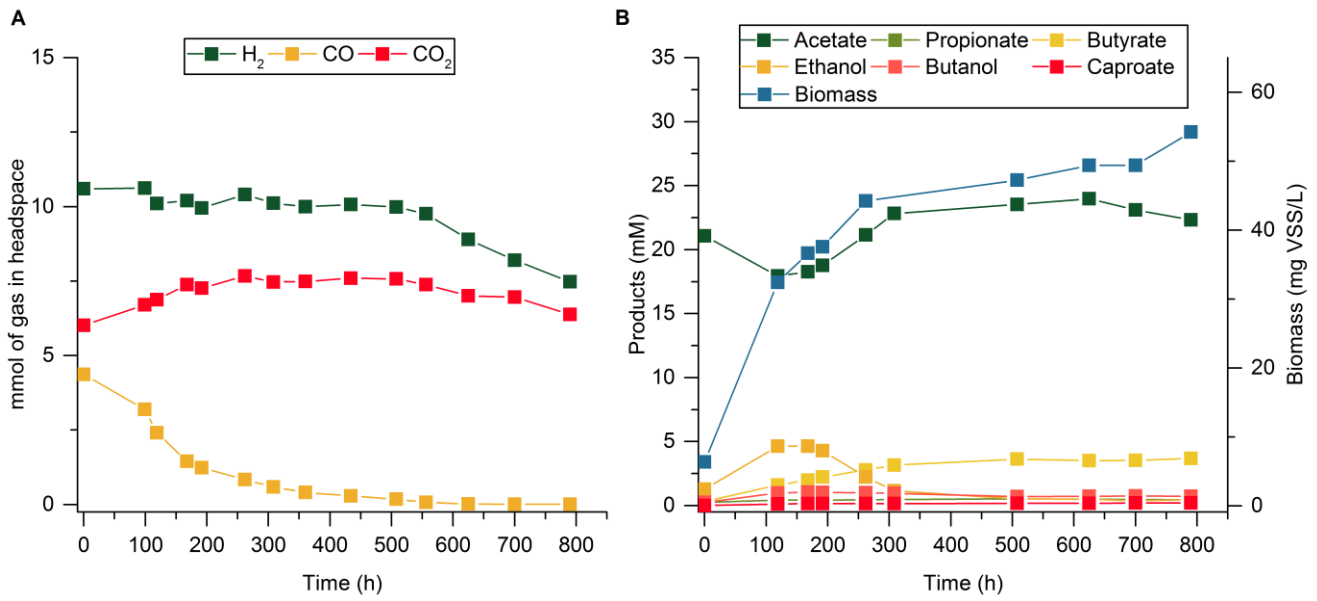


Figure 10. Fermentation profile of enrichment HT5YE-Ac at transfer T3(replicate 2). **A** Gas composition of the headspace (mmol). **B** Concentration of products in the fermentation broth (mM) and microbial growth (mg VSS/L).

Manuscript III

“Enrichment of mesophilic and thermophilic mixed microbial consortia for syngas biomethanation: the role of kinetic and thermodynamic competition”



Enrichment of Mesophilic and Thermophilic Mixed Microbial Consortia for Syngas Biomethanation: The Role of Kinetic and Thermodynamic Competition

Antonio Grimalt-Alemany¹ · Mateusz Łężyk² · David M. Kennes-Veiga¹ · Ioannis V. Skiadas¹ · Hariklia N. Gavala¹

Received: 11 September 2018 / Accepted: 21 January 2019
© Springer Nature B.V. 2019

Abstract

Mixed culture-based syngas biomethanation is a robust bioconversion process with high versatility in terms of exploitable feedstocks and potential applications, as it could be operated independently, or coupled to anaerobic digestion systems and in-situ biogas upgrading processes. Typically, the syngas biomethanation consists in the stepwise conversion of syngas into methane through a number of catabolic routes, which may vary considerably depending on the operating conditions. In this study, two enrichments were performed at 37 °C and 60 °C to investigate the effect of the incubation temperature on the microbial selection process and the dominant catabolic routes followed. This was carried out through the characterization of the catabolic routes and the microbial composition of the enriched cultures, and a thermodynamic feasibility study on their metabolic networks. The enrichments resulted in two stable microbial consortia with different patterns of activity. The mesophilic enriched consortium presented a more intricate metabolic network composed by four microbial trophic groups, where acetoclastic methanogenesis contributed to $64.9 \pm 8.3\%$ of the CH_4 production. The metabolic network of the thermophilic enriched consortium was much simpler, consisting in the syntrophic association of carboxydrotrophic hydrogenogens and hydrogenotrophic methanogens. This led to significant differences in methane productivity, corresponding to 1.83 ± 0.27 and 33.48 ± 0.90 mmol $\text{CH}_4/\text{g VSS/h}$ for the mesophilic and the thermophilic enriched consortium, respectively, which would potentially make the thermophilic consortium more suited for industrial applications. 16S rRNA gene amplicon analysis indicated the presence of strains with similarity to *Acetobacterium* sp., *Methanospirillum hungatei*, *Methanospirillum stamsii* and *Methanotherix* sp. at mesophilic conditions, and *Thermincola carboxydiphila* and *Methanothermobacter* sp. at thermophilic conditions, implying a role in the conversion of syngas. The thermodynamic feasibility study demonstrated that the microbial selection was not driven solely by kinetic competition, since thermodynamic limitations also played a significant role defining the dominant catabolic routes.

Keywords Syngas · Carbon monoxide · Hydrogen · Methane · Mixed cultures · Thermodynamics

Statement of Novelty

In this study, stable mesophilic and thermophilic enriched microbial consortia able to fully convert syngas into CH_4 were developed. The enrichments had a strong effect on the catabolic routes dominating the conversion of syngas. Furthermore, the thermodynamic analysis of the metabolic network of the enriched consortia demonstrated that the microbial selection through the enrichments was not solely dictated by the kinetics of the microbial community, since the thermodynamic limitation of several biochemical reactions also played an important role defining the activity of the enriched consortia. The findings show that analyzing the thermodynamics and applying thermodynamic control

Electronic supplementary material The online version of this article (<https://doi.org/10.1007/s12649-019-00595-z>) contains supplementary material, which is available to authorized users.

✉ Hariklia N. Gavala
hnga@kt.dtu.dk; hari_gavala@yahoo.com

¹ Department of Chemical and Biochemical Engineering, Technical University of Denmark, Søtofts Plads 229, 2800 Kgs. Lyngby, Denmark

² Institute of Environmental Engineering, Faculty of Civil and Environmental Engineering, Poznan University of Technology, Berdychowo 4, 60-965 Poznan, Poland

over the metabolic routes followed in the bioconversion can contribute significantly to optimizing the operational conditions favoring high productivities in mixed-culture based industrial processes.

Introduction

The increasing energy demands along with the need of replacing fossil resources have motivated a paradigm shift towards sustainable production of commodity chemicals and biofuels. One of such chemicals with a high versatility in terms of potential applications is biomethane, as it can be used either for heat and power generation, direct injection into the gas grid or as a transportation fuel [1]. Additionally, recent findings point at methane as a potential platform chemical to bio-synthesize a number of high added value products such as single cell protein, polyhydroxyalkanoates and extracellular polysaccharides [2].

The production of biomethane can take place through several conversion routes and from a wide variety of feedstocks. The conventional process for biomethane (or biogas) production is the anaerobic digestion process, which has long been applied for the treatment of wastewater and different types of organic wastes from the agricultural sector [3, 4]. However, when it comes to recalcitrant biomasses, the anaerobic digestion process typically suffers from low conversion efficiencies due to the presence of refractory biomass fractions [5]. One of the alternatives to overcome the low biodegradability of recalcitrant biomasses is the gasification of either the solid effluent fraction from anaerobic digesters or the whole biomass into synthesis gas, a mixture of primarily H_2 , CO and CO_2 , which can be further converted biologically into methane through the syngas biomethanation process. Both gasification and syngas biomethanation present a number of inherent merits. On one hand, applying thermochemical conversion methods provides higher conversion efficiency and broadens the range of exploitable feedstocks as any type of biomass can be gasified regardless of recalcitrance or toxicity, including non-fermentable by-products and biomass fractions, forestry residues and municipal solid wastes [6]. On the other hand, the biomethanation of synthesis gas constitutes a multi-purpose process as it can be used for converting biomass-derived syngas and CO/CO_2 -rich off-gas streams from several industrial processes into methane and carbon dioxide [7], or as an in-situ biogas upgrading technology by addition of an external H_2 supply to the biomethanation unit [8]. Therefore, the syngas biomethanation process holds a significant application potential either as a stand-alone technology or integrated in current anaerobic digestion systems for improving the biomass conversion efficiency and the methane content of the gaseous outlet.

The anaerobic microbial conversion of synthesis gas into CH_4 supports growth of a variety of microbial trophic groups and can take place through different catabolic routes. Direct conversion of H_2/CO_2 into CH_4 by hydrogenotrophic methanogens is widespread among methanogenic archaea and has been well studied. On the other hand, direct conversion of CO into CH_4 is rare and, so far, only a few species have been found to be capable of carboxydrotrophic methanogenesis, with all of them presenting rather long doubling times [9–12]. When using open mixed microbial consortia though, the direct biomethanation of CO has never been reported as carboxydrotrophic methanogens are generally inhibited by relatively low partial pressures of CO (P_{CO}) and are easily outcompeted by other faster-growing carboxydrotrophic microbial groups such as carboxydrotrophic acetogens or hydrogenogens [13–15]. As a result, the biomethanation of syngas typically requires the syntrophic association of several microbial trophic groups and comprises a rather complex network of biochemical reactions mainly including the biological water–gas shift reaction, carboxydrotrophic acetogenesis, homoacetogenesis, hydrogenotrophic methanogenesis and acetoclastic methanogenesis [1]. However, the dominance of each of the catabolic routes has been shown to shift depending on the operating conditions applied. Navarro et al. [13] studied the effect of the P_{CO} using a mesophilic granular sludge and found that acetoclastic methanogenesis was dominant at P_{CO} below 0.5 atm., while the carbon flux shifted towards syntrophic acetate oxidation and hydrogenotrophic methanogenesis when increasing the P_{CO} to 1 atm. Similar observations were made when studying the effect of the incubation temperature as carboxydrotrophic acetogenesis was found to be gradually replaced by carboxydrotrophic hydrogenogenesis when increasing the incubation temperature from 45 °C onwards, which consequently changed the dominant catabolic routes leading to methane [14]. This illustrates the dynamic nature of microbial communities, which respond rapidly to changes in environmental conditions by adjusting the structure of their microbial population towards the most efficient catabolic routes.

Studying changes in the microbial community structure and activity when exposed to different operating conditions is thus fundamental for understanding the population dynamics determining the outcome of microbial conversion processes. The evolution of the activity and composition of syngas-converting methanogenic microbial communities upon exposure to syngas as the sole carbon and energy source using mesophilic and thermophilic anaerobic sludges has been recently studied through microbial enrichments in batch mode [15, 16]. However, both of these enrichment studies resulted in the development of enriched cultures with limited methanogenic potential, as significant amounts of acetate remained unconverted in the fermentation broth due to the absence of certain methanogenic microbial groups in

the mixed cultures. Thus, this work focuses on the development of both mesophilic and thermophilic syngas-converting methanogenic enriched cultures with high product selectivity towards CH_4 . The goal of this study is to characterize the syngas conversion routes utilized by open mixed microbial consortia enriched at different temperatures as well as to assess the role of kinetic and thermodynamic competition in defining the microbial interactions present in each enriched consortium as a result of the microbial selection process. This is carried out by analyzing the catabolic routes employed by the enriched consortia through specific activity tests, determining their microbial composition based on 16S rRNA gene amplicon sequencing, and studying the thermodynamics of their metabolic networks.

Materials and Methods

Growth Medium

The growth medium used in all experiments corresponded to a modified basal anaerobic (BA) medium composed by 7 stock solutions. The composition of the stock solutions was the following: salts solution (NH_4Cl , 100 g/l; NaCl , 10 g/l; $\text{MgCl}_2 \cdot 6\text{H}_2\text{O}$, 10 g/l; $\text{CaCl}_2 \cdot 2\text{H}_2\text{O}$, 5 g/l), vitamins solution (biotin, 2 mg/l; folic acid, 2 mg/l; pyridoxine-HCl, 10 mg/l; riboflavin-HCl, 5 mg/l; thiamine-HCl, 5 mg/l; cyanocobalamine, 0.1 mg/l; nicotinic acid, 5 mg/l; p-aminobenzoic acid, 5 mg/l; lipoic acid, 5 mg/l; D-pantothenic acid hemicalcium salt, 5 mg/l), trace metal solution ($\text{FeCl}_2 \cdot 4\text{H}_2\text{O}$, 2000 mg/l; H_3BO_3 , 50 mg/l; ZnCl_2 , 50 mg/l; CuCl_2 , 30 mg/l; $\text{MnCl}_2 \cdot 4\text{H}_2\text{O}$, 50 mg/l; $(\text{NH}_4)_6\text{Mo}_7\text{O}_{24} \cdot 4\text{H}_2\text{O}$, 50 mg/l; AlCl_3 , 50 mg/l; $\text{CoCl}_2 \cdot 6\text{H}_2\text{O}$, 50 mg/l; NiCl_2 , 50 mg/l; $\text{Na}_2\text{SeO}_3 \cdot 5\text{H}_2\text{O}$, 100 mg/l; $\text{Na}_2\text{WO}_4 \cdot 2\text{H}_2\text{O}$, 60 mg/l), sodium bicarbonate solution (NaHCO_3 , 52 g/l), potassium phosphate dibasic solution (K_2HPO_4 , 152 g/l), chelating agent solution (Nitrilotriacetic acid, 1 g/l) and reducing agent solution ($\text{Na}_2\text{S} \cdot 9\text{H}_2\text{O}$, 25 g/l). The medium was prepared by adding 10 ml/l of salts solution, 10 ml/l of vitamins solution, 1 ml/l of trace metal solution, 50 ml/l of sodium bicarbonate solution, 2 ml/l of potassium phosphate dibasic solution, 20 ml/l of chelating agent solution, 10 ml/l of reducing agent solution (added after sealing the flasks under anaerobic conditions) and distilled water up to 1 l.

Inoculum and Microbial Enrichment Experiments

A mixture of two different types of anaerobic sludge was used as inoculum for mesophilic and a thermophilic microbial enrichment. The two anaerobic sludges used were collected from the Lundtofte Wastewater Treatment plant (Denmark) and from a lab-scale anaerobic digester fed solely with manure (at Chemical and Biochemical Engineering

Department, Technical University of Denmark). Prior to inoculation, the anaerobic sludges were mixed in equal amounts (1/1 v/v) while flushing with N_2 to ensure anaerobic conditions. The Total Suspended Solids concentration (TSS) and the Volatile Suspended Solids concentration (VSS) of the mixture of anaerobic sludges corresponded to 25.4 ± 0.1 g TSS/l and 15.3 ± 0.2 g VSS/l, respectively.

A batch enrichment technique was used in the mesophilic and the thermophilic enrichment series, which consisted in the successive transfer of the active enrichment cultures into flasks with fresh medium and synthetic syngas mixture (H_2 , CO and CO_2). Both enrichments comprised a total of 5 transfers using a constant initial partial pressure of gases and an inoculum size of 15% v/v. The enrichments were performed in duplicates, using the individual experiment with the highest CH_4 yield as inoculum for the next set of duplicates. The two series of enrichment experiments were performed in 330 ml flasks with an active volume of 100 ml. A volume of 85 ml of medium was first added to the flasks, flushed with H_2 to ensure anaerobic conditions and sealed with rubber stoppers and screw plugs. After sealing the flasks, additional H_2 , CO and CO_2 were added to the flasks anaerobically up to a final partial pressure after inoculation of 1.3 atm (P_{H_2}), 0.4 atm (P_{CO}) and 0.3 atm (P_{CO_2}) at 25 °C using a precision pressure indicator (model CPH6400, WIKA, Germany). The final P_{CO_2} decreased to approximately 0.2 atm due to solubilization in the medium. The incubation temperature corresponded to 37 °C for the mesophilic enrichment and 60 °C for the thermophilic enrichment. All flasks were incubated in a rotary shaker incubator at 100 rpm. The average initial pH of the enrichment after inoculation was 6.99 ± 0.16 at mesophilic conditions and 7.08 ± 0.14 at thermophilic conditions. A bicarbonate buffer was used to prevent significant changes in the pH during the fermentations. Mesophilic and thermophilic control experiments with no addition of syngas to evaluate the contribution of the organic matter from the inoculum to the overall product recovery were incubated at the same conditions with a headspace composition of 1.7 atm of N_2 and 0.3 atm of CO_2 (0.2 atm final P_{CO_2}). The headspace composition of the fermentations was monitored every second day and liquid samples were withdrawn at the beginning and at the end of each transfer.

Identification of Catabolic Routes

The analysis of the catabolic routes employed by the mesophilic and the thermophilic enriched microbial consortia was carried out by combining specific activity tests with either CO , H_2/CO_2 or acetate as the only substrate and the use of sodium 2-bromoethanesulfonate (BES) (15 mM) for inhibiting methanogenic archaea and allowing the identification of intermediate products used by each enriched microbial consortium. The initial experimental conditions used for

each experiment, including initial partial pressure of gases, acetate concentration and addition of BES, are summarized in Table 1. All experiments were carried out in triplicates in 330 ml flasks using an active volume of 100 ml and an inoculum size of 20% v/v, which corresponded to an initial VSS concentration of 23.7 ± 2.5 mg VSS/l for the mesophilic enrichment culture and 10.1 ± 0.4 mg VSS/l for the thermophilic. Mesophilic and thermophilic active enrichment cultures from transfer T6 (not shown) were used as inoculum for the mesophilic and the thermophilic experiments, respectively. Anaerobic conditions were secured as described above and the partial pressure of each gas was adjusted using a precision pressure indicator (model CPH6400, WIKA, Germany). The average initial pH after inoculating was 7.33 ± 0.12 for all experiments at mesophilic conditions, and 7.16 ± 0.02 at thermophilic conditions. Significant pH changes during the fermentations were prevented by using a bicarbonate buffer (0.2 bar P_{CO_2} and 31 mM of $NaHCO_3$). All flasks were incubated in a rotary shaker incubator at 100 rpm. The incubation temperature for experiments at mesophilic conditions corresponded to 37 °C, and at thermophilic conditions to 60 °C. Gaseous and liquid samples for monitoring headspace composition, metabolites concentration and microbial biomass growth along the fermentations were withdrawn at least once a day for all experiments.

Analytical Methods

The composition of the headspace (H_2 , CO , CO_2 and CH_4) was analyzed using a gas chromatograph (model 8610C, SRI Instruments, USA) with a thermal conductivity detector and two packed columns, a Molsieve 13X column (6' \times 1/8") and a silica gel column (6' \times 1/8") connected in series with a rotating valve. The column temperature conditions were: 65 °C for 3 min, temperature ramp of 10 °C/min up to 95 °C and a second ramp of 24 °C/min from 95 to 140 °C. Liquid samples were analyzed for volatile fatty acids (VFA) and alcohols using a High Performance Liquid Chromatograph (Shimadzu, USA) equipped with a refractive index detector and an Aminex HPX-87H column (Bio-Rad, USA) at 63 °C. The flow rate of the eluent (12 mM H_2SO_4 solution) corresponded to 0.6 ml/min. Microbial biomass

growth was monitored based on the absorbance of liquid samples (600 nm) using a spectrophotometer (DR2800, Hach Lange). The absorbance of the liquid samples was correlated to the concentration of Volatile Suspended Solids (VSS) determined according to standard methods for each of the enriched microbial consortia [17].

DNA Isolation and Amplicon Sequencing

Samples for extraction of total genomic DNA were collected at the late exponential phase (day 4) of fermentations performed in triplicates, corresponding to transfer T7 of the mesophilic and the thermophilic microbial enrichments. Total genomic DNA was isolated from triplicate samples using PowerSoil™ DNA Isolation Kit (Qiagen, Denmark) following manufacturer recommendations. DNA samples were submitted to Macrogen Inc. (Korea) for 16S rRNA amplicon library preparation and sequencing using Illumina Miseq instrument (300 bp paired-end sequencing). Libraries were prepared according to 16S Metagenomic Sequencing Library Preparation Protocol (Illumina, Part #15044223, Rev. B), with Herculanase II Fusion DNA Polymerase Nextera XT Index Kit V2. Amplification of V3 and V4 region of 16S rRNA gene was carried out with Pro341F (5'-CCTACG GGNBGCASCAG-3') and Pro805R (5'-GACTACNVGGG TATCTAATCC-3') from Takahashi et al. [18], while amplification of V4 and V5 region was performed with 515FB (5'-GTGYCAGCMGCCGCGGTAA-3') and 926R (5'-CCG YCAATTYMTTTRAGTTT-3') from Walters et al. [19].

Analysis of 16S rRNA Gene Amplicons

Remaining read-through adapters were clipped using cutadapt [20]. Subsequently, paired reads were merged using usearch-fastq_mergepairs, allowing for 80% identity and up to 10 mismatches in the alignment. Only merged reads containing primer sequences were kept and primer sequences were stripped for subsequent analysis. Subsequently, filtering, generation of Operational Taxonomic Units (OTUs) and mapping of reads to OTUs was performed using the UPARSE/unoise3 pipeline [21]. In brief, reads were quality filtered using usearch-fastq_filter and maximum expected error threshold to 1.0 and uniques identified using

Table 1 Initial partial pressure of gases, concentration of acetate and BES concentration used in the specific activity tests performed at mesophilic and thermophilic conditions

	H_2 (atm)	CO (atm)	CO_2 (atm)	N_2 (atm)	$NaCH_3COO$ (mM)	BES (mM)
CO + BES	–	0.4	0.2	1.4	–	15
H_2/CO_2 + BES	0.8	–	0.2	1	–	15
H_2/CO_2	0.8	–	0.2	1	–	–
Acetate	–	–	0.2	1.8	25	–
H_2/CO_2 + CO	1.0	0.4	0.2	0.4	–	–

usearch-fastx_uniques. Only reads with abundance more than 8 were kept. These were denoised and chimera-filtered using UNOISE3 [21]. Taxonomy names were assigned to OTUs using SINTAX [22] and SILVA v132 LTP database of 13,899 curated 16S sequences using 0.8 bootstrap confidence threshold [23]. To create OTU table, unfiltered reads were mapped to OTUs using usearch-otutab. Sample data from replicate runs were collapsed based on the median count and each sample was normalized to the depth of the sample with least-mapped counts. Downstream analyses were performed with Qiime and STAMP [24].

Thermodynamic Feasibility

The thermodynamics of the metabolic network was evaluated based on the Gibbs free energy change ($\Delta_r G^\circ$) of the overall biochemical reactions present in each of the enriched microbial consortia. Standard Gibbs free energies of formation ($\Delta_f G^\circ$) and standard enthalpies of formation ($\Delta_f H^\circ$) used were obtained from Alberty [25] and Amend and Shock [26]. The $\Delta_r G^\circ$ were first corrected for temperature and ionic strength according to the Gibbs–Helmholtz equation (Eq. 1) and the extended Debye–Hückel equation (Eq. 2) [25].

$$\Delta_r G'_i(T) = \Delta_r G^\circ_i(298.15K) \cdot \frac{T}{298.15K} + \Delta_r H^\circ_i(298.15K) \cdot \frac{298.15K - T}{298.15K} \quad (1)$$

$$\Delta_r G^\circ_i(I) = \Delta_r G^\circ_i(I = 0) - \frac{RTAz_i^2 I^{1/2}}{1 + BI^{1/2}} \quad (2)$$

where z_i is the charge number of compound i , I is the ionic strength of the medium, A was calculated as a function of temperature according to Alberty [25] and B is an empirical constant that takes a value of $1.6 \text{ l}^{1/2} \text{ mol}^{-1/2}$ within a range of ionic strength of 0.05–0.25 M [25]. Subsequently, the Gibbs free energy change of the reactions considered ($\Delta_r G'_T$) was corrected for the actual partial pressure of gases and concentration of metabolites according to Eq. 3, and the effect of the pH was corrected as described in Steinbusch et al. [27].

$$\Delta_r G'_T = \Delta_r G^\circ_T(I = 0.08M) + RT \ln \frac{[C]^c [D]^d}{[A]^a [B]^b} \quad (3)$$

The thermodynamic potential factor (F_T), calculated according to Eq. 4, was introduced by Jin and Bethke [28] to include thermodynamic consistency in kinetic models (e.g. $\mu = \mu_{\max} \cdot S/(k_s + S) \cdot F_T$) by considering the energy released and the energy conserved through a specific metabolic pathway. However, in this study, F_T calculations were used to identify possible bioenergetic limitations affecting the

rate of conversion of the biochemical reactions composing the metabolic network of the enriched consortia under the operating conditions found experimentally, as described in Grimalt-Alemanly et al. [29], and to determine the minimum threshold concentration of substrate for each microbial group considered. The F_T was calculated according to Eqs. 4 and 5.

$$F_T = 1 - \exp\left(-\frac{\Delta G_A - \Delta G_C}{\chi RT}\right) \quad (4)$$

$$\Delta G_C = Y_{ATP} \cdot \Delta G_p \quad (5)$$

where ΔG_A equals to $-\Delta_r G'_T$ in kJ per reaction; ΔG_C is the energy conserved calculated based on the ATP yield of each metabolic pathway multiplied by the Gibbs free energy of phosphorylation (ΔG_p); and χ is the average stoichiometric number, which can be approximated by the number of times a rate-determining step takes place through a metabolic pathway. When $\Delta G_A \gg \Delta G_C$, F_T approaches 1, which indicates that there is a strong thermodynamic driving force for a specific reaction to proceed forward, and thus the rate of the reaction is strictly dependent on the kinetic properties of the microbial species in question. When $\Delta G_A \approx \Delta G_C$, F_T approaches 0, the thermodynamic drive is low and F_T has a strong effect on the reaction rate, indicating that the reaction rate is thermodynamically controlled. When ΔG_A is equal to or lower than ΔG_C , F_T is 0 or negative, respectively, and the thermodynamic drive for the reaction to proceed forward disappears and the metabolism stops.

F_T calculations for acetogenic growth on H_2/CO_2 and CO were performed using an ATP yield of 0.33 mol ATP/mol acetate and 1.66 mol ATP/mol acetate, respectively, calculated using the H^+/Na^+ translocation described in Bertsch and Müller [30] for *Acetobacterium woodii* and an ATP synthesis stoichiometry of 3 H^+/Na^+ per ATP formed. The reverse reaction for syntrophic acetate oxidation and the syntrophic propionate oxidation reaction were assumed to have an ATP yield of 0.33 mol ATP/mol acetate or propionate [31]. The hydrogenogenesis was assumed to translocate one H^+ across the membrane per mol of CO through an energy-conserving hydrogenase, which would result in an ATP yield of 0.33 mol ATP/mol CO using an ATP synthesis stoichiometry of 3 H^+ per ATP synthesized. Lastly, both aceticlastic and hydrogenotrophic methanogenesis were assumed to be performed by species without cytochromes with an ATP yield of 0.5 mol ATP/mol CH_4 resulting from the translocation of 6 Na^+ (1 mol ATP invested in acetate activation) and 2 Na^+ across the membrane, respectively, and using an ATP synthesis stoichiometry of 4 Na^+ per ATP formed [32]. The rate-determining step for hydrogenotrophic and aceticlastic methanogenesis was assumed to be the translocation of Na^+ by the methyl transferase complex (Mtr). The ATP yields and χ used for F_T calculations are summarized in Table 2. To account for uncertainties in the ATP yields used, three

different values of ΔG_p covering a rather broad range were considered in F_T calculations, corresponding to 45 kJ/mol ATP, 50 kJ/mol ATP and 55 kJ/mol ATP.

Results and Discussion

Enrichment of Mesophilic and Thermophilic Mixed Cultures

A mixture of mesophilic anaerobic sludges was used as initial inoculum in a mesophilic and a thermophilic microbial enrichment to generate two stable enriched cultures with the ability to convert syngas into CH_4 and CO_2 as the only end products. Despite the initial inoculum was adapted to mesophilic conditions and had not been previously exposed to synthesis gas, both mesophilic and thermophilic enrichment cultures presented hydrogenotrophic and carboxydrotrophic activity. Both enrichment cultures were able to convert synthesis gas into CH_4 as the main product from the first transfer of the enrichment, with only a short lag phase of around 2 days. The native carboxydrotrophic ability of the anaerobic sludge was anticipated, since CO is a necessary intermediate for the autotrophic fixation of CO_2 by acetogenic bacteria and for the aceticlastic energy metabolism of methanogenic archaea [33, 34]. However, more striking was the fact that the thermophilic enrichment culture did not present any apparent negative effect caused by the drastic change in incubation temperature at transfer T0 when compared to the mesophilic enrichment culture. Similar observations were made by Sipma et al. [14] when incubating a mesophilic

anaerobic sludge at 55 °C using CO as the only carbon and energy source, as they observed that the anaerobic sludge became rapidly adapted to the higher incubation temperature. This suggests that thermophilic microorganisms prevail in mesophilic anaerobic sludge microbial communities, and illustrates the high adaptability of mixed cultures when facing drastic changes in operating conditions.

The product recovery of the fermentations carried out by the mesophilic and the thermophilic cultures was relatively stable along the enrichment (Fig. 1). The contribution of the residual activity of the inoculum to the total product recovery was only significant at transfer T0, where the production of acetate and CH_4 in control experiments corresponded to 6.6% and 14.1% of the total product recovery for the mesophilic and the thermophilic enrichment cultures, respectively (Fig. 1). Both enrichments rapidly reached a stable activity with an average CH_4 yield in the last four transfers of $83.1 \pm 1.5\%$ of the stoichiometric yield at mesophilic conditions and $90.1 \pm 1.6\%$ at thermophilic conditions. However, the mesophilic enrichment presented acetate accumulation at transfer T1 as the culture was transferred before acetate could be fully converted to CH_4 . Consequently, the fermentation time was extended considerably in subsequent transfers to avoid washing out the aceticlastic methanogenic microbial group from the enrichment culture. In turn, the enrichment at thermophilic conditions allowed much faster transfers of the culture with no negative effects on the product selectivity towards CH_4 , since significant acetate production was only observed at the beginning of the enrichment (Fig. 1).

The results obtained here for both the mesophilic and the thermophilic enrichments differed quite significantly from previous enrichment studies. A study on the enrichment of a thermophilic mixed culture reported that the CH_4 production was suppressed along the microbial enrichment, and this was attributed to the inhibition of methanogenesis by the presence of CO [15]. However, in their study, the initial P_{CO} was increased from 0.09 to 0.18 atm at the third transfer, which probably limited the adaptability of the culture due to the advanced stage of the enrichment, as it is likely that the enrichment had initially selected for methanogenic species with low tolerance to CO. In the present study, the initial P_{CO} was kept constant at 0.4 atm along the whole thermophilic microbial enrichment, which probably favored the prompt selection of hydrogenotrophic methanogenic species with higher tolerance to CO, allowing a complete conversion of syngas into CH_4 . Similarly, recent work on the enrichment of mesophilic mixed cultures using a multi-orifice baffled bioreactor (MOBB) sludge as initial inoculum reported a partial conversion of syngas into CH_4 with acetate accumulation in the fermentation broth, which was attributed to a possible inhibition of aceticlastic methanogens due to the toxicity of CO [16]. In the present study, similar observations were made at transfer T1, where acetate started accumulating in

Table 2 Overall biochemical reactions, ATP yield and average stoichiometric number used in thermodynamic potential factor (F_T) calculations

Stoichiometry of biochemical reactions	ATP yield (mol per reaction)	χ	Ref.
Acetogenesis			
$4 \text{H}_2 + 2 \text{CO}_2 \rightarrow \text{CH}_3\text{COOH} + 2 \text{H}_2\text{O}$	0.33	1	[30]
$4 \text{CO} + 2 \text{H}_2\text{O} \rightarrow \text{CH}_3\text{COOH} + 2 \text{CO}_2$	1.66	5	[30]
Hydrogenogenesis			
$\text{CO} + \text{H}_2\text{O} \rightarrow \text{H}_2 + \text{CO}_2$	0.33	1	Calculated
Syntrophic fatty acid oxidation			
$\text{CH}_3\text{CH}_2\text{COOH} + 2 \text{H}_2\text{O} \rightarrow \text{CH}_3\text{COOH} + 3 \text{H}_2 + \text{CO}_2$	0.33	1	[31]
$\text{CH}_3\text{COOH} + 2 \text{H}_2\text{O} \rightarrow 4 \text{H}_2 + 2 \text{CO}_2$	0.33	1	[31]
Methanogenesis			
$4 \text{H}_2 + \text{CO}_2 \rightarrow \text{CH}_4 + 2 \text{H}_2\text{O}$	0.5	2	[32]
$\text{CH}_3\text{COOH} \rightarrow \text{CO}_2 + \text{CH}_4$	0.5	2	Calculated

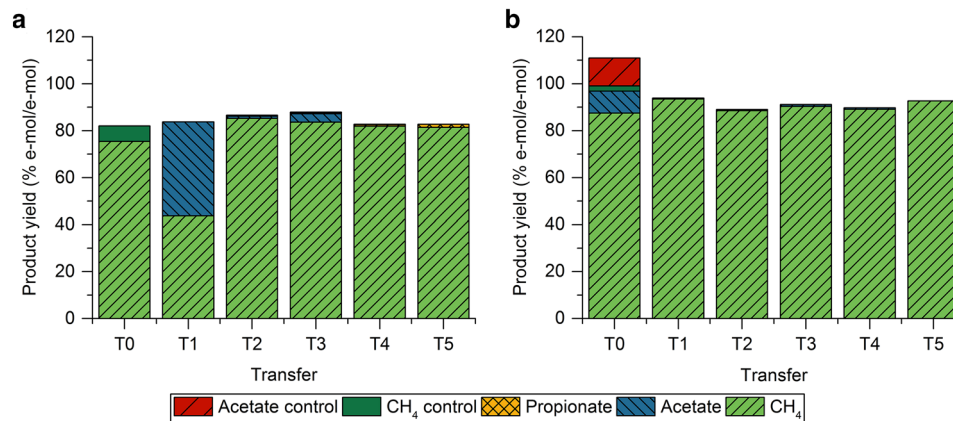


Fig. 1 **a** Product yields and total product recovery for the mesophilic culture along the enrichment. **b** Product yields and total product recovery for the thermophilic culture along the enrichment. The product yields are given as percentage of the stoichiometric yield (% e-mol/e-mol) and correspond to the duplicate experiment used to

inoculate the subsequent fermentation. Product yields from control experiments correspond to the estimated contribution of the organic matter present in the inoculum to the overall product recovery. Note that product yield observed in control experiments was negligible after transfer T0

the fermentation broth possibly due to inhibition of acetoclastic methanogens (Fig. 1a). However, in this case, extending the fermentation time enabled the activity of the acetoclastic methanogenic microbial trophic group once CO was depleted, and thus, allowed the full conversion of syngas into CH₄.

Identification of Catabolic Routes and their Specific Activities

The microbial enrichments, carried out in batch mode, were expected to select for the fastest growing microbial trophic groups at mesophilic and thermophilic conditions, diverting thus the carbon flux through the most efficient catabolic routes converting syngas into CH₄ and CO₂ in each case. Noticeable differences were found when comparing the fermentation profiles of the two enriched microbial consortia, which suggested different patterns of activity. The fermentation of syngas by the mesophilic enriched consortium typically resulted in transient production of acetate as intermediate product and propionate as a minor end by-product, while the evolution of intermediate products was not apparent when using the thermophilic enriched culture (Fig. 2). Additionally, the maximum specific CH₄ productivity of the mesophilic enriched consortium was one order of magnitude lower than that of the thermophilic consortium, namely 1.83 ± 0.27 and 33.48 ± 0.90 mmol CH₄/g VSS/h respectively (Table 4), which also indicated significant differences in the catabolic routes employed by each enriched microbial consortium since such difference in CH₄ productivity could not be solely attributed to the anticipated increase in reaction rates due to the increase of incubation temperature.

The conversion of CO by the mesophilic and the thermophilic microbial consortium using BES for inhibiting methanogenic archaea resulted in the production of different metabolites, which indicated that the microbial trophic group metabolizing CO was different in each consortium (Table 3 and Online Resource 1—fig. S1a). The mesophilic enriched consortium was found to produce acetate as the main end-product (0.17 ± 0.01 mol/mol CO) and propionate as a secondary metabolite (0.01 ± 0.00 mol/mol CO) (Table 3). Several microbial groups have been reported to grow on CO producing significant amounts of acetic acid including carboxydrotrophic acetogens, methanogens, hydrogenogens and sulfate-reducers [11, 35–37]. Nonetheless, among these microbial groups, only carboxydrotrophic acetogens have been described to produce acetic acid as the main product at mesophilic conditions. Additionally, the addition of the methanogenic inhibitor BES and the lack of sulfate in the growth medium prevented the growth of carboxydrotrophic methanogens and sulfate-reducers, leading thus to the conclusion that carboxydrotrophic acetogens were the microbial group responsible for the conversion of CO at mesophilic conditions. In turn, the conversion of CO by the thermophilic enriched consortium in presence of BES resulted in the production of H₂ as the main end-product (0.68 ± 0.01 mol/mol CO) and acetic acid as the only secondary metabolite (0.04 ± 0.01 mol/mol CO) (Table 3 and Online Resource 1—fig. S1b). However, acetic acid was not observed as intermediate product when the thermophilic microbial consortium was exposed to syngas (Fig. 2b), and no acetoclastic activity was found in this microbial consortium (Table 3). This indicated that acetic acid was produced only when CO was used as the sole carbon source, which could only be explained by a partial metabolic shift from

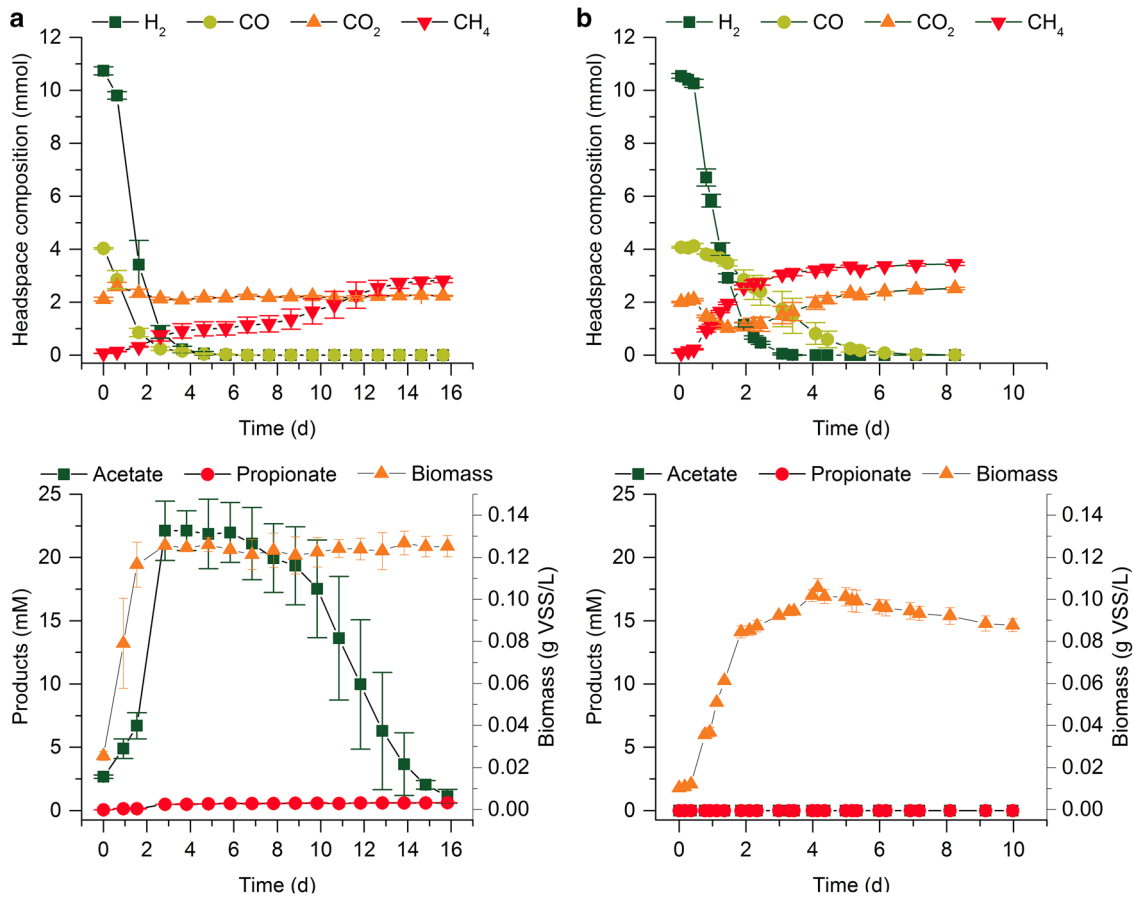


Fig. 2 a Fermentation profile for the mesophilic enriched microbial consortium after 6 transfers for substrates, products and biomass, respectively. b Fermentation profile for the thermophilic enriched

microbial consortium after 6 transfers for substrates, products and biomass, respectively

Table 3 Product yields and overall product recovery for the specific activity tests using the mesophilic and the thermophilic enriched microbial consortia

	Product recovery (% e-mol/e-mol)	Acetate yield (mol/mol)	Propionate yield (mol/mol)	H ₂ yield (mol/mol)	CH ₄ yield (mol/mol)
Mesophilic microbial consortium					
CO+BES	73.7±3.9	0.17±0.01	0.01±0.00	–	–
H ₂ /CO ₂ +BES	84.7±2.5	0.21±0.01	–	–	–
H ₂ /CO ₂ ^a	92.8±0.3 ^a	–	–	–	0.23±0.00 ^a
Acetate	81.5±0.9	–	–	–	0.82±0.01
H ₂ /CO ₂ +CO	81.5±0.1	–	0.004±0.000	–	0.20±0.00
Thermophilic microbial consortium					
CO+BES	84.6±2.7	0.04±0.01	–	0.68±0.01	–
H ₂ /CO ₂ +BES	No activity	–	–	–	–
H ₂ /CO ₂	91.4±0.9	–	–	–	0.23±0.00
Acetate	No activity	–	–	–	–
H ₂ /CO ₂ +CO	92.2±1.7	–	–	–	0.23±0.00

^aThe product recovery and the CH₄ yield corresponds to the overall yield including the conversion of acetic acid through acetoclastic methanogenesis. The specific hydrogenotrophic CH₄ yield and product recovery corresponds to 0.24±0.01 mol/mol H₂ and 95.4±5.6%, respectively

Table 4 Biomass yield and specific activities and productivities for the different microbial groups present in the mesophilic and the thermophilic enriched microbial consortia

	Biomass yield(g VSS/mol substrate)	Max. specific activity (mmol substrate/g VSS/h)			Max. specific productivity (mmol product/g VSS/h)			
		H ₂	CO	Acetate	Acetate	Propionate	H ₂	CH ₄
Mesophilic enriched consortium								
Carboxydrotrophic acetogens	2.45 ± 0.06	–	14.18 ± 2.31	–	2.53 ± 0.64	0.18 ± 0.03	–	–
Homoacetogens	0.54 ± 0.03	49.14 ± 10.70	–	–	7.36 ± 1.62	–	–	–
Hydrogenotrophic methanogens ^a	0.72 ± 0.03 ^a	46.12 ± 5.50 ^a	–	–	–	–	–	11.00 ± 1.31 ^a
Aceticlastic methanogens	0.57 ± 0.06	–	–	6.65 ± 1.77	–	–	–	6.44 ± 0.54
All microbial groups	0.87 ± 0.02	27.45 ± 1.23	14.87 ± 0.59	–	5.26 ± 0.91	0.10 ± 0.00	–	1.83 ± 0.27
Thermophilic enriched consortium								
Carboxydrotrophic hydrogenogens	0.82 ± 0.01	–	52.35 ± 1.72	–	1.61 ± 0.42	–	44.95 ± 4.11	–
Hydrogenotrophic methanogens	0.51 ± 0.01	244.26 ± 12.87	–	–	–	–	–	43.46 ± 1.52
All microbial groups	0.66 ± 0.01	165.75 ± 4.53	12.43 ± 1.16	–	–	–	–	33.48 ± 0.90

^aThe biomass yield, the maximum specific activity and productivity for hydrogenotrophic methanogens was estimated based on the biomass and acetate yield of homoacetogens determined in the experiments with H₂/CO₂ with BES addition

hydrogenogenesis to acetogenesis during the conversion of CO. Such a metabolic shift has been previously reported for the hydrogenogenic species *Carboxydotherrmus hydrogeniformans*, where the shift towards acetogenesis was attributed to the accumulation of CO₂ in the gas phase [37]. Thus, the product profile found in the experiments at thermophilic conditions using CO is probably the result of strictly hydrogenogenic growth being partially inhibited by the accumulation of H₂ and CO₂ rather than simultaneous acetogenic and hydrogenogenic growth.

Significant differences were also found when studying the catabolic routes for the conversion of H₂/CO₂ employed by each enriched microbial consortium. The experiments using the mesophilic enriched consortium with H₂/CO₂ as the sole substrate and addition of BES resulted in the production of acetic acid as the only end-metabolite (0.21 ± 0.01 mol/mol H₂), while in the experiments without BES addition, both acetic acid and methane were initially produced upon consumption of H₂/CO₂ and the acetic acid was further converted to CH₄ in a later stage of the fermentation (overall CH₄ yield of 0.23 ± 0.00 mol/mol H₂ and estimated CH₄ yield for the direct conversion of H₂/CO₂ of 0.24 ± 0.01 mol/mol H₂) (Online Resource 1, fig. S2a, S3a and S4a). On the other hand, the thermophilic consortium did not present any microbial activity in experiments with BES and acetate addition, and H₂/CO₂ was found to be converted strictly to CH₄ when BES was not added to the growth medium, resulting in a CH₄ yield of 0.23 ± 0.00 mol/mol H₂ (Online Resource 1, fig. S2b, S3b and S4b). This indicated that the

thermophilic enriched consortium metabolized H₂/CO₂ strictly through hydrogenotrophic methanogenesis, while in the mesophilic enriched consortium, both homoacetogenesis and hydrogenotrophic methanogenesis co-existed and competed for this substrate. The latter was further supported by the high similarity between the specific activity rates of the homoacetogenic and the hydrogenotrophic methanogenic microbial groups found for the mesophilic enriched consortium (Table 4).

Overall, the analysis of the patterns of activity of each microbial consortium revealed that the enrichment at different incubation temperatures resulted in the development of two enriched consortia with totally different levels of complexity in terms of microbial community structure, and activity rates (Table 4). As a result of the enrichment, the mesophilic enriched consortium presented a more intricate metabolic network composed by four different microbial trophic groups where aceticlastic methanogenesis contributed to 64.9 ± 8.3% of the CH₄ production, with the rest being produced through hydrogenotrophic methanogenesis. Thus, based on the maximum specific activities and productivities determined for this microbial consortium, at mesophilic conditions, aceticlastic methanogenesis was the main rate-limiting step of the conversion of syngas into CH₄ (Table 4). In turn, the enrichment at thermophilic conditions led to a much simpler metabolic network based on H₂ as the only intermediate product, resulting in the syntrophic association of only two different microbial trophic groups. This allowed achieving a more direct and much faster conversion

of syngas into CH_4 due to the higher turnover rates of H_2 when compared to that of acetate (Table 4). Additionally, the lower complexity of the thermophilic enriched consortium could also explain the higher overall CH_4 yield observed in experiments for syngas conversion at thermophilic conditions, as the involvement of less intermediate steps, mostly in the conversion of H_2 , reduced the carbon and energy losses during the microbial conversion (Table 3).

The specific activity tests allowed for determining the biomass yield for each microbial group composing the mesophilic and the thermophilic enriched consortia (Table 4). The biomass yields were consistent with the product recoveries found for each experiment since there is a reversely proportional correlation between them, where higher product recovery resulted in a lower biomass yield for the corresponding microbial group with the exception of the experiment with H_2/CO_2 at mesophilic conditions (Tables 3, 4). The carboxydrotrophic acetogenic microbial group was found to have the highest biomass yield, which could be explained by the high ATP yield of their metabolic pathway compared to the rest (Table 2). This probably favored the fact that growth of the aceticlastic methanogenic microbial group was not noticeable during the late stage of the fermentation of syngas at mesophilic conditions (Fig. 2a).

Previous work on the identification of the catabolic routes for the conversion of CO to CH_4 showed that the main CO conversion pathways shifted from acetogenesis to hydrogenogenesis when increasing the incubation temperature from 45 °C onwards [14]. However, several studies focusing on the conversion of CO using different anaerobic sludges showed that, despite the shift in the main catabolic routes between carboxydrotrophic acetogenesis and hydrogenogenesis, both of these reactions were available to the anaerobic sludge and occurred simultaneously during the conversion towards CH_4 [13, 14, 38]. In this study, the mesophilic enriched consortium was found to convert CO strictly through carboxydrotrophic acetogenesis, while the thermophilic converted CO exclusively via carboxydrotrophic hydrogenogenesis. Similarly, several studies showed that there is a strong competition for H_2 between homoacetogens and hydrogenotrophic methanogens in both mesophilic and thermophilic anaerobic sludges, although hydrogenotrophic methanogenesis is clearly favored at thermophilic conditions [39, 40]. In this study, a strong competition was also found between homoacetogens and hydrogenotrophic methanogens at mesophilic conditions, whereas hydrogenotrophic methanogenesis was the only H_2/CO_2 microbial conversion activity found at thermophilic conditions. Therefore, it seems that the microbial enrichment procedure applied in the present study based on batch operation and the incubation temperature selected the most efficient and fastest growing microbial groups at the specific conditions used, enhancing the

carbon flux through their corresponding catabolic pathways and demoting the slower pathways to a negligible activity.

Microbial Composition of Enriched Cultures

The number of raw reads for the sequenced libraries varied between 272,590 and 429,724 ($347,711 \pm 48,914$ on average). The number of OTUs generated using the V3-V4 region primer set corresponded to 2,373, while for the V4-V5 primer set corresponded to 2,285 OTUs. The percentage of reads mapped to OTUs ranged from a minimum of 65.7% for the anaerobic sludge used as initial inoculum to a maximum of 95.5% for the thermophilic enriched microbial consortium. The reads not mapped corresponded to reads of lower quality, chimeric or to true biological sequences that were not found among the OTUs (and were filtered out or wrongly assigned as chimeras). Despite small differences, the percentage of reads mapping to specific taxonomic lineages was highly consistent for the two primer sets used, indicating that both of them could be used for analysis of bacterial and archaeal communities in analyzed samples (Online Resource 1—fig. S5 and Online Resource 2).

The anaerobic sludge used as inoculum for the enrichments was found to be significantly different from the mesophilic and the thermophilic enriched consortia. While it is difficult to point to the dominant genera in the anaerobic sludge samples as the percentage of reads mapping to OTUs unassigned at genus level corresponded to 69.7% (Fig. 3), the major phyla included *Firmicutes*, *Proteobacteria*, *Bacteroidetes* (26.4%, 21.6%, 21.1% reads mapped, respectively, using 341F785R primer set). None of the genera identified in the anaerobic sludge was found in samples from the mesophilic or the thermophilic enriched consortium, which shows that the enrichment had a strong effect on the microbial composition of the cultures, reducing the complexity of the microbial communities. Alpha diversity, both in terms of the number of observed OTUs and calculated PD whole tree index (reflecting the phylogenetic distance between OTUs), was considerably higher in anaerobic sludge samples. Moreover, higher temperature conditions clearly resulted in less diverse microbial community (Online Resource 2).

The mesophilic enriched consortium presented the highest microbial diversity at genus level among the two enriched consortia. The dominant genera identified in this culture corresponded to *Acetobacterium* and *Methanospirillum*, with a percentage of reads mapping to these genera of 26.0% and 23.3%, respectively (Fig. 3). The species belonging to the genus *Acetobacterium* could not be identified; however, *Acetobacterium* species were likely responsible for the acetogenic growth on CO and H_2/CO_2 observed experimentally as several species from this genus have been found to be capable of carboxydrotrophic and homoacetogenic growth [41]. While having in mind the lower confidence of species

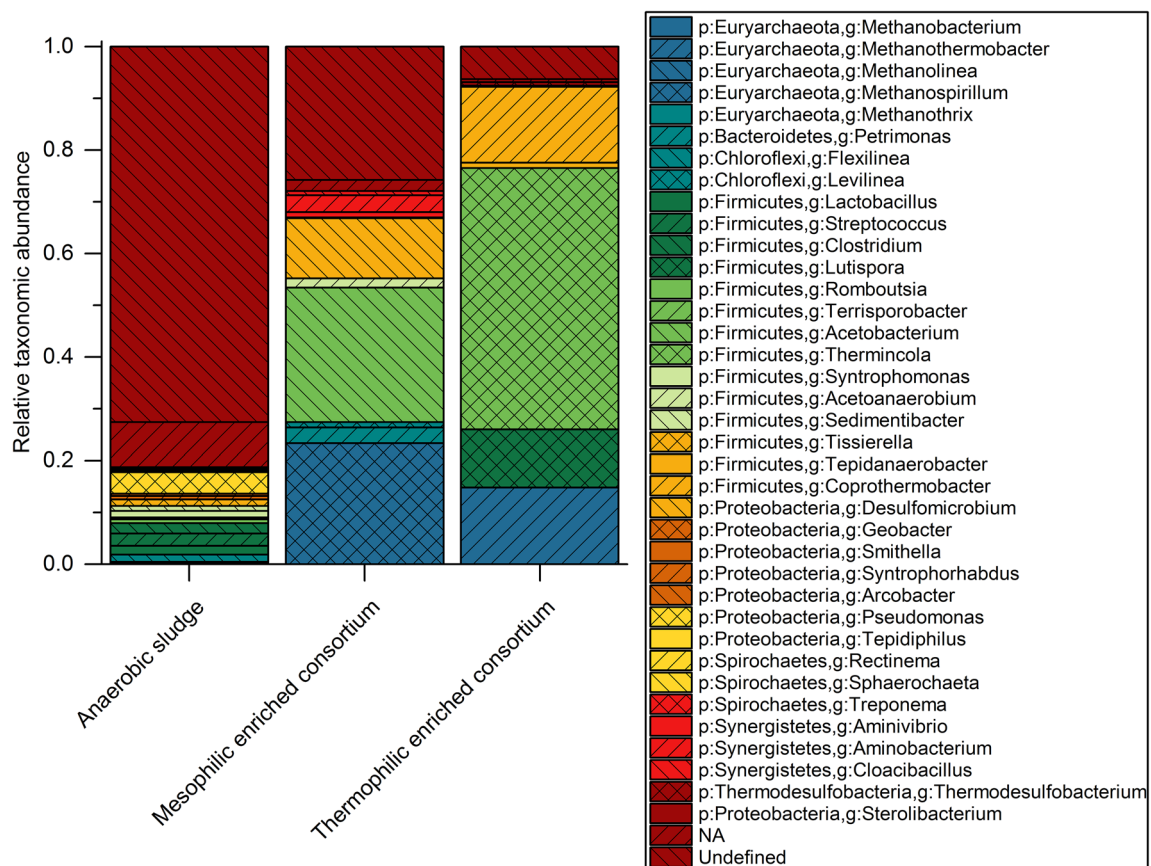


Fig. 3 Average relative taxonomic abundance of triplicate samples for the initial inoculum used and the mesophilic and thermophilic enriched microbial consortia at genus level using the V3-V4 region

assignment in 16S amplicon sequencing studies [42], 15.8% and 2.4% of mapped 341F785R reads corresponded to OTUs assigned as *Methanospirillum hungatei* and *Methanospirillum stamsii*, respectively (Fig. 3). It is likely that these or closely related species carried out the conversion of H_2/CO_2 into CH_4 as both of them have been reported to be strict hydrogenotrophic methanogens [43]. Another genus identified with relatively high abundance was *Desulfomicrobium* (11.7% of reads mapped), most likely corresponding to the species *Desulfomicrobium escambiense*. This relative abundance would suggest a possible role during the conversion of either CO or H_2/CO_2 . However, several species closely related to *Desulfomicrobium escambiense* were found to be incapable of autotrophic growth in absence of sulfate and were not able to grow on acetate or propionate, for which the role of this species during the fermentation is yet to be elucidated since the only source of sulfur in the growth medium used was in the form of sulfide [44]. Aceticlastic methanogenesis is a metabolic process performed exclusively by methanogenic euryarchaea from the order *Methanosarcinales* [45]. While none of the observed OTUs

primer set. NA corresponds to the sum of all genera with relative abundance below 0.5% in the individual samples before calculating the average

in thermophilic enrichment samples were assigned to *Methanosarcinales*, less than 0.5% or reads corresponded to this order in mesophilic microbial community. The presence of aceticlastic methanogenic genera was in fact expected as this reaction was clearly observed in the specific activity tests. Low abundance of reads mapping to this microbial group could be explained by the fact that sampling was performed during the late exponential phase of the fermentation, possibly before the aceticlastic microbial group became active (Fig. 2a). As shown in “[Identification of Catabolic Routes and their Specific Activities](#)” section, small amounts of propionate remained unconverted at the end of the fermentation, which would indicate that syntrophic fatty acid oxidizing bacteria did not play a significant role during the conversion. However, a small percentage of the reads mapped corresponded to the genus *Geobacter* (0.2% using V3-V4 primer set and 0.5% using V4-V5 primer set), within which some species have been reported to be able of syntrophic fatty acid oxidation (Online resource 2, Table 5) [46]. This indicates that propionate oxidation could have occurred to a limited extent during the fermentation. Two other genera belonging

to the phylum Synergistetes corresponding to *Aminivibrio* and *Aminobacterium* were found to have higher relative abundances (1.0% and 3.3% of reads mapping to corresponding OTUs, respectively), although several species from these genera are not capable of syntrophic propionate or acetate oxidation and are probably associated with the degradation of amino acids originating from cell debris [47].

According to the results obtained in “[Identification of Catabolic Routes and their Specific Activities](#)” section, the thermophilic enriched consortium presented a simpler metabolic network when compared to that of the mesophilic enriched consortium. This is consistent with the results obtained in the analysis of the microbial composition. As shown in Fig. 3, this microbial community was dominated by the genus *Thermincola* with a 47.9% of reads mapping to OTUs assigned to the species *Thermincola carboxydiphila*. *Thermincola carboxydiphila* has been reported to be an obligate carboxydrotrophic hydrogenogen, which indicates that it was responsible for the conversion of CO into H₂ and CO₂ observed during the specific activity tests [48]. Similarly, the conversion of H₂/CO₂ into CH₄ by hydrogenotrophic methanogens observed experimentally was confirmed by the fact that 14.8% of the reads mapped to *Methanothermobacter* OTUs, as species belonging to this genus have been reported to be capable of autotrophic growth. In fact, the species *Methanothermobacter thermoautotrophicus* and *Methanothermobacter marburgensis* belonging to this genus were found to be capable of growth on both H₂/CO₂ and CO [9, 12]. Direct carboxydrotrophic methanogenesis is not likely in this enriched culture though given the high relative abundance of the obligate carboxydrotrophic hydrogenogen *Thermincola carboxydiphila*. Other species identified with a significant relative abundance were *Lutispora thermophila* and *Coprothermobacter proteolyticus*, representing a 9.6% and 14.7% of reads mapping to these species, respectively (Fig. 3). Nonetheless, the role of these species during the fermentation is still uncertain as none of them is capable of autotrophic growth, and both are usually associated to environments with abundant proteinaceous material [49].

The analysis of the microbial composition of the enrichment cultures allowed for identifying the dominant microbial trophic groups present in both mesophilic and thermophilic microbial consortia. Overall, the microbial composition found was in agreement with the catabolic routes identified for each enriched consortium in “[Identification of Catabolic Routes and their Specific Activities](#)” section as most of the dominant genera identified could be associated with a specific microbial activity. Additionally, the results obtained here were highly consistent with other batch enrichment studies performed at similar conditions as the genera *Acetobacterium* and *Methanospirillum* were also found to be predominant by Arantes et al. [16] at mesophilic conditions and the genus *Thermincola* by Alves et al. [15] at thermophilic

conditions. This indicates that the microbial selection process is somewhat independent of the inoculum used for the enrichment and shows high reproducibility, since microbial communities with very different initial microbial composition converged towards enriched cultures with high similarity as a result of the microbial selection driven by the operating conditions used. However, more systematic enrichment and sequencing studies are necessary to investigate this phenomenon.

Microbial Selection and Competition for Common Substrates

In “[Identification of Catabolic Routes and their Specific Activities](#)” and “[Microbial Composition of Enriched Cultures](#)” sections, it was shown that the mesophilic and the thermophilic microbial enrichments resulted in the selection of different microbial groups, leading to different patterns of activity in each microbial consortium. As the enrichments were carried out in batch mode with initially high partial pressure of H₂/CO₂ and CO, the microbial selection was expected to be dictated by the kinetic properties of the different microbial groups. However, several reactions composing the metabolic network of these enriched consortia proceed rather close to thermodynamic equilibrium, for which the competition for H₂/CO₂, CO or acetic acid could also be affected by possible bioenergetic limitations. Therefore, a thermodynamic analysis of the metabolic network was carried out in order to investigate further the effect of the temperature and other operational parameters on the rate of the biochemical reactions prevailing in each consortium and to identify possible bioenergetic limitations explaining their different patterns of activity.

The analysis of the effect of the temperature on the thermodynamics of H₂-consuming reactions revealed that the $\Delta_r G'_T$ of both homoacetogenesis and hydrogenotrophic methanogenesis was significantly affected by the change in incubation temperature. As shown in Fig. 4a, the $\Delta_r G'_T$ of both homoacetogenesis and hydrogenotrophic methanogenesis become less negative as the temperature increases, which indicates that the thermodynamic driving force for these reactions to proceed forward decreases with increasing temperatures. Nonetheless, the fact that the thermodynamic potential factor (F_T) approaches 1 in both cases suggests that, in fact, the rate of these reactions would not be affected by changes in $\Delta_r G'_T$ as these reactions would release enough free energy to satisfy the energy conservation requirements of their corresponding metabolic pathways regardless of the incubation temperature (Fig. 4b). At the initial fermentation conditions, the activity rate of these reactions would then be strictly subject to kinetic control, which implies that the result of the competition for H₂ would be dependent on the maximum specific growth rate (μ_{max}) of these two microbial

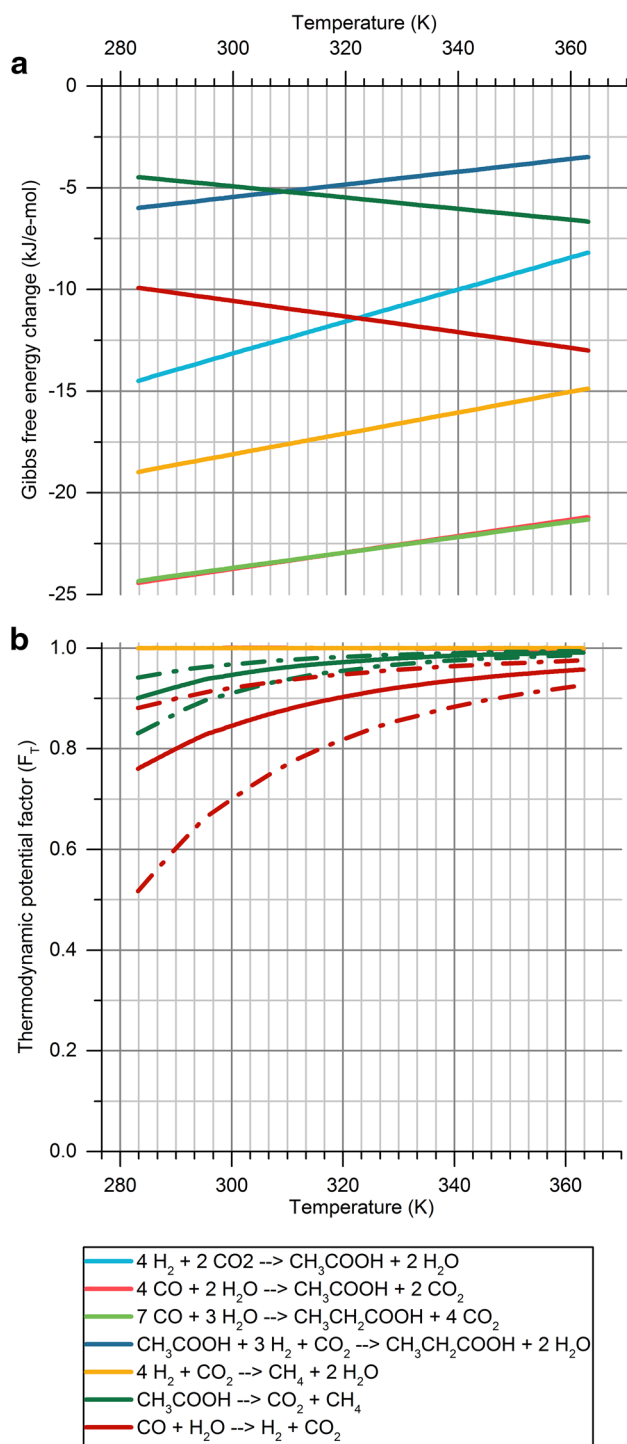


Fig. 4 **a** Gibbs free energy change as a function of temperature normalized to e-mol of electron donor for each of the biochemical reactions considered at the initial enrichment conditions. The operating conditions considered were P_{H_2} of 1.3 atm, P_{CO_2} of 0.2 atm, P_{CO} of 0.4 atm, acetic acid concentration of 0.001 M, propionate concentration of 0.0001 M, pH 7 and ionic strength of 0.08 M. **b** Thermodynamic potential factor (F_T) as a function of temperature for each of the biochemical reactions considered at the initial enrichment conditions. Solid lines represent F_T calculated using a ΔG_p of 50 kJ/mol of ATP. Dashed lines represent the upper and lower boundaries of F_T when using a ΔG_p of 45 and 55 kJ/mol of ATP, respectively

groups. Therefore, the competition for H_2 would be expected to favor hydrogenotrophic methanogens when increasing the temperature as it has been shown that the positive effect of the temperature on μ_{max} is more pronounced for hydrogenotrophic methanogens, with homoacetogens being able to compete for H_2 only at psychrophilic and mesophilic conditions [39, 40, 50].

The main CO conversion pathways identified in this study corresponded to carboxydutrophic acetogenesis and hydrogenogenesis, found to be predominant at mesophilic and thermophilic conditions, respectively. Analyzing the $\Delta_r G'_T$ as a function of temperature showed that both of these reactions should be feasible at the temperature range considered, with acetogenesis becoming less exergonic with increasing temperatures and hydrogenogenesis being favored by the increase of temperature (Fig. 4a). However, the analysis of the F_T revealed that, although the hydrogenogenesis is feasible at all temperatures, the rate of this reaction becomes thermodynamically limited at low temperatures due to the high initial P_{H_2} used in the experiments. As illustrated in Fig. 4b, this reaction approaches its limits of feasibility as the temperature decreases, with the F_T decreasing from a minimum of 0.86 at 60 °C to 0.77 at 37 °C when considering a ΔG_p of 55 kJ/mol of ATP and an ATP yield of 0.33 mol ATP/mol CO. This thermodynamic limitation is applicable only at the initial fermentation conditions with high P_{H_2} though, as F_T would rapidly approach 1 as soon as H_2 started to be consumed. Nevertheless, this suggests that thermodynamics could have played a role in the microbial selection process during the enrichment at mesophilic conditions, as this initial thermodynamic limitation could have given an initial competitive advantage to the acetogenic microbial group. The kinetic properties of these microbial trophic groups appear to be consistent with the latter since carboxydutrophic acetogens have been shown to perform better at mesophilic conditions (with minimum reported doubling times of 1.5 h at mesophilic conditions [35] and 7 h at thermophilic conditions [51]), while the carboxydutrophic hydrogenogenic growth rate seems to be favored at thermophilic conditions (with minimum reported doubling times of 5.7 h at mesophilic conditions [52] and 1 h at thermophilic conditions [53]). Thus, both kinetics and thermodynamics may have contributed to the outcome of the competition for CO found at the experimental conditions tested.

The fermentation of synthesis gas at mesophilic conditions resulted in the accumulation of propionic acid as a minor end product, which was not completely converted to CH_4 . Navarro et al. [13] made similar observations when using anaerobic sludge for the biomethanation of CO, as varying amounts of propionic acid were produced depending on the initial P_{CO} used in batch experiments. The production of propionic acid could take place through several reactions e.g. through the direct conversion of CO, or through the

reduction of acetic acid using H_2 and CO_2 . As shown in the thermodynamic analysis, both reactions are feasible at mesophilic conditions due to the high initial partial pressure of CO , H_2 and CO_2 since $\Delta_r G'_T$ is negative and the F_T value approaches 1 in both cases (Fig. 4). Nevertheless, the fact that propionic acid was not produced in experiments using H_2/CO_2 and was produced only in experiments containing CO indicates that the direct conversion of CO into propionic acid was the most likely pathway. Therefore, propionic acid was probably a by-product of the carbon flux diverted towards biomass synthesis during the conversion of CO as this would be consistent with the high biomass yield observed for carboxydrotrophic acetogens (Table 4).

According to the catabolic routes identified in “**Identification of Catabolic Routes and their Specific Activities**” section, it seems that the main syntrophic interactions prevailing in the enriched microbial consortia were limited to cross-feeding relationships, since the participation of strict syntrophic microorganisms such as syntrophic fatty acid oxidizing bacteria could not be observed experimentally. Of course, it is likely that the microbial community as a whole benefited from the synergistic action of the different microbial groups involved in the conversion, e.g. the continuous removal of acetate and H_2 by methanogenic archaea probably had a positive effect on the conversion of CO by carboxydrotrophic acetogens and hydrogenogens, respectively. However, as shown in the specific activity tests, these reactions could easily proceed forward even when methanogenic growth was inhibited, indicating that their microbial interaction was not as necessary as it is the case for syntrophic fatty acid oxidizing bacteria. As discussed above, the experiments at mesophilic conditions resulted in the accumulation of propionate as a final product, which was apparently not converted through syntrophic propionate oxidation. Similarly, acetate was found to be converted strictly through aceticlastic methanogenesis with no apparent participation of syntrophic acetate oxidizers. Nevertheless, the presence of *Geobacter* sp. (with a relative read abundance of 0.5% using the V4-V5 primer set) suggested a limited participation of syntrophic fatty acid oxidation reactions along the fermentation. Additionally, other studies focusing on the biomethanation of CO and H_2 have shown that both propionate and acetate can be converted through the microbial interaction between syntrophic fatty acid oxidizers and hydrogenotrophic methanogens [13, 54]. This can be explained by the thermodynamic feasibility of these reactions under the specific operating conditions found in this study. The limits of thermodynamic feasibility as a function of a specific product or substrate for each reaction can be approximated based on the concentration at which F_T reaches a value of 0, as this indicates that the metabolism ceases and the biochemical reaction reaches its maximum threshold concentration of product or its minimum threshold

concentration of substrate at which it is feasible. As shown in Fig. 5b, the minimum threshold concentration of acetate for aceticlastic methanogens at the experimental conditions was estimated to range between 75 nM and 600 nM, which is consistent with experimentally determined threshold acetate concentrations for this microbial group [55]. Considering the concentration of metabolites in the fermentation broth and the gas phase at the end of the experiments with syngas, the conversion of propionate to acetate, H_2 and CO_2 would then be thermodynamically feasible only at acetate concentrations either equal or below the minimum threshold for aceticlastic methanogens (Fig. 5b). This indicates that aceticlastic methanogens were not able to keep the acetate concentration at levels low enough for allowing complete syntrophic propionate oxidation. Similarly, at the time of the fermentation with the maximum acetate concentration, the extent of the syntrophic interaction between hydrogenotrophic methanogens and syntrophic acetate oxidizers was intrinsically limited by the thermodynamic feasibility of these reactions, as hydrogenotrophic methanogenesis and syntrophic acetate oxidation reaction share the same minimum and maximum threshold P_{H_2} , respectively (Fig. 5a). However, both syntrophic acetate and propionate oxidation reactions are at the edge of their feasibility with respect to the minimum threshold for hydrogenotrophic and aceticlastic methanogens, which suggests that these reactions could have taken place to a limited extent, keeping the concentration of acetate and propionate at their minimum threshold during the fermentation. Therefore, the fact that syntrophic fatty acid oxidation reactions had a limited participation during the fermentation and that aceticlastic methanogenesis was the dominant catabolic route converting acetate to CH_4 cannot be attributed to kinetic competition, but to the limits of thermodynamic feasibility of these reactions under these specific operating conditions.

At mesophilic conditions, aceticlastic methanogenesis became the dominant catabolic route despite being the main rate-limiting step of the conversion due to the thermodynamic limitation of syntrophic acetate oxidation. However, syntrophic fatty acid oxidizers have been shown to be capable of fast growth with doubling times of 6–8 h at mesophilic conditions [46], which indicates that these should be able to outcompete aceticlastic methanogens as long as the syntrophic fatty acid oxidation is feasible. Therefore, the overall productivity of the mesophilic enriched consortium could be significantly boosted by favoring operating conditions allowing the syntrophic acetate oxidation. One way of achieving this would be reducing the P_{CO_2} in the gas phase either by optimizing the initial composition of syngas or by supplying additional H_2 in order to increase the minimum threshold of acetate concentration for syntrophic acetate oxidizers, which would make hydrogenotrophic methanogenesis the

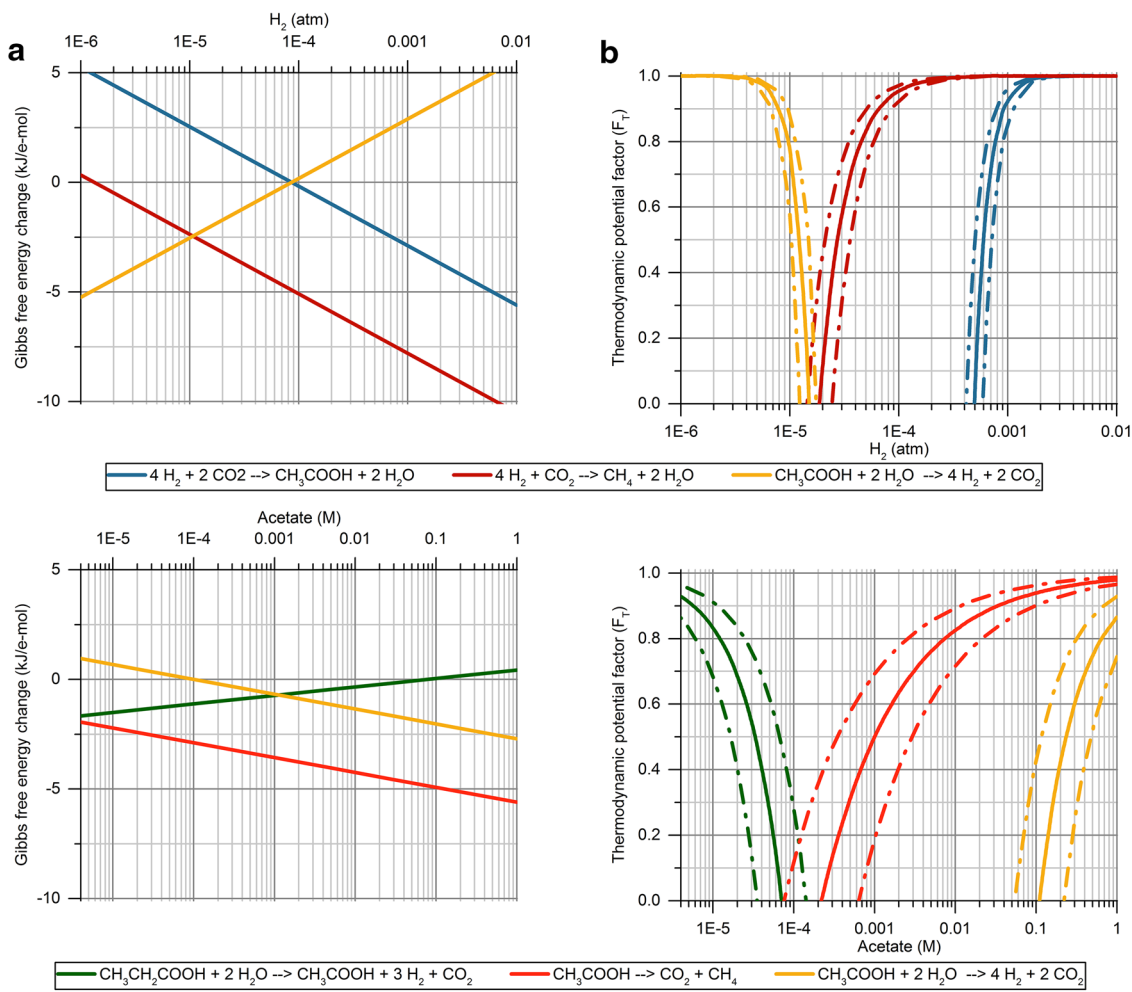


Fig. 5 a Gibbs free energy change ($\Delta_r G'_T$) and thermodynamic potential factor (F_T) as a function of P_{H_2} for hydrogenotrophic methanogenesis, homoacetogenesis and syntrophic acetate oxidation at the fermentation time with maximum acetate concentration. The operating conditions considered were P_{CO_2} of 0.2 atm, P_{CH_4} of 0.1 atm, acetate concentration of 0.022 M, temperature of 37 °C, pH 6.8 and ionic strength of 0.08 M. **b** Gibbs free energy change ($\Delta_r G'_T$) and thermodynamic potential factor (F_T) as a function of acetate concentration for aceticlastic methanogenesis and syntrophic propionate and acetate oxidation at the final fermentation conditions. The operating condi-

tions considered were P_{H_2} of 0.00002 atm [determined by the minimum threshold of H_2 for hydrogenotrophic methanogens (Fig. 5a)], P_{CO_2} of 0.2 atm, P_{CH_4} of 0.28 atm, propionate concentration of 0.0006 M, temperature of 37 °C, pH 7 and ionic strength of 0.08 M. The $\Delta_r G'_T$ shown was normalized to e-mol of electron donor for each of the biochemical reactions considered. Solid lines for F_T represent F_T calculated using a ΔG_p of 50 kJ/mol of ATP. Dashed lines represent the upper and lower boundaries of F_T when using a ΔG_p of 45 and 55 kJ/mol of ATP, respectively

dominant CH_4 production pathway. In this case, applying thermodynamic control for driving a shift in the catabolic routes of the mesophilic enriched consortium towards syntrophic acetate oxidation would be especially beneficial under continuous operating mode, as shorter hydraulic retention times (HRT) could be applied, resulting in higher overall CH_4 productivities. It should be noted though, that under continuous operation the gas conversion efficiency would become a crucial parameter for keeping P_{H_2} and P_{CO_2} at levels low enough to allow a significant syntrophic acetate oxidation.

Conclusions

Highly specialized microbial consortia for the biomethanation of syngas at mesophilic and thermophilic conditions were obtained through enrichments in batch mode. Both microbial consortia were shown to be able to convert syngas into CH_4 with high product selectivity, presenting a stable activity over several transfers. The CH_4 yield obtained corresponded to $81.5 \pm 0.1\%$ and $92.2 \pm 1.7\%$ of the stoichiometric yield and the maximum specific CH_4 productivity

was 1.83 ± 0.27 and 33.48 ± 0.90 mmol CH₄/g VSS/h for the mesophilic and the thermophilic enriched consortium, respectively. The incubation temperature was found to be a crucial operating parameter affecting the microbial composition of the enriched cultures, the catabolic routes employed by each of them and the microbial activity rates. Both the specific activity tests and the microbial composition analysis confirmed that the mesophilic and the thermophilic enriched consortia presented drastically different patterns of activity. Additionally, the thermodynamic feasibility analysis of their metabolic networks revealed that the competition for common substrates was not solely driven by kinetic competition, as the thermodynamic limitation of several reactions under the experimental process conditions also played an important role defining the microbial structure of the enriched consortia and the dominant catabolic routes. As a result, the mesophilic enriched consortium presented a more intricate metabolic network than the thermophilic consortium, which ultimately limited the CH₄ production rate due to the fact that acetoclastic methanogenesis was the dominant catabolic route leading to CH₄. This indicates that, in principle, the thermophilic consortium could be more suitable for industrial applications owing to the higher CH₄ production rate derived from the faster turnover rates of H₂ as intermediate metabolite. However, the possibility of applying thermodynamic control over catabolic routes employed by the mesophilic enriched consortium, shifting from acetoclastic methanogenesis to syntrophic acetate oxidation, could also favor a significant improvement in the CH₄ production rate both in batch and continuous processes as hydrogenotrophic methanogenesis would become the dominant methanogenic pathway.

Acknowledgements This work was financially supported by the Technical University of Denmark (DTU) and Innovation Foundation-DK in the frame of SYNFERON project.

Compliance with Ethical Standards

Conflict of interest The authors declare that they have no conflict of interest.

References

- Grimalt-Alemany, A., Skiadas, I.V., Gavala, H.N.: Syngas biomethanation: state-of-the-art review and perspectives. *Biofuels Bioprod. Biorefining* **12**, 139–158 (2018)
- Cantera, S., Muñoz, R., Lebrero, R., Lopez, J.C., Rodríguez, Y., García-Encina, P.A.: Technologies for the bioconversion of methane into more valuable products. *Curr. Opin. Biotechnol.* **50**, 128–135 (2018)
- Holm-Nielsen, J.B., Al Seadi, T., Oleskowicz-Popiel, P.: The future of anaerobic digestion and biogas utilization. *Bioresour. Technol.* **100**, 5478–5484 (2009)
- Batstone, D.J., Viridis, B.: The role of anaerobic digestion in the emerging energy economy. *Curr. Opin. Biotechnol.* **27**, 142–149 (2014)
- Hendriks, A.T.W.M., Zeeman, G.: Pretreatments to enhance the digestibility of lignocellulosic biomass. *Bioresour. Technol.* **100**, 10–18 (2009)
- Kumar, A., Jones, D.D., Hanna, M.A.: Thermochemical biomass gasification: a review of the current status of the technology. *Energies* **2**, 556–581 (2009)
- Asimakopoulos, K., Gavala, H.N., Skiadas, I.V.: Reactor systems for syngas fermentation processes: a review. *Chem. Eng. J.* **348**, 732–744 (2018)
- Luo, G., Angelidaki, I.: Integrated biogas upgrading and hydrogen utilization in an anaerobic reactor containing enriched hydrogenotrophic methanogenic culture. *Biotechnol. Bioeng.* **109**, 2729–2736 (2012)
- Daniels, L., Fuchs, G., Thauer, R.K., Zeikus, J.G.: Carbon monoxide oxidation by methanogenic bacteria. *J. Bacteriol.* **132**, 118–126 (1977)
- O'Brien, J.M., Wolkin, R.H., Moench, T.T., Morgan, J.B., Zeikus, J.G.: Association of hydrogen metabolism with unitrophic or mixotrophic growth of *Methanosarcina barkeri* on carbon monoxide. *J. Bacteriol.* **158**, 373–375 (1984)
- Rother, M., Metcalf, W.W.: Anaerobic growth of *Methanosarcina acetivorans* C2A on carbon monoxide: an unusual way of life for a methanogenic archaeon. *Proc. Natl. Acad. Sci. USA* **101**, 16929–16934 (2004)
- Diender, M., Pereira, R., Wessels, H.J.C.T., Stams, A.J.M., Sousa, D.Z.: Proteomic analysis of the hydrogen and carbon monoxide metabolism of *Methanothermobacter marburgensis*. *Front. Microbiol.* **7**, 1–10 (2016)
- Navarro, S.S., Cimpoaia, R., Bruant, G., Guiot, S.R.: Biomethanation of syngas using anaerobic sludge: shift in the catabolic routes with the CO partial pressure increase. *Front. Microbiol.* **7**, 1–13 (2016)
- Sipma, J., Lens, P.N.L., Stams, A.J.M., Lettinga, G.: Carbon monoxide conversion by anaerobic bioreactor sludges. *FEMS Microbiol. Ecol.* **44**, 271–277 (2003)
- Alves, J.I., Stams, A.J.M., Plugge, C.M., Alves, M.M., Sousa, D.Z.: Enrichment of anaerobic syngas-converting bacteria from thermophilic bioreactor sludge. *FEMS Microbiol. Ecol.* **86**, 590–597 (2013)
- Arantes, A.L., Alves, J.I., Stams, A.J.M., Alves, M.M., Sousa, D.Z.: Enrichment of syngas-converting communities from a multi-orifice baffled bioreactor. *Microb. Biotechnol.* (2017). <https://doi.org/10.1111/1751-7915.12864>
- APHA: Standard Methods for the Examination of Water and Wastewater. American Public Health Association/American Water Works Association/Water Pollution Control Federation, Washington, DC (1997)
- Takahashi, S., Tomita, J., Nishioka, K., Hisada, T., Nishijima, M.: Development of a prokaryotic universal primer for simultaneous analysis of bacteria and archaea using next-generation sequencing. *PLoS ONE* **9**, e105592 (2014)
- Walters, W., et al.: Transcribed spacer marker gene primers for microbial community surveys. *mSystems* **1**, e0009-15 (2015)
- Martin, M.: Cutadapt removes adapter sequences from high-throughput sequencing reads. *EMBnet J* **17**, 10–12 (2011)
- Edgar, R.C.: UNOISE2: improved error-correction for Illumina 16S and ITS amplicon sequencing. *BioRxiv* <https://doi.org/10.1101/081257> (2016)
- Edgar, R.C.: SINTAX: a simple non-Bayesian taxonomy classifier for 16S and ITS sequences. *BioRxiv* <https://doi.org/10.1101/074161> (2016)

23. Yarza, P., et al.: The all-species living tree project: a 16S rRNA-based phylogenetic tree of all sequenced type strains. *Syst. Appl. Microbiol.* **31**, 241–250 (2008)
24. Dhariwal, A., Chong, J., Habib, S., King, I.L., Agellon, L.B., Xia, J.: MicrobiomeAnalyst: a web-based tool for comprehensive statistical, visual and meta-analysis of microbiome data. *Nucleic Acids Res.* **45**, 180–188 (2018)
25. Alberty, R.A.: *Thermodynamics of Biochemical Reactions*. John Wiley & Sons, Inc, New Jersey (2003)
26. Amend, J.P., Shock, E.L.: Energetics of overall metabolic reactions of thermophilic and hyperthermophilic Archaea and bacteria. *FEMS Microbiol. Rev.* **25**, 175–243 (2001)
27. Steinbusch, K.J.J., Hamelers, H.V.M., Buisman, C.J.N.: Alcohol production through volatile fatty acids reduction with hydrogen as electron donor by mixed cultures. *Water Res.* **42**, 4059–4066 (2008)
28. Jin, Q., Bethke, C.M.: The thermodynamics and kinetics of microbial metabolism. *Am. J. Sci.* **307**, 643–677 (2007)
29. Grimalt-Alemany, A., Łężyk, M., Lange, L., Skiadas, I.V., Gavala, H.N.: Enrichment of syngas-converting mixed microbial consortia for ethanol production and thermodynamics-based design of enrichment strategies. *Biotechnol. Biofuels* **11**, 1–22 (2018)
30. Bertsch, J., Müller, V.: Bioenergetic constraints for conversion of syngas to biofuels in acetogenic bacteria. *Biotechnol. Biofuels* **8**, 1–12 (2015)
31. Lingen, H.J., Van Plugge, C.M., Fadel, J.G., Kebreab, E.: Thermodynamic driving force of hydrogen on rumen microbial metabolism: a theoretical investigation. *PLoS ONE* **11**, e0161362 (2016)
32. Kaster, A., Moll, J., Parey, K., Thauer, R.K.: Coupling of ferredoxin and heterodisulfide reduction via electron bifurcation in hydrogenotrophic methanogenic archaea. *Proc. Natl. Acad. Sci.* **108**, 2981–2986 (2011)
33. Diekert, G., Wohlfarth, G.: Metabolism of homoacetogens. *Antonie Van Leeuwenhoek* **66**, 209–221 (1994)
34. Oelgeschläger, E., Rother, M.: Carbon monoxide-dependent energy metabolism in anaerobic bacteria and archaea. *Arch. Microbiol.* **190**, 257–269 (2008)
35. Lorowitz, W.H., Bryant, M.P.: *Peptostreptococcus productus* strain that grows rapidly with CO as the energy source. *Appl. Environ. Microbiol.* **47**, 961–964 (1984)
36. Parshina, S.N., Kijlstra, S., Henstra, A.M., Sipma, J., Plugge, C.M., Stams, A.J.M.: Carbon monoxide conversion by thermophilic sulfate-reducing bacteria in pure culture and in co-culture with *Carboxydotherrmus hydrogenoformans*. *Appl Microbiol Biotechnol* **68**, 390–396 (2005)
37. Henstra, A.M., Stams, A.J.M.: Deep conversion of carbon monoxide to hydrogen and formation of acetate by the anaerobic thermophile *Carboxydotherrmus hydrogenoformans*. *Int. J. Microbiol.* (2011). <https://doi.org/10.1155/2011/641582>
38. Guiot, S.R., Cimpoaia, R.: Potential of wastewater-treating anaerobic granules for biomethanation of synthesis gas. *Environ. Sci. Technol.* **45**, 2006–2012 (2011)
39. Sipma, J., Lettinga, G., Stams, A.J.M., Lens, P.N.L.: Hydrogenogenic CO conversion in a moderately thermophilic (55 °C) sulfate-fed gas lift reactor: competition for CO-derived H₂. *Biotechnol. Prog.* **22**, 1327–1334 (2006)
40. Liu, R., Hao, X., Wei, J.: Function of homoacetogenesis on the heterotrophic methane production with exogenous H₂/CO₂ involved. *Chem. Eng. J.* **284**, 1196–1203 (2015)
41. Diekert, G., Ritter, M.: Carbon monoxide fixation into the carboxyl group of acetate during growth of *Acetobacterium woodii* on H₂ and CO₂. *FEMS Microbiol. Lett.* **17**, 299–302 (1983)
42. Nguyen, N., Warnow, T., Pop, M., White, B.: A perspective on 16S rRNA operational taxonomic unit clustering using sequence similarity. *NPJ. Biofilms Microbiomes*, **2**, (2016)
43. Patel, G.B., Roth, L.A., Van den Berg, L., Clark, D.S.: Characterization of a strain of *Methanospirillum hungatii*. *Can. J. Microbiol.* **22**, 1404–1410 (1976)
44. Genthner, B.R.S., Friedman, S.D., Devereux, R.: Reclassification of *Desulfovibrio desulfuricans* Nomay 4 as *Desulfomicrobium nowegicum* comb. nov. and confirmation of *Desulfomicrobium escambiense* (corrig., formerly “*escambium*”) as a new species in the genus *Desulfomicrobium*. *Int. J. Syst. Bacteriol.* **47**, 889–892 (1997)
45. Fournier, G.P., Gogarten, J.P.: Evolution of acetoclastic methanogenesis in *Methanosarcina* via horizontal gene transfer from cellulolytic clostridia. *J. Bacteriol.* **190**, 1124–1127 (2008)
46. Cord-ruwisch, R., Lovley, D.R.: Growth of *Geobacter sulfurreducens* with acetate in syntrophic cooperation with hydrogen-oxidizing anaerobic partners. *Appl. Environ. Microbiol.* **64**, 2232–2236 (1998)
47. Hamdi, O., et al.: *Aminobacterium thunnarium* sp. nov., a mesophilic, amino acid-degrading bacterium isolated from an anaerobic sludge digester, pertaining to the phylum Synergistetes. *Int. J. Syst. Evol. Microbiol.* **65**, 609–614 (2015)
48. Sokolova, T.G., Kostrikin, N.A., Chernyh, N.A., Kolganova, T.V., Tourova, T.P., Bonch-osmolovskaya, E.A.: *Thermincola carboxydiphila* gen. nov., sp. nov., a novel anaerobic, carboxydo-trophic, hydrogenogenic bacterium from a hot spring of the Lake Baikal area. *Int. J. Syst. Evol. Microbiol.* **55**, 2069–2073 (2005)
49. Shiratori, H., et al.: *Lutispora thermophila* gen. nov., sp. nov., a thermophilic, spore-forming bacterium isolated from a thermophilic methanogenic bioreactor digesting municipal solid wastes. *Int. J. Syst. Evol. Microbiol.* **58**, 964–969 (2008)
50. Kotsyurbenko, O.R., Glagolev, M.V., Nozhevnikova, A.N., Conrad, R.: Competition between homoacetogenic bacteria and methanogenic archaea for hydrogen at low temperature. *FEMS Microbiol. Ecol.* **38**, 153–159 (2001)
51. Savage, M.D., Wu, Z., Daniel, S.L., Lundie, L.L., Drake, H.L.: Carbon monoxide dependent chemolithotrophic growth of *Clostridium thermoautotrophicum*. *Appl. Environ. Microbiol.* **53**, 1902–1906 (1987)
52. Kerby, R.L., Ludden, P.W., Roberts, G.P.: Carbon monoxide-dependent growth of *Rhodospirillum rubrum*. *J. Bacteriol.* **177**, 2241–2244 (1995)
53. Slepova, T.V., et al.: *Carboxydocella sporoproducens* sp. nov., a novel anaerobic CO-utilizing/H₂-producing thermophilic bacterium from a Kamchatka hot spring. *Int. J. Syst. Evol. Microbiol.* **56**, 797–800 (2006)
54. Wang, W., Xie, L., Luo, G., Zhou, Q., Angelidaki, I.: Performance and microbial community analysis of the anaerobic reactor with coke oven gas biomethanation and in situ biogas upgrading. *Biore-sour. Technol.* **146**, 234–239 (2013)
55. Westermann, P., Ahring, B.K., Mah, R.A.: Threshold acetate concentrations for acetate catabolism by aceticlastic methanogenic bacteria. *55*, 514–515 (1989)

Publisher's Note Springer Nature remains neutral with regard to jurisdictional claims in published maps and institutional affiliations.

Enrichment of mesophilic and thermophilic mixed microbial consortia for syngas biomethanation: the role of kinetic and thermodynamic competition – Electronic Supplementary Material (Online Resource 1)

Journal: Waste and Biomass Valorization

Antonio Grimalt-Alemany¹, Mateusz Łężyk^{1,2}, David M. Kennes-Veiga¹, Ioannis V. Skiadas¹ and Hariklia N. Gavala^{1*}

*Correspondence: hnga@kt.dtu.dk, hari_gavala@yahoo.com

¹Department of Chemical and Biochemical Engineering, Technical University of Denmark, Søtofts Plads 229, 2800 Kgs. Lyngby, Denmark.

²Current address: Institute of Environmental Engineering, Faculty of Civil and Environmental Engineering, Poznan University of Technology, Berdychowo 4, 60-965 Poznań, Poland.

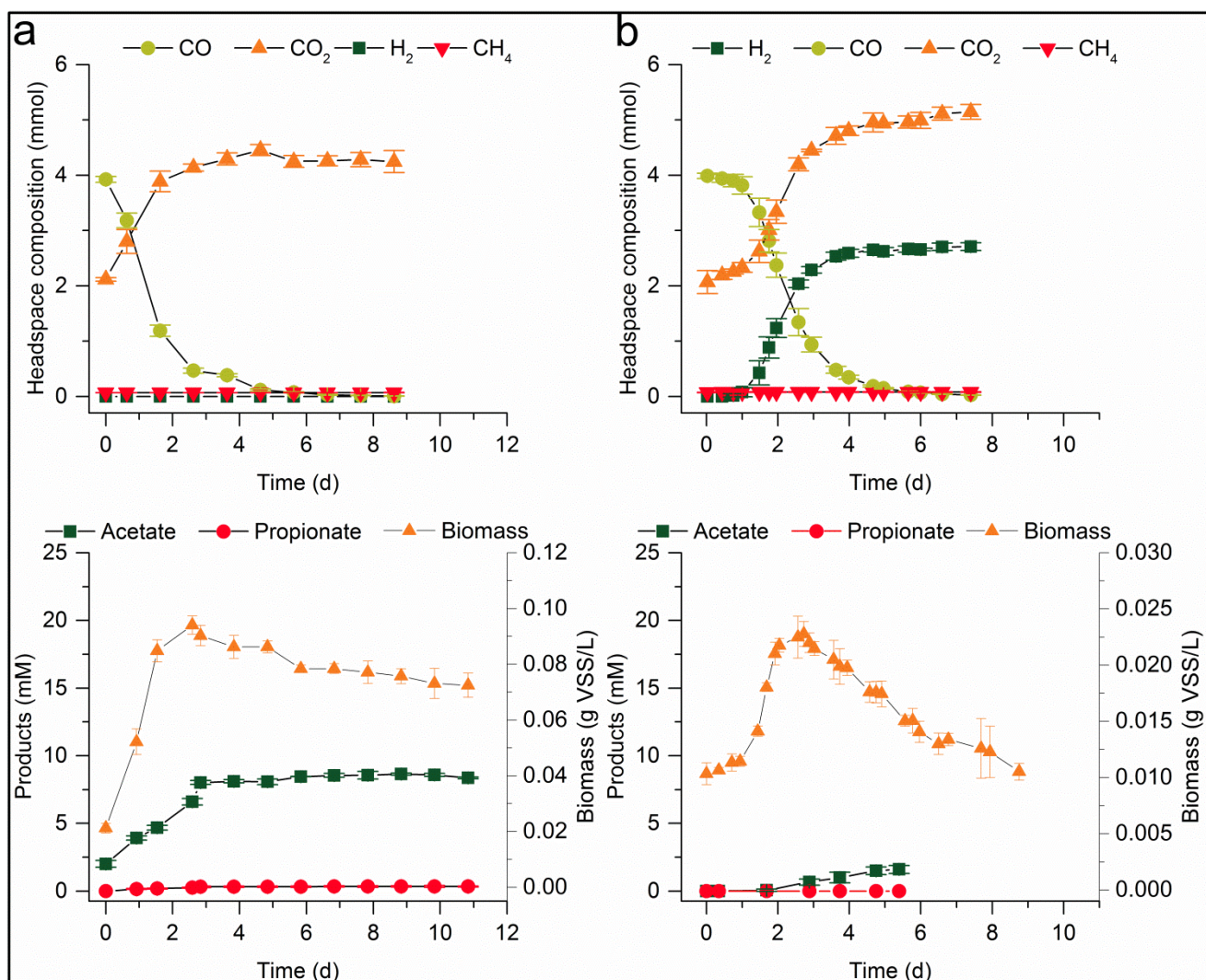


Figure S1.a. Fermentation profile for the specific activity test with CO and BES using the mesophilic enriched microbial consortium. **b.** Fermentation profile for the specific activity test with CO and BES using the thermophilic enriched microbial consortium.

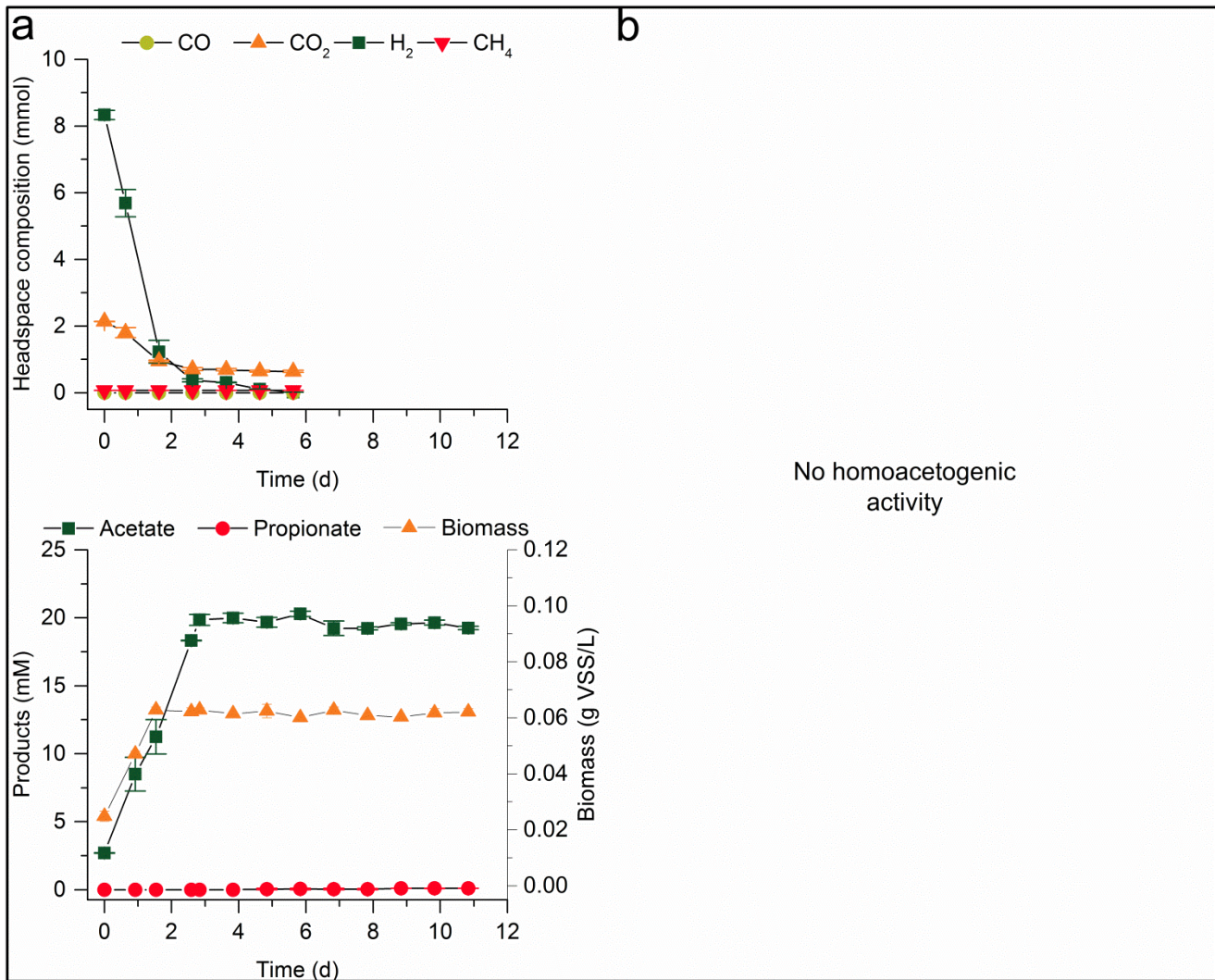


Figure S2. a. Fermentation profile for the specific activity test with H₂/CO₂ and BES using the mesophilic enriched microbial consortium. **b.** Fermentation profile for the specific activity test with H₂/CO₂ and BES using the thermophilic enriched microbial consortium.

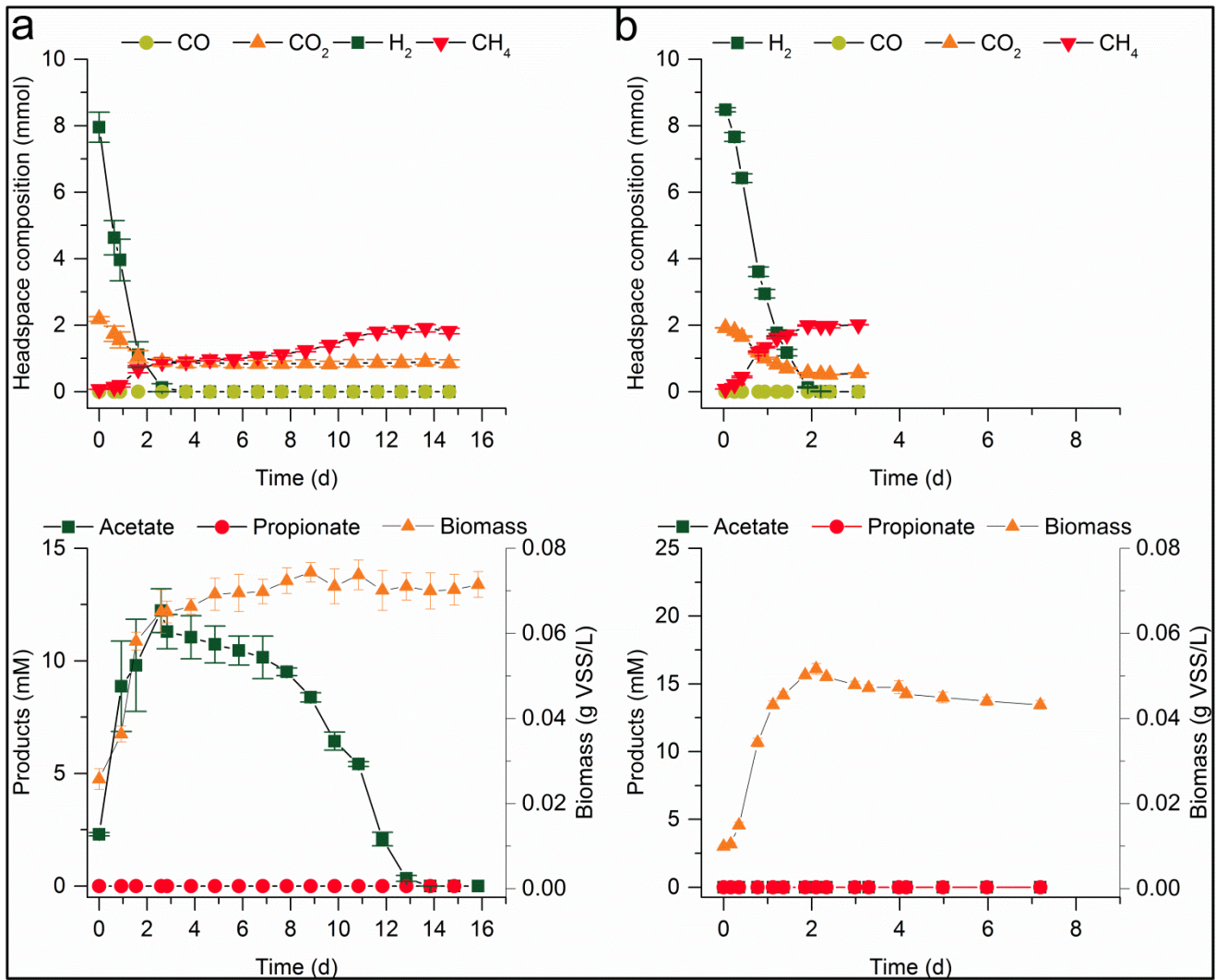


Figure S3. a. Fermentation profile for the specific activity test with H₂/CO₂ using the mesophilic enriched microbial consortium. **b.** Fermentation profile for the specific activity test with H₂/CO₂ using the thermophilic enriched microbial consortium.

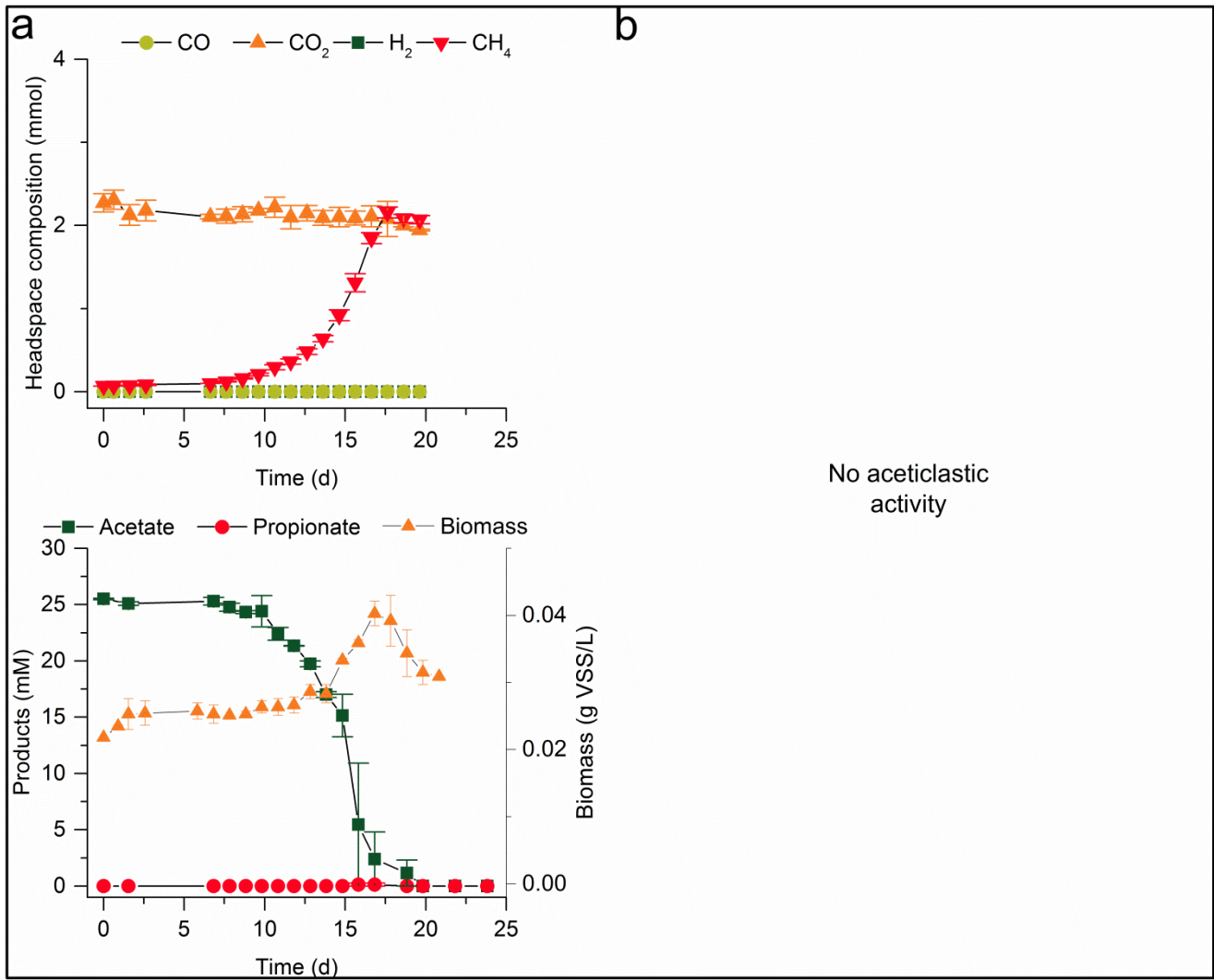


Figure S4. a. Fermentation profile for the specific activity test with acetate using the mesophilic enriched microbial consortium. This experiment was performed in duplicates. **b.** Fermentation profile for the specific activity test with acetate using the thermophilic enriched microbial consortium.

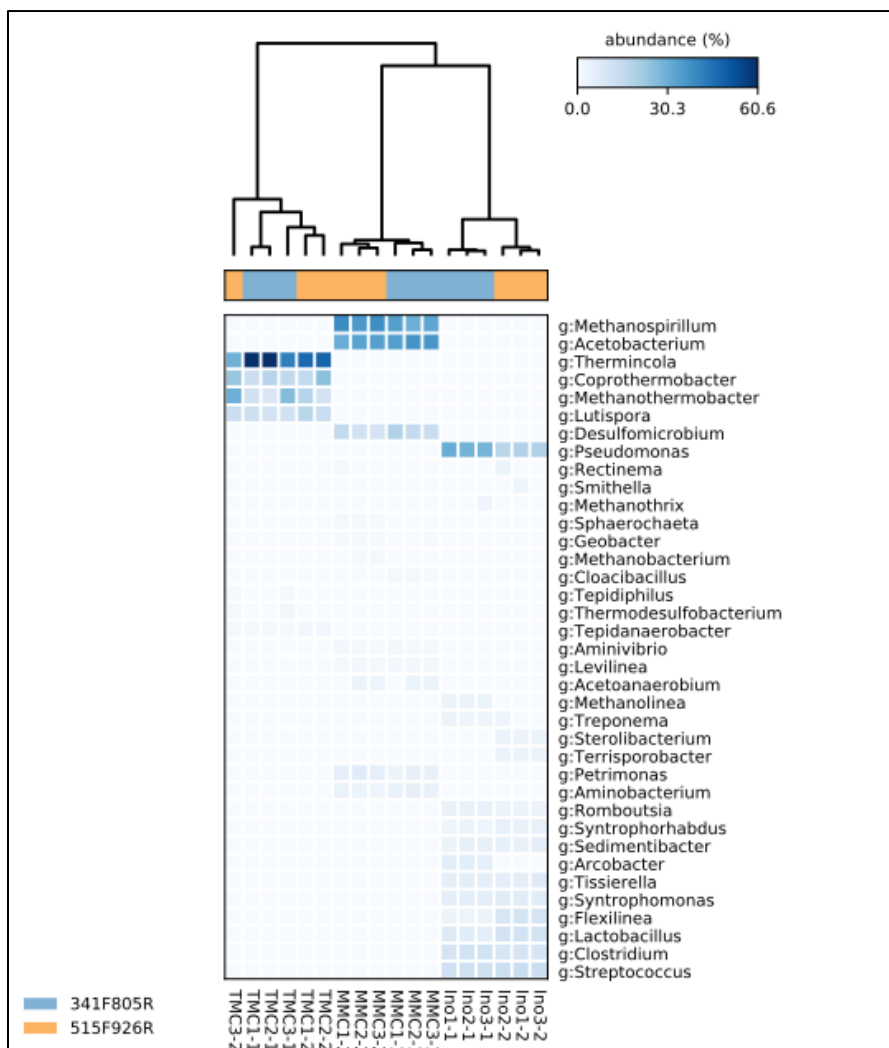


Figure S5. Heatmap comparing the results for relative taxonomic abundance obtained with the two primer sets used. Primer set 1 corresponds to 16S rRNA V3-V4 region primer set (341F805R) and primer set 2 corresponds to 16S rRNA V4-V5 region primer set (515F926R). Ino corresponds to the anaerobic sludge samples, MMC stands for mesophilic microbial consortium and TMC for thermophilic microbial consortium.

Manuscript IV

**“Modeling of Syngas Biomethanation and Control of Catabolic Routes of
Mesophilic and Thermophilic Mixed Microbial Consortia”**

Modeling of Syngas Biomethanation and Control of Catabolic Routes of Mesophilic and Thermophilic Mixed Microbial Consortia

*Antonio Grimalt-Aleman, Konstantinos Asimakopoulos, Ioannis V. Skiadas, Hariklia N. Gavala**

Department of Chemical and Biochemical Engineering, Technical University of Denmark, Søltofts Plads 229, 2800 Kgs. Lyngby, Denmark

*Correspondence: hnga@kt.dtu.dk, hari_gavala@yahoo.com

Abstract

The syngas biomethanation process is a promising bioconversion route due to its high versatility, as it could be applied as a stand-alone technology, coupled to gasification plants or integrated in anaerobic digestion or bioelectrochemical conversion systems. The biomethanation of syngas typically takes place through a rather complex network of interspecific metabolic interactions, which may vary significantly depending on the operating conditions applied and the diversity of microbial groups present. In this work, the syngas biomethanation process carried out by mesophilic and thermophilic mixed microbial consortia was modelled based on batch experiments. All microbial growth processes included were made thermodynamically consistent through the thermodynamic potential factor, which allowed for predicting metabolic shifts between the main catabolic routes employed by the microbial consortia. After parameter identifiability analysis, parameter estimation and determination of the overall mass transfer coefficients for all gases, the two models developed were able to successfully describe the performance of the mesophilic and thermophilic consortium. According to the kinetic parameters estimated, the superiority of the thermophilic microbial consortium in terms of specific CH_4 productivity was found to derive from the faster turnover rates of the intermediate metabolite used by this culture, H_2 , compared to that of acetate, used by the mesophilic microbial consortium. Based on the cross-feeding and mutual exclusion microbial interactions included in the models, the possibility of directing the microbial activity through the control of the catabolic routes employed by mixed microbial consortia was evaluated. The results showed that the limitations related to product selectivity typically encountered in continuous syngas biomethanation processes could be overcome by applying catabolic route control strategies based on the modulation of the mass transfer coefficients or the partial pressure of CO_2 .

Highlights

- Mesophilic and thermophilic syngas biomethanation were successfully modelled for the first time.

- Thermodynamically-consistent growth models allowed thermodynamic competition predictions.
- Thermodynamic limitation on carboxydophilic hydrogenogens triggers acetate production.
- Microbial activity can be directed through catabolic route control.

Keywords

Syngas biomethanation, biogas, mixed cultures, modeling, kinetic parameters, thermodynamics

1. Introduction

Biomethane has become a product of increasing interest, not only due to its potential contribution to reducing greenhouse gas emissions, but also owing to its versatility in terms of potential applications as it may be used for storage of surplus electricity, as energy carrier in households and the transportation sector, or as a platform chemical for the upcoming biotechnological industry [1]. The commercial production of biomethane (or biogas) is currently dominated by the anaerobic digestion (AD) process, mainly applied to wastewater sludge, agricultural residues and organic effluents from the industry. However, other biomethane production technologies under development have been gaining attention in recent years in order to facilitate the interconversion between energy carriers, broaden the range of feedstocks currently available to AD systems, and increase their energy efficiency. Examples of these technologies are bio-electrochemical or H₂-mediated power-to-gas (BEP2G) systems, and the catalytic methanation of either CO₂ or biomass-derived synthesis gas [2,3]. Another promising approach combining several aspects of these technologies is the biomethanation of synthesis gas, which typically consists of the gasification of an organic feedstock into synthesis gas (a mixture of mainly H₂, CO and CO₂) and its further biological conversion into methane [4]. The potential of the syngas biomethanation lies in its high operational flexibility and high efficiency. On one hand, one of the main advantages of this process derives from the gasification step, as it allows for a significant increase of the energy efficiency due to the conversion of the lignin fraction of lignocellulosic biomasses, which accounts for 25-35% of their energy content [5]. Additionally, there is a wide array of other feedstocks that could be used in this process, ranging from a large variety of organic wastes that could be gasified into syngas, to CO/CO₂ rich industrial off-gases along with H₂ originating from water electrolysis [6,7]. On the other hand, the syngas biomethanation process is highly versatile as it could be applied as a stand-alone technology, integrated in AD or BEP2G systems, or coupled to gasification plants with a fluctuating demand of heat and power as an alternative outlet. For example, according to Guiot et al. [8], coupling AD of the digestible fraction of municipal solid waste (MSW) with the gasification of the recalcitrant fraction could result in an increase of CH₄ production from 15 to

88 m³ STP per ton of MSW. Furthermore, the conversion of syngas into CH₄ seems to be an interesting option to avoid energy losses in the form of heat when compared to combined heat and power (CHP) generation. The overall energy efficiency of gasification of woody biomass with a dual fluidized bed gasifier and CHP generation was estimated to be 67%, with a corresponding net electrical efficiency of 27% (heat recovered with a thermal efficiency of 40%), while the overall efficiency of producing CH₄ instead would be 51.2%, with the advantage of the higher flexibility of CH₄ as product and the possibility of efficient transportation and long-term storage [9,10].

The biomethanation of syngas has been demonstrated using both monocultures, co-cultures and undefined mixed microbial consortia (MMC) [8,11–13]. Although there are a few strains of methanogens able to convert both H₂/CO₂ and CO into CH₄, these are easily inhibited by CO and present long doubling times when growing on CO as substrate. Two of these species, *Methanothermobacter thermoautotrophicus* and *Methanothermobacter marburgensis*, also exhibit a clear preference for H₂/CO₂ over CO [14], which limits their applicability in continuous processes. In turn, the biomethanation of syngas by undefined MMC typically takes place through the syntrophic association of several microbial trophic groups, comprising a rather complex network of biochemical reactions. These include mainly carboxydrotrophic hydrogenogenesis and acetogenesis, homoacetogenesis, hydrogenotrophic methanogenesis, aceticlastic methanogenesis and syntrophic fatty acid oxidation [15]. Their interspecific metabolism allows them to circumvent the methanogenic inhibition by CO and to be more efficient converting syngas into CH₄ as they are able to divert the carbon through the most efficient catabolic routes depending on the operating conditions. Additionally, the fact that sterilization is not necessary improves the economic feasibility of the process [16]. On the downside, the use of MMC often entails a higher complexity derived from the microbial interactions between different trophic groups involved in the process, ultimately resulting in a poor understanding and limited process control. Thus, gaining better understanding on the activity of MMC is fundamental for the further development of the mixed culture-based syngas biomethanation process.

Modeling of biological processes has proven to be a valuable tool for providing a better understanding and control over their performance and facilitating operation and optimization tasks. Most microbial trophic groups with a role in syngas biomethanation have been kinetically characterized in the frame of monoculture studies using Monod or modified Monod models. Vega et al. [17] modelled the growth of the acetogen *Ruminococcus productus* on CO using the Andrew model to study the effect of the gas loading rate and the volumetric mass transfer on the conversion rate of CO in stirred tank and bubble column reactors. Similarly, the hydrogenogen *Carboxydotherrmus hydrogeniformans* was characterized kinetically to study the effects of the partial pressure of CO (P_{CO}) and the ratio substrate/microbial biomass on the activity of the culture [18]. The growth kinetics of

other microbial trophic groups such as hydrogenotrophic and acetoclastic methanogens have also been studied [19,20]. Nevertheless, a model able to simulate the dynamics of the biomethanation of syngas carried out by MMC has not been proposed yet.

In this work, two structured models were developed with the purpose of modeling the syngas biomethanation process carried out by mesophilic and thermophilic MMC. The structure of the models accounts for simultaneous growth of different microbial trophic groups and other physicochemical processes such as acid dissociation and gas-liquid mass transfer. Additionally, in order to add thermodynamic consistency to the models, the thermodynamic potential factor (F_T) derived by Jin & Bethke [21] was included in all microbial growth processes, with which each microbial trophic group is only active within the boundaries of thermodynamic feasibility of their corresponding metabolic pathways. This increases the predictive capacity of the models as it allows for simulation of kinetic and thermodynamic competition, and for changes in the main catabolic routes as a function of the operating conditions, e.g. shifts between acetoclastic methanogenesis and syntrophic acetate oxidation. After calibrating the models through parameter estimation and performing an identifiability analysis, the validity of the models was tested outside the experimental region used for calibration to investigate possible CO inhibition phenomena. Additionally, the effect of the mass transfer on the competition for H_2 between homoacetogens and hydrogenotrophic methanogens, the competition for acetate between acetoclastic methanogens and syntrophic acetate oxidizers and the dynamics of the product distribution of hydrogenogenic growth on CO were investigated based on model simulations. Based on these, possible operational strategies for improving the control over the dominant catabolic pathways leading to CH_4 are discussed. Modeling syngas biomethanation and the successful simulation of kinetic versus thermodynamic competition come with a high novelty element and a high application potential, not only for syngas fermentation but also other bioprocesses based on mixed microbial consortia, where thermodynamic limitations may become important and critical for the final products distribution.

2. Materials and Methods

2.1. Medium composition and mixed microbial cultures

A modified basic anaerobic (BA) medium was used in all experiments. The medium was composed by 7 stock solutions with the following composition: 10 ml/l of salts solution (NH_4Cl , 100 g/l; $NaCl$, 10 g/l; $MgCl_2 \cdot 6H_2O$, 10 g/l; $CaCl_2 \cdot 2H_2O$, 5 g/l), 1 ml/l of trace metal solution ($FeCl_2 \cdot 4H_2O$, 2000 mg/l; H_3BO_3 , 50 mg/l; $ZnCl_2$, 50 mg/l; $CuCl_2$, 30 mg/l; $MnCl_2 \cdot 4 H_2O$, 50 mg/l; $(NH_4)_6Mo_7O_{24} \cdot 4 H_2O$, 50 mg/l; $AlCl_3$, 50 mg/l; $CoCl_2 \cdot 6H_2O$, 50 mg/l; $NiCl_2$, 50 mg/l; $Na_2SeO_3 \cdot 5H_2O$, 100 mg/l; $Na_2WO_4 \cdot 2H_2O$, 60 mg/l), 10 ml/l of vitamins solution (biotin, 2

mg/l; folic acid, 2 mg/l; pyridoxine-HCl, 10 mg/l; riboflavin-HCl, 5 mg/l; thiamine-HCl, 5 mg/l; cyanocobalamine, 0.1 mg/l; nicotinic acid, 5 mg/l; p-aminobenzoic acid, 5 mg/l; lipoic acid, 5 mg/l; D-pantothenic acid hemicalcium salt, 5 mg/l), 20 ml/l of chelating agent solution (Nitrilotriacetic acid, 1 g/l), 2 ml/l of potassium phosphate dibasic solution (K_2HPO_3 , 152 g/l), 50 ml/l of sodium bicarbonate solution ($NaHCO_3$, 52 g/l), 10 ml/l of reducing agent solution ($Na_2S \cdot 9H_2O$, 25 g/l) and distilled water up to 1 L.

The enrichment cultures used as inocula in experiments carried out at mesophilic and thermophilic conditions corresponded to two different MMC previously enriched at mesophilic and thermophilic conditions, respectively. Both enriched cultures originated from the same initial mixture of anaerobic sludges and were enriched using a synthetic syngas mixture as the only carbon and electron source as described in Grimalt-Alemany et al. [22].

2.2. Experimental setup

The calibration (parameter estimation) and validation of the models were performed largely based on a dataset from previous work [22] consisting of one experiment with syngas and 4 specific activity tests with either only CO , H_2/CO_2 or acetate as the only substrates combined with the methanogenic inhibitor sodium 2-bromoethanesulfonate (BES). This dataset was extended with 4 additional experiments, where the initial P_{H_2} was fixed to 1 atm and the initial P_{CO} varied from 0.2 atm to 0.8 atm. The complete experimental setup used for both parameter estimation and validation of the mesophilic and the thermophilic model is summarized in table 1. It should be noted that specific activity tests resulting in no microbial activity when using the thermophilic MMC, namely experiments with H_2/CO_2+BES and acetate, were not included in the dataset for parameter estimation.

All experiments were performed in 330 ml flasks with a final working volume of 100 ml. The flasks were first filled with 85 ml of medium and flushed with either N_2 or H_2 to create anaerobic conditions. After sealing the flasks with rubber stoppers and screw lids, the composition of the headspace was adjusted to the corresponding partial pressures given in table 1. The pressure of each gas was adjusted using a precision pressure indicator (CPH6400, WIKA, Germany) while working at 25 °C. The incubation temperature at mesophilic conditions corresponded to 37 °C, and at thermophilic conditions to 60 °C. All flasks were incubated at 100 rpm using an orbital shaker Gio Gyrotory (New Brunswick Scientific Co., USA) with an orbit diameter of 2.54 cm at mesophilic conditions, and a MaxQ2000 (Thermo Scientific, USA) with an orbit diameter of 1.90 cm at thermophilic conditions. The initial pH of the cultures corresponded to an average of 7.2 ± 0.1 at both mesophilic and thermophilic conditions. Samples from the gas and liquid phase were withdrawn at least once a day for monitoring the headspace composition, the concentration of metabolites in the liquid and the microbial biomass growth.

Table 1. Initial partial pressure of gases, acetate and BES concentration used in the complete experimental setup. The use of each dataset is also described. PE stands for parameter estimation and V for validation.

	H ₂ (atm)	CO (atm)	CO ₂ (atm)	N ₂ (atm)	NaCH ₃ COO (mM)	BES (mM)	Dataset use	Ref.
<i>Mesophilic microbial consortium</i>								
CO + BES	-	0.4	0.2	1.4	-	15	PE	[22]
H ₂ /CO ₂ + BES	0.8	-	0.2	1.0	-	15	PE	[22]
H ₂ /CO ₂	0.8	-	0.2	1.0	-	-	PE	[22]
Acetate	-	-	0.2	1.8	25	-	PE	[22]
H ₂ /CO ₂ + CO	1.0	0.2	0.2	0.6	-	-	V	
H ₂ /CO ₂ + CO	1.0	0.4	0.2	0.4	-	-	PE	
H ₂ /CO ₂ + CO	1.0	0.6	0.2	0.2	-	-	V	
H ₂ /CO ₂ + CO	1.0	0.8	0.2	-	-	-	V	
<i>Thermophilic microbial consortium</i>								
CO + BES	-	0.4	0.2	1.4	-	15	PE	[22]
CO + BES	-	0.8	0.2	1.0	-	15	PE	
H ₂ /CO ₂	0.8	-	0.2	1.0	-	-	PE	[22]
H ₂ /CO ₂ + CO	1.0	0.4	0.2	0.4	-	-	PE	[22]
H ₂ /CO ₂ + CO	1.0	0.2	0.2	0.6	-	-	V	
H ₂ /CO ₂ + CO	1.0	0.4	0.2	0.4	-	-	V	
H ₂ /CO ₂ + CO	1.0	0.6	0.2	0.2	-	-	V	
H ₂ /CO ₂ + CO	1.0	0.8	0.2	-	-	-	V	

2.3. Mass transfer coefficient ($k_L a$) experimental determination

The mass transfer coefficient ($k_L a$) of H₂, CO, CH₄ and CO₂ was determined in duplicate experiments in 330 ml flasks incubated at the same conditions as the mesophilic and thermophilic experiments, namely, at 100 rpm using a Gio Gyrotory shaker at 37 °C and a MaxQ2000 shaker at 60 °C, respectively. The method used is based on monitoring the evolution of the concentration of the gases in the liquid phase over time in abiotic experiments. For this purpose, a volume of 100 ml of medium was added to the flasks, and these were flushed with N₂ and sealed with rubber stoppers and screw plugs. The rubber stoppers had two ports, with one connecting to the gas phase and the other to the liquid phase. The port connected to the gas phase was connected to a bag filled with a synthetic syngas mixture of H₂ (45%), CO (20%), CH₄ (10 %) and CO₂ (25%), and the port connected to the liquid phase served as liquid sampling port. Before the beginning of the experiment and with valves closed, vacuum was created in the flasks using a vacuum pump for allowing a fast diffusion of the gas into the headspace of the flasks. The experiment started when the valve connecting the bag and the headspace of the flasks was opened, letting the synthetic syngas mixture rapidly flow into the bottle. To ensure that the gas composition of the bag and the flask was the same, vacuum was rapidly created in the flasks a second time with the valves closed, subsequently opening the valve connecting the bag and the headspace of the flask once again. Liquid samples (8 ml) were transferred into anaerobic serum vials with a total volume of 11 ml and were heated

to 100 °C for 30 min, from which a 100 µl gas sample was taken using a gas tight syringe to determine the gaseous composition.

2.4. Analytical methods

Gaseous samples containing H₂, CO, CO₂ and CH₄ were analyzed using a gas chromatograph (8610C, SRI Instruments, USA) equipped with a thermal conductivity detector, and a Molsieve 13X packed column (6' x 1/8") and a silica gen column (6' x 1/8") connected in series through a rotating valve. The temperature of the oven was maintained at 65 °C for 3 min, followed by a ramp of 10°C/min up to 95°C and a second ramp of 24°C/min from 95°C to 140°C. Volatile fatty acids (VFA) determination was carried out using a High Performance Liquid Chromatograph (Shimadzu, USA) equipped with a refractive index detector and an Aminex HPX-87H column (Bio-Rad, USA) at 63°C and a flow of 0.6 ml/min of 12 mM H₂SO₄ eluent solution. Microbial biomass growth was measured based on the optical density (OD) of the liquid samples at 600 nm using a spectrophotometer (DR2800, Hach Lange). The OD was then correlated to the concentration of Volatile Suspended Solids (VSS) determined according to standard methods [23].

2.5. Models description

Two structured models were designed, each of them intended for modelling mesophilic and thermophilic syngas biomethanation process in batch mode. Each model presented a different structure according to the catabolic routes employed by its corresponding MMC (see section 3.1). The mesophilic and thermophilic models comprised 25 and 18 dynamic state variables, respectively, corresponding to the concentration of gaseous compounds in the gas and the liquid phase, the different microbial biomass groups involved in the conversion and the different carbonate, acetate and propionate species. A total of 20 and 12 processes were considered in the mesophilic and thermophilic models, respectively, including microbial growth, maintenance and decay, acids dissociation and gas-liquid mass transfer.

A number of control functions were included in the models in the form of control factors for modeling of microbial growth processes. These control factors were taken into account upon multiplication with the specific growth rate equations.

All microbial growth processes were made thermodynamically consistent by including a thermodynamic potential factor (F_T) [21]. The F_T was calculated as follows:

$$F_T = \begin{cases} 1 - \exp\left(-\frac{\Delta G_A - \Delta G_C}{\chi RT}\right), & \Delta G_A \geq \Delta G_C \\ 0, & \Delta G_A \leq \Delta G_C \end{cases} \quad (1)$$

$$\Delta G_C = Y_{ATP} \cdot \Delta G_p \quad (2)$$

where ΔG_A equals to the negative Gibbs free energy change ($-\Delta_r G'$) of each biochemical reaction in kJ per reaction corrected for temperature, ionic strength and reactants concentration as described in Grimalt-Aleman et al. [22]; ΔG_C is the free energy conserved through each metabolic pathway calculated by multiplying the ATP yield with the Gibbs free energy of phosphorylation (ΔG_p), assumed to have a value of 15 kJ/mol ATP; and χ corresponds to the number of times a rate-determining step takes place through a metabolic pathway. F_T approaches 0 when $\Delta G_A \approx \Delta G_C$, indicating that the thermodynamic drive is low and that the reaction rate is thermodynamically controlled. When $\Delta G_A \leq \Delta G_C$, F_T becomes 0, which indicates that the thermodynamic drive for the reaction to proceed forward disappears and the metabolism stops. Consequently, the growth rate is strictly kinetically controlled through the Monod model when the biochemical reaction is far from thermodynamic equilibrium, and thermodynamically controlled when the reaction approaches its thermodynamic feasibility limits.

The lag phase period for each microbial trophic group considered and the inhibition of the methanogenesis due to the addition of the specific inhibitor BES was modelled according to eq. 3 and 4, respectively, where t represents time, t_{lag} corresponds to the duration of the lag phase and C_{BES} is the concentration of BES. According to eq. 3, $f_{lag, i}$ deactivates the microbial growth process of the corresponding microbial trophic group i until time t reaches the end of the lag phase. Similarly, f_{BES} (eq. 4) deactivates methanogenic growth in those experiments where BES was added to the growth medium.

$$f_{lag} = \begin{cases} 1, & t \geq t_{lag} \\ 0, & t \leq t_{lag} \end{cases} \quad (3)$$

$$f_{BES} = \begin{cases} 1, & C_{BES} = 0 \text{ mM} \\ 0, & C_{BES} = 15 \text{ mM} \end{cases} \quad (4)$$

The inhibition due to low pH was included only for methanogenic microbial groups as described in ADM1 [24] according to eq. 5. The parameters pHUL (pH upper limit) and pHLL (pH lower limit) correspond to the pH values at which a specific microbial group is not inhibited, and is fully inhibited, respectively.

$$I_{pH} = \begin{cases} \exp\left(-3 \cdot \left(\frac{pH - pHUL}{pHUL - pHLL}\right)^2\right), & pH \leq pHUL \\ 1, & pH \geq pHUL \end{cases} \quad (5)$$

The mesophilic syngas biomethanation model considered growth of 6 microbial trophic groups, including carboxydrotrophic acetogens, homoacetogens, hydrogenotrophic methanogens, aceticlastic methanogens,

syntrophic acetate oxidizers and syntrophic propionate oxidizers. The specific growth rate of carboxydrotrophic acetogens (μ_{carb}) was assumed to depend on the dissolved CO (CO_{aq}) in the liquid phase as the only source of carbon and electrons, and was described by eq. 6. Both homoacetogenic (μ_{hom}) and hydrogenotrophic methanogenic (μ_{hyd}) specific growth rates depended on dissolved H_2 (H_{2aq}) as the limiting substrate during the fermentations, and were described according to eq. 7 and 8. The acetoclastic methanogenic specific growth rate (μ_{ac}) was assumed to depend on the total acetate concentration (Ac_{tot}) consisting of the sum of undissociated and dissociated species, and was defined according to eq. 9. Lastly, the specific growth rate of syntrophic acetic and propionic acid oxidizers, μ_{SAO} and μ_{SPO} respectively, was described by eq. 10 and 11. As syntrophic fatty acid oxidation reactions often operate very close to thermodynamic equilibrium, it is likely that including both Monod model and F_T in the model would result in an overlapping effect on the growth rate. Therefore, in this case, the specific growth rates of these microbial groups were assumed to be strictly thermodynamically controlled through F_T in order to avoid redundant control of their growth kinetics (eq. 10 and 11).

$$\mu_{carb} = \frac{\mu_{max,carb} \cdot CO_{aq}}{k_{s,carb} + CO_{aq}} \cdot F_{T,carb} \cdot f_{lag,carb} \quad (6)$$

$$\mu_{hom} = \frac{\mu_{max,hom} \cdot H_{2aq}}{k_{s,hom} + H_{2aq}} \cdot F_{T,hom} \cdot f_{lag,hom} \quad (7)$$

$$\mu_{hyd} = \frac{\mu_{max,hyd} \cdot H_{2aq}}{k_{s,hyd} + H_{2aq}} \cdot F_{T,hyd} \cdot I_{pH,hyd} \cdot f_{lag,hyd} \cdot f_{BES} \quad (8)$$

$$\mu_{ac} = \frac{\mu_{max,ac} \cdot Ac_{tot}}{k_{s,ac} + Ac_{tot}} \cdot F_{T,ac} \cdot I_{pH,ac} \cdot f_{lag,ac} \cdot f_{BES} \quad (9)$$

$$\mu_{SAO} = \mu_{max,SAO} \cdot F_{T,SAO} \quad (10)$$

$$\mu_{SPO} = \mu_{max,SPO} \cdot F_{T,SPO} \quad (11)$$

The thermophilic model assumed growth of two different microbial trophic groups, namely carboxydrotrophic hydrogenogens and hydrogenotrophic methanogens. As in the mesophilic model, the specific growth rate of hydrogenotrophic methanogens (μ_{hyd}) was assumed to depend on H_{2aq} (eq. 12). In this case, the inhibition due to low pH was not included for simplicity as, due to the fact that acids were not produced during the fermentation, the pH was not expected to play a significant role. The carboxydrotrophic hydrogenogenic specific growth rate (μ_{carb_hyd}) depended on CO_{aq} and was described by eq. 13. In contrast to the other microbial groups, carboxydrotrophic hydrogenogens presented the particularity of shifting their product from H_2 to acetic acid depending on the operating conditions [22]. In this work, it was hypothesized that this metabolic shift could be

modelled based on the thermodynamic feasibility of the conversion of CO into H₂ and CO₂, where the product yield (Y_{H₂} and Y_{Ac}), defined by the fraction of e-mol diverted to each product from CO, changes proportionally to F_{T,carb_hyd} from H₂ to acetic acid when the production of H₂ starts to be thermodynamically limited (eq.14 and 15). Consequently, the thermodynamic feasibility of μ_{carb_hyd} was ultimately dependent on the production of acetate from CO defined by F_{T,carb_ac}. Another particularity of the carboxydrotrophic hydrogenogenic microbial group was that the production of acetic acid seemed not to be associated to growth. This was modelled by including a specific maintenance rate as described in eq. 16. According to eq. 16, the specific maintenance rate is proportional to the specific growth rate of this microbial group (μ_{carb_hyd}), the fraction of e-mols diverted to acetate, described by (1 - F_{T,carb_hyd}), and a_{carb_hyd}, which reflects the severity of the maintenance cost. When 0 < a_{carb_hyd} < 1, there is partial growth associated to the production of acetic acid; a_{carb_hyd} = 1 when there is no growth associated to the production of acetic acid; and a_{carb_hyd} > 1 when there is an increased maintenance cost associated to the production of acetic acid.

$$\mu_{hyd} = \frac{\mu_{max,hyd} \cdot H_{2aq}}{k_{s,hyd} + H_{2aq}} \cdot F_{T,hyd} \cdot f_{lag,hyd} \quad (12)$$

$$\mu_{carb_hyd} = \frac{\mu_{max,carb_hyd} \cdot CO_{aq}}{k_{s,carb_hyd} + CO_{aq}} \cdot F_{T,carb_ac} \cdot f_{lag,carb_hyd} \quad (13)$$

$$Y_{H_2,carb_hyd} = F_{T,carb_hyd} \cdot Y_{e-mol/CO} / n_{e-mol/mol H_2} \quad (14)$$

$$Y_{Ac,carb_hyd} = (1 - F_{T,carb_hyd}) \cdot Y_{e-mol/CO} / n_{e-mol/mol Ac} \quad (15)$$

$$m_{s,carb_hyd} = a_{carb_hyd} \cdot \mu_{carb_hyd} \cdot (1 - F_{T,carb_hyd}) \quad (16)$$

Microbial biomass decay was described in the same way for all microbial trophic groups and was assumed to follow first-order kinetics according to eq. 17. The net growth rate was then calculated by subtracting the specific maintenance (m_s) and decay rates (k_d) from the growth rates (μ).

$$r_d = k_d \cdot X \quad (17)$$

The physicochemical processes of gas-liquid mass transfer and acid dissociation were included in the two models. The gas-liquid mass transfer of all gases included as dynamic state variables was described by eq. 18, where k_La represents the overall mass transfer coefficient multiplied by the specific transfer area, and H is the Henry's law constant, and C_g and C_{aq} represent the concentration of the gas in the gas and liquid phase, respectively. The dynamics of acid dissociation were described by converting the acid-base equilibrium equations into differential equations according to eq. 19, where k_a corresponds to the dissociation constant and k_f

is the rate of dissociation, which was assumed to take place at very fast rates (10^{10} d^{-1}), and C_i is the concentration of compound i .

$$\rho_T = k_L a \cdot (H \cdot C_g - C_{aq}) \quad (18)$$

$$\rho_{a/b} = k_f \cdot \left(C_a - \frac{C_b \cdot C_{H^+}}{k_a} \right) \quad (19)$$

Both Henry's constant (H) and acid dissociation constants (k_a) were corrected for temperature using Van't Hoff equation (eq. 20, represented by the generic constant K), where $-\Delta H^\circ$ stands for the standard enthalpy of solution ($-\Delta_{\text{sol}}H^\circ$) of a specific gas when correcting the Henry's law constants, and for the standard enthalpy of reaction ($-\Delta_{\text{rxn}}H^\circ$) when correcting the acid dissociation constants. The acid dissociation constants were also corrected for ionic strength according to Alberty [25] as described in eq. 21, where z_i is the charge number of compound i and $\sum v_i z_i^2$ is the change in z_i^2 in the reaction, I is the ionic strength of the medium, α is a constant calculated as a function of temperature and B is an empirical constant with a value of $1.6 \text{ L}^{1/2} \text{ mol}^{-1/2}$ within a range of ionic strength of 0.05-0.25 M [25].

$$K(T) = K^\circ \cdot \exp\left(\frac{-\Delta H^\circ}{R} \left(\frac{1}{T} - \frac{1}{T^\circ}\right)\right) \quad (20)$$

$$\ln K(I) = \ln K(I = 0) + \frac{\alpha I^{1/2} \sum v_i z_i^2}{1 + B I^{1/2}} \quad (21)$$

To reduce the number of parameters to be estimated, most parameters related to the F_T calculations, and all product and microbial biomass yields were determined based on experimental observations and largely derived from previous work on the same enrichment cultures used here [22]. In some cases, the biomass yields for the different microbial trophic groups were recalculated either taking into account only the early exponential growth phase or using additional experimental data. The values for all conversion yields, stoichiometric numbers and ATP yields used are summarized in table 2. The product yield coefficients for syntrophic fatty acid oxidation were calculated assuming a 100% e-mol recovery based on the biomass yields found in the literature [26,27]. Similarly to the yield coefficients, the t_{lag} of each microbial group was determined through experimental observation based on the profile of microbial biomass, substrate and product of each experiment. The initial biomass fractions corresponding to each microbial group were determined through simulation of the pre-culture used as inoculum in the experiments.

Table 2. Yield coefficients for biomass, products and ATP, and stoichiometric number (χ) for each microbial trophic group included in each model. The negative $Y_{\text{CO}_2/\text{S}}$ indicates consumption of CO_2 along with the main substrate (H_2). The biomass yield for syntrophic fatty acid oxidizers was extracted from Cord-Ruwisch et al. [26] and Leng et al. [27].

	Y_X (g VSS/mol substrate)	Y_{Ac} (mol/mol substrate)	Y_{Prop} (mol/mol substrate)	Y_{H_2} (mol/mol substrate)	Y_{CH_4} (mol/mol substrate)	Y_{CO_2} (mol/mol substrate)	χ	Y_{ATP} (mol/mol product)
<i>Mesophilic syngas biomethanation model</i>								
Carboxydrotrophic acetogens $4 \text{ CO} + 2 \text{ H}_2\text{O} \rightarrow \text{CH}_3\text{COOH} + 2 \text{ CO}_2$	2.21	0.17	0.01			0.47	5	1.66
Homoacetogens $4 \text{ H}_2 + 2 \text{ CO}_2 \rightarrow \text{CH}_3\text{COOH} + 2 \text{ H}_2\text{O}$	0.49	0.21				-0.43	1	0.33
Hydrogenotrophic methanogens $4 \text{ H}_2 + \text{CO}_2 \rightarrow \text{CH}_4 + 2 \text{ H}_2\text{O}$	0.72				0.23	-0.22	2	0.5
Aceticlastic methanogens $\text{CH}_3\text{COOH} \rightarrow \text{CO}_2 + \text{CH}_4$	0.57				0.82	0.95	2	0.5
Syntrophic acetate oxidizers $\text{CH}_3\text{COOH} + 2 \text{ H}_2\text{O} \rightarrow 4 \text{ H}_2 + 2 \text{ CO}_2$	2.30			3.80		1.90	1	0.33
Syntrophic propionate oxidizers $\text{CH}_3\text{CH}_2\text{COOH} + 2 \text{ H}_2\text{O} \rightarrow \text{CH}_3\text{COOH} + 3 \text{ H}_2 + \text{CO}_2$	2.80	0.96		2.86		0.96	1	0.33
<i>Thermophilic syngas biomethanation model</i>								
Carboxyd. hydrogenogens (growth - $F_{\text{T,carb,ac}}$) $\text{CO} + \text{H}_2\text{O} \rightarrow \text{H}_2 + \text{CO}_2$	0.88					0.85	5	1.66
Carboxyd. hydrogenogens (Product yield - $F_{\text{T,carb,hyd}}$) ^b		1.76 ^a		1.76 ^a			1 ^b	0.33 ^b
Hydrogenotrophic methanogens $4 \text{ H}_2 + \text{CO}_2 \rightarrow \text{CH}_4 + 2 \text{ H}_2\text{O}$	0.57				0.23	-0.23	2	0.5

^aThe $Y_{\text{H}_2/\text{CO}}$ and $Y_{\text{Ac}/\text{CO}}$ given correspond to the total product yield of carboxydrotrophic hydrogenogens expressed in e-mol products/mol substrate, calculated as the sum of e-mols from acetate and H_2 produced divided by the mols of CO consumed. ^bThe specific yield of H_2 ($Y_{\text{H}_2/\text{CO}}$), acetate ($Y_{\text{Ac}/\text{CO}}$) and the maintenance rate was modulated based on $F_{\text{T,carb,hyd}}$ according to eq. 1, 2 and 14-16.

The kinetic parameters of the model were initially adjusted according to values from the literature, and subsequently, model mismatches with the experimental data were corrected through parameter estimation. The initial value of the kinetic parameters used in the mesophilic and the thermophilic model is tabulated in table 3. The values chosen were based on kinetic parameters previously reported in the literature when possible. Little information is available on the decay rates (k_d) for each of the microbial groups considered, for which tentative values were selected based on manual fitting to the experimental data. Values for high and low pH inhibition factors of hydrogenotrophic and aceticlastic methanogens were manually fixed according to the range of values reported in the ADM1 [24]. The initial values of the overall gas-liquid mass transfer coefficients for each gas were tentatively fixed to 100 d^{-1} based on the minimum overall mass transfer coefficients reported for CO_2 in Siegrist et al. [28]. The kinetic parameters related to growth and decay of the syntrophic fatty acid oxidizing microbial groups were left out of the parameter estimation and identifiability analysis as the dataset was not expected to allow their estimation.

Table 3. Initial values of kinetic parameters used for the mesophilic and the thermophilic model. The parameters marked with “X” in the last column correspond to the parameters that were subject to experimental determination, manual tuning and least squares parameter estimation.

Parameters	Units	Initial Value	Ref.	Estimated
<i>Mesophilic model</i>				
$\mu_{\max, \text{carb}}$	d^{-1}	5.04	[17]	X
$k_{\text{s,carb}}$	M	4.0e-5	[17]	
$k_{\text{d,carb}}$	d^{-1}	3.5e-2		
$\mu_{\max, \text{hom}}$	d^{-1}	16.28		X
$k_{\text{s,hom}}$	M	2.31e-6	[29]	
$k_{\text{d,hom}}$	d^{-1}	4.6e-3		
$\mu_{\max, \text{hyd}}$	d^{-1}	2	[28]	X
$k_{\text{s,hyd}}$	M	1.56e-6	[24,29]	
$k_{\text{d,hyd}}$	d^{-1}	1.3e-3		
pHUL_{hyd}		6.6	[24]	
pHLL_{hyd}		5.9	[24]	
$\mu_{\max, \text{ac}}$	d^{-1}	0.37	[28]	X
$k_{\text{s,ac}}$	M	1.0e-3	[28]	
$k_{\text{d,ac}}$	d^{-1}	1.0e-2		
pHUL_{ac}		6.6	[24]	
pHLL_{ac}		5.9	[24]	
$\mu_{\max, \text{SAO}}$	d^{-1}	2.3	[26]	
$k_{\text{d,SAO}}$	d^{-1}	1.0e-3		
$\mu_{\max, \text{SPO}}$	d^{-1}	0.313	[27]	
$k_{\text{d,SPO}}$	d^{-1}	1.0e-3		
$K_{\text{L}}a_{\text{CO}}$	d^{-1}	100	[28]	X
$K_{\text{L}}a_{\text{H}_2}$	d^{-1}	100	[28]	X
$K_{\text{L}}a_{\text{CO}_2}$	d^{-1}	100	[28]	X
$K_{\text{L}}a_{\text{CH}_4}$	d^{-1}	100	[28]	X
<i>Thermophilic model</i>				
$\mu_{\max, \text{carb_hyd}}$	d^{-1}	7.44	[30]	X
$k_{\text{s,carb_hyd}}$	M	1.45e-3	[18]	
$k_{\text{d,carb_hyd}}$	d^{-1}	1.76e-1		
$\Delta G_{\text{carb_hyd}}$	kJ mol^{-1}	15	[22]	X
$a_{\text{carb_hyd}}$		1		X
$\chi_{\text{carb_hyd}}$		1	[22]	X
$\mu_{\max, \text{hyd}}$	d^{-1}	11.76	[31]	X
$k_{\text{s,hyd}}$	M	1.32e-4	[31]	
$k_{\text{d,hyd}}$	d^{-1}	3.5e-2		
$K_{\text{L}}a_{\text{CO}}$	d^{-1}	100	[28]	X
$K_{\text{L}}a_{\text{H}_2}$	d^{-1}	100	[28]	X
$K_{\text{L}}a_{\text{CO}_2}$	d^{-1}	100	[28]	X
$K_{\text{L}}a_{\text{CH}_4}$	d^{-1}	100	[28]	X

The stoichiometric coefficients corresponding to each of the processes for describing the behavior of all dynamic state variables included in the models are given in table 4. The volume of headspace (V_{h}) and liquid (V_{l}) used in the stoichiometric matrix (table 4) corresponds to 0.23 l and 0.1 l, respectively.

Table 4. Matrix of stoichiometric coefficients for the processes included in the mesophilic and thermophilic syngas biomethanation model. The value of the yield coefficients is given in table 2. The subscripts corresponding to each microbial group were not added in the yield coefficients for simplicity.

Processes	Rates	Stoichiometric coefficients																																				
		CO _{2(aq)}	H _{2(aq)}	CO _{2(aq)}	CH _{4(aq)}	Ac _{tot}	Prop _{tot}	X _{tot}	X _{carb}	X _{carb,hyd}	X _{hyd}	X _{hom}	X _{ac}	X _{SAO}	X _{SPO}	HAc	Ac ⁻	HP _{Prop}	Prop ⁻	H ⁺	OH ⁻	CO ₃ ⁻²	HCO ₃ ⁻	CO _g	H _{2g}	CO _{2g}	CH _{4g}											
Growth-Mesophilic																																						
Carb. acetogens	$\mu_{carb} \cdot X_{carb}$	-1/Y _X		Y _{CO2} /Y _X		Y _{HAc} /Y _X	1	1								Y _{HAc} /Y _X																						
Hydrog. methanogens	$\mu_{hyd} \cdot X_{hyd}$		-1/Y _X	Y _{CO2} /Y _X	Y _{CH4} /Y _X		1		1																													
Homoacetogens	$\mu_{hom} \cdot X_{hom}$		-1/Y _X	Y _{CO2} /Y _X		Y _{HAc} /Y _X	1			1						Y _{HAc} /Y _X																						
Aceticl. methanogens	$\mu_{ac} \cdot X_{ac}$			Y _{CO2} /Y _X	Y _{CH4} /Y _X	-1/Y _X	1				1					-1/Y _X																						
SAO	$\mu_{SAO} \cdot X_{SAO}$		Y _{H2} /Y _X	Y _{CO2} /Y _X		-1/Y _X	1						1			-1/Y _X																						
SPO	$\mu_{SPO} \cdot X_{SPO}$		Y _{H2} /Y _X	Y _{CO2} /Y _X		Y _{HAc} /Y _X	-1/Y _X	1						1																								
Decay-Mesophilic																																						
Carb. acetogens	$k_{d,carb} \cdot X_{carb}$								-1	-1																												
Hydrog. methanogens	$k_{d,hyd} \cdot X_{hyd}$								-1		-1																											
Homoacetogens	$k_{d,hom} \cdot X_{hom}$											-1																										
Aceticl. methanogens	$k_{d,ac} \cdot X_{ac}$																																					
SAO	$k_{d,SAO} \cdot X_{SAO}$																																					
SPO	$k_{d,SPO} \cdot X_{SPO}$																																					
Growth-Thermophilic																																						
Carb. hydrogenogens	$\mu_{carb,hyd} \cdot X_{carb,hyd}$	-1/Y _X	Y _{H2} /Y _X	Y _{CO2} /Y _X		Y _{HAc} /Y _X	1	1								Y _{HAc} /Y _X																						
Hydrog. methanogens	$\mu_{hyd} \cdot X_{hyd}$		-1/Y _X	Y _{CO2} /Y _X	Y _{CH4} /Y _X		1		1																													
Maintenance-Thermophilic																																						
Carb. hydrogenogens	$m_{s,carb,hyd} \cdot X_{carb,hyd}$																																					
Decay-Thermophilic																																						
Carb. hydrogenogens	$k_{d,carb,hyd} \cdot X_{carb,hyd}$																																					
Hydrog. methanogens	$k_{d,hyd} \cdot X_{hyd}$																																					
Acid dissociation																																						
Acetic acid/Acetate	$\rho_{HAc/Ac}$																																					
Prop. acid/Propionate	$\rho_{HProp/Prop}$																																					
CO ₂ /HCO ₃ ⁻	$\rho_{CO2/HCO3}$																																					
HCO ₃ ⁻ /CO ₃ ⁻²	$\rho_{HCO3/CO3}$																																					
Mass transfer																																						
CO	$\rho_{T,CO}$		V _h /V _l																																			
H ₂	$\rho_{T,H2}$			V _h /V _l																																		
CO ₂	$\rho_{T,CO2}$				V _h /V _l																																	
CH ₄	$\rho_{T,CH4}$					V _h /V _l																																

2.6. Parameter estimation and identifiability analysis

The models were implemented in Matlab (Mathworks, USA) and the equations describing the dynamic state variables included in each model were solved numerically using the stiff solver ode15s. The parameter estimation was conducted using a non-weighted least squares method for the minimization of the objective function S (eq. 22), where y corresponds to the set of experimental measurements and $f(\theta)$ to the model predictions. The minimization algorithms used were unconstrained `fminsearch`, and `lsqnonlin` for confirmation of the solution. The model outputs and experimental measurements considered in the minimization of the sum of squares corresponded to CO_g , H_{2g} , CH_{4g} , Ac_{tot} and X_{tot} .

$$S(y, \theta) = \sum (y - f(\theta))^2 \quad (22)$$

The uncertainty of the estimated parameters ($\hat{\theta}$) was evaluated based on the 95% confidence interval of each parameter. The confidence intervals were calculated based on the covariance matrix ($\text{cov}(\hat{\theta})$), which was determined through a linear approximation method using the Jacobian matrix (F) according to eq. 23-25 [32]. $S_{\min}(y, \hat{\theta})$ corresponds to the minimum value of the objective function, s^2 is an estimation of the variance from the residuals of the model outputs, n is the number of experimental measurements, p is the number of estimated parameters.

$$s^2 = \frac{S_{\min}(y, \hat{\theta})}{n-p} \quad (23)$$

$$\text{cov}(\hat{\theta}) = s^2 (F' \cdot F)^{-1} \quad (24)$$

$$\hat{\theta}_{1-\alpha} = \hat{\theta} \pm t_{N-p}^{\alpha/2} \sqrt{\text{diag cov}(\hat{\theta})} \quad (25)$$

A local sensitivity analysis was performed on the model outputs mentioned above in order to evaluate the sensitivity of the model outputs at the neighboring values of the estimated parameters as described in Sin et al. [33]. The perturbation factor size used was 1% of the corresponding parameter values ($\varepsilon = 1e-2$). The non-dimensional sensitivity (sr) and the relative non-dimensional sensitivity were calculated using the nominal value of the parameters (θ^0), a scaling factor corresponding to the average values of each model output over the time frame of the experiments (\bar{y}), and the Euclidean norm according to eq. 26 and 27.

$$sr = \frac{dy}{d\theta} \cdot \frac{\theta^0}{\bar{y}} \quad (26)$$

$$snorm = \frac{sr}{\|sr\|} \quad (27)$$

The parameter identifiability analysis conducted for determining uniquely identifiable parameter subsets was based on the sensitivity measure (δ_j^{msqr}) and the collinearity index (γ_K) [33,34]. The sensitivity measure δ_j^{msqr} was calculated according to eq. 28 considering the sensitivities of all parameters and variables from all experiments used for parameter estimation (table 1). The collinearity index γ_K was calculated for the experiments with syngas subject to parameter estimation and the variable X_{tot} , as this variable contained information about all microbial growth processes from which the rest of model outputs depended. The collinearity index γ_K was calculated for all possible combinations of parameters using eq. 29 and 30, where the subscript K indicates the parameter subset evaluated and λ_K represents the eigenvalues of the normalized sensitivity matrix for the same parameter subset.

$$\delta_j^{msqr} = \sqrt{\frac{1}{N} \sum_i^N (sr_{ij}^2)} \quad (28)$$

$$\gamma_K = \frac{1}{\sqrt{\min \lambda_K}} \quad (29)$$

$$\lambda_K = \text{eigen}(snorm_K^T \cdot snorm_K) \quad (30)$$

The threshold of γ_K values above which a specific parameter subset is poorly identifiable was determined empirically [34]. Since the parameter identifiability measures used in the analysis are of local nature and evaluate only the neighbouring values of the estimated parameters, the process of parameter estimation and identifiability analysis was iterated as suggested by Brun et al. [34]. During initial iterations, unknown parameters not previously reported in the literature or parameters causing significant model mismatch, outside the identifiable parameter subsets, were tuned manually before performing parameter estimation [34].

3. Results and Discussion

3.1. Behavior of microbial consortia and yield coefficients consistency

The MMC used in the experiments were the result of two microbial enrichments, with each of them being performed at mesophilic and at thermophilic conditions. As a result of the microbial selection during the enrichments, the two MMC presented significant differences in their microbial composition and their dominant catabolic routes leading to CH_4 . A brief description of the microbial groups involved in the conversion is given below to justify the model structure selected in each case. For more details on the microbial activity of the cultures, the reader is referred to Grimalt-Aleman et al. [22].

The mesophilic culture presented a rather complex metabolic network, where CO was converted into acetate and propionate by carboxydrotrophic acetogens, and H₂/CO₂ was converted into both acetate and CH₄ simultaneously by homoacetogens and hydrogenotrophic methanogens, respectively. Acetate was then further converted to CH₄ by aceticlastic methanogens. In previous work on these same cultures, it was hypothesized that neither acetate nor propionate were converted through syntrophic fatty acid oxidation in significant amounts based on the fact that these reactions were not thermodynamically feasible under the experimental conditions of the study [22]. Nevertheless, the mesophilic model was built considering growth of all microbial trophic groups with a possible role during the conversion, also including syntrophic fatty acid oxidizers in order to improve the predictive capacity of the model as these reactions could become available when changing the operating conditions.

In turn, the thermophilic culture was much simpler, comprising only carboxydrotrophic hydrogenogens carrying out the conversion of CO into H₂ and CO₂, and hydrogenotrophic methanogens, which converted all H₂/CO₂ strictly into CH₄. The carboxydrotrophic hydrogenogenic microbial group presented a dynamic behavior depending on the operating conditions. When hydrogenotrophic methanogens were inhibited with BES (table 1), carboxydrotrophic hydrogenogens diverted a part of the carbon originating from CO into acetate instead of H₂ and CO₂; whereas when they were grown in syntrophic association with hydrogenotrophic methanogens, only H₂ and CO₂ were produced. Therefore, the structure selected for the thermophilic model was consistent with these observations and the model included a dynamic product yield for carboxydrotrophic hydrogenogens (eq. 15).

Table 5. Total e-mol recovery accounting for microbial biomass and all products found for each microbial group based on the yield coefficients used. The composition of the biomass was assumed to be C₅H₇O₂N.

	Biomass (% e-mol/e-mol)	Products (% e-mol/e-mol)	Recovery (% e-mol/e-mol)
<i>Mesophilic microbial consortium</i>			
Carboxydrotrophic acetogens	19.5%	73.7%	93.2%
Homoacetogens	4.4%	84.7%	89.1%
Hydrogenotrophic methanogens	6.3%	95.4%	101.8%
Aceticlastic methanogens	1.3%	81.5%	82.7%
Syntrophic acetate oxidizers	5.1%	94.9%	100.0%
Syntrophic propionate oxidizers	3.5%	96.5%	100.0%
<i>Thermophilic microbial consortium</i>			
Carboxydrotrophic hydrogenogens	7.8%	87.9%	95.7%
Hydrogenotrophic methanogens	5.0%	91.4%	96.4%

The consistency of the yield coefficients used in the models for each microbial group was evaluated based on the electron balance (table 5). In most cases, the total e-mol recovery calculated based on the yield coefficients determined experimentally was within a 10% difference from complete recovery. This suggests that the yield coefficients were correct as the small percentage of e-mols missing could be attributed to inefficiencies of the

microbial metabolism due to maintenance costs, understood as energy expenditures not translated into apparent microbial growth [35].

3.2. Parameter importance and identifiability analysis

The selection of parameters to be estimated was performed through iterative parameter estimation and identifiability analysis based on the sensitivity measure ∂_j^{msqr} and the collinearity index γ_K . According to Brun et al. [34], for a parameter subset to be identifiable, it is required that (i) the model outputs are sensitive to the parameters in question and (ii) that the parameters composing a specific parameter subset do not have collinear dependence among them, as this would result in multiple parameter values yielding the same output.

The results of the parameter significance analysis through the sensitivity measure ∂_j^{msqr} revealed common trends for both mesophilic and thermophilic models (fig.1). Both models coincided in the fact that the mass transfer of H_2 and CO exerted a strong influence on several model outputs, and that the maximum specific growth rates (μ_{max}) seemed to be systematically more important than the half-saturation constants (k_s) within the same microbial group. Besides k_{LaH_2} and k_{LaCO} , the output variables of the mesophilic model were influenced by several kinetic parameters including $\mu_{\text{max,carb}}$, $k_{\text{s,carb}}$, $\mu_{\text{max,hom}}$, $\mu_{\text{max,hyd}}$, $k_{\text{s,hyd}}$, $\mu_{\text{max,ac}}$ and $k_{\text{s,ac}}$; while other parameters related to the pH inhibition and k_{LaCO_2} and k_{LaCH_4} had no effect during the experiments used for calibration. In the thermophilic model, the kinetic parameters μ_{max} and k_s of both carboxydrotrophic hydrogenogens and hydrogenotrophic methanogens were also found to have a significant effect on the model outputs. However, the most important parameters affecting the model outputs of the thermophilic model, besides k_{LaH_2} and k_{LaCO} , were related to the specific maintenance rate and the thermodynamic feasibility of the carboxydrotrophic hydrogenogenesis, namely $a_{\text{carb_hyd}}$, $\Delta G_{\text{carb_hyd}}$ and $\chi_{\text{carb_hyd}}$.

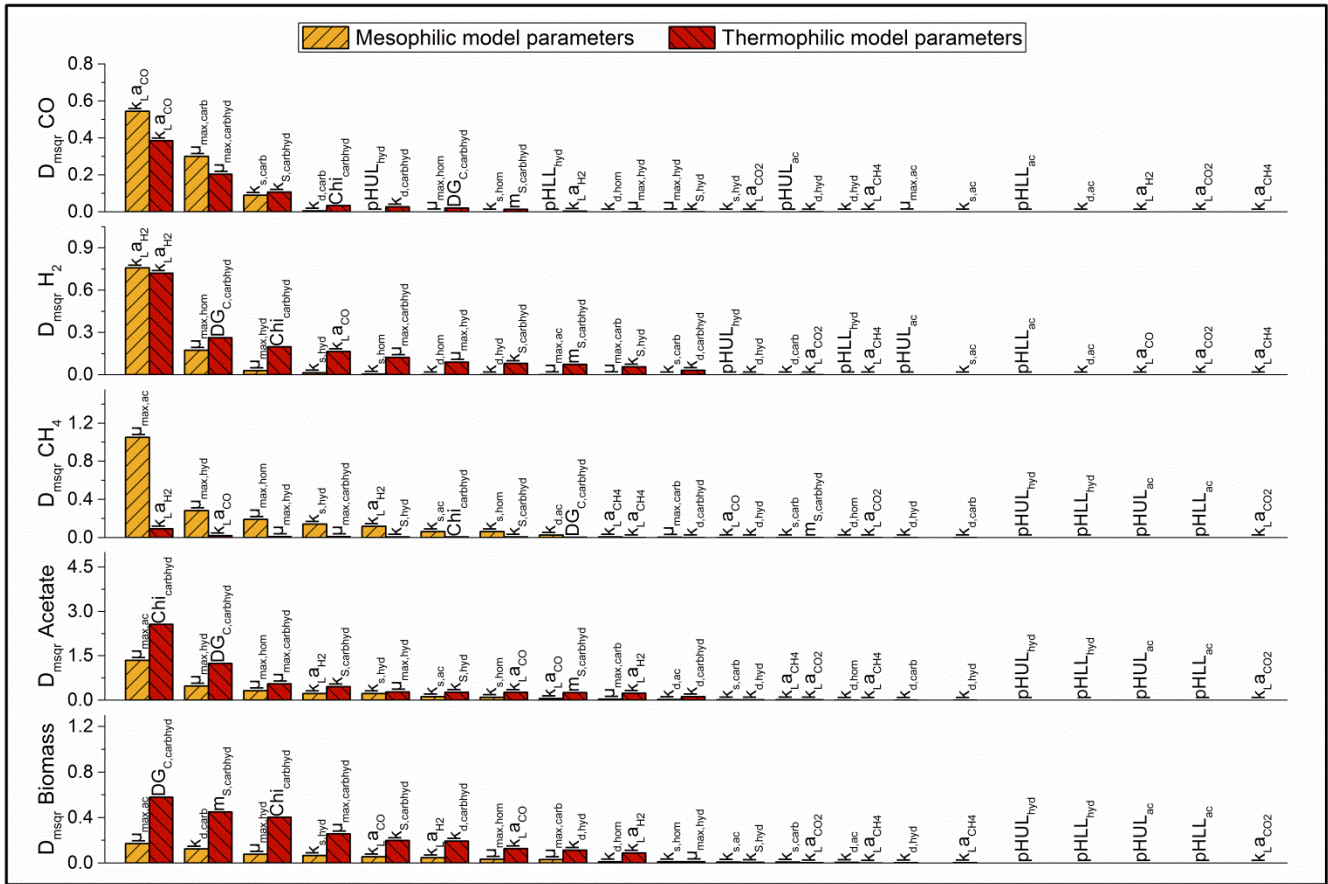


Figure 1. Parameter significance ranking based on the sensitivity measure $\hat{\sigma}_j^{\text{msqr}}$ for the model outputs used for parameter estimation in both mesophilic and thermophilic syngas biomethanation model.

Analyzing the collinearity of candidate parameters to be estimated showed that, as expected, not all parameters with an influence on the model outputs were identifiable. After several iterations, the threshold γ_K values determining the unique identifiability of a specific parameter combination were found to be below approx. 5 and 25 for the mesophilic and the thermophilic model, respectively (table 6). As shown in table 6, the datasets used for model calibration could not support the estimation of parameter combinations including both μ_{max} and k_s of the same microbial group, even when estimating only two parameters in the case of the mesophilic syngas biomethanation model [36,37]. Similarly, the importance of $k_L a_{\text{H}_2}$ and $k_L a_{\text{CO}}$ and their high collinearity with other parameters in both models would also limit the identifiability of other kinetic parameters if these were included, as other parameters would have to be fixed manually instead (table 6). Therefore, the $k_L a$ coefficient was determined experimentally for all gases in order to maximize the number of kinetic parameters estimated. The parameters of the mesophilic model finally selected for parameter estimation corresponded to $\mu_{\text{max,carb}}$,

$\mu_{\max,\text{hyd}}$ and $\mu_{\max,\text{ac}}$, with the parameter $\mu_{\max,\text{hom}}$ being manually tuned beforehand. In the case of the thermophilic model, the parameters selected were $\mu_{\max,\text{carb_hyd}}$, $\mu_{\max,\text{hyd}}$, $\Delta G_{\text{C,carb_hyd}}$ and $a_{\text{carb_hyd}}$, as it was not possible to include $\chi_{\text{carb_hyd}}$ due to the high collinearity of that specific parameter combination (table 6). Thus, the parameter $\chi_{\text{carb_hyd}}$ was fixed manually before performing the final parameter estimation.

Table 6. Collinearity index values for different parameter combinations. The first parameter combination of each model was selected for the final parameter estimation.

Subset size	Parameter combination					γ_K	
<i>Mesophilic model</i>							
3	$\mu_{\max,\text{carb}}$	$\mu_{\max,\text{hyd}}$	$\mu_{\max,\text{ac}}$			1.42	Identifiable
2	$\mu_{\max,\text{carb}}$	$k_{\text{s,carb}}$				7.17	Non-identifiable
4	$\mu_{\max,\text{carb}}$	$\mu_{\max,\text{hom}}$	$\mu_{\max,\text{hyd}}$	$\mu_{\max,\text{ac}}$		9.42	Non-identifiable
4	$\mu_{\max,\text{carb}}$	$\mu_{\max,\text{hom}}$	$\mu_{\max,\text{hyd}}$	$k_{\text{L}}a_{\text{CO}}$		12.36	Non-identifiable
4	$\mu_{\max,\text{carb}}$	$\mu_{\max,\text{hom}}$	$\mu_{\max,\text{hyd}}$	$k_{\text{L}}a_{\text{H}_2}$		11.41	Non-identifiable
<i>Thermophilic model</i>							
4	$\mu_{\max,\text{carb_hyd}}$	$\mu_{\max,\text{hyd}}$	$\Delta G_{\text{C,carb_hyd}}$	$a_{\text{carb_hyd}}$		23.98	Identifiable
2	$\mu_{\max,\text{carb_hyd}}$	$k_{\text{s,carb_hyd}}$				13.09	Identifiable
5	$\mu_{\max,\text{carb_hyd}}$	$\mu_{\max,\text{hyd}}$	$\Delta G_{\text{C,carb_hyd}}$	$a_{\text{carb_hyd}}$	$\chi_{\text{carb_hyd}}$	262.67	Non-identifiable
5	$\mu_{\max,\text{carb_hyd}}$	$\mu_{\max,\text{hyd}}$	$\Delta G_{\text{C,carb_hyd}}$	$\chi_{\text{carb_hyd}}$	$k_{\text{L}}a_{\text{CO}}$	414.88	Non-identifiable
5	$\mu_{\max,\text{carb_hyd}}$	$\mu_{\max,\text{hyd}}$	$\Delta G_{\text{C,carb_hyd}}$	$\chi_{\text{carb_hyd}}$	$k_{\text{L}}a_{\text{H}_2}$	122.42	Non-identifiable

3.3. Determination of mass transfer coefficients

The $k_{\text{L}}a$ coefficients of all gases were determined through abiotic experiments in order to rule out any possible effect on the estimation of other kinetic parameters and to allow a more accurate estimation of the kinetic parameters selected. As shown in fig. 2A, the method used for the experimental determination of the $k_{\text{L}}a$ coefficients presented good reproducibility. The $k_{\text{L}}a$, determined by linearizing the solution of eq. 18 (where the slope corresponded to $-k_{\text{L}}a$), corresponded to 2.59 h^{-1} (0.0431 min^{-1}) and 2.61 h^{-1} (0.0435 min^{-1}) for CO at mesophilic and thermophilic conditions, respectively (fig. 2B). The $k_{\text{L}}a_{\text{H}_2}$ found was 4.18 h^{-1} (0.0697 min^{-1}) and 3.81 h^{-1} (0.0635 min^{-1}) at mesophilic and thermophilic conditions, respectively (fig. 2B). The $k_{\text{L}}a$ for CO₂ corresponded to 3.23 h^{-1} (0.0539 min^{-1}) and 2.41 h^{-1} (0.0403 min^{-1}) at mesophilic and thermophilic conditions, respectively, and for CH₄ was 2.55 h^{-1} (0.0425 min^{-1}) and 2.41 h^{-1} (0.0401 min^{-1}) at mesophilic and thermophilic conditions, respectively (Supporting information file 1, fig. S1). Two different orbital shakers were used in this study, with the one used at mesophilic conditions having an orbit diameter of 2.54 cm and the one used at thermophilic conditions having 1.90 cm. Using orbital shakers with different orbit diameters may cause significant differences on the $k_{\text{L}}a$ when operating at the same agitation rate, with the $k_{\text{L}}a$ increasing with the orbit diameter [38]. Similarly, the temperature also exerts a significant influence on the $k_{\text{L}}a$, which increases with the

increase of temperature [39]. However, the small differences found at mesophilic and thermophilic conditions suggest that the orbit diameter and temperature effects on the mass transfer counterbalanced each other, as in this case the $k_{L}a$ coefficient at mesophilic and thermophilic conditions was comparable for all gases with the exception of CO_2 . Therefore, the differences observed in the performance of the two MMC used in this study can only be attributed to differences in their kinetic parameters and the catabolic routes employed by each of them.

The $k_{L}a$ coefficients found in these experiments performed in batch mode were lower than those generally reported in studies using continuous gas sparging and other configurations [40,41]. The difference between the $k_{L}a$ coefficients found in this and other studies indicates that the mass transfer was likely limiting during the fermentation, which in turn limited the microbial conversion rates. This does not imply that the kinetic parameters μ_{\max} and k_s were unidentifiable as, according to the sensitivity measure $\hat{\partial}_j^{\text{msqr}}$, both parameters exerted an effect on the model outputs. Additionally, the liquid phase was saturated with the gaseous substrates at the beginning of the experiments and presented significant changes in concentration in the liquid phase during the fermentation, which should allow the estimation of these parameters. Nonetheless, this emphasizes the importance of determining the $k_{L}a$ coefficients independently prior to the estimation of kinetic parameters, as this avoids undesirable interdependencies between kinetic parameters and $k_{L}a$ coefficients, and consequently improves the accuracy of the parameter estimation.

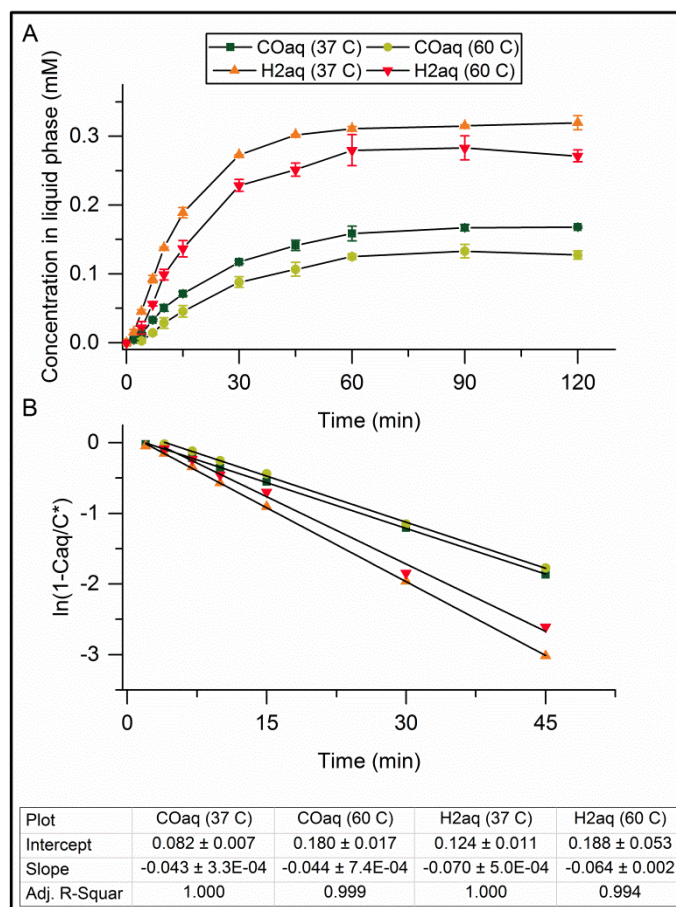


Figure 2. **A** Concentration of H₂ and CO in the liquid phase over time at mesophilic and thermophilic conditions. **B** Plot of linearized eq. 18 in the form $\ln(1-C_{aq}/(H \cdot C_g)) = -k_L a \cdot t$ used to determine k_{LaCO} and k_{LaH_2} at mesophilic and thermophilic conditions.

3.4. Parameter estimation

The results of the parameter estimation for the selected parameters are given in table 7. All estimated parameters presented low correlation among them, with the maximum correlation factor corresponding to 0.373 for parameters of the thermophilic MMC, which confirms that these parameters were uniquely identifiable (table 7). However, it should be noted that the parameters $\mu_{max,hom}$ (in the model for mesophilic conditions), χ_{carb_hyd} and $k_{s,carb_hyd}$ (in the model for thermophilic conditions) were tuned manually before performing least squares parameter estimation and that all other k_s parameters were fixed according to values reported in the literature.

Table 7. Value of estimated parameters for the mesophilic and thermophilic MMC along with their standard deviation (SD), 95% confidence intervals (CI 95) and correlation matrix. Values for $\mu_{\max, \text{hom}}$, $k_{s, \text{carb_hyd}}$ and $\chi_{\text{carb_hyd}}$ were fixed manually prior to the least squares parameter estimation.

Parameters	Estimated parameters	SD	Lower CI 95	Upper CI 95	Correlation matrix			
Mesophilic microbial consortium								
$\mu_{\max, \text{carb}}$ (d^{-1})	3.910	0.001	3.908	3.911	1.000			
$\mu_{\max, \text{hyd}}$ (d^{-1})	5.026	0.029	4.969	5.083	-0.024	1.000		
$\mu_{\max, \text{ac}}$ (d^{-1})	0.667	0.001	0.665	0.669	-0.031	-0.265	1.000	
$\mu_{\max, \text{hom}}$ (d^{-1})	8.140							
Thermophilic microbial consortium								
$\mu_{\max, \text{carb_hyd}}$ (d^{-1})	10.927	0.050	10.828	11.025	1.000			
$\mu_{\max, \text{hyd}}$ (d^{-1})	11.106	0.009	11.089	11.124	0.373	1.000		
$\Delta G_{\text{C, carb_hyd}}$ (kJ/mol H_2)	8.288	0.039	8.211	8.365	-0.283	0.088	1.000	
$a_{\text{carb, hyd}}$	2.390	0.001	2.388	2.392	0.116	-0.079	-0.027	1.000
$\chi_{\text{carb_hyd}}$	2							
$k_{s, \text{carb_hyd}}$ (M)	1.45e-4							

After experimental determination of $k_{\text{L}}a$ and model fitting to the experimental data, the mesophilic syngas biometanation model was able to describe satisfactorily the behavior of the mesophilic MMC as it can be seen that all model variables followed closely the experimental measurements (fig. 3 and 4A, and supplementary information file fig. S2, S3 and S4). The value of the estimated parameters for hydrogenotrophic ($\mu_{\max, \text{hyd}}$) and acetoclastic methanogens ($\mu_{\max, \text{ac}}$) were consistent with average values previously reported for other anaerobic sludges and the species *Methanosaeta concilii* GP-6 and *Methanosarcina mazeii* S-6, which were within a range of 1.4-12 d^{-1} for hydrogenotrophs and 0.3-1.4 d^{-1} for acetoclastic methanogens [24,42,43]. Similarly, the parameter $\mu_{\max, \text{carb}}$ was also comparable and slightly below the μ_{\max} value of 5.04 d^{-1} found by Vega et al. [17] for *Ruminococcus productus* (f. *Peptostreptococcus productus*) growing on CO, from where the value for $k_{s, \text{carb}}$ was extracted.

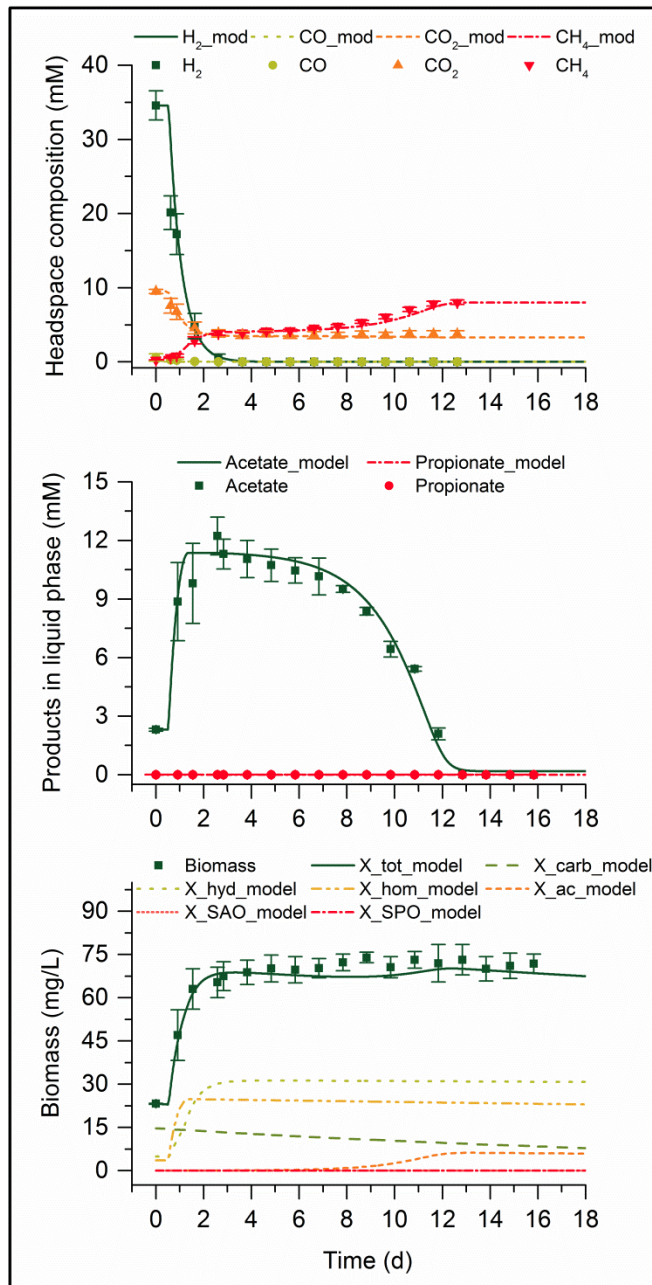


Figure 3. Model fitting to experiment at mesophilic conditions with initial P_{H_2} and P_{CO_2} of 0.8 atm and 0.2 atm, respectively.

Based on the parameter values and the model structure selected for the mesophilic MMC, confirmed by the good fit to the experimental data, the performance of the culture could be fully described by considering metabolic cross-feeding interactions using acetate as intermediate metabolite and mutual exclusion interactions regarding the competition for H₂. According to the parameters μ_{max} and k_s for hydrogenotrophic methanogens and homoacetogens (5.03 d⁻¹ and 1.56e-6 M, and 8.14 d⁻¹ and 2.31e-6 M, respectively) and in line with the findings

of Kotsyurbenko et al. [44], the competition for H_2 should favor growth of homoacetogens at high H_2 concentrations in the liquid phase, whereas hydrogenotrophic methanogens should be able to outcompete homoacetogens when the concentration of H_2 started to be limiting during the fermentation. This can be observed in the microbial growth profile of these two microbial groups in fig. 3 and 4A, where homoacetogens become dominant at the initial stage of the fermentation and hydrogenotrophic methanogens outgrow homoacetogens when H_2 becomes limiting. Due to the combined kinetic and thermodynamic competition found here between these two microbial groups, it can be anticipated that $k_{1,a_{H_2}}$ exerts a strong influence on the outcome of the competition for H_2 as this parameter determines the concentration of H_2 in the liquid phase. As it will be discussed in section 3.6.1, this parameter could be used as a tool for modulating the dominant H_2 conversion pathways. Regarding the use of acetate as intermediate for CH_4 production, the mesophilic MMC was clearly dominated by aceticlastic methanogens. According to the model fittings, aceticlastic methanogenesis was practically the only reaction with a significant role during the experiments used for model calibration (fig. 3, 4A, and supplementary information file fig. S4). Syntrophic acetate oxidizers did not participate in the conversion of acetate in any experiment used for model calibration, with the exception of the one supplemented with acetate as the only substrate, where the higher initial concentration of acetate and the absence of H_2 in the initial headspace composition allowed for the syntrophic acetate oxidation to become thermodynamically feasible and contribute to the production of CH_4 in cooperation with hydrogenotrophic methanogens (Supplementary Information file, fig. S4). Similarly, syntrophic propionate oxidation did not take place during the experiments used for calibration as this reaction was not thermodynamically feasible under the specific operating conditions of these experiments.

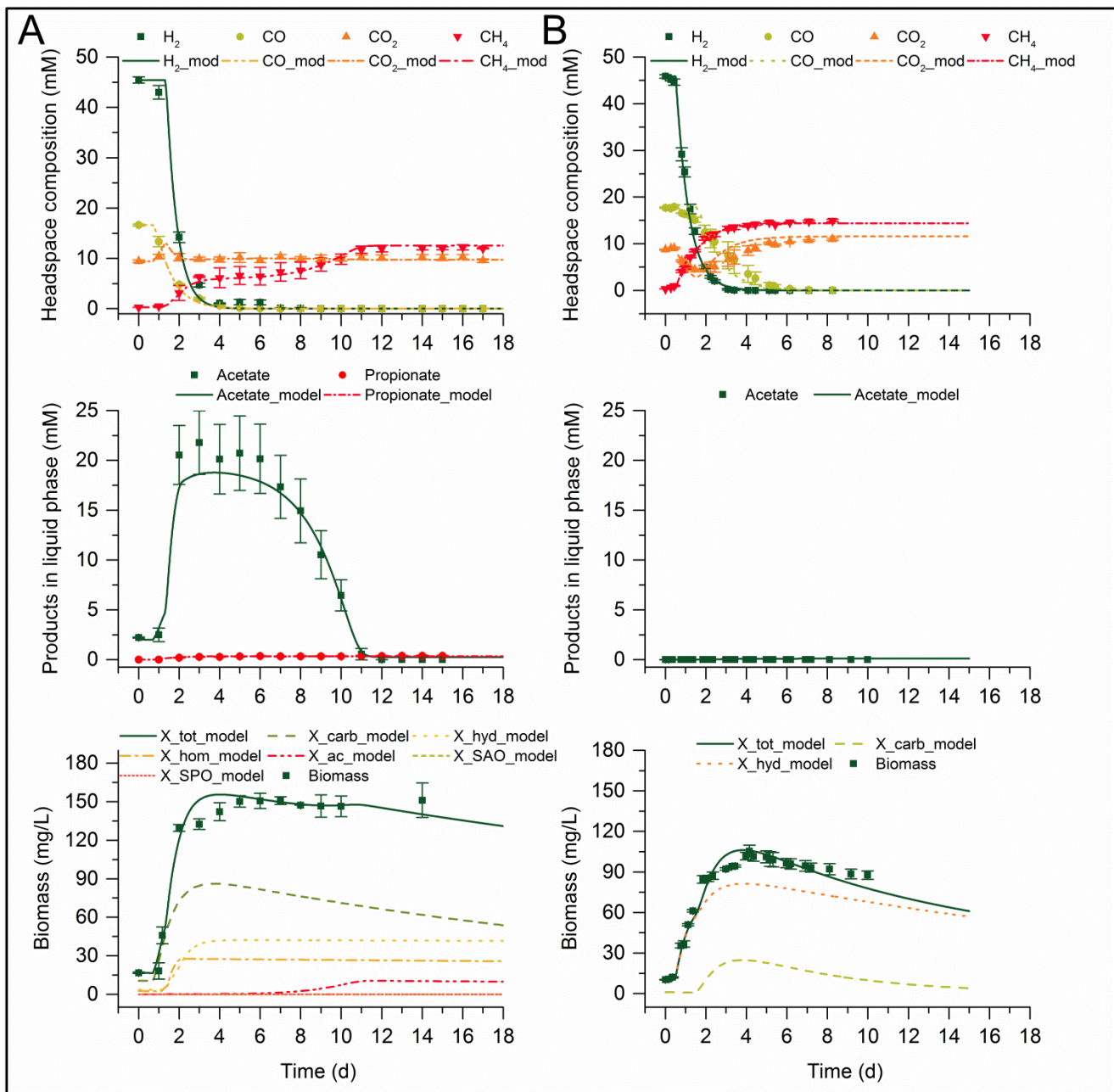


Figure 4. **A** Model fitting to experiment at mesophilic conditions with P_{H_2} , P_{CO} and P_{CO_2} of 1.0 atm, 0.4 atm and 0.2 atm, respectively. **B** Model fitting to experiment at thermophilic conditions with P_{H_2} , P_{CO} and P_{CO_2} of 1.0 atm, 0.4 atm and 0.2 atm, respectively.

The thermophilic syngas biomethanation model also described satisfactorily the behavior of the thermophilic MMC after fitting the model to the experimental data (fig. 4B and 5, and supplementary information file fig. S5). The model was not able to fully describe the period of reduced CO conversion activity at the initial stage of the fermentation between day 3 and 5 when grown at an initial P_{CO} of 0.8 (fig. 5B). However, once the culture reached exponential growth phase, all model variables followed closely the experimental measurements in the

experiments used for model calibration. The estimated parameter $\mu_{\max,\text{hyd}}$ found (10.93 d⁻¹) was very similar to the μ_{\max} value of 11.76 d⁻¹ previously reported by Schönheit et al. [31] for *Methanothermobacter marburgensis* (f. *Methanobacterium thermoautotrophicum* strain Marburg) growing on H₂/CO₂, from where the value for $k_{s,\text{hyd}}$ was extracted. Kinetic characterization studies on carboxydrotrophic hydrogenogens are very limited. To the best knowledge of the authors, there is only one study reporting kinetic parameters for carboxydrotrophic hydrogenogenic growth, corresponding to the species *Carboxydotherrmus hydrogenoformans* [18]. The estimated value of $\mu_{\max,\text{carb_hyd}}$ found here was consistent with the range of μ_{\max} values 3.07-12.93 d⁻¹ obtained in their study, from where the k_s value was originally extracted [18]. However, in this case the value for $k_{s,\text{carb_hyd}}$ was manually reduced 10-fold in order to obtain biologically relevant values for $\mu_{\max,\text{carb_hyd}}$. The least squares estimation of this parameter using their original k_s value (1.45e-3 M) resulted in a $\mu_{\max,\text{carb_hyd}}$ of 57.31 d⁻¹ and a doubling time (t_d) of 0.29 h, which is much shorter than the minimum t_d ever reported for any carboxydrotrophic hydrogenogenic species corresponding to 1h for *Carboxydocella sporoproducens* [45]. In previous work, the microbial composition analysis of the thermophilic MMC used here indicated that the hydrogenogenic conversion of CO was carried out by a species closely related to *Thermincola Carboxydiphila* [22]. Based on the $\mu_{\max,\text{carb_hyd}}$ value of 10.93 d⁻¹ finally determined, the minimum t_d of this microbial group would correspond to 1.52 h and would be consistent with the minimum t_d of 1.3 h previously reported for *Thermincola Carboxydiphila* [46], which confirms that the kinetic parameters obtained in the present study were biologically relevant.

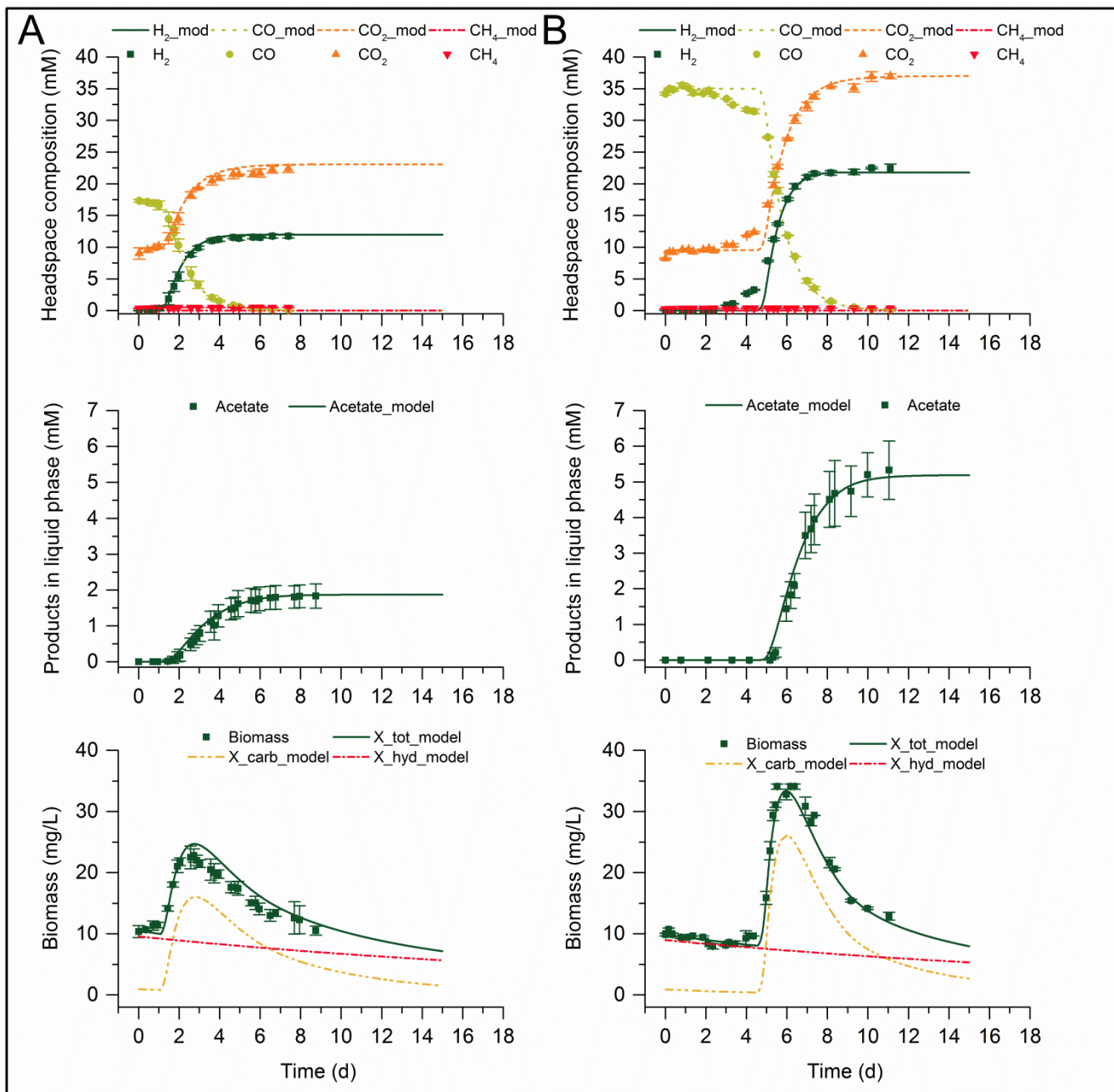


Figure 5. **A** Model fitting to experiment with initial P_{CO} of 0.4 atm and BES addition at thermophilic conditions. **B** Model fitting to experiment with initial P_{CO} of 0.8 atm and BES addition at thermophilic conditions.

As mentioned above, the carboxydotrophic hydrogenogenic microbial group presented a dynamic behavior depending on the operating conditions. The conversion of CO was directed strictly towards H_2 and CO_2 when carboxydotrophic hydrogenogens were grown in syntrophic association with hydrogenotrophic methanogens (fig. 4B), while CO was partially converted into acetate when hydrogenotrophic methanogens were inhibited and H_2 and CO_2 started to accumulate in the headspace (fig. 5). As shown in fig. 5A, the fermentation of CO with an

initial gaseous concentration of CO of 17.3 mM resulted in the production of 11.97 mM of H₂ in the gas phase and 1.87 mM of acetate in the liquid phase, while doubling the initial concentration of CO to 35 mM resulted in the production of 21.79 mM of H₂ in the gas phase and 5.19 mM of acetate in the liquid phase (fig. 5B). This indicated that the ratio of H₂/acetate produced during the fermentation was not constant and depended on the concentration of CO, H₂ and CO₂. Similarly, the biomass concentration profile of these experiments could not be described by strictly substrate-dependent Monod kinetics and a first-order decay rate as the biomass yield seemed to be variable along the fermentation. Both phenomena, the dynamic product and biomass yield, were successfully modelled using eq. 14, 15 and 16, which assume that the yield of H₂ and acetate is directly proportional to the degree of thermodynamic limitation of the conversion of CO into H₂ determined through $F_{T,carb_hyd}$, and that the biomass growth is affected by a maintenance term dependent on a_{carb_hyd} and $F_{T,carb_hyd}$. According to this model, H₂ is the main product of carboxydrotrophic hydrogenogenic metabolism and acetate is a by-product resulting from the thermodynamic limitation of the hydrogenogenesis in order to allow growth on CO when production of H₂ starts to be limited. Additionally, the fact that the value for a_{carb_hyd} of 2.39 obtained here was above 1 indicated that the production of acetate was associated with an increased maintenance cost, possibly related to the synthesis of enzymes needed to excrete acetate as a by-product, and resulted in no net biomass formation. The minimum threshold of Gibbs free energy change for the conversion of CO into H₂/CO₂ defined by $\Delta G_{C,carb_hyd}$ was found to be 8.28 kJ/mol H₂. This value is much lower than the theoretical minimum quantum of metabolically convertible energy (ΔG_{min}) needed in biochemical conversions given by the free energy needed for the translocation of one H⁺ across the membrane, approximately -20 kJ/mol [47]. Nevertheless, more recent findings demonstrated that microbial metabolism can be sustained with much lower minimum energy requirements in several anaerobic microbial groups, including syntrophic fatty acid oxidizers, hydrogenotrophic methanogens and sulfate-reducing bacteria [48,49]. Additionally, the value of $\Delta G_{C,carb_hyd}$ found here is consistent with the findings of Henstra & Stams [50] when studying the ΔG_{min} of *Carboxydotherrmus hydrogenoformans*, where it was found that the ΔG_{min} for H₂ production was around 3 kJ/mol. It should be noted though that the final acetate concentration could not be determined in their study since it fell below their minimum detection levels, which limited the accuracy and probably underestimated the ΔG_{min} value for the production of H₂.

3.5. Models validation and CO inhibition phenomena

The two models were validated with experiments using a fixed initial P_{H₂} and P_{CO₂} of 1 atm and 0.2 atm, respectively, and varying initial P_{CO} from 0.2 atm to 0.8 atm. The simulation of the profile of the headspace composition and the concentration of products in the liquid phase described quite accurately the experimental data in all experiments with small deviations only in the concentration of acetate at mesophilic conditions

(supplementary information file, fig. S6-S12). On the other hand, the simulation of the biomass concentration profile in thermophilic experiments at an initial P_{CO} of 0.6 atm and 0.8 atm presented a considerable overestimation when compared to the experimental measurements. However, the biomass concentration measurements of these experiments seemed to be inconsistent, since the maximum biomass concentrations found at an initial P_{CO} of 0.6 atm (83 mg/L) and 0.8 atm (83 mg/L) were lower than that of the experiment at a P_{CO} of 0.4 atm (93 mg/L) (Supplementary Information file, fig. S10, S11 and S12). Additionally, the fact that the profile of H_2 , CO , CO_2 and CH_4 were well described by the model reveals inconsistencies in the biomass concentration profile as the former should also be affected by the lower biomass concentration. Thus, it can be concluded that the disagreement between the observed and simulated biomass concentration profiles at thermophilic conditions was caused by experimental errors. Overall, despite the deviations in these two experiments, the maximum apparent specific activities for H_2 and CO and the maximum specific CH_4 productivities based on experimental measurements were in agreement with the simulation-based calculations, which show that the model described satisfactorily the performance of the MMC outside the experimental region used for model calibration (fig. 6).

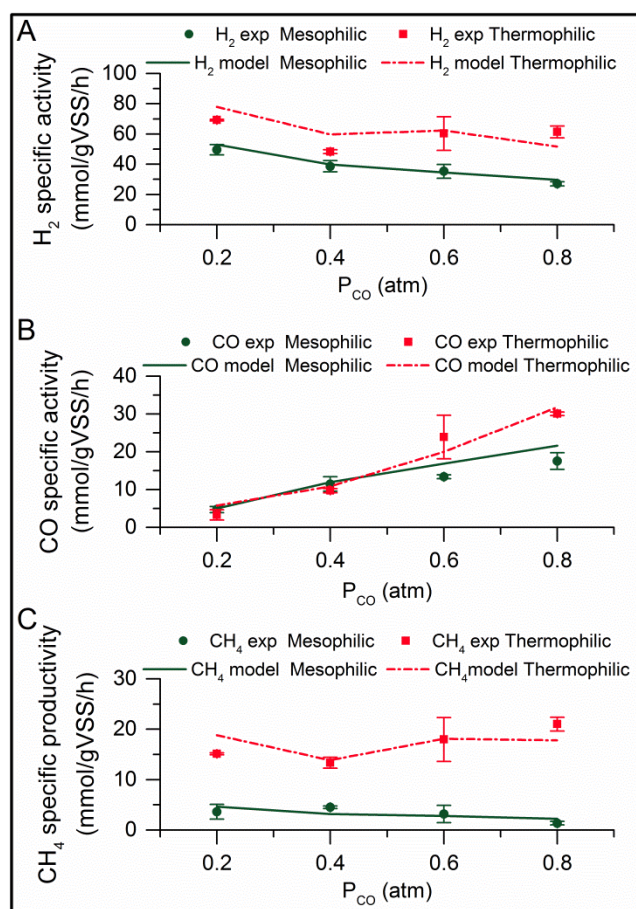


Figure 6. **A** Maximum apparent specific activity for H₂ at varying initial P_{CO} calculated based on experimental measurements and simulations using the same time points. **B** Maximum apparent specific activity for CO at varying initial P_{CO} calculated based on experimental measurements and simulations using the same time points. **C** Maximum apparent specific CH₄ productivity at varying initial P_{CO} calculated based on experimental measurements and simulations using the same time points. It should be noted that the initial P_{CO} given in the x axis corresponds to P_{CO} at 25°C; the effective initial gas partial pressure was higher in both mesophilic and thermophilic conditions due to the increase of temperature during incubation.

The decreasing trend in maximum apparent specific activity of H₂ when increasing the initial P_{CO} found in both mesophilic and thermophilic experiments could be interpreted as a possible inhibition of the homoacetogenic and hydrogenotrophic methanogenic microbial groups due to the higher initial P_{CO} (fig. 6). Nevertheless, the fact that inhibition parameters were not included in the models and that the simulated H₂ maximum specific activities were in agreement with the experimentally calculated indicate that these microbial groups were not affected by CO inhibition phenomena. Instead, the decrease in H₂ maximum specific activity could be attributed to the lower percentage of H₂-consuming microbial groups over the whole MMC when increasing the initial P_{CO}, which changes according to the initial ratio of P_{H₂}/P_{CO}. Other possible CO inhibition phenomena could be expected for the acetoclastic methanogenic microbial group. Several studies have reported inhibitory effects on the acetoclastic methanogenic microbial group due to high P_{CO} in both batch and continuous operating mode with concomitant acetate accumulation [12,51,52]. However, the dataset used in this study could not support the estimation of CO inhibition parameters for this microbial group since the acetoclastic activity typically started once CO was practically depleted with no apparent effect on the acetate conversion rates. Thus, the dataset should be extended with data from continuous mode experiments in order to enable the estimation of CO inhibition parameters. On the other hand, inhibition of the acetoclastic methanogenesis due to low pH could be observed when using an initial P_{CO} of 0.8 atm at mesophilic conditions due to the accumulation of acetate in the fermentation broth (Supplementary Information file, fig. S8). According to the model, the acetate conversion found in this experiment from day 6 could be partially attributed to the syntrophic acetate oxidation catabolic route, which also contributed to the alleviation of the pH inhibition on acetoclastic methanogens (Supplementary Information file, fig. S8).}

The thermophilic MMC was clearly superior in terms of maximum apparent specific productivity of CH₄ when compared to the mesophilic MMC. Based on model simulations, the maximum apparent specific productivity of CH₄ found at an initial P_{CO} of 0.2 atm for the thermophilic MMC (18.8 mmol/g VSS/d) was four times higher than that of the mesophilic (4.6 mmol/g VSS/d), and this difference increased with increasing initial P_{CO}. The higher microbial activity rate found when increasing the incubation temperature could be expected as, generally, thermophilic microorganisms present higher growth rates than mesophilic. According to the estimated kinetic parameters, the carboxydrotrophic microbial trophic group presented a much higher μ_{\max} at thermophilic conditions than at mesophilic conditions, namely 10.93 d⁻¹ and 3.91 d⁻¹ respectively. Nevertheless, if the biomass

yield is considered together with the μ_{\max} , the corresponding k_{\max} of the hydrogenogen (9.62 mmol CO/mg VSS/d) would be only slightly higher than that of the acetogen (8.64 mmol CO/mg VSS/d), which is also reflected in figure 6B. Similarly, the $\mu_{\max,hyd}$ of thermophilic hydrogenotrophic methanogens (11.11 d⁻¹) was much higher than that of the mesophilic (5.03 d⁻¹), but the $k_{s,hyd}$ of the thermophilic was two orders of magnitude lower indicating a much lower substrate affinity. Therefore, such difference in the maximum specific CH₄ productivity cannot be solely explained by the kinetic parameters of the microbial groups present in each MMC, and it is necessary to include the catabolic routes followed towards CH₄ as a major factor determining the overall microbial activity rates. In this case, the thermophilic culture was found to be favored by the faster turnover rates of H₂ as intermediate metabolite along with the fact that H₂ was strictly converted to CH₄, while the productivity of the mesophilic culture was hindered by the strong competition for H₂ between homoacetogens and hydrogenotrophic methanogens and the fact that the slower aceticlastic methanogenesis was the dominant catabolic route leading to CH₄.

3.6. Control over dominant catabolic routes in microbial consortia

Although characteristics like metabolic redundancy and microbial diversity are generally the main assets of MMC in terms of adaptability and resiliency, in some cases, these may also be a clear disadvantage when the carbon is metabolized through suboptimal catabolic routes leading to lower overall productivities. Therefore, an effective way of improving the performance of MMC would be gaining control over the dominant catabolic routes employed through the conversion as this would allow for maximizing the product selectivity, yield and productivity of the process. This would be highly desirable not only from an industrial application perspective, but also for the enrichment and isolation of e.g. specific microbial groups or novel species carrying out specific biotransformations.

Gaining control over the performance of MMC requires knowledge on which are the main mechanisms and parameters determining the outcome of the fermentation. The models developed here were able to describe the performance of the mesophilic and thermophilic MMC by considering cross-feeding interactions, mutualistic interactions, and mutual exclusion interactions based on kinetic and thermodynamic competition among different microbial groups, all of which determined the dominant catabolic routes leading to CH₄. Based on these interactions, two possible strategies for controlling the catabolic routes employed by the MMC are demonstrated through model simulations: the first using kinetic control through the mass transfer, and the second using thermodynamic control through the P_{CO_2} .

3.6.1. Kinetic control - Mass transfer

As stated above, one of the main limitations of the mesophilic MMC derived from the competition for H_2 between homoacetogens and hydrogenotrophic methanogens, which resulted in a significant fraction of carbon from syngas diverted towards acetic acid as intermediate metabolite. The kinetic parameters found and the thermodynamics of these microbial groups suggest that the competition for H_2 is both kinetically and thermodynamically driven, where high H_2 concentration in the liquid phase should favor the dominance of the homoacetogenic microbial group, while hydrogenotrophic methanogens should be able to outperform homoacetogens at limiting H_2 concentrations. According to this, the concentration of H_2 in the liquid phase should be a key parameter determining the dominant H_2/CO_2 catabolic route employed by the MMC. Therefore, the possibility of controlling these catabolic routes through the modulation of the H_2 gas-to-liquid mass transfer rate was evaluated based on model simulations in batch mode with varying k_La coefficient values.

The simulations revealed that the mass transfer exerts a strong effect on the concentration of H_2 in the liquid phase during exponential growth, and consequently determines the result of the competition between homoacetogens and hydrogenotrophic methanogens. As shown in figure 7A, the simulations of the H_2 conversion using the lower range of evaluated k_La values resulted in a drastic drop in the concentration of H_2 in the liquid, whereas using the higher range of k_La values resulted in a H_2 concentration profile approaching saturation levels until H_2 was depleted. Consequently, high mass transfer rates should favor growth of homoacetogens due to the higher concentration of H_2 in the liquid during the fermentation, while low mass transfer rates should allow for hydrogenotrophic methanogens to consume most of the H_2 since its concentration in the liquid should be very low from the beginning of the fermentation. This is shown in figure 7B, where it can be seen that, according to the model, hydrogenotrophic methanogens would become dominant at k_La coefficients below 200 d^{-1} while homoacetogens would dominate above that value. In this case, the model simulations predict that the relative abundance of homoacetogens would not reach values significantly higher than 65% in the simulations, since (i) both microbial groups are able to grow simultaneously at high H_2 concentrations during batch operation and (ii), independently of the k_La coefficient used, H_2 would always decrease to concentrations low enough to allow for considerable growth of hydrogenotrophic methanogens. This control strategy based on the modulation of the mass transfer would be a valuable tool for the enrichment and isolation of species from specific microbial groups competing for gaseous substrates when operating in batch mode or even for bioaugmentation operational strategies. It should be noted though that, in terms of industrial application, this catabolic route control strategy would only be applicable to processes operating in batch mode or continuous mode under plug-flow regime, since the typically substrate-limiting conditions found in CSTR-like reactors would neglect the effect of the mass transfer on the H_2 concentration in the liquid, making it strictly dependent

on the liquid dilution rate. Additionally, the effect of the mass transfer on the productivity of CH₄ should be evaluated carefully since decreasing the mass transfer rate would also result in lower overall productivity of the system.

While the mass transfer rate may exert a strong effect on the dominant H₂-converting catabolic routes, the effect of changing the mass transfer on the conversion of CO would be strictly related to the microbial activity rate. The mesophilic MMC presented only one carboxydrotrophic microbial group, and consequently, changes in the mass transfer would not affect the catabolic routes converting CO. In this case, the effect of the mass transfer would be limited to the CO conversion rate and the productivity of acetate.

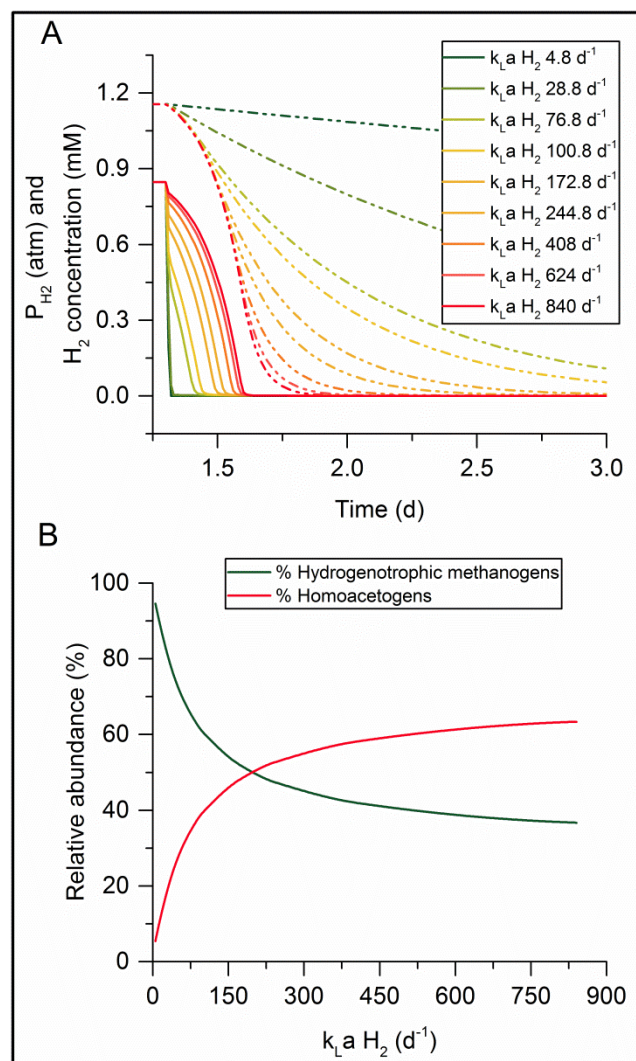


Figure 7. **A** Simulation of the conversion of H₂ over time by homoacetogens and hydrogenotrophic methanogens using different k_La_{H₂} values. Dashed lines represent the P_{H₂} of the headspace and solid lines represent the concentration of H₂ in the liquid phase. **B** Relative abundance of hydrogenotrophic methanogens and homoacetogens at the end of the fermentation plotted as a function of k_La_{H₂}.

3.6.2. Thermodynamic control – P_{CO_2}

The examples of thermodynamics-based control of the catabolic routes given here are intended to circumvent some of the issues related to reduced product selectivity typically encountered in both mesophilic and thermophilic syngas biomethanation processes.

At mesophilic conditions, although the process generally presents high product selectivity towards CH_4 (>65% e-mols recovered as CH_4), acetate and other volatile fatty acids (VFAs) tend to accumulate as by-products of the process accounting for up to 20-25% of the e-mols contained in syngas in some cases [12]. The reason for which VFAs remain unconverted in the liquid phase is typically attributed to the inhibition of the acetoclastic microbial group due to the presence of CO [51–53]. Therefore, alternative configurations involving a two-stage process for conversion of syngas into acetate and subsequent acetate conversion into CH_4 have been proposed to circumvent the CO inhibition of this microbial group [54]. In this work, an alternative strategy applying thermodynamic control over acetate-converting catabolic routes is proposed, which would allow for circumventing the inhibition of the acetoclastic methanogens by steering the acetate conversion towards syntrophic acetate oxidation, achieving a complete conversion of syngas into CH_4 in a single-stage process. Additionally, μ_{max} values reported for syntrophic fatty acid oxidizers (0.4-2.7 d^{-1}) are generally higher than those of acetoclastic methanogens (0.4-1.4 d^{-1}) [24,26], for which shifting the dominant acetate-converting catabolic route towards syntrophic acetate oxidation would result not only in much lower VFAs concentration remaining as by-products, but most probably with higher CH_4 productivity as higher dilution rates could be applied.

Syntrophic acetate oxidizers typically play a negligible role during syngas biomethanation due to the high CO_2 content in the off-gas stream given that often CO_2 is in stoichiometric excess in syngas [12], which renders this reaction thermodynamically unfeasible. However, this catabolic route could be enabled by reducing the P_{CO_2} to levels low enough so that this reaction becomes thermodynamically feasible. The possibility of applying this catabolic route control strategy was evaluated through model simulations with varying fixed P_{CO_2} using acetate as the only substrate in order to make the syntrophic acetate oxidation reaction initially feasible. The results of the simulations revealed that, according to the kinetic parameters used in the mesophilic model, syntrophic acetate oxidizers would be able to compete for acetate and dominate the culture below a P_{CO_2} of 0.01 atm, and would present a relative abundance over 90% when decreasing the P_{CO_2} down to 0.0015 atm. (fig. 8A). The strong influence of the P_{CO_2} on the thermodynamic feasibility of the syntrophic acetate oxidation can also be observed through a plot of the evolution of the thermodynamic potential factor (F_T) during fermentations at varying P_{CO_2} (fig. 8B). This figure shows that the syntrophic acetate oxidation would be strictly thermodynamically controlled when operating at P_{CO_2} above 0.1 atm, with F_T values below 1 at all times and

would approach its limits of thermodynamic feasibility during the early stage of the fermentation, while operating at P_{CO_2} below 0.1 atm would allow for kinetic control of the conversion rate (F_T values of 1 implying no thermodynamic limitation and higher conversion rates) for much longer during the fermentation (fig. 8B). Therefore, it should be possible to engineer the operating conditions to drive a shift of the dominant acetate-converting catabolic route from aceticlastic methanogenesis to syntrophic acetate oxidation when operating in continuous mode at mesophilic conditions. At thermophilic conditions, achieving this metabolic shift would be even easier given that the thermodynamic feasibility of the syntrophic acetate oxidation increases with the incubation temperature. In practice, this catabolic route control strategy could be applied either by optimizing the syngas composition used as feedstock or by supplying additional H_2 originating from e.g. water electrolysis.

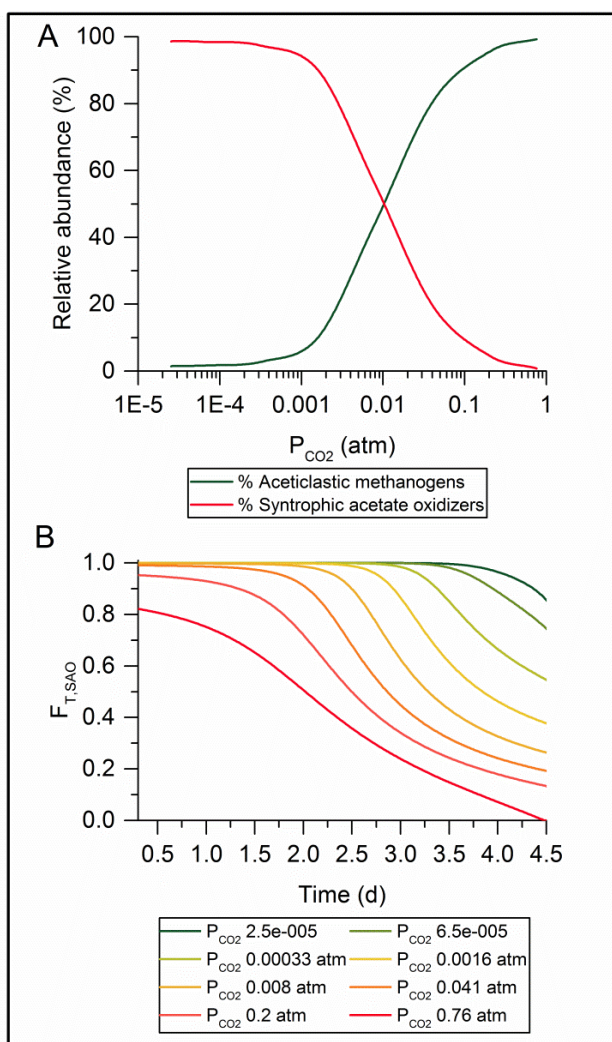


Figure 8. **A** Relative abundance of aceticlastic methanogens and syntrophic acetate oxidizers as a function of P_{CO_2} in both fermentation using acetate (initial concentration of 25 mM) as the only substrate. **B** Simulation of the evolution of the thermodynamic potential factor for syntrophic acetate oxidation ($F_{T,SAO}$) during the course of acetate fermentations using different fixed P_{CO_2} .

Similarly to mesophilic conditions, the product selectivity of the thermophilic syngas biomethanation process is also often limited by the partial production of acetate as a by-product. Even when using a co-culture composed by *C. hydrogenoformans* and *M. thermoautotrophicus*, where CO would be expected to be converted strictly into H₂/CO₂, the amount of carbon diverted towards acetate accounted for 7.9-15.4% of the product distribution in Cmol basis [55]. The acetogenic capabilities of the carboxydophilic hydrogenogen *C. hydrogenoformans* when grown alone have been shown previously [50]. In previous work, it was demonstrated that the thermophilic enriched MMC used here, dominated by the carboxydophilic hydrogenogen *T. carboxydiphila*, is also capable of partial production of acetate from CO when methanogens are inhibited (fig. 5) [22]. In this work, it was found that, in the thermophilic MMC, the production of acetate from CO is triggered by the thermodynamic limitation of the conversion of CO into H₂/CO₂ when the latter start to accumulate in the headspace. This dynamic product yield was modelled through $F_{T,carb,hyd}$ based on eq. 14 and 15. According to this, the metabolic shift from hydrogenogenesis towards acetogenesis could be controlled through the thermodynamic feasibility of the hydrogenogenesis, which could be achieved by modulating the P_{CO₂} since decreasing P_{CO₂} would result in higher thermodynamic drive for the hydrogenogenesis. This is shown in figure 9, where it can be seen that the thermodynamic feasibility of the hydrogenogenesis is highly sensitive to changes in P_{CO₂} and that the product selectivity towards H₂ could be increased from 68% to 95% by decreasing P_{CO₂} from 0.27 atm to 0.0027 atm. Therefore, modulating P_{CO₂} could allow for minimizing the formation of acetate as by-product in thermophilic syngas biomethanation processes, which could be achieved either through the optimization of the syngas composition or by addition of external H₂ originating from e.g. water electrolysis.

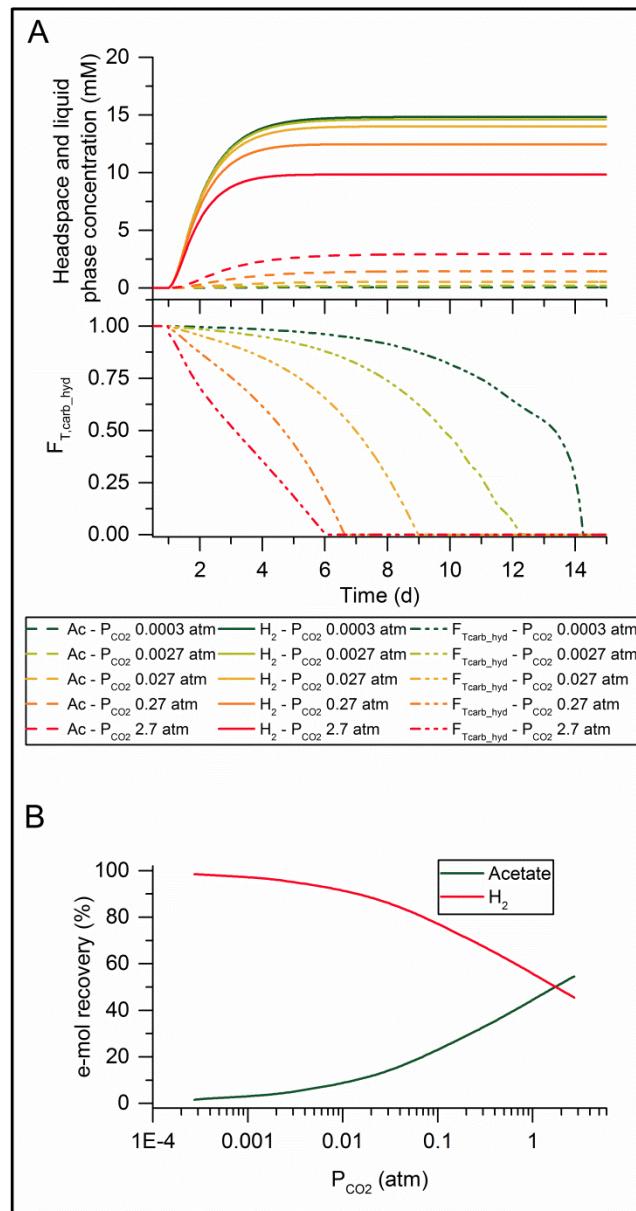


Figure 9. **A** Simulation of H_2 and acetate concentration profiles and evolution of the thermodynamic potential factor for carboxydrotrophic hydrogenogenesis ($F_{T,carb,hyd}$) during the fermentation of CO (0.4 atm) with BES addition using different fixed P_{CO_2} . **B** Percentage of e-mols recovered as H_2 and acetate as a function of P_{CO_2} when fermenting CO with addition of BES to inhibit methanogenic archaea.

4. Conclusions

To the best knowledge of the authors, the models developed in this work constitute the first attempt of modeling the syngas biomethanation process at mesophilic and thermophilic conditions. After parameter estimation and determination of the overall mass transfer coefficients for all gases, both models were able to describe satisfactorily the performance of syngas-converting MMC used here in terms of microbial interactions, microbial

specific activities and overall CH₄ productivity over time. All microbial growth processes included in the models were made thermodynamically consistent, which allowed for predicting metabolic shifts between different catabolic routes available to the MMC, at both mesophilic and thermophilic operating conditions. Based on the microbial interactions considered in the models, several strategies for directing the microbial activity by controlling the catabolic routes employed by the MMC were identified. The results revealed that the limitations typically found in syngas biomethanation processes related to product selectivity and, to some extent, to CH₄ productivity could be addressed by applying either kinetic or thermodynamic control over the catabolic routes employed by the MMC.

Nomenclature

$\Delta_r G'$	Corrected Gibbs free energy change of reaction
ΔG_A	Free energy available given by $-\Delta_r G'$
ΔG_C	Gibbs free energy conserved
Y_{ATP}	ATP yield
ΔG_p	Gibbs free energy of phosphorylation
χ	Average stoichiometric number
ΔG_{min}	Minimum threshold $\Delta_r G'$ of a biochemical reaction
t_{lag}	Duration of lag phase period
pH _{UL}	Upper limit of pH with no inhibition
pH _{LL}	Lower limit of pH with complete inhibition
μ	Specific growth rate
μ_{carb}	μ for carboxydrotrophic acetogens
μ_{carb_hyd}	μ for carboxydrotrophic hydrogenogens
μ_{hom}	μ for homoacetogens
μ_{hyd}	μ for hydrogenotrophic methanogens
μ_{ac}	μ for acetoclastic methanogens
μ_{SAO}	μ for syntrophic acetate oxidizers
μ_{SPO}	μ for syntrophic propionate oxidizers
$\mu_{max, i}$	Maximum specific growth rate for microbial group i
$k_{S, i}$	Saturation constant for microbial group i
$m_{S, i}$	Specific maintenance rate for microbial group i
a_i	Measure of maintenance cost severity for microbial group i

$F_{T,i}$	Thermodynamic potential factor for microbial group i
$k_{d,i}$	Specific decay rate for microbial group i
$k_{La,i}$	Overall mass transfer coefficient for compound i
δ_j^{msqr}	Sensitivity measure for parameter j
γ_K	Collinearity index for parameter subset k

Acknowledgements

This work was financially supported by the Technical University of Denmark (DTU) and Innovation Foundation-DK in the frame of SYNFERON project.

Conflict of Interest

The authors declare that they have no conflict of interest.

References

- [1] Bagi Z, Ács N, Böjti T, Kakuk B, Rákhely G, Strang O, et al. Biomethane: The energy storage, platform chemical and greenhouse gas mitigation target. *Anaerobe* 2017;46:13–22. doi:10.1016/j.anaerobe.2017.03.001.
- [2] Geppert F, Buisman C, Liu D, van Eerten-Jansen M, ter Heijne A, Weidner E. Bioelectrochemical Power-to-Gas: State of the Art and Future Perspectives. *Trends Biotechnol* 2016;34:879–94. doi:10.1016/j.tibtech.2016.08.010.
- [3] Younas M, Loong Kong L, Bashir MJK, Nadeem H, Shehzad A, Sethupathi S. Recent Advancements, Fundamental Challenges, and Opportunities in Catalytic Methanation of CO₂. *Energy and Fuels* 2016;30:8815–31. doi:10.1021/acs.energyfuels.6b01723.
- [4] Asimakopoulos K, Gavala HN, Skiadas IV. Reactor systems for syngas fermentation processes: A review. *Chem Eng J* 2018;732–44. doi:10.1016/j.cej.2018.05.003.
- [5] Daniell J, Köpke M, Simpson S. Commercial Biomass Syngas Fermentation. *Energies* 2012;5:5372–417. doi:10.3390/en5125372.
- [6] Kumar A, Jones DD, Hanna MA. Thermochemical Biomass Gasification: A Review of the Current Status

of the Technology. *Energies* 2009;2:556–81. doi:10.3390/en20300556.

- [7] Redl S, Diender M, Ølshøj T, Sousa DZ, Toftgaard A. Exploiting the potential of gas fermentation. *Ind Crop Prod* 2017;106:21–30. doi:10.1016/j.indcrop.2016.11.015.
- [8] Guiot SR, Cimpioia R. Potential of Wastewater-Treating Anaerobic Granules for Biomethanation of Synthesis Gas. *Environ Sci Technol* 2011;45:2006–12.
- [9] François J, Abdelouahed L, Mauviel G, Feidt M, Rogaume C, Mirgaux O, et al. Estimation of the energy efficiency of a wood gasification CHP plant using Aspen Plus. *Chem Eng Trans* 2012;29:769–74. doi:10.3303/CET1229129.
- [10] Michailos S, Emenike O, Ingham D, Hughes KJ, Pourkashanian M. Methane production via syngas fermentation within the bio-CCS concept: A techno-economic assessment. *Biochem Eng J* 2019;150:107290. doi:10.1016/j.bej.2019.107290.
- [11] O’Brien JM, Wolkin RH, Moench TT, Morgan JB, Zeikus JG. Association of hydrogen metabolism with unitrophic or mixotrophic growth of *Methanosarcina barkeri* on carbon monoxide. *J Bacteriol* 1984;158:373–5.
- [12] Asimakopoulos K, Gavala HN, Skiadas IV. Biomethanation of Syngas by Enriched Mixed Anaerobic Consortia in Trickle Bed Reactors. *Waste and Biomass Valorization* 2019. doi:10.1007/s12649-019-00649-2.
- [13] Klasson KT, Cowger JP, Ko CW, Vega JL, Clausen EC, Gaddy JL. Methane production from synthesis gas using a mixed culture of *R. rubrum*, *M. barkeri*, and *M. formicicum*. *Appl Biochem Biotechnol* 1990;24–25:317–28.
- [14] Diender M, Pereira R, Wessels HJCT, Stams AJM, Sousa DZ. Proteomic Analysis of the Hydrogen and Carbon Monoxide Metabolism of *Methanothermobacter marburgensis*. *Front Microbiol* 2016;7:1–10. doi:10.3389/fmicb.2016.01049.
- [15] Grimalt-Alemany A, Skiadas IV., Gavala HN. Syngas biomethanation: State-of-the-art review and perspectives. *Biofuels, Bioprod Biorefining* 2018;12:139–58. doi:10.1002/bbb.1826.
- [16] Kleerebezem R, van Loosdrecht MC. Mixed culture biotechnology for bioenergy production. *Curr Opin Biotechnol* 2007;18:207–12. doi:10.1016/j.copbio.2007.05.001.

- [17] Vega JL, Clausen EC, Gaddy JL. Design of bioreactors for coal synthesis gas fermentations. *Resour Conserv Recycl* 1990;3:149–60. doi:10.1016/0921-3449(90)90052-6.
- [18] Zhao Y, Cimpoia R, Liu Z, Guiot SR. Kinetics of CO conversion into H₂ by *Carboxydotherrmus hydrogenoformans*. *Appl Microbiol Biotechnol* 2011;91:1677–84. doi:10.1007/s00253-011-3509-7.
- [19] Ako OY, Kitamura Y, Intabon K, Satake T. Steady state characteristics of acclimated hydrogenotrophic methanogens on inorganic substrate in continuous chemostat reactors. *Bioresour Technol* 2008;99:6305–10. doi:10.1016/j.biortech.2007.12.016.
- [20] Pan X, Angelidaki I, Alvarado-Morales M, Liu H, Liu Y, Huang X, et al. Methane Production from Formate, Acetate and H₂/CO₂; focusing on kinetics and microbial characterization. *Bioresour Technol* 2016;218:796–806. doi:10.1016/j.biortech.2016.07.032.
- [21] Jin Q, Bethke CM. The thermodynamics and kinetics of microbial metabolism. *Am J Sci* 2007;307:643–77. doi:10.2475/04.2007.01.
- [22] Grimalt-Aleman A, Łężyk M, Kennes-Veiga DM, Skiadas I V., Gavala HN. Enrichment of mesophilic and thermophilic mixed microbial consortia for syngas biomethanation: the role of kinetic and thermodynamic competition. *Waste and Biomass Valorization* 2019. doi:10.1007/s12649-019-00595-z.
- [23] APHA, AWWA, WEF. *Standard Methods for the Examination of Water and Wastewater*. 20th Ed. Washington DC: 1997.
- [24] Batstone DJ, Keller J, Angelidaki I, Kalyuzhnyi S., Pavlostathis S., Rozzi A, et al. The IWA Anaerobic Digestion Model No 1 (ADM1). *Water Sci Technol* 2002;45:65–73. doi:10.2166/wst.2008.678.
- [25] Alberty RA. *Thermodynamics of Biochemical Reactions*. New Jersey: John Wiley & Sons, Inc; 2003.
- [26] Cord-ruwisch R, Lovley DR. Growth of *Geobacter sulfurreducens* with Acetate in Syntrophic Cooperation with Hydrogen-Oxidizing Anaerobic Partners. *Appl Environ Microbiol* 1998;64:2232–6.
- [27] Leng L, Yang P, Singh S, Zhuang H, Xu L, Chen W. A review on the bioenergetics of anaerobic microbial metabolism close to the thermodynamic limits and its implications for digestion applications. *Bioresour Technol* 2018;247:1095–106. doi:10.1016/j.biortech.2017.09.103.
- [28] Siegrist H, Vogt D, Garcia-Heras JL, Gujer W. Mathematical model for meso- and thermophilic anaerobic sewage sludge digestion. *Environ Sci Technol* 2002;36:1113–23. doi:10.1021/es010139p.

- [29] Ni BJ, Liu H, Nie YQ, Zeng RJ, Du GC, Chen J, et al. Coupling glucose fermentation and homoacetogenesis for elevated acetate production: Experimental and mathematical approaches. *Biotechnol Bioeng* 2011;108:345–53. doi:10.1002/bit.22908.
- [30] Kim MS, Bae SS, Kim YJ, Kim TW, Lim JK, Lee SH, et al. Co-dependent H₂ production by genetically engineered *Thermococcus onnurineus* NA1. *Appl Environ Microbiol* 2013;79:2048–53. doi:10.1128/AEM.03298-12.
- [31] Schönheit P, Moll J, Thauer RK. Growth Parameters ($K_{s,s}$, μ_{max} , Y_s) of *Methanobacterium thermoautotrophicum*. *Arch Microbiol* 1980;127:59–65.
- [32] Sin G, Gernaey KV. Data handling and parameter estimation. *Exp. METHODS WASTEWATER Treat.*, IWA Publishing Company; 2016, p. 201–34.
- [33] Sin G, Meyer AS, Gernaey KV. Assessing reliability of cellulose hydrolysis models to support biofuel process design — Identifiability and uncertainty analysis. *Comput Chem Eng J* 2010;34:1385–92. doi:10.1016/j.compchemeng.2010.02.012.
- [34] Brun R, Martin K, Siegrist H, Gujer W, Reichert P. Practical identifiability of ASM2d parameters — systematic selection and tuning of parameter subsets. *Water Res* 2002;36:4113–27.
- [35] Van Bodegom P. Microbial maintenance: A critical review on its quantification. *Microb Ecol* 2007;53:513–23. doi:10.1007/s00248-006-9049-5.
- [36] Kalafatakis S, Skiadas IV., Gavala HN. Determining butanol inhibition kinetics on the growth of *Clostridium pasteurianum* based on continuous operation and pulse substrate additions. *J Chem Technol Biotechnol* 2019:1–8. doi:10.1002/jctb.5919.
- [37] Reichart P. AQUASIM 2.0 - Computer Program for the Identification and Simulation of Aquatic Systems. Dubendorf: EAWAG; 1998.
- [38] Klöckner W, Gacem R, Anderlei T, Raven N, Schillberg S, Lattermann C. Correlation between mass transfer coefficient $k_L a$ and relevant operating parameters in cylindrical disposable shaken bioreactors on a bench-to-pilot scale. *J Biol Eng* 2013;7:1–14.
- [39] Ferreira A, Ferreira C, Teixeira JA, Rocha F. Temperature and solid properties effects on gas-liquid mass transfer. *Chem Eng J* 2010;162:743–52. doi:10.1016/j.cej.2010.05.064.

- [40] Munasinghe PC, Khanal SK. Syngas fermentation to biofuel: Evaluation of carbon monoxide mass transfer coefficient (k_{La}) in different reactor configurations. *Biotechnol Prog* 2010;26:1616–21. doi:10.1002/btpr.473.
- [41] Orgill JJ, Atiyeh HK, Devarapalli M, Phillips JR, Lewis RS, Huhnke RL. A comparison of mass transfer coefficients between trickle-bed, Hollow fiber membrane and stirred tank reactors. *Bioresour Technol* 2013;133:340–6. doi:10.1016/j.biortech.2013.01.124.
- [42] Schmidt JE, Ahring BK. Immobilization patterns and dynamics of acetate-utilizing methanogens immobilized in sterile granular sludge in upflow anaerobic sludge blanket reactors. *Appl Environ Microbiol* 1999;65:1050–4.
- [43] Pavlostathis SG, Giraldo-Gomez E. Kinetics of Anaerobic Treatment: A Critical Review. *Crit Rev Environ Control* 1991;21:411–90.
- [44] Kotsyurbenko OR, Glagolev M V., Nozhevnikova AN, Conrad R. Competition between homoacetogenic bacteria and methanogenic archaea for hydrogen at low temperature. *FEMS Microbiol Ecol* 2001;38:153–9. doi:10.1016/S0168-6496(01)00179-9.
- [45] Slepova T V., Sokolova TG, Lysenko AM, Tourova TP, Kolganova T V., Kamzolkina O V., et al. *Carboxydocella sporoproducens* sp. nov., a novel anaerobic CO-utilizing/H₂-producing thermophilic bacterium from a Kamchatka hot spring. *Int J Syst Evol Microbiol* 2006;56:797–800. doi:10.1099/ijs.0.63961-0.
- [46] Sokolova TG, Kostrikina NA, Chernyh NA, Kolganova T V., Tourova TP, Bonch-Osmolovskaya EA. *Thermincola carboxydiphila* gen. nov., sp. nov., a novel anaerobic, carboxydotrophic, hydrogenogenic bacterium from a hot spring of the Kae Baikal area. *Int J Syst Evol Microbiol* 2005;55:2069–73. doi:10.1099/ijs.0.63299-0.
- [47] Schink B. Energetics of Syntrophic Cooperation in Methanogenic Degradation. *Microbiol Mol Biol Rev* 1997;61:262–80.
- [48] Jackson BE, McInerney MJ. Anaerobic microbial metabolism can proceed close to thermodynamic limits. *Nature* 2002;415:454–6.
- [49] Hoehler TM, Alperin MJ, Albert DB, Martens CS. Apparent minimum free energy requirements for methanogenic Archaea and sulfate-reducing bacteria in an anoxic marine sediment. *FEMS Microbiol*

Ecol 2001;38:33–41. doi:10.1016/S0168-6496(01)00175-1.

- [50] Henstra AM, Stams AJM. Deep Conversion of Carbon Monoxide to Hydrogen and Formation of Acetate by the Anaerobic Thermophile *Carboxydotherrmus hydrogenoformans*. Int J Microbiol 2011;2011:1–4. doi:10.1155/2011/641582.
- [51] Esquivel-elizondo S, Krajmalnik-brown R, Miceli J, Cesar III. Impact of carbon monoxide partial pressures on methanogenesis and medium chain fatty acids production during ethanol fermentation. Biotechnol Bioeng 2018;115:341–50. doi:10.1002/bit.26471.
- [52] Navarro SS, Cimpoaia R, Bruant G, Guiot SR. Biomethanation of Syngas Using Anaerobic Sludge: Shift in the Catabolic Routes with the CO Partial Pressure Increase. Front Microbiol 2016;7:1–13. doi:10.3389/fmicb.2016.01188.
- [53] Luo G, Wang W, Angelidaki I. Anaerobic digestion for simultaneous sewage sludge treatment and CO biomethanation: process performance and microbial ecology. Environ Sci Technol 2013;47:10685–93. doi:10.1021/es401018d.
- [54] Luo G, Jing Y, Lin Y, Zhang S, An D. A novel concept for syngas biomethanation by two-stage process: Focusing on the selective conversion of syngas to acetate. Sci Total Environ 2018;645:1194–200. doi:10.1016/j.scitotenv.2018.07.263.
- [55] Diender M, Uhl PS, Bitter JH, Stams AJM, Sousa DZ. High Rate Biomethanation of Carbon Monoxide-Rich Gases via a Thermophilic Synthetic Coculture. ACS Sustain Chem Eng 2018;6:2169–76. doi:10.1021/acssuschemeng.7b03601.

Modeling of Syngas Biomethanation and Control of Catabolic Routes of Mesophilic and Thermophilic Mixed Microbial Consortia (Supplementary Information File 1)

*Antonio Grimalt-Alemany, Konstantinos Asimakopoulos, Ioannis V. Skiadas, Hariklia N. Gavala**

*Correspondence: hnga@kt.dtu.dk, hari_gavala@yahoo.com

Department of Chemical and Biochemical Engineering, Technical University of Denmark, Søtofts Plads 229, 2800 Kgs. Lyngby, Denmark

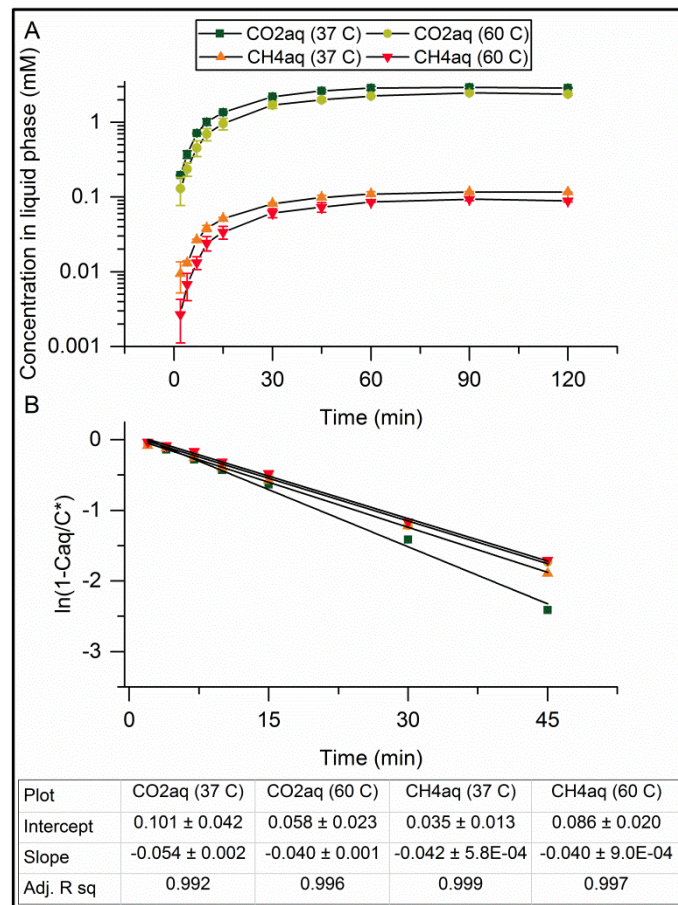


Figure S1. **A** Concentration of CO₂ and CH₄ in the liquid phase over time at mesophilic and thermophilic conditions. **B** Plot of linearized eq. 18 in the form $\ln(1-C_{aq}/(H \cdot C_g)) = -k_L a \cdot t$ used to determine $k_{L a_{CO_2}}$ and $k_{L a_{CH_4}}$ at mesophilic and thermophilic conditions.

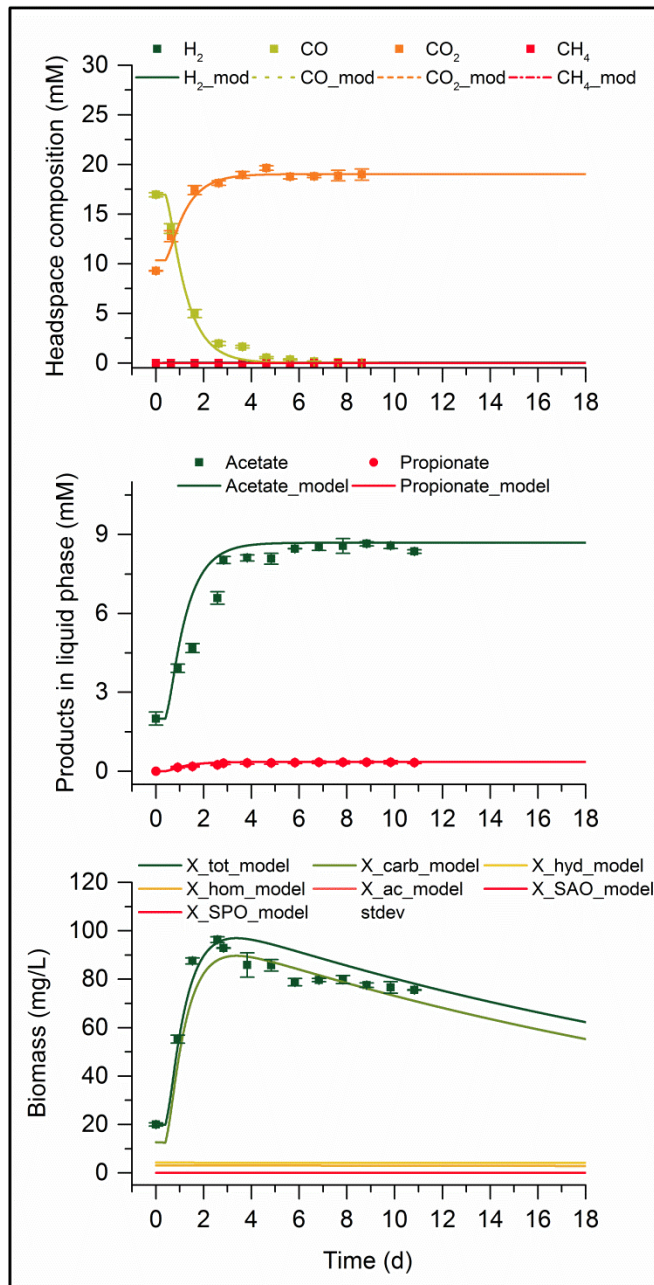


Figure S2. Model fitting to experiment at mesophilic conditions with addition of BES to inhibit methanogenic growth and an initial P_{CO} of 0.4 atm.

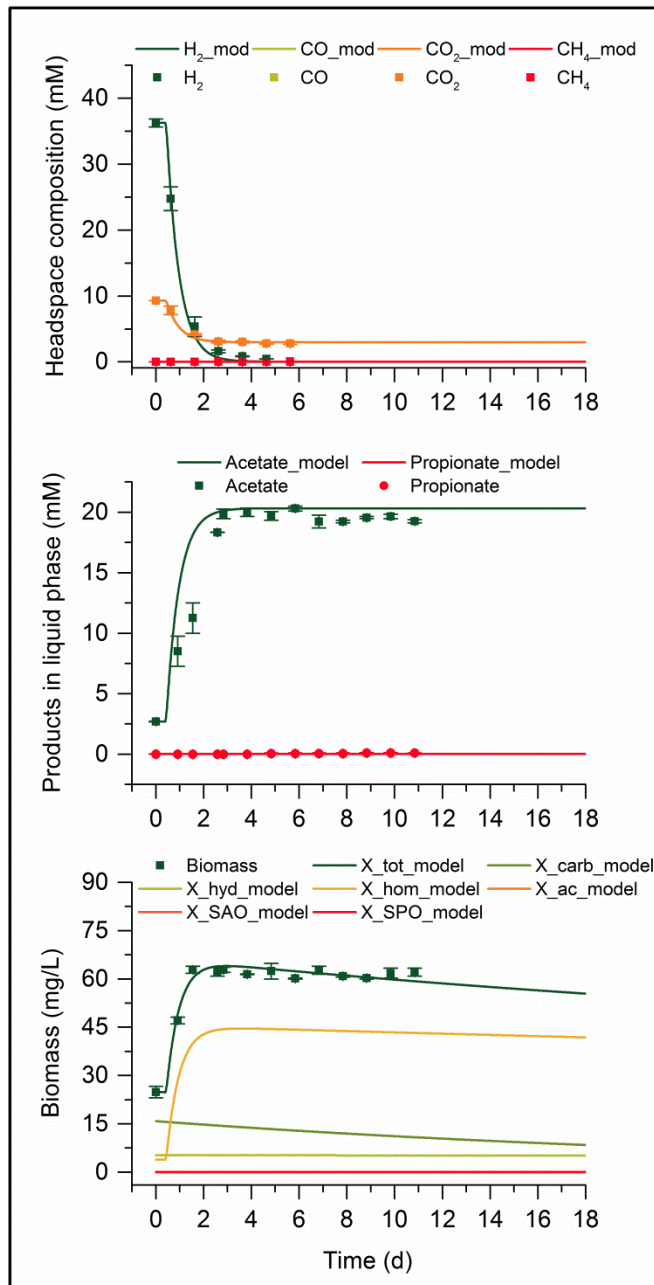


Figure S3. Model fitting to experiment at mesophilic conditions with addition of BES to inhibit methanogenic growth and an initial P_{H_2} and P_{CO_2} of 0.8 atm and 0.2 atm, respectively.

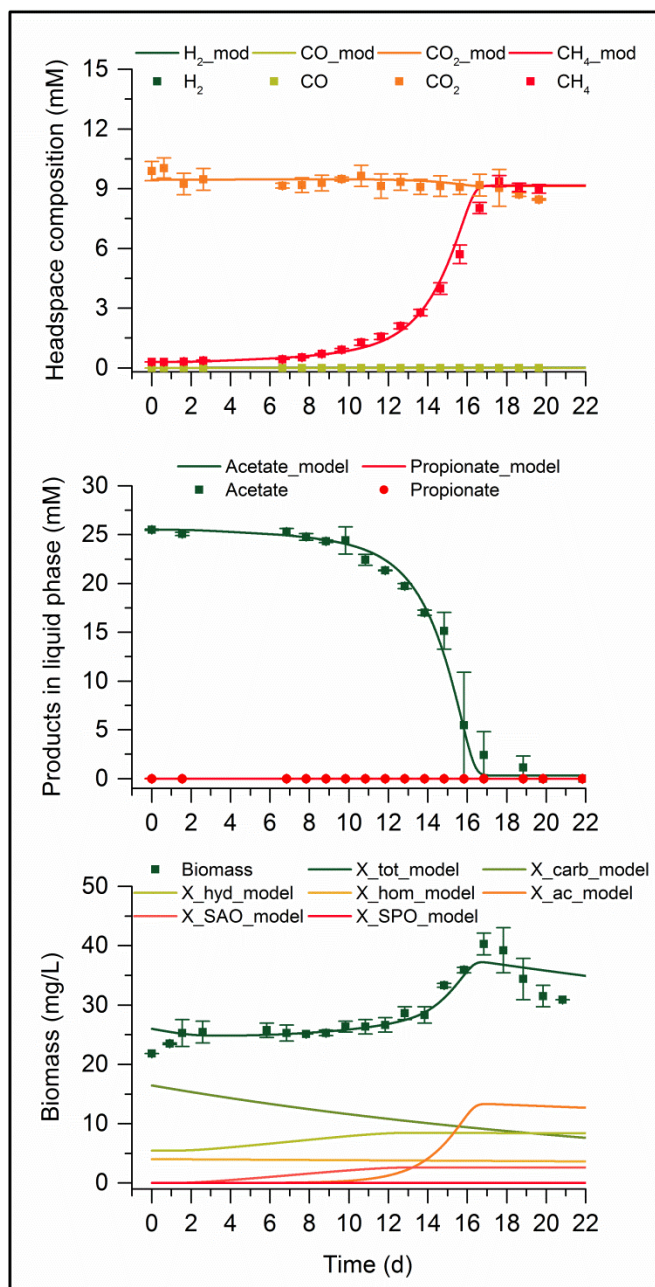


Figure S4. Model fitting to experiment at mesophilic conditions with addition of acetate (25 mM) as the only substrate.

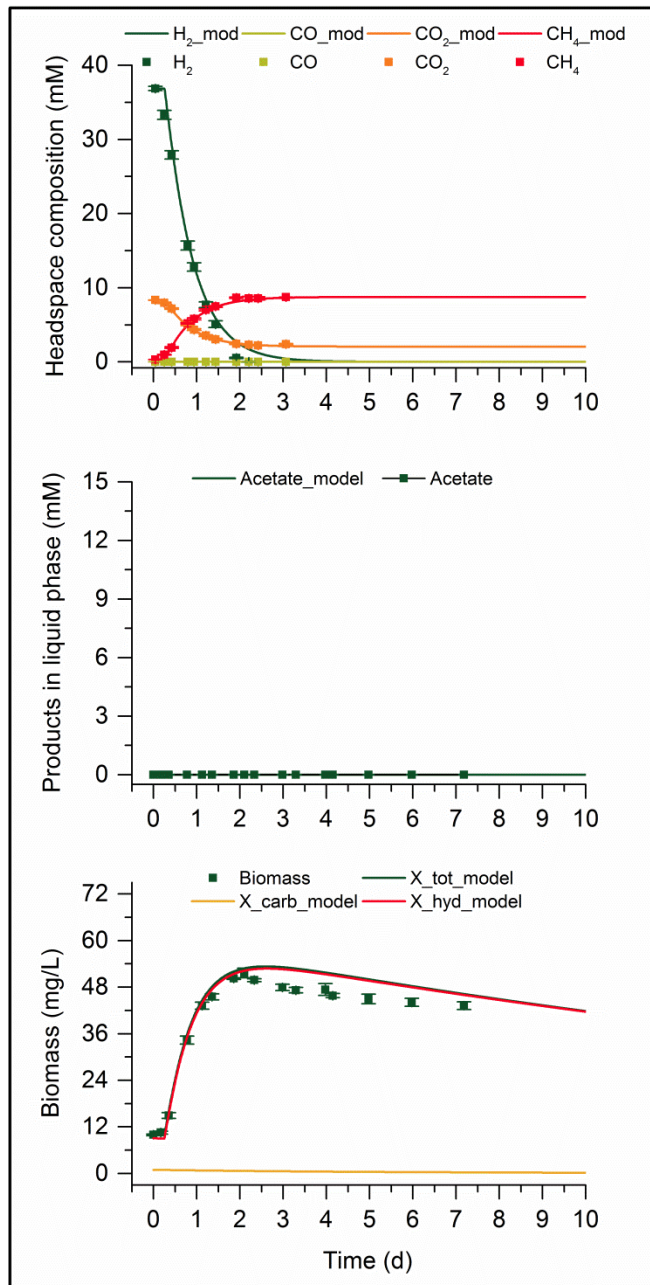


Figure S5. Model fitting to experiment at thermophilic conditions with an initial P_{H_2} and P_{CO_2} of 0.8 atm and 0.2 atm, respectively.

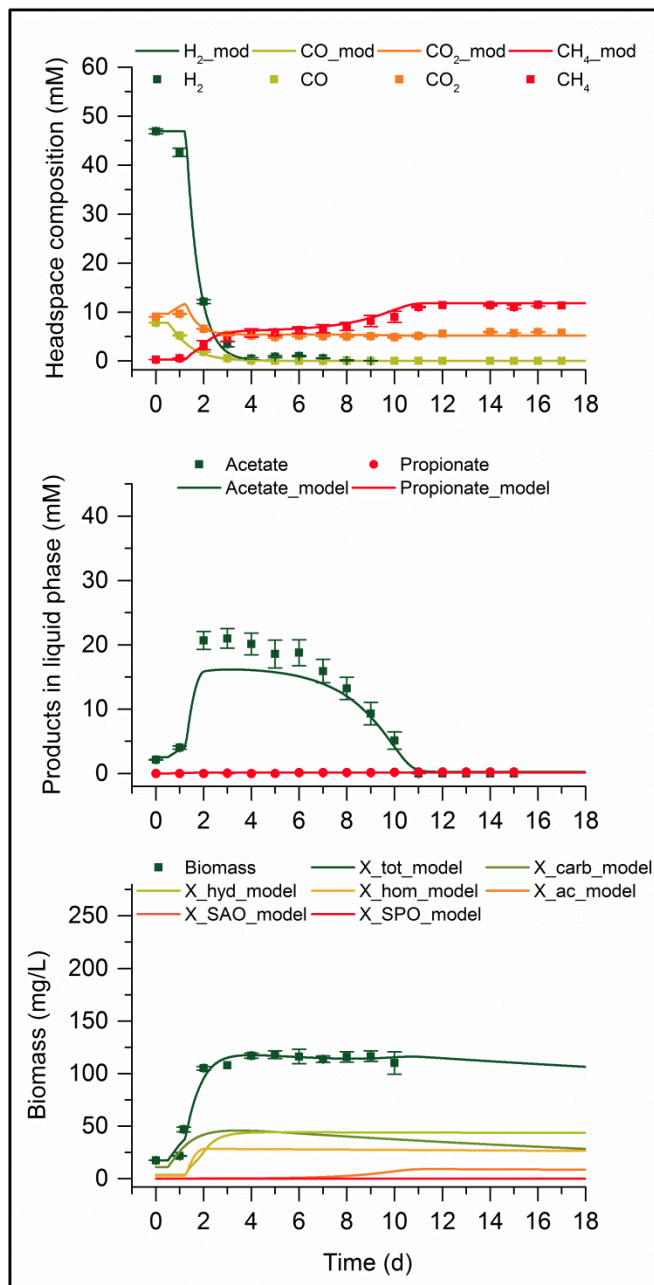


Figure S6. Simulation of validation experiment at mesophilic conditions and an initial P_{H_2} , P_{CO_2} and P_{CO} of 1 atm, 0.2 atm and 0.2 atm, respectively.

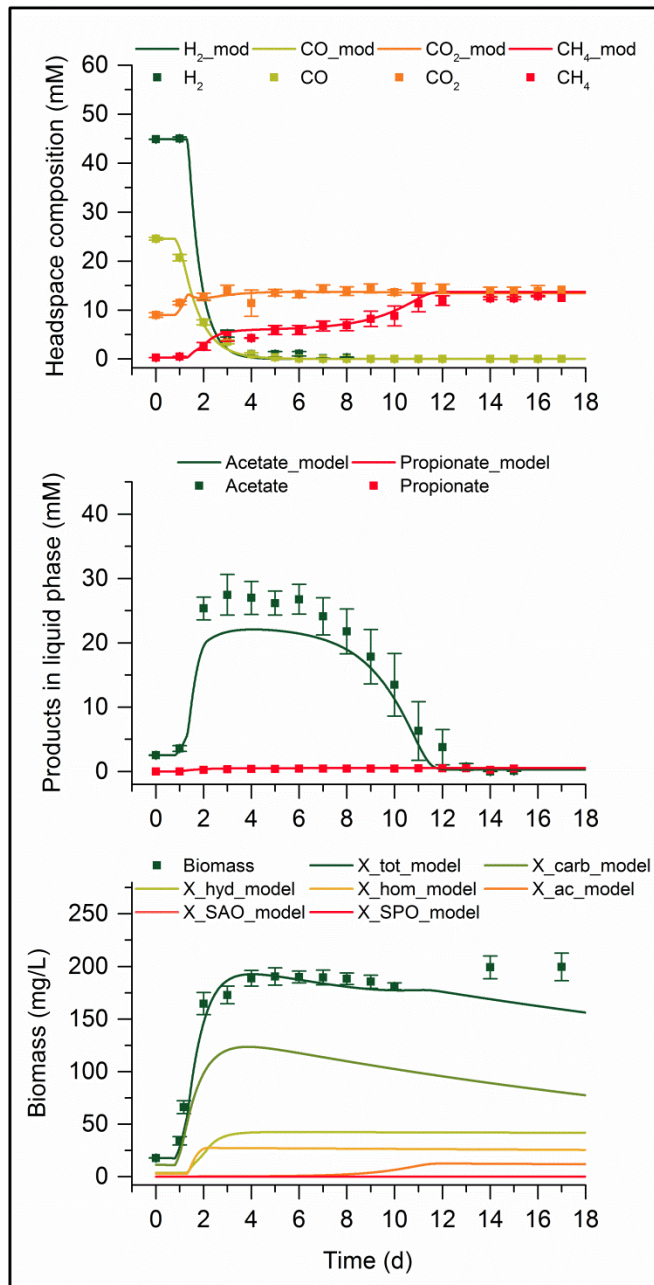


Figure S7. Simulation of validation experiment at mesophilic conditions and an initial P_{H_2} , P_{CO_2} and P_{CO} of 1 atm, 0.2 atm and 0.6 atm, respectively.

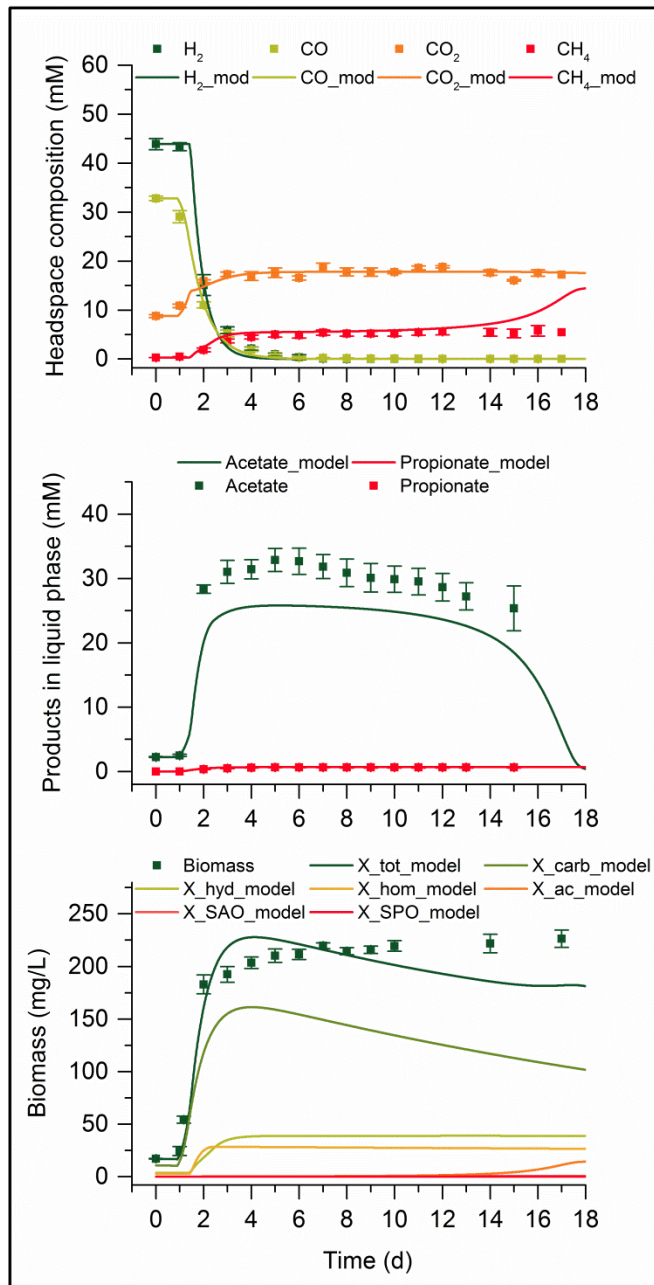


Figure S8. Simulation of validation experiment at mesophilic conditions and an initial P_{H_2} , P_{CO_2} and P_{CO} of 1 atm, 0.2 atm and 0.8 atm, respectively.

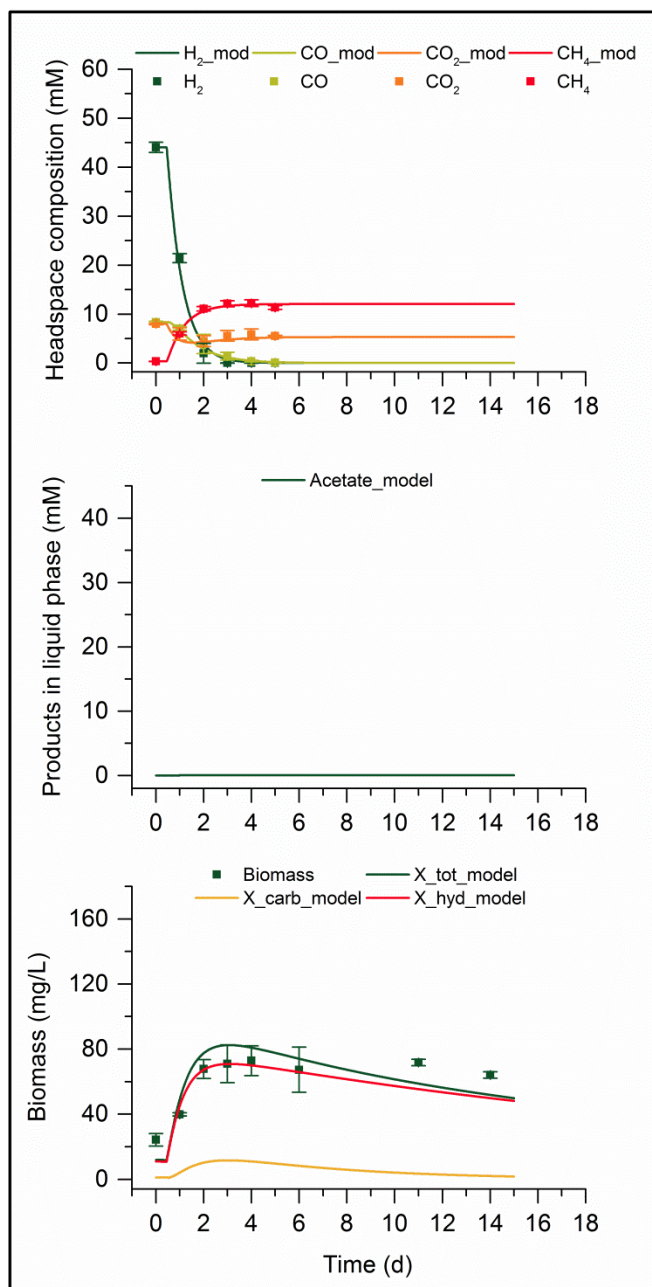


Figure S9. Simulation of validation experiment at thermophilic conditions and an initial P_{H_2} , P_{CO_2} and P_{CO} of 1 atm, 0.2 atm and 0.2 atm, respectively.

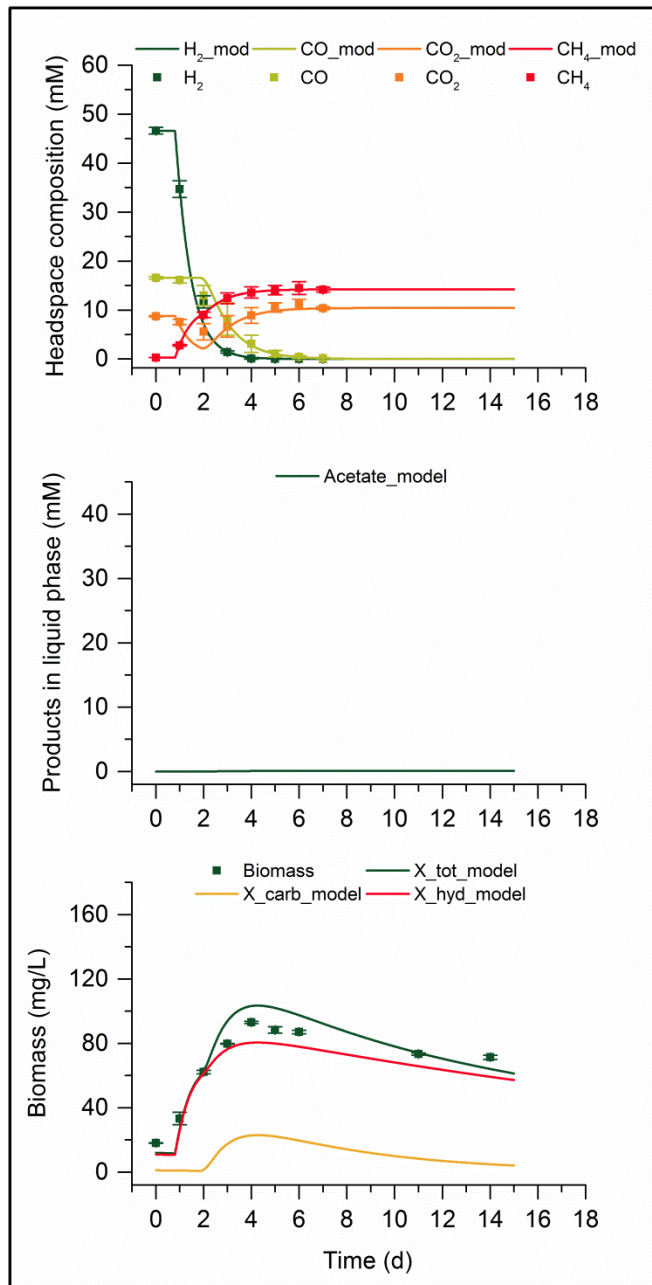


Figure S10. Simulation of validation experiment at thermophilic conditions and an initial P_{H_2} , P_{CO_2} and P_{CO} of 1 atm, 0.2 atm and 0.4 atm, respectively.

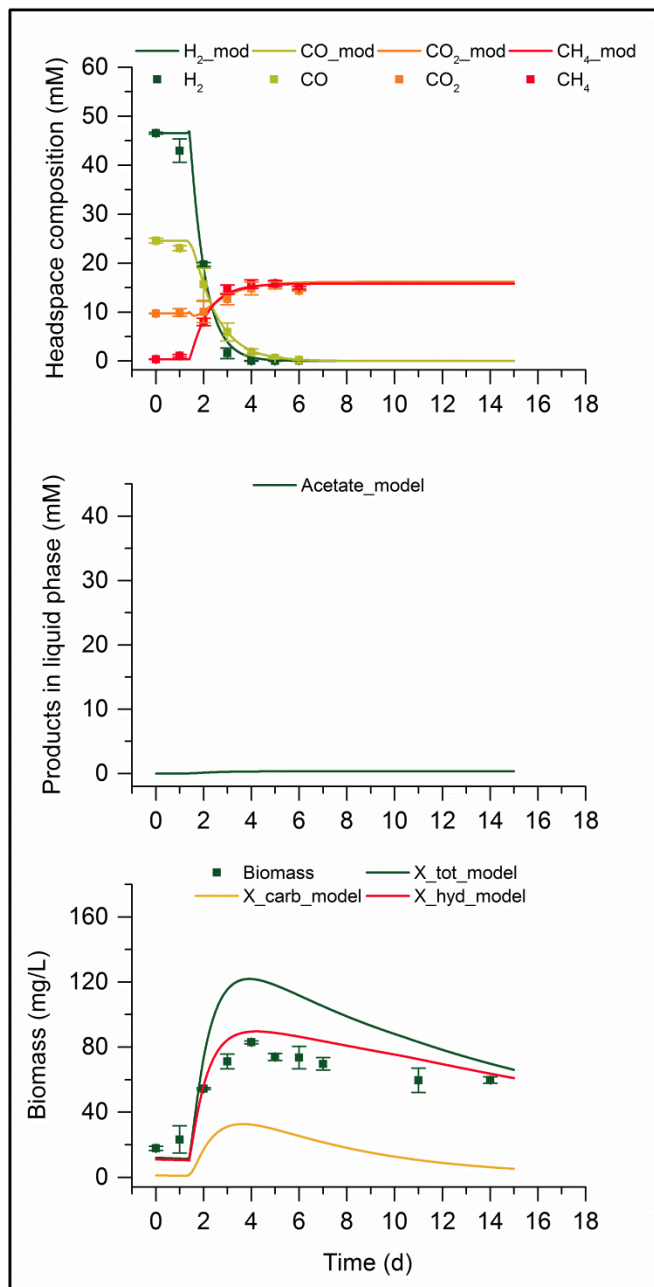


Figure S11. Simulation of validation experiment at thermophilic conditions and an initial P_{H_2} , P_{CO_2} and P_{CO} of 1 atm, 0.2 atm and 0.6 atm, respectively.

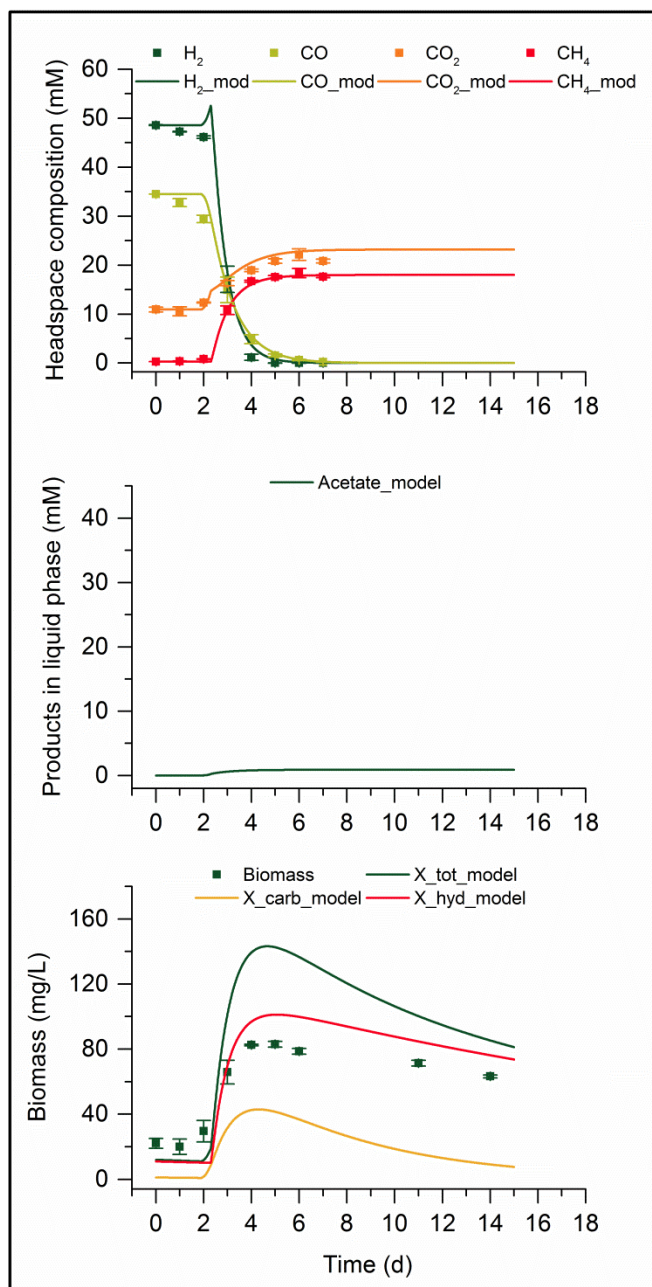


Figure S12. Simulation of validation experiment at thermophilic conditions and an initial P_{H_2} , P_{CO_2} and P_{CO} of 1 atm, 0.2 atm and 0.8 atm, respectively.

Manuscript V

“Cryopreservation and fast recovery of enriched syngas-converting microbial communities”

Cryopreservation and fast recovery of enriched syngas-converting microbial communities

Antonio Grimalt-Aleman¹, Mateusz Łężyk², Konstantinos Asimakopoulos¹, Ioannis V. Skiadas¹, Hariklia N. Gavala^{1}*

*Correspondence: hnga@kt.dtu.dk, hari_gavala@yahoo.com

¹Department of Chemical and Biochemical Engineering, Technical University of Denmark, Søtofts Plads 229, 2800 Kgs. Lyngby, Denmark

² Institute of Environmental Engineering, Faculty of Civil and Environmental Engineering, Poznan University of Technology, Berdychowo 4, 60-965 Poznań, Poland.

Abstract

Over the last decades, the use of mixed microbial communities has attracted increasing scientific attention due to their potential biotechnological applications in several emerging technological platforms such as the carboxylate, bioplastic, syngas and bio-electrochemical synthesis platforms. However, this increasing interest has not been accompanied by a parallel development of suitable cryopreservation techniques for microbial communities. While cryopreservation methods for the long-term storage of axenic cultures are well established, their effectiveness in preserving the microbial diversity and functionality of microbial communities has rarely been studied. In this study, the effect of the addition of different cryopreservation agents on the long-term storage of microbial communities at -80°C was studied using a stable enrichment culture converting syngas into acetate and ethanol. The cryopreservation agents considered in the study were glycerol, dimethylsulfoxide, polyvinylpyrrolidone, Tween 80 and yeast extract, as well as with no addition of cryopreservation agent. Their effectiveness was evaluated based on the microbial activity recovery and the maintenance of the microbial diversity and community structure upon revival of the microbial community. The results showed that the commonly used glycerol and no addition of cryopreservation agent were the least recommendable methods for the long-term frozen storage of microbial communities, while Tween 80 and polyvinylpyrrolidone were overall the most effective. Among the cryoprotectants studied, polyvinylpyrrolidone and especially Tween 80 were the only ones assuring reproducible results in terms of microbial activity recovery and microbial community structure preservation.

1. Introduction

The climate crisis and the foreseen future scarcity of fossil resources have motivated a paradigm shift towards the sustainable production of commodity chemicals, biomaterials and biofuels, where microbial production systems have much to contribute. Traditionally, axenic cultures have been the cornerstone of the biotechnological industry. Nevertheless, arising from the need of treating and revalorizing the large amount of waste generated in our societies, over the last decades, a new biotechnological field has emerged by combining elements from environmental and industrial biotechnology, in which the functional redundancy and resilience of microbial communities are harnessed for simultaneous waste treatment and product maximization [1]. This mixed culture biotechnology field is currently expanding beyond the conventional anaerobic digestion process towards the development of new technological platforms based on highly specialized microbial communities [2,3]. Examples of these platforms, where the use of mixed cultures has attracted scientific attention, are the carboxylate platform, bioplastics, bio-electrochemical systems and the syngas platform [4]. For instance, in the case of syngas fermentation, trickle bed bioreactors were recently suggested as a potential solution for the typically encountered mass-transfer limitations and low cell concentrations of syngas fermentation units, due to their high surface-to-volume ratio [5,6]. However, the attached microbial growth of these bioreactor configurations may make them especially prone to contamination, for which the use of mixed microbial communities would be especially convenient at industrial scale since these do not require sterile operation and there is low risk of contamination. Despite the increasing scientific interest in mixed-culture-based production systems, the preservation of these mixed microbial communities and the reproducibility of their performance after long-term storage has not been thoroughly investigated. In fact, neither natural nor engineered microbial communities are available in any culture collection yet [7–9].

Preservation methods for the long-term frozen storage of axenic cultures are well established. The effectiveness of the cryopreservation is affected by several factors such as species, strain, physiological state of the cells, cell density, cryopreservation agent (CPA) used, cooling and thawing rate, storage temperature and duration of the storage [10,11]. Among these, the choice of CPA is a crucial factor determining the survival rate and viability of the culture upon reactivation [12]. A large variety of CPAs have been successfully used in bacteria including serum albumin, skimmed milk, yeast extract, malt extract, Tween 80, polyvinylpyrrolidone (PVP), dimethylsulfoxide (DMSO) and glycerol, among many others. Generally, different protection mechanisms can be distinguished based on the permeability of the cell membrane and cell wall to the CPA, which can be categorized as permeant, semipermeant and non-permeant CPAs [10,13]. According to Hubálek [12], all effective permeant CPAs are highly hydrophilic and form strong hydrogen bonds with water, which reduce salt toxicity and prevent excessive dehydration and formation of large ice crystals within the cells. On the other

hand, non-permeable CPAs do not interact with the cell membrane or the cell wall, instead these adsorb on the surface of the membrane and increase the viscosity of the liquid inhibiting growth of ice crystals and keeping the ice structure amorphous [12]. Permeable CPAs like glycerol or DMSO are broadly used due to historical reasons and their apparently more universal effectiveness, but non-permeable CPAs such as PVP have also been proven equally or more effective than the latter in some cases. For instance, comparing the effect of PVP, DMSO and glycerol on the viability of the gram-positive *Streptococcus mutans* GS-5 and the gram-negative *Fusobacterium nucleatum* F-1 and *Selenomonas sputigena* 1304 after frozen storage in liquid nitrogen showed that PVP was the most effective among the three CPAs [14]. Thus, no single CPA or cryopreservation method is ideal for all species. When it comes to mixed microbial communities, an additional factor expected to play a determining role is the cell density. According to Malik [11], high cell density, between 10^6 and 10^8 cells per ml, is recommended to ensure cell viability after long-term cryopreservation. However, the inherent richness of species of microbial communities, with an important fraction of their microbial diversity being poorly represented in terms of relative abundance, makes this task practically inviable. Therefore, it can be anticipated that one of the challenges in the long-term storage of mixed microbial communities lies in the preservation of their complete structure, including their abundant minority groups.

Studies on the cryopreservation and reactivation of engineered mixed microbial communities have been rather limited so far. The short-term storage (three weeks) of microbial communities using DMSO, glycerol and no addition of CPA was investigated based on the activity and microbial composition of a thermophilic enrichment culture growing on switchgrass [15]. In turn, long-term cryopreservation studies (2-17 months) focused so far on the effect of the storage temperature with and without addition of glycerol, DMSO and a complex medium (DMSO combined with trehalose and tryptic soy broth) as CPAs on the preservation of nitrifying and denitrifying microbial consortia, a methanotrophic microbial community and fecal biomass [16–18]. However, to the best knowledge of the authors, the effectiveness of long-term cryopreservation of microbial communities using CPAs other than glycerol and DMSO has not been investigated yet. In this study, a highly specialized acetogenic microbial community converting syngas was generated through a microbial enrichment in continuous mode. The enrichment culture was then used to evaluate the effect of a variety of CPAs on the long-term cryopreservation of the activity and microbial composition of the microbial community. The range of CPAs already tested (no CPA addition, DMSO and glycerol) was extended with a non-permeant CPA (PVP), a complex freezing medium (yeast extract) and a surfactant (Tween 80), all of which have been reported to be as effective as glycerol or DMSO for the cryopreservation of specific bacteria [14,19,20].

2. Materials and Methods

2.1. Growth medium composition

A modified basic anaerobic (BA) medium was used in all experiments, which consisted of several stock solutions. The composition of stock solution was as follows: salt solution (NH_4Cl , 100 g/l; NaCl , 10 g/l; $\text{MgCl}_2 \cdot 6\text{H}_2\text{O}$, 10 g/l; $\text{CaCl}_2 \cdot 2\text{H}_2\text{O}$, 5 g/l), sodium sulfate solution (Na_2SO_4 , 100 g/l); vitamins solution according to Wolin et al. [21], modified ATCC 1754 trace metal solution ($\text{Fe}(\text{NH}_4)_2(\text{SO}_4)_2 \cdot 6\text{H}_2\text{O}$, 800 mg/l; H_3BO_3 , 10 mg/l; $\text{ZnSO}_4 \cdot 7\text{H}_2\text{O}$, 200 mg/l; $\text{CuCl}_2 \cdot 2\text{H}_2\text{O}$, 20 mg/l; $\text{MnSO}_4 \cdot \text{H}_2\text{O}$, 1000 mg/l; $\text{Na}_2\text{MoO}_4 \cdot 2\text{H}_2\text{O}$, 20 mg/l; AlCl_3 , 10 mg/l; $\text{CoCl}_2 \cdot 6\text{H}_2\text{O}$, 200 mg/l; $\text{NiSO}_4 \cdot 6\text{H}_2\text{O}$, 20 mg/l; Na_2SeO_3 , 18.3 mg/l; $\text{Na}_2\text{WO}_4 \cdot 2\text{H}_2\text{O}$, 22.5 mg/l; nitrilotriacetic acid, 2000 mg/l), dipotassium hydrogen phosphate solution ($\text{K}_2\text{HPO}_4 \cdot 3\text{H}_2\text{O}$, 200 g/l), yeast extract solution (yeast extract, 25 g/l) and reducing agent solution ($\text{Na}_2\text{S} \cdot 9\text{H}_2\text{O}$, 25 g/l).

The medium was prepared in deionized water by adding 20 ml/l of salts solution, 20 ml/l of sodium sulfate solution, 10 ml/l of vitamins solution, 10 ml/l of trace metal solution, 4 ml/l of dipotassium hydrogen phosphate solution, 20 ml/l of yeast extract solution, and 2 ml/l of reducing agent solution added in anaerobic conditions. In batch activity tests, the initial pH of the medium was adjusted by substituting the dipotassium hydrogen phosphate solution by a 50 mM phosphate buffer using two stock solutions ($\text{K}_2\text{HPO}_4 \cdot 3\text{H}_2\text{O}$, 200 g/l; and KH_2PO_4 , 136 g/l).

2.2. Inoculum source and microbial enrichment

In order to increase the initial diversity of the microbial community, the inoculum used in the microbial enrichment consisted of a mixture of two different anaerobic sludges, collected from the Lundtofte Wastewater Treatment plant (Denmark) and from a lab-scale anaerobic digester fed with manure (Department Chemical and Biochemical Engineering, Technical University of Denmark). Prior to inoculation, the anaerobic sludges were mixed in equal amounts while flushing with N_2 to create anaerobic conditions. The mixture of anaerobic sludges underwent a heat-shock treatment in order to suppress the methanogenic activity. The heat-shock treatment was carried out by heating the mixture of anaerobic sludges and maintaining the temperature above 90°C for 15 min while flushing with N_2 .

The mixed microbial community used for studying the effect of adding different CPAs was generated through a microbial enrichment in continuous mode using syngas as the only carbon and energy source. A 2 L stirred tank bioreactor (Biostat B, Sartorius Stedim Biotech GmbH, Germany) with a working volume of 2 L was used for performing the enrichment. The bioreactor was equipped with an external vacuum pump (N86AP12DCB, KNF, Sweden) to allow the recirculation of the exhaust gas, and with a mass flow controller (Bronkhorst,

Netherlands) for adjusting the syngas inflow. The pH was measured using a pH/ORP probe (Easyferm Plus VP 225, Hamilton, Switzerland) and was automatically regulated through the addition of 1 M KOH and 0.5 M HCl.

Throughout the whole enrichment, the temperature was maintained at 37 °C, the agitation speed was adjusted to 300 rpm and the gas recirculation rate was set to 1.7 L/min. The heat-treated mixture of sludges was inoculated into the bioreactor (without prior acclimatization of the inoculum to CO) using an inoculum size of 5% v/v in order to initiate the enrichment. The microbial enrichment started in batch mode at a pH of 5 and a continuous inflow of 10 ml/min of syngas containing 45% of H₂, 20% of CO, 25% of CO₂ and 10% of N₂. Once the batch fermentation finished, the bioreactor started to be operated in continuous mode with a hydraulic retention time (HRT) of 5.1±0.3 days and a syngas inflow of 10 ml/min. The pH was allowed to decrease freely until a pH of 4.5 was reached and later on the pH was maintained constant at pH 4.5. After 25 days of operation in continuous mode when steady state was reached, the HRT was set to 2.4±0.1 days and the syngas inflow was increased to 25 ml/min in order to keep a similar ratio of syngas/medium supply. Once steady state was reached at HRT 2.4 days, the HRT was set back to 5.1±0.5 days setting the syngas inflow back to 10 ml/min.

2.3. Cryopreservation agents and storage of microbial community

After 78 days of operation, the enriched microbial community was preserved frozen at -80 °C using different CPAs, namely glycerol, dimethylsulfoxide, polyvinylpyrrolidone, Tween 80, yeast extract and without addition of any CPA. All CPA solutions were prepared in anaerobic serum vials of 10 ml using a CPA solution volume of 2 ml and were sealed with rubber stoppers and aluminum crimps after creating anaerobic conditions by flushing with N₂. All serum vials were inoculated with 5 ml samples of actively growing culture with a cell density of $1.23 \cdot 10^8 \pm 0.22 \cdot 10^8$ cells/ml, measured using a hemocytometer. Prior to inoculation, glycerol, yeast extract and Tween 80 CPA solutions were autoclaved at 121 °C for 15 min in sealed anaerobic serum vials, the solution with dimethylsulfoxide was filter-sterilized and injected into previously sterilized anaerobically sealed serum vials, and polyvinylpyrrolidone (PVP-15K) was solubilized in sterile ultrapure water and injected into sterile anaerobically sealed serum vials. The concentration of glycerol in the CPA solution was adjusted to a final concentration after inoculation of 15% w/v and the solution was left to equilibrate 45 min at room temperature after inoculation. The final concentration of dimethylsulfoxide after sample inoculation corresponded to 10% w/v and the solution was equilibrated for 45 min at room temperature after inoculation. The polyvinylpyrrolidone solution was adjusted to a final concentration of 3% w/v and was equilibrated for 10 min at room temperature after inoculation of the sample. The final concentration of the yeast extract solution corresponded to 2% w/v and the solution was equilibrated for 10 min at room temperature after inoculation. The solution with Tween 80 was adjusted to a final concentration of 1% w/v and was left to equilibrate for 10 min at room temperature after inoculation. Lastly, the fermentation broth containing actively growing culture was also

injected into previously sterilized anaerobically sealed serum vials without addition of any CPA. After the equilibration time, all serum vials were fast frozen by submerging them into liquid nitrogen for 2 min and were preserved at -80 °C for 7 months until reactivation.

2.4. Activity recovery tests

The recovery of the microbial activity after 7 months of frozen storage for each CPA was evaluated by comparing the results of batch activity tests inoculated with the frozen cultures to the results obtained in a reference batch fermentation inoculated directly with the actively growing enriched microbial community from the bioreactor at the 78th day of operation (when samples of the culture were subjected to cryopreservation). The syngas composition used in all batch activity tests corresponded to 50% H₂, 20% CO, 10% CO₂ and 20% N₂.

All batch activity tests were performed in triplicates using 330 ml serum flasks with an active volume of 100 ml. The modified BA medium supplemented with a 50 mM phosphate buffer was added to the flasks, which were flushed with H₂ to create anaerobic conditions and sealed with rubber stoppers and screw plugs. After the flasks were anaerobically sealed, all flasks were autoclaved at 121 °C for 15 min. Vitamins and yeast extract solution were filter-sterilized and added into the flasks after sterilization, and the reducing agent solution was filter-sterilized and added into the flasks prior to inoculation. The remaining gases (CO, CO₂ and N₂) were filter-sterilized and added to the flasks up to a total pressure of 2 atm using a precision pressure indicator (CPH6400, WIKA, Germany), so that the final partial pressure of H₂, CO, CO₂ and N₂ corresponded to 1 atm, 0.4 atm, 0.2 atm and 0.4 atm, respectively. After inoculation, the fermentation flasks were incubated at 37 °C and 100 rpm. The initial pH of all batch activity tests corresponded to an average of 5.7±0.1. Control experiments were performed in triplicates at the same incubation conditions with no addition of gaseous substrates, adjusting the composition of the headspace to 1.8 atm of N₂ and 0.2 atm of CO₂.

Prior to inoculation, all frozen cultures were thawed by incubating the serum vials at 37 °C for 30 min. The reference batch activity tests using the culture from the bioreactor and the frozen culture with no addition of CPA were inoculated using an inoculum size of 1% v/v, and the remaining frozen cultures were inoculated using an inoculum size of 1.4% v/v to correct for the dilution of the biomass after mixing with the CPAs.

2.5. DNA extraction and amplicon sequencing

Samples for microbial composition analysis were collected from the bioreactor and from all batch activity tests. During the microbial enrichment, 11 samples of 5 ml were collected from the bioreactor on day 1, 13, 23, 35, 37, 44, 51, 52, 56, 70 and 78. Samples from all batch activity tests (5 ml) were collected at the end of the fermentation during stationary growth phase. Total genomic DNA was isolated from all samples using the

DNeasy Blood & Tissue Kit, following manufacturer recommendations for Gram-positive bacteria (Qiagen, Denmark). DNA samples were submitted to Macrogen Inc. (Korea) for 16S rRNA amplicon library preparation and sequencing using Illumina Miseq instrument (300 bp paired-end sequencing). The libraries were prepared according to 16S Metagenomic Sequencing Library Preparation Protocol (Part #15044223, Rev. B) using Herculase II Fusion DNA Polymerase Nextera XT Index Kit V2. Regions V3 and V4 of the 16S rRNA gene were amplified using the primers Pro341F (5'-CCTACGGGNBGCASCAG-3') and Pro805R (5'-GACTACNVGGGTATCTAATCC-3') from Takahashi et al. [22]. Raw sequences obtained in this study were deposited in NCBI SRA database with BioProject ID: PRJNA565688 (BioSample accessions: SAMN12769536-SAMN12769543).

2.6. Analysis of 16S rRNA gene amplicons

All reads containing primers were trimmed with cutadapt and untrimmed reads were discarded [23]. Paired reads were merged using usearch-fastq_mergepairs, allowing for 10 mismatches in the alignment and a 90% identity, and were quality filtered using usearch-fastq_filter with a maximum expected error threshold of 1.0 [24]. Filtered reads were then derreplicated to identify uniques using vsearch-derep_fulllength [25]. Generation of operational taxonomic units (OTUs) and mapping of merged reads to OTUs was performed using the UPARSE pipeline [24], where uniques with higher abundance than two were kept and reads with at least 99% identity were considered in the OTU counts. Taxonomic assignment to OTUs was carried out using SINTAX and the database SILVA v132 LTP using a 0.8 bootstrap confidence threshold [26,27]. Downstream analyses including Shannon diversity index and Principal Coordinate analysis (PCoA) were performed using the Phyloseq R package [28].

2.7. Analytical methods

The exhaust gas from the bioreactor and the headspace of the fermentation flasks was analyzed using a gas chromatograph (8610C, SRI Instruments, USA) equipped with a thermal conductivity detector and two packed columns, a Molsieve 13X column (6' x 1/8") and a silica gel column (6' x 1/8") connected in series with a rotating valve. The temperature of the oven was held at 65°C for 3 min, followed by a first temperature ramp of 10°C/min up to 95°C and a second ramp of 24°C/min from 95°C to 140°C. Liquid samples were analyzed for volatile fatty acids and alcohols through a High Performance Liquid Chromatograph (Shimadzu, USA) equipped with a refractive index detector and an Aminex HPX-87H column (Bio-Rad, USA). The temperature of the oven was held constant at 63°C and the flow rate of the mobile phase (H₂SO₄ 12 mM) was 0.6 ml/min. Microbial growth was monitored indirectly through the absorbance of the liquid samples at 600 nm using a spectrophotometer (DR2800, Hach Lange).

2.8. Calculations

The recovery of the microbial activity after long-term frozen storage was carried out by comparing the maximum apparent product yields and the maximum volumetric productivities observed experimentally in reactivated cultures to the ones observed in the reference batch fermentation. The maximum apparent product yield, expressed in e-mols of product per e-mols of syngas consumed, was determined according to eq. 1 using the time points with maximum concentration for each product, where $n_{(i)}$ is the number of moles of compound i , and n_{e-i} is the number of e-mols per mol of compound i .

$$Y_i \left(\frac{e\text{-mol product}}{e\text{-mol substrate}} \right) = \frac{(n_{(i)} \text{ produced} - n_{(i)} \text{ control}) \cdot n_{e-i}}{n_{H_2} \text{ consumed} \cdot n_{e-H_2} + n_{CO} \text{ consumed} \cdot n_{e-CO}} \quad (1)$$

The maximum volumetric productivity for each product was calculated according to eq. 2, where t_j represents the time at measurement number j , C_{i,t_j} corresponds to the concentration of product i at time point t_j and n is the number of measurements. Experimental measurements were taken on a daily basis.

$$Q_{p,i} (mmol \cdot l^{-1} \cdot d^{-1}) = \max \left\{ \frac{C_{i,t_j} - C_{i,t_{j-1}}}{t_j - t_{j-1}} : j = 1, \dots, n \right\} \quad (2)$$

The overall distance between the maximum product yields and volumetric productivities of the reactivated cultures and the reference experiment was calculated through the standardized Euclidean distance, computed for each of the triplicates according to eq. 3 and 4.

$$D_{A,ref} = \sqrt{\sum_{i=1}^N \frac{1}{s_i^2} (Q_{p,i} - Q_{p,i,ref})^2} \quad (3)$$

$$D_{Y,ref} = \sqrt{\sum_{i=1}^N \frac{1}{s_i^2} (Y_i - Y_{i,ref})^2} \quad (4)$$

where $D_{A,ref}$ and $D_{Y,ref}$ is the weighted Euclidean distance associated to volumetric productivities and product yields, respectively; $Q_{p,i}$ and $Q_{p,i,ref}$ represent the productivity of product i for the reactivated culture and the reference, respectively; Y_i and $Y_{i,ref}$ represent the yield of product i for the reactivated culture and the reference, respectively; s_i^2 corresponds to the standard deviation of all values of variable i (including all experiments); and N is the number of variables, in this case, acetate, ethanol, butyrate, butanol and 1,3-propanediol (1,3-PDO). In order to account for the variability of the triplicates in reactivated cultures, the weighed Euclidean distance to each of the triplicates of the reference experiment was computed for each of the triplicates of the reactivated cultures. Then, the average distance was plotted along with the standard deviation.

3. Results and Discussion

3.1. Microbial enrichment in continuous mode

The microbial enrichment was intended to generate a microbial community dominated by acetogenic bacteria able to convert both H_2/CO_2 and CO into acetate and ethanol. The heat-shock treatment of the anaerobic sludge mixture successfully inhibited methanogenic growth since methane was not detected along the whole enrichment process. On the other hand, the presence of 2 g/l of sodium sulfate in the medium could have favored growth of spore-forming sulfate-reducing bacteria, mainly belonging to the genera *Desulfotomaculum* and *Desulfosporosinus*, which would be detrimental for the production of acetate and ethanol as these could be partially oxidized to CO_2 [29]. However, the high product recovery observed along the whole enrichment, above 80% in all operating conditions tested, suggested that this microbial group was not present in the enriched microbial community. Additionally, neither methanogenic archaea nor sulfate-reducing bacteria were detected in the enriched microbial community according to the microbial composition analysis.

The product spectrum of the microbial community was clearly dominated by acetate and ethanol, although other products like butyrate and butanol (and traces of propionate, iso-butyrate and caproate) were also detected (fig.1). During start-up in batch mode, a maximum concentration of 257.6 mM of acetate and 48.5 mM of ethanol was obtained. Nevertheless, when continuous operation started, the concentration of acetate dropped significantly and stabilized within a range of 100-125 mM during the rest of the enrichment. In turn, the production of ethanol was found to be strongly affected by the HRT, ranging from a minimum concentration of 17.5 ± 0.1 mM at steady state with 2.36 days of HRT, to 40.9 ± 1.6 mM at steady state with 5.09 days of HRT. This suggested that ethanol was probably produced through the reduction of acetate using either H_2 or CO, as higher HRT should allow for higher extent of this reaction. Several acetogenic species typically used in syngas fermentation processes, such as *Clostridium ljungdahlii*, *Clostridium autoethanogenum* and *Clostridium ragsdalei*, have been reported to be able to convert syngas into ethanol either directly through aldehyde dehydrogenase or indirectly through acetaldehyde-ferredoxin oxidoreductase by reducing intracellular acetate [30]. However, Gonzalez-Cabaleiro et al. [31] pointed out that the reduction of acetate into ethanol using an electron donor, such as H_2 or CO, could also be an independent energy-yielding metabolic bioconversion. According to this, it is possible that, in this case, ethanol was not produced by a single species, but by the microbial interaction between several species coupling the production of acetate to its further reduction into ethanol.

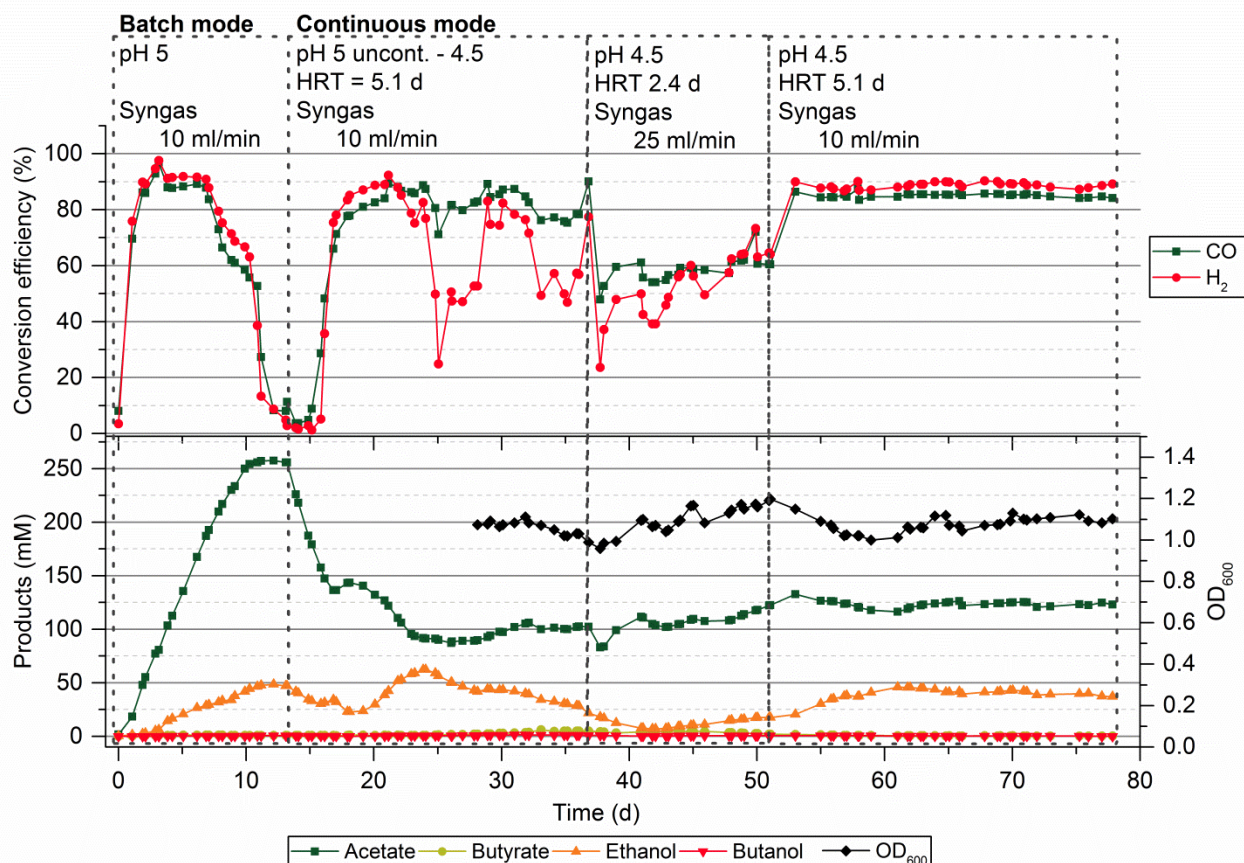


Figure 1. Conversion efficiency and product concentration profile during the microbial enrichment under batch and continuous operation. Changes in operating conditions are noted above the graph. The initial lag phase of the anaerobic sludge after inoculation is not included in the graph.

A low pH (4.5) was selected in order to prevent a significant conversion of acetate and ethanol into butyrate through the chain elongation reaction, as the latter has been reported to be inhibited either by low pH (below 5.2) or by the high concentration of undissociated acids at low pH [32–35]. However, during the first phase of continuous operation (between days 13 and 37) and despite the low pH, the concentration of butyrate started to increase gradually until a maximum concentration of 6.0 mM was reached, which accounted for $8.0 \pm 1.0\%$ of the e-mols diverted to products (fig. 1). The production of butyrate could take place either by direct production from syngas, or by an independent metabolic activity through the chain elongation reaction. *Clostridium carboxidivorans* is an example of those species able to produce butyrate and butanol directly from CO, although it is not clear whether these are mainly produced directly or through re-assimilation of other metabolites [36,37]. On the other hand, acetate and ethanol can also be elongated to butyrate by species that are not able to consume syngas, such as *Clostridium kluyveri* [35]. In any case, decreasing the HRT from 5.12 days to 2.36 days resulted in a sharp drop in the concentration of butyrate until the end of the enrichment, even when the HRT was

increased again to 5.09 days, which indicated that the species carrying out the chain elongation to butyrate was nearly washed out by the higher dilution rate (fig. 1). However, the fact that the concentration of butyrate was not zero when changing the HRT back to 5.09 days suggested a residual chain-elongating activity. Thus, it can be concluded that butyrate was likely produced in syntrophic association with other syngas-converting species.

The analysis of the microbial composition showed that, as expected, the microbial community was clearly dominated by acetogenic bacteria belonging to the family *Clostridiaceae*. The dominant families, corresponding to *Clostridiaceae*, *Enterobacteriaceae* and *Pseudomonadaceae*, were established in the microbial community from the first day of active fermentation (fig. 2). However, despite their early establishment, based on the Shannon diversity index, a significant reduction in the complexity of the microbial community was observed as the enrichment progressed, which suggested a gradual specialization of the microbial community (ESM 1, fig. 1). Within the family *Clostridiaceae*, the most abundant species was closely related to *C. ljungdahlii* (1.00 bootstrap confidence), which represented a significant percentage of the reads mapped in all samples ranging from 45.5% to 83.4% (ESM 1, table 2). Other OTUs from this family with high relative abundance of reads at some point during the enrichment mapped to species closely related to *C. luticellarii* (with a maximum of 28% of the reads mapped) and *Clostridioides manganotii* (with a maximum of 2.5% of the reads). Other *Clostridium* spp. with lower percentage of reads were also identified. The high abundance of reads mapping to *C. ljungdahlii* indicated that this species potentially metabolized a large fraction of the syngas supplied. Nevertheless, when operating at 5.12 days and 2.36 days of HRT (days 13-51), its relative abundance dropped sharply while reads corresponding to *C. luticellarii* increased from 0.3% at the end of batch operation to 28.0% and 13.4% on days 44 and 52, respectively. *C. luticellarii* was recently isolated and has not been tested for its potential hydrogenotrophic or carboxydophilic ability yet [38]. However, the high abundance of this species in the enrichment and the fact that it is closely related to *C. ljungdahlii* suggest a possible syngas-converting activity [38]. Additionally, *C. luticellarii* was also found to be responsible for the chain-elongating activity observed in an open culture bioreactor [39], which could explain the appearance of butyrate in the product profile of the enrichment. Within families *Enterobacteriaceae* and *Pseudomonadaceae*, reads mapping to a *Pseudomonas* sp. and another species likely belonging to the genus *Klebsiella* (0.45 bootstrap confidence) reached a maximum abundance of 17.8% on day 35 and 12.2% on day 23, respectively, although both of them represented around 2% of the reads mapped at the end of the enrichment (fig.2). Overall, the composition of the microbial community was found to be very stable when reaching steady state under continuous operation but highly sensitive to changes in the operating conditions, responding to these changes with rearrangements in the dominant species.

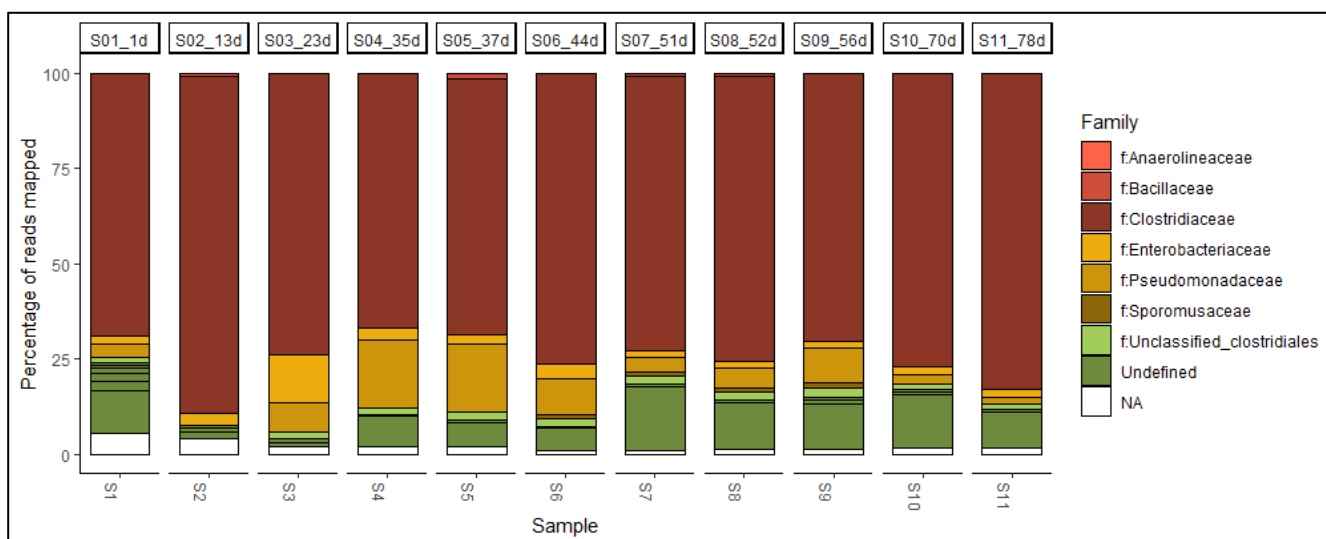


Figure 2. Relative abundance of reads mapped to OTUs at family taxonomic level during the microbial enrichment. The corresponding day when the sample was taken is given above the columns. NA corresponds to reads mapped to OTUs assigned to families with a percentage of reads below 0.5%.

3.2. Recovery of microbial activity

Along the enrichment, a highly specialized microbial community dominated by *Clostridium* spp. and able to produce acetate and ethanol with high syngas conversion efficiency was generated. This enriched microbial community was then used to inoculate a batch fermentation in order to provide a reference for comparison with the reactivated microbial communities after 7 months of frozen storage using different CPAs.

Besides the change in operating mode from continuous to batch in the reference batch experiments, the pH was increased from 4.5 to 5.7 in order to prevent a drop in pH above inhibitory levels during batch fermentation and allow for complete substrate consumption. The different operating conditions promoted changes in the product distribution of the batch reference experiments basically derived from (i) the higher initial pH, which promoted the chain elongation, and (ii) the batch operating mode, which allowed for growth of species that had lower affinity for the substrates and were previously outcompeted under continuous operation. As a result of these changes, acetate and ethanol were partially converted into butyrate and further reduced to butanol, probably by species that thrived in batch mode and were poorly represented during the enrichment, resulting in a maximum apparent yield for each product along the fermentation of $60.0 \pm 7.6\%$ of acetate (88 h), $38.0 \pm 6.8\%$ of ethanol (111 h), $22.5 \pm 5.8\%$ of butyrate (126 h) and $12.2 \pm 2.1\%$ of butanol (126 h) in e-mol basis (fig. 3). Under ideal cryopreservation conditions, the reactivated microbial communities were expected to undergo the same metabolic changes observed in reference experiments upon cultivation in batch fermentation flasks.

All frozen microbial communities were successfully revived upon cultivation in batch fermentation flasks. There were no differences in the lag phase duration of the reactivated cultures when compared to reference experiments (24 h), with the exception of the enriched community preserved using glycerol as CPA. When using glycerol as CPA, the culture started growing in less than 24 h; however, the culture presented diauxic-like growth as the conversion of syngas did not start until a considerable amount of the glycerol added along with the inoculum was consumed (48 h).

The ability of the microbial community to convert syngas into acetate and ethanol was successfully preserved when DMSO, PVP, Tween 80 and yeast extract were used as CPAs. With these CPAs, the maximum yield of acetate and ethanol varied between 87.6-99.5% and 87.9-92.4% of the maximum yield obtained in reference experiments, respectively (fig. 3). Their volumetric productivity rates followed the same trends as the maximum yields, although with generally lower relative recovery in most cases, ranging from 62.8% to 79.6% for acetate and from 73.6% to 104.0% for ethanol (fig. 3). This indicated that the dominant microbial species, likely responsible for the conversion of syngas into acetate and ethanol, were well preserved during frozen storage. Nevertheless, notable differences were observed in the maximum yield of butyrate and butanol, which suggested that the viability of less abundant species performing secondary reactions like the chain elongation and the reduction of butyrate into butanol was severely affected after frozen storage. Among these CPAs, PVP seemed to present the best activity recovery, reflected in a maximum yield for butyrate and butanol of 23.0% and 30.9% of that of the reference, respectively (fig. 3). In turn, DMSO presented the lowest yield of butyrate and butanol, corresponding to 11.9% and 13.6% of the reference, respectively. It should be noted though that the butyrate- and butanol-producing activity was maintained in these reactivated microbial communities, and full activity recovery would probably take place upon continued operation.

As opposed to the aforementioned CPAs, the reactivation of the microbial community stored using no CPA resulted in important differences in terms of maximum product yields and volumetric productivities. The acetate and ethanol producing activity of the microbial community was still present upon revival, which indicated that the dominant species converting syngas were adequately preserved. However, the reactivated culture exhibited a negligible butyrate and butanol yield and productivity (fig. 3). In fact, only traces of butanol and butyrate were detected, with the latter being produced in only one of the triplicate experiments. This suggested that concentration of cells played an important role during the preservation without CPA, as it seems that highly abundant species (likely converting syngas) were appropriately preserved and poorly represented species (likely performing chain elongation) had the lowest survival rates among all preservation conditions tested.

The activity recovery found when using glycerol as CPA also indicated that the culture was considerably affected upon reactivation. However, in this case, the main differences observed derived from the fact that glycerol was metabolized along with syngas during the reactivation. Despite the microbial community was enriched for almost 80 days using syngas as the only carbon and energy source, the enriched culture still presented the ability to metabolize glycerol. Consequently, syngas and glycerol were co-metabolized resulting in a drastically different final product distribution (despite the correction for control experiments). A good example of these differences is the production of a considerable amount of 1,3-propanediol (1,3-PDO), which constituted the second major product of the fermentation (fig. 3). Other significant differences arising from the co-metabolism of syngas and glycerol were the higher productivity of butyrate and reduced productivity of ethanol compared to the reference (fig. 3). This drastic change in the product distribution could imply that the composition of the reactivated microbial community was also strongly affected.

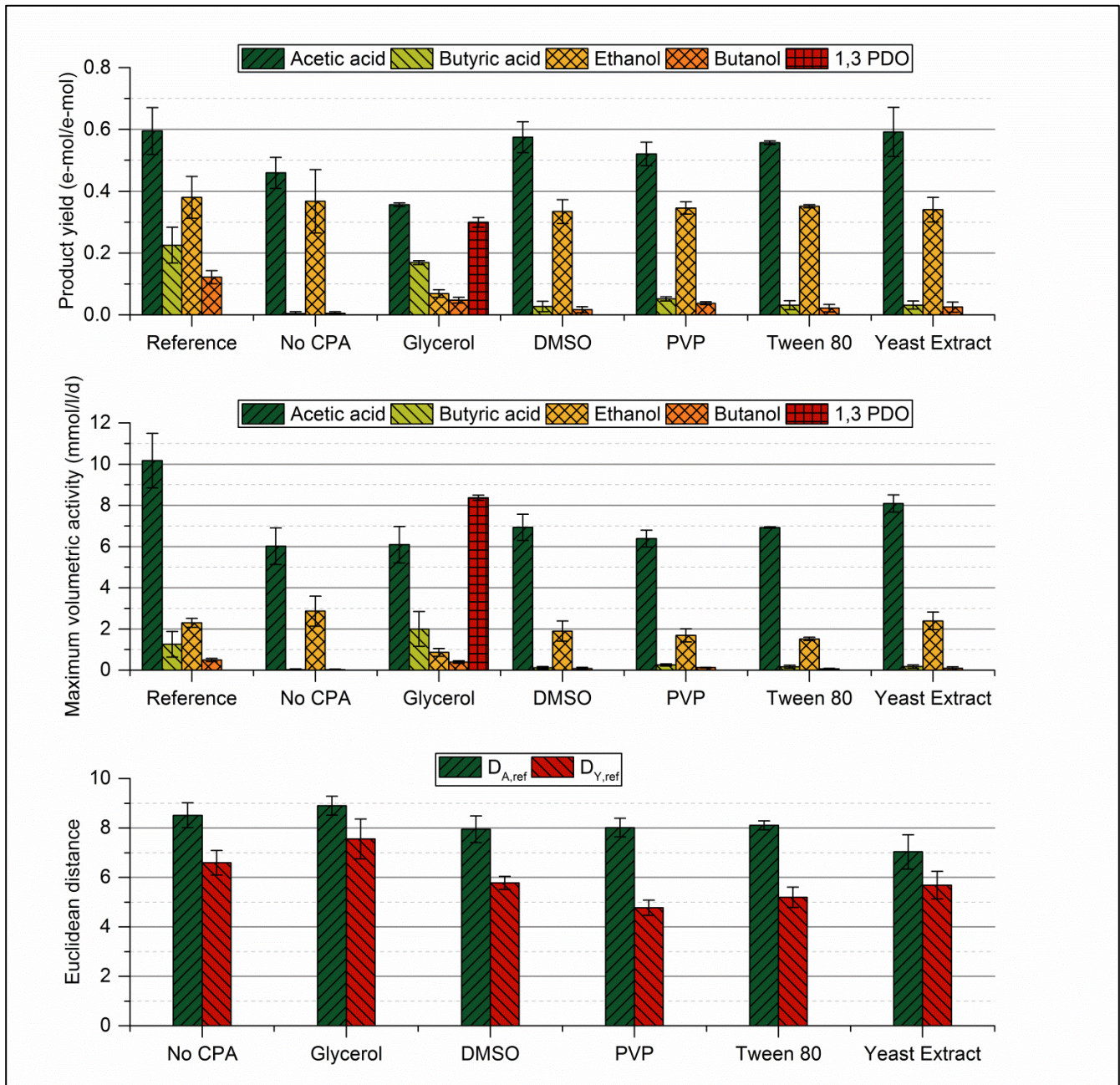


Figure 3. Maximum apparent product yield and maximum volumetric productivity of each product for reference experiments (fresh microbial community) and reactivated microbial communities after long-term frozen storage using different CPAs, and Euclidean distance to the reference for each CPA based on the maximum product yields ($D_{Y,ref}$) and maximum productivities ($D_{A,ref}$). Note that the maximum product yields do not correspond to the final product yields, but to the yield in the time points where the maximum concentration of each product was observed. The maximum product yields were corrected for the production from control experiments.

Generalized loss of activity upon revival after long-term cryopreservation was previously reported when attempting to recover the original activity of fecal biomass cultivated anaerobically and denitrifying sludge [16,18]. These observations are in line with the findings of Vlaeminck et al. [17] when studying the influence of

storage temperature on the preservation of aerobic and anaerobic ammonium-oxidizing bacteria, since a loss of activity upon reactivation was observed regardless of the storage temperature and conditions. The results of this study are in agreement with the above since a generally lower maximum product yield and productivity was observed in all reactivated microbial communities when compared to reference experiments. Based on the loss of activity in secondary biochemical conversions like the chain elongation and the reduction of butyrate to butanol, it can be concluded that the relative activity recovery depended strictly on the initial concentration of viable cells of each species upon reactivation. This is consistent with the loss in relative cell viability after long-term frozen storage typically reported for axenic cultures [40].

The effectiveness of the long-term cryopreservation of an industrial denitrifying sludge at -80°C without CPA addition and with glycerol were previously compared by Laurin et al. [16]. These authors concluded that the preservation of the microbial community was clearly more effective when glycerol was added in the freezing medium based on its higher activity recovery. In this study, the cryopreservation without CPA addition resulted in drastic differences in the performance of the reactivated microbial community and the reference, as the reactivated culture presented negligible butyrate and butanol productivities. In turn, all products found in reference experiments were also observed upon reactivation of the microbial community preserved with glycerol, which suggested that the cryopreservation with glycerol was more effective than without CPA addition. However, the effects of glycerol as cryoprotectant could not be thoroughly evaluated in terms of activity recovery since the product distribution of these experiments was severely influenced by the co-metabolism of syngas and glycerol. When working with anaerobic microorganisms, instead of separating the cells by centrifugation prior to inoculation, a common practice to minimize the toxicity of the CPA is to dilute the freezing medium 100-200 times upon inoculation into the growth medium [11]. This protocol was also followed for recovering the activity of an enriched microbial community growing on switchgrass using glycerol [15]. However, the effects of glycerol on the product recovery, if any, were not reported in the study. Based on the present study though, the use of glycerol as CPA for achieving a fast microbial activity recovery is not recommended for microbial communities without separation of the biomass prior to reactivation.

Previous studies also showed that cryopreservation with DMSO was more effective than without CPA addition using different microbial communities [15,18]. This observations are in line with the findings of this study since DMSO was clearly more effective than not adding any CPA. Nonetheless, in this study, PVP, Tween 80 and yeast extract were found at least as effective as DMSO in terms of activity recovery. Based on the Euclidean distance between the maximum product yields ($D_{Y,ref}$) of the reactivated microbial communities and that of the reference microbial community, PVP seemed to be the most effective CPA. The differences between the $D_{Y,ref}$ of PVP and the other CPAs tested though were only statistically significant for DMSO (p-value 0.026), glycerol (p-

value 0.027) and when no CPA was added (p-value 0.018). No statistically significant differences were found between the $D_{Y,ref}$ of PVP, Tween 80 and yeast extract.

3.3. Preservation of the microbial composition

After the batch reference experiments, the microbial community maintained the same community structure as the enrichment culture from the bioreactor as it presented a high abundance of reads mapping to the family *Clostridiaceae* (sample S11_78d in fig. 2 and S1_Ref in fig. 4A). However, there were some differences arising from the change in operating conditions, such as the higher percentage of reads mapping to *Enterobacteriaceae* spp. (8.5-8.7% compared to 2.3% in the bioreactor), the lower percentage of reads mapping to *Pseudomonaceae* spp. (0.013-0.02% compared to 1.9% in the bioreactor) and the appearance of *Enterococcaceae* spp. (1.07-1.08% of reads mapped), previously lower than 0.05% in the bioreactor. Another significant difference was found within family *Clostridiaceae*. While the community structure of the enriched microbial community from the bioreactor was dominated by the putative species *C. ljungdahlii*; after the batch reference experiments, the microbial community presented a more even structure with multiple abundant OTUs corresponding to different *Clostridium* spp. (fig. 4B). The dominant OTUs within family *Clostridiaceae* corresponded to a species closely related to *C. ljungdahlii* (1.00 bootstrap confidence) and two *Clostridium* spp. with closest but low similarity to *C. carboxidivorans* (0.53 bootstrap confidence) and *C. nitrophenolicum* (0.48 bootstrap confidence). This rapid shift in the relative abundance of *Clostridiaceae* spp. resulting from the change in operating conditions demonstrates the high functional redundancy of the enriched microbial community, as the latter quickly adapted to the change in operating mode and pH with rearrangements in the community structure maintaining its functionality. The high percentage of reads mapping to *Clostridiaceae* spp. was indicative of an important role during the fermentation of syngas. Both *C. ljungdahlii* and *C. carboxidivorans* are well known for their hydrogenotrophic and carboxydrotrophic abilities, with *C. carboxidivorans* being able to synthesize butyrate and butanol from syngas, besides acetate and ethanol [36,41]. In turn, a species closely related to *C. nitrophenolicum* was identified in an enrichment culture reducing acetate into ethanol using syngas as electron donor [42], which suggested that this could possibly be the role of this species during the batch reference experiments.

All reactivated microbial communities after long-term frozen storage exhibited a similar microbial community structure at family level, which suggested that all CPAs used were able to preserve the most abundant species of the microbial community. Nevertheless, a few differences were identified when comparing to the reference microbial composition at this taxonomic level. The microbial communities preserved without CPA addition and with DMSO, PVP, Tween 80 and yeast extract presented a higher percentage of reads mapping to *Enterobacteriaceae* spp. corresponding to a range of 8.1-19.4%, compared to 8.5-8.7% in the reference microbial community (fig. 4A). The biggest deviation at this taxonomic level was found in the microbial

community preserved with glycerol, where *Enterobacteriaceae* spp. and *Enterococcaceae* spp. reached a maximum of 32.7% and 5.7% of reads mapped, respectively, compared to 8.7% and 1.0% in the reference microbial community (fig. 4A). The higher relative abundance of reads mapping to *Enterobacteriaceae* spp. and *Enterococcaceae* spp. when using glycerol as CPA could be clearly attributed to the consumption of the glycerol added along with the inoculum, as glycerol metabolism is widespread in *Enterobacteriaceae* spp. and *Enterococcaceae* spp. [43,44]. Nevertheless, a possible role of these families in microbial communities preserved with other CPAs, justifying the generalized increase in percentage of reads mapped in all reactivated cultures, could not be identified.

Analyzing the family *Clostridiaceae* in more detail revealed considerable differences in the cryopreservation of the dominant species belonging to this family depending on the CPA used. The microbial community preserved without addition of CPA presented an almost negligible percentage of reads mapping to the *Clostridium* sp. with closest similarity to *C. carboxidivorans*, corresponding to 3.7%, 0.006% and 0.002% in the triplicates, compared to 34.4-48.4% in the reference microbial community (fig. 4B). Assuming that this species was involved in the production of butyrate and butanol [36], its low abundance would explain the negligible productivity of these products found in this reactivated microbial community. Glycerol was found to be ineffective for the preservation of the *Clostridium* sp. with closest similarity to *C. nitrophenolicum* as reads mapping to this OTU corresponded to 0.07-0.20% compared to 10.7-17.6% in the reference microbial community (fig. 4B). In turn, when DMSO and yeast extract were used as CPAs, the three dominant *Clostridium* spp. were present in the microbial community, but these exhibited a high variability in their relative abundance across triplicates (fig. 4B). Overall, PVP and Tween 80 were the only CPAs resulting in high reproducibility in the relative abundance of these OTUs across triplicates as well as low variability upon reactivation when compared to the reference microbial community. Therefore, given the strong link found between these *Clostridium* spp. and the functionality of the microbial community, it is obvious that PVP and Tween 80 were the most reliable CPAs as these were the only ones warranting reproducible results upon reactivation. Further investigation on whether the microbial community will eventually revert to its original state upon continued operation in sequential batch fermentations is needed for the other CPAs.

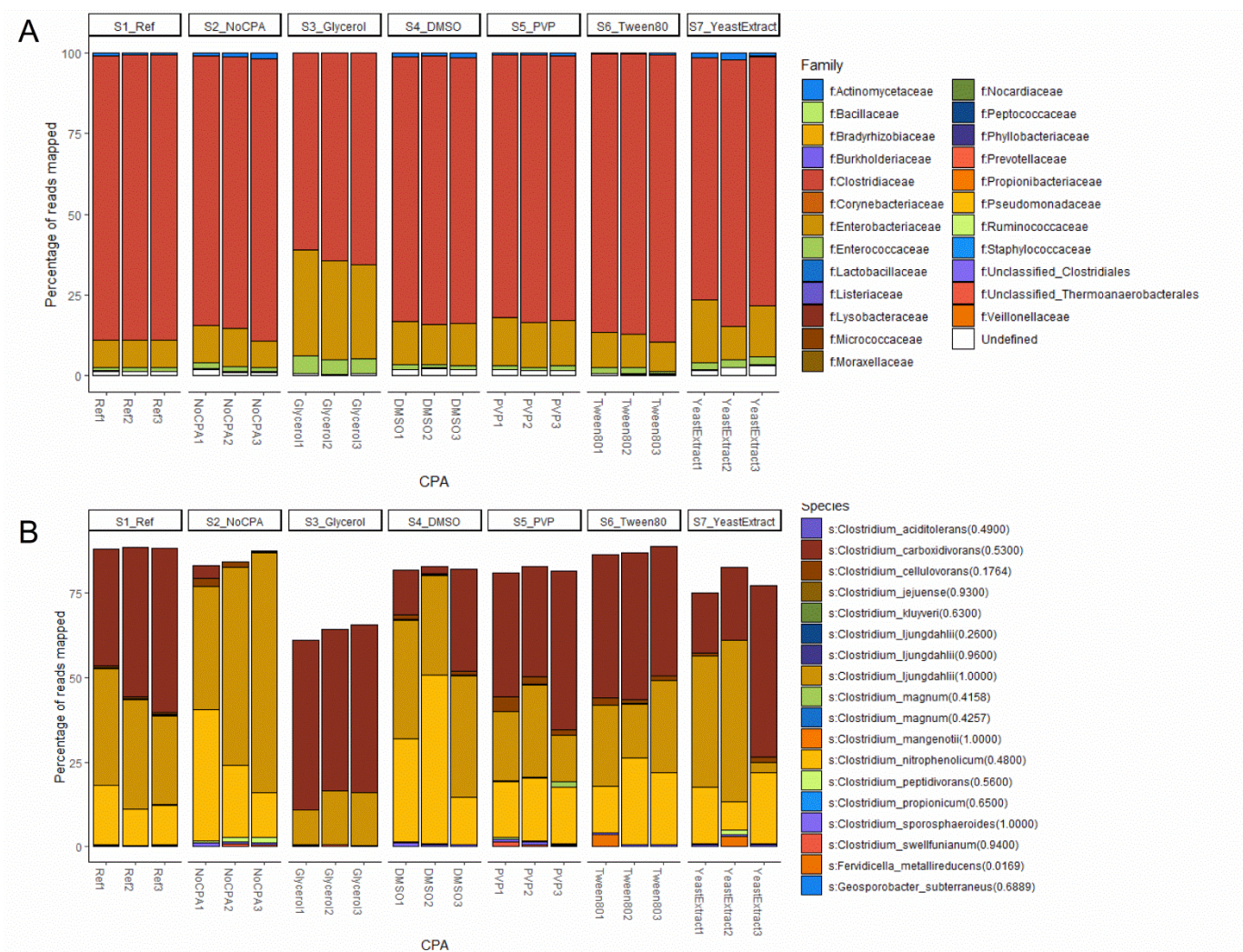


Figure 4. A Relative abundance of reads mapped to OTUs at family taxonomic level in reference microbial community and reactivated microbial communities after long-term frozen storage using different CPAs. OTUs with a bootstrap confidence measure at family level below the bootstrap confidence threshold of 0.8 were categorized as Undefined. **B** Relative abundance of reads mapping to *Clostridiaceae* spp. in reference microbial community and reactivated microbial communities after long-term frozen storage using different CPAs. The bootstrap confidence measure is given in brackets.

An overview of the OTUs identified in the reference and all reactivated microbial communities is provided in fig. 5 along with their relative abundance and the highest possible level of taxonomic assignment using a bootstrap confidence of 0.80. Considerable differences were found in species with minor representation in the microbial community since several OTUs present in the reference microbial community were absent after cryopreservation using the different CPAs, and vice versa. Glycerol is one of the most notable examples of this as several OTUs within the *Clostridium* cluster were absent in this microbial community (fig. 5). On the contrary, the microbial community preserved using PVP exhibited the highest amount of species not present in the reference microbial community. This is also reflected in fig. 6A, where it is shown that the microbial

communities preserved using glycerol and PVP presented the lowest and highest average Shannon diversity index.

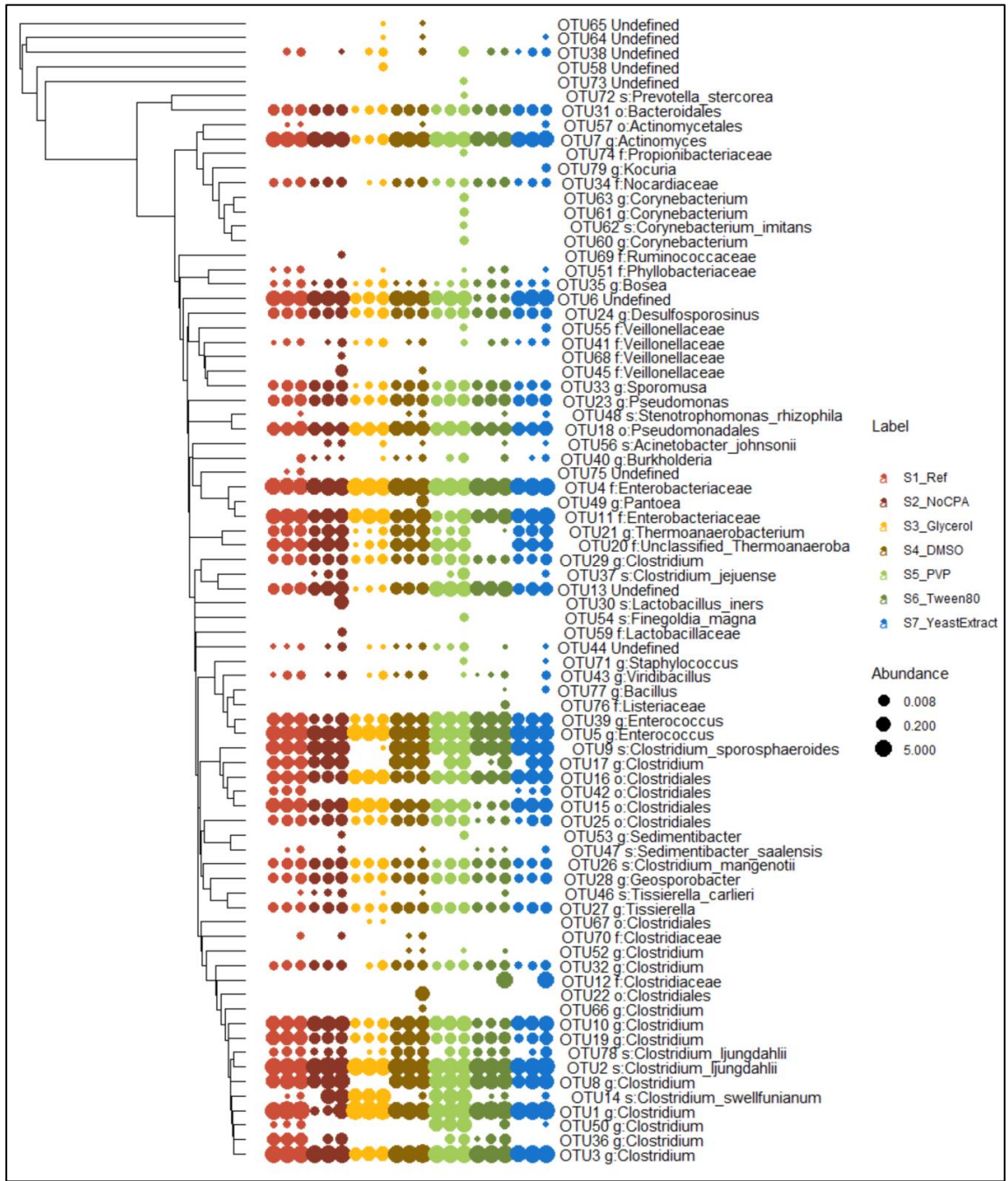


Figure 5. Phylogenetic tree of OTU sequences identified in reference microbial community and reactivated microbial communities, and relative abundance of reads mapped to OTUs for triplicates of the reference microbial community and reactivated microbial communities after long-term frozen storage using different CPAs. Taxonomy was assigned at the highest possible taxonomic level based on a bootstrap confidence threshold of 0.80.

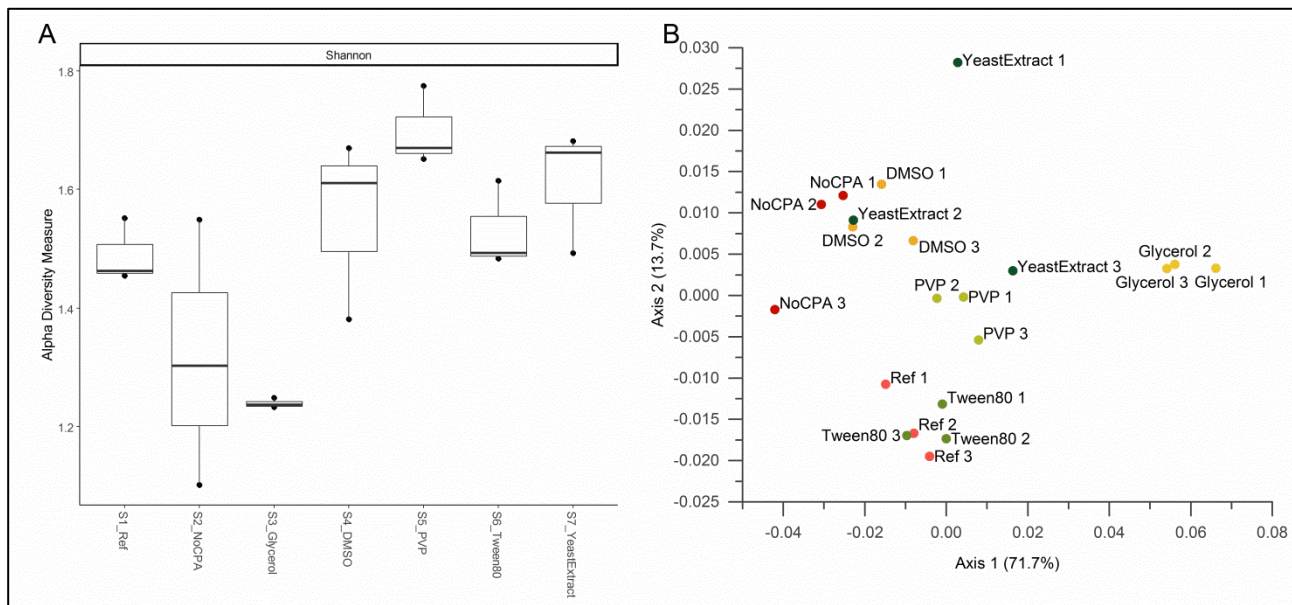


Figure 6. **A** Alpha diversity measure based on the Shannon diversity index for the reference microbial community and all reactivated microbial communities after cryopreservation using different CPAs. **B** Principal Coordinate Analysis (PCoA) on Unifrac distances between samples from the reference microbial community and all reactivated microbial communities. The percentage of variability explained in the ordination of samples by each axis is given in the axis label.

Previous work on the cryopreservation of microbial communities from fecal samples showed that frozen storage without addition of CPA resulted in a drastic loss of bacterial cell viability, while using glycerol as CPA increased the viability to levels similar to unfrozen samples [45]. However, these authors also pointed out that glycerol was not equally effective for preserving all bacterial species. Yu et al. [15] found that the cryopreservation without addition of CPA resulted in high variability in the composition of the reactivated microbial community, whereas both glycerol and DMSO, despite changes in the overall microbial community composition, were able to retain the dominant species after short-term cryopreservation. In line with this, Kerckhof et al. [18] reported loss of OTUs after cryopreservation in different microbial communities, even when adding DMSO and DMSO + tryptic soy and trehalose, although the general community structure was maintained.

In this study, the long-term cryopreservation without CPA addition and with addition of glycerol was not able to maintain the microbial diversity and functionality of the microbial community upon reactivation. These two storage conditions resulted in the lowest alpha diversity (fig. 6A) upon reactivation, and several *Clostridium* spp. with an important role in the microbial community were missing. This is also reflected in their large Unifrac distances to the reference samples (fig. 6B). It should be noted though that some changes in the structure of the microbial community preserved with glycerol could be attributed to the glycerol metabolism of the microbial community (e.g. the increase in *Enterobacteriaceae* spp. and *Enterococcaceae* spp.) rather than to its

effectiveness as cryoprotectant. DMSO was found to be more effective than glycerol and not adding CPA in maintaining the microbial community structure and its microbial diversity (fig. 6A). Nevertheless, among all CPAs tested, PVP and Tween 80 were found to be the most reliable as these were the only CPAs warranting high reproducibility in the composition of the family *Clostridiaceae*, which was clearly linked to the functionality of the microbial community. Based on the Unifrac distances to the reference microbial community samples though, Tween 80 was the most effective CPA in preserving the overall microbial community structure (fig. 6B).

From a biotechnological perspective, both fast activity recovery and preservation of the microbial community diversity and structure are indispensable requirements upon reactivation. On one hand, a fast activity recovery is crucial in mixed-culture-based bioprocesses in order to minimize the start-up time needed to reach stable operation after an eventual process shutdown. On the other hand, preserving the functional redundancy of microbial communities after frozen storage is essential for maintaining a healthy and functional microbial community, given that functional redundancy is the main asset against eventual process disturbances in mixed-culture-based bioprocesses. In this sense, the development of cryopreservation methods satisfying both of these requirements is necessary for the further advancement of mixed-culture-based biotechnological applications.

4. Conclusions

In this work, a highly specialized and stable microbial community converting syngas into mainly acetate and ethanol, and dominated by *Clostridium* spp., was generated through a microbial enrichment in continuous mode. The enriched microbial community presented high functional redundancy as it rapidly responded to changes in operating conditions with rearrangements in its community structure while maintaining its functionality. The preservation of this microbial community, evaluated based on the microbial activity recovery and microbial composition of reactivated cultures, was found to be affected by the cryopreservation agents used during frozen storage. All reactivated microbial communities presented differences in terms of activity and community structure when compared to the reference microbial community. Considering the storage protocols used, not adding cryopreservation agent and using glycerol for assisting the cryopreservation were found the least recommendable storage methods both for achieving a fast activity recovery upon revival of the microbial community and for preserving the microbial diversity. DMSO was found to be more suitable for the cryopreservation of the microbial community than the latter. However, PVP and especially Tween 80 were the only cryoprotectants warranting reproducible results in terms of both fast activity recovery and maintenance of the microbial community structure after long-term frozen storage. Overall, this work provided alternative and more effective cryopreservation methods than those commonly used for preserving anaerobic mixed microbial

communities, which contribute to further advancing in this important, yet poorly developed, research area. Further research in this direction is still necessary.

References

- [1] Kleerebezem R, van Loosdrecht MC. Mixed culture biotechnology for bioenergy production. *Curr Opin Biotechnol* 2007;18:207–12. doi:10.1016/j.copbio.2007.05.001.
- [2] Batstone DJ, Viridis B. The role of anaerobic digestion in the emerging energy economy. *Curr Opin Biotechnol* 2014;27:142–9. doi:10.1016/j.copbio.2014.01.013.
- [3] Agler MT, Wrenn B a, Zinder SH, Angenent LT. Waste to bioproduct conversion with undefined mixed cultures: the carboxylate platform. *Trends Biotechnol* 2011;29:70–8. doi:10.1016/j.tibtech.2010.11.006.
- [4] Marshall CW, LaBelle E V., May HD. Production of fuels and chemicals from waste by microbiomes. *Curr Opin Biotechnol* 2013;24:391–7. doi:10.1016/j.copbio.2013.03.016.
- [5] Asimakopoulos K, Gavala HN, Skiadas I V. Reactor systems for syngas fermentation processes: A review. *Chem Eng J* 2018;732–44. doi:10.1016/j.cej.2018.05.003.
- [6] Asimakopoulos K, Gavala HN, Skiadas I V. Biomethanation of Syngas by Enriched Mixed Anaerobic Consortia in Trickle Bed Reactors. *Waste and Biomass Valorization* 2019. doi:10.1007/s12649-019-00649-2.
- [7] Emerson D, Wilson W. Giving microbial diversity a home. *Nat Rev Microbiol* 2009;7:758. doi:10.1038/nrmicro2246.
- [8] Sievers M. Culture Collections in the Study of Microbial Diversity, Importance. *Encycl Metagenomics* 2013:1–5. doi:10.1007/978-1-4614-6418-1.
- [9] Dominguez Bello MG, Knight R, Gilbert JA, Blaser MJ. Ensure the Health of Future Generations. *Science (80-)* 2018;362:33–5.
- [10] Singh SK, Baghela A. Cryopreservation of Microorganisms. *Mod. Tools Tech. to Understand Microbes*, Cham, Switzerland: Springer International Publishing AG; 2017, p. 321–33. doi:10.1007/978-3-319-49197-4_20.
- [11] Malik KA. Cryopreservation of bacteria with special reference to anaerobes. *World J Microbiol*

Biotechnol 1991;7:629–32. doi:10.1007/BF00452850.

- [12] Hubálek Z. Protectants used in the cryopreservation of microorganisms. *Cryobiology* 2003;46:205–29. doi:10.1016/S0011-2240(03)00046-4.
- [13] Tao D, Li PH. Classification of plant cell cryoprotectants. *J Theor Biol* 1986;123:305–10. doi:10.1016/S0022-5193(86)80245-4.
- [14] Gilmour MN, Turner G, Berman RG, Krenzer AK. Compact liquid nitrogen storage system yielding high recoveries of gram-negative anaerobes. *Appl Environ Microbiol* 1978;35:84–8.
- [15] Yu C, Reddy AP, Simmons CW, Simmons BA, Singer SW, Vandergheynst JS. Preservation of microbial communities enriched on lignocellulose under thermophilic and high-solid conditions. *Biotechnol Biofuels* 2015;8:1–13. doi:10.1186/s13068-015-0392-y.
- [16] Laurin V, Labbé N, Juteau P, Parent S, Villemur R. Long-term storage conditions for carriers with denitrifying biomass of the fluidized, methanol-fed denitrification reactor of the Montreal Biodome, and the impact on denitrifying activity and bacterial population. *Water Res* 2006;40:1836–40. doi:10.1016/j.watres.2006.03.002.
- [17] Vlaeminck SE, Geets J, Vervaeren H, Boon N, Verstraete W. Reactivation of aerobic and anaerobic ammonium oxidizers in OLAND biomass after long-term storage. *Appl Microbiol Biotechnol* 2007;74:1376–84. doi:10.1007/s00253-006-0770-2.
- [18] Kerckhof FM, Courtens ENP, Geirnaert A, Hoefman S, Ho A, Vilchez-Vargas R, et al. Optimized cryopreservation of mixed microbial communities for conserved functionality and diversity. *PLoS One* 2014;9:1–14. doi:10.1371/journal.pone.0099517.
- [19] Calcott PH, MacLeod RA. The survival of *Escherichia coli* from freeze-thaw damage: the relative importance of wall and membrane damage. *Can J Microbiol* 1975;21:1960–8. doi:10.1139/m75-284.
- [20] Baumann DP, Reinbold GW. Freezing of Lactic Cultures. *J Dairy Sci* 1966;49:259–64. doi:10.3168/jds.s0022-0302(66)87846-3.
- [21] Wolin EA, Wolin MJ, Wolfe RS. Formation of methane by bacterial extracts. *J Biol Chem* 1963;238:2882–6. doi:10.1016/S0016-0032(13)90081-8.
- [22] Takahashi S, Tomita J, Nishioka K, Hisada T, Nishijima M. Development of a Prokaryotic Universal

Primer for Simultaneous Analysis of Bacteria and Archaea Using Next-Generation Sequencing. PLoS One 2014;9:e105592. doi:10.1371/journal.pone.0105592.

- [23] Martin M. Cutadapt removes adapter sequences from high-throughput sequencing reads. EMBnet J 2011;17:10–2.
- [24] Edgar RC. UPARSE: Highly accurate OTU sequences from microbial amplicon reads. Nat Methods 2013;10:996–8. doi:10.1038/nmeth.2604.
- [25] Rognes T, Flouri T, Nichols B, Quince C, Mahé F. VSEARCH: a versatile open source tool for metagenomics. PeerJ 2016;4:e2584. doi:10.7717/peerj.2584.
- [26] Edgar RC. SINTAX: a simple non-Bayesian taxonomy classifier for 16S and ITS sequences. BioRxiv 2016. doi:http://dx.doi.org/10.1101/074161.
- [27] Yarza P, Richter M, Euzeby J, Amann R, Schleifer K, Ludwig W, et al. The All-Species Living Tree project: A 16S rRNA-based phylogenetic tree of all sequenced type strains. Syst Appl Microbiol 2008;31:241–50. doi:10.1016/j.syapm.2008.07.001.
- [28] McMurdie PJ, Holmes S. Phyloseq: An R Package for Reproducible Interactive Analysis and Graphics of Microbiome Census Data. PLoS One 2013;8:e61217. doi:10.1371/journal.pone.0061217.
- [29] Castro H F, Williams N H, Ogram A. Phylogeny of sulfate-reducing bacteria. FEMS Microbiol Ecol 2000;31:1–9.
- [30] Bengelsdorf FR, Poehlein A, Linder S, Erz C, Hummel T, Hoffmeister S, et al. Industrial acetogenic biocatalysts: A comparative metabolic and genomic analysis. Front Microbiol 2016;7:1–15. doi:10.3389/fmicb.2016.01036.
- [31] González-Cabaleiro R, Lema JM, Rodríguez J, Kleerebezem R. Linking thermodynamics and kinetics to assess pathway reversibility in anaerobic bioprocesses. Energy Environ Sci 2013;6:3780–9. doi:10.1039/c3ee42754d.
- [32] Kenealy WR, Waselefsky DM. Studies on the substrate range of *Clostridium kluyveri*; the use of propanol and succinate. Arch Microbiol 1985;141:187–94. doi:10.1007/BF00408056.
- [33] Grootsholten TIM, Kinsky dal Borgo F, Hamelers HVM, Buisman CJN. Promoting chain elongation in mixed culture acidification reactors by addition of ethanol. Biomass and Bioenergy 2013;48:10–6.

doi:10.1016/j.biombioe.2012.11.019.

- [34] Ganigué R, Sánchez-paredes P, Bañeras L, Colprim J. Low Fermentation pH Is a Trigger to Alcohol Production , but a Killer to Chain Elongation. *Front Microbiol* 2016;7:1–11. doi:10.3389/fmicb.2016.00702.
- [35] Richter H, Molitor B, Diender M, Sousa DZ. A Narrow pH Range Supports Butanol , Hexanol , and Octanol Production from Syngas in a Continuous Co-culture of *Clostridium ljungdahlii* and *Clostridium kluyveri* with In-Line Product Extraction. *Front Microbiol* 2016;7:1–13. doi:10.3389/fmicb.2016.01773.
- [36] Zhang J, Taylor S, Wang Y. Effects of end products on fermentation profiles in *Clostridium carboxidivorans* P7 for syngas fermentation. *Bioresour Technol* 2016;218:1055–63. doi:10.1016/j.biortech.2016.07.071.
- [37] Ramió-pujol S, Ganigué R, Bañeras L, Colprim J. Incubation at 25 ° C prevents acid crash and enhances alcohol production in *Clostridium carboxidivorans* P7. *Bioresour Technol* 2015;192:296–303. doi:10.1016/j.biortech.2015.05.077.
- [38] Wang Q, Wang CD, Li CH, Li JG, Chen Q, Li YZ. *Clostridium luticellarii* sp. nov., isolated from a mud cellar used for producing strong aromatic liquors. *Int J Syst Evol Microbiol* 2015;65:4730–3. doi:10.1099/ijsem.0.000641.
- [39] De Smit SM, De Leeuw KD, Buisman CJN, Strik DPBTB. Continuous n-valerate formation from propionate and methanol in an anaerobic chain elongation open-culture bioreactor. *Biotechnol Biofuels* 2019;12:1–16. doi:10.1186/s13068-019-1468-x.
- [40] Kanmani P, Satish Kumar R, Yuvaraj N, Paari KA, Pattukumar V, Arul V. Effect of cryopreservation and microencapsulation of lactic acid bacterium *Enterococcus faecium* MC13 for long-term storage. *Biochem Eng J* 2011;58–59:140–7. doi:10.1016/j.bej.2011.09.006.
- [41] Köpke M, Held C, Hujer S, Liesegang H, Wiezer A, Wollherr A, et al. *Clostridium ljungdahlii* represents a microbial production platform based on syngas. *Proc Natl Acad Sci* 2010;107:13087–92. doi:10.1073/pnas.1011320107.
- [42] Grimalt-Aleman A, Łężyk M, Lange L, Skiadas I V, Gavala HN. Enrichment of syngas-converting mixed microbial consortia for ethanol production and thermodynamics-based design of enrichment strategies. *Biotechnol Biofuels* 2018;11:1–22. doi:10.1186/s13068-018-1189-6.

- [43] Murarka A, Dharmadi Y, Yazdani SS, Gonzalez R. Fermentative utilization of glycerol by *Escherichia coli* and its implications for the production of fuels and chemicals. *Appl Environ Microbiol* 2008;74:1124–35. doi:10.1128/AEM.02192-07.
- [44] Murakami N, Oba M, Iwamoto M, Tashiro Y, Noguchi T, Bonkohara K, et al. L-Lactic acid production from glycerol coupled with acetic acid metabolism by *Enterococcus faecalis* without carbon loss. *J Biosci Bioeng* 2016;121:89–95. doi:10.1016/j.jbiosc.2015.05.009.
- [45] Waite DW, Deines P, Taylor MW. Quantifying the impact of storage procedures for faecal bacteriotherapy in the critically endangered New Zealand Parrot, the Kakapo (*Strigops habroptilus*). *Zoo Biol* 2013;32:620–5. doi:10.1002/zoo.21098.

Manuscript VI

**“Syngas Biomethanation with Exogenous H₂ Supply for the Production of
Natural Gas Grade Biomethane”**

Syngas Biomethanation with Exogenous H₂ Supply for the Production of Natural Gas Grade Biomethane

Konstantinos Asimakopoulos¹, Antonio Grimalt-Alemany¹, Christoffer Lundholm-Høffner¹, Hariklia N. Gavala¹, Ioannis V. Skiadas¹

¹Department of Chemical and Biochemical Engineering, Technical University of Denmark, Søtofts Plads 229, 2800 Kgs. Lyngby, Denmark

Highlights

- A new index was introduced for the quality of the syngas composition
- Stoichiometric CO₂ excess was alleviated with in-situ exogenous H₂ supply
- Higher CH₄ productivity achieved at 60 °C compared to 37 °C
- Natural gas grade biomethane was produced
- Thermodynamic limitations on microbial metabolism were verified

Keywords

Syngas biomethanation; trickle bed reactor; mixed microbial consortia; carbon sequestration; natural gas; thermodynamics

Abstract

Biomass gasification generates a gas mixture (syngas) that constitutes a rich source of carbon and energy for the production of second-generation renewable fuels such as biomethane. However, the produced syngas composition (H₂/CO/CO₂) cannot be converted to natural gas grade biomethane due to stoichiometric limitations. The present study introduces the concept of biomass gasification coupled to syngas biomethanation with in-situ exogenous H₂ supply for the production of biomethane able to be injected in the natural gas grid. Syngas biomethanation was executed by mixed microbial consortia in a trickle bed reactor at 37 °C and 60 °C. The assessment of the effects of the net inlet gas composition was performed according to a proposed syngas quality index ($SQI = \frac{\%H_2 + \%CO}{\%CO_2 + \%CO}$), which is founded on the stoichiometry of the reactions converting syngas to CH₄. The ideal syngas composition has a SQI = 4. Values below 4 correspond to a stoichiometric carbon-moles excess while values above 4 correspond to a stoichiometric electron-moles excess. It was demonstrated that switching the SQI from 1.44 to 3.67 increased the CH₄ content in the outlet of the reactor from 30% to 72%, accompanied by an at least 1.2-fold increase of the CH₄ productivity. A SQI of 4.78 (>4) resulted in a significant deterioration of the quality of the produced biomethane due to a high content (52%-54%) of unconverted H₂ and because of thermodynamic limitations on carboxydrotrophic hydrogenogenesis in thermophilic conditions. Production of natural gas grade biomethane (97.2% CH₄ content) was feasible at a SQI = 3.98.

1. Introduction

A key element of the route towards a biobased economy is the detoxification of the global energy production from fossil fuels and the transition to green energy with net-zero CO₂ emissions. Biomethane is considered an important renewable fuel for the implementation of the directives of the European Commission because it can supplant natural gas, serve as a fuel for transport applications [1] and as a platform chemical in a wide range of chemical and biochemical processes [2]. Consequently, the development of innovative technologies for the sustainable production of biomethane has recently attracted scientific attention [3].

An emerging technology presenting high potential is biomass gasification followed by syngas biomethanation by mixed microbial consortia (MMC) [4]. The thermochemical conversion of biomass produces a gas mixture (mainly CO, CO₂ and H₂) called synthesis gas or syngas, the composition of which depends primarily on the gasification conditions, such as temperature and pressure [5], and the mechanical design of the gasifier [6]. Syngas can be, subsequently, converted to biomethane by microorganisms, which, in contrast to chemical catalysts, present higher resiliency to impurities (inhibitory compounds), last longer, are cheaper, and their selectivity is independent of the syngas composition [7]. Furthermore, syngas biomethanation is performed at mild temperatures (30 °C – 70 °C) and atmospheric pressure.

Temperature has a strong impact on the metabolic pathways via which CO is converted to biomethane due to the growth of different microbial communities at different temperature ranges [8,9]. Under mesophilic conditions CO is mainly converted to acetate by carboxydrotrophic acetogens through the Wood-Ljungdahl pathway and then acetate is converted to CH₄ by aceticlastic methanogens [10,11]. In turn, in thermophilic conditions CO is mainly consumed by carboxydrotrophic hydrogenogens through the biological water-gas shift reaction [9]. Regardless of the temperature level, the biological conversion of H₂ and CO₂ to CH₄ is performed by archaea known as hydrogenotrophic methanogens [12]. Apart from the aforementioned principal metabolic pathways, other bioreactions that may occur are homoacetogenesis, syntrophic acetate oxidation and carboxydrotrophic methanogenesis [4]. Syntrophic acetate oxidation is thermodynamically unfavorable under standard conditions, and thus it can typically occur under very low partial pressures of H₂ [10].

The selectivity of anaerobic MMC to CH₄ as an end product can be increased with acclimation/microbial enrichment procedures, i.e. the successive transfers of actively growing MMC under the appropriate batch operating conditions [10], or the long term exposure to a specific anaerobic environment [11]. The latter showed that a 45 days exposure of an anaerobic sludge to CO increased its conversion yield to CH₄ from 8% to 90% [11]. In another study, long term acclimation of sludge samples to 5% CO decreased the lag phase from 5 h to 1 h at

55 °C and from 15 h to 3 h at 70 °C when inoculated in serum vials under batch operation with H₂:CO₂:CO ratio of 80:16:5 as a substrate [13]. The aim of the microbial enrichment practices is the selection of the most competitive microbial groups for the targeted bioconversion (syngas to CH₄ in this case).

Table 1. Equations of biological reactions performed by mixed microbial consortia when grown on syngas and their standard Gibbs free energy change.

Metabolism	Reaction	$\Delta G^{0'}$ (kJ·mol ⁻¹)
Carboxydrotrophic acetogenesis	4 CO + 2 H ₂ O → CH ₃ COOH + 2 CO ₂	-176
Aceticlastic methanogenesis	CH ₃ COOH → CH ₄ + CO ₂	-31
Carboxydrotrophic hydrogenogenesis	CO + H ₂ O → CO ₂ + H ₂	-20
Hydrogenotrophic methanogenesis	CO ₂ + 4 H ₂ → CH ₄ + 2 H ₂ O	-131
Homoacetogenesis	2 CO ₂ + 4 H ₂ → CH ₃ COOH + 2 H ₂ O	-104
Syntrophic acetate oxidation	CH ₃ COOH + 2 H ₂ O → 2 CO ₂ + 4H ₂	+104
Carboxydrotrophic methanogenesis	4 CO + 2 H ₂ O → CH ₄ + 3 CO ₂	-211

The syngas composition determines the quality of the biomethane that will be produced from the biomethanation process. According to the stoichiometry of the reactions presented in Table 1, the ideal syngas composition should satisfy the equation: $SQI = \frac{\%H_2 + \%CO}{\%CO_2 + \%CO} = 4$ (eq. 1), when CH₄ is the targeted product. This is, however, not the case with the available biomass gasification technologies which result in a Syngas Quality Index (SQI) between 1 and 2 [14,15]. As a result, the produced gas from syngas biomethanation consists of a high fraction of CO₂, which demands further upgrade before its injection to the natural gas grid. An attractive alternative to the present downstream processing technologies is the in-situ exogenous H₂ supply to the syngas biomethanation unit in order to counterbalance the stoichiometric excess of CO₂ [16]. To comply with the biobased circular economy agenda, H₂ should derive from sustainable sources, such as water electrolysis from the surplus electricity produced from solar panels or wind turbines [17]. The described concept is under the power-to-gas framework which is founded on the fact that the electricity grid gets periodically overcharged due to intermittent fluctuations of the weather conditions [18]. An important advantage of this technology is, not only the exploitation of the surplus electricity, but also the carbon sequestration from the conversion of the remaining CO₂ to CH₄. Several small-scale and large-scale projects focusing on anaerobic digestion with in-situ or ex-situ H₂ injection have been developed over the last 10 years, most of which are located in Germany and Denmark [19]. Nevertheless, to the best of our knowledge, this is the first study that addresses the concept of biomass gasification coupled with syngas biomethanation including in-situ upgrade of biomethane to natural gas grade levels.

The limiting factors of syngas fermentation processes are the mass transfer of the sparingly soluble syngas components (H_2 and CO) to the water based media along with the low concentrations of microbes [20]. A solution is the use of a bioreactor configuration that can circumvent both of them simultaneously. A bioreactor that fulfills these specifications is the trickle bed reactor and has recently been on the spotlight for biological hydrogen methanation processes [17,21–23]. Trickle bed bioreactors consist of a fixed bed with high surface to volume ratio, where biofilm is formed and converts the gaseous substrate flowing co-currently or counter-currently to the recirculating trickling liquid flow [24]. Biofilms are viscoelastic aggregates of cells embedded in a matrix that protects them from dehydration and inhibitory toxic compounds, thus allowing for a high cell density and long cell retention time in the reactor [25]. A recent review has shown that bioreactors with biofilms provide higher gas-to-liquid mass transfer rates than conventional stirred tank and bubble column reactors and thus, they are more suitable for syngas biomethanation [26]. Furthermore, as a recent research study has shown [27], trickle bed reactors can have a key role in the power-to-gas framework since they can be put in a standby mode for up to 8 days at 25 °C and then get restarted without negative effects on the biomethanation performance.

While several studies focus on biological hydrogen methanation for biogas upgrade [28], syngas biomethanation has not yet received the attention it deserves. Recent research activities show potential in this technology, when the major challenges it faces are properly addressed [29–33]. The aim of this study was to assess the impacts of exogenous H_2 supply on syngas biomethanation performed by enriched mixed microbial consortia in a trickle bed reactor under mesophilic and thermophilic conditions. In addition, the role of thermodynamics and its effects on the microbial interactions under different syngas compositions was investigated. To our knowledge, this is the first study that addresses the effect of the syngas composition on syngas biomethanation by MMC at two different temperatures (37 °C and 60 °C) in a trickle bed reactor operated at continuous mode.

2. Materials and Methods

2.1 Inocula

The inocula employed in the present study were enriched mixed microbial consortia deriving from a mixture of two anaerobic sludges. Their preparation can be described in the following steps: i) Collection of sludge (a) from the Lundtofte Wastewater Treatment plant (Lundtofte, Denmark) and sludge (b) from a lab-scale manure treating anaerobic digester (Chemical Engineering Department, Technical University of Denmark), ii) Mixing of sludge (a) and (b) in equal volumes so as to increase the initial microbial diversity, iii) The mixed sludge underwent a

batch enrichment process under mesophilic (37 °C) and thermophilic conditions (60 °C), which is thoroughly described in a previous study [10]. Briefly, the mixed sludge was initially injected in an anaerobically sealed serum vial (15% volume of sludge per total volume) with growth medium and a headspace gas composition of 1.3 atm H₂, 0.4 atm CO and 0.3 atm CO₂. When active growth in the exponential phase was observed the culture from the first vial was used as inoculum (15% v/v) for the second vial with the same headspace gas composition and growth medium (transfer – one). Five successive transfers were performed at each temperature and the actively growing culture of the last transfer was used as inoculum for the respective mesophilic and thermophilic trickle bed reactor.

2.2 Growth Medium

A modified basic anaerobic medium (BA) was used to buffer the pH in the reactor at 7 and to provide the necessary trace elements and nutrients to the microbes. The following stock solutions were used for the preparation of the BA: Solution A contained NH₄Cl-100 g·l⁻¹, NaCl-10 g·l⁻¹, MgCl₂·6H₂O-10 g·l⁻¹ and CaCl₂·2H₂O-5 g·l⁻¹; Solution B contained KH₂PO₄-17.7 g·l⁻¹; Solution C contained K₂HPO₄-151.6 g·l⁻¹; Solution D contained NaHCO₃-52 g·l⁻¹; Trace Metal Solution (TMS) contained FeCl₂·4H₂O-2 g·l⁻¹, H₃BO₃-0.05 g·l⁻¹, ZnCl₂-0.05 g·l⁻¹, CuCl₂-0.03 g·l⁻¹, MnCl₂·4H₂O-0.05 g·l⁻¹, (NH₄)₆Mo₇O₂₄·5H₂O-0.05 g·l⁻¹, AlCl₃-0.05 g·l⁻¹, Na₂SeO₃·5H₂O-0.1 g·l⁻¹ and Na₂WO₄·2H₂O-0.06 g·l⁻¹; Solution E contained nitrilotriacetic acid (NTA)-1 g·l⁻¹; Vitamin Solution (VS) contained vitamins B7-2 mg·l⁻¹, B6-10 mg·l⁻¹, B2-5 mg·l⁻¹, B1-5 mg·l⁻¹, B12-0.1 mg·l⁻¹, folic acid-2 mg·l⁻¹, nicotinic acid-5 mg·l⁻¹, P-aminobenzoic acid-5 mg·l⁻¹, thiotic acid-5 mg·l⁻¹ and DL-pantothenic acid-5 mg·l⁻¹; and Solution F contained Na₂S-25 mg·l⁻¹. Solution F was prepared anaerobically in an anaerobically sealed serum vial by adding Na₂S to distilled H₂O after flushing for 20 min with N₂ to remove solubilized O₂.

The volumes of each stock solution per liter of medium were: A-10 ml, B-100 ml, C-100 ml, D-50 ml, TMS-4 ml, E-15 ml, VS-40 ml and F-40 ml. The stock solutions were added in 641 ml of distilled H₂O. Solution F was added with a syringe after flushing the rest mixture with N₂ for 20 min and sealing it anaerobically with a butyl rubber stopper. Fresh medium was prepared in a weekly basis.

2.3 Trickle Bed Reactor

The design of the bioreactor configuration was a modified version of a unit presented in a previous study [29]. Fig. 1 shows the schematic diagram of the setup and the direction of the flow of the fluids in it. The molar composition of the inlet gas mixture was suggested from an external partner (Danish Gas Technology Center) as

the produced gas from the gasification of wood pellets in an allothermal fluidized bed gasifier utilizing steam as a fluidization and gasification agent. The suggestion for the syngas composition was 45% H₂, 25% CO₂, 20% CO and 10% CH₄; in this study CH₄ was replaced with N₂ in order to avoid having the product in the inlet.

Syngas (45% H₂, 25% CO₂, 20% CO and 10% N₂) and high purity H₂ (>99.99%) were supplied from two different gas cylinders (AGA Industrielle gasser; 1, 18) to the trickle bed column (4). The flow of each gas was regulated with a mass flow controller (Bronkhorst; 3, 20) through the LabVIEW PC software (NATIONAL INSTRUMENTS) and the available flow range was between 0 and 10 ml·min⁻¹ with a 0.1 ml·min⁻¹ increment. The volume of the packed bed was 180 ml with a height/diameter ratio of 4.18 and contained polypropylene/polyethylene packing material (BioFLO 9 – Smoky Mountain Biomedica, USA) with a density of 1 g·cm⁻³ and a surface area of 800 m²·m⁻³. Developed biofilm on the packing material converted the supplied gas mixture to biomethane as it flowed downwards through the trickle bed column. The produced biomethane entered the headspace of a liquid reservoir (5) and, afterwards, it exited the reactor flowing through a gas sampling port (8), a foam trap (9) and a gas flowmeter (Ritter; 10). The trickle bed column and the liquid reservoir were made of borosilicate glass and had a double wall that allowed for temperature control. Water was pumped at a high speed from a water bath with internal sensor (Julabo) to the outer walls of the trickle bed column and the liquid reservoir securing a stable temperature in the reactor.

The liquid broth was continuously recirculated from the reservoir to the trickle bed column with a peristaltic pump (Watson Marlow; 7) at a constant flow rate of 200 ml·min⁻¹. Homogenous mixing of the liquid broth in the reservoir was achieved with a magnetic stirrer (IKA, 17) operated at 200 rpm and liquid samples were obtained from a liquid sampling port (6). The direction of the liquid flow was co-current to the gas flow (top-to-bottom). Moreover, fresh medium was introduced in the recirculation line with a peristaltic pump (Cole Parmer, 14) from an anaerobically sealed vessel (13) at an HRT of 8 days. A compressible gas bag (12) filled with N₂ was connected with the headspace of the vessel (13) so as to prevent O₂ entrance to the vessel and avoid vacuum creation as the medium was pumped out of it. Liquid effluent was removed from the unit with the use of a peristaltic pump (Cole Parmer, 15) operating always at the same speed with pump 14 so as to preserve a constant liquid volume of 220 ml in the reactor and a constant HRT of 8 d.

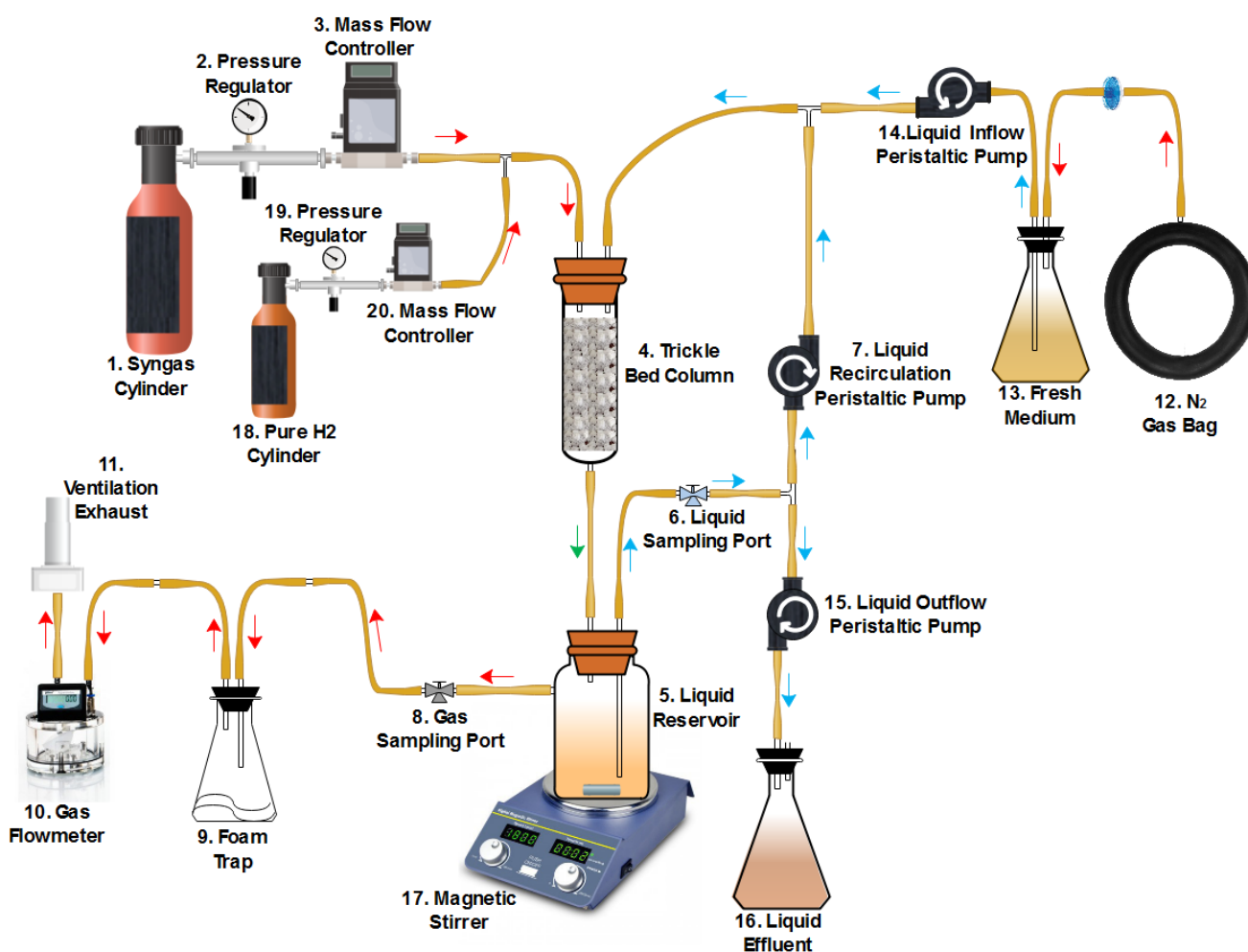


Figure 1. Schematic diagram of the trickle bed reactor. The design of the setup was a modified version of a module used in a previous study [29] from the same research group. Red arrows depict the flow of fluids in the gas phase, light blue arrows depict the flow of fluids in the liquid phase, and green arrows depict the combined flow of gas and liquid fluids.

2.4 Analytical Methods

The composition of the gas phase at the exit of the reactor was analyzed with the use of a SRI 8610C gas chromatograph (GC) equipped with a Molsieve 13 x column, a silica gel column, a rotating valve and a TCD detector. The Molsieve 13 x column separated H_2 , O_2 , N_2 , CH_4 and CO while the silica gel column separated CO_2 . The rotating valve determined the direction of the flow of the mobile phase (helium) through the columns. Gas samples (100 μ l) were collected from the gas sampling port (Fig. 1 – 8) with a Hamilton gas tight syringe and were directly injected, without storage, in the GC. The applied analysis method can be split in two phases. In phase 1 helium flowed first through the silica gel column and then through the Molsieve 13 x column while

the temperature was stable at 65 °C for 3 min followed by a 10 °C·min⁻¹ temperature ramp until 95 °C. In phase 2 the direction of the flow of the mobile phase was reversed and a 24 °C·min⁻¹ temperature ramp was applied until a final temperature of 140 °C was reached.

The analysis of the concentration of volatile fatty acids (VFAs) and alcohols was performed with high performance liquid chromatography (Shimadzu, USA). The analyzed compounds were acetate, propionate, isobutyrate, butyrate, caproate, valerate, isovalerate, ethanol and 1-butanol. The chromatograph was equipped with refractive index detector and an Aminex HPX-87H column (Bio-Rad, USA). The mobile phase consisted of H₂SO₄ 12 mM and was set at 600 µl·min⁻¹. Liquid samples were collected from the liquid sampling port (Fig. 1 – 6) and were stored in HPLC vials. 40 µl from each vial were analyzed for 43 min at 63 °C for the detection of the aforementioned compounds. Liquid and gas samples were collected on a daily basis.

2.5 Calculations

The produced gas from the biological trickle bed reactor was defined as biomethane regardless of the CH₄ content in it or the content of the other gases. In addition, a new index was introduced in the present study for the determination of the stoichiometric quality of the inlet gas. The syngas quality index was calculated as $SQI = \frac{\%H_2 + \%CO}{\%CO_2 + \%CO}$ and is based on the stoichiometric reactions presented in Table 1. Assuming no carbon losses to cell growth and maintenance and byproducts, when the SQI takes values below 4 the available carbon moles are more than the available electron moles for the production of CH₄ as the end product, and when the SQI takes values above 4 the available electrons moles are in an excess. When the SQI takes a value of 4 the available electron moles are in perfect stoichiometry with the available carbon moles for the production of CH₄. The ideal stoichiometric SQI = 4 will be mentioned hereafter as SQI_{Id} (Syngas Quality Index Ideal).

The volume specific productivity of CH₄ (Q_{CH_4}) was calculated as the mmol of CH₄ produced per liter of bed volume per unit of time [mmol·l_{bed}⁻¹·h⁻¹] by multiplying the concentration of CH₄ [mmol·ml⁻¹] in the gas sampling port with the volume specific total gas outflow rate [ml·l_{bed}⁻¹·h⁻¹]. The conversion of the amount of the gas compounds from liters to moles was performed with the ideal gas law at 1 atm and 298 K. Moreover, the conversion efficiencies of CO, CO₂ and H₂ were calculated as $R_i = \frac{Q_i^{in} - Q_i^{out}}{Q_i^{in}} 100\%$, where Q is the volume specific flow rate of each component i. Furthermore, the electron recovery or electron yield is represented in this study with “Y_j” and refers to the percentage of the released electron moles from the consumption of the electron donors (CO and H₂) that were fixed to each product j (j: CH₄, VFAs and Unidentified sinks that correspond

primarily to cell biomass and incidentally to potential undetected byproducts). The calculation of “ Y_j ” is thoroughly explained in a previous study [29]. All the detected VFAs were summed together to facilitate the presentation of the results. The HRT [d] was calculated as the total liquid volume in the reactor [220 ml] divided by the liquid medium outflow rate [27.5 ml·d⁻¹]. Finally, the empty bed residence time (EBRT) [h] is the quotient of the division of the volume of the bed [180 ml] by the total gas inflow rate [ml·h⁻¹]. The results presented in this study are under steady state operation and a steady state was considered when the gas effluent composition did not change more than 1% for every individual gas compound for three consecutive days.

2.6 Startup of the reactors and description of the experimental conditions

Before inoculation, the trickle bed column and the liquid reservoir were covered with black tape to avoid any potential photosynthetic growth. They were also flushed with N₂ overnight to establish an anaerobic environment. After inoculation (10% volume of inoculum per total liquid volume in the reactor) with an actively growing culture of enriched mixed microbial consortia, the pumping speed of the recirculation pump was set at 200 ml·min⁻¹, the HRT at 8 d and the flow from the syngas cylinder at 1 ml·min⁻¹. Based on previous experience these conditions were retained for 1 month in order to secure a stable biofilm [29]. The described procedure was applied for both mesophilic (37 °C) and thermophilic (60 °C) conditions.

The full set of experiments performed in this study is presented in Table 2 and contains 15 operating conditions, seven of them at 37 °C and eight at 60 °C. The chosen parameters allow for a direct comparison between mesophilic and thermophilic conditions, between a higher EBRT (3 h) and a lower EBRT (1.5 h) and, most importantly, shed light on the impact of the inlet gas composition (or the SQI) on the biomethanation process. Operating condition 15 was tested in order to assess the results from a stoichiometrically ideal syngas composition (SQI_{id} = 4).

The inlet gas composition was dependent on the flow rate from the syngas cylinder and the high purity H₂ cylinder. For example, at a total inflow rate of 1 ml·min⁻¹, in order to increase the SQI from 1.44 to 2.93 the flowrate from the syngas cylinder should drop from 1 ml·min⁻¹ to 0.6 ml·min⁻¹ and the flowrate from the H₂ cylinder should increase from 0 ml·min⁻¹ to 0.4 ml·min⁻¹. In this case the inlet gas composition changes from 45% H₂, 20% CO, 25% CO₂ and 10% N₂ to 67% H₂, 12% CO, 15% CO₂ and 6% N₂. The aforementioned example refers to operating conditions No. 1 and No. 2 in Table 2.

Table 2. Overview of the tested experimental conditions. Syngas cylinder column refers to the percentage of the total flow supplied from the syngas cylinder and H₂ cylinder column refers to the percentage of the total flow supplied from the pure H₂ cylinder. The Inlet molar

gas composition column refers to the final gas composition of gas entering the reactor. The Syngas Quality Index (SQI) is calculated according to eq. 1.

No.	Temperature (°C)	Total Inflow rate (ml·min ⁻¹)	Syngas cylinder (%)	H ₂ cylinder (%)	EBRT (h)	Inlet molar gas composition (%)				SQI
						H ₂	CO	CO ₂	N ₂	
1	37	1.0	100	0	3.0	45	20	25	10	1.44
2	37	1.0	60	40	3.0	67	12	15	6	2.93
3	37	1.0	50	50	3.0	72.5	10	12.5	5	3.67
4	37	1.0	40	60	3.0	78	8	10	4	4.78
5	37	2.0	100	0	1.5	45	20	25	10	1.44
6	37	2.0	60	40	1.5	67	12	15	6	2.93
7	37	2.0	50	50	1.5	72.5	10	12.5	5	3.67
8	60	1.0	100	0	3.0	45	20	25	10	1.44
9	60	1.0	60	40	3.0	67	12	15	6	2.93
10	60	1.0	50	50	3.0	72.5	10	12.5	5	3.67
11	60	1.0	40	60	3.0	78	8	10	4	4.78
12	60	2.0	100	0	1.5	45	20	25	10	1.44
13	60	2.0	60	40	1.5	67	12	15	6	2.93
14	60	2.0	50	50	1.5	72.5	10	12.5	5	3.67
15	60	1.5	47	53	2.0	74.3	9.3	11.7	4.7	3.98

2.7 Thermodynamic feasibility study

2.7.1 Computational Methods

The thermodynamics of hydrogenotrophic methanogenesis, syntrophic acetate oxidation and carboxydophilic hydrogenogenesis were evaluated based on the Gibbs free energy change ($\Delta_r G'_T$) and the thermodynamic potential factor (F_T) of net biochemical reactions [10]. Briefly, the standard Gibbs free energies of formation ($\Delta_f G^\circ$) and standard enthalpies of formation ($\Delta_f H^\circ$) used were extracted from Alberty [34]. $\Delta_f G^\circ$ were corrected for temperature (310 K and 333 K) and ionic strength (0.25 M) according to eq. 1 and 2, where z_i corresponds to the charge number of compound i , I is the ionic strength of the medium [34], B is an empirical constant that takes a value of $1.6 \text{ L}^{1/2} \text{ mol}^{-1/2}$ within a range of ionic strength of 0.05-0.25 M, and A was calculated as a function of temperature according to Alberty [34]. The $\Delta_r G'_T$ was then corrected for partial pressure of gases and concentration of acetate according to eq. 3, and the effect of the pH was taken into account as described in Steinbusch et al. [35].

$$\Delta_f G'_i(T) = \Delta_f G^\circ_i(298.15 K) \cdot \frac{T}{298.15 K} + \Delta_f H^\circ_i(298.15 K) \cdot \frac{298.15 K - T}{298.15 K} \quad (1)$$

$$\Delta_f G^\circ_i(I) = \Delta_f G^\circ_i(I = 0) - \frac{RTAz_i^2 I^{1/2}}{1 + BI^{1/2}} \quad (2)$$

$$\Delta_r G'_T = \Delta_r G^\circ_T(I = 0.25 M) + RT \ln \frac{[C]^c [D]^d}{[A]^a [B]^b} \quad (3)$$

The F_T , derived by Jin & Bethke [36], was used to study the feasibility of the microbial interaction between hydrogenotrophic methanogens and syntrophic acetate oxidizers and was calculated according to eq. 4 and 5, where ΔG_A represented $-\Delta_r G'_T$ in kJ per reaction; ΔG_C corresponds to the energy conserved calculated as a function of the ATP yield of each metabolic pathway and the Gibbs free energy of phosphorylation (ΔG_p); and χ represents the average stoichiometric number. F_T values above zero ($\Delta G_A = \Delta G_C$) indicate that the reaction is feasible as the ΔG_A is greater than ΔG_C . When F_T approaches 1, at $\Delta G_A \gg \Delta G_C$, there is a strong thermodynamic driving force for the reaction to proceed forward, and thus the rate of the reaction can be considered strictly dependent of the kinetics of the microbial species carrying out the conversion. In turn, when F_T approaches 0, at $\Delta G_A \approx \Delta G_C$, the thermodynamic driving force of the reaction is low and the reaction rate can be considered thermodynamically controlled.

$$F_T = 1 - \exp\left(-\frac{\Delta G_A - \Delta G_C}{\chi RT}\right) \quad (4)$$

$$\Delta G_C = Y_{ATP} \cdot \Delta G_p \quad (5)$$

F_T calculations for hydrogenotrophic methanogenesis were made assuming a conservative ATP yield of 0.5 mol ATP/mol CH_4 resulting from the translocation of 2 Na^+ across the membrane and an ATP synthesis stoichiometry of 4 Na^+ per ATP formed [37]. χ for hydrogenotrophic methanogenesis was calculated assuming that the rate-determining step was the translocation of Na^+ by the methyl transferase complex (MTR). The syntrophic acetate oxidation was assumed to have a ΔG_C of 12 kJ/mol of acetate as found by Jackson & McInerney [38] for syntrophic fatty acid oxidizers. The carboxydrotrophic hydrogenogenesis was assumed to translocate one H^+ across the membrane per mol of CO , which would result in an ATP yield of 0.33 mol ATP/mol CO by using an ATP synthesis stoichiometry of 3 H^+ per ATP synthesized [10]. All ΔG_C calculations were made using a ΔG_p of 45 kJ/mol ATP. The ΔG_C , ATP yields and χ used for F_T calculations are summarized in table 3.

Table 3. Overall biochemical reactions, ATP yield and average stoichiometric number used in thermodynamic potential factor (FT) calculations. FT calculations were not used for carboxydrotrophic hydrogenogenesis and thus the average stoichiometric number (χ) is not given.

Stoichiometry of biochemical reactions	ΔG_c (kJ per reaction)	ATP yield (mol per reaction)	χ	Ref.
Carboxydrotrophic hydrogenogenesis $\text{CO} + \text{H}_2\text{O} \rightarrow \text{H}_2 + \text{CO}_2$	14.85	0.33		[10]
Syntrophic acetate oxidation $\text{CH}_3\text{COOH} + 2 \text{H}_2\text{O} \rightarrow 4 \text{H}_2 + 2 \text{CO}_2$	12		1	[39]
Methanogenesis $4 \text{H}_2 + \text{CO}_2 \rightarrow \text{CH}_4 + 2 \text{H}_2\text{O}$	22.5	0.5	2	[38]

2.7.2 Experimental Confirmation of Thermodynamic Interpretations

The thermodynamic analysis of the effect of the syngas composition on syntrophic acetate oxidation and hydrogenotrophic methanogenesis in mesophilic conditions was performed by switching from a SQI = 2.83 to a SQI = 3.67 at an EBRT of 2.3 h and an HRT of 8 d. The total duration of this study was 21 days.

In thermophilic conditions, the thermodynamic interpretation of the effects of the increase of the SQI on carboxydrotrophic hydrogenogenesis was performed at an EBRT = 3 h and an HRT = 8 d. The duration of the study was 12 days, during which two SQI transitions were performed (2.93 \rightarrow 3.67 \rightarrow 4.78).

The aforementioned experiments were performed after the completion of the experiments described in section 2.6 for the interpretation of observations made during the main core of the study.

3. Results and Discussion

3.1 Effect of the SQI/syngas composition on the performance of the trickle bed reactors

Eight operating conditions were selected for the assessment of the impact of different syngas compositions (SQI) on syngas biomethanation. Half of them were under mesophilic conditions (No. 1 – 4) and the rest under thermophilic conditions (No. 8 – 11). The EBRT at these operating conditions was 3.0 h (total flow 1 ml·min⁻¹). The tested SQIs were 1.44, 2.93, 3.67 and 4.78. SQI = 1.44 corresponded to the scenario when no supply of exogenous H₂ takes place, SQI = 2.93 and SQI = 3.67 addressed the effects of the partial pressure/content of the syngas components, as the SQI_{ld} was approached, and SQI = 4.78 allowed for an assessment of the consequences of a stoichiometric excess of H₂ on syngas biomethanation (Table 2).

An increase of the SQI from 1.44 to 3.67 resulted in a respective increase of the conversion efficiency of CO₂ from 44.7% to 92.7% in mesophilic conditions and from 26.7% to 86.0% in thermophilic conditions (Fig. 2c). This was also reflected in the excess gas composition where the percentage of CO₂ in biomethane decreased from 33.7% to 4.0% and from 41.7% to 7.4% in mesophilic and thermophilic conditions, respectively (Fig. 2b). When the SQI was further increased to 4.78, CO₂ was fully converted in both temperatures and a high H₂ percentage was observed in the produced biomethane (54.9% in mesophilic and 52.7% in thermophilic conditions). Furthermore, approaching the SQI_{ld}, the fraction of CH₄ in the produced gas increased from 31.0% (SQI = 1.44) to 71.7% (SQI = 3.67) in mesophilic conditions and from 32.4% (SQI = 1.44) to 71.2% (SQI = 3.67) in thermophilic conditions but, when the SQI was set over the SQI_{ld}, CH₄ plummeted back to 32.4% and 28.7% (Fig. 2b), respectively. The aforementioned results indicated that the described stoichiometry from H₂, CO and CO₂ to CH₄ in Table 1 was strictly followed in the trickle bed reactor from the MMC independent of the temperature. Note that the increase of the percentage of N₂ in biomethane (Fig. 2b) does not imply N₂ production. It occurs due to the fact that, stoichiometrically, there are 3 reacting gas compounds and only one produced gas compound. In addition, a fraction of the gas reactants was used for synthesis of cell biomass and liquid byproducts.

An interesting difference between mesophilic and thermophilic conditions was that at SQI = 4.78 partial inhibition of the carboxydrotrophic activity at 60 °C (Fig. 2c) was observed ($R_{CO} = 54.0\%$), while no apparent inhibition occurred at 37 °C ($R_{CO} = 90.6\%$). This observation is discussed and explained in detail in section 3.5.

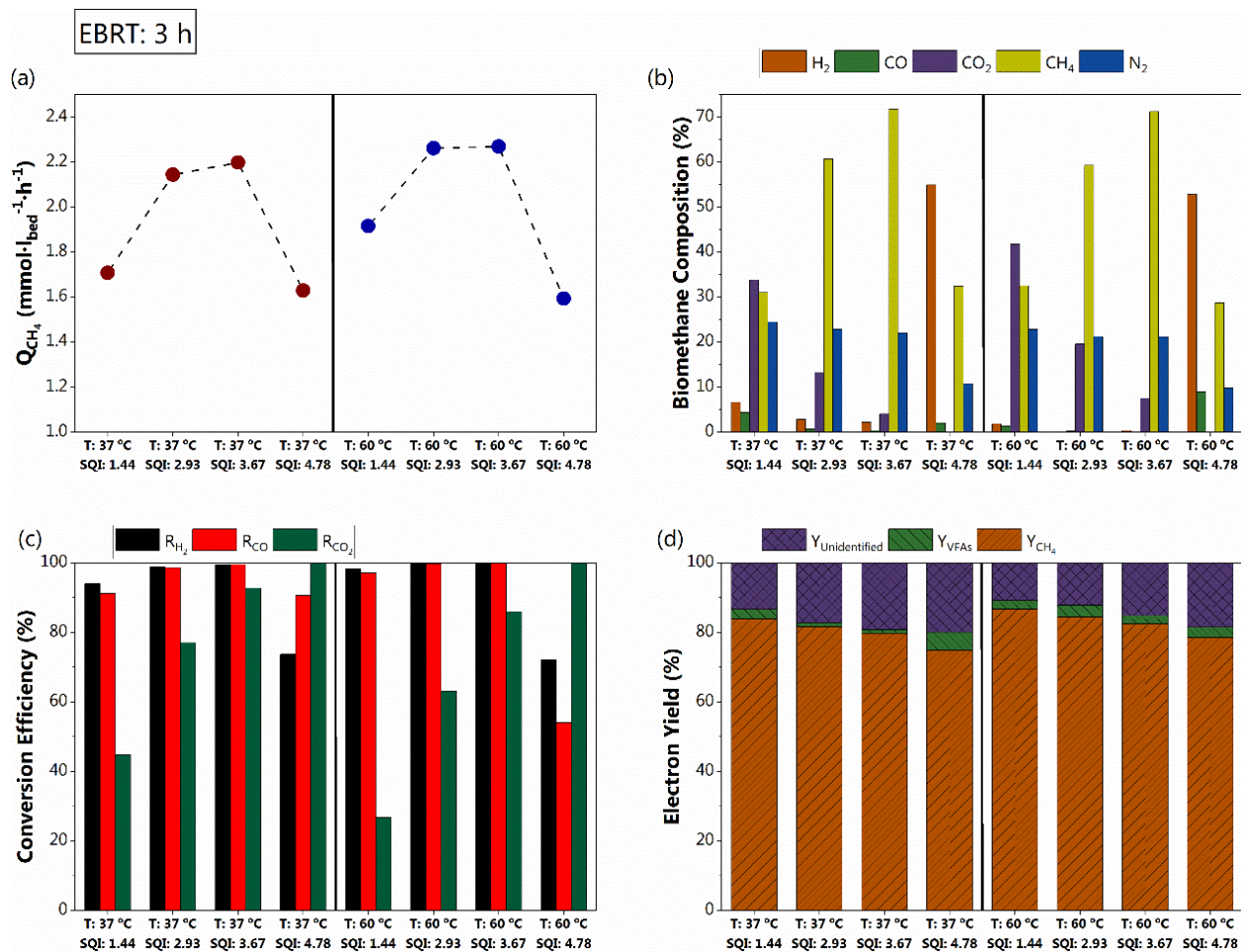


Figure 2. Effect of the syngas quality index (SQI) or the syngas composition on [(a) volume specific CH₄ productivity, (b) produced biomethane composition, (c) conversion efficiency of the substrate and (d) electron yield to CH₄, VFAs, and other unidentified sinks] at 1 ml·min⁻¹ total gas inflow rate. In graph (a) the brown dots correspond to mesophilic conditions (No. 1 – 4) and the blue dots on thermophilic conditions (No. 8 – 11). In graph (d) Y_{Unidentified} corresponds mainly to cell biomass synthesis and maintenance, and potentially other liquid byproducts not detected in the present study.

The volume specific CH₄ productivity increased in both mesophilic and thermophilic conditions when exogenous H₂ was supplied (Fig. 2a). More specifically, by raising the SQI from 1.44 to 2.93, the achieved CH₄ productivity increased from 1.71 and 1.92 to 2.14 and 2.26 in mesophilic and thermophilic conditions, respectively. This was expected since an increase of the SQI at a constant inflow rate increases the convertible C-moles for CH₄ production (Table 4), and thus higher CH₄ productivity can be achieved. As it is shown in Table 4, there is an important distinction between the stoichiometrically maximum convertible carbon moles and the inflow rate of carbon in the reactor. This distinction is not intuitively obvious since at a constant gas inflow rate (constant EBRT) increasing the SQI from 1.44 to 2.93 corresponds to the decrease of the flow from the syngas cylinder from 1.0 ml·min⁻¹ to 0.6 ml·min⁻¹ and the increase of the flow from the high purity H₂ cylinder

from 0 ml·min⁻¹ to 0.4 ml·min⁻¹, and thus the inflow rate of the carbon in the reactor at SQI = 2.93 is 60% of the one at SQI = 1.44. Nevertheless, based on the stoichiometry of the biological reactions (Table 1), at SQI = 1.44 only 36% of the supplied carbon is stoichiometrically convertible to CH₄, while at SQI = 2.93 the convertible carbon to CH₄ increases to 73% (Table 4).

Regarding the electron yield, it was observed that in both temperatures the electron yield to biomass ($Y_{\text{Unidentified}}$) presented an upward trend (Fig. 2d) with the increase of the SQI, and consequently, the electron yield to CH₄ decreased. The cause of this could be a potential change of the microbial populations and the microbial metabolism in the biofilm because of the lower partial pressure of CO and the higher partial pressure of H₂. Jing et al. [39] showed that CO addition in anaerobic granular sludge converting wastewater, changed significantly the microbial communities. At SQI = 4.78 the volume specific CH₄ productivity dropped harshly compared to the SQI = 3.67 both in mesophilic and thermophilic conditions while the minimum electron yield to CH₄ was observed.

Table 4. Distinction of the total supply of carbon in the reactor vs the stoichiometrically available carbon for CH₄ production. Stoichiometrically means that it is assumed that no carbon is used for synthesis of cell biomass or production of liquid byproducts. The fourth column refers to the percentage of the stoichiometrically available carbon for CH₄ production over the total carbon supplied. If the percentage is below 100% the carbon supply is in stoichiometric excess, and if it is above 100% the carbon supply is in stoichiometric deficiency.

SQI	Volume specific carbon inflow rate (C·mmol·l _{bed} ⁻¹ ·h ⁻¹)		Stoichiometrically maximum convertible carbon flow rate for CH ₄ production (C·mmol·l _{bed} ⁻¹ ·h ⁻¹)		Percentage of convertible carbon over the total carbon supply
	EBRT = 3 h	EBRT = 1.5 h	EBRT = 3 h	EBRT = 1.5 h	
1.44	6.05	12.10	2.20	4.40	36%
2.93	3.63	7.26	2.66	5.32	73%
3.67	3.02	6.04	2.77	5.54	92%
4.78	2.42	4.84	2.90	5.80	120%

Overall, the major observations from this set of experiments were: a) as the SQI increased towards the SQI_{Id}, the quality of the produced biomethane was significantly improved, the electron yield to CH₄ was slightly decreased and the CH₄ productivity was increased, and b) surpassing the SQI_{Id} resulted in much lower CH₄ productivity, lower electron yield to CH₄ and a high percentage of H₂ in biomethane. Consequently, the exogenous H₂ supply should be regulated at flowrates that result in an inflow gas composition with SQI close to 4 and SQIs higher

than 4 should be avoided. It is noteworthy that the trickle bed reactor responded efficiently to exogenous hydrogen addition and according to the anticipated stoichiometry both in mesophilic and thermophilic conditions.

3.2 Impacts of temperature on syngas biomethanation with respect to the SQI

The assessment of the impacts of temperature on syngas biomethanation at different SQIs was performed at a total gas inflow rate of $2 \text{ ml}\cdot\text{min}^{-1}$ (EBRT = 1.5 h) and was based on six operating conditions. Operating conditions No. 5, 6 and 7 correspond to mesophilic conditions at SQIs 1.44, 2.93 and 3.67, respectively, while operating conditions No. 12, 13 and 14 correspond to thermophilic conditions at the same SQIs (Table 2).

The thermophilic trickle bed reactor achieved higher CH_4 productivity and higher conversion efficiency of the electron donors (CO and H_2) at each SQI tested compared to the mesophilic trickle bed reactor, (Fig. 3a and Fig. 3c). The superiority of the thermophilic reactor can also be observed from the biomethane composition (Fig. 3b), where, at SQI = 3.67, the percentage of CH_4 was 72.0% at thermophilic conditions and 46.4% at mesophilic conditions. This observation is in line with relevant research activities reporting that the specific carboxydrotrophic methanogenic activity of an anaerobic sludge at $60 \text{ }^\circ\text{C}$ was 5 times higher than at $35 \text{ }^\circ\text{C}$ [9], and that a 5.3 fold increase of the maximum specific hydrogenotrophic activity was achieved at $60 \text{ }^\circ\text{C}$ compared to $37 \text{ }^\circ\text{C}$ in batch experiments performed with MMC and syngas as the only available substrate [10]. In the present study at thermophilic conditions CO and H_2 were almost fully converted at the three examined SQIs (EBRT = 1.5 h). On the other hand, at mesophilic conditions at SQI = 1.44 the conversion efficiency of CO and H_2 was 67.5% and 70.8%, respectively, and at SQI = 3.67 the conversion efficiency of CO and H_2 was 85.1% and 87.0%. In another study with a thermophilic synthetic coculture (*Carboxydotherrmus hydrogenoformans* and *Methanothermobacter thermoautotrophicus*) and a gas mixture (66.6% H_2 and 33.3% CO) with a SQI = 3, the fraction of CH_4 in the produced gas was 72% (96% of the stoichiometric fraction = 75%) [40], while in this study at a similar SQI of 2.93 the fraction of CH_4 in the produced gas was 58.8% (98.3% of the maximum stoichiometric fraction = 59.8% {The reason why the stoichiometric CH_4 fraction has a big difference between the two studies, despite the close proximity of the SQI, is because in the present study 10% N_2 was contained in the syngas cylinder. Without an inert gas, a SQI = 2.93 corresponds to a maximum stoichiometric CH_4 fraction of 73.3%}). This shows that the MMC have the capability to perform syngas biomethanation as effectively as defined cocultures, a noteworthy observation taking also into account that reactors operated with MMC do not demand sterilization prior to inoculation and do not face any risk of contamination.

Even though the conversion efficiency of H_2 was just 1.9% higher than the conversion efficiency of CO at mesophilic conditions at SQI = 3.67, the inflow rate of H_2 was 7.25 times higher than the inflow rate of CO , thus

indicating a 7.4 times higher conversion rate of H₂ over CO at the tested EBRT. This observation is in accordance with a research study employing anaerobic sludge and blast furnace gas (20% CO, 16% CO₂ and 64% H₂) as a substrate, where the specific hydrogenotrophic activity was 18 times higher than the specific carboxydrotrophic activity under batch operation at 37 °C [16].

The decrease of the percentage/partial pressure of CO in the gas inflow from 20% to 12% and 10% resulted in improved conversion efficiency of the electron donors (H₂ and CO) in mesophilic conditions (Fig. 3c), thus implying an inhibitory effect of CO on the metabolism of the developed biofilm. Guiot et al. [9] reported a steep increase of the consumption of CO by anaerobic granules for the production of CH₄ when its partial pressure dropped below 0.15 atm (15%).

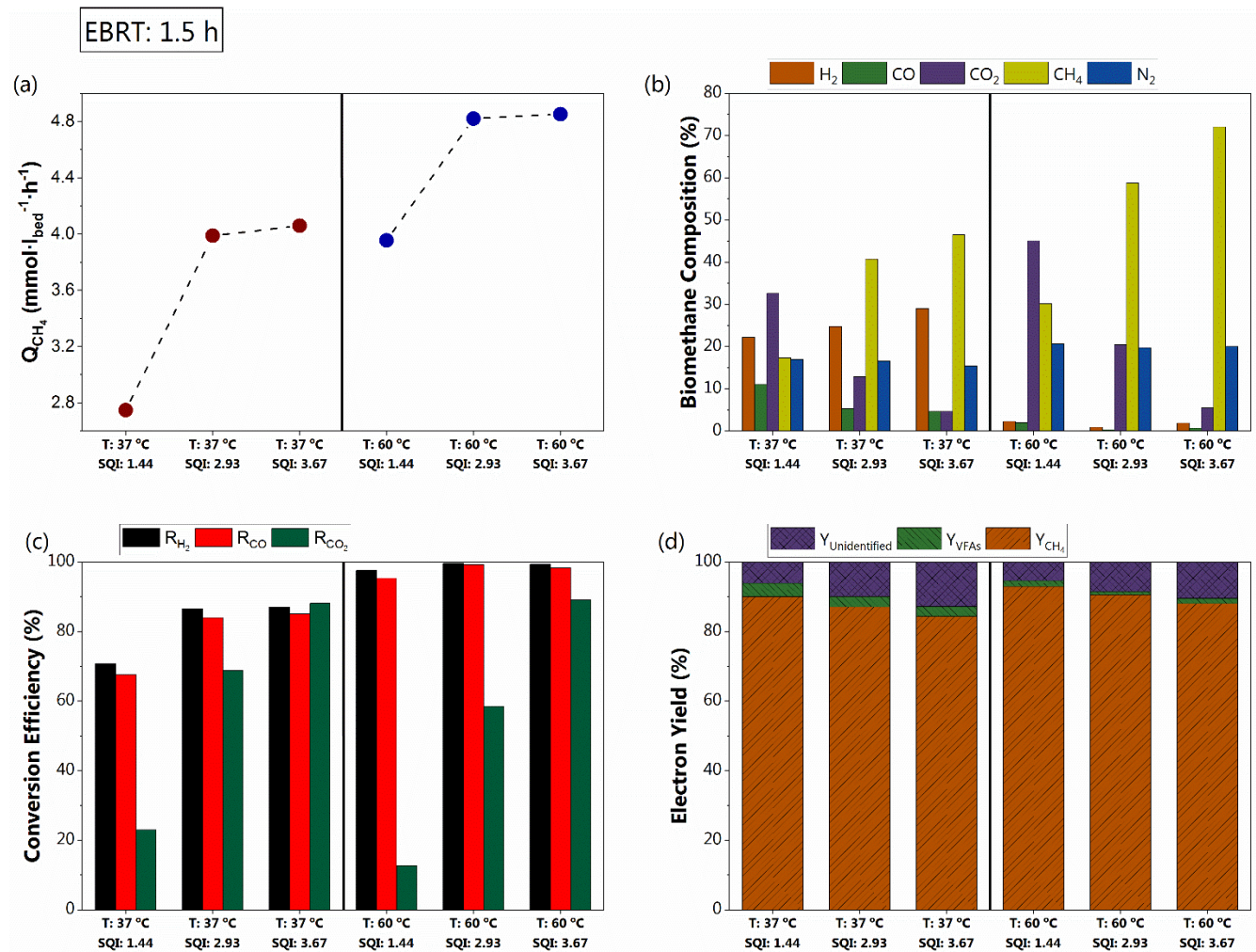


Figure 3. Effect of the temperature on [(a) volume specific CH₄ productivity, (b) produced biomethane composition, (c) conversion efficiency of the substrate and (d) electron yield to CH₄, VFAs and other unidentified sinks] at 2 ml·min⁻¹ total gas inflow rate. In graph (a)

the brown dots correspond to mesophilic conditions (No. 5 – 7) and the blue dots on thermophilic conditions (No. 12 – 14). In graph (d) $Y_{\text{Unidentified}}$ corresponds to cell biomass synthesis and potentially other liquid byproducts not detected in the present study.

Regarding the electron yield to CH_4 (Fig. 3d) no significant differences were observed between mesophilic and thermophilic conditions, whereas an at least 2-fold higher electron yield to VFAs was observed in mesophilic conditions at each SQI tested. Nevertheless, the electron yield to VFAs was lower than 5% in all operating conditions examined in the present study, thus pointing out a high selectivity of the enriched mixed microbial consortia to CH_4 independent of the temperature. The low yields to VFAs were also important from a microbiological perspective since it has been reported that acetate inhibits hydrogenotrophic methanogenesis and diverts the carbon flow towards homoacetogenesis [41].

3.3 Effect of the EBRT on syngas biomethanation with respect to the SQI

The required data for the assessment of the effect of the EBRT on syngas biomethanation are included in Fig. 2 and Fig. 3 which correspond to an EBRT of 3 h (total inflow rate of $1 \text{ ml}\cdot\text{min}^{-1}$) and an EBRT of 1.5 h (total inflow rate of $2 \text{ ml}\cdot\text{min}^{-1}$), respectively. Comparing the electron yield to CH_4 (Y_{CH_4}) and biomass ($Y_{\text{Unidentified}}$) (Fig. 2d and Fig. 3d), it was deduced that when the supply of substrate was doubled, the losses to biomass decreased in both mesophilic and thermophilic conditions at all SQIs tested, and thus the electron yield to CH_4 increased. For example, at $\text{SQI} = 3.67$ and a total gas inflow rate of $1 \text{ ml}\cdot\text{min}^{-1}$ the $Y_{\text{Unidentified}}$ was 19.3% and 15.1% at mesophilic and thermophilic conditions, respectively, whereas at $\text{SQI} = 3.67$ and a total gas inflow rate of $2 \text{ ml}\cdot\text{min}^{-1}$ the $Y_{\text{Unidentified}}$ was 12.7% and 10.4%, respectively. The aforementioned results indicated that the demanded electron moles for microbial cell growth and maintenance were not linearly correlated with the substrate supply rate.

Schwede et al. [32] performed batch mesophilic (38°C) experiments with non-acclimated anaerobic sludge and a headspace syngas composition of 48.4% H_2 , 26.4% CO_2 , 23.3% CO and 1.9% CH_4 which, coincidentally, has a $\text{SQI} = 1.44$ and achieved a 50% electron yield to CH_4 . In the present study at the same SQI in mesophilic conditions a much higher electron yield of 84% and 90% was observed at an EBRT of 3 h and 1.5 h, respectively. This indicates a better selectivity of the enriched MMC used in this study, albeit the comparison of a batch reactor with a continuous reactor should be done cautiously.

Furthermore, in section 3.1 (EBRT = 3 h) it was mentioned that as the SQI approached the SQI_{Id} , the volume specific CH_4 productivity (Fig. 2a) increased in both mesophilic and thermophilic conditions and this observation was attributed to the big increase of the stoichiometrical convertible carbon to CH_4 (Table 4). The same expected trend was observed at an EBRT of 1.5 h. When the convertible carbon supply was increased from

4.40 C·mmol·l_{bed}⁻¹·h⁻¹ (SQI = 1.44) to 5.32 C·mmol·l_{bed}⁻¹·h⁻¹ (SQI = 2.93), the volume specific CH₄ productivity was increased from 2.75 mmol·l_{bed}⁻¹·h⁻¹ to 3.99 mmol·l_{bed}⁻¹·h⁻¹ in mesophilic conditions and from 3.95 mmol·l_{bed}⁻¹·h⁻¹ to 4.82 mmol·l_{bed}⁻¹·h⁻¹ in thermophilic conditions. Subtracting the convertible carbon supply at SQI = 2.93 from the one at SQI = 1.44 equals to an increase of 0.92 C·mmol·l_{bed}⁻¹·h⁻¹. In thermophilic conditions the achieved increase in CH₄ productivity from SQI = 1.44 to 2.93 was 4.82-3.95 = 0.87 C·mmol·l_{bed}⁻¹·h⁻¹ (94.6% of the increase of the molar carbon supply), while in mesophilic conditions the respective increase was 3.99-2.75 = 1.24 C·mmol·l_{bed}⁻¹·h⁻¹ (134.8% of the increase of the carbon mole supply). These values can be explained by looking at the conversion efficiency the electron donors (H₂ and CO), which in mesophilic conditions increased from 70.8% to 86.5% for H₂ and from 67.5% to 84.0% for CO (Fig. 3c), while in thermophilic conditions they were almost fully converted in both SQIs.

Overall, the major outcome from the comparison of the two EBRTs was that the lower EBRT enhanced the selectivity to CH₄ and decreased the carbon and energy losses for the synthesis and maintenance of cell biomass (Fig 2d and Fig 3d). Furthermore, it can be concluded that an increase of the SQI led to a decrease of the electron yield to CH₄ irrespective of the temperature and the EBRT. In addition, in thermophilic conditions the electron donors (CO and H₂) were almost fully converted (>98%) in both EBRTs at SQIs < 4. This was not the case, though, at mesophilic conditions where a drop of the EBRT from 3 h to 1.5 h led to a decrease of the conversion efficiency of H₂ and CO at all SQIs < 4, thus indicating that the uptake rate of the substrate from the biofilm could not keep up with the increase of the supply rate of the substrate in the mesophilic reactor.

3.4 Operation of the thermophilic trickle bed reactor at the SQI_{Id}

Due to the fact that the mass flow controllers had an increment of 0.1 ml·min⁻¹, the closest value to the SQI_{Id} that could be achieved was 3.98 at a total gas inflow rate of 1.5 ml·min⁻¹ (Syngas Cylinder: 0.7 ml·min⁻¹ and high purity H₂ cylinder: 0.8 ml·min⁻¹). The conversion efficiency of the substrate at SQI = 3.98 was 99.7% for H₂, 99.0% for CO and 97.2% for CO₂, resulting in a biomethane composition of 77.3% CH₄, 1.4% CO₂, 1.0% H₂, 0.4% CO and 19.9% N₂ (Fig. 4). As expected, the CO₂ content (1.4%) in biomethane was the lowest amongst all operating conditions tested with a SQI < 4. Additionally, at SQI = 3.98 the fraction of CH₄ (77.3%) in biomethane was the highest observed in the present study.

In section 2.3, it was stated that the syngas composition in the syngas cylinder was chosen according to a suggestion from a collaborating company with expertise in gasification technologies, and that a slight modification from this suggestion was made by replacing 10% CH₄ with 10% N₂. Assuming that CH₄ had not been substituted by N₂, the content of CH₄ in biomethane at SQI = 3.98 would be 97.2%. The Upper Wobbe

Index of biomethane with a gas composition of 97.2% CH₄, 1.0% H₂, 0.4% CO and 1.4% CO₂ is 51.76 MJ·Nm⁻³ (calculated based on ISO 6976:2016), a value that lies within the allowed bandwidth for substitution of natural gas in the European Union. For example, in France the allowed range is 48.24 – 56.52 MJ·Nm⁻³ and in Germany 46.1 – 56.5 MJ·Nm⁻³ [17]. Furthermore, the presented gas composition complies with additional requirements such as CO₂ content < 2% and H₂ content < 5% [17]. As a result, operating the trickle bed reactor with the enriched MMC at a SQI \cong SQI_{ld} can produce a gas mixture able to be injected in the natural gas grid without the need of downstream processing applications.

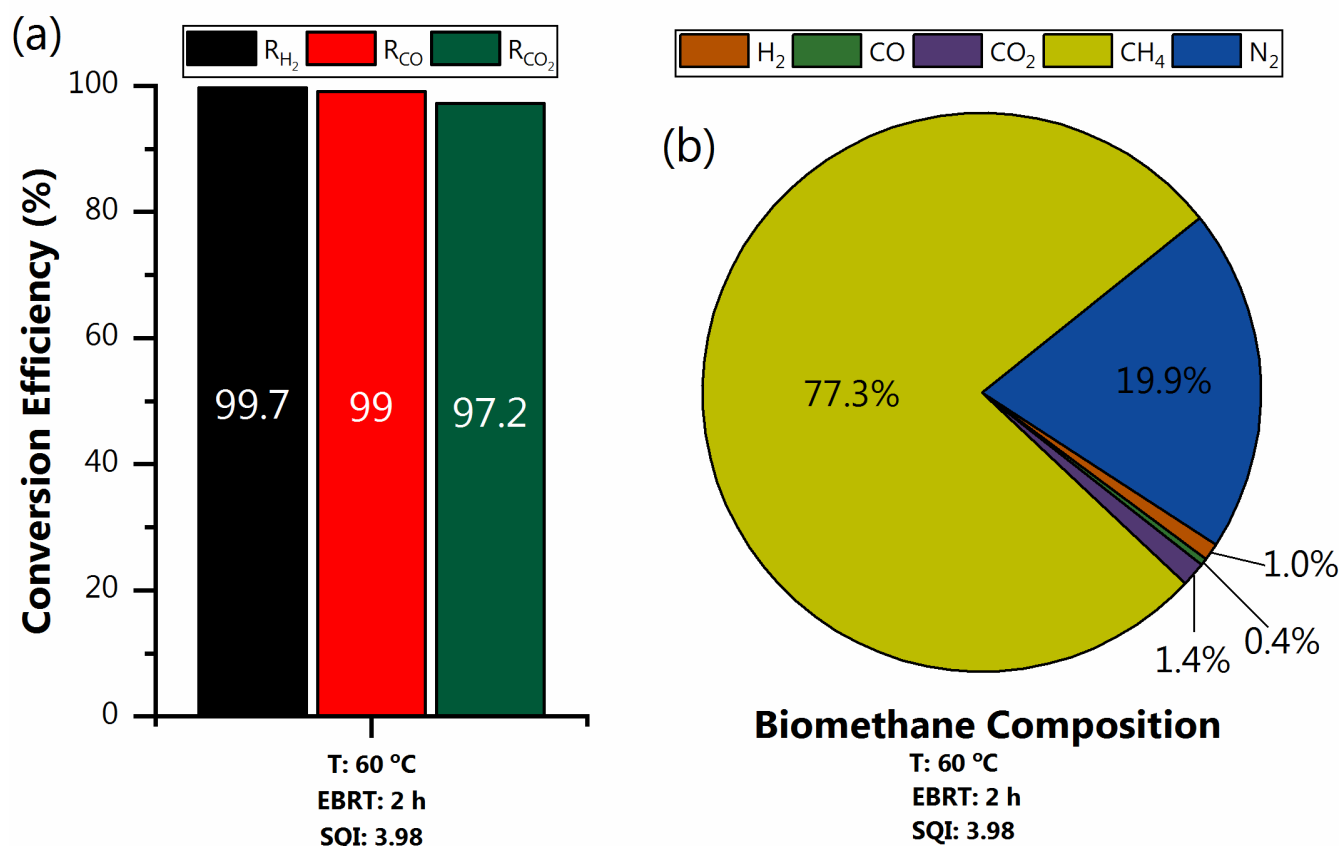


Figure 4. (a) Conversion Efficiency of H₂, CO and CO₂ at SQI = 3.98, temperature = 60 °C and EBRT = 2 h. (b) Biomethane composition at SQI = 3.98 and EBRT = 2 h.

3.5 Thermodynamic interpretation of the effect of H₂ and CO₂ on catabolic routes

In the sections above, it was demonstrated that the addition of exogenous H₂ to a synthetic syngas mixture might allow for producing a natural gas grid standard biomethane as well as increasing the CH₄ productivity in both

mesophilic and thermophilic trickle bed reactors. Based on previous work on the same enriched microbial consortia, an additional expected benefit from the addition of exogenous H_2 was a significant reduction in byproducts formation [10]. In this study, the electron yield to VFAs did not exceed 5% in any of the conditions tested. However, other studies including mixed and co-cultures reported a rather high fraction of e-mols diverted to VFAs of 10% and higher during the biomethanation of syngas [29,40,42].

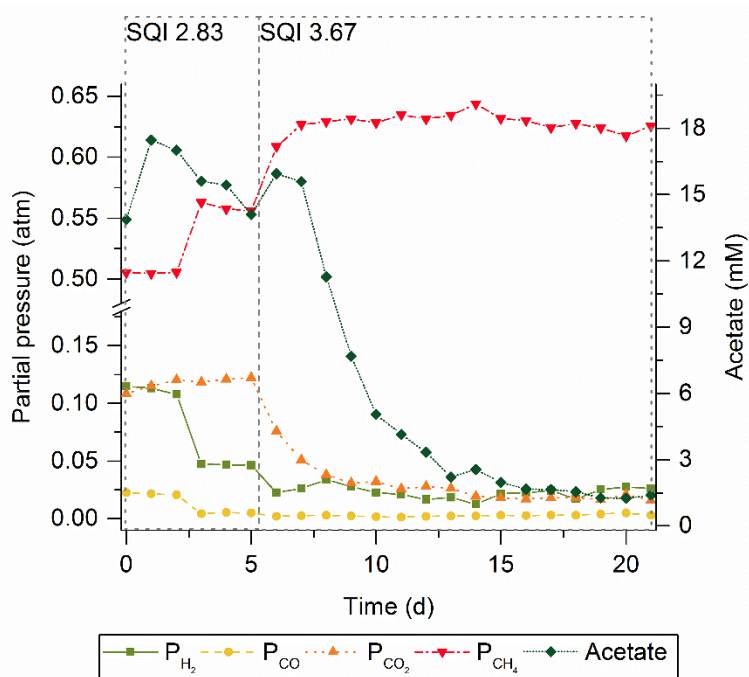


Figure 5. Partial pressure of gases in the effluent and acetate concentration profile of the mesophilic trickle bed reactor operated in continuous mode at SQI 2.83 and 3.67.

Reduction of the net VFAs production, through control of the active catabolic routes used by the mesophilic microbial consortium, was evaluated based on the effects of the decreasing P_{CO_2} during a transient state from a SQI = 2.83 to a SQI = 3.67. As shown in Fig. 5, the P_{CO_2} exerted a clear effect on the concentration of acetate at mesophilic conditions. Decreasing the P_{CO_2} from 0.12 atm to 0.016 atm (and the P_{H_2} from 0.11 atm to around 0.02 atm) resulted in a twelve-fold decrease in the acetate concentration in the reactor, which corresponded to a drop in the respective electron yield from 3.4% to 0.4%. In this case, the higher acetate conversion could not be attributed to a higher aceticlastic activity since the latter should not be significantly affected by changes in CO_2 concentration in the liquid at the range tested. Additionally, in previous work it was found that this microbial group was probably absent in this enriched microbial consortium [43]. Instead, the higher acetate conversion activity could be explained by the fact that the syntrophic interaction between syntrophic acetate oxidizers (SAO)

and hydrogenotrophic methanogens (HM) was enabled or significantly enhanced from the drop of the concentration of H_2 and CO_2 in the liquid. The thermodynamic feasibility of this syntrophic interaction was evaluated through the thermodynamic potential factor (F_T), which takes values above zero when a specific biochemical reaction is thermodynamically feasible. According to F_T calculations as a function of P_{H_2} and P_{CO_2} using the process conditions found experimentally, the syntrophic interaction between SAO and HM would not be possible at a P_{CO_2} of 0.1 atm since HM would not be able to decrease the P_{H_2} to levels low enough to allow syntrophic acetate oxidation (fig.6). However, decreasing the concentration of CO_2 in the liquid to levels equivalent to a P_{CO_2} of 0.001 atm would make this syntrophic interaction clearly feasible, as it can be seen that both HM and SAO could be active at the same range of H_2 concentrations (intersection of the yellow and red line corresponding to $P_{CO_2} = 0.001$ in fig. 6b). Considering that the CO_2 concentration in the liquid should be significantly below its saturation level due to the fact that there is net consumption of CO_2 , it can be concluded that the drop in acetate concentration was due to a higher syntrophic acetate oxidation activity. Therefore, paradoxically, adding exogenous H_2 to the mesophilic trickle bed reactor favored a higher acetate conversion into H_2 and CO_2 by SAO (and ultimately into CH_4 by HM), resulting in lower byproduct formation.

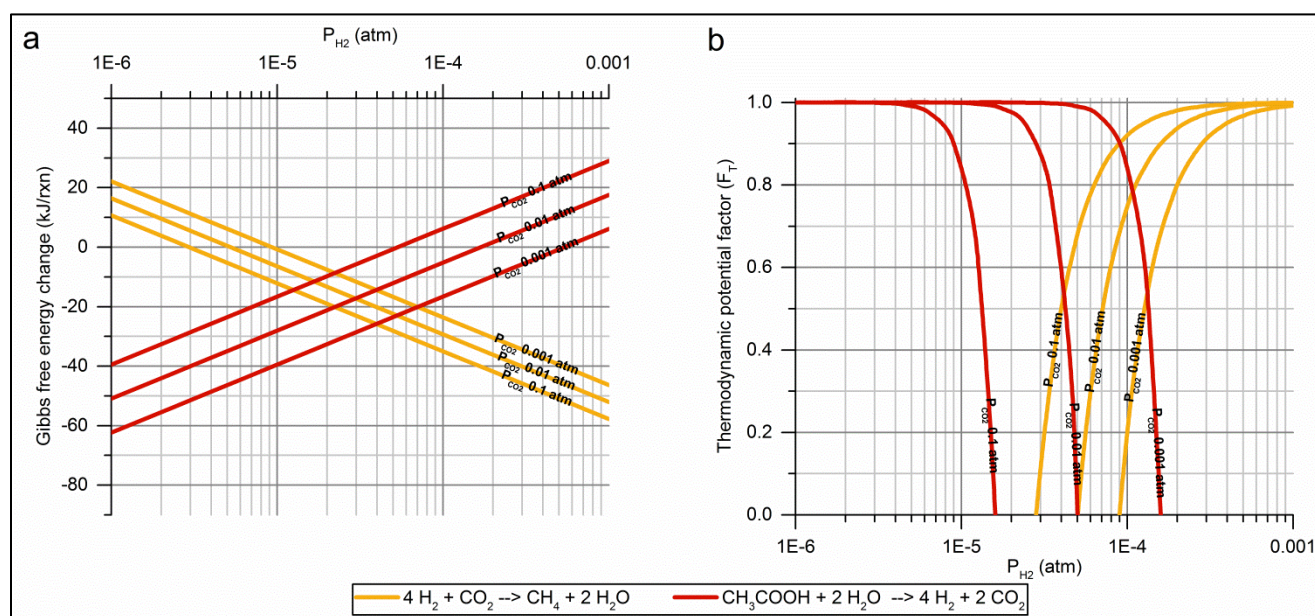


Figure 6. (a) Gibbs free energy change ($\Delta_r G'_{310K}$) as a function of P_{H_2} in kJ per reaction (according to the stoichiometry given in table 3) for hydrogenotrophic methanogenesis and syntrophic acetate oxidation calculated at different P_{CO_2} . (b) Thermodynamic potential factor (F_T) as a function of P_{H_2} for hydrogenotrophic methanogenesis and syntrophic acetate oxidation calculated at different P_{CO_2} . The operating conditions considered in the calculations were P_{CO_2} of 0.1 atm, 0.01 atm and 0.001 atm; P_{CH_4} of 0.6 atm; acetate concentration of 17 mM; temperature of 310 K; pH 7.4; and ionic strength of 0.25 M.

In previous work it was shown that the carboxydrotrophic and hydrogenotrophic microbial groups present in the thermophilic microbial consortium used here corresponded strictly to HM and carboxydrotrophic hydrogenogens [10,43]. Consequently, the VFA production observed in the thermophilic reactor was attributed to the acetogenic metabolism of carboxydrotrophic hydrogenogens, which has been shown to be dependent on the intrinsic thermodynamic limitation of the hydrogenogenesis [44,45]. The high sensitivity of the thermodynamic feasibility of the carboxydrotrophic hydrogenogenesis is shown in figure 7, where it can be seen that the minimum threshold P_{CO} is strongly affected by changes in P_{H_2} and P_{CO_2} (with the minimum threshold P_{CO} changing 6 orders of magnitude depending on P_{H_2} and P_{CO_2}). According to this, decreasing the P_{CO_2} through the addition of exogenous H_2 at SQIs < 4 would be expected to result in lower acetate concentrations in the reactor, as this should make carboxydrotrophic hydrogenogenesis more exergonic. The effect of the P_{CO_2} on carboxydrotrophic hydrogenogenesis and the formation of acetate as byproduct was evaluated experimentally through the increase of the SQI from 2.93 to 3.67 and 4.78, where the H_2 supply was increased gradually to achieve a lower P_{CO_2} . In this case, the decrease of the P_{CO_2} from 0.23 atm to 0.07 atm resulted only in a modest decrease in the acetate concentration from 16.8 mM (electron yield of 3.1%) to 11.4 mM (electron yield of 2%), probably due to the fact that the CO_2 concentration was not low enough to avoid acetate production (Fig. 8). It should be noted, though, that the production of acetate in thermophilic conditions also occurs due to the high abundance of dead cell scavengers such as the proteolytic genera *Coprothermobacter* and *Lutispora* [43]. Subsequently, adding excess H_2 to decrease further the P_{CO_2} resulted in a drastic drop in the conversion of CO arising from the increase in P_{H_2} and the saturated concentration of H_2 in the liquid, which limited the thermodynamic feasibility of hydrogenogenesis. This shows that the partial inhibition of carboxydrotrophic hydrogenogenesis in thermophilic conditions abovementioned (see section 3.1), observed at SQI of 4.78, was grounded on a thermodynamic limitation of this reaction.

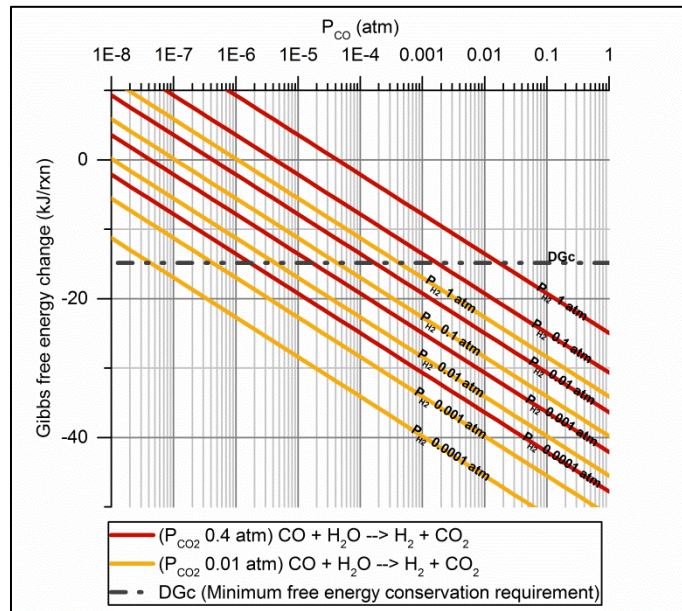


Figure 7. Gibbs free energy change ($\Delta_r G'_{333K}$) as a function of P_{CO} in kJ per reaction for carboxydrotrophic hydrogenogenesis calculated using different P_{H_2} and P_{CO_2} . The dashed line indicates the minimum energy conservation requirements (ΔG_c or ΔG_{min}) assumed for carboxydrotrophic hydrogenogenesis and the minimum threshold P_{CO} at each of the conditions considered. The calculations were made using a P_{H_2} of 1 atm, 0.1 atm, 0.01 atm, 0.001 atm and 0.0001 atm; P_{CO_2} of 0.4 atm and 0.01 atm; and temperature of 333 K.

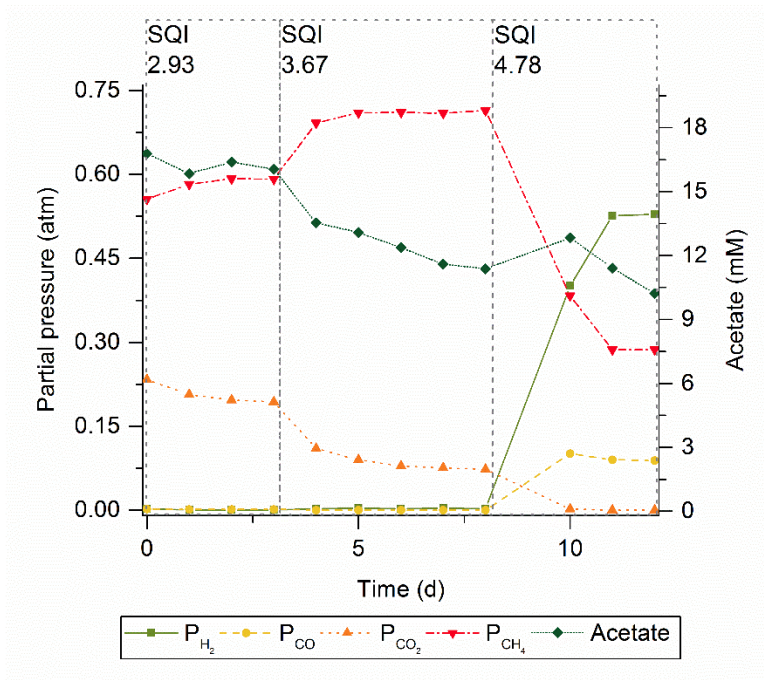


Figure 8. Partial pressure of gases and acetate concentration profile of the thermophilic trickle bed reactor operated in continuous mode at SQI 2.93, 3.67 and 4.78.

4. Conclusions

Based on the stoichiometry of the biological reactions leading to the production of CH₄ when syngas is used as the sole carbon and electron donor, a new index (the syngas quality index, SQI) was introduced for the assessment of the impacts of syngas composition on syngas biomethanation. The results of the performed experiments showed an enhancement of the CH₄ productivity and the content of CH₄ in the effluent gas of the reactor under both mesophilic and thermophilic conditions, when exogenous H₂ was supplied at increasing SQIs < 4. At an empty bed residence time (EBRT) of 1.5 h and a temperature of 60 °C, increasing the SQI from 1.44 to 3.67 resulted in an increase of the volume specific CH₄ productivity from 3.95 mmol·l_{bed}⁻¹·h⁻¹ to 4.85 mmol·l_{bed}⁻¹·h⁻¹ and the CH₄ content in the produced gas from 30% to 72%. When a SQI = 3.98 (the stoichiometrically ideal is 4) was applied, it was portrayed that natural gas grade biomethane complying with the criteria for introduction to the natural gas grid of European countries can be produced. Furthermore, increase of the SQI above 4 resulted in a big drop of the CH₄ productivity and the CH₄ content due to the high stoichiometrical excess of H₂ that remained unconverted. An additional outcome was the superior biomethanation performance of the trickle bed reactor under thermophilic conditions compared to mesophilic conditions independent of the net inlet syngas composition. Finally, it was demonstrated that observed changes in the catabolic routes of the mixed microbial consortia related to carboxydrotrophic hydrogenogenesis, syntrophic acetate oxidation, hydrogenotrophic methanogenesis and acetogenesis could be explained thermodynamically, and therefore, potentially induced by applying thermodynamic control strategies.

Considering the scale-up of this process, the major conclusions of this study are that it is preferable to operate the reactor at thermophilic conditions and that it is of vital important to regulate the flow of the additional H₂ supply to levels that will produce a net inlet gas composition in the proximity of a SQI = 4, and preferably slightly lower since stoichiometric excess of H₂ causes thermodynamic limitations to the carboxydrotrophic hydrogenogenic metabolism in thermophilic conditions.

Acknowledgements

This work was financially supported by the Technical University of Denmark (DTU) and Innovation Fund Denmark in the frame of SYNFERON project.

References

- [1] H. Li, D. Mehmood, E. Thorin, Z. Yu, Biomethane Production Via Anaerobic Digestion and Biomass Gasification, *Energy Procedia*. 105 (2017) 1172–1177. doi:10.1016/j.egypro.2017.03.490.
- [2] Z. Bagi, N. Ács, T. Böjti, B. Kakuk, G. Rákhely, O. Strang, M. Szuhaj, R. Wirth, K.L. Kovács, Biomethane: The energy storage, platform chemical and greenhouse gas mitigation target, *Anaerobe*. 46 (2017) 13–22. doi:10.1016/j.anaerobe.2017.03.001.
- [3] B. Lecker, L. Illi, A. Lemmer, H. Oechsner, Biological hydrogen methanation – A review, *Bioresour. Technol.* 245 (2017) 1220–1228. doi:10.1016/j.biortech.2017.08.176.
- [4] A. Grimalt-Alemany, I. V. Skiadas, H.N. Gavala, Syngas biomethanation: state-of-the-art review and perspectives, *Biofuels, Bioprod. Biorefining*. 12 (2018) 139–158. doi:10.1002/bbb.1826.
- [5] E.G. Pereira, J.N. da Silva, J.L. de Oliveira, C.S. Machado, Sustainable energy: A review of gasification technologies, *Renew. Sustain. Energy Rev.* 16 (2012) 4753–4762. doi:https://doi.org/10.1016/j.rser.2012.04.023.
- [6] A. Molino, S. Chianese, D. Musmarra, Biomass gasification technology: The state of the art overview, *J. Energy Chem.* 25 (2016) 10–25. doi:10.1016/j.jechem.2015.11.005.
- [7] S. Ghosh, R. Chowdhury, P. Bhattacharya, Mixed consortia in bioprocesses: role of microbial interactions, *Appl. Microbiol. Biotechnol.* 100 (2016) 4283–4295. doi:10.1007/s00253-016-7448-1.
- [8] J. Sipma, P.N.L. Lens, A.J.M. Stams, G. Lettinga, Carbon monoxide conversion by anaerobic bioreactor sludges, *FEMS Microbiol. Ecol.* 44 (2003) 271–277. doi:10.1016/S0168-6496(03)00033-3.
- [9] S.R. Guiot, R. Cimpoaia, G.G. Carayon, Potential of wastewater-treating anaerobic granules for biomethanation of synthesis gas, *Environ. Sci. Technol.* 45 (2011) 2006–2012. doi:10.1021/es102728m.
- [10] A. Grimalt-Alemany, M. Łężyk, D.M. Kennes-Veiga, I. V. Skiadas, H.N. Gavala, Enrichment of Mesophilic and Thermophilic Mixed Microbial Consortia for Syngas Biomethanation: The Role of Kinetic and Thermodynamic Competition, *Waste and Biomass Valorization*. (2019). doi:10.1007/s12649-019-00595-z.
- [11] S.S. Navarro, R. Cimpoaia, G. Bruant, S.R. Guiot, Biomethanation of Syngas Using Anaerobic Sludge:

- Shift in the Catabolic Routes with the CO Partial Pressure Increase, *Front. Microbiol.* 7 (2016) 1188. doi:10.3389/fmicb.2016.01188.
- [12] R.K. Thauer, A. Kaster, H. Seedorf, W. Buckel, Methanogenic archaea: ecologically relevant differences in energy conservation, *Nat. Rev. Microbiol.* 6 (2008) 579–591. doi:10.1038/nrmicro1931.
- [13] F. Bu, N. Dong, S. Kumar Khanal, L. Xie, Q. Zhou, Effects of CO on hydrogenotrophic methanogenesis under thermophilic and extreme-thermophilic conditions: Microbial community and biomethanation pathways, *Bioresour. Technol.* 266 (2018) 364–373. doi:10.1016/j.biortech.2018.03.092.
- [14] R.M. Slivka, M.S. Chinn, A.M. Grunden, Gasification and synthesis gas fermentation: an alternative route to biofuel production, *Biofuels.* 2 (2011) 405–419. doi:10.4155/bfs.11.108.
- [15] A.S. Mednikov, A Review of Technologies for Multistage Wood Biomass Gasification, *Therm. Eng.* (2018). doi:10.1134/s0040601518080037.
- [16] Y. Wang, C. Yin, Y. Liu, M. Tan, K. Shimizu, Z. Lei, Z. Zhang, I. Sumi, Y. Yao, Y. Mogi, Biomethanation of blast furnace gas using anaerobic granular sludge via addition of hydrogen, *RSC Adv.* 8 (2018) 26399–26406. doi:10.1039/C8RA04853C.
- [17] L. Rachbauer, G. Voithl, G. Bochmann, W. Fuchs, Biological biogas upgrading capacity of a hydrogenotrophic community in a trickle-bed reactor, *Appl. Energy.* 180 (2016) 483–490. doi:10.1016/j.apenergy.2016.07.109.
- [18] M. Thema, T. Weidlich, M. Hörl, A. Bellack, F. Mörs, F. Hackl, M. Kohlmayer, J. Gleich, C. Stabenau, T. Trabold, M. Neubert, F. Ortloff, R. Brotsack, D. Schmack, H. Huber, D. Hafenbradl, J. Karl, M. Sterner, Biological CO₂-Methanation: An Approach to Standardization, *Energies.* 12 (2019) 1670. doi:10.3390/en12091670.
- [19] M. Thema, F. Bauer, M. Sterner, Power-to-Gas: Electrolysis and methanation status review, *Renew. Sustain. Energy Rev.* 112 (2019) 775–787. doi:10.1016/j.rser.2019.06.030.
- [20] M. Yasin, N. Jang, M. Lee, H. Kang, M. Aslam, A. Bazmi, Bioreactors , gas delivery systems and supporting technologies for microbial synthesis gas conversion process by, *Bioresour. Technol. Reports.* (2019).
- [21] H. Porté, P.G. Kougiyas, N. Alfaro, L. Treu, S. Campanaro, I. Angelidaki, Process performance and

- microbial community structure in thermophilic trickling biofilter reactors for biogas upgrading, *Sci. Total Environ.* 655 (2019) 529–538. doi:10.1016/j.scitotenv.2018.11.289.
- [22] M. Burkhardt, T. Koschack, G. Busch, Biocatalytic methanation of hydrogen and carbon dioxide in an anaerobic three-phase system, *Bioresour. Technol.* 178 (2015) 330–333. doi:10.1016/j.biortech.2014.08.023.
- [23] D. Strübing, B. Huber, M. Lebuhn, J.E. Drewes, K. Koch, High performance biological methanation in a thermophilic anaerobic trickle bed reactor, *Bioresour. Technol.* 245 (2017) 1176–1183. doi:10.1016/j.biortech.2017.08.088.
- [24] F.S. Mederos, J. Ancheyta, J. Chen, Review on criteria to ensure ideal behaviors in trickle-bed reactors, *Appl. Catal. A Gen.* (2009). doi:10.1016/j.apcata.2008.11.018.
- [25] M. Edel, H. Horn, J. Gescher, Biofilm systems as tools in biotechnological production, *Appl. Microbiol. Biotechnol.* 103 (2019) 5095–5103. doi:10.1007/s00253-019-09869-x.
- [26] K. Asimakopoulos, H.N. Gavala, I. V. Skiadas, Reactor systems for syngas fermentation processes: A review, *Chem. Eng. J.* 348 (2018) 732–744. doi:10.1016/j.cej.2018.05.003.
- [27] D. Strübing, A.B. Moeller, B. Mößnang, M. Lebuhn, J.E. Drewes, K. Koch, Anaerobic thermophilic trickle bed reactor as a promising technology for flexible and demand-oriented H₂/CO₂ biomethanation, *Appl. Energy.* 232 (2018) 543–554. doi:10.1016/j.apenergy.2018.09.225.
- [28] I. Angelidaki, L. Treu, P. Tsapekos, G. Luo, S. Campanaro, H. Wenzel, P.G. Kougias, Biogas upgrading and utilization: Current status and perspectives, *Biotechnol. Adv.* 36 (2018) 452–466. doi:10.1016/j.biotechadv.2018.01.011.
- [29] K. Asimakopoulos, H.N. Gavala, I. V. Skiadas, Biomethanation of Syngas by Enriched Mixed Anaerobic Consortia in Trickle Bed Reactors, *Waste and Biomass Valorization.* (2019). doi:10.1007/s12649-019-00649-2.
- [30] K. Chandolias, E. Pekgenc, M.J. Taherzadeh, Floating Membrane Bioreactors with High Gas Hold-Up for Syngas-to-Biomethane Conversion, *Energies.* 12 (2019) 1046. doi:10.3390/en12061046.
- [31] F. Lü, K. Guo, H. Duan, L. Shao, P. He, Exploit Carbon Materials to Accelerate Initiation and Enhance Process Stability of CO Anaerobic Open-Culture Fermentation, *ACS Sustain. Chem. Eng.* 6 (2018)

2787–2796. doi:10.1021/acssuschemeng.7b04589.

- [32] S. Schwede, F. Bruchmann, E. Thorin, M. Gerber, Biological Syngas Methanation via Immobilized Methanogenic Archaea on Biochar, *Energy Procedia*. 105 (2017) 823–829. doi:10.1016/j.egypro.2017.03.396.
- [33] S. Westman, K. Chandolias, M. Taherzadeh, Syngas Biomethanation in a Semi-Continuous Reverse Membrane Bioreactor (RMBR), *Fermentation*. 2 (2016) 8. doi:10.3390/fermentation2020008.
- [34] R.A. Alberty, *Thermodynamics of Biochemical Reactions*, John Wiley & Sons, Inc, New Jersey, 2003.
- [35] K.J.J. Steinbusch, H.V.M. Hamelers, C.J.N. Buisman, Alcohol production through volatile fatty acids reduction with hydrogen as electron donor by mixed cultures, *Water Res.* 42 (2008) 4059–4066. doi:10.1016/j.watres.2008.05.032.
- [36] Q. Jin, C.M. Bethke, The thermodynamics and kinetics of microbial metabolism, *Am. J. Sci.* 307 (2007) 643–77. doi:10.2475/04.2007.01.
- [37] A. Kaster, J. Moll, K. Parey, R.K. Thauer, Coupling of ferredoxin and heterodisulfide reduction via electron bifurcation in hydrogenotrophic methanogenic archaea, 108 (2011) 2981–2986. doi:10.1073/pnas.1016761108.
- [38] B.E. Jackson, M.J. McInerney, Anaerobic microbial metabolism can proceed close to thermodynamic limits, *Nature*. 415 (2002) 454–6.
- [39] Y. Jing, S. Campanaro, P. Kougias, L. Treu, I. Angelidaki, S. Zhang, G. Luo, Anaerobic granular sludge for simultaneous biomethanation of synthetic wastewater and CO with focus on the identification of CO-converting microorganisms, *Water Res.* 126 (2017) 19–28. doi:10.1016/j.watres.2017.09.018.
- [40] M. Diender, P.S. Uhl, J.H. Bitter, A.J.M. Stams, D.Z. Sousa, High Rate Biomethanation of Carbon Monoxide-Rich Gases via a Thermophilic Synthetic Coculture, *ACS Sustain. Chem. Eng.* 6 (2018) 2169–2176. doi:10.1021/acssuschemeng.7b03601.
- [41] L. Rachbauer, R. Beyer, G. Bochmann, W. Fuchs, Characteristics of adapted hydrogenotrophic community during biomethanation, *Sci. Total Environ.* 595 (2017) 912–919. doi:10.1016/j.scitotenv.2017.03.074.
- [42] A.L. Arantes, J.I. Alves, A.J.M. Stams, M.M. Alves, D.Z. Sousa, Enrichment of syngas-converting

communities from a multi-orifice baffled bioreactor, *Microb. Biotechnol.* 11 (2018) 639–646. doi:10.1111/1751-7915.12864.

- [43] K. Asimakopoulos, M. Łężyk, A. Grimalt-Alemany, A. Melas, Z. Wen, H.N. Gavala, I. V. Skiadas, Temperature Effects on Syngas Biomethanation Performed in a Trickle Bed Reactor, *Submitt. to Chem. Eng. J.* (2019).
- [44] A.M. Henstra, A.J.M. Stams, Deep Conversion of Carbon Monoxide to Hydrogen and Formation of Acetate by the Anaerobic Thermophile *Carboxydotherrmus hydrogenoformans*, *Int. J. Microbiol.* 2011 (2011) 1–4. doi:10.1155/2011/641582.
- [45] A. Grimalt-Alemany, K. Asimakopoulos, I. V. Skiadas, H.N. Gavala, Modeling of Syngas Biomethanation and Control of Catabolic Routes of Mesophilic and Thermophilic Mixed Cultures, *Submitt. to Appl. Energy.* (2019).